ADVANCES IN EXPERIMENTAL MEDICINE AND BIOLOGY

Volume 592

REGULATORY MECHANISMS OF STRIATED MUSCLE CONTRACTION

Edited by
Setsuro Ebashi,
Iwao Ohtsuki

Springer

REGULATORY MECHANISMS OF STRIATED MUSCLE CONTRACTION

ADVANCES IN EXPERIMENTAL MEDICINE AND BIOLOGY

Recent Volumes in this Series

Volume 586
CURRENT TOPICS IN COMPLEMENT
Edited by John D. Lambris

Volume 587
NEW TRENDS IN CANCER FOR THE 21st CENTURY
Edited by Antonio Llombart-Bosch, Jose López-Guerrero and Vincenzo Felipe

Volume 588
HYPOXIA AND EXERCISE
Edited by Robert C. Roach, Peter D. Wagner, and Peter H. Hackett

Volume 589
NEURAL CREST INDUCTION AND DIFFERENTIATION
Edited by Jean-Pierre Saint-Jeannet

Volume 590
CROSSROADS BETWEEN INNATE AND ADAPTIVE IMMUNITY
Edited by Peter D. Katsikis

Volume 591
SOMATIC CELL NUCLEAR TRANSFER
Edited by Peter Sutovsky

Volume 592
REGULATORY MECHANISMS OF STRIATED MUSCLE CONTRACTION
Edited by Setsuro Ebashi and Iwao Ohtsuki

Volume 593
MICROARRAY TECHNOLOGY AND CANCER GENE PROFILING
Edited by Simone Mocellin

Volume 594
MOLECULAR ASPECTS OF THE STRESS RESPONSE
Edited by Peter Csermely and Laszlo Vigh

REGULATORY MECHANISMS OF STRIATED MUSCLE CONTRACTION

Edited by

Setsuro Ebashi
National Institute of Physiological Sciences
Okazaki, Japan

and

Iwao Ohtsuki
The Jikei University School of Medicine
Tokyo, Japan

Springer

Proceedings of the symposium entitled “Regulatory Proteins of Striated Muscle – Structure, Function and Disorder (33rd NIPS Conference),” held at Okazaki, Japan, October 25–28, 2005, and supported by the following organizations: National Institute of Physiological Sciences (NIPS), The Jikei University School of Medicine, Japan Science and Technology Agency (ERATO-Actin Dynamics Project), Uehara Memorial Foundation for Life Sciences, Sankyo Life Science Foundation, Naito Memorial Foundation, Kato Memorial Fund for Diseases, and Zenyaku Kogyo Co. Ltd

ISSN 0065 2598

ISBN-10 4-431-38451-0 Springer Tokyo Berlin Heidelberg New York
ISBN-13 978-4-431-38451-9 Springer Tokyo Berlin Heidelberg New York

Library of Congress Control Number: 2006935370

Printed on acid-free paper

Typesetting: SNP Best-set Typesetter Ltd., Hong Kong
Printing and binding: Kato Bunmeisha, Japan

CONTENTS

III. REGULATION IN CARDIAC MUSCLE AND DISORDERS

IV. REGULATION BY MYOSIN

V. EXCITATION-CONTRACTION COUPLING AND DISORDER

PREFACE

The discovery of troponin by Professor Setsuro Ebashi opened a new era for research into the regulation of striated muscle contraction. This volume is the proceedings of the symposium held at Okazaki, Japan, in 2005 celebrating the 40th anniversary of that discovery.

Professor Ebashi started his work on muscle contraction when he was a young researcher, immediately after World War II, having been inspired by the book *Chemistry of Muscular Contraction* by Albert Szent-Györgyi. He was fascinated by the dynamic features of the contractile processes performed by the two contractile proteins, myosin and actin, in the presence of ATP. However, he wondered about the mechanism by which muscle relaxes after contraction. He proceeded with biochemical studies of muscle relaxation and found in 1952 that a factor present in the supernatant of the suspension of minced frog skeletal muscle caused relaxation of glycerinated muscle fibers. Based on this finding and succeeding work, he came to the conclusion that the relaxation of contracted muscle was caused by the uptake of calcium ions from the cytosol into the relaxing factor (sarcoplasmic reticulum). His work greatly contributed to elucidating the entire processes of excitation–contraction coupling, particularly the role of calcium ions in triggering the contractile response of myofibrils.

Then he found that superprecipitation of actomyosin, i.e., an in vitro contraction model, became sensitive to calcium ion concentration in the presence of a protein factor other than myosin and actin. This factor showed some similarity to tropomyosin, which had been reported by Bailey, and thus was called native tropomyosin.

When I started working in Professor Ebashi's laboratory in 1963 as a graduate student, he was working very hard with his wife to characterize the biochemical properties of native tropomyosin. Tropomyosin, reported by Bailey, was actually isolated by isoelectric precipitation from native tropomyosin, but it did not confer any calcium sensitivity to actomyosin. In 1965, Professor Ebashi succeeded in isolating a new protein named "troponin" from native tropomyosin, which, in association with tropomyosin, made actomyosin sensitive to calcium ions. With a series of studies in the 1960s, the molecular basis for the regulation of muscle contraction was established. Since that time, troponin has been the central object in research on the regulation of striated muscle contraction. Properties of troponin, which consists of three different components, have been extensively investigated as revealing insights into a representative calcium-receptive and calcium-regulatory protein.

Professor Ebashi and I sincerely hoped that this volume would become a milestone for future developments in the study of the regulation of muscle contraction and related biomedical sciences. I would like to express my profound gratitude to all contributors for their heartfelt cooperation.

Finally, I regret to say that Professor Ebashi passed away in July. Although he could not see this volume through to publication, every detail of the book should be in accord with his long-lasting interest in muscle science. He was a great pioneer in the molecular biology of the regulation of muscle contraction.

Iwao Ohtsuki
August 2006

October 19, 2005

Dear Ebashi-san,

On this anniversary of the discovery of troponin, I would like to add a few words to all the praise of this great achievement – in a letter, since to my great regret I cannot be at the symposium in person.

What in my eyes made this work so outstanding and so successful was that it was all based on one concept: calcium triggers muscle contraction. Also, your interpretation of this concept was unusually broad for its day, extending calcium signaling beyond myofibrillar shortening to other processes essential to muscle contraction as a whole, such as the rapid release of fuel at the beginning of contraction. To show what I mean I would like to trace the elegant progression of this work in a few words.

When I first met you in 1958 or 1959, you had just started to look for evidence that calcium was the activator of myofibrillar contraction. If it was, you reasoned, relaxation should be caused by calcium removal from myofibrils and actomyosin. This implied that the relaxing factor should act by removing calcium from myofibrils. Thus, in Lipmann's laboratory you were searching for calcium binding by what was then called the particulate relaxing factor. More than that, you were searching for ATPase-dependent calcium binding because you had shown earlier that the relaxing action of the relaxing factor disappeared when its intrinsic ATPase activity was destroyed. You found what you searched for.

During this same period I heard you give a seminar discussing the other aspect of this argument: myofibrils should relax whenever calcium was removed; for instance they should relax in the presence of chelating agents. In 1961 you published a paper that demonstrated this. The concept that calcium removal from myofibrils was responsible for relaxation was new: do you remember how it was roundly rejected by nearly everybody in the field at the 1962 Dedham Conference?

The basis for the rejection was that a mixture of highly purified actin and myosin – in contrast to myofibrils or actomyosin extracted as the complex between the two proteins – always contracted on ATP addition, even after the complete removal of calcium by EDTA. However, you persisted, because you knew you were right. The experiments with purified actomyosin drove you to search for a calcium-sensitive structural protein that might have been removed during the preparation of actin. In 1963 you announced in *Nature* that "native tropomyosin" was the protein responsible for the calcium regulation of actomyosin contraction. In 1965 you, Fumiko [Ebashi] and Ayako Kodama succeeded in isolating the small protein that made native tropomyosin different from pure tropomyosin and was responsible for calcium sensitivity. You named this protein troponin, and some years later Iwao Ohtsuki in your laboratory showed that it was bound to the I-bands of the myofibrils.

The evidence that calcium signaling extended beyond myofibrillar shortening came in 1967, when, in collaboration with Eijiro Ozawa and Keizo Hosoi, you showed that the

low calcium concentrations that initiated actomyosin contraction simultaneously also activated phosphorylase kinase, thereby triggering the explosive breakdown of glycogen, which supplies the fuel for contraction. In my recollection this was the first time that a messenger was shown to integrate a program rather than control a single reaction.

Ten years after the beginning of your series of discoveries, in 1968, you and Makoto Endo put together the whole calcium story in muscle in a beautiful review discussing in depth the role of calcium in every aspect of muscle contraction. Do you remember the feeling of doom during the student riots, when you wondered whether the review might be your last paper? I vividly remember your fear that the students might completely destroy your laboratories and thus put an end to your scientific career.

This did not happen, and instead your laboratory became one of the centers of muscle research, attracting frequent visitors. I remember fondly the enthusiastic group of young collaborators and students surrounding you, the freshness of the discussions, and the extremely generous hospitality we all received. It was a wonderful time.

I wish I could have told you this in person.

Annemarie Weber

The most important development in muscle science since the 1950s has been the discovery of the troponin–tropomyosin system and the light it has thrown on the mechanisms involved in the regulation of contraction in striated muscle. Indeed, I believe when the mechanism of regulation is completely elucidated it will lead to a further understanding of the interaction of actin and myosin itself. In view of Setsuro Ebashi's outstanding discovery and the further contributions of many of his colleagues, it is entirely appropriate that the celebration of the fortieth anniversary of this achievement should be made in Japan.

It grieves me very much that because of the current state of my health it would not be wise, and would certainly be very uncomfortable, for me to make the long journey required to attend this important meeting. Because of my long interest in this field I find this hard to bear. It is the one meeting I would wish to attend and renew acquaintance with many friends and colleagues of long standing. To them I convey my good wishes.

As one of the few muscle biochemists to visit Japan soon after the war, I was fortunate to meet in 1953 the individuals who were beginning to lay the foundations of the outstanding Japanese contributions to muscle science. Associated with Hiroshi Kumagai was a promising young scientist, Setsuro Ebashi, who was sedimenting out a relaxing factor fraction from muscle homogenates. Koscak Maruyama was a somewhat precocious graduate student and Fumio Oosawa and Yuji Tonomura were laying the foundations of their careers. My visit was somewhat unconventional, for I was enjoying a six-week tour of Japan as the Manager of the Cambridge University Rugby Team.

Setsuro Ebashi once commented to me that as rugby players we were treated like princes whereas life was very hard for him and his colleagues. It was clear from the visits to laboratories and muscle scientists made when I could sneak away from my duties that the funding of Japanese universities and research was still suffering from the war. I was, however, impressed with what had been achieved with very limited resources. Perhaps the most impressive event witnessed during my visit was Reiji Natori's demonstration of the skinned fibre preparation, then unknown in the West. In his laboratory he had a single muscle fibre mounted under a drop of oil. After sharpening a matchstick he amazed me by running it carefully along the fibre, detaching the membrane and leaving the myofibrils exposed.

Iwao Ohtsuki has made important contributions to the structure of the troponin complex and we are fortunate that he and his colleagues have organized this meeting at such an appropriate time. He deserves our sincere thanks for all his efforts and the efficient way he has carried them out. May I hope that when the meeting ends we shall have a mechanism for the molecular function of troponin with which we all agree.

S.V. Perry
October 19, 2005

I

HISTORICAL ASPECTS

1

BIOLOGICAL ACTIONS OF CALCIUM

Andrew Fielding Huxley

1.1. HISTORICAL

This meeting is being held to celebrate a great advance that was made forty years ago by Professor Setsuro Ebashi. This was the discovery of the substance "troponin",[1] a component of the thin filaments of striated muscle of vertebrates. A few years earlier,[2] Ebashi had given direct evidence that calcium ions, at a concentration of a few micromolar, cause contraction of actomyosin preparations. This was a remarkable achievement, since at that time calcium chelators were not available, and the level of calcium impurities had to be kept down by extreme care in preparation of his solutions. This observation was made while Ebashi was spending a year in the laboratory of Fritz Lipmann in New York. On his way back to Japan in 1960, he passed through Britain and took the opportunity of coming to Cambridge to visit Alan Hodgkin and myself. He told us of his observations, and also said that Lipmann had been unwilling to accept that anything as simple as a calcium ion could perform such an important and specific function, and that this had delayed Ebashi's publication of his results. Later, Ebashi told me that he had been much encouraged by my enthusiastic response to what he told us.

A little earlier, the importance of calcium in muscle contraction was shown by Professor Annemarie Weber,[3] using a biochemical, not a physiological, approach. This was a demonstration that actomyosin preparations would hydrolyse ATP only if calcium was present at micromolar (or higher) concentration.

The earliest indications of the importance of calcium in biological systems were given in the 1880s in two papers[4,5] by Sydney Ringer of University College Hospital, London. Both of these papers described experiments in which the contractions of the ventricle of a frog heart were recorded during perfusion with various solutions. The second draws attention to the fact that the saline (0.75% NaCl) used in the first paper was made up not with distilled water but with tap water, and shows that when distilled water was used the ventricle failed to contract. He showed that the difference was due to the presence in tap water of calcium. He found that contractions were well maintained if calcium chloride and potassium chloride were added to the saline at concentrations of about 0.5 and 1.3 mM respectively. The resulting solution was what has become familiar as "Ringer's Solution."

Trinity College, Cambridge, UK

Regulatory Mechanisms of Striated Muscle Contraction
Edited by Ebashi and Ohtsuki, Springer, 2007

The next step was taken in 1913 by G.R.Mines[6] of Cambridge (England) who showed that a heart perfused with a calcium-free solution still gave more or less normal action potentials, although there was no mechanical response. In the next year, he moved to Canada and was appointed Professor of Physiology at McGill University, Montreal. Tragically, he died soon after his move, during an experiment on respiration that he was performing on himself, alone in the laboratory. He was only 28 years of age. He was an exceptionally brilliant individual and his early death was a great loss to physiology.

No major progress on the functions of calcium was made between the two world wars. Interest in calcium was however maintained by a series of articles by L.V Heilbrunn of the University of Pennsylvania, which he summarised in a review in 1940.[7] He described the contractions that were produced when a damaged muscle fibre was immersed in solutions of calcium chloride at a series of concentrations of which the lowest was a little over 20 mM – four orders of magnitude greater than what was found later to produce a maximal contraction! A role of calcium – again at millimolar concentrations – was also proposed by Kenneth Bailey,[8] a distinguished muscle biochemist at Cambridge (England) who committed suicide when accused of homosexual activity. A later paper by Heilbrunn and Wiercinski[9] showed that a local contraction could be caused by injecting calcium chloride into a muscle fiber.

1.2. RELAXING FACTORS

The idea of a "relaxing factor" was introduced in 1951 by B. B. Marsh[10,11] who was working in Kenneth Bailey's laboratory. Marsh was following the time course of the decrease in volume of a preparation of fragmented muscle fibers, presumably due to the contractile material undergoing contraction. There was a delay of some minutes before this decrease in volume began, and it was accompanied by a decrease in the concentration of adenosine triphosphate in the preparation. This delay could be increased, and the contraction could be reversed, by adding supernatant from muscle fragments suspended in isotonic potassium chloride and centrifuged. Marsh concluded that this supernatant contained a "relaxing factor" that was normally present in the sarcoplasm of muscle, and in 1953 Lorand[12] proposed that this factor was the enzyme creatine phoshpokinase. Marsh's results were extended by J. R. Bendall,[13] also working in Bailey's laboratory, and in 1954 Bendall proposed that the factor was the enzyme myokinase.[14]

1.3. ACTIVATION OF MUSCLE BY CALCIUM

At about the same time, a major step forward was made by Emil Bozler of Ohio State University. He showed[15] that the substance EDTA (a chelator of calcium ions) imitates all the effects of the relaxing factor and concluded correctly that calcium ions are necessary for contraction. I remember discussing this result with a biochemist, and was again met with disbelief on the grounds that such a function could not be done by anything as simple as an inorganic ion. However, Bozler's interpretation has been universally confirmed, and it has become standard practice to use EDTA (or the still stronger chelator EGTA) to ensure that muscle remains in a relaxed state. Nevertheless, suggestions that the "factor" was an organic compound were still being made ten years later.[16]

1.4. ATPASE IN MUSCLE

Myosin, probably what we now call actomyosin, was recognized in 1939 by Engelhardt and his wife Ljubimova in Moscow[17] as being the main enzyme in muscle responsible for the hydrolysis of adenosine triphosphate. Then in 1948 Kielley and Meyerhof[18] found that myosin-free preparations from muscle had ATPase activity, and in 1952 it was shown by Perry[19] and by Hasselbach[20] that this activity was associated with a microsomal fraction. These microsomes have since been recognized as fragments of the lateral vesicles of the "triads" seen in electron micrographs by Porter and Palade[21] in the spaces between the myofibrils. In intact muscle these lateral vesicles contain stores of calcium, some of which is released when an action potential passes down the central element, which is a tubule continuous with the surface membrane of the fibre. If a negative electric pulse is applied through a micropipette to the mouth of one of these tubules, only the corresponding I-band (frog[22]) or half I-band (lizard[23] or crab[24]) responds by shortening.

1.5. OTHER ACTIONS OF CALCIUM

Since the work that I have mentioned, calcium has been shown to have very important actions as a co-factor for many enzymes. These will no doubt be discussed by other contributors to this symposium, but I will not say anything about them as I am no expert in this field.

1.6. REFERENCES

1. S. Ebashi, and A. Kodama, A new protein factor promoting aggregation of tropomyosin. *J. Biochem.* **58**, 107–108 (1965).
2. S. Ebashi, Third component participating in the superprecipitation of "natural actomyosin." *Nature, London*, **200**, 1010 (1963).
3. A. Weber, On the role of calcium in the activity of adenosine-5'-triphosphate hydrolysis by actomyosin. *J. biol. Chem.* **234**, 2764–2769 (1959).
4. S. Ringer, Concerning the influence exerted by each of the constituents of blood on the contraction of the ventricle. *J. Physiol.* **3**, 380–393 (1882).
5. S. Ringer, A further contribution regarding the influence of the different constituents of the blood on the contraction of the heart. *J. Physiol.* **4**, 29–42 (1883).
6. G. R. Mines, On functional analysis by the action of electrolytes. *J. Physiol.* **46**, 188–235 (1913).
7. L. V. Heilbrunn, The action of calcium on muscle protoplasm. *Physiol. Zool.* **13**, 88–94 (1940).
8. K. Bailey, Myosin and adenosinetriphosphatase. *Biochem. J.* **36**, 121–139 (1942).
9 L. V. Heilbrunn, and F. J. Wiercinski, The action of various cations on muscle protoplasm. *J. cell. comp. Physiol.* **29**, 15–32 (1947).
10. B. B. Marsh, A factor modifying muscle fibre synaeresis. *Nature*, **167**, 1065–1066 (1951).
11. B. B. Marsh, The effects of adenosine triphosphate on the fibre volume of a muscle homogenate. *Biochim. biophys. Acta* **9**, 247–260 (1952).
12. L. Lorand, Adenosinetriphosphate-creatine transphosphorylase as relaxing factor of muscle. *Nature*, **172**, 1181 (1953).
13. J. R. Bendall, Further observations on a factor (the "Marsh" factor) effecting relaxation of ATP-shortened muscle-fibre models, and the effect of Ca and Mg ions upon it. *J. Physiol.* **121**, 232–254 (1953).
14. J. R. Bendall, The relaxing effect of myokinase on muscle fibres; its identity with the "Marsh" factor. *Proc. R. Soc. Lond. B* **142**, 409–426 (1954).

15. E. Bozler, Relaxation in extracted muscle fibers. *J. gen. Physiol*. **38**, 149–159 (1954).
16. K. Uchida, and W. F. H. M. Mommaerts, Modification of the contractile responses of actomyosin by cyclic adenosine 3′,5′ phosphate. *Biochem. biophys. Res. Commun.* **10**, 1–3 (1963).
17. V. A. Engelhardt, and M. N. Ljubimova, Myosin and adenosine triphosphatase. *Nature*, **144**, 668–669 (1939).
18. W. W. Kielley, and O. Meyerhof, Studies on the adenosine triphosphatase of muscle II. A new magnesium-activated adenosinetriphosphatase. *J. biol. Chem*. **176**, 591–601 (1948).
19. S. V. Perry, The ATPase of lipoprotein granules isolated from muscle. *Biochim. biophys. Acta*. **8**, 499–509 (1952).
20. W. Hasselbach, Die Diffusionskonstante des Adenosintriphosphats im inneren der Muskelfaser. *Z. Naturforsch*. **7b**, 334–337 (1952).
21. K. R. Porter, and G. E. Palade, Studies on the endoplasmic reticulum. III. Its form and distribution in striated muscle cells. *J. biophys. biochem. Cytol.* **3**, 269–300 (1957).
22. A. F. Huxley, and R. E. Taylor, Local activation of striated muscle fibres *J. Physiol*. **144**, 426–441 (1958).
23. A. F. Huxley, and R. W. Straub, Local activation and interfibrillar structures in striated muscle. *J. Physiol.* **143**, 40–41*P* (1958).
24. A. F. Huxley, and L. D. Peachey, Local activation of crab muscle. *J. Cell Biol.* **23**, 107A (1964).

2

PROFESSOR EBASHI'S JOURNEY TOWARD THE DISCOVERY OF TROPONIN: A PERSONAL RECOLLECTION

Makoto Endo

I first met Dr. Setsuro Ebashi in 1954, when he was an instructor (or assistant professor) in the Department of Pharmacology, the University of Tokyo, and I was an undergraduate student. Our group of students was doing some experiments on dogs in the corner of the department, which Professor Ebashi had kindly allowed us to use. He was quite kindhearted, but when talking with him one immediately recognized his brilliance, and his penetrating eyes aroused a feeling of awe in us. I did not realize it then, but this was the time when he was establishing the fact that the essential principle of Marsh's relaxing factor is not a soluble enzyme such as creatine kinase or myokinase, but a microsomal ATPase described by Kielley and Myerhof in 1948.[1]

When Hiroshi Kumagai and Ebashi organized the 1957 conference on muscle at the International House in Tokyo, which J. Gergely mentioned in his chapter, I was an intern in the University of Tokyo Hospital and was still wondering where to work. Shortly afterward, following Ebashi's suggestion I finally decided to join Kumagai's laboratory and became a graduate student there in April 1958. Ebashi was then working on the mechanism of relaxation by the relaxing factor. He appreciated Bozler's work, which demonstrated that EDTA causes relaxation as the relaxing factor does,[2] and assumed that the removal of Ca^{2+} might cause the relaxation. He compared the Ca^{2+}-binding activity of various chelating agents and their relaxing activity, but found no parallelism at all between the two activities. I clearly remember that his wife and trusted co-worker Fumiko Ebashi presented the negative results at a regional meeting of the Japanese Pharmacological Society and concluded that the mechanism had nothing to do with Ca^{2+}.[3] I felt that it might be too early to exclude the possibility simply on the grounds that parallelism was absent. However, because it was the conclusion of such a brilliant scientist, and because I, just a beginner then, had no possible alternative explanation in mind, I did not make any comment. To my later regret, I felt that if I had made some comment at that time, I might have risen in Professor Ebashi's esteem.

Faculty of Medical Care and Health, Saitama Medical University, Kawagoe Building, 21-7 Wakitahoncho, Kawagoe 350-1123, Japan

Regulatory Mechanisms of Striated Muscle Contraction
Edited by Ebashi and Ohtsuki, Springer, 2007

Disappointed by the negative results, Ebashi joined Fritz Lipmann's laboratory in New York at the end of 1958. He was inclined to shift his field of research there to enzymology, but Lipmann advised him to continue his own research on muscle. Ebashi later greatly appreciated this advice. As a result, continuing his work on muscle, he soon realized that in his previous calculation of Ca^{2+}-binding activity, Mg^{2+}-binding of chelating agents had not been taken into account. Recalculations revealed a striking parallelism between the Ca^{2+}-binding activity of chelating agents in experimental conditions and their relaxing activity.[4] Convinced that Ca^{2+} was the key substance, he then set out to prove that ATP-induced superprecipitation of actomyosin requires the presence of Ca^{2+}, and indeed he did demonstrate that a micromolar level of Ca^{2+} was necessary for the reaction.[5] He carried out this experiment without using a Ca^{2+} buffer, and for this purpose he expended tremendous effort to completely remove contaminated Ca^{2+} from all the experimental system including the actomyosin preparation. He later confessed that he would never repeat such difficult experiments again. He then showed that the relaxing factor is nothing but the fragmented sarcoplasmic reticulum (in fact, the triad is seen in his relaxing factor preparation), and that it strongly accumulates Ca^{2+} in the presence of ATP, thereby removing Ca^{2+} from the medium.[6] As A. F. Huxley wrote in his chapter, Lipmann was unwilling to accept that anything as simple as Ca^{2+} could perform such an important action as regulating the contraction–relaxation cycle. For this reason, it took almost two years for Lipmann and Ebashi to publish their seminal paper.

On these grounds established in New York, Ebashi first suggested the present scheme of excitation–contraction coupling, that action potential evoked at the surface membrane somehow sends a signal through T-tubules to the sarcoplasmic reticulum to cause the release of Ca^{2+} that had accumulated during the relaxing and resting period.[7]

During his stay at Lipmann's laboratory, Ebashi was appointed as a full professor at the University of Tokyo in 1959, a triple promotion of rank by skipping the ranks of lecturer and associate professor, which was and still is extremely rare in Japanese universities. I had hoped it would be possible but never believed it would actually occur because of the conservative nature of Japanese universities.

However beautiful Ebashi's results, and in spite of the fact that Annemarie Weber also showed that Ca^{2+} is essential for actomyosin ATPase activity,[8] most of the biochemists at that time preferred organic materials to Ca^{2+} as a key substance to regulate the contraction–relaxation cycle. At the Conference on Biochemistry of Muscle Contraction held in Dedham (Massachusetts, USA) in May 1962, the idea that the mechanism of relaxation by the relaxing factor is a result of a hypothetical soluble relaxing substance produced by that factor was predominant over the Ca^{2+} theory.[9] Ebashi himself thought that the weakest point in the Ca^{2+} theory was the fact demonstrated clearly by Weber and Winicur that "synthetic" actomyosin (a mixture of myosin and actin prepared separately) with certain actin preparations was quite insensitive to Ca^{2+}.[10] He assumed that actin might be denatured in such a preparation insensitive to Ca^{2+}, and he was determined to prove it. Ebashi declared to Weber as well as to F. Oosawa, the head of a leading research group working on actin in Japan, that he would carry out such work on actin to be fair to them. He started the experiments immediately after he came back to Tokyo from Dedham.

He worked very hard for this purpose, harder than before. During the daytime, he had to engage in teaching and administrative work as the youngest professor on the faculty. Afterward, he would start his experiments every evening, always continuing

them until after midnight. I witnessed this for only a few months, because I left Tokyo in September 1962 to join A. F. Huxley's laboratory in London. About one year later I received in London a preprint of Ebashi's paper that was to be published in *Nature*. In it was the description that a third component (besides myosin and actin) is required for "natural actomyosin" to be sensitive to Ca^{2+}.[11] Ebashi's original idea (denaturation of actin) was wrong in a sense, but its direction was absolutely correct. The third protein component had many characteristics similar to those of tropomyosin, but the original tropomyosin discovered by K. Bailey did not have the Ca^{2+}-sensitizing action. Therefore, Ebashi called the component "native tropomyosin." At just that time, a Royal Society Symposium on muscle was held in London, and I had the honor of introducing Ebashi's results, shortly before their publication, during the discussion of the structure and function of thin filament at the meeting.[12]

Ebashi then inquired into the problem of the difference between Bailey's tropomyosin and "native tropomyosin" and he soon found that "native tropomyosin" was a complex of tropomyosin and a new protein troponin.[13] This time he thought from the beginning that "native tropomyosin" might have some other protein component. After returning to Tokyo from London, I enjoyed working on the localization of "native tropomyosin," tropomyosin, and troponin in myofibrils in relation to striation patterns with fluorescence microscopy,[14] before turning to Ca^{2+} release experiments.

2.1. REFERENCES

1. H. Kumagai, S. Ebashi, and F. Takeda, Essential relaxing factor in muscle other than myokinase and creatine phosphokinase. *Nature* **176**, 166–168 (1955).
2. E. Bozler, Relaxation in extracted muscle fibers. *J. Gen. Physiol.* **38**, 149–159 (1954).
3. F. Ebashi, and S. Ebashi, On the substances that cause relaxation of glycerinated muscle. (in Japanese) *Folia Pharmacol. Jap.* **55**, 31§ (1959).
4. S. Ebashi, Calcium binding and relaxation in the actomyosin system. *J. Biochem.* **48**, 150–151 (1960).
5. S. Ebashi, Calcium binding activity of vesicular relaxing factor. *J. Biochem.* **50**, 236–244 (1961).
6. S. Ebashi, and F. Lipmann, Adenosine triphosphate-linked concentration of calcium ions in a particulate fraction of rabbit muscle. *J. Cell Biol.* **14**, 389–400 (1962).
7. S. Ebshi, The role of "relaxing factor" in contraction-relaxation cycle of muscle. *Progr. Theoret. Phys. (Kyoto) Suppl.* **17**, 35–40 (1961).
8. A. Weber, On the role of calcium in the activity of adenosine 5′-triphosphate hydrolysis by actomyosin. *J. Biol. Chem.* **234**, 2764–2769 (1959).
9. H. H. Weber, Introduction (to "Interaction of myosin and actin"), in: *Biochemistry of Muscle Contraction*, edited by J. Gergely (Little, Brown and Co., Boston, 1964), pp. 193–198.
10. A. Weber, and S. Winicur, The role of calcium in the superprecipitation of myosin. *J. Biol. Chem.* **236**, 3198–3202 (1961).
11. S. Ebashi, Third component participating in the superprecipitation of "natural actomyosin." *Nature* **200**, 1010 (1963).
12. M. Endo, Comment. *Proc. Roy. Soc. Lond.* **B160**, 500 (1964).
13. S. Ebashi, and A. Kodama, A new protein factor promoting aggregation of tropomyosin. *J. Biochem.* **58**, 107–108 (1965).
14. M. Endo, Y. Nonomura, T. Masaki, I. Ohtsuki, and S. Ebashi, Localization of native tropomyosin in relation to striation patterns. *J. Biochem.* **60**, 605–608 (1966).

3

HIGHLIGHTS OF THE HISTORY OF CALCIUM REGULATION OF STRIATED MUSCLE

John Gergely

3.1. INTRODUCTION

First of all, I should like to express my gratitude for the invitation, making it possible for me to participate in the celebration of the fortieth anniversary of the discovery of troponin by Professor Ebashi and his colleagues. This discovery opened up new vistas of the regulation of striated muscle contraction and the role of ionized calcium in it.

I first met Dr. Ebashi in 1957 having been invited to a meeting at the International House in Tokyo organized by Professor Kumagai, and, then Assistant Professor, Setsuro Ebashi. That meeting revealed the progress our Japanese colleagues had made in various aspects of muscle biochemistry and physiology during the years following the end of World War II. It opened up new paths of communication among European, American and Japanese scientists, and was followed by many meetings in the subsequent years where the exchange of ideas continued and friendships which had begun in 1957 flourished. Sadly, many of those present in 1957, among them Hiroshi Kumagai, Koscak Maruyama, Yuji Tonomura, Shizuo Watanabe, Koloman Laki, and Wayne Kielley are not with us anymore.

One item of great interest at the 1957 meeting was a presentation by Ebashi following up a 1955 publication by Professor Hiroshi Kumagai, Setsuro Ebashi, and Fumiko Takeda – now Mrs. Ebashi,[1] That publication had thrown new light on the problem of the so-called relaxing factor that had been confusing those working on muscle during the preceding years. I thought a brief look at this part of muscle history would be appropriate before turning to troponin.

There is something I should like to make clear. This is not a report on new work, nor is it a conventional review of a field or topic with full bibliographic backing. It is looking back over half a century, pointing to some key events involving Ebashi, and, if appropriate, related work by others.

Boston Biomedical Research Institute; Harvard Medical School; Massachusetts General Hospital, Boston, MA, USA

Regulatory Mechanisms of Striated Muscle Contraction
Edited by Ebashi and Ohtsuki, Springer, 2007

3.2. RELAXING FACTOR AND CALCIUM IONS

In the early fifties B. B. Marsh[2,3] in Great Britain found that the shrinking of the volume of low-speed centrifuged homogenized muscle – attributable to the contraction of myofibrils (syneresis) – could be reversed by calcium and a factor in the supernatant, hence named the relaxing factor. Known enzymes, such as creatine kinase and myokinase, were considered as candidates for the role of relaxing factor. This was changed when Ebashi and his colleagues published the paper showing that the relaxing factor was sedimentable at high speed and possessed properties identifying it with an ATPase of a particulate nature described by Kielley and Meyerhof[4–6] in 1948. Work with chelators such as EDTA led to the suggestion that the relaxing factor somehow may be involved in the removal of Ca^{2+}. Rigorous analysis of experiments with various levels of ATP, Ca^{2+} and Mg^{2+} led Annemarie Weber[7,8] to the conclusion that contraction and ATPase activity are Ca^{2+}-dependent.

During his stay in the US with Fritz Lipmann at the Rockefeller Institute Ebashi established that the relaxing factor actually contains vesicles carrying an ATPase and functions as a Ca^{2+} pump removing Ca^{2+} from the sarcoplasm leading to relaxation.[9] These vesicular elements were formed from fragments of what became known as the sarcoplasmic reticulum. Hasselbach and Makinose too, independently discovered an ATPase dependent Ca^{2+} pump.[10] Interestingly, at about the same time that the relaxing factor became recognized as the controller of contraction and relaxation of muscle, cell biologists had brought to light an almost forgotten Italian investigator, E. Veratti, who in 1902 described tubular structures in muscle which, as we now know, correspond to the sarcoplasmic reticulum.[11]

3.3. NATIVE TROPOMYOSIN AND TROPONIN

A new era opens with the discovery of troponin by Ebashi and his colleagues. By 1962 tropomyosin, a muscle protein discovered in 1946 by K. Bailey[12] was a well characterized entity, and there had been indications of its possible interaction with actin. The report by Jean Hanson and Jack Lowy[13] of the structure of actin filaments stimulated thinking about possible tropomyosin-actin filament structures. Ebashi and his colleagues, in light of earlier reports on actomyosin preparations that lacked Ca^{2+}-sensitivity, turned to looking for a missing component required for Ca^{2+}-sensitive actin myosin interaction. This led to the discovery of a protein sharing many similarities with, yet differing in some respects from, tropomyosin.[14] They named it native tropomyosin but soon found that although "native tropomyosin" did indeed contain tropomyosin there was an additional component that became known as troponin.[15,16] Shortly after the discovery Ebashi's group established that troponin was a Ca^{2+}-binding protein with an obvious role in the regulation of the muscle contraction and relaxation.[17] Ohtsuki and his colleagues[18] in Ebashi's laboratory identified troponin with distinct entities along the thin filament separated by 400A, an important step in the troponin story.[19–21]

In the meantime a number of investigators became interested in the study of troponin and it became clear that troponin is actually made up of two or more components with distinct functions. One had Ca^{2+}-binding properties and another inhibited actomyosin ATPase.[22,23] It was more difficult to establish the existence of additional components

because of the possibility of the presence of fragments that had resulted from proteolysis.[24] Marion Greaser, in our laboratory, using a then new technique, viz. SDS polyacrylamide gel electrophoresis, was able to identify a new component in addition to the Ca-binding and inhibitory one; the three were named TnC, TnI and TnT, referring to calcium binding, inhibition of ATPase activity, and tropomyosin binding, respectively.[25,26] The existence of three troponin components and the above nomenclature was generally accepted at the 1972 Cold Spring Harbor Symposium on muscle, a meeting which has become a landmark in the history of muscle studies.

Once the amino acid sequence of TnC had been determined[27] it became possible to look for the calcium binding sites. This was greatly helped by the work of Kretsinger and his colleagues[28,29] on parvalbumin, a Ca^{2+}-binding protein first found in fish muscle. They established the atomic structure of Ca^{2+}-binding sites in parvalbumin by x-ray crystallography leading to the concept of the EF-hand, the E and the F being reference to two alpha helical regions found flanking a sequence that constituted the actual Ca-binding loop. There were two such structures in each parvalbumin molecule, and comparison of the amino acid sequences of parvalbumin and TnC led to the identification of four such binding sites in the latter. Direct measurements of Ca^{2+} binding proved the existence of four binding sites in each TnC molecule, a pair of high affinity, and a pair of lower affinity. The higher affiniy sites were also able to bind Mg^{2+}. Comparison of the Ca^{2+}-binding constants to TnC and the Ca^{2+} concentration dependence of actomyosin ATPase activity in the presence of tropomyosin and troponin identified the lower affinity sites as the regulatory ones.[30,31] Ca^{2+} binding studies on TnC fragments indicated that the specific sites were in the N-terminal region.[32,33] A study of the Ca^{2+} dependence of the availability of carboxyl groups on whole TnC for chemical modification also identified the N-terminal region of TnC as the location of the regulatory Ca^{2+} sites.[34]

The amino acid sequences of TnI and TnT were also determined, which opened the way for searching for regions of functional significance, e.g. effects on actomyosin ATPase activity, superprecipitation of actomyosin, or contraction of glycerinated fibers. The smallest fragment of TnI possessing inhibitory activity was identified as residues 104–115.[35,36] (for reviews thus far see[37,38])

3.4. ATOMIC STRUCTURE OF TROPONIN C ESTABLISHED

A new era opened in the mid eighties with two laboratories,[39,40] reporting the atomic structure of troponin C. There were two domains, also referred to as lobes, each having two helix-loop-helix sequences, binding sites for Ca^{2+} or Mg^{2+}. It came as a surprise that the two halves were connected by a long helix, – formed by the junction of two helices, one from each lobe – which became known as the central helix; in an earlier model based on the structure of parvalbumin two parvalbumin-like units would be joined by having the two halves facing each other locked, as it were, together.[41] James and his colleagues[42] noted that the N-terminal and C-terminal lobes differed in an important respect; the N terminal region, which was devoid of Ca^{2+} in the crystals, appeared in a closed conformation, whereas the Ca^{2+}-bound C terminal region was open, exposing what is referred to as the hydrophobic patch. They proposed a model in which the activation of the actomyosin system and initiation of contraction would be due to the opening up of the N-terminal lobe of TnC by Ca^{2+}, producing an overall structure similar to the open structure of

the C terminal region, They had proposed that the region opening up under the influence of Ca^{2+} would be the site to which TnI would bind thus being removed from actin and permitting the activation of the actomyosin system. Shortly thereafter two reports appeared showing that prevention of the opening of the Ca^{2+} sensitive N terminal domain of troponin C led to loss of function of TnC. Both of these reports relied on using genetic engineering techniques to exchange amino acids in positions where effects on the opening of he N-lobe would be expected, one by introducing Cys residues leading to the formation of a disulfide bridge;[43] and the other by changing the electrical charge[44] by replacing a Glu residue with Lys, which was expected to stabilize the closed form. It should be noted that later work showed that in cardiac TnC site 1 in the N-terminal domain did not bind Ca^{2+} and binding to site 2 alone did not lead to the opening of the hydrophobic patch unless TnI binding also took place.[46]

3.5. STEPS TOWARDS A COMPLETE STRUCTURE OF TROPONIN

In the following ten years or so numerous studies were carried out to make use of genetic engineered mutants suitable for the placement of reporter groups to indicate changes in structure. Mutants are also used for the placement of so-called donor and acceptor molecules in order to apply Forster's resonance energy transfer (FRET) method, making it possible to determine intra- or intermolecular distances. Nuclear magnetic resonance technique, small angle and neutron X-ray diffraction were also among the tools found useful in this period. Reviews covering this period give a detailed insight into these developments.[46,47] It became clear that in addition to the inhibitory region of TnI that at low Ca^{2+} levels interacts with a portion of TnC roughly corresponding to the central helix, another segment became identified as being a key element in regulation, often referred to as a switch or trigger, interacting with the hydrophobic N-lobe patch.[48–50] I would refrain from getting into details oin this decade since a number of the presentations at this Conference will cover them.

What I consider a milestone in the effort to understand the regulation of muscle contraction on an atomic level is the determination of the crystal structure by Maeda and his colleagues[51] of the complex of an N-terminal portion of TnI bound to the C-lobe of TnC. They also included a predicted structure for two key portions of TnI; namely, the inhibitory region flanking the long helix in the central portion of TnC and the helical structure that was previously identified as part of the switch region interacting with the N-lobe of TnC. This work came to full blossoming with another paper from the Maeda lab involving cardiac TnC and larger fragments of TnI and TnT.[52] The structure, involves coiled coil interactions between fragments of TnI and TnT; such interaction was previously suggested based on amino acid sequences characteristic of heptads present in alpha helical coiled coils.[53] A recent paper from Fletterick's laboratory[54] dealing with the structure of skeletal troponin and its interaction with TnI and TnT fragments including the effects of calcium on the structure is an important contribution to the current picture of subunit interactions in troponin. Recent work[55] also in the program of this conference, considering troponin structure in the framework of relaxed and Ca-activated thin filaments, opens up new vistas in relating structure and function in contraction and relax-

ation. Some lack of agreement concerning the orientation of the troponin complex with respect to the polarity of the thin filaments remains to be resolved.

Structural changes in the thin filament on activation were proposed some thirty years ago involving the azimuthal movement of the tropomyosin strand attached to an actin filament resulting in a two-state model.[56,57] A three-state model was eventually derived from kinetic and structural studies proposing three positions for tropomyosin on interaction with actin influenced by myosin S-1, Ca^{2+} and ATP.[58,59] Recently EM studies were carried out on interacting thick and thin filaments; 3-D reconstruction of thin filaments under relaxing, Ca^{2+} activated, and rigor conditions has shown three distinct positions of tropomyosin in agreement with the 3-state model.[60] There are some unresolved questions about steric blocking versus allosteric mechanisms of regulation. The former implies that in the relaxed state there is direct competition between myosin heads and tropomyosin for the same binding sites on actin. In the allosteric model tropomyosin binding induces changes in the actin structure which affect myosin binding that could take place at different binding sites. Perry and his colleagues seem to favor the allosteric mechanism.[61,62] In a recent paper they offer NMR evidence for distinct binding sites for myosin and tropomyosin.[63] It is unfortunate that Sam Perry is not present to argue his case. For a suggestion to combine the steric and allosteric views see.[64] Recent studies on tropomyosin (for a review see[65]; and Sarah Hitchcock at this conference) may also have a bearing on achieving a consensus in this area.

An important and challenging aspect of current research has been the interest in relating basic research to medical problems. Again one might refer to the ongoing work connected with anomalies in the Ca^{2+}-handling system involving what is known as the ryanodine receptor and its relation to malignant hyperthermia, (see Y. Ogawa, this Cooference). Various cardiomyopathies are the result of mutations in which the primary problem is in troponin.[66] Findings in this area may lead to drugs designed to interact with and change the behavior of protein constituents underlying a disease There are reciprocal effects of research connecting medical and basic research.[67] Changes of medical interest induced by a mutation in the structure of a protein may lead to the recognition of some new property or interaction that is part of the normal physiological mechanism but may have been missed in research directed at the proteins themselves.

Ebashi's research has laid down the foundations in several areas of research. First of all, the role of Ca^{2+} in the control of muscle contraction and relaxation became firmly established. In connection with this he and his colleagues led the road to the recognition of the cellular components that play a role in the storage of Ca^{2+} and control the free Ca^{2+} levels in muscle. By now we refer to these as sarcoplasmic reticulum and T tubules and their role is now considered under the heading Excitation Contraction Coupling (see M. Endo's presentation in this Conference). The third area, which is central to this Conference involves the troponin/tropomyosin system that contains the receptor of Ca^{2+}. There is no greater tribute to Setsuro Ebashi than the ongoing research forty years after the discovery of troponin answering questions about biochemical biophysical mechanisms relating to the structure of proteins and their interaction as an ensemble within muscle.

In closing I would like to say thank you, Setsuro, for all you have done for basic scientists and clinicians. I know you must enjoy the sight of the ripening of the fruits of your original research.

3.6. REFERENCES

1. H. Kumagai, S. Ebashi, and F. Takeda, Essential relaxing factor in muscle other than myokinase and creatine phosphokinase, *Nature* **176**, 166 (1955).
2. B. B. Marsh, A factor modifying muscle fibre syneresis, *Nature* **167**, 1065–1066 (1951).
3. B. B. Marsh, The effects of adenosine triphosphate on the fibre volume of a muscle homogenate, *Biochim. Biophys. Acta* **9**, 247–260 (1952).
4. W. W. Kielley, and O. Meyerhof, A new magnesium-activated adenosinetriphosphatase from muscle, *J. Biol. Chem*. **174**, 387–388 (1948).
5. W. W. Kielley, and O. Meyerhof, Studies on adenosinetriphosphatase from muscle. II. A new magnesium-activated adenosinetriphosphatase, *J. Biol. Chem*. **176**, 591–601 (1948).
6. W. W. Kielley, and O. Meyerhof, Studies on adenosinetriphosphatase from muscle. III, The lipoprotein nature of the magnesium-activated adenosinetriphosphatase, *J. Biol. Chem*. **183**, 391–401 (1950).
7. A. Weber, On the role of calcium in the activity of adenosine 5'-triphosphate hydrolysis by actomyosin, *J. Biol. Chem*. **234**, 2764–2769 (1959).
8. A. Weber, and S. Winicur, The role of calcium in the superprecipitation of myosin, *J. Biol. Chem*. **236**, 3198–3202 (1961).
9. S. Ebashi, and F. Lipmann, Adenosine triphosphate-linked concentration of calcium ions in a particulate fraction of rabbit muscle, *J. Cell. Biol.* **14**, 389–400 (1962).
10. W. Hasselbach, and M. Makinose, The calcium pump of the relaxing granules of muscle and its dependence on ATP-splitting, *Biochem. Z*. **196**, 518–528 (1961).
11. K. R. Porter, The sarcoplasmic reticulum. Its recent history and present status, *J. Biophys. Biochem. Cytol.* **10**, 219–226 (1961).
12. K. Bailey, Tropomyosin: a new asymmetric protein of muscle, *Nature* **57**, 368–369 (1946).
13. J. Hanson, and J. Lowy, The structure of F-actin and of actin filaments isolated from muscle, *J. Mol. Biol.* **6**, 46–60 (1963).
14. S. Ebashi, Third component participating in the superprecipitation of 'natural actomyosin'. *Nature* (*London*) **200**, 1010 (1963).
15. S. Ebashi, and A. Kodama, A new protein factor promoting aggregation of tropomyosin, *J. Biochem. (Tokyo*) **58**, 107–108 (1965)
16. S. Ebashi, and A. Kodama, Interactio n of troponin with F-actin in the presence of tropomyosin, *J. Biochem. (Tokyo*) **59**, 425–426 (1966).
17. S. Ebashi, F. Ebashi, and A. Kodama, Troponin as the Ca^{2+} receptive protein in the contractile system, *J. Biochem. (Tokyo*) **62**, 137–138, (1965).
18. I. Ohtsuki, T. Masaki, Y. Nonomura, and S. Ebashi, Periodic distribution of troponin along the thin filament, *J. Biochem*. **61**, 817–819 (1967)
19. S. Ebashi, and M. Endo, Calcium ion and muscle contraction, *Prog. Biophys. Mol. Biol.* **18**, 123–183 (1968).
20. S. Ebashi, M. Endo, and I. Ohtsuki, Control of muscle contraction. *Q. Rev. Biophys.* **2**, 351–384 (1969).
21. A. Weber, Energized calcium transport and relaxing factors, in: *Current Topics in Bioenergetics*, Vol. 1, edited by D. R. Sanadi (New York, Academic Press, 1966), pp. 203–249.
22. D. J. Hartshorne, and H. Mueller, Fractionation of troponin into two distinct proteins. *Biochem. Biophys. Res. Commun.* **31**, 647–653 (1968).
23. M. C. Schaub, and S. V. Perry, The relaxing factor system of striated muscle. Resolution of the troponin complex into inhibitory and calcium ion-sensitizing factors and their relatonship to tropomyosin, *Biochem. J.* **115**, 993–1004 (1969).
24. S. Ebashi, T. Wakabayashi, and F. Ebashi, Troponin and its components, *J. Biochem. (Tokyo*) **69**, 441–445 (1971).
25. M. L. Greaser, and J. Gergely, Reconstitution of troponin activity from three protein components, *J. Biol. Chem.* **246**, 4226–4233 (1971).
26. M. L. Greaser, and J. Gergely, Purification and properties of the components from troponin, *J. Biol. Chem.* **248**, 2125–2133 (1973).
27. J. H. Collins, J. D. Potter, M. J. Wilshire, and N. Jackman, The amino acid sequence of rabbit skeletal muscle: gene replication and homology with Ca-binding proteins from carp and hake muscle, *FEBS Lett.* **36**, 268–272 (1973).

28. C. E. Nockolds, R. H. Kretsinger, C. E, Coffee, and R. A. Bradshaw, Structure of a calcium-binding carp protein, *Proc. Natl. Acad. Sci. USA* **69**, 581–584 (1972).
29. R. H. Kretsinger, and C. E. Nockolds, Carp muscle and calcium binding proteins II. Structure determination and general description, *J. Biol. Chem.* **248**, 3313–3316 (1973).
30. J. D. Potter, and J. Gergely, Troponin, tropomyosin and actin interactions in the Ca^{2+} regulation of muscle contrction, *Biochemistry* **13**, 2697–2703 (1974).
31. J. D. Potter, and J. Gergely, The calcium and magnesium binding sites on troponin and their role in the regulation of myofibrillar adenosine triphosphatase, *J. Biol. Chem.* **250**, 4628–4633 (1975).
32. W. Drabikowski, Z. Grabarek, and B. Barylko, Degradation of the Tn-C component of troponin by trypsin, *Biochim. Biophys. Acta* **490**, 216–224 (1977).
33. P. C. Leavis, S. S. Rosenfeld, J. Gergely, Z. Grabarek, and W. Drabikowski, Proteolytic fragments of troponin C. Localization of high and low affinity Ca^{2+} binding sites and interactions with troponin I and troponin T, *J. Biol. Chem.* **253**, 5452–5459 (1978).
34. I. L. Sin, R. Fernandes, and D. Mercola, Direct identification of the high and low affinity calcium binding sites of troponin-C, *Biochem. Biophys. Res. Commun.* **82**, 1132–1139 (1978).
35. H. Syska, J. M. Wilkinson, R. J. Grand, and S. V. Perry, The relationship between biological activity and primary structure of troponin I from white skeletal muscle of the rabbit, *Biochem. J.* **153**, 375–387 (1976).
36. J. A. Talbot, and R. S. Hodges, Synthetic studies on the inhibitory region of rabbit skeletal troponin I. Relationship of amino acid sequence to biological activity, *J. Biol. Chem.* **256**, 2798–2802 (1981).
37. P. C. Leavis, and J. Gergely, Thin filament proteins and thin filament-linked regulation of vertebrate muscle contraction, *Crit. Rev. Biochem. Mol. Biol.* **16**, 235–305 (1984).
38. I. Ohtsuki, K. Maruyama, and S. Ebashi, Regulatory and cytoskeletal proteins of vertebrate skeletal muscle, in: *Advances in Protein Chemistry,* Vol. 38, edited by C. B. Anfinsen, J. T. Edsall, and F. M. Richards (Academic Press, Inc. Orlando, 1986), pp. 1–68.
39. O. Herzberg, and M. N. James, Structure of the calcium regulatory muscle protein troponin-C at 2.8 A resolution. *Nature* **313**, 653–659 (1985).
40. M. Sundaralingam, R. Bergstrom, and G. Strasburg, Molecular structure of troponin C from chicken skeletal muscle at 3-angstrom resolution, *Science* **227**, 945–948 (1985)
41. R. H. Kretsinger, and C. D. Barry, The predicted structure of the calcium-binding component of troponin, *Biochim. Biophys. Acta* **405**, 40–52 (1975).
42. O. Herzberg, J. Moult, and M. N. James, A model for the Ca^{2+}-induced conformational transition of troponin C. A trigger for muscle contraction, *J. Biol. Chem.* **261**, 2638–2644 (1986).
43. Z. Grabarek, R. Y. Tan, J. Wang, T. Tao, and J. Gergely, Inhibition of mutant troponin C activity by an intra-domain disulphide bond, *Nature* **345**, 132–135 (1990).
44. K. Fujimori, M. Sorenson, O. Herzberg, J. Moult, and F. C. Reinach, Probing the calcium-induced conformational transition of troponin C with site-directed mutants [see comments], *Nature* **345**, 182–184 (1990)
45. S. K. Sia, M. X. Li, L. Spyracopoulos, S. M. Gagne, W. Liu, J. A. Putkey, B. C. Sykes, Structure of cardiac muscle troponin C unexpectedly reveals a closed regulatory domain, *J. Biol. Chem.* **272**, 18216–18221 (1997).
46. A. M. Gordon, E. Homsher, and M. Regnier, Regulation of contraction in striated muscle, *Physiol. Rev.* **80**, 853–924 (2000).
47. H. C. Cheung, Calcium-induced molecular and structural signaling in striated muscle contraction, in: *Molecular Control Mechanisms in Striated Muscle Contraction*, edited by R. J. Solaro, and R. L. L. Moss (Kluwer Acad. Publishers, Dordrecht, 2002), pp. 199–246.
48. R. T. McKay, B. P. Tripet, J. R. Pearlstone, L. B. Smilley, and B. D. Sykes, Defining the region of troponin-I that binds to troponin-C, *Biochemistry* **38**, 5478–5489 (1999).
49. B. P. Tripet, J. E. Van Eyk, and R. S. Hodges, Mapping of a second actin tropomyosin and a second troponin C binding site within the C terminus of troponin I, and their importance in the Ca2+-dependent regulation of muscle contraction, *J. Mol. Biol.* **271**, 728–750 (1997).
50. Y. Luo, J. L. Wu, B. Li, K. Langsetmo, J. Gergely, and T. Tao, Photocrosslinking of benzophenone-labeled single cysteine troponin I mutants to other thin filament proteins, *J. Mol. Biol.* **296**, 899–910 (2000).
51. D. G. Vassylyev, S. Takeda, S. Wakatsuki, K. Maeda, and Y. Maeda, Crystal structure of troponin C in complex with troponin I fragment at 2.3A resolution, *Proc. Natl. Acad. Sci. USA* **95**, 4847–4852 (1998).

52. S. Takeda, A. Yamashita, K. Maeda, and Y. Maeda, Structure of the core domain of human cardiac troponin in the Ca^{2+}-saturated form, *Nature* **424**, 35–41 (2003).
53. R. Stefancsik, P. K. Jha, and S. Sarkar, Identification and mutageness of a highly conserved domain in troponin T responsible for troponin I binding: potential role for coiled coil interaction, *Proc. Natl. Acad. Sci. USA* **96**, 957–962 (1998).
54. M. V. Vinogradova, D. B. Stone, G. G. Malanina, C. Karatzaferi, R. Cooke, R. A. Mendelson, R. J. Fletterick, Ca^{2+}-regulated structural changes in troponin, *Proc. Natl. Acad. Sci. USA* **102**, 5038–5043 (2005).
55. K. Murakami, F. Yumoto, S. Y. Ohki, T. Yasunaga, M. Tanokura, and T. Wakabayashi, Structural basis for Ca^{2+}-regulated muscle relaxation at interaction sites of troponin with actin and tropomyosin, *J. Mol. Biol.* **352**, 178–201 (2005).
56. H. E. Huxley, Structural changes in the actin- and myosin-containing filaments during contraction, *Cold Spring Harb. Symp. Quant. Biol.* **37**, 361–376 (1973).
57. J. C. Haselgrove, X-ray evidence for a conformational change in the actin-containing filaments of vertebrate striated muscle, *Cold Spring Harb. Symp. Quant. Biol.* **37**, 341–352 (1973).
58. D. F. A. McKillop, and M. A. Geeves, Regulation of the interaction between actin and myosin subfragment 1: evidence for three states of the thin filament, *Biophys. J.* **65**, 693–701 (1993).
59. M. A. Geeves, and S. S. Lehrer, The muscle thin filament as a classical M. cooperative/allosteric regulatory system, *J. Mol. Biol.* **277**, 1081–1089 (1998).
60. R. Craig, and W. Lehman, Crossbridge and tropomyosin positions observed in native, interacting thick, and thin filaments, *J. Mol. Biol.* **311**, 1027–1036 (2001).
61. S. V. Perry, Troponin I: inhibitor or facilitator? *Mol. Cell. Biochem.* **190**, 9–32, (1999).
62. S. V. Perry, What is the role of tropomyosin in the regulation of muscle contraction? *J. Muscle Res. Cell Motil.* **24**, 593–596 (2003).
63. V. B. Patchell, C. E. Gallon, J. S. Evans, Y. Gao, S. V. Perry, and B. A. Levine, The regulatory effects of tropomyosin and troponin-I on the interaction of myosin loop regions with F-actin, *J. Biol. Chem.* **280**, 14469–14475 (2005).
64. L. S. Tobacman, Structure and regulation of cardiac and skeletal muscle thin filaments, in: *Molecular Control Mechanisms in Striated Muscle Contraction*, edited by R. J. Moss, and R. L. Salaro (Klewer, Dordrecht, 2002), pp. 143–162.
65. J. H. Brown, and C. Cohen, Regulation of muscle contraction by tropomyosin and troponin: how structure illuminates function, in: *Advances in Protein Chemistry*, Vol. 7, edited by F. M. Richards, D. S. Eisenberg, and J. Kuriyan, (Elsevier Academic Press, Amsterdam, 2005), pp. 121–165.
66. M. X. Li, X. Wang, and B. D. Sykes, Structural based insights into the role of troponin in cardiac muscle pathophysiology, *J. Muscle Res. Cell Motil.* **25**, 559–579 (2004).
67. T. Kobayashi, and R. J. Solaro, Calcium, thin filaments and the integrative biology of cardiac contractility, *Ann. Rev. Physiology* **67**, 9–67 (2005).

II

REGULATION BY TROPONIN AND TROPOMYOSIN

4

TROPONIN: STRUCTURE, FUNCTION AND DYSFUNCTION

Iwao Ohtsuki

4.1. INTRODUCTION

A Ca^{2+}-sensitizing protein factor first isolated from minced muscle showed some similarity to the previously found tropomyosin in amino acid composition and was thus considered to be a native form of tropomyosin (Bailey, 1946; 1948; Ebashi, 1963; Ebashi and Ebashi, 1964). In 1965, however, a new protein was found in this protein factor in addition to tropomyosin and named troponin (Ebashi and Kodama, 1965). The discovery of troponin triggered a new era of the molecular biology of the regulation of muscle contraction. Troponin was shown to be the Ca^{2+}-receptive protein for the Ca^{2+}-sensitive contraction in striated muscle. In the absence of Ca^{2+}, troponin in association with tropomyosin suppresses the contractile interaction between myosin and actin, and this suppression is removed by an action of Ca^{2+} on troponin to activate the contraction (Ebashi et al., 1968). An electron microscopic study revealed that troponin is distributed along the thin filament at regular intervals of about 40 nm, and this finding led to the construction of a model of thin filament as an ordered assembly of troponin, tropomyosin and actin (Ohtsuki et al., 1967; Ebashi et al., 1969). By these studies, the molecular basis of the Ca^{2+}-regulation of muscle contraction was established.

In this chapter I will overview the studies on troponin covering from its structure and function to genetic dysfunction.

4.2. PERIODIC DISTRIBUTION OF TROPONIN

It was in early April, 1966 that I observed the location of troponin by using its antibody in myofibrillar structure in an electron microscope. It was then found that the antibody against troponin formed 24 transverse striations with regular intervals in the thin filament region of chicken skeletal myofibrils (Ohtsuki et al., 1967; Ohtsuki, 1974) (Figure 4.1). This finding indicated that troponin is distributed regularly along the entire length of thin filaments and that the positions of troponin molecules in neighboring thin

Department of Physiology, The Jikei University School of Medicine, Tokyo, Japan

Regulatory Mechanisms of Striated Muscle Contraction
Edited by Ebashi and Ohtsuki, Springer, 2007

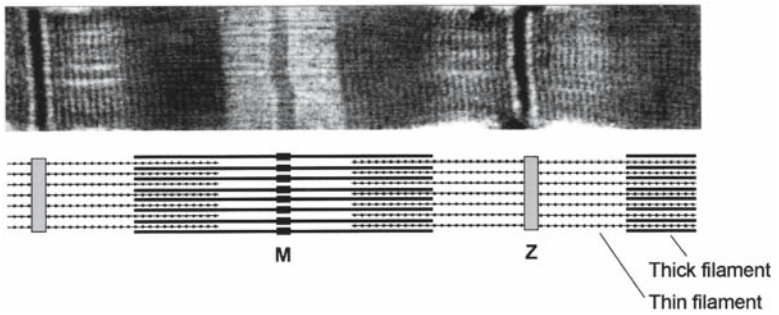

Figure 4.1. Electron micrograph of chicken skeletal myofibril treated with anti-troponin antibody. The antibody forms 24 regular transverse striations along the entire thin filament region. A periodic distribution of troponin along each thin filament is schematically illustrated in the lower portion of the figure. From Ebashi et al. (1969).

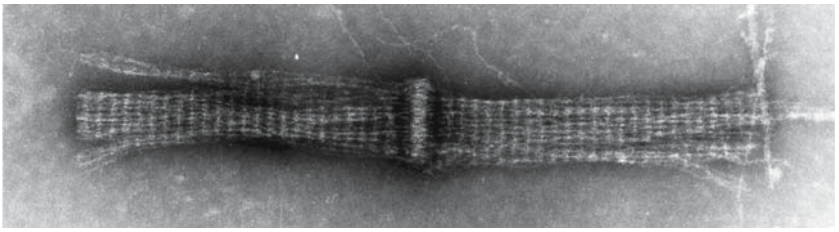

Figure 4.2. Electron micrograph of the separated thin filaments stained by anti-troponin antibody. Anti-troponin distributes with regular intervals of 38.2 nm along thin filaments extending on both sides of Z-band. From Ohtsuki (1974).

filaments are in register. This was confirmed by the observation that anti-troponin is distributed along each of the separated thin filaments at 38 nm intervals (Figure 4.2).

The regular 38 nm interval length of troponin along the thin filament corresponds to the length of the filamentous tropomyosin molecule which has a strong tendency to form end-to-end filaments (Tsao et al., 1951; Ooi et al., 1962). It was then deduced that two end-to-end tropomyosin filaments, with a troponin attached to a specific region of each molecule, are distributed along actin double strands in the thin filament. Based on this consideration, a molecular model of the thin filament was presented (Ebashi et al., 1969) (Figure 4.3A). In this structure, double-stranded actin molecules form a core of the filament and two end-to-end filaments of fibrous tropomyosin molecules lie in the grooves of actin double strands almost in register. Troponin binds to the specific region of each tropomyosin and one troponin period covers the length of a chain of seven actin molecules along a single strand. The molecular ratio of 7 : 1 : 1 for actin, tropomyosin, and troponin in the model was in accord with the biochemical stoichiometry of these proteins in muscle (Ebashi et al., 1968).

The detailed observation of separated thin filaments showed that the filament free end is apart about two-thirds of the 38 nm period length from the terminal location of the anti-troponin antibody (Figure 4.2). Structural analysis of troponin-tropomyosin parac-

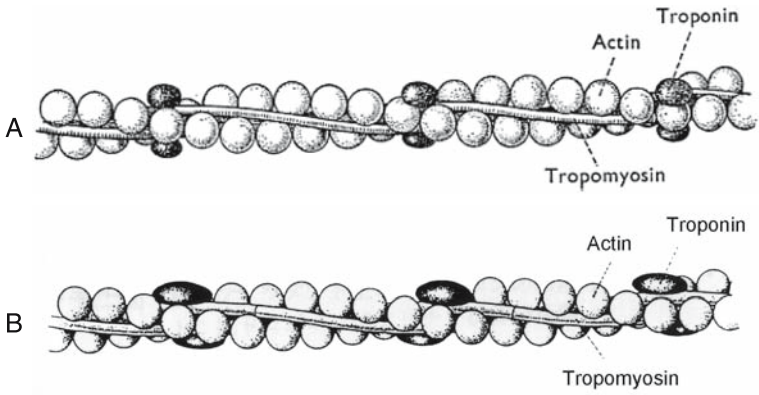

Figure 4.3. Molecular arrangement of troponin, tropomyosin and actin in the thin filament. (A) From Ebashi et al. (1969). (B) From Ebashi (1974).

rystals actually demonstrated that troponin binds to the region two-thirds of the molecular length from one end of the filamentous tropomyosin molecule. The formation of the narrow transverse anti-troponin striations also indicate that the two sets of troponin-tropomyosin in each troponin period are almost in register along the filament axis. But, at the same time, the two troponin-tropomyosins would make essentially the same specific interaction with actin double strands, and thus they must be shifted by about half actin size with each other, according to the helical symmetry of actin double strands (Ohtsuki, 1974). These considerations are included in the refined model in Figure 4.3B, where the filament has the structural polarity along its axis; the filament top is located on the left side (Ebashi, 1974). In the absence of Ca^{2+}, troponin in association with tropomyosin, suppresses the contractile interaction of double stranded actin with myosin. The action of Ca^{2+} on troponin releases the inhibition by troponin-tropomyosin on actin molecules and then the contractile interaction is activated.

4.3. TROPONIN COMPONENTS

In 1968, it was reported that troponin was composed of activating factor and inhibitory factor (Hartshorne and Mueller, 1968). The activating factor is known now as troponin C, while the essential component of the inhibitory factor is troponin I (Schaub and Perry, 1969). Detailed studies revealed that there is a third factor called troponin T that binds to tropomyosin (Greaser & Gergely, 1971; Ebashi, 1972). The inhibitory action of troponin I on actomyosin in the presence of tropomyosin represents the inhibition of contractile interaction of actomyosin by troponin-tropomyosin in the absence of Ca^{2+}. This inhibition by troponin I is neutralized by troponin C irrespective of Ca^{2+}-concentrations when troponin T is absent. The contractile interaction becomes sensitive to Ca^{2+} only in the concurrent presence of troponins C, I and T (Ohtsuki et al., 1986). Troponin is not a mere assembly of three protein units but its regulatory function is controlled by the dynamic interactions between the three different components. Troponin T is the

integrating component of the regulatory function of troponin complex and its structure and function are discussed briefly in the following section.

4.4. TROPONIN T

The presence of two domains in the troponin T molecule was first indicated by immunoelectron microscopic investigation (Ohtsuki, 1975). It was found that anti-troponin T antibody formed a definitively wider band than those of troponin C or I in each 38 nm period along the thin filament, and detailed observation revealed that the wide band of anti-troponin T consisted of a pair of lines that were separated by a distance of about 13 nm along the thin filament, strongly suggesting the axial arrangement of the two domains of troponin T molecule. Subsequent biochemical studies demonstrated that troponin T was split into two subfragments by mild treatment with chymotrypsin (Ohtsuki, 1979). Upon gradually increasing the KCl concentrations in eluting solution, two peaks were eluted from a SE-Sephadex ion exchange column to which a chymotryptic digest of troponin T had been added. The first eluted subfragment was named troponin T_1 and the second was named troponin T_2. The antibodies against two troponin T subfragments of chicken skeletal muscle were raised in rabbits and their location along thin filaments was studied electron microscopically. As a result, it was found that anti-troponin T_1 and anti-troponin T_2 were located on the Z-band side and the filament-top side of the wide band formed by anti-troponin T (Figure 4.4).

The biochemical properties of troponin T and its subfragments are summarized in the following. This protein is a single peptide of 259 residues with a high percentage of

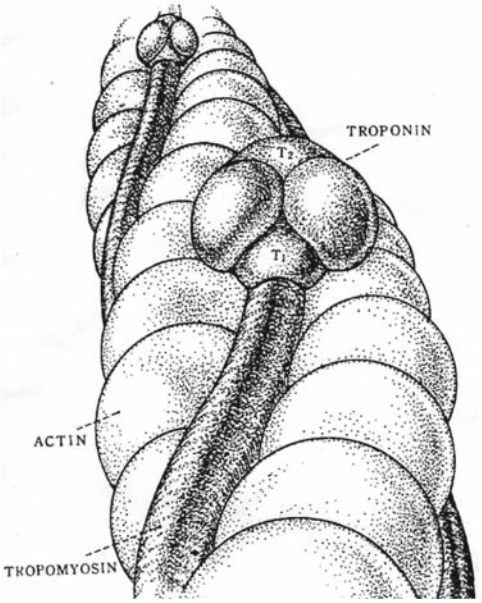

Figure 4.4. Arrangement of troponin T_1- and T_2- regions along the thin filament. The Z-line and the filament-top are located at the near side and far side of the figure, respectively. From Ohtsuki (1980).

which are charged (Pearlstone et al., 1976). The charged residues are distributed along the entire sequence, but it is noticed that the N-terminal region is rich in acidic residues, while the C-terminal region is rich in basic residues. This highly charged protein is insoluble under physiological low ionic strength conditions and becomes soluble only at high ionic strength conditions. This insoluble nature of troponin T under physiological low ionic strength conditions made it difficult to study the properties of troponin T, but this problem was overcome to a great extent by the production of soluble subfragments, one of which retains the Ca^{2+}-regulating ability. Troponin T from rabbit skeletal muscle was split into two subfragments, troponin T_1 and T_2, by the mild treatment with chymotrypsin. Troponin T_1 is a fragment of the N-terminal 158-residues (MW 18,700), whereas troponin T_2 (or T2α) is a fragment of the C-terminal 101-residues (MW 11,900). Troponin T_1 binds strongly to tropomyosin, whereas troponin T_2 interacts with tropomyosin, troponin I, and troponin C (Tanokura et al., 1982; 1983). The tropomyosin-binding region in troponin T_1 is located in the helix-rich region of residues 71 – 151(CB2) (Jackson et al., 1975), which probably forms a coiled-coil interacting structure with tropomyosin. The Ca^{2+}-sensitizing activity of troponin T resides in the smaller C-terminal subfragment, troponin T_2 (Ohtsuki et al., 1981). Both the Ca^{2+}-sensitizing action and tropomyosin-binding ability of troponin T_2 are greatly diminished when the C-terminal 17 residues are removed. The Ca^{2+}-sensitizing action of troponin T is therefore closely correlated with the binding stability to tropomyosin through the C-terminal region of troponin T_2. A fragment devoid of the N-terminal 45 residues of troponin T (a 26 K fragment) was also produced by endogenous proteases, calpain or cathepsin D (Ohtsuki et al., 1984; Pan et al., 1991). This fragment shows essentially the same Ca^{2+}-sensitizing and tropomyosin-binding activity as intact troponin T does, indicating that the N-terminal residues are not critical for the Ca^{2+}-regulatory function.

The troponin T molecule is a rod-shaped particle of approximately 17 nm length as observed under an electron microscope by using rotary shadow technique. But troponin T within troponin C·I·T complex shows polymorphic shapes as follows (Ohtsuki et al., 1988). The troponin C·I·T complex, immediately after its isolation from minced muscle, has a globular shape of 13×9 nm in size. In the globular troponin particle, rod-shaped troponin T is folded around a small head region mostly composed of troponin C·I. During the course of storage, the troponin T rod is gradually unfolded from the head portion, forming bent tails of various lengths extending from the lateral side of the head region, and finally forms a straight tail of 17 nm length extending from the center of the small head region. It is well known that a water solution of fresh troponin is fluid and transparent, but it becomes highly viscous and frequently turbid during the course of storage. This would be due to delicate changes in the interactions between troponin components after isolation from muscle and would be related to the polymorphic shapes of troponin. The Ca^{2+}-sensitizing ability is highest in fresh troponin and becomes lower during the course of storage. In order to explore the regulatory mechanisms of the troponin complex at the atomic level, a quaternary structure prediction of the globular troponin was attempted (Nagano and Ohtsuki, 1982). Recently, the crystallographic structures of the core domain (troponin C·I·T_2 complex) from human cardiac troponin and chicken skeletal troponin were determined (Takeda et al., 2003; Vinogradova et al., 2005). It will be crucial to determine the molecular arrangement of troponin ternary complex in the native thin filament to clarify the mechanisms of troponin under physiological conditions.

4.5. ASPECTS OF THE REGULATORY MECHANISMS BY TROPONIN

The essential roles of troponin components in the Ca^{2+}-regulation of muscle contraction are as follows (Ohtsuki et al., 1986). The inhibition of the contractile interaction by troponin-tropomyosin in the absence of Ca^{2+} is exerted by the inhibitory action of tropnin I. The presence of tropomyosin is required for the inhibitory activity of troponin I and the inhibition by troponin I is removed (or neutralized) by troponin C regardless of Ca^{2+}-concentrations. The Ca^{2+}-sensitivity of the contraction is conferred only in the concurrent presence of troponin C, I and T. Troponin T apparently makes the neutralizing action of troponin C sensitive to Ca^{2+}-concentrations.

Troponin I forms a stable complex with troponin C, and the troponin C·I complex binds to tropomyosin-actin only in the absence of Ca^{2+}, though the troponin C·I complex does not show the inhibitory activity even in the absence of Ca^{2+}. The action of Ca^{2+} on troponin C intensifies the interaction of troponin C with troponin I and then troponin I is dissociated from actin-tropomyosin, but troponin I complexed with troponin C binds to actin-tropomyosin so weakly that troponin I can not exert its inhibitory activity even in the absence of Ca^{2+}. Troponin T confers the inhibitory activity to the troponin I-troponin C complex in the absence of Ca^{2+}.

Recent crystallographic analysis of the core domain structure of troponin C·I·T_2 demonstrated that troponin T_2 and troponin I form a coiled-coil backbone structure within the IT-arm region of the core domain (Takeda et al., 2003; Vinogradova et al., 2005). The IT-arm region would be fixed stably to tropomyosin through two tropomyosin binding regions of troponin T: the C-terminal region of troponin T_2 and the helical region in troponin T_1. The tropomyosin binding through the C-terminal region of troponin T_2 would pivot the position of the inhibitory region of troponin I and its C-terminal side region onto actin-tropomyosin so as to make the inhibitory action of troponin I fully active, whereas the binding to tropomyosin through troponin T_1 would stabilize the overall position of the core domain of troponin along the thin filament.

In the thin filament, the position of troponin I is considered to be determined through the binding of troponin T to tropomyosin. At the same time, it has been shown by biochemical studies that troponin I itself inhibits the contractile interaction between myosin and actin in the presence of tropomyosin, while the inhibitory action of troponin I is very weak in the absence of tropomyosin (Perry, 1999). This suggests that a certain structural relationship also exists between troponin I and tropomyosin along actin double strands, though no specific interactions between these two proteins have been presented. In accord with this consideration, an immunoelectron microscopic examination showed that anti-troponin I formed transverse striations along the bundle of troponin I-tropomyosin-actin filaments with regular intervals of 38 nm (Ohtsuki and Shiraishi, 2002). Since the 38 nm length just corresponds to the molecular length of tropomyosin, this finding indicates that troponin I molecules are distributed along each actin-tropomyosin filament with 38 nm periodicity and that each troponin I molecule is located at a specific region of each tropomyosin molecule along the tropomyosin-actin filament. The anti-troponin I molecules formed the bundle of filaments by crosslinking troponin I molecules in the neighboring filaments, and the subsequent formation of transverse narrow anti-troponin I striations along the bundle of filaments would indicate that two molecules of troponin I and hence two tropomyosin molecules in each 38 nm period align almost in register along each actin filament. It is very conceivable that two tropomyosin molecules in each 38 nm period bind

cooperatively to the grooves of actin double strands and that the binding of tropomyosin to actin at the specific region of tropomyosin causes the increase in the affinity of the specific actin molecule to troponin I. Seven actin molecules covered by one tropomyosin are not equal in their affinity to troponin I, but the specific actin should have a high affinity to troponin I.

The essential roles of troponin components in the Ca^{2+} regulation are demonstrated by the removal and reconstitution of troponin components *in situ* in glycerinated skeletal muscle fibers (Hatakenaka and Ohtsuki, 1992). By treating the fibers with excess troponin T at slightly acidic as well as slightly high ionic strength conditions, the intrinsic troponin C·I·T complex in the fibers is replaced by the added troponin T. As a result, both troponin C and troponin I disappear from the fibers and the steady state tension stays at a level of about 70% of the maximum tension irrespective of Ca^{2+}-concentrations. By the reconstitution of troponin I, the tension is fully suppressed and, by the further addition of troponin C, the original Ca^{2+} sensitivity of the contraction is restored. These findings indicate that the contraction of muscle fibers is inhibited by the inhibitory action of troponin I and activated by Ca^{2+} through the neutralizing action of troponin C in the presence of troponin T. A level of about 70% of the maximum tension after removal of troponin C and I is consistent with the *in vitro* finding that the maximum activation of actomyosin-tropomyosin in the presence of the troponin C·I·T complex is slightly but definitely higher than that in the absence of the troponin C·I·T complex (Ohtsuki et al., 1986).

Although this activating action of troponin is a minor mechanism of troponin in vertebrates under physiological conditions, it is a predominant mechanism of scallop troponin (Shiraishi et al., 1999). A recent study on the properties of troponin I fragments from scallop striated muscle demonstrated that a fragment containing the inhibitory region and its N-terminal side sequence of troponin I completely replaced a whole troponin I molecule in terms of the Ca^{2+}-dependent activating activity of the scallop troponin complex, while a fragment containing the inhibitory region and its C-terminal side sequence did not show any Ca^{2+}-regulatory activity in the troponin complex (Tanaka et al., 2005). It was also shown that a fragment containing the inhibitory region and its N-terminal region of rabbit skeletal troponin I was involved in the activating action, whereas a fragment containing the inhibitory region and its C-terminal side sequence showed the suppression-desuppression-type Ca^{2+}-regulating activity in the troponin complex. These findings suggest that the N-terminal side region of troponin I that binds to troponin T_2 and the C-domain of troponin C, is not a mere structural core of troponin complex but is functionally engaged in the activating action of troponin. The activating action of troponin is enhanced by two missense mutations of human cardiac troponin T that cause hypertrophic cardiomyopathy (Nakaura et al., 1999b).

4.6. DYSFUNCTION BY TROPONIN MUTATIONS

Over the last 15 years, genetic analyses have revealed that inherited cardiomyopathies, i.e., hypertrophic (HCM), dilated (DCM) and restrictive (RCM) cardiomyopathies, are caused by a large number of mutations of genes for various cardiac sarcomeric as well as cytoskeletal proteins including cardiac troponin components (Fatkin and Graham, 2002; Ahmad et al., 2005). It has been shown that more than 60 mutations in genes for human cardiac troponin components are associated with inherited cardiomyopathies;

troponin T mutations (>30) in HCM and DCM, troponin I mutations (>30) in HCM, DCM and RCM, and two troponin C mutations in HCM and DCM.

4.6.1. Cardiac Troponin T Mutations

Hypertrophic cardiomyopathy (HCM) is an autosomal dominant disease that is characterized by ventricular hypertrophy and impaired diastolic function with a high incidence of sudden death in youth. The presence of inherited cardiomyopathy associated with the mutations of cardiac troponin components was first indicated by a report showing that two missense mutations (Ile79Asn, Arg92Gln) and a splice donor site mutation (Intron16$G_1 \rightarrow A$) of human cardiac troponin T gene were linked to HCM (Thierfelder et al., 1994). Functional analysis of these mutations was carried out by using the procedure for exchanging three troponin components in skinned fibers *in situ* that had been developed in my laboratory at Kyushu University (Hatakenaka and Ohtsuki, 1991; 1992). At first, mutants of two missense mutations (Ile79Asn, Arg92Gln) of troponin T were expressed in E. coli and purified. These mutant proteins were incorporated into permeabilized rabbit cardiac muscle, by employing the *in situ* troponin-exchange technique. The Ca^{2+}-activation profiles of force generation of the fibers containing the troponin T mutants were then compared with those of the muscle fibers containing wild-type troponin T. As a result, it was found that the free Ca^{2+}-concentrations required for the force generation of the fibers containing mutant troponin T was lower than that in the fibers containing wild-type troponin T, while no significant changes were observed in other parameters, such as the maximum force or cooperativity (Morimoto et al., 1998). The splice donor site mutation produced two truncated mutants of troponin T; one mutant lacks the C-terminal 14 residues ($TnT_{\Delta 14}$) and the other lacks the C-terminal 28 residues with 7 novel residues ($TnT_{\Delta 28+(7)}$). Both mutants showed the marked Ca^{2+}-sensitizing effect, while the maximum force was not affected by the $TnT_{\Delta 14}$ mutation but depressed by the $TnT_{\Delta 28+(7)}$ mutation (Nakaura et al., 1999a). Essentially the same results were obtained on the myofibrillar ATPase activity (Yanaga et al., 1999).

Subsequent investigations using the *in situ* troponin-exchange technique revealed that most examined mutations (Ile79Asn, Arg92Leu, Arg92Gln, Arg92Trp, Arg94Leu, Ala104Val, Arg130Cys, ΔGlu160, Glu163Arg, Ser179Phe, Lys273Glu, Arg278Cys, $TnT_{\Delta 14}$, $TnT_{\Delta 28+(7)}$) had the Ca^{2+}-sensitizing effect on the skinned fiber force development, while the maximum force level was not significantly affected by most of these mutations (Morimoto et al., 1999; Szczesna et al., 2000; Morimoto et al., 2002; Lu et al., 2003; Venkatraman et al., 2003; Harada and Potter, 2004) (Figure 4.5). These findings strongly indicate that the increase in the Ca^{2+}-sensitivity of force generation is the main functional consequence of the HCM-causing troponin T mutations. At the same time, two HCM-causing mutations (Phe110I, Glu244Asp) showed variable effects that depend on the animal species of skinned muscles. The Phe110I mutation did not show the Ca^{2+}-sensitizing effect but showed the large potentiation of the maximum force of rabbit cardiac muscle, whereas this mutation caused the Ca^{2+}-sensitizing effect and decreased maximum activity of porcine cardiac muscle (Nakaura et al., 1999b; Szczesna et al., 2000). The Glu244Asp mutation caused the increased Ca^{2+}-sensitivity and the increased maximum force level of rabbit cardiac muscle, whereas the mutation caused the increased maximum force level without the Ca^{2+}-sensitization of the force development of porcine cardiac muscle (Nakaura et al., 1999b; Harada and Potter 2004). These discrepancies however

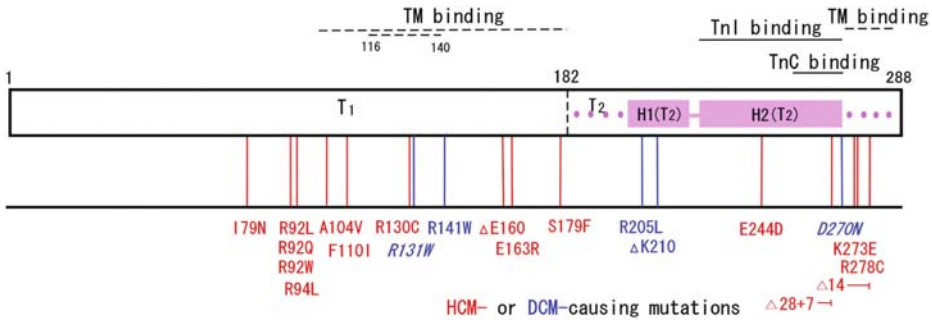

Figure 4.5. Distribution of HCM- and DCM-causing mutations along the amino acid sequence of human cardiac troponin T. Nineteen mutations, of which skinned fiber analyses were carried out, are indicated in the figure; HCM-causing mutations in red letters: DCM-causing mutations in blue letters. Two DCM-causing mutations (*R131W, D270N in blue italic letters*) were analysed by actomyosin ATPase and in vitro motility assays. Two helical regions, H1(T2) (residues 203–222) and H2(T2) (residues 225–271) of troponin T_2 in the IT-arm region of the core domain structure are indicated in the sequence (Takeda et al., 2003). The H2(T2) forms a coiled-coil with H2(I) of troponin I. The H1(T2) includes a part of homologous sequence for actin binding of chicken skeletal troponin T (Oliveira et al., 2000). The region of residues 114–138 is homologous to the region of residues 112–136 of bovine cardiac troponin T that is critical for tropomyosin binding (Hinkle and Tobacman, 2003).

suggest that the enhanced maximum force generation, in addition to the Ca^{2+}-sensitiztion, is the functional consequence of these mutations related to the pathogenesis of the HCM.

Dilated cardiomyopathy (DCM) is a syndrome characterized by cardiac dilation and systolic dysfunction, often leading to heart failure. A deletion mutation (ΔLys210) and a missense mutation (Arg141Trp) in the gene of human cardiac troponin T associated with DCM were reported (Kamisago et al., 2000; Li et al., 2001). Functional analysis of these mutations demonstrated that both mutations caused the Ca^{2+} desensitization of force generation without significant changes in the maximum activation (Morimoto et al., 2002; Lu et al., 2003). At the same time, Venkatraman et al. (2003) reported the Ca^{2+}-desensitization of skinned porcine cardiac muscle activation by the Lys210 deletion mutation, though they did not detect significant changes in the Ca^{2+}-sensitivity by the Arg141Trp mutation. Mirza et al. (2005) also showed the Ca^{2+}-desensitizing effect of two missense DCM-causing mutations (Arg141Trp, Arg205Leu) on the skinned muscle force of guinea pig heart trabeculae, and they showed that the Ca^{2+}-desensitization of actomyosin ATPase and in vitro motility assays was caused by five DCM-causing troponin T mutations (Arg131Trp, Arg141Trp, Arg205Leu, ΔLys210, Aps270Asn). These findings strongly suggest that the decreased Ca^{2+}-sensitivity of force generation is the critical functional consequence of the DCM-causing mutations of troponin T. The Ca^{2+}-desensitizing effect was also demonstrated on the force generation of skinned left ventricular muscle from mouse heart in which the Lys210 deletion mutation had been knocked-in (Morimoto et al., 2005).

In twitch contraction in cardiac muscle, the level of force generation reached by Ca^{2+} is usually submaximal and therefore the force generation in both systolic and diastolic phases is affected greatly by the changes in Ca^{2+} sensitivity (Rüegg, 1986). The increased Ca^{2+} sensitivity enhances systolic contraction and delays diastolic relaxation, whereas the

decreased Ca^{2+} sensitivity depresses systolic contraction. These changes are consistent with the difference in characteristic features between the two cardiomyopathies; the HCM is characterized by ventricular hypertrophy and impaired diastolic relaxation, while the DCM is characterized by dilation of the ventricular wall and reduced systolic function. This supports the importance of the change in the Ca^{2+}-sensitivity of contraction as a pathogenic cause leading to inherited cardiomyopathy.

4.6.2. Cardiac Troponin I Mutations

Mutations in genes for human cardiac troponin I are involved in HCM and RCM. One mutation (Ala2Val) that causes DCM was also reported recently.

Six HCM-causing mutations in human cardiac troponin I were first reported (Arg-145Gly, Arg145Gln, Arg162Trp, ΔLys182, Gly203Ser, Lys206Gln) (Kimura et al., 1997) (Figure 4.6). The Ca^{2+}-sensitizing action of these mutations was demonstrated by a study on skinned cardiac muscle force generation and myofibrillar ATPase activity using the *in situ* troponin-exchange technique (Takahashi-Yanaga et al., 2001). Two mutations, Arg145Gly and Arg145Gln, that are located within the inhibitory region, caused almost the same Ca^{2+}-sensitization with an elevated minimum force but no significant change in the maximum activation. Similar effects were observed by the Arg-162Trp mutation located at the N-terminal end of the H4(I). The ΔLys183 deletion mutation in the H4(I) shows the Ca^{2+}-sensitizing effect without changes in either the maximum or minimum force level. Two mutations, Gly203Ser and Lys206Gln, in the C-terminal end region of the molecule have a small marginal Ca^{2+}-sensitizing effect on the skinned fiber force generation. An Arg21Cys mutation that cause HCM, was reported to have the Ca^{2+}-sensitizing effect on the skinned fiber force development (Gomes et al., 2005).

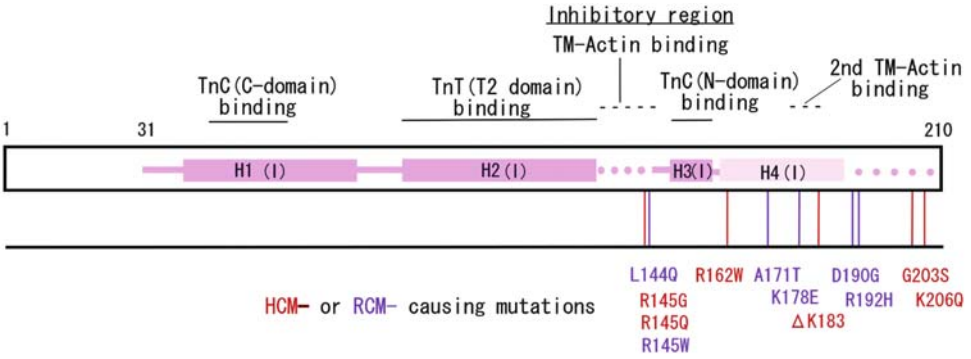

Figure 4.6. Distribution of HCM- and RCM-causing mutations along the sequence of human cardiac troponin I. The sites of mutations, of which skinned fiber analyses were carried out, are indicated as follows; HCM-causing mutations in red letters: RCM-causing mutations in purple letters. Position of four helical regions (H1(I), residues 42–80: H2(I), residues 90–136: H3(I), residues150–159:H4(I), residues 161–189) are indicated based on the core domain structure of troponin CIT_2 (Takeda et al., 2003). The H2(I) forms a coiled-coil with the H2(T2) of troponin T. The H3(I) is homologous to the part of the second troponin C binding region (signal segment) of skeletal troponin I, and the H4(I) includes the region of residues 176–184 that is homologous to the second actin-tropomyosin binding region of skeletal troponin I (Tripet et al., 1997).

In 2003, six mutations in genes for human cardiac troponin I were found to be associated with idiopathic restrictive cardiomyopathy (RCM) (Mogensen et al., 2003a). This genetic disorder is the least common among inherited cardiomyopathies and characterized by impaired diastolic filling of the left ventricle with normal or near normal systolic function and ventricular wall thickness. These RCM-causing mutations (Leu144Gln, Arg145Trp, Ala171Thr, Lys178Glu, Asp190Gly, Arg192His) showed the Ca^{2+}-sensitizing effect on the skinned fiber force generation and actomyosin ATPase activity (Yumoto et al., 2005). The Ca^{2+}-sensitizing effect by the RCM-causing mutations is larger than that by the HCM-causing mutations. The Ca^{2+}-sensitization by the RCM-causing mutations is in the order of Lys178Glu >Arg192His ≈ Arg145Trp > Leu144Gln ≈ Ala171Thr > Asp-190Gly, whereas the Ca^{2+}-sensitization by the six HCM-causing mutations of troponin I is in the order of Arg145Gly > Arg145Gln ≈ ΔLys183 > Arg162Trp > Lys206Gln ≥ Gly203Ser (Takahashi-Yanaga et al., 2001; Yumoto et al., 2005). The elevation of the minimum force at low Ca^{2+}-concentrations was observed in all six RCM-causing mutations and four HCM-causing troponin I mutations. The maximum activation of force generation is depressed by four RCM-causing mutations (Leu144Gln, Arg145Trp, Ala171Thr, Arg192His) but no significant change is caused by any of HCM-causing mutations. As a whole, the Ca^{2+}-activation profiles are affected to a greater extent by the RCM-causing mutations than by the HCM-causing mutations. It was reported that the Asp190Gly mutation, which shows the smallest Ca^{2+}-sensitizing effect among the six RCM-causing mutations caused both RCM and HCM in the same family (Mogensen et al., 2003a). This finding suggests that the two genetic disorders are caused by similar mechanisms and that a small but definite difference in the amplitude of the Ca^{2+}-sensitizing effect plays a role in determining clinical phenotypes of HCM and RCM. Both the HCM- and RCM-causing mutations of troponin I are distributed mostly in the inhibitory region and its C-terminal side region of the molecule, both of which are necessary for the Ca^{2+}-regulatory action of troponin I (Figure 4.6).

Examinations using troponin I fragments ($TnI_{129–210}$) demonstrated that the Lys-178Glu mutation, which shows the largest Ca^{2+}-sensitizing effect, decreased the inhibitory affinity of the troponin I fragment to actin-tropomyosin without change in the maximum level of inhibition and also decreased the EC_{50} of the neutralizing action of troponin C. By the two dimensional NMR analysis, it was demonstrated that the Lys-178Glu mutation of the $TnI_{129–210}$ fragment causes structural changes in the restricted region of residues177–181 (Yumoto et al., 2005), which is included in the region corresponding to the second actin-tropomyosin-binding region of chicken skeletal troponin I (Tripet et al., 1997). The local conformational changes by the Lys178Glu mutation would make the inhibitory action of troponin I less efficient and thereby render the neutralization by troponin C more efficient. As a result, the contraction would become more sensitive to Ca^{2+}.

4.6.3. Cardiac Troponin C Mutations

One HCM-causing mutation (Leu29Gln) of human cardiac troponin C was reported (Hoffman et al., 2001). This mutation is located in the first one (site I; non-functional) of four EF-hand motifs of the molecule. There has been no functional study. A DCM-causing mutation (Gly159Asp) was also reported (Mogensen et al., 2003b) and this mutation has no Ca^{2+}-sensitizing action on the skinned fiber force generation, but it slows the rate of

force development (Preston et al., 2004). Recently this mutation was reported to decrease the Ca^{2+} sensitivity of acto-S1 ATPase activity (Mirza et al., 2005).

4.6.4. Troponin Mutations and Ca^{2+}-Regulatory Mechanisms

A large number of cardiomyopathy-causing mutations of cardiac troponin components have been reported. *In situ* functional studies of these troponin mutations have revealed that distinct changes in the Ca^{2+}-activation profiles of contraction are caused by the troponin mutations for three types of cardiomyopathies, HCM, DCM and RCM. An increased Ca^{2+}-sensitivity of contraction is produced by the HCM- and RCM-causing mutations, and the Ca^{2+}-sensitivity increase by the RCM-causing mutations is larger than that by the HCM-causing mutations. On the other hand, a decrease in Ca^{2+}-sensitivity is caused by the DCM-causing mutations. These findings strongly indicate that the modulation of Ca^{2+}-sensitivity is the crucial functional consequence leading to the three types of inherited cardiomyopathies.

In order to explore the pathogenesis of the inherited cardiomyopathies caused by troponin mutations, it is essential to develop appropriate animal models of these disorders. Transgenic mice of HCM-causing mutations of troponin T and I have been produced, but HCM-model mice with ventricular hypertrophy are not available (Knollman and Potter, 2001; Knollman et al., 2003). Recently, a knock-in mouse model of DCM caused by a deletion mutation of troponin T was produced (Morimoto et al., 2005). In this case, skinned cardiac muscle from the mutant mouse showed the decreased Ca^{2+}-sensitivity of force generation. The mutant heart was enlarged with ventricular dilation and impaired systolic function. The mutant mice were associated with a high incidence of sudden death without any sign of heart failure.

The core domain of the troponin $C{\cdot}I{\cdot}T_2$ complex consists of an IT-arm region and a regulatory head region (Takeda et al., 2003). The IT-arm is the structural core of the troponin complex and is fixed to tropomyosin through the two regions of troponin T: the helical tropomyosin-binding region of troponin T_1 and the C-terminal region of troponin T_2. The regulatory head (N-domain of troponin C and H3(I) of troponin I), which is connected with the IT-arm by a flexible linker, is the Ca^{2+}-receptive site for the regulation of contraction. The inhibitory region of troponin I and its C-terminal side region of the molecule, are engaged in the suppression-desuppression type Ca^{2+}-regulatory mechanism: the suppression of actin-tropomyosin by troponin I from interacting with myosin in the absence of Ca^{2+} and the neutralization of the suppression by troponin I through the Ca^{2+}-binding to the N-domain of troponin C. In this respect, the N-domain of troponin C competes with actin-tropomyosin for the troponin I Ca^{2+} dependently.

Most mutations of troponin T and I are located outside of the core domain; instead they are distributed in the regions that interact with actin and tropomyosin. The HCM-causing troponin T mutations would impair the interactions of troponin T with tropomyosin to increase the Ca^{2+}-sensitivity, whereas the DCM-causing mutations of troponin T would modulate the interactions of troponin T with tropomyosin or actin to decrease the Ca^{2+}-sensitivity. The HCM- and RCM-causing mutations of troponin I are located mostly in the inhibitory region and its C-terminal sequence of the molecule, and these mutations would impair the inhibitory action of troponin I and/or modulate the neutralizing action of troponin C and consequently increase the Ca^{2+}-sensitivity of contraction.

At the present time, the detailed mechanisms by which the functional consequences of various mutations of troponin components converge in the Ca^{2+}-sensitizing or Ca^{2+}-desensitizing effect are not yet clear. Detailed investigations especially on the interactions between the thin filament proteins will be required to fully elucidate the features of the pathogenesis of these disorders due to troponin mutations. Studies along this line will also contribute to clarifying the physiological mechanisms of Ca^{2+}-regulation of the contraction underlying these disorders.

4.7. REFERENCES

Ahmad, F., Seidman, J. G., and Seidman, C. E., 2005, The genetic basis for cardiac remodeling, *Annu. Rev. Genomics Hum. Genet.* **6**:185–216.

Bailey, K., 1946, Tropomyosin: a new asymmetric protein component of muscle, *Nature (London)* **157**:368–369.

Bailey, K., 1948, Tropomyosin: a new asymmetric protein component of the muscle fibril, *Biochem. J.* **43**:271–279.

Ebashi, S., 1963, Third component participating in the superprecipitation of "natural actomyosin", *Nature (London)*, **200**:1010.

Ebashi, S., 1972, Troponin and its components, *J. Biochem.* **72**:787–790.

Ebashi, S., 1974, Regulatory mechanism of muscle contraction with special reference to the Ca-troponin-tropomyosin system, *Essays Biochem.* **10**:1–36.

Ebashi, S., and Ebashi. F., 1964, A new protein component participating in the superprecipitation of myosin B, *J. Biochem.* **55**:604–613.

Ebashi, S., Endo, M., and Ohtsuki, I., 1969, Control of muscle contraction, *Q. Rev. Biophys.* **2**:351–384.

Ebashi, S., and Kodama, A., 1965, A new protein factor promoting aggregation of tropomyosin, *J. Biochem.* **58**:107–108.

Ebashi, S., Kodama, A., and Ebashi, F., 1968, Troponin 1. Preparation and physiological function, *J. Biochem.* **64**:465–477.

Fatkin, D., and Graham, R. M. 2002, Molecular mechanism of inherited cardiomyopathies, *Physiol. Rev.* **82**:945–980.

Gomes, A. V., Harada, K., and Potter, J. D., 2005, A mutation in the N-terminal of troponin I that is associated with hypertrophic cardiomyopathy affects the Ca^{2+}-sensitivity, phosphorylation kinetics and proteolytic susceptibility of troponin. *J. Mol. Cell. Cardiol.* **39**:754–765.

Greaser, M. L., and Gergely, J., 1971, Reconstitution of troponin activity from three protein components, *J. Biol. Chem.* **246**:4226–4233.

Harada, K., and Potter, J. D., 2004, Familial hypertrophic cardiomyopathy mutations from different functional regions of troponin T result in different effects on the pH- and Ca^{2+}-sensitivity of cardiac muscle contraction. *J. Biol. Chem.* **279**:14488–14495.

Hartshorne, D. J., and Mueller, H., 1968, Fractionation of troponin into two distinct proteins, *Biochem. Biophys. Res. Commun.* **31**:647–653.

Hatakenaka, M., and Ohtsuki, I., 1991, Replacement of three troponin components with cardiac troponin components within single glycerinated skeletal muscle fibers, *Biochem. Biophys. Res. Commun.* **181**:1022–1027.

Hatakenaka, M., and Ohtsuki, I., 1992, Effect of removal and reconstitution of troponins C and I on the Ca^{2+}-activated tension development of single glycerinated rabbit skeletal muscle fibers, *Eur. J. Biochem.* **205**:985–993.

Hinkle, A., and Tobacman, L. S., 2003, Folding and function of troponin tail domain. Effects of cardiomyopathic troponin T mutations, *J. Biol. Chem.* **278**:506–513.

Hoffman, B., Schmidt-Traub, H., Perrot, A., Osterziel, K. J., and Gessner R., 2001, First mutation in cardiac troponin C, L29Q, in a patient with hypertrophic cardiomyopathy, *Hum. Mutat.* **17**:524.

Jackson, P., Amphlett, G. W., and Perry, S. V. 1975, The primary structure of troponin T and the interaction with tropomyosin, *Biochem. J.* **151**:85–97.

Kamisago, M., Sharma, S. D., DePelma, S. R., Solomon, S., Sharma, P., McDonough, B., Smool, L., Mullen, M. P., Woolf, P. K., Wigle, E. D., and Seidman, C. E., 2000, Mutations in sarcomere protein genes as a cause of dilated cardiomyopathy, *N. Engl. J. Med.* **343**:1688–1696.

Kimura, A., Hara, H., Park, J. E., Nishi, H., Satoh, M., Takahashi, M., Hiroi, S., Sasaoka, T., Ohbuchi, N., Nakamura, T., Koyanagi, T., Hwang, T. H., Choo, J. A., Chung, K. S., Hasegawa, A., Nagai, R., Okazaki, O., Nakamura, H., Matsuzaki, M., Sakamoto, T., Toshima, H., Koga, Y., Imaizumi, Y., and Sasazuki, T., 1997, Mutations in the cardiac troponin I gene associated with hypertrophic cardiomyopathy, *Nat. Genet.* **16**:379–382.

Knollman, B. C., Kirchhof, P., Sirenko, S. G., Degan, H., Greene, A. E., Schober, T., Mackow, J. C., Fabritz, L., Potter, J. D., and Morad, M., 2003, Familial hypertrophic cardiomyopathy-linked mutant troponin T causes stress-induced ventricular tachycardia and Ca^{2+}-dependent action potential remodeling, *Circ. Res.* **92**:428–436.

Knollman, B. C., and Potter, J. D., 2001, Altered regulation of cardiac muscle contraction by troponin T mutations that cause familial hypertrophic cardiomyopathy, *Trends Cardiovasc. Med.* **11**:206–212.

Li, D., Czernuszewicz G. Z., Gonzalez, O., Tapscott, T., Karibe, A., Durand, J. B., Brugada, R., Hill, R., Gregoritch, J. M., Anderson, J. L., Quinones M., Bachinski, L. L., and Roberts, R., 2001, Novel cardiac troponin T mutation as a cause of familial dilated cardiomyopathy, *Circulation* **104**:2188–2193.

Lu, Q-W., Morimoto, S., Harada, K., Du, C-K., Takahashi-Yanaga, F., Miwa, Y., Sasaguri, T., and Ohtsuki, I., 2003, Cardiac troponin T mutation found in dilated cardiomyopathy stabilizes the troponin T-tropomyosin interaction and causes Ca^{2+} desensitization, *J. Mol. Cell. Cardiol.* **35**:1421–1427.

Mirza, M., Marston, S., Willott, R., Ashley, C., Mogensen, J., McKenna, W., Robinson, P., Redwood, C., and Watkins, H., 2005, Dilated cardiomyopathy mutations in three thin filament regulatory proteins results in a common functional phenotype, *J. Biol. Chem.* **280**:28498–28506.

Mogensen, J., Kubo, T., Duque, M., Uribe, W., Shaw, A., Murphy, R., Gimeno, J. R., Elliott, P., and Mckenna, W. J., 2003a, Idiopathic restrictive cardiomyopathy is part of the clinical expression of cardiac troponin I mutations, *J. Clin. Invest.* **111**:209–216.

Mogensen, J., Murphy, R. T., Shaw, A., Bahl, A., Elliott, P. M., and McKenna, W. J., 2003b, Cardiac troponin C, and T mutations in 238 patients with idiopathic dilated cardiomyopathy; Prevalence, clinical features and impact on the troponin complex, *Circulation* **108**:IV–50.

Morimoto, S., Du, C.-K., Ohta, M., Lu, Q.-W., Harada, K., Nishii, K., Yamamura, K., and Ohtsuki, I., 2005, A knock-in mouse model for familial dilated cardiomyopathy caused by the mutation ΔK210 in cardiac troponin I, *Biophys. J.* **88**(1):Part 2.480a.

Morimoto, S., Lu, Q-W., Harada, K., Takahashi-Yanaga, F., Minakami, R., Ohta, M., Sasaguri, T., and Ohtsuki, I., 2002, Ca^{2+} desensitizing effect of a deletion mutation delta-K210 in cardiac troponin T that causes familial dilated cardiomyopathy, *Proc. Natl. Acad. Sci. USA* **99**:913–918.

Morimoto, S., Nakaura, H., Yanaga, F., and Ohtsuki, I., 1999, Functional consequences of a carboxy terminal missense mutation Arg278Cys in human cardiac troponin T, *Biochem. Biophys. Res. Commun.* **261**:79–82.

Morimoto, S., Yanaga, F., Minakami, R., and Ohtsuki, I., 1998, Ca^{2+}-sensitizing effects of the mutations at Ile-79 and Arg-92 of troponin T in hypertrophic cardiomyopathy, *Am. J. Physiol.* **275**:C200–C207.

Nagano, K., and Ohtsuki, I., 1982, Prediction of approximate quaternary structure of troponin complex, *Proc. Japan Acad.* **58**(Ser.B):73–77.

Nakaura, H., Morimoto, S., Yanaga, F., Nakata, M., Nishi, N., Imaizumi, Y., and Ohtsuki, I., 1999a, Functional changes in troponin T by a splice donor site mutation that causes hypertrophic crdiomyopathy, *Am. J. Physiol.* 277, C225–C232.

Nakaura, H., Yanaga, F., Ohtsuki, I., and Morimoto, S., 1999b, Effects of missense mutations Phe110Ile and Glu244Asp in human cardiac troponin T on force generation in skinned cardiac muscle fibers, *J. Biochem.* **126**:457–460.

Ohtsuki, I., 1974, Localization of troponin in thin filament and tropomyosin paracrystal, *J. Biochem.* **75**:753–765.

Ohtsuki, I., 1975, Distribution of troponin components in the thin filament studied by immunoelectron microscopy, *J. Biochem.* **77**:633–639.

Ohtsuki, I., 1979, Molecular arrangement of troponin T in thin filament, *J. Biochem.* **86**:491–497.

Ohtsuki, I. 1980, Functional organization the troponin-tropomyosin system, in: *Muscle Contraction; Its Regulatory Mechanisms*, S. Ebashi, K. Maruyama, M. Endo, eds, Jpn Sci. Soc. Press, Tokyo, Springer-Verlag, Berlin, Heidelbeng, New York, pp. 237–250.

Ohtsuki, I., Maruyama, K, and Ebashi, S., 1986, Regulatory and cytoskeletal proteins of vertebrate skeletal muscle, *Adv. Protein Chem.* **38**:1–68.

Ohtsuki I., Masaki, T., Nonomura, Y, and Ebashi, S. 1967, Periodic distribution of troponin along thin filament, *J. Biochem*. **81**:817–819.

Ohtsuki, I., Onoyama, Y., and Shiraishi, F., 1988, Electron microscopic study of troponin, *J. Biochem*. **103**: 913–919.

Ohtsuki, I., and Shiraishi, F., 2002, Periodic binding of troponin C·I and troponin I to tropomyosin-actin filaments, *J. Biochem*. **131**:739–743.

Ohtsuki, I., Shiraishi, F., Suenaga, N., Miyata, T., and Tanokura, M., 1984, 26K fragment of troponin T from rabbit skeletal muscle, *J. Biochem*. **95**:1337–1342.

Ohtsuki, I., Yamamoto, K., and Hashimoto, K., 1981, Effect of two C-terminal side chymotryptic subfragments on the Ca^{2+} sensitivity of superprecipitation and ATPase activities of actomyosin, *J. Biochem*. **90**: 259–261.

Oliveira, D. M., Nakaie, C. R., Sousa, A. D., Farah, C. S., and Reinach, C., 2000, Mapping the domain of troponin T responsible for the activation of actomyosin ATPase activity. Identification of residues involved in binding to actin, *J. Biol. Chem.* **275**:27513–27519.

Ooi, T., Mihashi, K., and Kobayashi, H., 1962, On the polymerization of tropomyosin, *Arch. Biochem. Biophys*. **98**:1–11.

Pan, B.-S., Gordon, A. M., and Potter, J. D., 1991, Deletion of the first 45 NH_2-terminal residues of rabbit skeletal troponin T strengthens binding of troponin to immobilized tropomyosin, *J. Biol. Chem*. **266**: 12432–12438.

Pearlstone, J. R., Carpenter, M. R., Johnson, P., and Smillie, L. B., 1976, Amino-acid sequence of tropomyosin binding component of rabbit skeletal muscle troponin, *Proc. Natl. Acad. Sci. USA* **73**: 1902–1906.

Perry, S. V., 1999, Troponin I: inhibitor or facilitator, *Mol. Cell. Biochem*. **190**:9–32.

Preston, L., Lipscomb, S., Robinson, P., Watkins, H., Redwood, C., Mogensen, J., and Ashley, C., 2004, Mechanical effect of human cardiac troponin C mutation Gly159Asp in exchanged rabbit psoas fibers, *Biophys. J.* **86**:396a.

Rüegg, J. C., 1986, *Calcium in Muscle Activation*, Springer-Verlag, Berlin, Tokyo, pp. 165–200.

Schaub, M. C., and Perry, S. V., 1969, The relaxing protein system of striated muscle, *Biochem. J.* **1155**: 903–1004.

Shiraishi, F., Morimoto, S., Nishita, K., Ojima, T., and Ohtsuki, I., 1999, Effects of removal and reconstitution of myosin regulatory light chain and troponin C on the Ca^{2+}-sensitive ATPase activity of myofibrils from scallop striated muscle, *J. Biochem*. **126**:1020–1024.

Szczesna, D., Zhang, R., Zhao, J., Jones, M., Guzman, G., and Potter, J. D., 2000, Altered regulation of cardiac muscle contraction by troponin T mutations that cause familial hypertrophic cardiomyopathy, *J. Biol. Chem*. **275**:624–630.

Takahashi-Yanaga, F., Morimoto, S., Harada, K., Minakami, R., Shiraishi, F., Ohta, M., Lu, Q-W., Sasaguri, T., and Ohtsuki, I., 2001, Functional consequences of the mutations in human cardiac troponin I gene found in familial hypertrophic cardiomyopathy, *J. Mol. Cell. Cardiol*. **33**:2095–2107.

Takeda, S., Yamashita, A., Maeda, K., and Maeda, Y., 2003, Structure of the core domain of human cardiac troponin in the Ca^{2+}-saturated form, *Nature*, **424:**35–41.

Tanaka, H., Takeya, Y., Doi, T., Yumoto, F., Tanokura, M., Ohtsuki, I., Nishita, K. and Ojima, T. 2005, Comparative studies on the functional roles of NH_2- or COOH-terminal region of molluskan and vertebrate troponin-I, *FEBS J.* **272**(17):4475–4486.

Tanokura, M., Tawada, Y., and Ohtsuki, I., 1982, Chymotryptic subfragments of troponin T from rabbit skeletal muscle. I. Determination of the primary structure, *J. Biochem*. **91**:1257–1265.

Tanokura, M., Tawada, Y., Ono, A., and Ohtsuki, I., 1983, Chymotryptic subfragments of troponin T from rabbit skeletal muscle. Interaction with tropomyosin, troponin I and troponin C, *J. Biochem*. **93**: 331–337.

Thierfelder, L., Watkins, H., MacRae, C., Lamas, R., McKenna, W., Vosberg, H. P., Seidman, J. G., and Seidman C. E., 1994, α-Tropomyosin and cardiac troponin T mutations cause familial hypertrophic cardiomyopathy, *Cell*, **77**:701–712.

Tripet, B., Van Eyk, J. E., and Hodges, R. S., 1997, Mapping of a second actin-tropomyosin and a second troponin C binding site within the C terminus of troponin I, and their importance in the Ca^{2+}-dependent regulation of muscle contraction, *J. Mol. Biol*. **271**:726–750.

Tsao, T.-C., Bailey, K., and Adair, G. S., 1951, The size, shape and aggregation of tropomyosin particles, *Biochem. J.* **49**:27–36.

Venkatraman, G., Harada, K., Gomes, A. V., Kerrick, W. G., and Potter, J. D., 2003, Different functional properties of troponin T mutants that cause dilated cardiomyopathy, *J. Biol. Chem*. **278**:41670–41676.

Vinogradova, M. V., Stone, D. B., Malanina, G. G., Karatzaferi, C., Cooke, R., Mendelson, R. A., and Fletterick, R. J., 2005, Ca^{2+}-regulated structural changes in troponin, *Proc. Natl. Acad. Sci. USA*, **102**:5038–5043.

Yanaga, F., Morimoto, S., and Ohtsuki, I., 1999, Ca^{2+} sensitization and potentiation of the maximum level of myofibrillar ATPase activity caused by mutations of troponin T found in familial hypertrophic cardiomyopathy, *J. Biol. Chem*. **274**:8806–8812.

Yumoto, F., Lu, Q-W., Morimoto, S., Tanaka, H., Kono, N., Ojima, T., Takahashi-Yanaga, F., Miwa, Y., Sasaguri, T., Nishita, K., Tanokura, M., and Ohtsuki, I., 2005, Drastic Ca^{2+}sensitization of myofilament associated with a small structural change in troponin I in inherited restrictive cardiomyopathy, *Biochem. Biophys. Res. Commun.* **338**:1519–1526.

5

FROM THE CRYSTAL STRUCTURE OF TROPONIN TO THE MECHANISM OF CALCIUM REGULATION OF MUSCLE CONTRACTION

Yuichiro Maeda[1,2,3], Yasushi Nitanai[1,2] and Toshiro Oda[1,2]

5.1. INTRODUCTION

In 2003, we published the crystal structures of the core domains of human cardiac muscle troponin (Takeda et al., 2003). Thus, for the first time we were able to visualize the architecture of the molecule; and to see how the three components (TnC, TnI and TnT) fold together to form the troponin molecule. Moreover, our molecular switch mechanism was confirmed, which was previously proposed (Vassylyev et al., 1998) based on the crystal structure of a much smaller complex (the full length TnC in complex with TnI (1–47), a short N-terminal fragment of TnI, both from rabbit skeletal muscle troponin). Namely, a C-terminal TnI segment (117–126 in the rabbit skeletal troponin sequence), directly downstream from the "inhibitory region" (104–115), forms an amphipathic α-helix and interacts with the hydrophobic pocket of the TnC N-lobe in a [Ca^{2+}]-dependent manner. This binding removes the inhi-bitory region from actin-tropomyosin, and thereby relieves the inhibitory action of TnI.

In spite of this progress, our understanding of the mechanism of troponin-linked calcium regulation of muscle contraction was far from complete. Actually, we felt that we stood at the starting point, facing a mountain of questions to address. For example, we do not know how and where on the actin-tropomyosin filament the troponin core domain resioles. More importantly, how the signal of Ca/up/2+/-binding to troponin C transfers to the actin-tropomyosin filament. In this review article, we shall discuss our strategy to progress from the atomic structure to an understanding of the mechanism of the troponin-linked Ca^{2+}-regulation. Recent analyses of the relationships between cardiomyopathy-causing mutations and functional aberrations should provide crucial information for our understanding of the relationship between the dynamic properties of troponin and the mechanisms of Ca^{2+}-regulation.

[1] ERATO Actin Filament Dynamics Project, c/o RIKEN Harima Institute SPring-8 Center, [2]Lab for Structural Biochemistry, RIKEN Harima Institute SPring-8 Center, Sayo, Hyogo, and [3]Division of Biological Sciences, Graduate School of Science, Nagoya University, Nagoya, Japan

Regulatory Mechanisms of Striated Muscle Contraction
Edited by Ebashi and Ohtsuki, Springer, 2007

5.2. TWO ELEMENTARY MECHANISMS

Ebashi and his colleagues (Ebashi and Endo, 1968; Ebashi et al., 1969) emphasized that the troponin-linked regulation of muscle contraction is predominantly due to the inhibition of actomyosin interactions at low ($<10^{-6}$ M) [Ca^{2+}], which is removed at high [Ca^{2+}]. However, subsequent efforts by Ohtsuki and his colleagues indicated that the activation should also have significant contributions.

First, they carefully measured the effects of the selective removal of troponin from the contractile apparatus on the calcium sensitivity of the force generated by demembranated rabbit skeletal muscle fibers. For this experiment (Hatakenaka and Ohtsuki, 1992), the endogenous troponin was replaced by exogenous TnT (precisely, a fragment thereof). It was known that the replacement of troponin by TnT is functionally equivalent to the removal of troponin. The results clearly indicated that, when troponin was completely removed, the level of the generated force was [Ca^{2+}]-independent and reached about 70% of the maximal force that was generated before the treatment. This indicates that 70% of the maximal force is generated by the mechanism that is inhibited at the low [Ca^{2+}] and relieved at the high [Ca^{2+}], while the remaining 30% is due to an activation mechanism that is associated with the presence of troponin (Figure 5.1).

Second, the skeletal muscle of the Akazara scallop is regulated by dual systems, the myosin-linked system as well as the troponin-linked system. The myosin-linked system is specialized for the mechanism of inhibition/removal of inhibition, while the troponin-linked system confers the activation (Shiraishi et al., 1999). Interestingly, the mechanism of activation remains when only the N-fragment of TnI (including only the N-terminal half up to the inhibitory region) is present together with the other components of the actin-tropomyosin-troponin complex. In contrast, the addition of the C-fragment of TnI (including only the C-terminal half downstream from the inhibitory region) did not confer [Ca^{2+}]-dependent force generation (Figure 5.2C) (Tanaka et al., 2005). Consistent with this, a similar experiment performed with rabbit skeletal muscle proteins dissected the

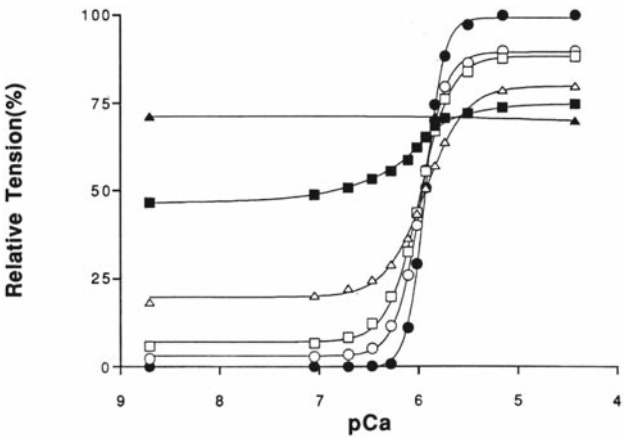

Figure 5.1. The [Ca^{2+}]-dependent forces generated by glycerinated rabbit skeletal muscle fiber from which the endogenous troponin was extracted to various extents. Different symbols correspond to different extents of troponin extraction. From (Hatakenaka and Ohtsuki, 1992) with permission.

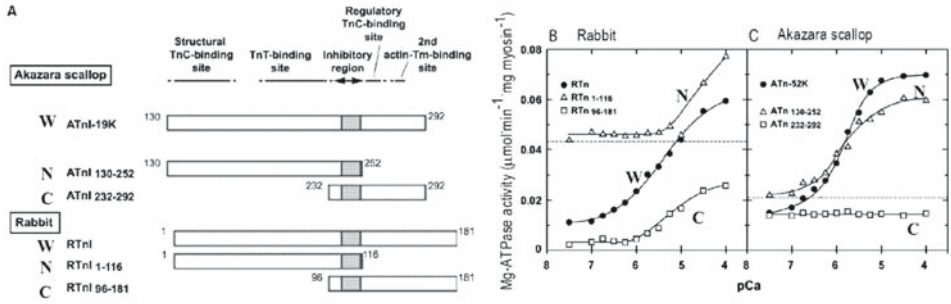

Figure. 5.2. Dissection of the troponin-linked regulation mechanism into two elementary mechanisms. **A**: The TnI constructs used. W, whole TnI; N, N-terminal fragment; C, C-terminal fragment. Residues 1–129 of Akazara scallop are not expressed (missing) in the major isoform of TnI. **B** and **C**, Actomyosin ATPase rates versus [Ca^{2+}] at 15°C. Modified from (Tanaka et al., 2005).

Ca^{2+}-regulation into two elementary mechanisms: The inhibition/removal of inhibition dependent on [Ca^{2+}], but not the activation, was restored if the C-fragment of TnI (including the inhibitory region) was present, while the [Ca^{2+}]-dependent activation was restored if the N-fragment of TnI (including the inhibitory region) was present (Figure 5.2B).

These findings indicated that the troponin-linked regulatory mechanism of muscle contraction is generally decomposed into two elementary mechanisms: mechanism-1 for inhibition/removal of inhibition and mechanism-2 for activation, and both are [Ca^{2+}]-dependent.

5.3. TROPONIN VARIANTS WHICH CAUSE CARDIOMYOPATHY

Cardiomyopathy is caused by mutations of proteins in the contractile apparatus, including troponin. Ohtsuki, Morimoto and their colleagues at Kyushu University have analyzed the functional aberrations of disease-causing troponin mutants in more than 30 patients. The mutants of human cardiac troponin were expressed in and purified from *E.coli*. They introduced the mutant proteins into glycerinated rabbit cardiac fibers by the use of their original refined techniques of replacing endogenous troponin by exogenous counterparts. By establishing these measuring procedures, they obtained an accurate and reproducible relationship between the force generated by the glycerinated fibers and the free [Ca^{2+}] of the bathing solution. Lately, many mutations have been identified as causes of a particular disease. However, in few diseases, functional aberration can be identified in *in vitro* experiments. According to the force-pCa relationships obtained from individual troponin mutants, the functional aberrations have been classified into three types (Figure 5.3). Type I indicates hyper [Ca^{2+}] sensitivity, type II shows hypo [Ca^{2+}] sensitivity, and type III is associated with increased forces by about 20% without altering the [Ca^{2+}] sensitivity.

It is interesting to note that the classification seems to be consistent with the view that the troponin-linked regulation of muscle contraction can be decomposed into two elementary mechanisms. The functional aberrations of types I and II in cardiomyopathy

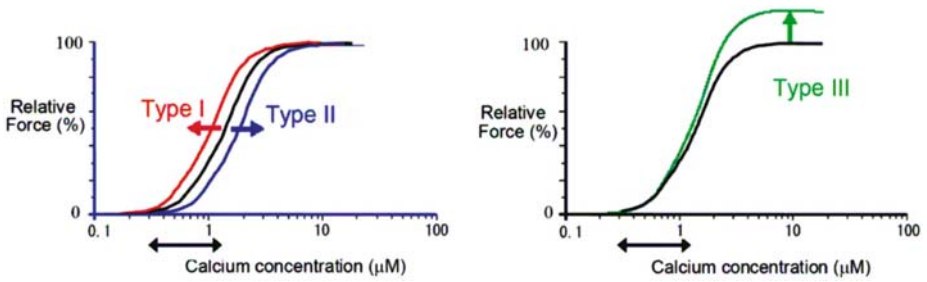

Figure 5.3. Three types of functional aberrations found with troponin mutants that cause cardiomyopathy. The arrows below the abscissa indicate the physiological ranges of intracellular [Ca^{2+}].

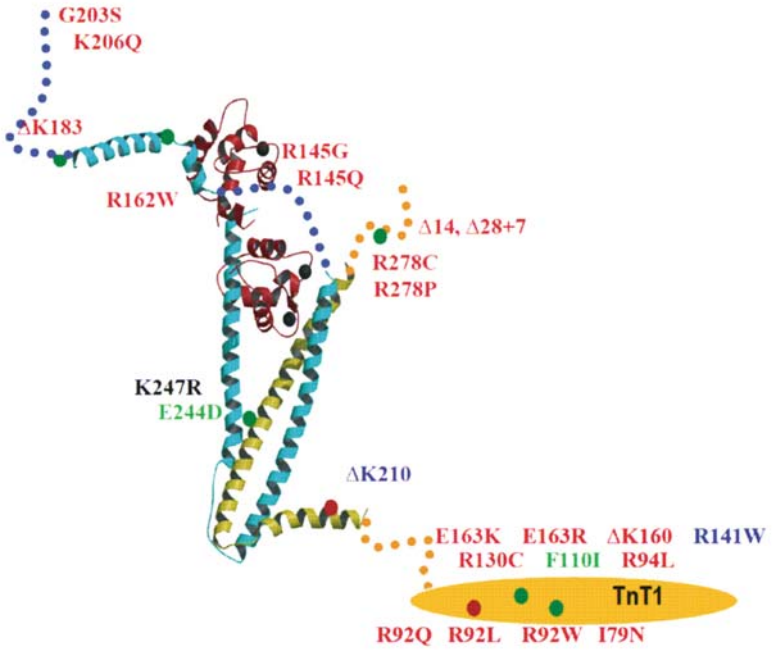

Figure 5.4. The loci of mutations that cause cardiomyopathy, marked on the crystal structure according to the same color-codes as in Figure 3.4. A ribbon model of the cardiac troponin crystal structure (Takeda et al., 2003); TnC, red; TnI, cyan; TnT2, yellow. The dotted lines indicate the segments that were included in the crystals but lacked defined electron densities. TnT1 was not included in the crystal.

patients must be caused by abnormalities in mechanism-1, while those of type III must originate from the excessive activity of the mechanism-2.

How are these findings related to the structure of troponin? In Figure 5.4, the loci of some disease causing mutations are marked on our crystal structure of the troponin core-domain, and are color-coded according to the type of functional aberration. This map indicates two things. First, the majority of the disease-causing mutations occur on the polypeptide segments for which electron densities were not defined in the crystal, presumably because the segments are mobile. From a functional point of view, these segments

either connect two structural domains or form interfaces with tropomyosin and/or actin. This reinforces the crucial importance of knowing the atomic structure of the entire complex of troponin-tropomyosin-actin, including the mobile loops and the binding interfaces. Second, the disease-causing mutations in one particular type of functional aberration are not restricted to a particular structural domain, but are scattered throughout the molecule. In other words, a particular mechanism does not reside in a particular structural domain of the protein, although it may be associated with a dynamic property of the molecule.

5.4. AMINO ACID REPLACEMENTS AT THE MIDDLE OF THE COILED-COIL

Only a few cardiomyopathy-causing mutations have been mapped to the IT arm of the troponin core domain (Figure 5.5A). Here we focus our attention on two mutations, E244D and K247R of TnT2, which occur in the middle of the coiled-coil formed between TnI and TnT. E244D reportedly shows potentiation of the maximum level of ATPase activity (Type III) (Yanaga et al., 1999), as well as additional Ca^{2+}-sensitization (Type I) when the force is measured from the fibers (Nakaura et al., 1999). A Spanish patient who suffered from severe hypertropic cardiomyopathy (HCM) was found to carry K247R (Garcia-Castro et al., 2003), but the functional consequence of this mutation has not yet been analyzed.

Before we start discussing the possible mechanisms of how these mutations cause functional aberrations, we should know more about the structure and possible dynamics

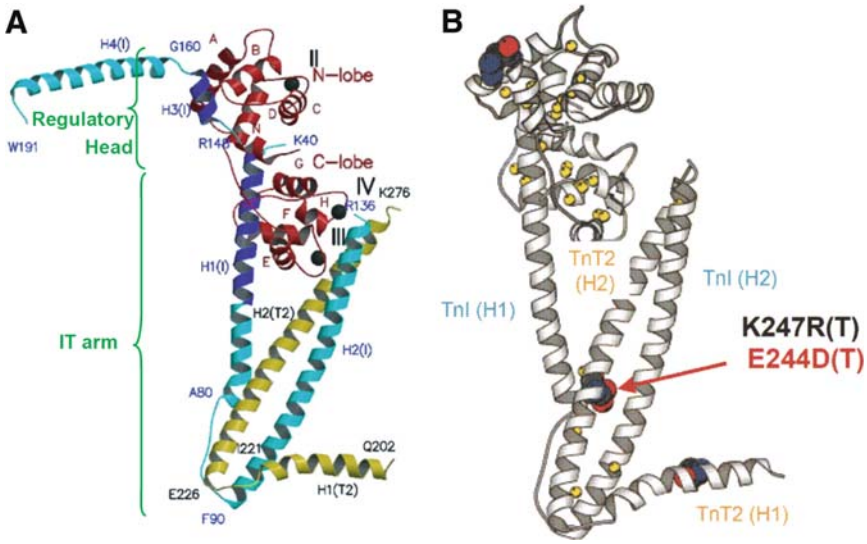

Figure 5.5. Ribbon models of the crystal structure of the human cardiac troponin core domain (Takeda et al., 2003). **A**: TnC, red; TnI, blue and cyan; TnT2, yellow. **B**: Two disease-causing mutations on TnT in the crystal structure.

of the loci where these mutations occur. The following discussions indicate that the loci are in a critical site of the troponin core-domain.

First, in order to define the mechanical and dynamic properties of the parts of the molecule near the loci, we performed a normal mode analysis of the thermal fluctuations of the troponin core-domain, based on the elastic network approximation (Tirion, 1996; Bahar et al., 1997). The troponin core domain was approximated by an elastic body in which each pair of C_α carbons within a distance of 8 Å were connected by a spring with a common constant. It was remarkable that all four of the slowest modes of structural fluctuations were global bending of the core-domain in various directions with different azimuth angles about the longitudinal axis, and that in each mode, the molecule bends close to the loci of the mutations (data not shown). This result may be consistent with the overall shape of the molecule, as the core-domain is elongated and is narrowest at the loci. When the molecule is viewed as in Figure 5.5, the molecule becomes wider as one goes from the loci upward. This is because the α-helix TnI (H1) merges close to the loci, in a fixed angle relative to the coiled-coil axis. At the top, i.e. the C-termini of the coiled-coil, the triangle formed by TnI (H1) and the coiled-coil is the widest. At this end, the structure may also be stiff, because the TnC C-lobe interacts tightly with both the coiled-coil and TnI (H1). On the other hand, at the lower part no bulky mass is attached to the coiled-coil, except for the α-helix TnT2 (H1), which merges with the coiled-coil at the bottom.

Second, a close inspection of the crystal structure indicates that the loci of the mutations are in the bent region of the coiled-coil. The coiled-coil axis is not straight, but is bent at two points in opposite directions: the first and second bends are close to the two helical turns below and above the position of K247, respectively (Figure 5.6A,B). The profile of the local bending angle (the black curve in Figure 5.6C) confirms that at each level, the coiled-coil is bent by about 8–10 degrees.

Third, the arrangement of the side chains near the loci of the mutations reveals a characteristic structure, which is referred to as “a pair of triads” (Figure 5.7).

(1) K247 of TnT2 and R111 of TnI are at the *a* position in the heptad repeat of the coiled-coil, facing each other at the same level along the coiled-coil axis. Since both are basic and repulsive to each other, and since both are bulky, the side chains of these residues are directed outwards, away from the axis of the coiled-coil, leaving a cavity at the core of the coiled-coil. The occurrence of two basic residues at the *a* positions and the side chain arrangement must destabilize the coiled-coil.

(2) The side chain of K247(a) forms hydrogen bonds with E244(at *e* position) of TnT2 and with E110(*g*) of TnI, forming a triad outside of the coiled-coil. Since two out of the three residues belong to TnT2, this triad is referred to as the triad on the TnT-side.

(3) Another triad (the triad on the TnI-side) is formed by R111(*a*) of TnI with D108(*e*) of TnI and E246(*g*) of TnT2.

(4) The pair of these two triads is symmetric around the coiled-coil axis, and probably stabilizes the coiled-coil structure.

(5) The surroundings of each triad are differ from each other. The triad on the TnT-side is located in a more crowded environment, where the space is restricted by the merging of TnI-H1, whereas the triad on the TnI-side is in a less crowded environment, since TnT2-H1 is still far away.

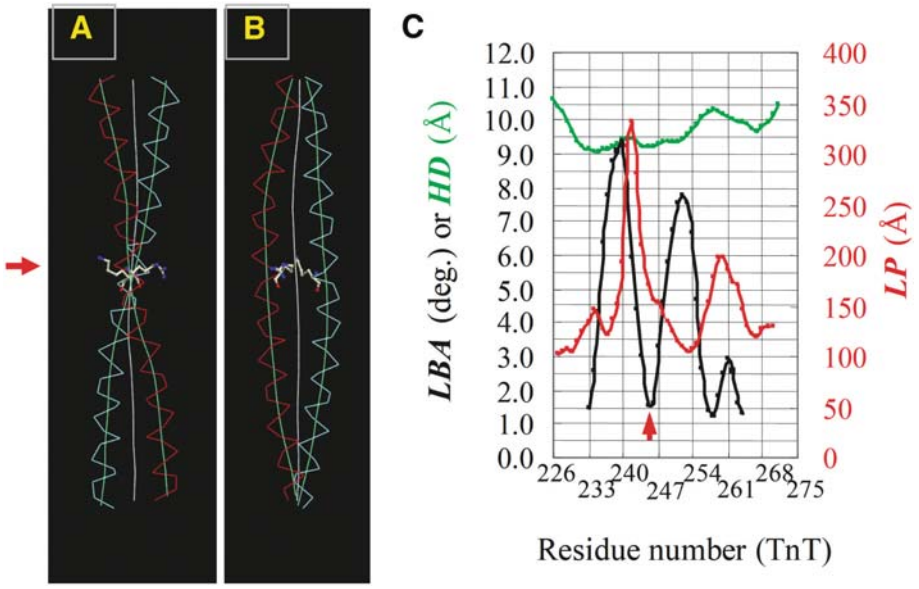

Figure 5.6. Bend of the coiled-coil around the loci of disease causing mutations. **A** and **B**: The axes of the coiled-coil (white line), and those of the two α-helices (green lines). **A** and **B** differ in the viewing direction by 90 degrees. The red arrow and the side chains in the wire model indicate K247 (TnT) and R111 (TnI). **C**: The helix distance (HD, green curve), the local bending angle (LBA, black curve) and the local pitch (LP, red curve) are plotted versus the residue numbers of TnT. The red arrow indicates the position of K247.

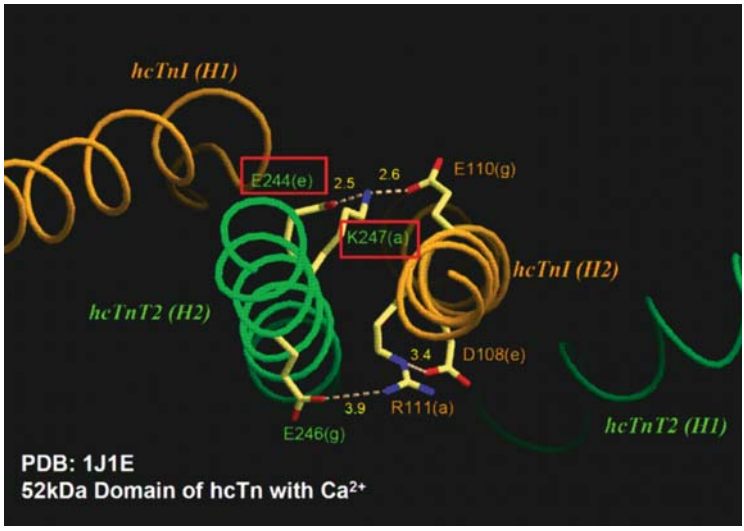

Figure 5.7. "A pair of triads" at the level of E244 and K247, viewed from the C-terminal end of the coiled-coil of the IT arm. In this diagram, TnT2 is green, while TnI is beige. Hydrogen bonds are indicated by the yellow dotted lines labeled with inter-atomic distances.

5.5. POSSIBLE MECHANISM OF FUNCTIONAL ABERRATIONS

Although the pair of triads has not been described in the crystal structures of coiled-coils, this structural motif should play important roles in the dynamics, and therefore in the physiological functions, of troponin. This is supported by the fact that the pair of triads is well conserved among the troponin species from different tissues and animals (Figure 5.8).

By taking the aforementioned considerations into account, we may speculate about the mechanisms by which these mutations cause cardiomyopathy.

First, the loci of these mutations are at a critical positions, where the coiled-coil, as well as the entire core-domain of troponin, may dynamically bend. Thus, the bending frequency and the amplitude, and therefore the compliance, as well as the bending direction might be altered upon subtle changes of the structure.

Second, a change in the side chain volume on the (crowded) TnT-side may greatly influence the dynamic properties of the bending region.

Third, a change in the electrostatic properties of the side chains may also affect the dynamic properties.

The three points described below are consistent with the above hypothesis, although they do not necessarily prove the hypothesis. (1) Both of the known disease-causing mutations, E244D and K247R, occur only on the crowded TnT-side, and no such mutation has been described on the opposite TnI-side. (2) Both of the mutations are associated with small changes in the side chain volume, a decrease in E244 and an increase in K247, without a change in the electrostatic properties. (3) In the Akazara scallop muscle troponin, which is specialized for [Ca^{2+}]-dependent activation, the residue corresponding to E244 of human cardiac muscle TnT is Ala, which occupies a substantially smaller volume. This smaller volume may cause the excessive activation in the Akazara troponin.

In conclusion, we hypothesize that the dynamic bending of the coiled-coil, and therefore the entire core-domain, at around K247 of TnT2 should be highly tuned. Thus, any significant perturbation which makes the bending region more flexible should cause excessive activation, which is the type III functional aberration found in cardiomyopathy patients.

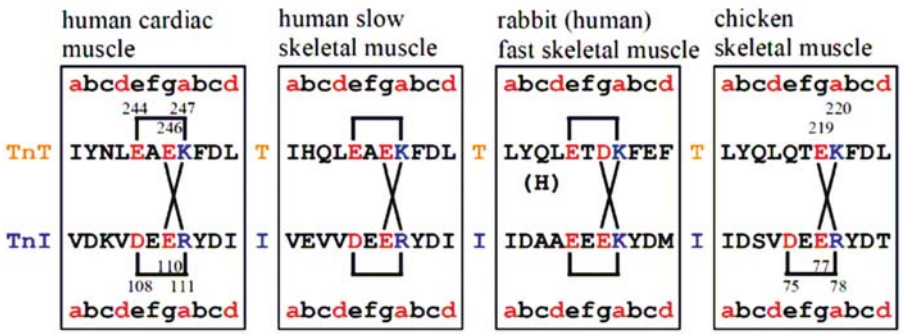

Figure 5.8. Amino acid sequences of the coiled-coil around the loci of the mutations, in various troponin species. In each box, the upper and lower rows are the sequences of TnT and TnI, respectively. The heptad-peptide repeats are indicated on the top and bottom rows. Acidic and basic residues are indicated by letters in red and blue, respectively.

5.6. HOW TO PROVE THE PROPOSED MECHANISM

In order to prove the hypothesis, we may perform mutation experiments. Some of our preliminary results may be interpreted in terms of the hypothesis. In any case, the functional aberration of an individual mutant troponin should be specified by measuring the actomyosin ATPase rate and/or the [Ca^{2+}]-dependent force generation. However, since the structure that is responsible for the dynamic bending of the coiled-coil consists of at least 6 residues (a pair of triads), the number of mutations to be tested should be enormous. Moreover, the functional characterization alone would make it impossible to interpret these results.

It would be quite desirable to measure the dynamic parameters directly from the wild type troponin and the disease-causing mutants. Among the various methods available, protein NMR may allow us to characterize the dynamic bending of the core-domain. Until recently, the application of NMR to a protein complex like troponin (46–52 kDa for the core-domain) has been not realistic, except for recording signals from mobile segments, since there has been a severe molecular size limitation. This limitation has now been relieved by the invention of the SAIL-NMR method by Kainosho and his colleagues (Kainosho et al., 2006). In this method, a minimum number of atoms are replaced by isotopes, so that the NMR spectra obtained from SAIL-protein are much less crowded. This makes it possible to measure proteins as large as 50–80 kDa. Moreover, the structure can be determined much more accurately, as compared with conventional methods.

To understand the troponin-linked regulation mechanisms at a molecular level, it would be quite useful to use disease-causing mutant proteins for measurements, and to perform measurements combining various techniques, such as X-ray protein crystallography, electron microscopy, protein NMR, and computational science. This is because, on one hand, since the atomic structure alone does not tell us much about the mechanism, it is essential to know the dynamic properties of the protein complex. On the other hand, from information about the dynamic properties of the complex, biologically relevant aspects could be selected. For this selection, our knowledge of the disease-causing mutations and the functional consequences of these mutations should play essential roles.

5.7. REFERENCES

Bahar, I., Atilgan, A. R., and Erman, B., 1997, Direct evaluation of thermal fluctuations in proteins using a single-parameter harmonic potential. *Fold Des.* **2**:173–181.

Ebashi, S., and Endo, M., 1968, Calcium ion and muscle contraction. *Prog. Biophys. Mol. Biol.* **18**:123–183.

Ebashi, S., Endo, M., and Otsuki, I., 1969, Control of muscle contraction. *Q. Rev. Biophys.* **2**:351–384.

Garcia-Castro, M., Reguero, J. R., Batalla, A., Diaz-Molina, B., Gonzalez, P., Alvarez, V., Cortina, A., Cubero, G. I., and Coto, E., 2 003, Hypertrophic cardiomyopathy: low frequency of mutations in the beta-myosin heavy chain (MYH7) and cardiac troponin T (TNNT2) genes among Spanish patients. *Clin. Chem.* **49**:1279–1285.

Hatakenaka, M., and Ohtsuki, I., 1992, Effect of removal and reconstitution of troponins C and I on the Ca^{2+}-activated tension development of single glycerinated rabbit skeletal muscle fibers. *Eur. J. Biochem.* **205**:985–993.

Kainosho, M., Torizawa, T., Iwashita, Y., Terauchi, T., Mei Ono, A., and Guntert, P., 2006, Optimal isotope labelling for NMR protein structure determinations. *Nature* **440**:52–57.

Nakaura, H., Yanaga, F., Ohtsuki, I., and Morimoto, S., 1999, Effects of missense mutations Phe110Ile and Glu244Asp in human cardiac troponin T on force generation in skinned cardiac muscle fibers. *J. Biochem. (Tokyo)* **126**:457–460.

Shiraishi, F., Morimoto, S., Nishita, K., Ojima, T., and Ohtsuki, I., 1999, Effects of removal and reconstitution of myosin regulatory light chain and troponin C on the Ca^{2+}-sensitive ATPase activity of myofibrils from scallop striated muscle. *J. Biochem. (Tokyo)* **126**:1020–1024.

Takeda, S., Yamashita, A., Maeda, K., and Maéda, Y., 2003, Structure of the core domain of human cardiac troponin in the Ca^{2+}-saturated form. *Nature* **424**:35–41.

Tanaka, H., Takeya, Y., Doi, T., Yumoto, F., Tanokura, M., Ohtsuki, I., Nishita, K., and Ojima, T., 2005, Comparative studies on the functional roles of N- and C-terminal regions of molluskan and vertebrate troponin-I. *FEBS J.* **272**:4475–4486.

Tirion, M. M., 1996, Large amplitude elastic motions in proteins from a single-parameter, atomic analysis. *Phys. Rev. Lett.* **77**:1905–1908.

Vassylyev, D. G., Takeda, S., Wakatsuki, S., Maeda, K., and Maéda, Y., 1998, Crystal structure of troponin C in complex with troponin I fragment at 2.3-Å resolution. *Proc. Natl. Acad. Sci. USA* **95**:4847–4852.

Yanaga, F., Morimoto, S., and Ohtsuki, I., 1999, Ca^{2+} sensitization and potentiation of the maximum level of myofibrillar ATPase activity caused by mutations of troponin T found in familial hypertrophic cardiomyopathy. *J. Biol. Chem.* **274**:8806–8812.

6

CA ION AND THE TROPONIN SWITCH

Maia V. Vinogradova, Deborah B. Stone, Galina G. Malanina,
Robert A. Mendelson and Robert J. Fletterick

6.1. INTRODUCTION

Muscle contraction as an event manifest by the sliding of myosin filaments along actin filaments was first proposed about fifty years ago by H. Huxley and J. Hanson (Huxley, 2004). This theory built a foundation for muscle research at the molecular level. A decade later the discovery of troponin by Professor S. Ebashi (Ebashi, 1963; Ebashi et al., 1967) highlighted the importance of regulation of muscle contraction and sparked numerous experimental studies of the mysterious protein troponin whose properties are now becoming understood at satisfying resolution.

The interactions of myosin and actin in the presence of ATP are Ca^{2+}-sensitive (Ebashi, 1960). Troponin and tropomyosin are parts of the regulatory machinery responsible for Ca^{2+} – activation of the actin-myosin complex formation (Gordon et al., 2000). Troponin, tropomyosin and actin compose a changing assembly that controls the availability of functional myosin binding sites in a three-state kinetic scheme: the myosin binding sites are blocked in the absence of Ca^{2+} ("blocked" state); some binding sites in the presence of Ca^{2+} are partially revealed ("closed" state); and all myosin binding sites are available when both Ca^{2+} and myosin are present ("open" state) (McKillop and Geeves, 1993). Positional changes of tropomyosin about the long axis of the actin filament characterize the three states (Xu et al., 1999). What is the role of troponin in the described events?

A working Ca^{2+}-receptor, troponin has three subunits: TnC, TnI and TnT (Greaser and Gergely, 1971). TnC, has four Ca^{2+}-binding sites. TnI, the modulator, inhibits ATP turnover by the actin-myosin complex. TnT, an integrator, links troponin together and binds tropomyosin (for review see Perry, 1998; Perry, 1999). Biochemical and structural studies of troponin defined substructures of troponin and identified the Ca^{2+}-induced movements within troponin. An important discovery was that the TnI fragment comprised of residues 117–128, termed the switch, moves out and in relative to TnC depending on the presence of Ca^{2+} (Pearlstone et al., 1997). The TnI segment 104–115 preceding the switch was shown to be responsible for almost full inhibition of myosin ATPase activity

Department of Biochemistry, UCSF

Regulatory Mechanisms of Striated Muscle Contraction
Edited by Ebashi and Ohtsuki, Springer, 2007

by troponin (Van Eyk et al., 1997). The crystal structures of TnC subunit in the absence and in the presence of Ca^{2+} revealed the conformational changes it undergoes upon Ca^{2+}-binding (Herzberg and James, 1988; Satyshur et al., 1988; Houdusse et al., 1997). The NMR structure of TnC with bound switch fragment of TnI advanced us further in understanding the structure of troponin complex and its regulatory mechanism (Slupsky and Sykes, 1995).

However, the full picture required the structure of the intact troponin complex. The decades of crystallization attempts were fruitless until a groundbreaking high-resolution crystal structure of the cardiac troponin core domain in the Ca^{2+}-saturated state was reported (Takeda et al., 2003). The structure of the troponin core domain comprising TnC, a truncated TnI and a proteolytic C-terminal fragment of TnT (TnT2) demonstrated the complex assembly through the TnI and TnT coiled coil interacting with the C-terminal domain of TnC. The N-terminal domain of TnC with the bound helical TnI switch was located away from the rest of the molecule. The TnC central linker and the TnI inhibitory segment were not visible. Although the crystal structure of the cardiac troponin unveiled the general plan of the complex assembly, we attempted crystallization of skeletal isoform of troponin to compare details and find information "missing" in the crystal structure of cardiac troponin. The cardiac and skeletal isoforms of troponin are distinct structurally and physiologically (Gordon et al., 2000; Maytum et al., 2003). The crystal structures of skeletal muscle troponin in both high-Ca^{2+} and low-Ca^{2+} states described here bring us information on the internal conformational changes within the troponin molecule upon Ca^{2+} binding and allow us to make a comparison between the tissue-specific isoforms of troponin.

6.2. CRYSTALLIZATION AND STRUCTURE DETERMINATION

Crystallizations of troponin were attempted in Edmonton at the University of Alberta, but the recent crystallization of skeletal muscle troponin was initiated in collaboration with the laboratory of Professor Robert Mendelson at UCSF. Dr. Mendelson and his colleagues studied the organization of troponin complex in the solution using neutron scattering and small angle X-ray diffraction (Stone et al., 1998; King et al., 2005). These careful experiments relied on the quality of the protein sample, its homogeneity and purity. The crystallization project owes its success to the quality of the protein sample preparation and using TnT2 rather than full length TnT which tended to cause aggregation. In 2000 Mendelson realized that the decrease observed in TnT2 associations in solution might aid crystallization.

The following recombinant constructs of chicken fast skeletal muscle troponin were used: the full length TnC (1-162) (the residue Ile130 replaces Thr130), the full length Cys-less TnI (1-182) and the C-terminal fragment of TnT (156-262), so called TnT2. TnC, TnI and TnT2 subunits were expressed and purified using procedures developed in Dr. Mendelson's laboratory (Stone et al., 1998; King et al., 2005). Prior to crystallization the ternary complex was isolated using gel-filtration on Superdex75 column. At this step the protein buffer contained either 1 mM $CaCl_2$ or 2 mM $MgCl_2$ and 1 mM EGTA (see Table 6.1).

The initial crystallization screening of troponin in the presence of Ca^{2+} resulted in crystals that appeared at +4°C as needles when the precipitant solution contained 20% ethanol, 0.1 M Tris, pH 8.5. These crystals were very difficult to work with due to the vola-

Table 6.1. Data collection and refinement statistics

	High Ca^{2+}	Ca^{2+} – free
Crystallization condition	Precipitant: 2.0 M phosphate, 0.2 M NaCl 0.1 M imidazole pH 8.0, 50 mM Anapoe 305 +4°C Protein buffer: 20 mg/ml, Hepes pH 7.5, 200 mM NaCl, 1 mM CaCl2, 1 mM DTT	Precipitant: 1.4 M sodium citrate, 0.1 M Hepes pH 7.5, +20°C Protein buffer: 20 mg/ml, Hepes pH 7.5, 200 mM NaCl, 2 mM MgCl2, 1 mM EGTA, 1 mM DTT
Space group	$P4_32_12$	$P4_32_12$
Unit cell (Å)	a = 138.608, b = 138.608, c = 83.676	a = 134.662, b = 134.662, c = 102.072
Data collection		
Resolution (Å)	3.0	7.0
Unique reflections	16088	1616
Observed reflections	275597	37739
Completeness (%)	95.9	93.9
R sym (%)	5.5	6.7
σ (on highest resolution shell)	2.0 (63.8/32.3)	2.0 (16.3/7.6)
Refinement		
R cryst (%)	**(25–3.0 Å)**	**(25–7.0 Å)**
R free (%)	28.2	35.8
R.m.s. deviation from ideality	33.3	35.9
Bonds (Å)		0.012
Angles (°)	0.011	1.9
Average B-factor	1.4	
($Å^2$)	56	1
Molecules per asymmetric unit	1	

tile properties of ethanol. They diffracted to a resolution of 9 Å which could not be improved by optimization of the crystallization conditions and cryo-protection procedures.

Another condition that yielded crystals of troponin in the presence of Ca^{2+} at +4°C contained 2.0 M phosphate, 0.2 M NaCl, 0.1 M imidazole pH 8.0. Despite their beautiful appearance, the diffraction quality of these crystals was still in the resolution range of 7–9 Å. The optimization of the precipitant composition using a variety of chemical additives provided a significant improvement in the diffraction quality of the crystals when either Anapoe305 or Anapoe405 was added to the original crystallization condition. The optimized crystals were used to collect the complete X-ray diffraction data set at a resolution of 3 Å (Table 6.1).

At the same time we carried out the screening for crystals of troponin in the absence of Ca^{2+}. However, no crystals of Ca^{2+}-free troponin were obtained when using the full length TnI subunit. After we had solved the crystal structure of Ca^{2+}-loaded troponin and compared it with crystal structure of cardiac troponin, we used this information to modify the troponin constructs used for crystallization. Two truncated versions of TnI (residues 1–137 and residues 1–129) (provided by Dr. Carlos Ramos) were tried for the troponin complex assembly and in crystallization. Troponin containing the truncated subunit TnI (residues 1–137) was crystallized at room temperature in the presence of 1.4 M sodium citrate, 0.1 M Hepes, pH 7.5. The crystals diffracted to a resolution of 7 Å and further attempts to improve their diffraction quality or to find another crystallization condition failed. Nevertheless, the complete X-ray diffraction data set was collected and was then successfully used for the troponin Ca^{2+}-free form structure determination.

The structure of troponin in the Ca^{2+}-activated state was determined by molecular replacement using atomic coordinates for the part of human cardiac troponin ternary complex (entry 1J1E). The search model contained TnT2 (residues 202–276 of cardiac troponin sequence) and TnC (residues 98–161 of cardiac troponin sequence). Various combinations of structural elements were tried as a search model and did not produce a molecular replacement solution apart from that one. The refined model of the Ca^{2+}-activated troponin was deposited to the Protein Data Bank with entry code 1YTZ.

For structure determination of the Ca^{2+}-free troponin the atomic coordinates of the Ca^{2+}-activated (Protein Data Bank entry 1YTZ) were used for molecular replacement. The search model was made of TnI and TnT2 subunits. The 7-Å data allowed us to determine the positions of α-helices in the structure of Ca^{2+}-free troponin unambiguously. During this process we were assured of unbiased structure models by careful and repeated study of electron density maps phased using fragments of the troponin model (Vinogradova et al., 2005). The electron density belonging to the most ordered loops was also clearly seen. The refined model of the Ca^{2+}-free troponin has the Protein Data Bank entry 1YV0.

6.3. CRYSTAL STRUCTURES OF TROPONIN

Even a cursory study of the crystal structure of troponin reveals why this protein was so difficult to crystallize. Although the components of the troponin complex that we used in crystallization were known to form a “globular domain” of troponin (Gordon et al., 2000), it hardly resembles a globe; troponin has a very non-compact structure.

In the Ca^{2+}-activated structure the internal symmetry formed by the α-helices of TnI (residues 58–102) and TnT2 (residues 200–245) is broken by the dumbbell shaped TnC whose central helix runs roughly perpendicular to the TnI-TnT2 coiled coil (Figure 6.1). The N-terminal helix of TnI (amino acids 8–48) and the TnI-TnT2 coiled coil hold the C-terminal domain of TnC. Helices B and C of the EF-hands in the regulatory domain of TnC are in the “open” conformation. The switch segment of TnI (amino acids 116–131) is bound to the regulatory domain of TnC between the helices of the opened EF-hands. The inhibitory segment of TnI (amino acids 104–115) is uniquely ordered as a loop that interacts with TnC. The electrostatic interactions with TnC and hydrophobic interactions with TnI stabilize the extended loop conformation of the inhibitory segment visualized in this troponin complex but disordered in cardiac troponin (Takeda et al., 2003) (Figure 6.2).

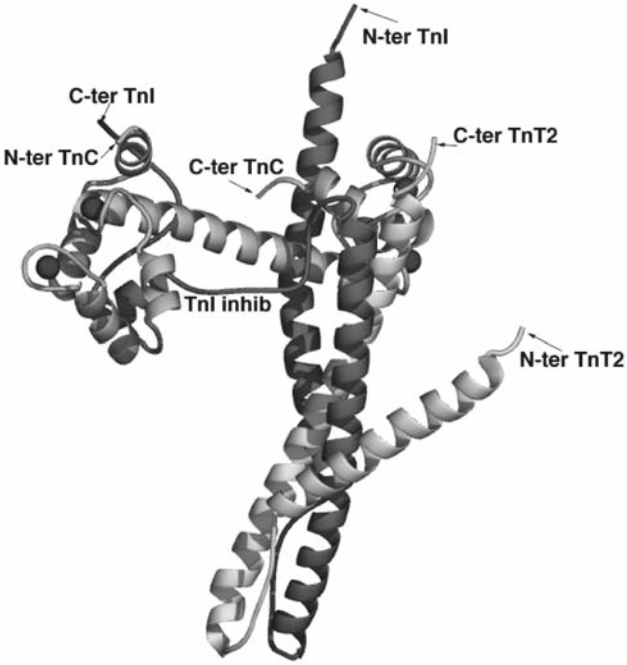

Figure 6.1. Structure of skeletal troponin complex in the Ca^{2+}-activated state. Calcium ions are shown as red spheres.

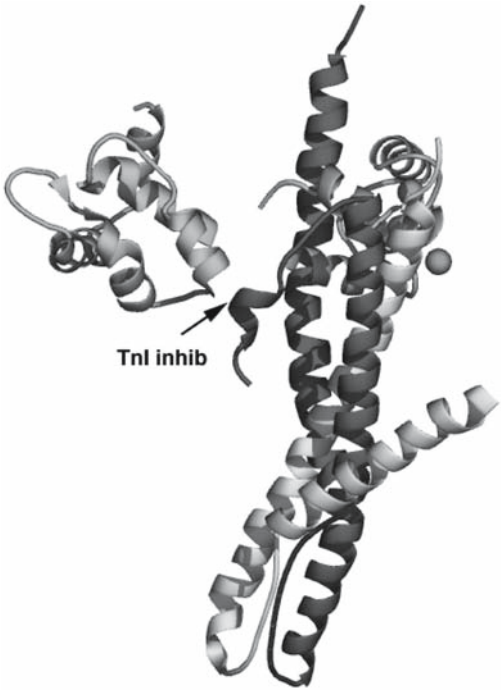

Figure 6.2. Comparison of the structures of chicken skeletal muscle troponin and human cardiac troponin in the Ca^{2+}- saturated state. The overall superposition is done by TnI + C-terminal domain of TnC + TnT2. The structure of cardiac troponin is as PDB entry 1J1E, chains D, E, F. The deviations are indicated with arrows. The conformations and positions of the C-termini of TnI and N-termini of TnT2 are heavily influenced by crystal lattice contacts in both structures.

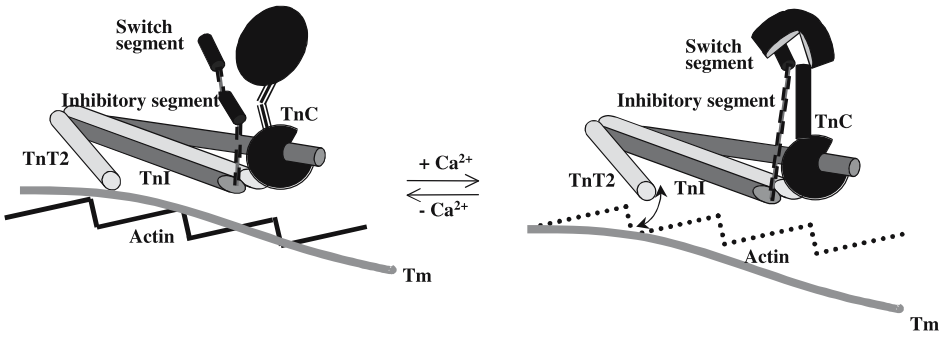

Figure 6.3. Structure of skeletal troponin complex in the Ca^{2+}-free state. Magnesium ions are shown as spheres. TnC central linker is disordered. Orientation of troponin is as in Figure 6.1.

In the Ca^{2+}-free structure of troponin (Figure 6.3) we observe that a loss of the Ca ions has only minor influence on the general architecture of the molecule. Thus, the TnI-TnT2 coiled coil, the N-terminal helices of TnI and of TnT2, and the C-terminal domain of TnC remain unchanged. The predicted conformational changes occur in the N-terminal domain of TnC: upon a loss of Ca ions the helices B and C move towards the helix D to close the previously opened hydrophobic pocket. The switch segment of TnI is no longer observed bound to this pocket. The central helix of TnC is apparently disordered and the N-terminal domain is free to rotate about 35° relative to its orientation in the Ca^{2+}-activated state. The inhibitory segment of TnI is released from the melted central helix of TnC and refolds into a short α-helix. In its new position this short TnI helix is stabilized by electrostatic interactions with the surface residues of the N-terminal domain of TnC among which the ionic bond between residues Arg108 of TnI and Glu56 of TnC appears to be the strongest. The loop preceding the inhibitory segment helix of TnI and a part of TnI from the TnI-TnT2 coiled coil form a "tip" which is highly ordered due to the hydrophobic interactions within it.

The effects of crystal packing may be great for non-globular proteins, especially ones that form an assembly that undergoes changes in conformation. Here, the crystal contacts permitting the formation of the crystal lattice of both Ca^{2+}-free and Ca^{2+}-activated troponins are very similar. The conformational change induced by Ca^{2+} causes the unit cell to swell while keeping the crystal contacts the same. There are no intermolecular crystal contacts in the region of the inhibitory segment of TnI and the TnC central linker. Hence these described conformations of the mutually stabilized structural elements are likely to be found *in vivo.*

6.4. MECHANISM OF TROPONIN REGULATION

Comparing the troponin structures shows an order-disorder transition around the central helix of TnC. Based on the analysis of the crystal structures we propose a basic structural mechanism of troponin regulation of muscle contraction. During muscle activation, we speculate that opening the N-terminal domain of TnC and repositioning of the TnI switch segment restores the helical conformation of the central helix of TnC and tugs

the TnI inhibitory segment from actin by dragging and stretching it along the central helix. In the presence of Ca^{2+} the TnI inhibitory segment loop and this helix are mutually stabilized. Upon closing of the pocket in the Ca^{2+}-free state of troponin in relaxed muscle, the switch segment is expelled and the TnC central linker loses its helical conformation. With a loss of stabilization by the TnC central helix, the TnI inhibitory segment is released and assumes a metastable α-helical conformation. In this alternate position, the inhibitory segment is supported by electrostatic interactions with surface residues of the TnC regulatory domain. Freed from TnC, the inhibitory segment forms its interaction with actin (Figure 6.4).

The surprising and satisfying observations made from these structures suggest that conformational change in troponin induced by Ca^{2+} does not involve the movements of the structural elements other than the C-terminal part of TnI including just the inhibitory and switch segments and N-terminal domain of TnC together with its central helix. The position of the TnI-TnT2 coiled coil and of the N-terminal helices of TnI and TnT2 are not affected by Ca^{2+}. Though the central helix of TnC melts upon the loss of Ca^{2+}, TnC retains its extended shape and its N-terminal domain occupies virtually the same location. The N-terminus of the TnI switch moves slightly. The observed shift agrees with a previously measured ~8 Å movement of the switch peptide away from TnC towards actin (Li et al., 2001). This observation and biochemical data of others (Kobayashi et al., 2000; Luo et al., 2000; Kobayashi et al., 2001; Kimura et al., 2002; Ferguson et al., 2003) suggest

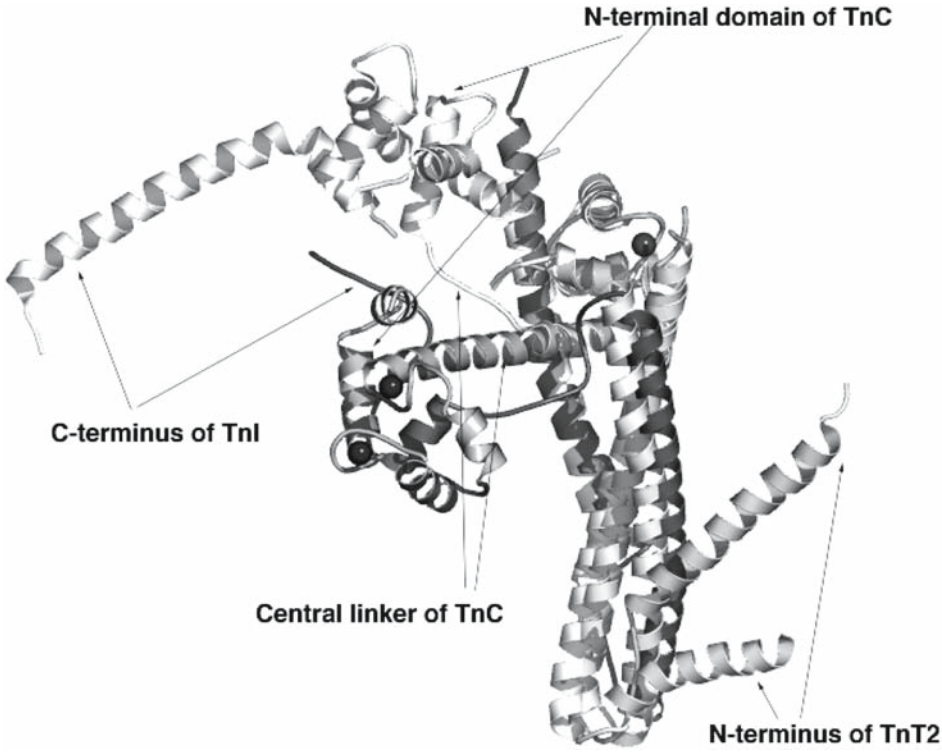

Figure 6.4. Cartoon representation of the conformational changes occurring in troponin during muscle contraction.

that the orientation of troponin on the thin filament does not change significantly by Ca^{2+} binding. This hypothesis was tested in 3D reconstructions of electron microscopy images of the activated and relaxed thin filaments by Prof. W. Lehman (unpublished data) and is sound.

The steric blocking mechanism (Potter and Gergely, 1974; Lehman et al., 1995; Lehman et al., 2001) further proposes that removal of the TnI inhibitory segment from actin affects the position of the bound tropomyosin that becomes less restrained and able to move on the actin surface. According to this model, troponin does not displace tropomyosin directly but rather the binding/dissociation of the TnI inhibitory peptide to/from actin modifies the actin surface and either creates or alters the tropomyosin binding site. Verification of this model requires a number of biological tests. The crystallization of the whole thin filament or higher resolution electron microscopy images will certainly address the proposed issues in the future.

6.5. STRUCTURAL DIFFERENCES BETWEEN SKELETAL AND CARDIAC ISOFORMS OF TROPONIN

Would troponins from cardiac and skeletal muscle act using the same mechanism? Although there are some differences in the Ca^{2+}-binding properties between two isoforms, it is likely that the mechanism of their function will be similar.

Comparison of the structures of cardiac (Takeda et al., 2003) and skeletal muscle troponins in the Ca^{2+}-bound states shows that both complexes share the organization of the subunits (Figure 6.2). Apart the expected differences (Gordon et al., 2000) inside the TnC Ca^{2+} regulatory domains, the location of these domains is different. Comparing the relative positions shows them 25 Å away from each other. The TnC Ca^{2+} regulatory domain is positioned in space by the central helix of TnC which is rigid in skeletal TnC while it is melted in cardiac TnC. Again we must consider whether, these differences are caused by crystal packing interactions. The crystal packing of skeletal troponin is less tight than in cardiac troponin (the solvent content is 66% vs 52% of in the skeletal and cardiac troponin crystals, respectively) and there are no crystal lattice interactions in the region of the TnC central helix. Likely resulting from the ordered central helix, the TnI inhibitory region is very well ordered in skeletal troponin while it is flexible and not visible in the cardiac troponin crystal structure.

Perhaps these changes in the central helix and configuration of the metal binding domains relate to function. The importance of the central linker for functionality of troponin was demonstrated repeatedly (Sheng et al., 1991; Ramakrishnan and Hitchcock-DeGregori, 1995; Ngai and Hodges, 2001). In solution, the flexibility of the central linker in cardiac troponin was reported to be higher than in skeletal troponin though the interactions of the cardiac specific N-terminal extension of TnI with N-terminal domain of TnC were shown to decrease it (Gaponenko et al., 1999; Abbott et al., 2000). Perhaps, the central helix of cardiac troponin is weaker than in skeletal troponin under the crystallization conditions. We speculate that in solution or *in vivo*, interactions with the missing cardiac specific N-terminal extension of TnI, and with inhibitory segment of TnI could assist stabilization of the central helix in cardiac troponin. Consistent with this idea, the extended conformation of TnC was observed *in situ* when using the small angle X-ray diffraction of the cardiac thin filaments (Matsumoto et al., 2004).

Thus, we conclude that the TnC central helix plays an important role in the mechanism of troponin regulation providing capturing of the TnI inhibitory segment in the presence of Ca^{2+}. However, we speculate that maintaining the central helix in cardiac troponin may require additional stabilization from the cardiac specific elements.

6.6. BINDING OF ANAPOE TO THE CA^{2+}-ACTIVATED TROPONIN

Opening of the EF-hands in the N-terminal domain of TnC induced by Ca^{2+} forms the hydrophobic pocket on the surface. The crystal structure of cardiac Ca^{2+}-bound TnC and the NMR structure of the cardiac Ca^{2+}-bound TnC in a complex with TnI switch peptide show that bepridil, a drug, can bind into this pocket (Wang et al., 2002). Likewise, Anapoe, a detergent agent used to optimize crystal quality for X-ray diffraction, binds to the pocket of Ca^{2+} – loaded skeletal troponin (Figure 6.5).

Binding of Anapoe is specific, supported by the numerous hydrophobic interactions with the side chains of both TnC and TnI. Physiological tests show that Anapoe has a noticeable positive effect on the Ca^{2+}-sensitivity of muscle contractions (Vinogradova et al., 2005) proving that its binding takes place in a potentially important site for modulation of the troponin activity.

Analysis of the pocket using the program LIGSITE (provided by Dr. G.Klebe from Philipps-University at Marburg, Germany) shows that the pocket is unique and highly

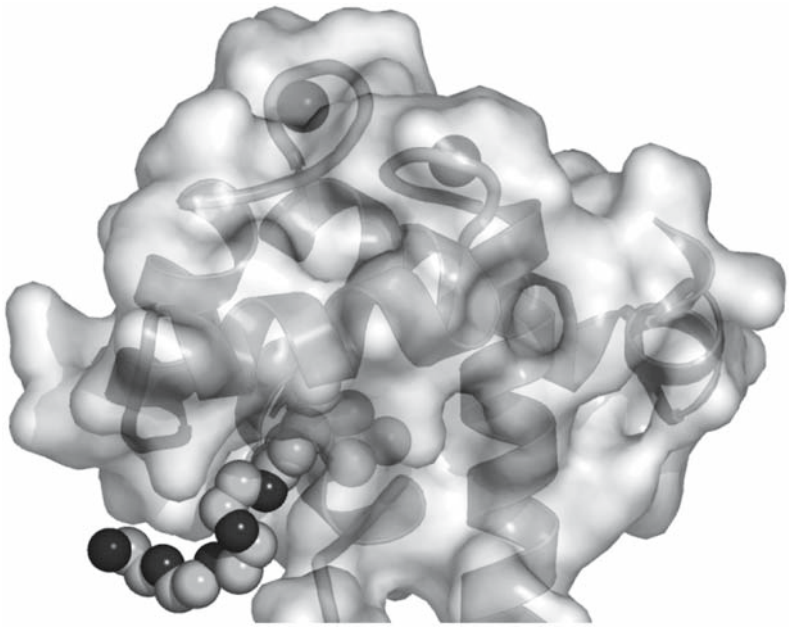

Figure 6.5. Binding of Anapoe to the N-terminal domain of TnC. The N-terminal domain of TnC with the bound TnI switch is shown as surface. A ribbon structure underneath the surface is for TnC and TnI. Ca ions are spheres. Anapoe is shown as space filled model.

hydrophobic, with a Met-rich environment. Apparently, the TnI switch cannot fulfil it completely. Part of the pocket remains exposed to the solvent even after the TnI switch binding.

Is there a natural ligand for troponin that acts as Anapoe or bepridil? This, as many other questions about the protein discovered by Professor S. Ebashi, is still to be answered in the future.

6.7. REFERENCES

Abbott, M. B., Gaponenko, V., Abusamhadneh, E., Finley, N., Li, G., Dvoretsky, A., Rance, M., Solaro, R. J., and Rosevear, P. R., 2000, Regulatory domain conformational exchange and linker region flexibility in cardiac troponin C bound to cardiac troponin I, *J. Biol. Chem.* **275**:20610–7.

Ebashi, S., 1960, Calcium binding and relaxation in the actomyosin system, *J. Biochem.* **48**:150–9.

Ebashi, S., 1963, Third component participating in the precipitation of "natural actomyosin", *Nature* **200**:1010–15.

Ebashi, S., Ebashi, F., and Kodama, A., 1967, Troponin as the Ca^{2+}-receptive protein in the contractile system, *J. Biochem.* **62**:137–8.

Ferguson, R. E., Sun, Y. B., Mercier, P., Brack, A. S., Sykes, B. D., Corrie, J. E., Trentham D. R., and Irving, M., 2003, In situ orientations of protein domains: troponin C in skeletal muscle fibers, *Mol. Cell* **11**:865–74.

Gaponenko, V., Abusamhadneh, E., Abbott, M. B., Finley, N., Gasmi-Seabrook, G., Solaro, R. J., Rance, M., and Rosevear, P. R., 1999, Effects of troponin I phosphorylation on conformational exchange in the regulatory domain of cardiac troponin C, *J. Biol. Chem.* **274**:16681–4.

Gordon, A. M., Homsher, E., and Regnier, M., 2000, Regulation of contraction in striated muscle, *Physiol. Rev.* **80**:853–924.

Greaser, M. L., and Gergely, J., 1971, Reconstitution of troponin activity from three protein components, *J. Biol. Chem.* **246**:4226–33.

Herzberg, O., and James, M. N., 1988, Refined crystal structure of troponin C from turkey skeletal muscle at 2.0 A resolution, *J. Mol. Biol.* **203**:761–79.

Houdusse, A., Love, M. L., Dominguez, R., Grabarek, Z., and Cohen. C., 1997, Structures of four Ca^{2+}-bound troponin C at 2.0 A resolution: further insights into the Ca^{2+}-switch in the calmodulin superfamily, *Structure* **5**:1695–711.

Huxley, H. E., 2004, Fifty years of muscle and the sliding filament hypothesis, *Eur. J. Biochem.* **271**:1403–15.

Kimura, C., Maeda, K., Maeda, Y., and Miki, M., 2002, Ca(2+)- and S1-induced movement of troponin T on reconstituted skeletal muscle thin filaments observed by fluorescence energy transfer spectroscopy, *J. Biochem. (Tokyo)* **132**:93–102.

King, W. A., Stone, D. B., Timmins, P. A., Narayanan, T., von Brasch, A. A., Mendelson, R. A., and Curmi. P. M., 2005, Solution structure of the chicken skeletal muscle troponin complex via small-angle neutron and X-ray scattering, *J. Mol. Biol.* **345**:797–815.

Kobayashi, T., Kobayashi, M., and Collins, J. H., 2001, Ca(2+)-dependent, myosin subfragment 1-induced proximity changes between actin and the inhibitory region of troponin I, *Biochim. Biophys. Acta* **1549**:148–54.

Kobayashi, T., Kobayashi, M., Gryczynski, Z., Lakowicz, J. R., and Collins, J. H., 2000, Inhibitory region of troponin I: Ca(2+)-dependent structural and environmental changes in the troponin-tropomyosin complex and in reconstituted thin filaments, *Biochemistry* **39**:86–91.

Lehman, W., Rosol, M., Tobacman, L. S., and Craig, R., 2001, Troponin organization on relaxed and activated thin filaments revealed by electron microscopy and three-dimensional reconstruction, *J. Mol. Biol.* **307**:739–44.

Lehman, W., Vibert, P., Uman, P., and Craig, R., 1995, Steric-blocking by tropomyosin visualized in relaxed vertebrate muscle thin filaments, *J. Mol. Biol.* **251**:191–6.

Li, Z., Gergely, J., and Tao, T., 2001, Proximity relationships between residue 117 of rabbit skeletal troponin-I and residues in troponin-C and actin, *Biophys. J.* **81**:321–33.

Luo, Y., Wu, J. L., Li, B., Langsetmo, K., Gergely, J., and Tao, T., 2000, Photocrosslinking of benzophenone-labeled single cysteine troponin I mutants to other thin filament proteins, *J. Mol. Biol.* **296**:899–910.

McKillop, D. F., and Geeves, M. A., 1993, Regulation of the interaction between actin and myosin subfragment 1: evidence for three states of the thin filament, *Biophys. J.* **65**:693–701.

Matsumoto, F., Makino, K., Maeda, K., Patzelt, H., Maeda, Y., and Fujiwara, S., 2004, Conformational changes of troponin C within the thin filaments detected by neutron scattering, *J. Mol. Biol.* **342**:1209–21.

Maytum, R., Westerdorf, B., Jaquet, K., and Geeves, M. A., 2003, Differential regulation of the actomyosin interaction by skeletal and cardiac troponin isoforms, *J. Biol. Chem.* **278**:6696–701.

Ngai, S. M., and Hodges, R. S., 2001, Structural and functional studies on Troponin I and Troponin C interactions, *J. Cell. Biochem*. **83**:33–46.

Pearlstone, J. R., Sykes, B. D., and Smillie, L. B., 1997, Interactions of structural C and regulatory N domains of troponin C with repeated sequence motifs in troponin I, *Biochemistry* **36**:7601–6.

Perry, S. V., 1998, Troponin T: genetics, properties and function, *J. Muscle Res. Cell Motil*. **19**:575–602.

Perry, S. V., 1999, Troponin I: inhibitor or facilitator, *Mol. Cell. Biochem*. **190**:9–32.

Potter, J. D., and Gergely, J., 1974, Troponin, tropomyosin, and actin interactions in the Ca^{2+} regulation of muscle contraction, *Biochemistry* **13**:2697–703.

Ramakrishnan, S., and Hitchcock-DeGregori, S. E., 1995, Investigation of the structural requirements of the troponin C central helix for function, *Biochemistry* **34**:16789–96.

Satyshur, K. A., Rao, S. T., Pyzalska, D., Drendel, W., Greaser, M., and Sundaralingam, M., 1988, Refined structure of chicken skeletal muscle troponin C in the two-calcium state at 2-A resolution, *J. Biol. Chem.* **263**:1628–47.

Sheng, Z. L., Francois, J. M., Hitchcock-DeGregori, S. E., and Potter, J. D., 1991, Effects of mutations in the central helix of troponin C on its biological activity, *J. Biol. Chem.* **266**:5711–5.

Slupsky, C. M., and Sykes, B. D., 1995, NMR solution structure of calcium-saturated skeletal muscle troponin C, *Biochemistry* **34**:15953–603.

Stone, D. B., Timmins, P. A., Schneider, D. K., Krylova, I., Ramos, C. H., Reinach, F. C., and Mendelson, R. A., 1998, The effect of regulatory Ca^{2+} on the in situ structures of troponin I and troponin C: a neutron scattering study, *J. Mol. Biol.* **281**:689–704.

Takeda, S., Yamashita, A., Maeda, K., and Maeda, Y., 2003, Structure of the core domain of human cardiac troponin in the Ca(2+)-saturated form, *Nature* **424**:35–41.

Van Eyk, J. E., Thomas, L. T., Tripet, B., Wiesner, R. J., Pearlstone, J. R., Farah, C. S., Reinach, F. C., and Hodges, R. S., 1997, Distinct regions of troponin I regulate Ca^{2+}-dependent activation and Ca^{2+} sensitivity of the acto-S1-TM ATPase activity of the thin filament, *J. Biol. Chem.* **272**:10529–37.

Vinogradova, M. V., Stone, D. B., Malanina, G. G., Karatzaferi, C., Cooke, R., Mendelson, R. A., and Fletterick, R. J., 2005, Ca(2+)-regulated structural changes in troponin, *Proc. Natl. Acad. Sci. USA* **102**:5038–43.

Wang, X., Li, M. X., and Sykes, B. D., 2002, Structure of the regulatory N-domain of human cardiac troponin C in complex with human cardiac troponin I147-163 and bepridil, *J. Biol. Chem.* **277**:31124–33.

Xu, C., Craig, R., Tobacman, L., Horowitz, R., and Lehman, W., 1999, Tropomyosin positions in regulated thin filaments revealed by cryoelectron microscopy, *Biophys. J.* **77**:985–92.

7

DISPOSITION AND DYNAMICS: INTERDOMAIN ORIENTATIONS IN TROPONIN

Ryan M.B. Hoffman and Brian D. Sykes

7.1. A PARADIGMATIC PROTEIN

When Galvani discovered the electrical regulation of muscle contraction science began an inexorable transformation. Observation of an inorganic trigger for a physiological event presaged the end of vitalism, the beginning of electrochemistry, and over 400 years of research into the first demonstrable biochemical machine: striated muscle. This molecular machine has been studied in various contexts, ranging from holistic (live muscle) to reductionist (purified molecules). Generations of scientists have, collectively, disassembled and reassembled the contractile apparatus of striated muscle, demonstrating an increasingly complete understanding of its function. In the process, high resolution structures[a] have been determined for most components of this machine. Given the relative orientation of these proteins in a muscle fiber, visualization of muscle contraction at the atomic level seems attainable. This effort is complicated by the inherent properties of proteins, specifically, proteins with conformationally heterogeneous native ensembles.

Ebashi discovered the tripartite molecular switch known as troponin (Tn),[1] which converts a sarcomeric [Ca^{2+}] fluctuation into physical motion. Tn is composed of troponin C (TnC): the calcium sensor, troponin I (TnI): the inhibitory protein, and troponin T (TnT), which couples Tn to tropomyosin.[b] First, the structure and function of TnC is discussed. Interactions between TnC and TnI are then discussed, culminating with a review of the most complete experimentally derived models of the Tn complex. We emphasize the role of conformational heterogeneity (disorder) in the determination and interpretation of domain-domain orientations in Tn.

Department of Biochemistry, University of Alberta, Edmonton, Alberta, Canada

[a] Here "structure" or "structural" refers to models of protein tertiary or quaternary structure. "Resolution" originates in the context of scattering methods (optics and diffraction), but is also used to refer to the "spatial precision of coordinates" in the context of structural models.

[b] Each protein can be characterized or referred to as separated N- or C-terminal domains, and as cardiac or (fast) skeletal paralogs. For example, "cCTnC" refers to the C-domain of cardiac troponin C. NTnC refers to the N-domain of TnC in both cardiac and skeletal systems.

Regulatory Mechanisms of Striated Muscle Contraction
Edited by Ebashi and Ohtsuki, Springer, 2007

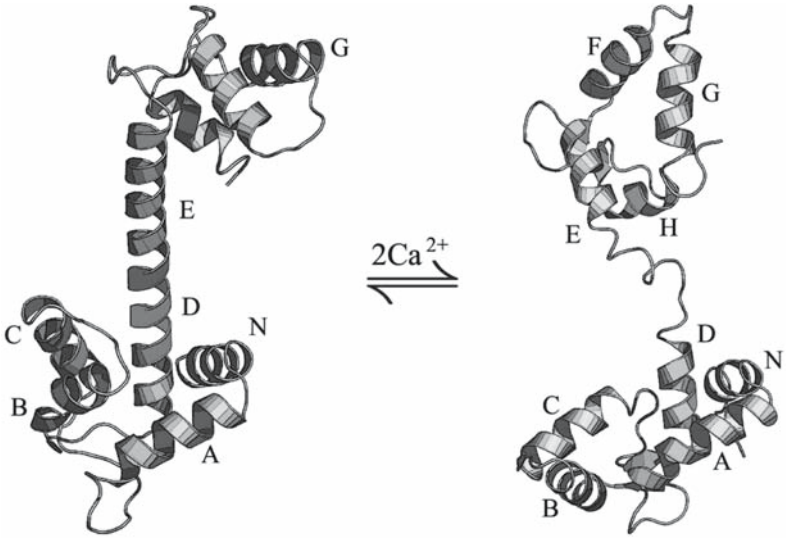

Figure 7.1. Initial regulatory changes in Tn: the crystal structure of turkey sTnC (PDB 5TNC[5]) has two Ca^{2+} occupying the C-terminal domain (ions not depicted). Binding of Ca^{2+} to the sNTnC stabilizes the open conformation, where the B and C helices have extended away from the N, A, and D helices (PDB 1TNW[6]). The disappearance of the DE linker is likely methodological in origin rather than consequential to Ca^{2+} activation. TnC seems to be predominantly extended when in the absence of other proteins, but on average, not as extended as would be expected from a completely α helical DE linker.

7.2. MODELS OF Ca^{2+}-ACTIVATION

7.2.1. The Ca^{2+} Sensor: TnC

TnC has two globular domains (designated N- and C-terminal) separated by a linker with 4 Ca^{2+} binding sites. Early efforts to characterize the biochemical significance of Ca^{2+} binding to sTnC implied sites 1 and 2 to be the actual regulatory sites, while sites 3 and 4 were "structural" or continuously metal-bound over a contractile cycle.[2] Initial crystallographic studies of TnC focused on avian skeletal isoforms.[3,4] TnC·2Ca^{2+} presented an elongated structure, with the globular N- and C-terminal domains being separated by an α helix (Figure 7.1, left[c]). The high affinity metal-binding sites (in CTnC) were occupied with ligands, whereas the regulatory sites (in NTnC) were unoccupied. These structures were interpreted as reflecting the contraction-inhibiting state.

Predictions of the structural impact of calcium binding to sites 1 and 2 were made. It was proposed that the structure of the calcium-activated N-terminal domain is similar in tertiary structure to the C-terminal domain.[7] A modeling study concluded that sNTnC·0Ca^{2+} can be continuously deformed into a Ca^{2+}-activated conformation without crossing physiologically inaccessible energetic barriers.[7] Experimental verification of the modeled Ca^{2+}-activated structure was accomplished in 1995 through high field NMR

[c] All Tn structures shown place NTnC in a similar orientation.

studies.[5] The solution structure of intact sTnC was also described that year[6] (Figure 7.1, right). This latter study determined the tertiary structure of the N- and C-terminal domains to high precision. The linker "helix" was unstructured due to an absence of NOE-derived distance restraints. This (negative) observation provided an experimentally-derived visualization of TnC consistent with ^{15}N T2 data demonstrating the extensive local dynamics in this region of TnC[8] and calmodulin (CaM).[9] The conclusions of earlier hydrodynamic[10,11] and computational[12] studies were reconciled with high resolution structural data. Studies of sTnC gave precise descriptions of Ca^{2+}-activation and qualitative insights into structural dynamics.

All of this motivated a detailed mechanistic hypothesis. Gagné et al proposed a mutational analysis into sTnC's mechanism.[13] Previous work had identified a conserved Glu residue (E41) at the second helix of the Ca^{2+}-binding site 1.[14] This residue coordinates Ca^{2+} through both of its acidic oxygens. In the apo (Ca^{2+}-free) state, E41 seems to form a salt bridge with K40. The salt bridge exists at the expense of strain introduced into the B helix. The relief of this strain, in the Ca^{2+}-activated state, stabilizes the sTnC's open conformation. This interpretation was supported by the NMR structure of sNTnC E41A, which binds Ca^{2+} but does not expose its hydrophobic pocket as a result.[13] The authors proposed that sNTnC E41A may be a suitable model for cNTnC in which site 1 is defunct.

7.2.2. The Case of cTnC

The successful experimental characterization of sTnC prompted a parallel characterization of the cardiac (and slow skeletal) isoform (cTnC). This protein was known to bind Ca^{2+} with a stoichiometry of 3 because of sequence divergence (an insertion, and substitutions) in site 1. The C-domain of cTnC binds Ca^{2+} with similar affinity to sTnC, but the affinity of site 2 differs. It was expected that compensatory sequence divergences in cNTnC would allow for relative stabilization of the open conformation, so that Ca^{2+}-binding to site 2 would promote this conformation, reconciling the cardiac Ca^{2+}-activation mechanism with the skeletal system.

Chicken cTnC was first solved in the activated ($3Ca^{2+}$-ligated) state[15] (Figure 7.2, center). Ca^{2+}-activated cNTnC, however, was found to be in a nearly closed conformation, almost identical to the conformation of cNTnC·$0Ca^{2+}$ (Figure 7.2, left). In the presence of switch peptide $cTnI_{147–163}$, cNTnC·$1Ca^{2+}$ assumes the open conformation (Figure 7.2, right). The results seemed to correlate the extent of Ca^{2+}-induced "opening" with the number of Ca^{2+} ions ligated in NTnC, but the characterization of sNTnC E41A suggest this is due to the stabilization of the open conformation due to the mechanical contributions from site 1. As discussed above, the closed-to-open conformational change does not appear to have a particularly large activation energy. The differences between sTnC and cTnC activation is probably not due to an additional driving force provided by the spontaneity of Ca^{2+} binding to site 1 of sTnC.

Knowledge of the native-state conformational exchange of the Ca^{2+}-activated N-domain prompted a hypothesis relating the structural thermodynamics between the N-domains of the skeletal and cardiac systems.[16] The explanation, still favored to date, is that the Ca^{2+}-activated cardiac isoform samples an open conformation with sufficient frequency to bind TnI, removing the inhibition of actomyosin ATPase. The interactions between TnC and TnI are now further discussed.

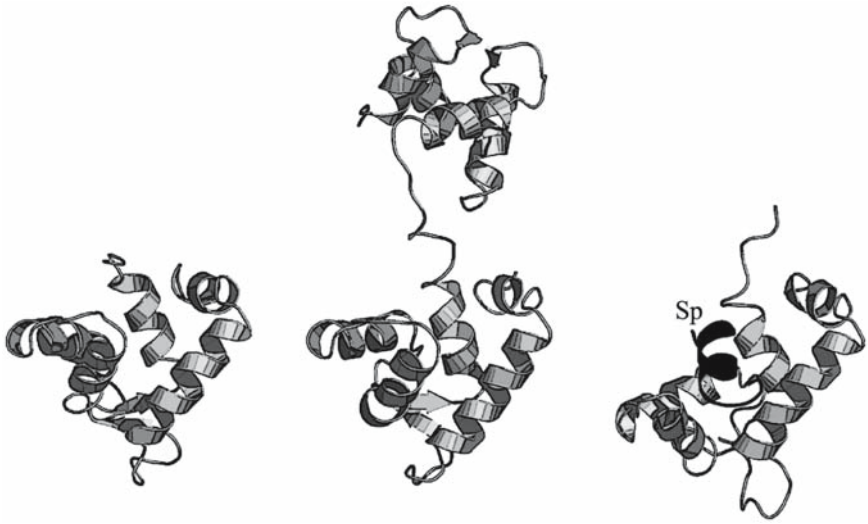

Figure 7.2. The structure of Ca^{2+}-saturated chicken cTnC (center, PDB 1AJ4) had a closed N-domain.[15] NMR structures of human cNTnC·0Ca^{2+} (left, 1SPY) and cNTnC·3Ca^{2+}·Sp (right, 1MXL) confirmed that cTnC undergoes Ca^{2+}- and Sp- dependent opening.

7.3. TOWARDS THE TN COMPLEX

7.3.1. The Inhibitory Protein: TnI

Tn acts as a mechanical switch in striated muscle contraction. Initial conformational changes produced in TnC are communicated to TnI, so-called due to its inhibitory properties. It binds a stretch of actin-tropomyosin, promoting the movement of tropomyosin, thereby obstructing the binding site for myosin on actin. The actual mode of coupling between troponin and actin-tropomyosin is further discussed below. The cardiac isoform of TnI (cTnI) has an N-terminal extension amounting to ~30 more residues than the skeletal isoform (sTnI). This region includes phosphorylation sites and interacts with the C-domain of TnC. Functional regions common to both isoforms span 6 helices that are C-terminal to cNTnI.[17] The stretch of TnI that disallows myosin-binding to actin ($cTnI_{128–147}$ or $sTnI_{96–115}$) is called "Ip." Ip is sandwiched between other functional regions of TnI. The switch region ($cTnI_{147–163}$ or $sTnI_{115–131}$) selectively binds to NTnC in the presence of Ca^{2+}. The switch region is abbreviated "Sp." Further C-terminal to Sp is a recently reported actin bindin domain ($sTnI_{131–182}$).[17,18]

7.3.2. The Ca^{2+}-activated cTn Core Complex

Tn and its constituent proteins are generally resilient to crystallization and therefore to characterization with crystal diffraction methods. Persistence does pay, however. Recent crystallographic studies have provided structures of large portions of the troponin complex, in both skeletal and cardiac systems. The cTn core complex structure, in the

calcium activated state (Figure 7.3) was presented by Maeda and coworkers.[19] This X-ray study afforded two models, each derived from distinct crystal forms, and refined to 2.6 and 3.3 Å resolution. Each model had two cTn molecules in the asymmetric unit, so the study determined the structures of four molecules of Tn. The two complexes crystallized lacked the N-terminal domain of $cTnT_{1–182}$, and varied in the length of the TnI component crystallized. One crystal contained $cTnI_{31–163}$, the other contained $cTnI_{31–210}$.

cTnI and cTnT are visualized as two pairs of alpha-helical chopsticks grasping TnC by its C-domain (see Figure 7.3). The two chopsticks interdigitate in a coiled-coil fold, forming the "IT arm." The C-terminus of cTnI, containing Sp and Ip, extends off of one chopstick, and interacts with cNTnC. The core Tn molecule shows two major subdomains, with the regulatory "head" containing cNTnC and cCTnI, and the IT arm containing cCTnC, cNTnI, and cTnT. The structures intimate a cascade of protein-protein interactions upon Ca^{2+} activation of cTnC, with the IT arm's orientation/stability being potentially modulated by cTnC activation (Figure 7.3).

These structures visualize many protein-protein interactions previously predicted by structural studies on smaller fragments of the Tn complex.[20] Prior results anticipated the coiled-coil interactions stabilizing the IT arm,[21] and the various contacts between TnI and TnC. The crystal structure, however, showed a novel orientation of cNTnC with respect to the remainder of the IT arm (see Figure 7.3). Takeda et al propose that the release of Ip from actin is accompanied by the movement of large portions of the TnI

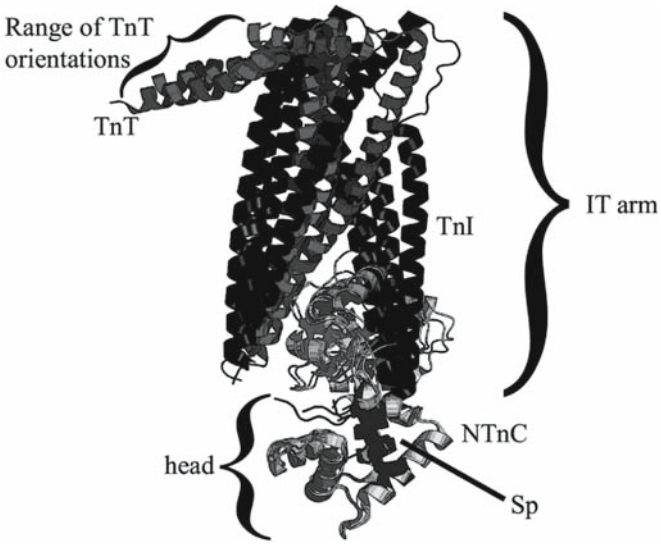

Figure 7.3. The cTn core complex structures presented by Takeda et al.[19] All Tn molecules reported are shown, superimposed on cNTnC. cTnC is depicted in light grey, cTnT in dark grey, and cTnI in black. The four replica Tn molecules show high internal consistency with respect to the cNTnC portion, however, the IT arm (all of cTnT and most of cTnI visualized here) assumes multiple orientations with respect to cNTnC. The DE linker is not visualized in the crystal structure. Most features of the quaternary structure, especially the contacts between cTnI (Sp, Rp, and Ip) and TnC, are as predicted from studies of smaller fragments of cTn.[20]

C-terminus.[19] The regions of Tn crystallized in this study, but rendered invisible due to disorder, are discussed further below.

7.3.3. Crystal Structures of Inhibited and Activated sTn Core Complex

Fletterick and coworkers recently reported the sTn core complex structure, in both Ca^{2+}-activated (resolved to 3 Å, Figure 7.4) and inactivated (7 Å, bottom of Figure 7.6) states.[22] As in the study by Takeda et al,[19] all of sTnC, most of sTnI ($sTnI_{1–182}$) [for Ca^{2+}-activated state] or $sTnI_{1–137}$ [for inactive state]), and sTnT2 ($sTnT_{156–262}$) were crystallized. Consistent with previous data, sTnI and sTnT form a pair of chopsticks grasping sCTnC, with the regulatory portion of TnI extending off the end of the C-terminal chopstick.

With cardiac and skeletal Tn core complex structures in hand, Vinogradova et al set out to draw comparisons between the two systems.[22] Attention is drawn to the central helix of TnC, which is intact and covisualized with Ip in the skeletal core complex, but not in the cardiac complex. The hydrophobic pocket of sNTnC is more open than cNTnC in the cTn structure by Takeda et al, confirming that Ca^{2+}-activated cNTnC does not expose as much hydrophobic surface as the skeletal isoform (even when bound to cSp). The authors propose that the substitution at position 84 of TnC (Q84 in sTnC, C84 in cTnC) helps to stabilize the relatively closed cNTnC·Ca^{2+}. Crystal structures of the core Tn complex thus corroborate the extensive protein-protein interactions predicted from high resolution studies of smaller portions of the troponin complex.[20] Still, portions of troponin evade visualization.

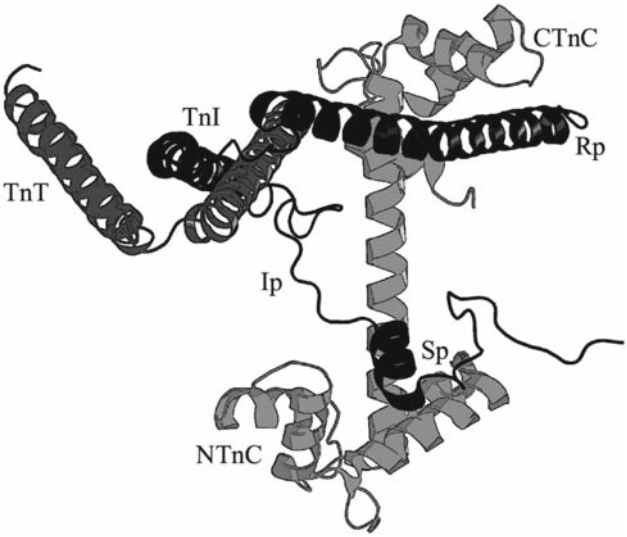

Figure 7.4. Structure of Ca^{2+}-activated sTn core complex (PDB 1YTZ). Most protein-protein interactions are similar to those observed in the cardiac system, but the DE linker is visualized as an α helix bound to the Ip region. This image shows sNTnC in a similar orientation to cNTnC (Figure 7.3), illustrating a highly dissimilar relative orientation of the head group with respect to the IT arm.

7.4. DISPOSITION AND DYNAMICS

7.4.1. Crystallographic Consensus

Structures of Tn do not have uniform resolution across the primary sequence. There is no widely accepted theory accounting for the regions of low precision. This is because the relationship between protein structural dynamics and resolution is complicated by methodological variables. NMR spectra can be compromised by spectral overlap, for example, which can reduce the number of distance restraints in an NMR structure. The crystallographic B factor is widely known to account for the combined effects of structural dynamics and imperfections in the crystal lattice. It is therefore quite difficult to interpret the disordered regions of a typical protein structure in terms of conformational dynamics, in the absence of additional data.

How can conformationally heterogeneous proteins crystallize given that alternate conformers lack chemical equivalence? We expect that crystal growth imposes selection from the native ensemble. Therefore, the actual proportion of the native-state ensemble represented by a crystal structure is unknown. For well structured proteins, the crystal structure is typically the most probable solution state conformation. For poorly structured proteins, this is not necessarily the case. Tn is intermediate between these extremes, having a high conformational homogeneity in many regions. These regions include the regulatory head and IT arm, when considered separately. These two lobes are coupled by the DE linker and by TnI.

Takeda et al interpret the four Tn molecules from two distinct crystal forms as reflecting the flexibility of the DE linker. When the four troponin core molecules are superimposed upon the cNTnC, the end of the IT arm sweeps out a distance of ~27 Å. This shows the N-domain sampling many orientations with respect to the IT arm. The authors assert the DE linker to be poorly structured "owing to the lack of specific interactions with the rest of the molecule"[19] which makes sense in the context of the local density model for B factors.[23] They cite the conclusions of mutational studies which suggest that deletions to the DE linker are not as deleterious to Tn function as substitutions that rigidify the structure. This interpretation alludes to the findings of Maeda and coworkers in a smaller cTnC·cTnI crystal structure.[24] As the DE linker and Ip regions were crystallized, but not visualized, the DE linker·Ip region likely has multiple conformations with respect to the bulk of the complex. It is possible that the DE linker·Ip region is stabilized by similar interaction in both sTn and cTn, but that this portion of the crystal ensemble is converged in the sTn structure[22] but not in the cTn structure.[19]

7.4.2. Disorder and Mechanism

Should the DE linker exhibit substantial structure in solution, its α helical conformation would ensure a fixed relative orientation between cNTnC and cCTnC, which would seem mechanistically significant given the quaternary structure of Tn. For example, sTnC's interdomain disposition in the sTn complex$_{22}$, is accurately predicted from the original crystal structure of sTnC·2Ca^{2+} (compare Figures 7.1 and 7.4). This is a consequence of canonical α helicity in the DE linker, in both of these structures. It is parsimonious to consider the intact α helix observed in the Ca^{2+}-activated sTn core complex,[22] and

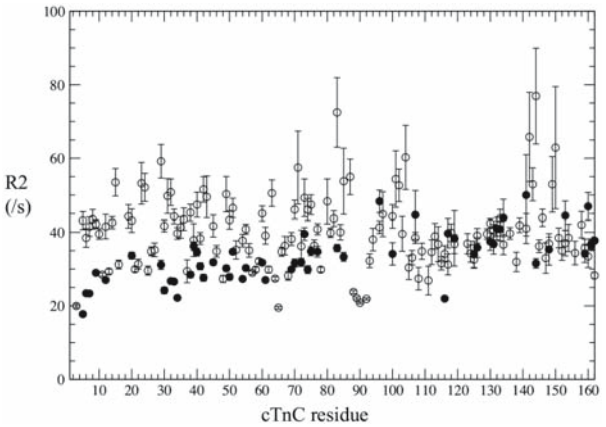

Figure 7.5. Backbone amide ^{15}N transverse relaxation rates (R2) as a function of sTnC residue. This plot is derived from a recent NMR study[27] of {^{2}H, ^{15}N}-labeled sTnC in uniformly ^{2}H-labeled sTn. The N-domain (residues 1–92) has smaller R2s than the remainder of the molecule in the sTnC·2Ca^{2+} state (filled circles) and sTnC·4Ca^{2+} states (open circles). This shows that sNTnC's rotational diffusion is weakly coupled to the bulk of the sTn molecule in the inactive state.

other crystal structures,[3,4] to be a substantially populated microstate in the native ensemble. However, evidence against the rigidity of the DE linker, in both TnC and calmodulin, has been previously presented. A crystallographic study reviewed a number of TnC structures and concluded that the central helix was indeed flexible.[25] The helix was intact in the structures reviewed in that study. Analysis of both Bragg and diffuse scattering of calmodulin crystals concluded that uncorrelated interdomain motions do exist at the expense of the rigidity of the central helix.[26] Newer data[27] show that Ca^{2+}-free sNTnC (assembled into the sTn complex) has a higher rate of rotational diffusion than the remainder of the Tn complex (see Figure 7.5). These newer observations are NMR data which can directly probe protein structural dynamics. Such dynamics do not preclude the DE linker's structure; rather, this structure is transient, or contingent on additional stabilizing factors. For example, cNTnC tumbles at a similar rate to the Tn complex in the Ca^{2+}-activated state.[27] This completely corroborates the structure of the sTn core complex.[22]

The hypothesis exists: the DE linker is rigid in the Ca^{2+}-activated state but not in the inhibited state.[22,27] Surely, a structured DE linker presents a stronger mechanical coupling of the head and IT arm, consistent with linker possessing the property of rigidity. It could be described accurately as "relatively rigid" when comparing the two states,[27] reflecting that the NTnC and CTnC are more strongly coupled in the Ca^{2+}-activated state. One may question whether this is actually a change in rigidity, however. If the DE linker alternates between being structured and disordered, it cannot be identified as "rigid" as in the "rigid body" approximation from mechanics,[d] but rather alternates between weakly and tightly constrained environments. For example, a pipe cleaner does not gain bonified rigidity upon insertion into a pipe stem. It simply becomes constrained. The DE linker may

[d] A rigid body's internal frame of reference remains untransformed in the presence of external forces. The definition of an internal reference frame implies that the orientation of the rigid body is irrelevant.

become more structured when bound to Ip but this does not make it inherently rigid. Although this point seems semantic, such language perpetuates the idea that the DE linker is converged upon a structured helix, in solution-state Tn·2Ca^{2+}.

7.4.3. Extending the Core Tn Complex: The Mobile Domain

Due to a slow rate of molecular tumbling, most of the NMR signals from ^{15}N-enriched sTnI in the ~52 kDa sTn complex were too broad to allow for assignment.[18,28] A subset of {^{1}H,^{15}N}-HSQC crosspeaks were sharp and dispersed, however, prompting their sequential assignment by Wakabayashi and coworkers.[18] These signals originate in a domain of sTnI C-terminal to sSp, residues 131–182 of chicken sTnI. This domain has higher rotational diffusion than the bulk of sTn and is named the mobile domain (sMd). NMR structures of sMd were determined, in the presence and absence of Ca^{2+}.[18] These observations prompted incorporation of sMd into cryo-EM (~25 Å resolution) structures of the thin filament. The combination of low resolution EM data with high resolution structures allowed for explicit visualization of Tn·thin filament interactions in the inactivated state.

Murakami et al. show how it is possible to define tertiary structure in the highly dynamic mobile domain.[18] The steady-state {^{1}H}-^{15}N NOE enhancement for this region averaged to 0.5. Compared with typical globular proteins, such NOE values are indicative of conformational exchange. The presence of interconverting conformers does not, however, preclude the presence of a native conformation. This means that the native state consists of a family of nearly isoenergetic but nonidentical conformers. This region of sTn was structured with NOE-derived distance restraints; secondary structures were further stabilized using hydrogen bond restraints.[18] Hydrogen bonds were assigned in regions of assignable secondary structure as indicated by canonical medium-range NOEs. So this study showcases the ability of the NOE to disclose long-range interactions in fluctuating protein structures. Other NMR observables such as the chemical shift, J-couplings and residual dipolar couplings, would be scaled down more extensively due to the averaging of multiple conformations, and would prove less useful when defining the native conformation. Indeed, in an independent study by Blumenschein et al,[28] Cα chemical shift analysis of sMd ($sTnI_{131–182}$) indicates sufficient intradomain conformational fluctuations to average the chemical shift to nearly random coil values.

7.4.4. Reconciling the Disorder: A Mechanism

The successful description of the Tn mobile domain, and the accompanying cryo-EM analysis,[18] allow for an elaboration on the mechanism of Tn-regulation of striated muscle contraction. Ip and sMd are attracted to the N- and C-termini of actin through long-range electrostatic forces. At low [Ca^{2+}], sIp and sMd bind to actin, in a conformation reminiscent to a "C clamp." The TnI·actin interactions localize the IT arm in a region suitable to displace tropomyosin. Ca^{2+}-activation of sNTnC allows for binding of sSp. This kinetically stable interaction disrupts the sIp·sMd·actin interactions enough for sIp to localize to the central helix of sTnC.

sMd is weakly or transiently structured. This does not preclude the conformational dispositions determined by Murakami et al.[18] Rather, our ability to define the region as highly mobile enriches the mechanistic picture. Conformational heterogeneity provides a means for TnI's C-terminus traversal between the Tn head and the thin filament.[28]

Conformational fluctuations confer a larger collision radius to a protein. Encounter-induced folding provides a mechanism for increasing the proportion of productive collisions out of total collisions. In other words, Md may be weakly structured to facilitate fast movements over large displacements, as previously suggested.[28] We visualize this mechanism in Figure 7.6. Our hypothesis is made more concrete by the invoking the fly-casting mechanism of molecular recognition, as described by Shoemaker, Portman and Wolynes.[29] Certainly, this mechanism has aspects discordant with conventional conceptions of structure-activity. The study of striated muscle contraction continues to guide us towards a richer understanding of biology and chemistry.

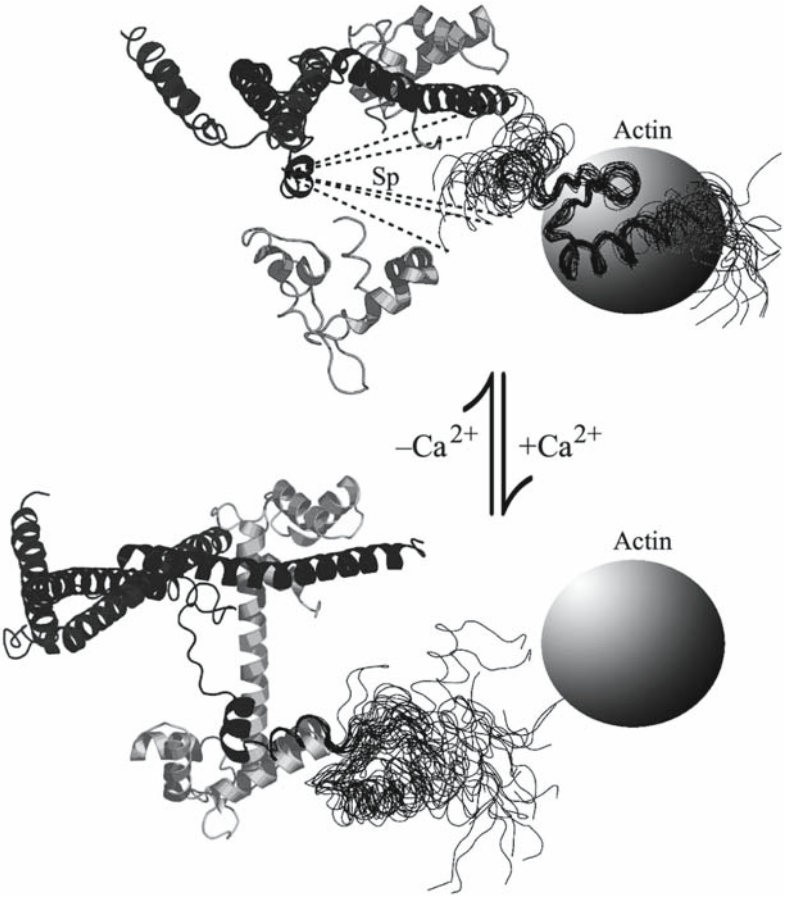

Figure 7.6. Fly-casting: traversing the actin-Tn gap using protein folding. The contraction-inhibited state is depicted (top) with the crystal structure of sTn (PDB 1YV0[22]) and the solution structure of sMd (PDB 1VDI[18]). Md is bound to actin (along with Ip, not depicted here), with the Md-Sp region being transiently structured. Ca^{2+} binding to sTnC allows for subsequent Sp binding, releasing Md from actin (bottom). The structures of Ca^{2+}-activated sTn (PDB 1YTZ) and sMd (PDB 1VDJ) when covisualized, suggest that Md can extend a large distance using its hinge regions, "fishing" for its binding partner.

7.5. ACKNOWLEDGMENTS

We are indebted to Dr. TMA Blumenschein, who brought the fly-casting mechanism to our attention. We thank Drs. MX Li, MNG James, SP Graether and DA Lindhout for productive discussions. This work was supported by the Canadian Institutes of Health Research and the Heart and Stroke Foundation.

7.6. REFERENCES

1. S. Ebashi, Regulatory mechanism of muscle contraction with special reference to the Ca-troponin-tropomyosin system. *Essays Biochem.* **10**, 1–36 (1974).
2. J. D. Potter, and J. Gergely, Troponin, tropomyosin, and actin interactions in the Ca^{2+} regulation of muscle contraction. *Biochemistry* **13**(13), 2697–2703 (1974).
3. O. Herzberg, and M. N. G. James, Common structural framework of the two Ca^{2+}/Mg^{2+} binding loops of troponin C and other Ca^{2+} binding proteins. *Biochemistry* **24**(20), 5298–5302 (1985).
4. M. Sundaralingam, R. Bergstrom, G. Strasburg, S. T. Rao, P. Roychowdhury, M. Greaser, and B. C. Wang, Molecular structure of troponin C from chicken skeletal muscle at 3-angstrom resolution. *Science* **227**(4689), 945–948 (1985).
5. S. M. Gagne, S. Tsuda, M. X. Li, L. B. Smillie, and B. D. Sykes, Structures of the troponin C regulatory domains in the apo and calcium-saturated states. *Nat. Struct. Biol.* **2**(9), 784–789 (1995).
6. C. M. Slupsky, and B. D. Sykes, NMR solution structure of calcium-saturated skeletal muscle troponin C. *Biochemistry* **34**(49), 15953–15964 (1995).
7. O. Herzberg, J. Moult, and M. N. G. James, A model for the Ca^{2+}-induced conformational transition of troponin C. A trigger for muscle contraction. *J. Biol. Chem.* **261**(6), 2638–2644 (1986).
8. C. M. Slupsky, *The NMR Solution Structure of Calcium-Saturated Skeletal Muscle Troponin C.* Ph.D. thesis, University of Alberta, Dept. of Biochemistry (1995).
9. N. Tjandra, H. Kuboniwa, H. Ren, and A. Bax, Rotational dynamics of calcium-free calmodulin studied by ^{15}N-NMR relaxation measurements. *Eur. J. Biochem.* **230**(3), 1014–1024 (1995).
10. A. C. Murray, and C. M. Kay, Hydrodynamic and optical properties of troponin A. Demonstration of a conformational change upon binding calcium ion. *Biochemistry* **11**(14), 2622–2627 (1972).
11. D. M. Byers, and C. M. Kay, Hydrodynamic properties of bovine cardiac troponin C. *Biochemistry* **21**(2), 229–233 (1982).
12. J. Gulati, A. B. Akella, H. Su, E. L. Mehler, and H. Weinstein, Functional role of arginine-11 in the N-terminal helix of skeletal troponin C: combined mutagenesis and molecular dynamics investigation. *Biochemistry* **34**(22), 7348–7355 (1995).
13. S. M. Gagne, M. X. Li, and B. D. Sykes, Mechanism of direct coupling between binding and induced structural change in regulatory calcium binding proteins. *Biochemistry* **36**(15), 4386–4392 (1997).
14. N. C. Strynadka, and M. N. G. James, Crystal structures of the helix-loop-helix calcium-binding proteins. *Annu. Rev. Biochem.* **58**, 951–998 (1989).
15. S. K. Sia, M. X. Li, L. Spyracopoulos, S. M. Gagne, W. Liu, J. A. Putkey, and B. D. Sykes, Structure of cardiac muscle troponin C unexpectedly reveals a closed regulatory domain. *J. Biol. Chem.* **272**(29), 18216–18221 (1997).
16. S. M. Gagne, M. X. Li, R. T. McKay, and B. D. Sykes, The NMR angle on troponin C. *Biochem. Cell Biol.* **76**(2–3), 302–312 (1998).
17. B. Tripet, J. E. Van Eyk, and R. S. Hodges, Mapping of a second actin-tropomyosin and a second troponin C binding site within the C terminus of troponin I, and their importance in the Ca^{2+}-dependent regulation of muscle contraction. *J. Mol. Biol.* **271**(5), 728–750 (1997).
18. K. Murakami, F. Yumoto, S.-Y. Ohki, T. Yasunaga, M. Tanokura, and T. Wakabayashi, Structural Basis for Ca^{2+}-regulated Muscle Relaxation at Interaction Sites of Troponin with Actin and Tropomyosin. *J. Mol. Biol.* **352**(1), 178–201 (2005).
19. S. Takeda, A. Yamashita, K. Maeda, and Y. Maeda, Structure of the core domain of human cardiac troponin in the Ca^{2+}-saturated form. *Nature* **424**(6944), 35–41 (2003).

20. B. D. Sykes, Pulling the calcium trigger. *Nat. Struct. Biol.* **10**(8), 588–589 (2003).
21. J. R. Pearlstone, and L. B. Smillie, The interaction of rabbit skeletal muscle troponin-T fragments with troponin-I. *Can. J. Biochem. Cell Biol.* **63**(3), 212–218 (1985).
22. M. V. Vinogradova, D. B. Stone, G. G. Malanina, C. Karatzaferi, R. Cooke, R. A. Mendelson, and R. J. Fletterick, Ca^{2+}-regulated structural changes in troponin. *Proc. Natl. Acad. Sci. USA* **102**(14), 5038–5043 (2005).
23. B. Halle, Flexibility and packing in proteins. *Proc. Natl. Acad. Sci. USA* **99**(3), 1274–1279 (2002).
24. D. G. Vassylyev, S. Takeda, S. Wakatsuki, K. Maeda, and Y. Maeda, The crystal structure of troponin C in complex with N-terminal fragment of troponin I. The mechanism of how the inhibitory action of troponin I is released by Ca^{2+}-binding to troponin C. *Adv. Exp. Med. Biol.* **453**, 157–167 (1998).
25. J. Soman, T. Tao, and G. N. J. Phillips, Conformational variation of calcium-bound troponin C. *Proteins* **37**(4), 510–511 (1999).
26. M. E. Wall, J. B. Clarage, and G. N. Phillips, Motions of calmodulin characterized using both Bragg and diffuse X-ray scattering. *Structure* **5**(12), 1599–1612 (1997).
27. T. M. A. Blumenschein, D. B. Stone, R. J. Fletterick, R. A. Mendelson, and B. D. Sykes, Calcium-dependent changes in the flexibility of the regulatory domain of troponin C in the troponin complex. *J. Biol. Chem.* **280**(23), 21924–21932 (2005).
28. T. M. A. Blumenschein, D. B. Stone, R. J. Fletterick, R. A. Mendelson, and B. D. Sykes, Dynamics of the C-terminal region of TnI in the troponin complex in solution. *Biophys. J.* 90(7), 2436–2444 (2006).
29. B. A. Shoemaker, J. J. Portman, and P. G. Wolynes, Speeding molecular recognition by using the folding funnel: the fly-casting mechanism. *Proc. Natl. Acad. Sci. USA* **97**(16), 8868–8873 (2000).

8

STRUCTURAL BASIS FOR CALCIUM-REGULATED RELAXATION OF STRIATED MUSCLES AT INTERACTION SITES OF TROPONIN WITH ACTIN AND TROPOMYOSIN

Kenji Murakami[1], Fumiaki Yumoto[2], Shin-ya Ohki[3], Takuo Yasunaga[4], Masaru Tanokura[2] and Takeyuki Wakabayashi[1]

8.1. INTRODUCTION

Muscle contraction, in general, is regulated by the intracellular calcium-ion concentration. Ca^{2+}-regulation in skeletal or cardiac muscle of vertebrate is mediated at the level of thin filaments consisting of actin, tropomyosin, and troponin. However, pure actin filaments themselves activate contraction irrespective of calcium concentration. Troponin,[1] together with tropomyosin, is required to regulate contraction.[2] Troponin consists of three subunits:[3] inhibitory TnI, Ca^{2+}-binding TnC, and tropomyosin-binding TnT. Troponin has an elongated shape and forms two structural regions, which are a long tail region containing the N-terminal region of TnT (TnT_1 (chicken skeletal residues 1–164 of TnT)[4]) and a globular head region containing TnI, TnC, and the C-terminal region of TnT [TnT_2 (chicken skeletal residues 165–263 of TnT)]. The globular head region plays a central role in regulating muscle contraction.[5]

Troponin as a ternary complex interacts with actin-tropomyosin through two kinds of sites: (i) Ca^{2+}-dependent binding through TnI; and (ii) almost Ca^{2+}-insensitive binding through TnT. TnT has two interaction sites: (i) the troponin tail region (TnT_1) that interacs with tropomyosin; and (ii) the N-terminal half of TnT_2 (chicken skeletal residues 157–193), which is essential for the binding of the globular head region of troponin (TnT_2-TnI-TnC complex) to actin. TnI plays a central role to inhibit the acto-myosin ATPase[6] resulting in the relaxation at low Ca^{2+}. The inhibitory region (residues 105–114

[1] Department of Biosciences, School of Science and Engineering, Teikyo University, Toyosatodai 1-1, Utsunomiya 320-8551, [2]Department of Applied Biological Chemistry, Graduate School of Agricultural and Life Sciences, University of Tokyo, Yayoi 1-1-1, Bunkyo-ku, Tokyo 113-8657, [3]Japan Advanced Institute of Science and Technology (JAIST), Asahidai 1-1, Tatsunokuchi, Ishikawa 923-1292, and [4]Department of Bioscience and Bioinformatics, Faculty of Computer Science and Systems Engineering, Kyushu Institute of Technology, Ooaza-kawazu 680-4, Iizuka, Fukuoka 820-850, Japan

Regulatory Mechanisms of Striated Muscle Contraction
Edited by Ebashi and Ohtsuki, Springer, 2007

of skeletal TnI) has been identified as a region responsible for inhibitory activity. This region binds to the N-terminal region of actin, in which the myosin-binding site is also located.[7–9] The C-terminal region of TnI (residues 130–182 of skeletal TnI) has been shown to be responsible for ~65% of total inhibitory activity.[10–11] Because the binding of this region to actin-tropomyosin is much weaker than that of the inhibitory region, the reason why the former is so important for full inhibitory activity has been unclear. The main purpose of this paper is to clarify this problem.

The interactions between troponin and actin are thought to be regulated by a "switch region" of TnI (skeletal residues 116–131, a second TnC-binding region) located between the inhibitory region and the C-terminal region of TnI. At low Ca^{2+}, the hydrophobic pocket in the N-domain of TnC closes and the switch region is suggested to move out of the hydrophobic pocket. Such Ca^{2+}-induced conformational changes of troponin are transmitted to actin, which now can interact with myosin heads to generate force.

The steric blocking model has been proposed for Ca^{2+}-regulation, in which the azimuthal positioning of tropomyosin on actin filament is critical. The tropomyosin shift appeared to be shown in three-dimensional images of regulated actin filaments by imposing helical symmetry. However, there have been two problems: (i) Troponin, which does not follow the helical symmetry of actin, might affect the position of tropomyosin in the reconstructed images; and (ii) troponin can not be visualized and the precise manner in which troponin induces the shift of tropomyosin remains to be clarified. To clarify these ambiguities we have applied the single particle analysis to electron cryo-micrographs of actin-tropomyosin-troponin and shown that the position of tropomyosin is affected by imposing the helical symmetry. More importantly, it revealed the Ca^{2+}-induced shift and transconformation of troponin. At low Ca^{2+}, troponin head was bifurcated and the actin-binding part of troponin, named the troponin arm was shown to emerge.[12] The estimated molecular mass of troponin arm was ~6 kDa. However, the limited resolution (~20 Å with Fourier shell correlation of 0.17; ~35 Å with that of 0.5) obscured its atomic details. In crystal structures of cardiac troponin,[13] the actin-binding regions of troponin were unclear and, crucially, it was not possible in these structures to visualize how troponin interacts with actin.

To overcome these problems, we applied NMR spectroscopy.[14] It was found that the core domain of troponin has an independent domain (~6.1 kDa), of which the NMR spectra could be analysed. NMR signals were sequentially assigned as representing residues 131–182 of TnI and atomic models could be calculated from NOE spectra both at low and high Ca^{2+}. The molecular mass and outline of the mobile domain were similar to those of the troponin arm. It was straight forward to dock the mobile domain into the cryo-EM density map. The molecular details of interactions between actin and the mobile domain could be visualized in the relaxed state. This in turn enabled the almost unique determination of the way to dock the whole crystal structure of the core domain[13] into the EM map.[12] Thus the molecular details of interactions between actin and troponin in the relaxed state were established. The resultant atomic model suggests how troponin causes the shift of tropomyosin to achieve muscle relaxation.

8.2. ELECTRON CRYO-MICROSCOPY AND THREE-DIMENSIONAL IMAGE RECONSTRACTION OF THIN FILAMENTS

Figure 8.1a shows a model of thin filaments. In Figure 8.1b, a composite model based on electron cryo-microscopy of thin filaments (tropomyosin and troponin) and X-ray crystallography of actin is shown.[16] According to the single particle analysis, thin filaments changed their conformation (Figure 8.2–8.3).[12] At low Ca^{2+}, troponin head was shifted by 30 Å towards the outer domain of actin and bifurcated (Figure 8.2b–d, left panels) and the actin-binding part of troponin, named the troponin arm was shown to emerge.[12] The estimated molecular mass of troponin arm was ~6 kDa.

It was also shown that Ca^{2+} caused tropomyosin shift, but its extent was not uniform and varied along its sequence (Figure 8.2).[12] Tropomyosin appeared to shift more in its C-terminal region (~35 Å, blocks VI and VII) than other regions (~12 Å, blocks II–IV).

8.3. IDENTIFICATION OF THE MOBILE DOMAIN IN THE TROPONIN TERNARY COMPLEX

The TnI-TnC-TnT_2 ternary complex with a molecular mass of ~52 kDa gave distinct signals with relatively narrow line widths in ^1H nuclear magnetic resonance (NMR) spectra. This indicated the existence of NMR-visible mobile residues in the complex.

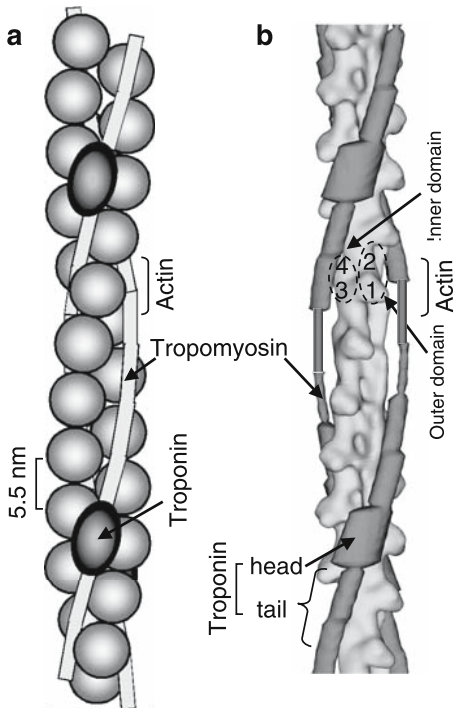

Figure 8.1. Thin filament model. (a) A schematic model of thin filaments from striated muscle.[15] (b) A composite model of thin filaments.[12] Tropomyosin and troponin part was from electron cryo-microscopy[12] and actin part was from X-ray crystallography of actin.[16]

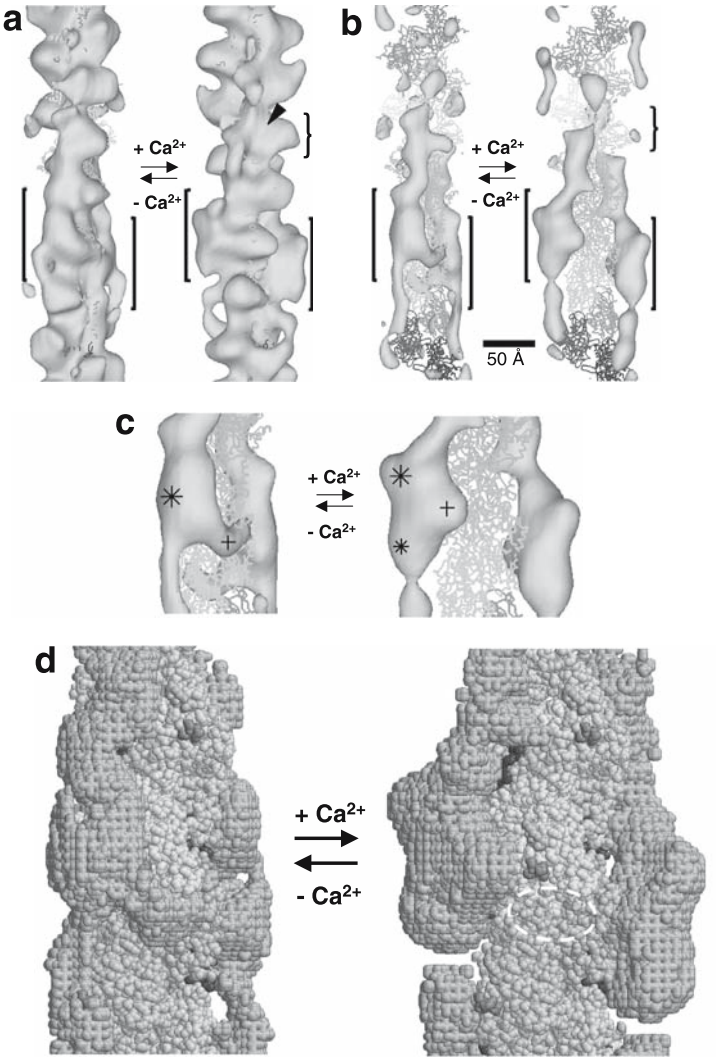

Figure 8.2. Ca^{2+}-induced comformational changes of thin filaments revealed by electron cryo-microscopy.[12] (a) Three-dimensional image of thin filaments. (b) Actin part was subtracted from the images shown in (a) so that only tropomyosin-troponin parts were visualized in solid models. Actin part was shown in wire models. (c) Close up view of (b). Asterisks indicate high density region. A cross indicates troponin arm. (d) Solid model corresponding to (c). Myosin-binding residues of actin were shown in darker gray.

Because of the large molecular mass, major portions of the troponin ternary complex gave broad signals. By applying standard triple resonance methods to uniformly ^{15}N- and/or ^{13}C- labelled TnI complexed with unlabelled TnC and TnT_2, the signals were sequentially identified as those from the C-terminal region of skeletal TnI (residues 131–182). Heteronuclear $\{^1H\}$-^{15}N NOE (ref. 40) showed clearly that most of the C-terminal region of TnI, with an average value of NOE = 0.5 except for its C-terminal 3 residues, took on a regular globular structure in the ternary complex irrespective of Ca^{2+}. This indicates that troponin

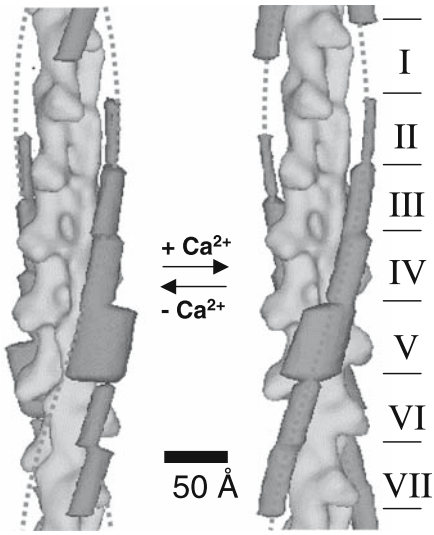

Figure 8.3. Locally averaged positions of tropomyosin and troponin.[12] Approximate positions of actins are labelled with Roman numerals.

assumes unusual molecular architecture, in which its portion constitutes a compact "mobile domain" tumbling independently of the rest of the molecule called the core domain.[13] A putative pivot point for tumbling, designated "hinge", appeared to be located between Gly127 and Lys131 of TnI, which is consistent with the observation that Gly127 (human cardiac Gly160) takes up multiple conformations in crystals.[13] Although NMR spectra of large complexes have been reported, portions giving signals were unstructured.

8.3.1. Atomic Structure of the Mobile Domain

Model solution structures of the mobile domain were computed using 577 or 514 distance restraints from NOESY spectra at low or high Ca^{2+}, respectively (Figure 8.4). The amino acid sequence of the mobile domain is shown in Figure 8.5d, together with that from human cardiac troponin. The size (40 × 20 × 15 Å) and the outline of the mobile domain were similar to those of the troponin arm at low Ca^{2+}. The mobile domain (Lys131-Ser182) contained three segments; a helix α4 (Val132-Leu140); a mini-globular subdomain (Val143-Lys167); and a helix α6 (Met170-Phe177), which were connected by a loop 1 (Lys141-Gln142) and a loop 3 (Ser168-Gly169) as shown in Figure 8.4b. A mini-globular subdomain was constructed from an antiparallel β-sheet (β1 and β2), a β-bulge (Glu146-Lys150), a loop 2 (Leu154-Val157) and a helix α5 (Gly158-Lys167) and resembled a zinc finger. The hydrophobic core of the mini-globular subdomain was formed by Val143, Leu154, Trp160, and Ile164 (Figure 8.4b). This hydrophobic core was stabilized also by long hydrophobic side chains (Lys141, Lys145, Arg155, and Arg161) and a salt bridge between Asp153 and Arg161. Figure 8.4c–e shows the superposition of 20 calculated structures of the mobile domain at low or high Ca^{2+}. Each of three segments was relatively well-defined structurally, whereas the spatial relations of the mini-globular subdomain to helices α4 and α6 were variable. Loop 1 provides the mobile domain with intra-domain flexibility, consistent with its high susceptibility to chymotrypsin. The inter-domain flexibility at the hinge and the intra-domain flexibility

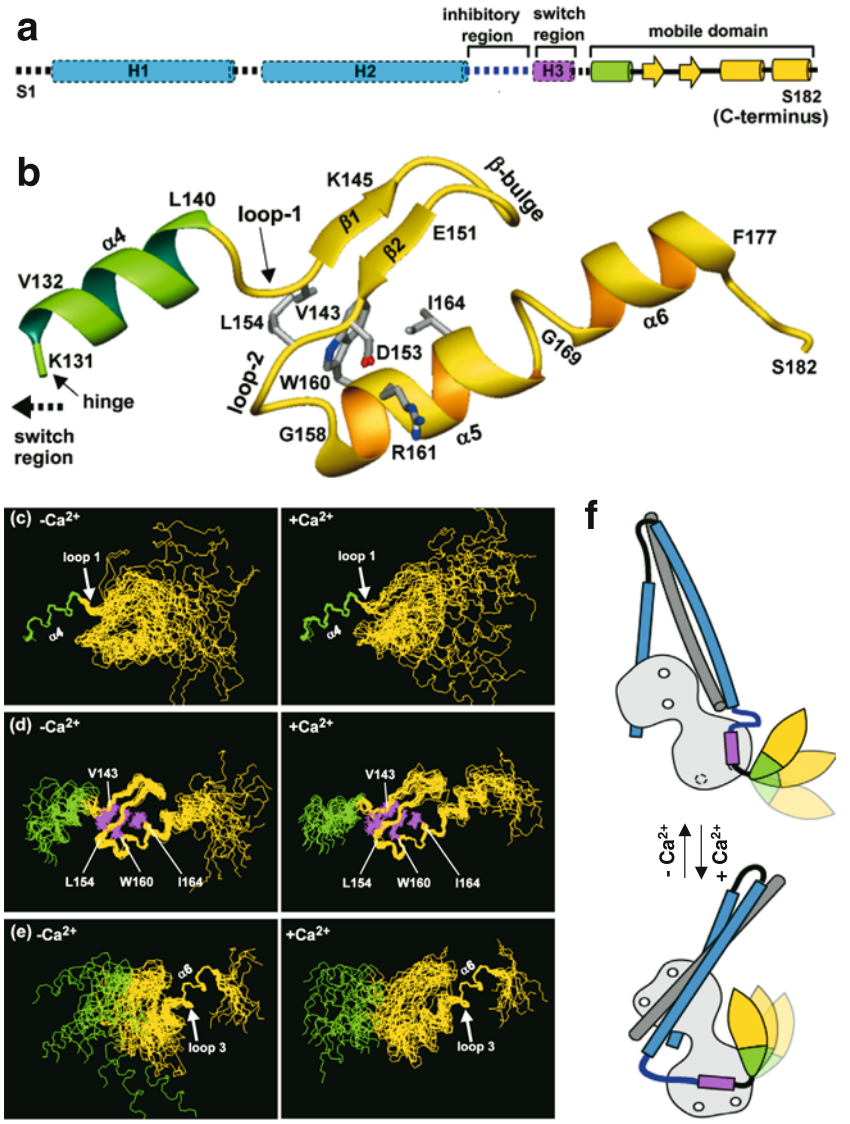

Figure 8.4. Solution NMR structure of the ~6.1 kDa mobile domain in the TnI-TnC-TnT_2 ternary complex (~52 kDa).[14] (a) A scheme for TnI. (b) A ribbon model of the NMR solution structure of the mobile domain in the ternary complex at low Ca^{2+}. (c–e) Twenty low-energy structures superimposed by aligning various part. (f) A schematic model of Ca^{2+}-induced changes of troponin core domain.

at loop 1 and loop 3 would favour induced-fitting of the mobile domain to bind to actin at low Ca^{2+}.

The global fold of the mini-globular subdomain in the mobile domain was established by long-range NOEs involving the hydrophobic core (Val143, Leu154, Trp160, and Ile164) and long hydrophobic side chains (Lys141, Lys145, Arg155, and Arg161) in the vicinity of the hydrophobic core. Many long- and medium-range NOEs could be observed in the

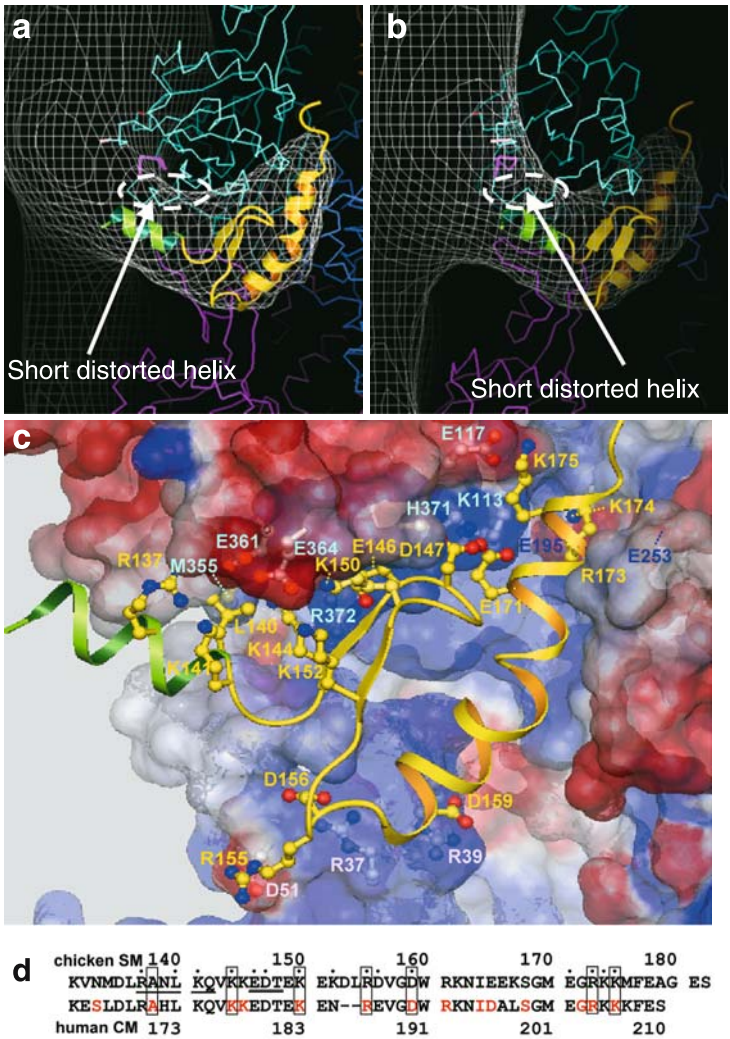

Figure 8.5. Docking of the mobile domain into the EM map.[14] (a) The mobile domain was docked into the troponin arm (gray contour lines).[12] Mobile domain (α4, light green; other parts, yellow) is shown in ribbon. Actin is shown in wire (b) is rotated by 40° with respect to (a). (c) Solid model of three actins showing their surface electrostatic potential and the ribbon model of the mobile domain. The interacting residues of the mobile domain with actin are shown in ball-and-stick. (d) Sequence of the mobile domain together with human cardiac sequence. Actin-interacting residues are indicated with dots. Residues that showed Ca^{2+}-induced change in chemical shift are underlined. Residues related to human cardiomyopathy are coloured red, and are enclosed with boxes if they were involved in interaction with either actin or the core domain of troponin.

hydrophobic core. Val143, Leu154, Trp160, and Ile164 have 26, 32, 54, and 50 long – ($i - j > 4$) and medium – ($i - j = 2$, 3, or 4) range NOE restraints, respectively.

Figure 8.4f shows the schematic model for the ternary complex of troponin based on X-rya crystallography[13] and NMR spectroscopy.[14]

8.3.2. Interaction of Actin with the Mobile Domain at Low Ca^{2+}

The atomic details of interactions between actin and the mobile domain at low Ca^{2+} could be established by docking the mobile domain into the troponin arm revealed in the 3D cryo-EM map of thin filament[12] at low Ca^{2+} (Figure 8.5a,b). The fitting of the mobile domain is based on two assumptions. First, helix α4 is tethered to the core domain. Second, the structure of the mobile domain is locally conserved, except for the hinge, loop 1, and loop 3. Then, the orientation and position of the mobile domain could be determined uniquely, because its shape was asymmetric and similar to that of the troponin arm. Considering the flexibility at loop 1 and loop 3, the dihedral angles of Gln142 in loop 1 and Gly169 in loop 3 were adjusted to optimize docking. The mobile domain lay in a cavity, which is surrounded by three actin monomers coloured in magenta, blue, and cyan in Figure 8.5a,b and located adjacent to the phalloidin-binding cavity.

The mobile domain interacted with actin mainly through salt bridges: Charged residues of the mobile domain faced against the actin surface with opposite electrostatic potential (Figure 8.5c). There were more than 10 putative salt bridges between the mobile domain and actin: (i) Basic residues (Arg137, Lys141, Lys144, Lys150, and Lys152) and acidic residues (Glu146-Asp147) of the mobile domain faced against acidic residues (Glu361 and Glu364) and basic residues (His371-Arg372) in the C-terminal region of cyan actin, respectively; (ii) Glu171, Arg173, Lys174, and Lys175 in α6 faced against Lys113, Glu253, Glu195, and Glu117 in the groove of actin double strands, respectively; and (iii) Arg155, Asp156, and Asp159 of the mobile domain faced against Asp51, Arg37, and Arg39 in the DNase I loop of magenta actin, respectively. There was also the possibilty of a hydrophobic interaction between Leu140 in α4 and Met355 of cyan actin. Actin-binding residues of TnI are indicated with dots in Figure 8.5d, in which the residues related to cardiomyopathy shown in red are enclosed with boxes if they interact with either actin or the core domain of troponin. Except for Ala138, all boxed residues interacting with actin are charged. This suggests the functional importance of the electrostatic interactions between actin and the mobile domain. It is consistent with the frequenct occurrence of human cardiomyopathy mutations in the charged residues of the mobile domain (Figure 8.5d).

To confirm the electrostatic nature of the binding of the mobile domain to actin filaments, we constructed two mutants of the mobile domain, which were a recombinant mobile domain and an extended one. The recombinant mobile domain (residues 128–182 fused to GFP) co-sedimented with actin filaments in a ratio of 1 : 1 in low salt solution, but the binding decreased linearly with the addition of salt down to a negligible level at ionic strength of ~150 mM (105 mM CH_3COOK). When the inhibitory and switch regions were fused to the mobile domain, the binding to actin filaments became much stronger (~10 times) and less sensitive to salt concentrations: A recombinant extended mobile domain (residues 104–182 fused to GFP) bound to actin with a dissociation constant of ~10 μM. Our results confirmed the previous qualitative data showing the importance of

residues 103–119 of TnI for actin binding: It was shown that $TnI_{103–182}$ binds to actin, whereas $TnI_{120–182}$ does not.[17]

The direct evidence for the location of the interaction interface between actin and the mobile domain was provided by the 3D cryo-EM reconstruction of actin filament decorated with a recombinant extended mobile domain. A region interpreted as fused GFP was located adjacent to the C-terminus of the mobile domain, and a region interpreted as the inhibitory and switch regions was located adjacent to the N-terminus of the mobile domain and consisted of two lobes. The upper lobe covered a cluster of acidic residues (Asp24 and Asp25) and the C-terminal half (Ileu345-Leu349) of the hydrophobic α-helix of actin. Probably Asp24 and Asp25 of actin face against a cluster of basic residues of the inhibitory region (Lys105, Lys107, Arg108, Arg112, and Arg113). A cluster of acidic residues in the N-terminal region of actin (Asp1, Glu2, Asp3, and Glu4) also may interact with the cluster of basic residues in the presence of other parts of troponin. The lower lobe lay near DNase I loop and was connected with the mobile domain. The mobile domain together with the inhibitory and switch regions surrounded the N- and C-terminal regions of actin in a C-clamp configuration.

8.4. DOCKING THE GLOBULAR HEAD REGION OF TROPONIN

Successful docking of the mobile domain to the EM map of thin filament[10] at low Ca^{2+} established the precise location of chicken skeletal Asn133 of TnI (rabbit skeletal Cys133), which is an important landmark to incorporate the available data. It was located in front of Gln353 of the subdomain 1 in the outer domain of actin, with the distance between two α-carbon atoms being ~7 Å. The ambiguity of the position of the α-carbon of Asn133 of TnI was ~3 Å in all directions. As a result, the core domain of troponin could be docked uniquely into the EM map of thin filament at low Ca^{2+} and a model containing actin and most of the globular head region of troponin at low Ca^{2+} was obtained (Figure 8.6). Combining the different pieces of information described below and taking advantage of the asymmetric shape of the core domain, the atomic structures could be docked almost uniquely into the EM map. The docking of the core domain of troponin was helped also by the successful docking of tropomyosin. Because the mass of tropomyosin could be observed separately from that of troponin in the blocks IV and VI (Figure 8.3), its azimuthal position on actin filament could be determined. Moreover, because the horizontal section of the EM map at the level above the core domain (in the block IV, Figure 8.3) was elliptic, the rotation angle around the axis of the coiled-coil structure of tropomyosin also could be determined. Thus, the coiled-coil structure of tropomyosin could be docked almost uniquely into the EM map. Even though the location of the inhibitory region and the switch region of TnI was determined as described in the section 8.3.2, these regions were not put into the vacant space of the EM map in front of Asp24 of actin, because of the lack of atomic structure information.

We considered the following points in generating our atomic model. First, residue Arg103 of TnI (human cardiac Arg136) adjacent to the inhibitory region was put near Asp24 in the N-terminal region of actin, which is also supported by the previous data. Second, Cys48 of TnI locating near the N-terminal tip of the coiled-coil region in the core domain was placed further from the mobile domain than the C-terminal one, because FRET measurement showed that it is 66 Å apart from residue 133 (chicken skeletal

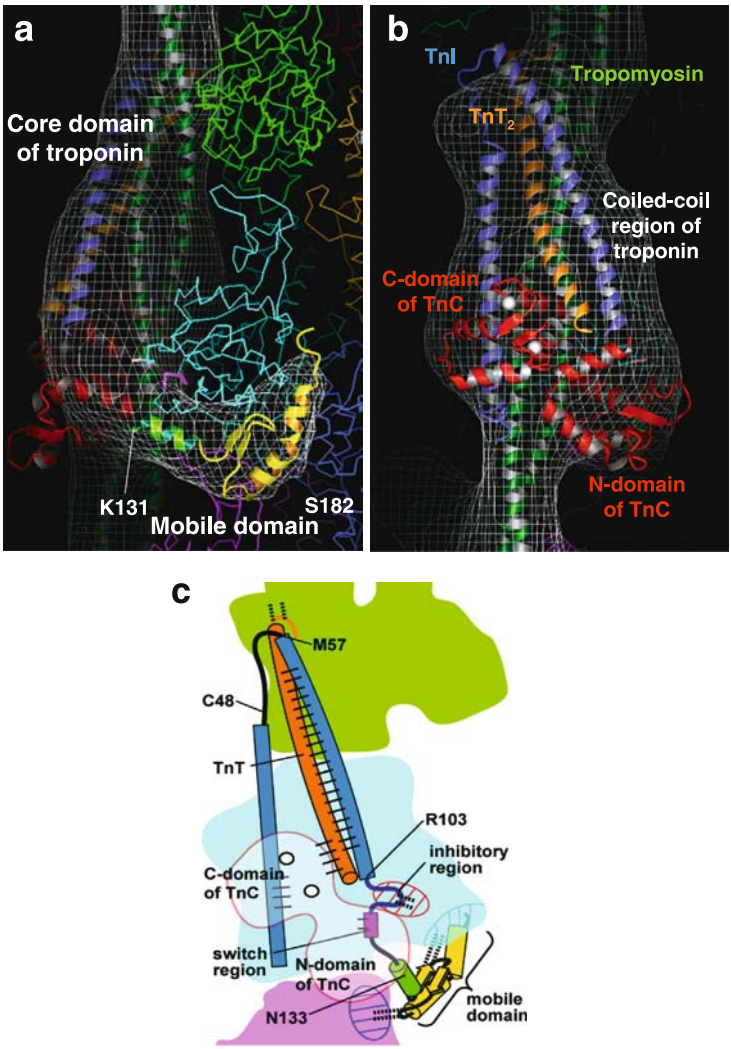

Figure 8.6. Docking the mobile domain and the core domain of troponin into 3D cryo-EM map of actin-tropomyosin-troponin[14] at low Ca^{2+}. (a) Densities due to troponin-tropomyosin[12] are shown with contour lines (gray). The N-domain of TnC in the core domain of troponin (PDB code 1J1D) was replaced with apo N-domain of TnC (PDB code 5TNC). Mobile domain (α4, light green; other parts, yellow), TnI (blue), TnT (orange), TnC (red), and tropomyosin (dark green) are shown in ribbon format. Ca^{2+} bound to high affinity sites in the C-domain of TnC are shown in spheres. Actin is shown in wire format and residues Asp24-Asp25 (red) and N-terminus (light pink) are shown in colour. The rotation angle is the same as that in Figure 8.5a,c. (b) is rotated by 100° with respect to (a). (c) General relation of actin with troponin at low Ca^{2+}. Colour scheme is the same as in (a)-(b). Dotted lines indicate actin-troponin interactions. Solid lines indicate interactions among troponin subunits. N-terminal region, C-terminal region, and DNase I loop of actin are hatched in red, dark gray (back side of cyan actin), and blue, respectively.

Asn133) of TnI.[18] The distance between α-carbon atoms of these residues was ~65 Å in our model. Third, the N-domain of TnC was placed near the mobile domain according to photo-crosslink experiments: the switch region locating adjacent to the helix α4 of the mobile domain was crosslinked to the N-domain of TnC. Fourth, the central linker region of TnC (D/E-linker) is reported to be flexible.[13,19–21] As a result of these constraints, the ambiguity of the position of the N-terminal tip of the coiled-coil region of core domain (Met57 (human cardiac Phe90) of TnI, Glu200 (human cardiac Glu226) of TnT) was ~3 Å in all directions and that of the C-terminal tip (Arg103 (human cardiac Arg136) of TnI, Asp243 (human cardiac Asn269) of TnT) was ~3 Å in z- and radial directions and ~6 Å in an azimuthal direction.

Although the fluctuation of the position of the N-domain of TnC may be caused due to the flexibility of the central linker region of TnC, the large part of the N-domain of TnC could be contained in the EM map. In our model, the central linker region of TnC was bent and the D helix of TnC was almost perpendicular to the E helix. The D helix of TnC was approximately perpendicular to the actin filament axis (100 ± 20°), although the rotation angle of N-domain of TnC around the D helix could not be determined. *In situ* orientation method using bifunctional fluorescent dyes[22] showed that the angle between the D helix and actin filament axis was 78 or 102°. Two EF-hands in the N-domain of TnC, which are poorly defined at low Ca^{2+}, were outside of the EM map, because the corresponding densities in the EM map are low probably due to their flexibility. Thus the relation between actin and most of the globular head region of troponin could be established unambiguously (Figure 8.6a–b). The coiled-coil region in the core domain was oriented at an angle of ~20° with respect to the helix axis of actin and was close to tropomyosin (Figure 8.6a–c). It is likely that the close contact between the coiled-coil region in the core domain and tropomyosin was the result of the shift of tropomyosin caused by the coiled-coil region of troponin as discussed below. There was a slight clash between tropomyosin and the N-terminal portion of the E helix of TnC. This clash can be avoided by the induced conformational disruption of the N-terminal portion of the E helix of TnC and/or tropomyosin.[12,23]

8.5. ATOMIC MODEL OF ACTIN-TROPOMYOSIN-TROPONIN

We have shown that the ~52 kDa TnI-TnC-TnT_2 ternary complex of troponin has an unusual architecture, in which a mobile domain (~6.1 kDa) tumbles independently of the core domain. The mobile domain showed an almost identical outline to that of the troponin arm and could be docked into the cryo-EM map of thin filament. The resolution of the reconstruction was ~35 Å (ref. 12). Recently, a more reasonable threshold for a density map calculated from a full set of image data has been proposed.[24] Judged by this threshold of ~0.14, the resolution of the reconstructed image is ~20 Å Still the ambiguity of our docking is one order of magnitude better than the nominal resolution of EM maps. This is consistent with the report by Wriggers and Birmanns:[25] Docking precision of atomic data into simulated 20 Å resolution maps is ~1 Å in average.

We established that the residue 133 of TnI was in front of Gln353 of actin with the ambiguity of ~3 Å. This allowed us to incorporate the previous structural and biochemical data so that we could dock uniquely the entire globular head region of troponin into the cryo-EM thin filament electron density map.[12] The resultant model showed how troponin

caused the shift of tropomyosin and explained why the N-terminal half of TnT_2 and the C-terminal region of TnI (the mobile domain) are so important for the full inhibitory activity.

8.5.1. Importance of the Unusual Molecular Architecture of Troponin

The spatial relation among myosin-binding regions (residues 24–28, 144–148, and 340–346 of actin),[26] the mobile domain, the inhibitory region, and the core domain on thin filament at low Ca^{2+} suggests the functional importance of the unusual molecular architecture of troponin. At low Ca^{2+}, myosin head and the inhibitory region compete for a partially overlapped binding region. In contrast, the binding region of the mobile domain is distinct from that of myosin head. Moreover, the attached myosin, of which binding has a positive cooperative effect on regulation,[5] physically restricts the path of the mobile domain to detach from actin. Therefore, myosin has to detach before the mobile domain detaches from actin. Considering a C-clamp configuration of the inhibitory region, the switch region, and the mobile domain, it is likely that the mobile domain plays a role in making a relaxed state more robust: It may work as a fail-safe molecular latch.

It appears to be strange that the affinity of the mobile domain for actin is not strong in spite of the interactions through a large number of salt bridges. Presumably the binding of the mobile domain with actin decreases the number of possible configurations of the mobile domain, because the degree of freedom of rotations of bonds at the hinge, loop 1, and loop 3 will be severely restricted. The same applies to the loops of actin involved in the binding. This will result in an unfavourable decrease in conformational entropy, which offsets the favourable enthalpy change due to the formation of salt bridges. This may account for the low affinity of the mobile domain for actin.

8.5.2. Mechanism of Tropomyosin Shift Caused by Troponin

By docking the globular head region of troponin into the cryo-EM map of thin filament[12] at low Ca^{2+}, we obtained a model for muscle relaxation of actin-tropomyosin-troponin (Figure 8.6c). This model is consistent with the proposal that the N-terminal end of the coiled-coil region in the core domain is tethered to actin through the N-terminal half of TnT_2 as previously suggested.[27] The N-terminal end of the coiled-coil region was located approximately in front of Pro307 in the subdomain 3 of actin. Considering the effect of crystalline packing on the crystal structure of the core domain, the N-terminal half of TnT_2 was not put into the model, but it is likely to play an important role in anchoring the entire globular head region to actin-tropomyosin filament irrespective of Ca^{2+}. To examine the importance of the residues 165–196, we have done binding assay to actin-tropomyosin by using two recombinant ternary complexes, TnI-TnC-$TnT_{197–263}$ and TnI-TnC-$TnT_{165–263}$: The deletion of the residues 165–196 reduced the binding ability of the ternary complex of troponin to actin-tropomyosin irrespective of Ca^{2+}. When the Ca^{2+} concentration decreases, the C-terminal end of the coiled-coil region in the core domain moves towards the outer domain of actin, because the inhibitory region and the mobile domain of TnI are attracted to and bind to the outer domain of actin. Then the coiled-coil region of the core domain would clash with tropomyosin if the latter had stayed in a

high-Ca^{2+} position (orange cylinder in Figure 8.7a–b). Therefore, the coiled-coil region of the Ca^{2+}-deprived core domain pushes tropomyosin towards the outer domain of actin until tropomyosin shifts to the low-Ca^{2+} position (green cylinder in Figure 8.7a–b).

The striking effect of the deletion of the residues 157–193 in the N-terminal half of TnT_2 on the inhibitory activity of the troponin ternary complex containing $TnT_{157–263}$ has been puzzling: The ternary complex containing $TnT_{157–263}$ almost loses its inhibitory activity, when the residues 157–193 are deleted.[27] In our model troponin needs two actin-anchoring sites at both ends of the coiled-coil region in the core domain to push

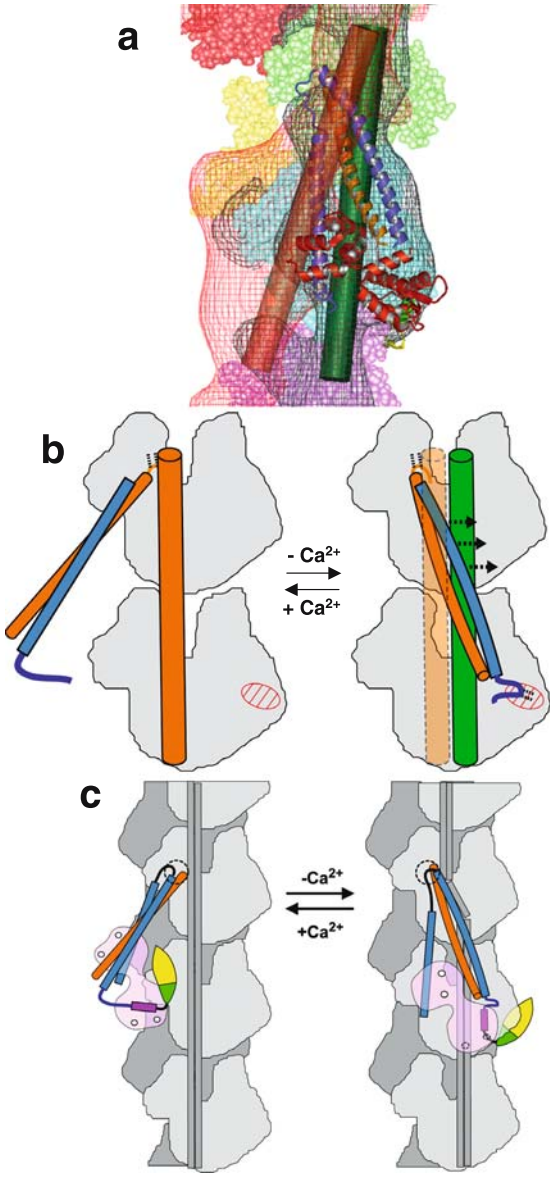

Figure 8.7. Proposed mechanism for Ca^{2+}-regulation of contraction of striated muscle with special reference to relationship between tropomyosin and the coiled-coil region of troponin.[14] (a) The coiled-coil region of troponin at low Ca^{2+} clashes with tropomyosin in a high-Ca^{2+} position (orange cylinder) but not with that in a low-Ca^{2+} position (green cylinder). Densities due to troponin-tropomyosin at low (gray) or high Ca^{2+} (orange) are shown with contour lines. Troponin at low Ca^{2+} is shown in ribbon format. Actin monomers are shown in solid model. Colour scheme for troponin and actin is same as in Figure 8.6. (b) Schematic models to show how the coiled-coil region pushes tropomyosin. (c) Proposed model for Ca^{2+}-regulation. The actin helix has been untwisted for clarity. The region near the N-terminal tip (encircled) of the coiled-coil region (orange, TnT_2; blue TnI) is tethered to actin through N-terminal half of TnT_2 (not shown) irrespective of Ca^{2+} concentration. At low Ca^{2+} (right panel), the inhibitory region (dark blue) and the mobile domain (light green and yellow) bind to the outer domain of actin, and pull the C-terminal end of the coiled-coil region, which pushes tropomyosin (gray) in a high-Ca^{2+} position towards the outer domain of actin until tropomyosin locates in a low-Ca^{2+} position. At high Ca^{2+} (left panel), the switch region (magenta) binds to the N-domain of TnC (pink) and pulls the inhibitory region and the mobile domain so that they detach from actin. Troponin tail (TnT_1, not shown) and/or tropomyosin will shift back towards the inner domain of actin. The uncovering of the outer domain of one actin is propagated to neighbouring actin monomers along the long-pitched actin helix at least towards the barbed-end direction (bottom of the illustration).

tropomyosin. Therefore our model can explain these puzzling data, because the coiled-coil region in the troponin ternary complex containing $TnT_{194–263}$ instead of $TnT_{157–263}$ can not anchor to actin filament at its N-terminal end and consequently the coiled-coil region becomes incapable of pushing tropomyosin towards the outer domain of actin. Thus, in our model it is natural that the N-terminal half of TnT_2 plays an important role in closed-to-blocked state transitions in the three-state model.[28]

8.5.3. A Proposed Model for Ca^{2+} Regulation

Figure 8.7c shows our proposed model for regulatory mechanism of striated muscle. Because both the inhibitory region and the mobile domain have nett positive charges, they tend to be attracted by strong electrostatic field towards the N- and C-terminal regions of actin.[29] At low Ca^{2+}, the inhibitory region and the mobile domain bind to the outer domain of actin in a C-clamp configuration. Then they pull the C-terminal end of the coiled-coil region towards the outer domain of actin. Thereby, the coiled-coil region clashes sterically with tropomyosin and pushes it towards the outer domain of actin. Upon binding of Ca^{2+} to TnC, the switch region binds to the opened hydrophobic pocket in the N-domain of TnC, which weakens the interaction of the inhibitory region and the mobile domain with actin. Now the globular head region of troponin anchors to actin only through the N-terminal half of TnT_2, and can rotate around the pivot (encircled in Figure 8.7c). In our previous model,[12] the N-domain of TnC was assumed to move less than the C-domain at low Ca^{2+}, because the precise location of the residue 133 of TnI was not known. However, in the present model, the N-domain of TnC moved more than that in the previous model. This is because the residue 133 could be located in front of Gln353 of actin at low Ca^{2+}. When tropomyosin is relieved from the steric stress, it shifts back towards the inner domain of actin. Uncovering of the outer domain of one actin monomer will be propagated through TnT_1 and/or tropomyosin to neighbouring actin monomers along the long-pitched helices at least towards the barbed-end direction.[12] Myosin now can bind to uncovered outer domains of actin monomers to generate contraction.

8.6. SUMMARY

In summary, we have shown that the TnI-TnC-TnT_2 ternary complex (~52 kDa) has a mobile actin-binding domain (~6.1 kDa) that tumbles independently of the core domain.[14] By docking the mobile domain and the core domain into the cryo-EM map obtained for thin filaments[12] at low Ca^{2+}, a model for actin-troponin interaction has been obtained.[14] This model shows the atomic details of interactions of actin with the mobile domain and suggests the mechanism by which troponin generates a shift in the azimuthal position of tropomyosin in response to changes in Ca^{2+} levels. In this model the mobile domain of troponin interacts with three actins and one troponin interacts with four actin molecules. The relationship between myosin and the mobile domain suggests that the latter may work as a fail-safe latch to secure a relaxed state. The model also provides insights into many mutations associated with human cardiomyopathy and has implications for the function of other actin-binding proteins. Coordinates of the mobile domain have been deposited in the Protein Data Bank under accession codes 1VDI (low Ca^{2+}) and 1VDJ (high Ca^{2+}).

Chemical shifts of the mobile domain have been deposited in the BMRB under accession ID 18140.

8.7. ACKNOWLEDGEMENTS

This work was supported by the HFSP(Human Frontier Science Program) and the grant-in-aid from the Ministry of Education, Science, Technology and Sports of Japan to T.W. It was also supported by Center for Nano Materials and Technology, JAIST to S.O.

8.8. REFERENC ES

1. S. Ebashi, and A. Kodama, A new protein factor promoting aggregation of tropomyosin, *J. Biochem.* **58**, 107–108 (1965).
2. S. Ebashi, and M. Endo, Calcium ions and muscle contraction, *Prog. Biophys. Mol. Biol.* **18**, 123–183 (1968).
3. M. L. Greaser, and J. Gergely, Reconstitution of troponin activity from three protein components, *J. Biol. Chem.* **246**, 4226–4233 (1971).
4. I. Ohtsuki, Molecular arrangement of troponin-T in the thin filament, *J. Biochem.* **86**, 491–497 (1979).
5. C. S. Farah, and F. C. Reinach, The troponin complex and regulation of muscle-contraction, *FASEB J.* **9**, 755–767 (1995).
6. S. V. Perry, Troponin I: inhibitor or facilitator, *Mol. Cell. Biochem.* **190**, 9–32 (1999).
7. C. Toyoshima, and T. Wakabayashi, Three-dimensional image analysis of the complex of thin filaments and myosin molecules from skeletal muscle. V. Assignment of actin in the actin-tropomyosin subfragment-1 complex, *J. Biochem.* **97**, 245–263 (1985).
8. R. A. Milligan, and P. F. Flicker, Structural relationships of actin, myosin, and tropomyosin revealed by cryo-electron microscopy, *J. Cell Biol.* **105**, 29–39 (1987).
9. I. Rayment, H. M. Holden, M. Whittaker, C. B. Yohn, M. Lorenz, K. C. Holmes, and R. A. Milligan, Structure of the actin-myosin complex and its implications for muscle contraction, *Science*, **261**, 58–65 (1993).
10. C. S. Farah, C. A. Miyamoto, C. H. I. Ramos, A. C. R. Dasilva, R. B. Quaggio, K. Fujimori, L. B. Smillie, and F. C. Reinach, Structural and regulatory functions of the NH- and COOH-terminal regions of skeletal-muscle troponin-I, *J. Biol. Chem.* **269**, 5230–5240 (1994).
11. H. M. Rarick, X. H. Tu, R. J. Solaro, and A. F. Martin, The C terminus of cardiac troponin I is essential for full inhibitory activity and Ca^{2+} sensitivity of rat myofibrils, *J. Biol. Chem.* **272**, 26887–26892 (1997).
12. A. Narita, T. Yasunaga, T. Ishikawa, K. Mayanagi, and T. Wakabayashi, Ca^{2+}-induced switching of troponin and tropomyosin on actin filaments as revealed by electron cryo-microscopy, *J. Mol. Biol.* **308**, 241–261 (2001).
13. S. Takeda, A. Yamashita, K. Maeda, and Y. Maeda, Structure of the core domain of human cardiac troponin in the Ca^{2+}-saturated form, *Nature*, **424**, 35–41 (2003).
14. K. Murakami, F. Yumoto, S. Ohki, T. Yasunaga, M. Tanokura, and T. Wakabayashi, Structural basis for Ca^{2+}-regulated muscle relaxation at interaction sites of troponin with actin and tropomyosin, *J. Mol. Biol.* **352**, 178–201 (2005).
15. T. Wakabayashi, and S. Ebashi, Calcium signaling: motility (Actomyosin-Troponin system), in: *Encyclopedia of Biological Chemistry,* Vol. 1, edited by W. J. Lennarz, and M. D. Lane (Elsevier, Oxford, 2004), pp. 250–255.
16. W. Kabsch, H. G. Mannherz, D. Suck, E. F. Pai, and K. C. Holmes, Atomic structure of the actin:DNase I complex, *Nature* **347**, 37–44 (1990).
17. C. S. Farah, C. A. Miyamoto, C. H. I. Ramos, A. C. R. Dasilva, R. B. Quaggio, K. Fujimori, L. B. Smillie, and F. C. Reinach, Structural and regulatory functions of the NH- and COOH-terminal regions of skeletal-muscle troponin-I, *J. Biol. Chem.* **269**, 5230–5240 (1994).

18. Y. Luo, J. L. Wu, J. Gergely, and T. Tao, Troponin T and Ca^{2+} dependence of the distance between Cys48 and Cys133 of troponin I in the ternary troponin complex and reconstituted thin filaments, *Biochemistry* **36**, 11027–11035 (1997).
19. A. Houdusse, M. L. Love, R. Dominguez, Z. Grabarek, and C. Cohen, Structures of four Ca^{2+}-bound troponin C at 2.0 Å resolution: further insights into the Ca^{2+}-switch in the calmodulin superfamily, *Structure* **5**, 1695–1711 (1997).
20. D. G. Vassylyev, S. Takeda, S. Wakatsuki, and Y. Maeda, Crystal structure of troponin C in complex with troponin I fragment at 2.3-angstrom resolution, *Proc. Natl. Acad. Sci. USA* **95**, 4847–4852 (1998).
21. T. M. Blumenschein, D. B. Stone, R. J. Fletterick, R. A. Mendelson, and B. D. Sykes, Calcium-dependent changes in the flexibility of the regulatory domain of TnC in the troponin complex, *J. Biol. Chem.* **280**, 21924–21932 (2005).
22. R. E. Ferguson, Y. B. Sun, P. Mercier, A. S. Brack, B. D. Sykes, J. E. T. Corrie, D. R. Trentham, and M. Irving, *In situ* orientations of protein domains: troponin C in skeletal muscle fibers, *Mol. Cell* **11**, 865–874 (2003).
23. R. Maytum, F. Bathe, M. Konrad, and M. A. Geeves, Tropomyosin exon 6b is troponin-specific and required for correct acto-myosin regulation, *J. Biol. Chem.* **279**, 18203–18209 (2004).
24. P. B. Rosenthal, and R. Henderson, Optimal determination of particle orientation, absolute hand, and contrast loss in single-particle electron cryomicroscopy, *J. Mol. Biol*. **333**, 721–745 (2003).
25. W. Wriggers, and S. Birmanns, Using situs for flexible and rigid-body fitting of multiresolution single-molecule data, *J. Struct. Biol.* **133**, 193–202 (2001).
26. R. A. Milligan, Protein-protein interactions in the rigor actomyosin complex, *Proc. Natl. Acad. Sci. USA* **93**, 21–26 (1996).
27. B. Malnic, C. S. Farah, and F. C. Reinach, Regulatory properties of the NH_2- and COOH-terminal domains of troponin T. ATPase activation and binding to troponin I and troponin C, *J. Biol. Chem.* **273**, 10594–10601 (1998).
28. D. F. McKillop, and M. A. Geeves, Regulation of the interaction between actin and myosin subfragment 1: evidence for three states of the thin filament, *Biophys. J.* **65**, 693–701 (1993).
29. H. Nakamura, S. Nagashima, and T. Wakabayashi, Electrostatic field around the actin filament, in: *Synchrotron Radiation in the Biosciences*, edited by B. Chance, J. Deisenhofer, S. Ebashi, D. T. Goodhead, J. R. Helliwell, H. E. Huxley, T. Iizuka, J. Kirz, T. Mitsui, E. Rubenstein, N. Sakabe, T. Sasaki, G. Schmahl, H. B. Sturmann, K. Wütrich and G. Zaccai (Oxford University. Press, New York, 1994), pp. 502–508.

9

TROPOMYOSIN: REGULATOR OF ACTIN FILAMENTS

Sarah E. Hitchcock-DeGregori, Norma J. Greenfield and Abhishek Singh

9.1. INTRODUCTION

Cellular movement and function have long been known to depend on the actin cytoskeleton and its regulation. The actin cytoskeleton is the ultimate target of numerous cellular signaling pathways. The first signaling system understood in any detail was that of vertebrate skeletal muscle. Setsuro Ebashi, celebrated by this volume, was a pioneer through his role in showing that the calcium ion is the physiological regulator of muscle contraction followed by his landmark discovery and naming of troponin as the calcium ion receptor that regulates contraction through its interaction with tropomyosin and actin. Early work in the field is summarized in his remarkable 1968 review with M. Endo (Ebashi and Endo, 1968). There they put forth the evidence for a pathway by which activation of the muscle by an action potential would ultimately result in a contractile response consequent to the binding of calcium ion released from the sarcoplasmic reticulum to troponin bound to tropomyosin on the actin filament. The concept of a signaling cascade is now central to any thinking about signaling pathways as we attempt to understand such mechanisms at the molecular level. Whereas troponin is found only in striated muscles, tropomyosin is expressed in virtually all eucaryotic cells and is recognized to be a universal actin filament regulator, versatile in its function despite its deceptively simple coiled coil structure. In this chapter we give an overview of tropomyosin's multiple regulatory roles and insights into aspects of the structural basis for its functions, focusing on vertebrate forms. As such, this is a personal view rather than a comprehensive review that can be found elsewhere (Perry, 2001; Gunning et al., 2005).

9.2. TROPOMYOSIN, A COILED COIL ACTIN BINDING PROTEIN

Tropomyosin is a fully coiled-coil protein that cooperatively binds head-to-tail to actin filaments following the actin helix (Figure 9.1a) (Perry, 2001). Analysis of the tropomyosin sequence revealed periodicities in non-interface positions postulated to be

Department of Neuroscience and Cell Biology, Robert Wood Johnson Medical School, Piscataway, New Jersey 08854, USA

Regulatory Mechanisms of Striated Muscle Contraction
Edited by Ebashi and Ohtsuki, Springer, 2007

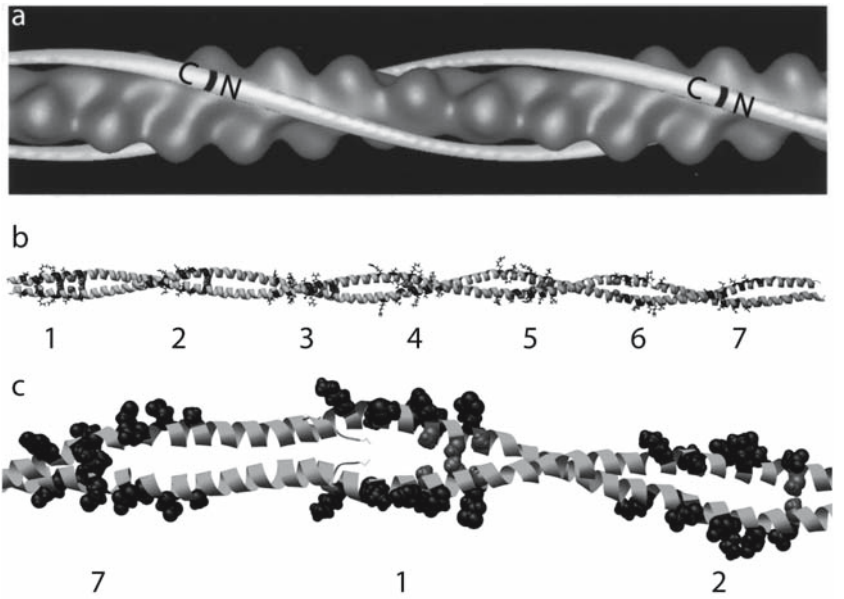

Figure 9.1. a. Surface view of the thin filament showing actin and muscle tropomyosin. The image is based on a helical image reconstruction of electron micrographs of F-actin-tropomyosin-troponin, $+Ca^{2+}$ (Xu et al., 1999). Tropomyosin forms a continuous strand along both sides of the helical actin filament such that one tropomyosin molecule spans the length of seven actin subunits. The tropomyosin molecules are associated N terminus-to-C terminus, shown on the figure. The thin filament is oriented so that the N terminus of tropomyosin and "minus" or "pointed" end of the actin filament (the end that binds tropomodulin, away from the Z-line) are at the left. Modified from a model prepared by Dr. William Lehman, Boston University School of Medicine, Boston, Massachusetts. b. Model of TM based on the 7 Å structure crystal structure, PDB entry 1C1G (Whitby and Phillips, 2000). The side chains of the periodic consensus residues are highlighted and the interface alanines within the consensus regions are space-filled. The numbers refer to the periodic repeats. c. The overlap region and the two periods on either side are enlarged, the side chains of the consensus residues and interface alanines are space-filled (Greenfield et al., 2006, J. Mol. Biol. in press).

seven quasi-equivalent actin binding sites along the length of one tropomyosin that correspond to the seven half-turns of the supercoil (Figure 9.1b) (McLachlan and Stewart, 1976; Phillips, 1986). The contribution of individual internal periodic repeats of striated muscle α-tropomyosin has been studied using deletion mutagenesis. If the five internal repeats are quasi-equivalent (the importance of the ends will be addressed below), then the consequences of deleting individual periods on actin affinity should be similar, and rather modest. Mutants with periods 2, 3, 4 or 6 deleted have similar affinities to each other, approximately 10-to-30 fold weaker than wildtype striated α-tropomyosin. However, deletion of period 5 results in loss of detectable binding (Hitchcock-DeGregori and Varnell, 1990; Hitchcock-DeGregori and An, 1996; Hammell and Hitchcock-DeGregori, 1997; Hitchcock-DeGregori et al., 2002). Similarly, substitution of tropomyosin sequence with a GCN4 leucine zipper only had severe consequences in period 5 (Hitchcock-DeGregori et al., 2002). The internal periods, when deleted singly or in multiples of two or three, do contribute in specific ways to tropomyosin's regulatory functions. For example, deletion of period 4 impairs activation of the regulated thin filament

in the presence of Ca^{2+} and activation by myosin whereas deletion of period 6 results in poor inhibition in the absence of Ca^{2+} (Landis et al., 1997; Landis et al., 1999; Tobacman and Butters, 2000; Hitchcock-DeGregori et al., 2001; Hitchcock-DeGregori et al., 2002).

What is special about period 5, a highly conserved region of tropomyosin encoded by a constitutively-expressed exon, for actin binding? In addition to the periodic repeat of non-interface residues, McLachlan and Stewart (1976) noted a periodic distribution of small non-polar amino acids (such as Ala) at the interface that they suggested would allow flexibility and bending of the tropomyosin supercoil on the actin filament helix, supported by an observed bend at an Ala cluster in a crystal structure of tropomyosin (Brown et al., 2001). While roughly periodic, the "Ala clusters" (Brown et al., 2001) or "destabilizing clusters" (Kwok and Hodges, 2004) do not always correspond to the Phillips repeats. Indeed, they are only *within* the period 1 and period 5 repeats (Figure 9.1b).

We made a series of mutants to learn if the position of the destabilizing residues within a periodic repeat is important for tropomyosin to bind to actin (Singh and Hitchcock-DeGregori, 2006). If the Ala cluster in period 5 is changed to canonical interface residues (Leu and Val), the stability of tropomyosin increases, and the actin affinity is severely weakened. The results show that local flexibility of the coiled coil is important for binding to the target actin filament. In a series of mutants designed to learn the contributions of interface instability vs the periodic consensus sequence for binding, we found that both are important. From the results we infer that periods 1 and 5, the two periods with Ala clusters within the periodic consensus repeat, contribute more to the overall actin affinity than the other five periods.

9.3. THE ENDS OF TROPOMYOSIN ARE IMPORTANT FUNCTIONAL DOMAINS

Another critical feature for tropomyosin function is the ends which are unresolved in the 7 Å crystal structure shown in Figure 9.1 (Whitby and Phillips, 2000). Encoded by alternatively-expressed exons, the ends overlap to form a complex on the actin filament that is the major mechanism for cooperative actin binding. Removal of either end results in loss of head-to-tail association, severely reduced actin affinity, and altered regulatory function (Ueno et al., 1976; Johnson and Smillie, 1977; Walsh et al., 1985; Heeley et al., 1989; Pan et al., 1989; Cho et al., 1990; Butters et al., 1993; Hammell and Hitchcock-DeGregori, 1996; Moraczewska and Hitchcock-DeGregori, 2000). Similarly, N-terminal modifications can modify the function of striated muscle tropomyosin. For example, an unacetylated N-terminal methionine reduces actin affinity and end-to-end association while the presence of additional amino acids at the N terminus can increase actin affinity (Heald and Hitchcock-DeGregori, 1988; Cho et al., 1990; Monteiro et al., 1994; Urbancikova and Hitchcock-DeGregori, 1994).

The structures of model peptides of the N terminus and the C terminus have been determined using NMR and X-ray diffraction (Greenfield et al., 1998; Brown et al., 2001; Li et al., 2002; Greenfield et al., 2003). Whereas the overlap region of the N terminus is a canonical coiled coil (Figure 9.2a), the extreme C terminus has a non-canonical, flexible structure. The helical chains are aligned in parallel in solution (Figure 9.2b) (Greenfield

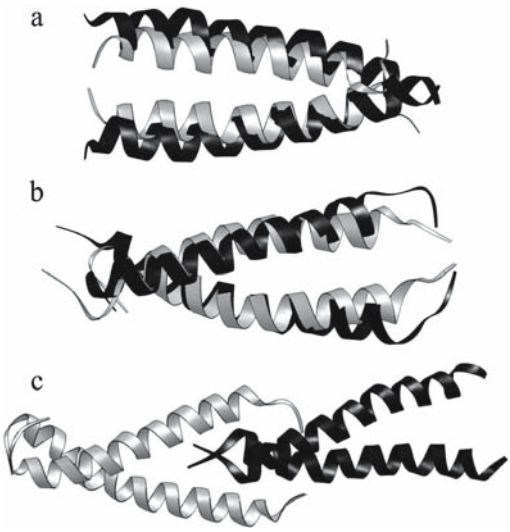

Figure 9.2. a. Comparison of the structure of the free N terminus of striated muscle tropomyosin (grey, PDB entry 1TMZ) (Greenfield et al., 1998) with the N terminus in the overlap complex (black). b. Comparison of the structure of free C terminus of striated muscle tropomyosin (grey, PDB entry 1MV4) (Greenfield et al., 2003) with the C terminus in the overlap complex (black). c. The overlap complex showing the C terminus (grey) and N terminus (black), (Greenfield et al., 2006, J. Mol. Biol. in press).

et al., 2003) and are splayed apart in the crystal structure consequent to binding the C terminus of another molecule (Li et al., 2002).

The structures of both the N terminus and C terminus change upon complex formation (Figure 9.2). The greatest change is in the C-terminal chains that splay apart, similar to the arrangement observed in the crystal structure of the C terminus alone, to accommodate the canonical N terminus (Figure 9.2b) (Greenfield et al., 2006). The ends overlap by 11 residues and the chains interlock in the complex: residues 1–11 at the N terminus and residues 274–284 at the C terminus (Figure 9.2c). Non-canonical interface residues not in the actual overlap region allow the flexibility for the C-terminal chains to separate and bind to the N terminus. Flexibility is required for complex formation. For example, mutation of Gln 263 at a *d* position to Leu, a canonical interface residue, reduces the ability of the C-terminal model peptide to bind to the N-terminal peptide and to form a ternary complex with a troponin T peptide (Greenfield et al., 2002). The N-terminal chains separate slightly to interact with the splayed C-terminal chains (Figure 9.2a). The resulting four-chained structure is flexible, and different from that of other four-helix bundles.

9.3.1. Significance of the Overlap Structure for Actin Binding and Regulatory Function

Knowledge of the structure and geometry of the overlap complex gives insights into the mechanisms of actin binding and regulatory functions of tropomyosin. In the overlap complex the observed planes of the N-terminal and C-terminal coiled coils are oriented

perpendicular to each other and the chains from the two ends interlock rather than form a planar overlap complex as in the McLachlan and Stewart model (1976). A consequence of the observed arrangement is that the postulated actin binding sites on the continuing cable of tropomyosin molecules would maintain the same orientation with respect to the actin filament. The consensus residues of period 1 start in the overlap region at residue 6, and those of period 7 end at residue 262, just before the overlap region (Figure 9.1c). The consensus sequences of two consecutive tropomyosin molecules would each have the same interactions with the actin monomers along its length. If the ends were to overlap in a planar fashion, only alternating tropomyosin molecules would have equivalent binding.

There is another interesting, and possibly significant consideration: in tropomyosins where the two chains are encoded by different genes, such as in αβ-tropomyosin found in vertebrate striated muscles, the site facing an actin monomer would come from alternate chains in sequential tropomyosin molecules on the filament since each period corresponds to a half-turn of the tropomyosin coiled coil. For example, site 5 of tropomyosin would come from the α-tropomyosin chain of one molecule and from the β-tropomyosin chain of the adjacent tropomyosin molecule on the actin filament. Similarly the orientation of the ends has structural consequences for the binding of troponin that spans from the middle of the molecule to the C terminus and includes the N terminus of the next molecule (Flicker et al., 1982; Hitchcock-DeGregori et al., 1988). This arrangement would seem to be important for cooperative regulation of cellular functions by tropomyosin, in particular Ca^{2+} regulation of muscle contraction by troponin-tropomyosin.

9.4. MULTIPLE FUNCTIONS FOR TROPOMYOSIN

Cooperative binding to actin filaments is a universal property of tropomyosin, and its presence alters the actin filament making it a cooperative structure. One fundamental effect of tropomyosin binding is to stiffen and mechanically stabilize the actin filament, modifying filament dynamics, as originally discovered in the Oosawa group (Fujime and Ishiwata, 1971). One consequence of a stiffer filament is that it is less susceptible to internal destabilization and severing by DNase I, gelsolin and cofilin, and nucleation of branches by the Arp2/3 complex (Hitchcock et al., 1976; Ishikawa et al., 1989; Bamburg, 1999; Blanchoin et al., 2001). Tropomyosin inhibits the binding of gelsolin and cofilin, as well as filament cross-linking proteins, to actin. Tropomyosin also inhibits depolymerization at the pointed, slow-growing end of the filament where, in striated muscles and red blood cells, it binds with tropomodulin to cap the pointed end (Broschat, 1990; Kostyukova and Hitchcock-DeGregori, 2004). In sum, tropomyosin stabilizes actin filaments by physically stiffening the filament as well as by inhibiting the activity of proteins that themselves destabilize actin. It is not surprising, therefore, that tropomyosin is absent from the leading edge, or lamellipodium, of cells where forward movement depends on rapid actin polymerization, the cofilin-dependent severing to create new ends, and Arp2/3-nucleated actin filaments (DesMarais et al., 2002).

The other crucial function of tropomyosin is its role in regulation. As detailed in other chapters in this volume, tropomyosin binds to troponin and is responsible for the cooperative activation of the striated muscle thin filament by Ca^{2+} and myosin. By its

interaction with troponin T in the troponin complex, tropomyosin positions troponin on the thin filament and determines the stoichiometry of one troponin per seven actins reviewed in (Perry, 2001). Tropomyosin also, through the end-to-end association that is strengthened *in vitro* by troponin, allows for the activation by Ca^{2+} to be cooperative, carrying the information along the actin filament by the lengths of multiple tropomyosin molecules. In smooth muscle and non-muscle cells, caldesmon acts through tropomyosin to regulate actin function, reviewed in (Wang, 2001).

It is now well-established that myosin binding to actin, in addition to Ca^{2+} binding to troponin C, cooperatively activates contraction (Bremel and Weber, 1972; Gordon et al., 2000). The cooperativity also depends on tropomyosin: tropomyosin increases the affinity of myosin heads for actin, and myosin increases the affinity of tropomyosin for actin (Eaton, 1976; Cassell and Tobacman, 1996). In the presence of tropomyosin, sub-stoichiometric amounts of myosin can activate the filament (Ishii and Lehrer, 1990; Geeves and Lehrer, 1994). While the specific effect of tropomyosin on myosin depends on the tropomyosin and the myosin isoforms, an effect, whether it be positive as in the case of skeletal proteins (Geeves and Lehrer, 1994), or negative in the case of certain non-muscle tropomyosins and actin (eg. (Tang and Ostap, 2001), is universal and can be considered a basic tropomyosin function. How it happens, however, remains to be resolved since a direct interaction between myosin and tropomyosin has never been convincingly demonstrated. Their binding sites on the actin filament are sufficiently close to suppose it would be a possibility.

9.5. MULTIPLE ISOFORMS OF TROPOMYOSIN

Tropomyosins are a family of coiled coil proteins highly conserved throughout phylogeny, yet with versatile cellular localizations and functions (Gunning et al., 2005). Developmentally regulated and tissue-specific expression of multiple genes (four in vertebrates) and alternatively spliced exons allows for isoform diversity. Additional variation can result from pairing of chains as homodimers or heterodimers in the two-chained coiled coil. The understanding of how different tropomyosin isoforms function differently is little understood, yet of biological and medical signficance. Similarly, isoform-specific tropomyosin binding proteins may remain to be discovered. While this is not the place for an extensive review of the subject, highlighting a few examples will serve to illustrate the scope of the relatively uncharted territory.

In vertebrates there are four tropomyosin genes, and many more isoforms result from alternative promoters and alternative exon splicing (Gunning et al., 2005). They are classified as short and long isoforms, with ~246 and ~284 residues, respectively, the result of alternative promotors. The alternative splicing of exons results in additional isoforms. In the TPM-1 gene (α-tropomyosin gene), for example, four of nine exons are alternatively-expressed exons, resulting in nine known tropomyosins (Figure 9.3). In all, the four vertebrate genes are known to express 23 polypeptides that could assemble into 23 different homodimers, and many more possible heterodimers, a number that is calculable but large. Most of these tropomyosins are expressed in non-muscle cells, and their specific functions are unknown. However, in certain cases they are known to affect cellular function in marked ways.

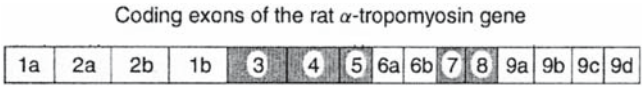

Figure 9.3. Schematic diagram of coding exons in the rat α-tropomyosin gene (Tpm1). Each block corresponds to a coding exon. Shaded exons are constitutively expressed in all tropomyosin isoforms; open blocks are alternatively expressed where one lettered exon is selected. The exon 9s are in their designated alphabetical order, not their order in genomic DNA. Exons 1a and exon 2a or 2b are expressed in long tropomyosins. In short tropomyosins exon 1b replaces exons 1a and 2 as a consequence of an alternate promotor.

9.5.1. Isoform-Specific Anti-Oncogenetic Effects of Tropomyosin

It has long been known that the reorganization of the cytoskeleton resulting in loss of stress fibers associated with malignant transformation of cells is correlated with down-regulation of high molecular weight tropomyosins and up-regulation of low molecular weight tropomyosins (Hendricks and Weintraub, 1981; Matsumura et al., 1983a; Cooper et al., 1985). The role of specific tropomyosin isoforms in regulating the neoplastic phenotype had been investigated in detail in breast carcinoma cells, as well as virally-transformed cell lines, by G.L.Prasad and his colleagues. TM1, encoded by the β- tropomyosin gene, widely-expressed in cells and smooth muscle, is down-regulated in primary breast tumors (Raval et al., 2003). The malignant phenotype is suppressed by expression of TM1 in transformed cells, resulting in restoration of stress fibers and inhibition of anchorage-independent growth (Braverman et al., 1996; Mahadev et al., 2002). The N-terminal sequence, but not the C-terminal sequence, is required for suppression of the neoplastic phenotype (Bharadwaj et al., 2005). What is striking is that TM2, a product of the α-tropomyosin gene, also widely-expressed in cells and smooth muscle, does not suppress the malignant phenotype (Braverman et al., 1996; Raval et al., 2003), though this may depend on the cell type (Gimona et al., 1996). How these two isoforms have such different effects on the cytoskeleton and cellular behavior is not understood.

9.5.2. Isoform-Specific Cellular Localizations of Tropomyosins and Their Effects on Cell Shape

Actin participates in diverse cellular functions, and it has been known for many years that the composition of actin filaments differs according to their functions and location within the cell (Matsumura et al., 1983b; Lin et al., 1988). Tropomyosin, which modifies the stability of tropomyosin and the ability of proteins to bind to actin, has a "ground floor" role in defining actin filament diversity. Gunning, Helfman and Lin and their colleagues have taken a lead in identifying and studying the localization of tropomyosin isoforms in cells through their development of specific antibodies, and found that over-expression of particular isoforms can dramatically affect cell shape, reviewed in (Gunning et al., 2005). Tropomyosin expression is developmentally regulated and many isoforms are tissue specific.

An example of how tropomyosin can dramatically affect cell shape is illustrated by the work of Bryce et al. (Bryce et al., 2003). Overexpression of two different isoforms in a neuroepithelial cell line has different effects on cell morphology and cell behavior. One widely-expressed isoform encoded by the γ-gene (TM5NM1) reduces the size of the

lamellipodium and the rate of cell migration while promoting the formation of stress fibers. In contrast, TMBr3, a brain-specific isoform encoded by the α-TM gene, increases the size of the lamellipodium, suppresses stress fibers, and increases the rate of cell motility. How these tropomyosins can essentially redirect the actin cytoskeleton is not understood, but certainly other proteins must be involved.

A particularly dramatic illustration of the specificity of tropomyosin targeting involves TM5NM1 that is found in stress fibers. Another tropomyosin encoded by the same gene that differs in only one exon, called TM5NM2, is localized to Golgi (Percival et al., 2004). These tropomyosins differ only in the sequence encoded by exon 6a (the α-TM equivalent of exons 6a and 6b shown in Figure 9.3). Again, the mechanism and functional importance are unknown.

9.5.3. Tropomyosin as a Regulator of the Mechanism of Cell Migration

The role of tropomyosin in regulating muscle contraction is well-established, but how it controls the organization of the cytoskeleton and cellular motility in living cells is poorly understood. Since the ends are so important for function, the use of fluorescent proteins, such as GFP, to localize the protein in living cells has been limited. Also there are no drugs that target tropomyosin as there are for actin filaments and microtubules.

Following from the overexpression work from the Gunning lab (for example (Bryce et al., 2003)), Gupton et al. showed that introduction of an exogenous tropomyosin into cells dramatically changes the dynamics of the actin cytoskeleton (analyzed using fluorescence speckle microscopy) and cell motility (Gupton et al., 2005). The lamellipodium of cells contains dynamic actin filaments with high concentrations of Arp2/3 complex and cofilin whereas deeper in the cell, as in the lamella, there are more stable filaments that contain tropomyosin and myosin II. Microinjection of skeletal muscle tropomyosin depletes Arp2/3 complex and cofilin from the lamellipodium but the cells still protrude at the leading edge and exhibit rapid cell migration. The tropomyosin-containing filaments are accompanied by myosin II, which is required for the cell migration. That is, the mechanism of cell migration changes from actin polymerization-driven to actin-myosin interaction-driven. Fluorescence speckle microscopy showed that tropomyosin altered the F-actin kinematics: it inhibited the rapid polymerization/depolymerization of actin filaments at the leading edge associated with dendritic nucleation of filaments by Arp2/3 complex coupled with cofilin severing (Pollard and Borisy, 2003). The results are consistent with the *in vitro* inhibition of Arp2/3 complex nucleation and cofilin severing by tropomyosin (Blanchoin et al., 2001; DesMarais et al., 2002).

9.6. CONCLUSIONS

In this brief review we have discussed some of the recent work and questions that involve tropomyosin and its regulatory function. Compared to troponin, in its middle age at 40 years, tropomyosin is a senior citizen. Indeed its golden years do indeed promise to be golden. With structures becoming available we are gaining insight into how a "simple" coiled coil can be so complex in its function. However, as ever in science, as we learn more we realize how little we know. How does tropomyosin make the thin filament cooperative? How does it communicate the signal of Ca^{2+} binding to troponin C along the thin filament? What are all those isoforms doing in non-muscle cells? Do

specific tropomyosins regulate specific myosins? Are there more binding partners? How are tropomyosins targeted to specific cytoskeletal domains – via the protein or the messenger RNA? Do some tropomyosin isoforms function other than on an actin filament? Answers will come from studies in model organisms using genetics (not reviewed here), molecular biology and biophysics, and live cell imaging studies.

9.7. ACKNOWLEDGMENTS

This research was supported by grants from the National Institutes of Health, RO1-GM36326 and RO1-GM63257.

9.8. REFERENCES

Bamburg, J. R., 1999, Proteins of the ADF/cofilin family: essential regulators of actin dynamics. *Annu. Rev. Cell Dev. Biol.* **15**:185–230.

Bharadwaj, S., Shah, V., Tariq, F., Damartoski, B., and Prasad, G. L., 2005, Amino terminal, but not the carboxy terminal, sequences of tropomyosin-1 are essential for the induction of stress fiber assembly in neoplastic cells. *Cancer Lett.* **229**:253–260.

Blanchoin, L., Pollard, T. D., and Hitchcock-DeGregori, S. E., 2001, Inhibition of the Arp2/3 complex-nucleated actin polymerization and branch formation by tropomyosin. *Curr. Biol.* **11**:1300–1304.

Braverman, R. H., Cooper, H. L., Lee, H. S., and Prasad, G. L., 1996, Anti-oncogenic effects of tropomyosin: isoform specificity and importance of protein coding sequences. *Oncogene* **13**:537–545.

Bremel, R. D., and Weber, A., 1972, Cooperation within actin filament in vertebrate skeletal muscle. *Nat. New Biol.* **238**:97–101.

Broschat, K. O., 1990, Tropomyosin prevents depolymerization of actin filaments from the pointed end. *J. Biol. Chem.* **265**:21323–21329.

Brown, J. H., Kim, K. H., Jun, G., Greenfield, N. J., Dominguez, R., Volkmann, N., Hitchcock-DeGregori, S. E., and Cohen, C., 2001, Deciphering the design of the tropomyosin molecule. *Proc. Natl. Acad. Sci. USA* **98**:8496–8501.

Bryce, N. S., Schevzov, G., Ferguson, V., Percival, J. M., Lin, J. J., Matsumura, F., Bamburg, J. R., Jeffrey, P. L., Hardeman, E. C., Gunning, P., and Weinberger, R. P., 2003, Specification of actin filament function and molecular composition by tropomyosin isoforms. *Mol. Biol. Cell* **14**:1002–1016.

Butters, C. A., Willadsen, K. A., and Tobacman, L. S., 1993, Cooperative interactions between adjacent troponin-tropomyosin complexes may be transmitted through the actin filament. *J. Biol. Chem.* **268**:15565–15570.

Cassell, M., and Tobacman, L. S., 1996, Opposite effects of myosin subfragment 1 on binding of cardiac troponin and tropomyosin to the thin filament. *J. Biol. Chem.* **271**:12867–12872.

Cho, Y. J., Liu, J., and Hitchcock-DeGregori, S. E., 1990, The amino terminus of muscle tropomyosin is a major determinant for function. *J. Biol. Chem.* **265**:538–545.

Cooper, H. L., Feuerstein, N., Noda, M., and Bassin, R. H., 1985, Suppression of tropomyosin synthesis, a common biochemical feature of oncogenesis by structurally diverse retroviral oncogenes. *Mol. Cell. Biol.* **5**:972–983.

DesMarais, V., Ichetovkin, I., Condeelis, J., and Hitchcock-DeGregori, S. E., 2002, Spatial regulation of actin dynamics: a tropomyosin-free, actin-rich compartment at the leading edge. *J. Cell Sci.* **115**: 4649–4660.

Eaton, B. L., 1976, Tropomyosin binding to F-actin induced by myosin heads. *Science* **192**:1337–1339.

Ebashi, S., and Endo, M., 1968, Calcium Ion and Muscle Contraction. *Prog. Biophys. Mol. Biol.* **18**: 125–183.

Flicker, P. F., Phillips, G. N., Jr., and Cohen, C., 1982, Troponin and its interactions with tropomyosin. An electron microscope study. *J. Mol. Biol.* **162**:495–501.

Fujime, S., and Ishiwata, S., 1971, Dynamic study of F-actin by quasielastic scattering of laser light. *J. Mol. Biol.* **62**:251–265.

Geeves, M. A., and Lehrer, S. S., 1994, Dynamics of the muscle thin filament regulatory switch: the size of the cooperative unit. *Biophys. J.* **67**:273–282.

Gimona, M., Kazzaz, J. A., and Helfman, D. M., 1996, Forced expression of tropomyosin 2 or 3 in v-Ki-ras-transformed fibroblasts results in distinct phenotypic effects. *Proc. Natl. Acad. Sci. USA* **93**:9618–9623.

Gordon, A. M., Homsher, E., and Regnier, M., 2000, Regulation of contraction in striated muscle. *Physiol. Rev.* **80**:853–924.

Greenfield, N. J., Montelione, G. T., Farid, R. S., and Hitchcock-DeGregori, S. E., 1998, The structure of the N-terminus of striated muscle alpha-tropomyosin in a chimeric peptide: nuclear magnetic resonance structure and circular dichroism studies. *Biochemistry* **37**:7834–7843.

Greenfield, N. J., Palm, T., and Hitchcock-DeGregori, S. E., 2002, Structure and interactions of the carboxyl terminus of striated muscle α-tropomyosin: It is important to be flexible. *Biophys. J.* **83**:2754–2766.

Greenfield, N. J., Swapna, G. V., Huang, Y., Palm, T., Graboski, S., Montelione, G. T., and Hitchcock-DeGregori, S. E., 2003, The structure of the carboxyl terminus of striated alpha-tropomyosin in solution reveals an unusual parallel arrangement of interacting alpha-helices. *Biochemistry* **42**:614–619.

Gunning, P. W., Schevzov, G., Kee, A. J., and Hardeman, E. C., 2005, Tropomyosin isoforms: divining rods for actin cytoskeleton function. *Trends Cell Biol.* **15**:333–341.

Gupton, S. L., Anderson, K. L., Kole, T. P., Fischer, R. S., Ponti, A., Hitchcock-DeGregori, S. E., Danuser, G., Fowler, V. M., Wirtz, D., Hanein, D., and Waterman-Storer, C. M., 2005, Cell migration without a lamellipodium: translation of actin dynamics into cell movement mediated by tropomyosin. *J. Cell. Biol.* **168**:619–631.

Hammell, R. L., and Hitchcock-DeGregori, S. E., 1996, Mapping the functional domains within the carboxyl terminus of alpha-tropomyosin encoded by the alternatively spliced ninth exon. *J. Biol. Chem.* **271**:4236–4242.

Hammell, R. L., and Hitchcock-DeGregori, S. E., 1997, The sequence of the alternatively spliced sixth exon of alpha-tropomyosin is critical for cooperative actin binding but not for interaction with troponin. *J. Biol. Chem.* **272**:22409–22416.

Heald, R. W., and Hitchcock-DeGregori, S. E., 1988, The structure of the amino terminus of tropomyosin is critical for binding to actin in the absence and presence of troponin. *J. Biol. Chem.* **263**:5254–5259.

Heeley, D. H., Smillie, L. B., and Lohmeier-Vogel, E. M., 1989, Effects of deletion of tropomyosin overlap on regulated actomyosin subfragment 1 ATPase. *Biochem. J.* **258**:831–836.

Hendricks, M., and Weintraub, H., 1981, Tropomyosin is decreased in transformed cells. *Proc. Natl. Acad. Sci. USA* **78**:5633–5637.

Hitchcock, S. E., Carisson, L., and Lindberg, U., 1976, Depolymerization of F-actin by deoxyribonuclease I. *Cell* **7**:531–542.

Hitchcock-DeGregori, S. E., and An, Y., 1996, Integral repeats and a continuous coiled coil are required for binding of striated muscle tropomyosin to the regulated actin filament. *J. Biol. Chem.* **271**:3600–3603.

Hitchcock-DeGregori, S. E., Lewis, S. F., and Mistrik, M., 1988, Lysine reactivities of tropomyosin complexed with troponin. *Arch. Biochem. Biophys.* **264**:410–416.

Hitchcock-DeGregori, S. E., Song, Y., and Greenfield, N. J., 2002, Functions of tropomyosin's periodic repeats. *Biochemistry* **41**:15036–15044.

Hitchcock-DeGregori, S. E., Song, Y., and Moraczewska, J., 2001, Importance of internal regions and the overall length of tropomyosin for actin binding and regulatory function. *Biochemistry* **40**:2104–2112.

Hitchcock-DeGregori, S. E., and Varnell, T. A., 1990, Tropomyosin has discrete actin-binding sites with sevenfold and fourteenfold periodicities. *J. Mol. Biol.* **214**:885–896.

Ishii, Y., and Lehrer, S. S., 1990, Excimer fluorescence of pyrenyliodoacetamide-labeled tropomyosin: a probe of the state of tropomyosin in reconstituted muscle thin filaments. *Biochemistry* **29**:1160–1166.

Ishikawa, R., Yamashiro, S., and Matsumura, F., 1989, Differential modulation of actin-severing activity of gelsolin by multiple isoforms of cultured rat cell tropomyosin. Potentiation of protective ability of tropomyosins by 83-kDa nonmuscle caldesmon. *J. Biol. Chem.* **264**:7490–7497.

Johnson, P., and Smillie, L. B., 1977, Polymerizability of rabbit skeletal tropomyosin: effects of enzymic and chemical modifications. *Biochemistry* **16**:2264–2269.

Kostyukova, A. S., and Hitchcock-DeGregori, S. E., 2004, Effect of the structure of the N terminus of tropomyosin on tropomodulin function. *J. Biol. Chem.* **279**:5066–5071.

Kwok, S. C., and Hodges, R. S., 2004, Stabilizing and destabilizing clusters in the hydrophobic core of long two-stranded alpha-helical coiled-coils. *J. Biol. Chem.* **279**:21576–21588.

Landis, C., Back, N., Homsher, E., and Tobacman, L. S., 1999, Effects of tropomyosin internal deletions on thin filament function. *J. Biol. Chem.* **274**:31279–31285.

Landis, C. A., Bobkova, A., Homsher, E., and Tobacman, L. S., 1997, The active state of the thin filament is destabilized by an internal deletion in tropomyosin. *J. Biol. Chem.* **272**:14051–14056.

Li, Y., Mui, S., Brown, J. H., Strand, J., Reshetnikova, L., Tobacman, L. S., and Cohen, C., 2002, The crystal structure of the C-terminal fragment of striated-muscle alpha-tropomyosin reveals a key troponin T recognition site. *Proc. Natl. Acad. Sci. USA* **99**:7378–7383.

Lin, J. J., Hegmann, T. E., and Lin, J. L., 1988, Differential localization of tropomyosin isoforms in cultured nonmuscle cells. *J. Cell. Biol.* **107**:563–572.

McLachlan, A. D., and Stewart, M., 1976, The 14-fold periodicity in alpha-tropomyosin and the interaction with actin. *J. Mol. Biol.* **103**:271–298.

Mahadev, K., Raval, G., Bharadwaj, S., Willingham, M. C., Lange, E. M., Vonderhaar, B., Salomon, D., and Prasad, G. L., 2002, Suppression of the transformed phenotype of breast cancer by tropomyosin-1. *Exp. Cell Res.* **279**:40–51.

Matsumura, F., Lin, J. J., Yamashiro-Matsumura, S., Thomas, G. P., and Topp, W. C. (1983a). Differential expression of tropomyosin forms in the microfilaments isolated from normal and transformed rat cultured cells. *J. Biol. Chem.* **258**:13954–13964.

Matsumura, F., Yamashiro-Matsumura, S., and Lin, J. J. (1983b). Isolation and characterization of tropomyosin-containing microfilaments from cultured cells. *J. Biol. Chem.* **258**:6636–6644.

Monteiro, P. B., Lataro, R. C., Ferro, J. A., and Reinach, F. C., 1994, Functional alpha tropomyosin produced in Escherichia coli. A dipeptide extension can substitute the amino-terminal acetyl group. *J. Biol. Chem.* **269**.

Moraczewska, J., and Hitchcock-DeGregori, S. E., 2000, Independent functions for the N- and C-termini in the overlap region of tropomyosin. *Biochemistry* **39**:6891–6897.

Pan, B. S., Gordon, A. M., and Luo, Z. X., 1989, Removal of tropomyosin overlap modifies cooperative binding of myosin S-1 to reconstituted thin filaments of rabbit striated muscle. *J. Biol. Chem.* **264**:8495–8498.

Percival, J. M., Hughes, J. A., Brown, D. L., Schevzov, G., Heimann, K., Vrhovski, B., Bryce, N., Stow, J. L., and Gunning, P. W., 2004, Targeting of a tropomyosin isoform to short microfilaments associated with the Golgi complex. *Mol. Biol. Cell* **15**:268–280.

Perry, S. V., 2001, Vertebrate tropomyosin: distribution, properties and function. *J. Muscle Res. Cell Motil.* **22**:5–49.

Phillips, G. N., Jr., 1986, Construction of an atomic model for tropomyosin and implications for interactions with actin. *J. Mol. Biol.* **192**:128–131.

Pollard, T. D., and Borisy, G. G., 2003, Cellular motility driven by assembly and disassembly of actin filaments. *Cell* **112**:453–465.

Raval, G. N., Bharadwaj, S., Levine, E. A., Willingham, M. C., Geary, R. L., Kute, T., and Prasad, G. L., 2003, Loss of expression of tropomyosin-1, a novel class II tumor suppressor that induces anoikis, in primary breast tumors. *Oncogene* **22**:6194–6203.

Singh, A., and Hitchcock-DeGregori, S. E., 2006, Dual requirement for flexibility and specificity for binding of the coiled coil tropomyosin to its target, actin. *Structure*, **14**:43–50.

Tang, N., and Ostap, E. M., 2001, Motor domain-dependent localization of myo1b (myr-1). *Curr. Biol.* **11**:1131–1135.

Tobacman, L. S., and Butters, C. A., 2000, A new model of cooperative myosin-thin filament binding [In Process Citation]. *J. Biol. Chem.* **275**:27587–27593.

Ueno, H., Tawada, Y., and Ooi, T., 1976, Properties of non-polymerizable tropomyosin obtained by carboxypeptidase A digestion. *J. Biochem. (Tokyo)* **80**:283–290.

Urbancikova, M., and Hitchcock-DeGregori, S. E., 1994, Requirement of amino-terminal modification for striated muscle alpha- tropomyosin function. *J. Biol. Chem.* **269**:24310–24315.

Walsh, T. P., Trueblood, C. E., Evans, R., and Weber, A., 1985, Removal of tropomyosin overlap and the co-operative response to increasing calcium concentrations of the acto-subfragment-1 ATPase. *J. Mol. Biol.* **182**:265–269.

Wang, C. L., 2001, Caldesmon and smooth-muscle regulation. *Cell Biochem. Biophys.* **35**:275–88.

Whitby, F. G., and Phillips, G. N., Jr., 2000, Crystal structure of tropomyosin at 7 Angstroms resolution. *Proteins* **38**:49–59.

Xu, C., Craig, R., Tobacman, L., Horowitz, R., and Lehman, W., 1999, Tropomyosin positions in regulated thin filaments revealed by cryoelectron microscopy. *Biophys. J.* **77**:985–992.

10

TROPOMYOSIN AND TROPONIN COOPERATIVITY ON THE THIN FILAMENT

Sabrina E. Boussouf and Michael A. Geeves

10.1. INTRODUCTION

The regulation of muscle contraction by the thin filament proteins tropomyosin (Tm) and troponin (Tn) has remained an area of interest since the proteins were first discovered 40 years ago.[1,2] Although we have learnt a great deal about the proteins themselves and the mechanism by which they regulate muscle contraction some aspects of the mechanism remain to be adequately explained. Our interest is in the cooperativity of the calcium regulatory process and this remains poorly understood and several different models have been proposed. At it simplest the essence of the problem can be simply outlined. In skeletal muscle the binding of calcium to the two regulatory sites of TnC is required for activation of muscle contraction. Isolated TnC binds the calcium cooperatively, as might be expected for a two-calcium-ion switch, with a hill coefficient (h) of between 1 & 2.[3,4] In contrast the calcium activation of isometric force in a skinned muscle fibre occurs with a much larger hill coefficient[5,6] leading to the idea that cooperativity extends beyond the single actin$_7$TmTn structural unit of the thin filament. Some models of muscle activation suggest the whole filament switches as a single unit while studies of the purified proteins in solution tend to indicate more limited cooperativity extending to only the nearest neighbour actin$_7$TmTn units. In this paper the reasons why the nature of the cooperativity remains a problem will be explored together with an overview of what our recent studies of the proteins in solution have revealed about thin filament cooperativity.

10.2. THE THREE STATES OF THE THIN FILAMENT AS SEEN BY MYOSIN AND THE NATURE OF THE COOPERATIVITY

To begin to explain why cooperativity has been a difficult problem to understand it is important to describe the complexity of the problem. To define the cooperativity we need to know what all of the significant components of the thin filament are; defined here as actin, Tm, the three subunits of Tn, (TnC, TnI and TnT) and myosin heads (or in solu-

Department of Biosciences, University of Kent, CT5 7NJ, UK

Regulatory Mechanisms of Striated Muscle Contraction
Edited by Ebashi and Ohtsuki, Springer, 2007

tion subfragment 1 or S1). We assume the other ancillary proteins of the sarcomere are not playing a major role in the event discussed here.

Next we need to know which of the proteins interact directly with each other. While these are reasonably well defined, not all are known. For example TnI has a calcium dependent interaction with TnC and an interaction with actin such that in the absence of calcium TnI binds weakly to TnC and strongly to actin. When calcium is bound to TnC the interaction with TnI becomes much stronger and disrupts the actin-TnI interaction. The recent crystal structures of Tn with and without calcium[7,8] have led to a simple picture of how this competition between actin and TnC for TnI might work at a structural level and this is shown as a pair of coupled equilibria in Figure 10.1 (see other chapters in this volume). In Figure 10.1. TnC and TnI are both shown as having two conformations and actin is shown playing a passive role. This may not be true, actin itself may undergo conformation changes but the evidence on this is still being debated (see below). The model in Figure 10.1. is adequate to explain some aspects of the calcium regulation switch but calcium binding to TnC can also be influenced by Tm, by TnT and by myosin. There must therefore be direct or indirect interactions between TnC and each of these proteins.

If the interactions between the components are defined and the number of conformations of each the component is defined then the total number of possible states can be calculated i.e. the total number of possible states of the thin filament regulatory unit. If for example TnC, TnI, TnT and Tm all had two possible conformations then there are $2^4 = 16$ possible combinations of states. Not all of these states will exist in the contracting muscle. Defining which are the significant states is one of the issues.

One reason why different views on the cooperativity arise is because the number of important states observed will depend upon what methods are used. These can be very different if observed by structural methods such as electron microscopy,[9] X-ray crystallography,[7,8] or NMR.[4] Different again when using fluorescent probes attached to the proteins[10–12] and different again when using a functional assay such as ATPase measurements,[13,14] motility assays[15,16] or isometric force development.[5,6]

Using assays which monitor the strong binding of myosin heads to thin filaments we have defined 3-functional states of the thin filament. These are now referred to as the

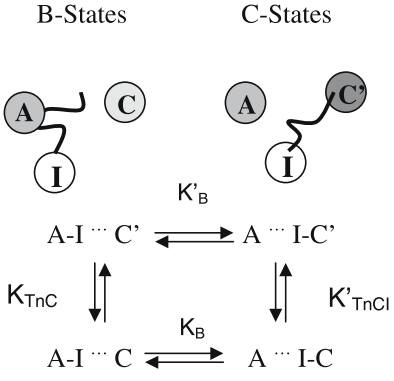

Figure 10.1. Conformational coupling between TnC, TnI and actin. If TnC has two conformations C and C′ with a calcium dependent equilibrium between the two, K_{TnC} (= [C]/[C′]) where C′ is the preferred form in the presence of calcium and C in the absence. Then the equilibrium constant K_B = [A + I-C]/[A-I + C] lies to the left i.e. the B state is preferred in which TnI interacts strongly with actin and weakly with TnC. In contrast K'_B lies to the right and C-states dominate in which TnI interacts strongly with TnC and weakly with actin.

B-state (*Blocked*, in which little productive binding of myosin to actin takes place); the C-state (*Closed* or calcium induced, in which myosin can bind relatively weakly to actin) and M-state (myosin induced or *Open,* in which productive, strong binding can occur). The model is illustrated in Figure 10.2a for a single actin monomer. The names of the three states have been modified since the model was originally proposed to emphasise the correspondence with the three actin.Tm structural states identified from helical imaging of electron micrographs of actin filaments.[17]

The cooperativity observed for myosin binding to actinTmTn filaments is illustrated in Figure 10.2b, which shows the 3-state model for a single actin$_7$TmTn structural unit. This illustrates the coupled equilibria between the three thin filament states and the equilibria for myosin binding. Thus in this illustration a single myosin head binding strongly to a specific actin can switch on the whole structural unit. If the K_B, B-to-C state switch described here is the same as the B-to-C switch illustrated for actin.TnI.TnC in Figure 10.1 then this provides a way to explain how the equilibria for myosin binding and calcium binding are coupled and therefore influence each other.

The problem in defining the cooperativity for a filament arises because there is no isolated structural or cooperative unit in the filament; the filament is continuous. The situation is more complex than the familiar cooperativity defined for oxygen binding to hemoglobin where each protein unit is an isolated independent tetramer. For the thin filament the real structural unit is 14 actins with two TmTn complexes because each Tm only

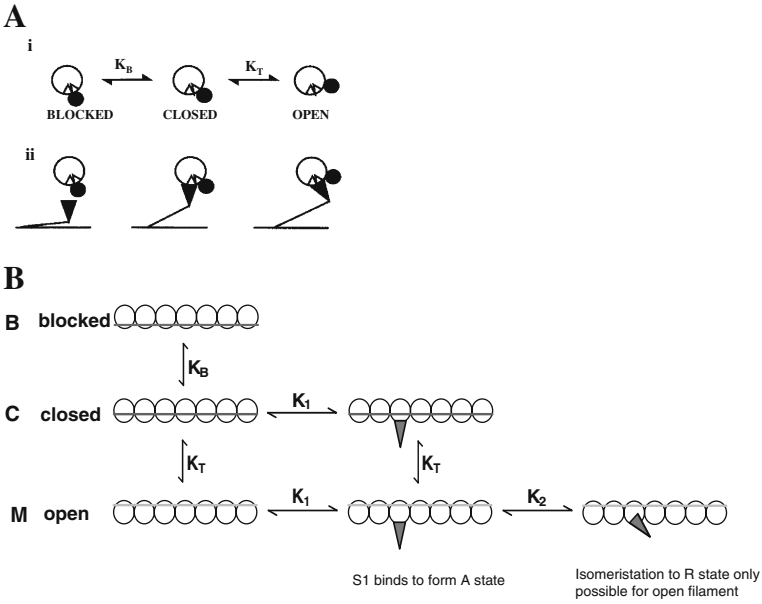

Figure 10.2. The 3-state model of thin filament regulation. (A) As seen from a single action monomer. i. The equilibrium between the three states in the absence of myosin. In the presence of calcium K_B >10 and K_T = 0.2. In the absence of calcium these are reduced to 0.3 and ≤0.2 respectively. ii. The binding of myosin heads to the three states. (B) The three states of the thin filament at the level of a single actin$_7$TmTn structural unit. The original names for the 3-states are given alongside the states with the one letter abbreviation used to correlate with the 3-structural states observed from electron micrographs.[17] See text for details.

interacts with one side of the actin filament. The Tm molecules polymerise head to tail along the actin filament and remain in direct contact with each other even when the average position of Tm on the surface of actin changes. Actins are also in contact with each other, these actin-actin and Tm-Tm contacts provide a route for continuous information exchange along the filament. As soon as the experimental data suggests that the cooperativity is greater than that which can be accounted for by a single structural unit the models for longer-range interaction become important. Three related classes of models have been proposed for longer-range cooperativity along an actin filament. The original model was proposed by T. L. Hill[18] in which TmTn units change state individually and in doing so influence the nearest neighbour TmTn structural units. This model was successful at defining equilibrium myosin binding data and has been extended in recent years to kinetic data for myosin binding by Chalovich and collaborators.[19] The original McKillop and Geeves[20] version of the 3-state model dealt only with the single isolated structural unit as the data at the time did not require longer-range cooperativity. In later versions the concept of an apparent cooperative unit *n* was introduced which, for a filament with few myosins bound, represents the averaged number of actin sites activated by the binding of a single myosin head to an actin filament. This model proposed that the signal propagation occurred through the continuous Tm-Tm strand along the surface of actin. This idea was developed into a formal mathematical description by David Smith.[21] The difference between a 3-state model with cooperativity between Tms and continuous worm-like-chain model is shown in Figure 10.3.

A third model, developed by Tobacman,[24] invoked actin-actin cooperativity that in principle can allow long distance propagation of actin structural changes along the filament. In practice the distance over which the signal can be propagated, as for other models, is limited by the energy required to switch-on each unit. Each of the models described above has been developed to address particular sets of *in vitro* data and currently none has been shown to cope with the full range of experimental data available.

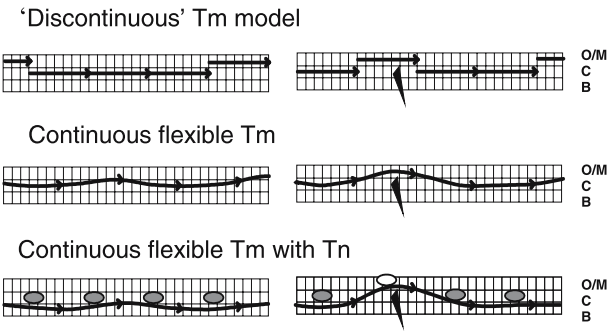

Figure 10.3. Models for longer range cooperativity between the actin$_7$TmTn structural units. Discontinuous model assumes individual Tm molecules can move between 3-positions on the surface of actin (blocked – closed – open). Strong TmTm contacts allow the movement of one Tm to influence the stability of its two neighbours. Continuous Flexible model assumes that Tm behaves as a continuous worm-like chain with a fixed probability of sections of Tm being displaced from the preferred closed position. In the presence of Tn and absence of calcium the position of Tm is pinned to actin by each TnI. With limited flexibility of Tm between each TnI site. Based on.[22,23]

A further class of models has been developed from muscle fibre studies but will not be dealt with here.

In the work presented here the description of cooperativity that has developed from the *in vitro* studies of the proteins in solution will be presented in the context of the 3-state model outlined in Figure 10.1–10.3.

10.3. PROBING THE MYOSIN INDUCED SWITCH BETWEEN THE C AND M STATES OF THE FILAMENT

These studies have been well documented in the literature[20,22,25] and so only a brief summary will be provided here. The experiment is an equilibrium titration in which myosin S1 is titrated into a solution of pyrene labelled actin and the fluorescence recorded as the myosin forms strongly bound states with actin. To perform the titration with the precision required relies on being able to use actin concentrations close to the overall K_d for binding, and under the conditions we routinely use, this means 50 nM actin. Under these conditions pure actin filaments bind myosin non-cooperatively and the binding isotherm is described by a hyperbola. In the presence of Tm or TmTn the myosin binding isotherm has the characteristic sigmoid shape of a cooperative binding reaction. The data can be well described by the equations derived for the 3-state model to yield the equilibrium constant for the switch between states (K_T), the myosin affinity for the two states (K_1, K_1K_2) and the size of the cooperative unit (n) which switches from C to M. K_T, K_1 & K_2 have little dependence upon the proteins used to assemble the thin filament (Tm isoform, Tn isoforms and components), but n varies considerably as shown in Table 10.1. A filament of actin and skeletal muscle Tm has a cooperative unit size of close to the structural unit size of 7, suggesting no strong Tm-Tm cooperativity. However, for smooth muscle Tm (and other non-muscle Tms) the cooperativity unit size is close to twice the structural unit size indicating significant Tm-Tm. cooperativity. It is well established that

Table 10.1. The influence of thin filament components on the apparent number of actin monomers switched on (C to M state) by a single myosin head binding to an actin filament

Thin filament	Apparent cooperative unit size (n)
Actin only	1
A.Tm	5–6[26]
A.smTn	10–12[23]
A.Tm5a	10–12[26]
A.TmTn + Ca^{2+}	10–12[26]
A.TmTn – Ca^{2+}	10–12[26]
A.TmTnT1	8–9[27]
A.TmTnICT2	6–7[27]

A – actin; Tm – skeletal muscle Tm; smTm – smooth muscle Tm; Tm5a – fibroblast; Tm isoform 5a; TnT1 N terminal fragment of troponin T; TnICT2 – troponin assembled from TnC, TnI and the C-terminal fragment of TnT.

smooth muscle Tm has much stronger Tm-Tm contacts, which may account for the increased cooperativity. Similarly the addition of Tn (in the presence of calcium) to actin. skeletal Tm induces an increase in cooperativity and this is due almost entirely to the N-terminal TnT_1 fragment of TnT that binds to the Tm-Tm overlap region. Note also that removal of calcium reduces the cooperative unit size back to a value close to 7. Our interpretation of this is that the strong TnI-actin contacts every 7th actin restricts the cooperativity to movement of Tm between these TnI sites.

10.4. PROBING THE CALCIUM INDUCED SWITCH BETWEEN THE B AND C-STATES OF THE FILAMENT

The kinetics of myosin, or more conveniently the myosin head, S1, binding to an actin filament provided a powerful tool to probe the state of the actin filament. It is important to emphasise that in the experiments described here S1 binding is used as a tool to probe the state of the filament. It does not matter which myosin is used, the experiment just probes the accessibility of the actin sites in the filament.

In the simplest experiment a large excess (10 fold) of actin is rapidly mixed with a small amount of S1 and the binding event is monitored by following the fluorescence of a pyrene label covalently attached to Cys-374 of actin. Such an experiment is shown in Figure 10.4 similar to that described by McKillop and Geeves.[20] S1 at 0.25 μM and actinTmTn at 2.5 μM (actin monomers) were rapidly mixed and an exponential change in fluorescence observed. In the presence of calcium the observed rate constant (k_{obs}) of the process was relatively fast at 4.5 s^{-1}. The value of k_{obs} was essentially similar when the experiment was repeated with a pure actin filament or with an actin.Tm filament. This suggests that the actinTmTn filament in the presence of calcium is similar to actin alone

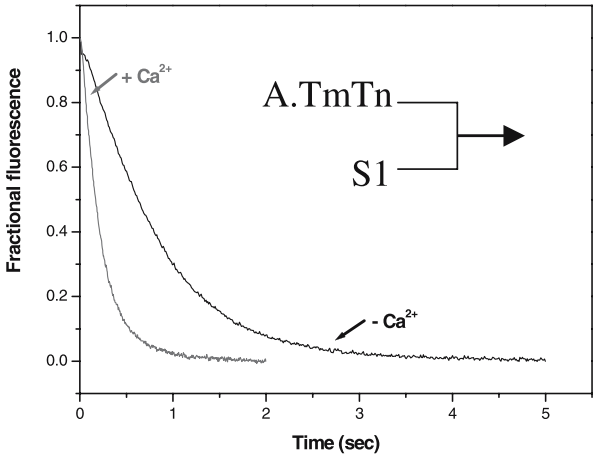

Figure 10.4. The calcium dependence of the rate of myosin binding to rabbit skeletal muscle thin filaments. The observed transients following 0.25 μM S1 binding to an excess of A.TmTn (2.5 μM actin monomers). The transients were well described by a single exponential with k_{obs} values of 4.5 and 1.2 s^{-1} for + and −Ca^{2+} respectively.[28]

and defines the fully "on-state" of the filament. When calcium was removed a similar amplitude of the exponential was observed but k_{obs} was reduced by a factor of 3–4. For a simple binding reaction the k_{obs} is defined by $k_{obs} = k$ [A], where [A] is the actin concentration and k is the intrinsic second order rate constant for S1 binding. The reduction in k_{obs} in the absence of calcium is then simply explained by a reduction in the availability of actin sites. If this is controlled by K_B, the equilibrium constant between B and C-state actin sites (K_B = [C-states]/[B-states]), then the fraction of available C-states is defined as

$$[\text{C-states}]/([\text{C-states}] + [\text{B-states}]) = K_B/(1 + K_B)$$

Thus in the absence of calcium

$$k_{obs} = k\ [\text{A}]\ \backslash K_B/(1 + K_B)$$

and the ratio of the values of k_{obs} in the presence and absence of calcium is $(1 + K_B)/K_B$. Thus if the ratio is equal to 4 the value of K_B is 0.33.

Subsequent experiments have shown that the reduction in the value of k_{obs} by removing calcium is independent of the type of myosin or of the nucleotide bound to myosin and is thus a property of the thin filament not the myosin used to probe the thin filament. In contrast the reduction in k_{obs} is a function of the calcium concentration and the type of Tn used in the experiment.

In Figure 10.5 the role of TnI in the formation of the B-state is probed. The experiment described in Figure 10.4 was repeated in Figure 10.5A as a control experiment. In Figure 10.5B the experiment was repeated but for an actin.Tm filament in the presence and absence of saturating TnI. A similar degree of inhibition of k_{obs} was observed indicating that the inhibition and hence the formation of the blocked state only requires TnI. Furthermore there is only a requirement for one TnI per actin$_7$Tm unit to induce the inhibition. TnI in the absence of Tm will inhibit myosin binding but requires one TnI per actin monomer for the full effect.

Tropomyosin isoforms have little influence upon the value of K_B but cardiac and skeletal Tn do influence the value of K_B. The data for these experiments is presented in Table 10.2 and show that K_B is similar for bacterially expressed αα-Tm, ββ-Tm and for native rabbit skeletal muscle Tm which is an approximately 50 : 50 mixture of αα and αβ Tm. In contrast the value of K_B is 0.35 for tissue purified rabbit skeletal muscle Tn and 0.60 for human cardiac Tn expressed in bacteria. Whether these differences reflect the differences between tissue purified and bacterially expressed protein remains to be defined.

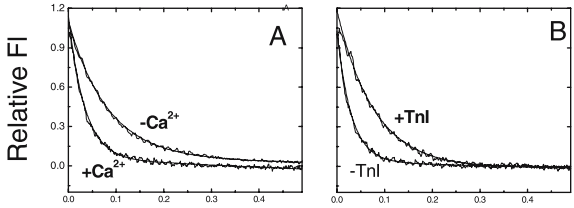

Figure 10.5. The role of TnI in the formation of the B-state. The effect of calcium and TnI on the observed transient for S1 binding to excess actin in thin filaments. (A) The effect of calcium on actin.Tm.Tn filaments. (B) The effect of addition of TnI only to actin.Tm filaments. Data from[29].

Table 10.2. The influence of Tm and Tn isoforms on K_B

Tm isoform	K_B	K_B
	SkTn	**cTn**
Native αα-Tm	0.35	0.55
αα-AS.Tm	0.35	0.66
ββ-AS.Tm	0.33	0.55
Sk.Tm	0.42	0.60

Native-Tm – Tm isolated from tissues and the αα isoform separated. Sk.Tm – Tm isolated from muscle tissue as mixed αα and αβ isoforms. AS.Tm bacterially expressed Tm with an Ala-Ser n-terminal extension used to mimic N-terminal acetylation. SkTn – Troponin isolated from rabbit skeletal muscle. cTn – bacterially expressed human cardiac troponin.[28]

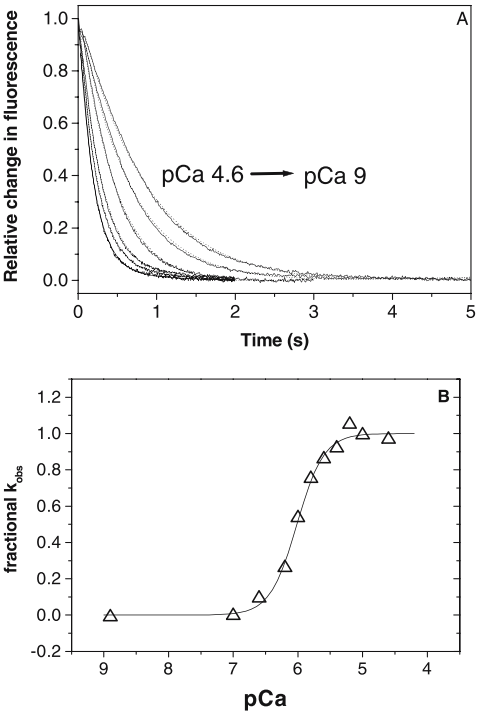

Figure 10.6. Calcium sensitivity of myosin binding to thin filaments. (A) The observed transients on mixing excess A.TmTn with S1 at different calcium concentrations between pCa 9 and 4.6. Each transient was well described by a single exponential. (B) A plot of the fractional change in k_{obs} as a function of pCa. The line represents the best fit to the hill equation with the mid-point at 6.02 with a hill coefficient of 1.5.[28]

The studies described so far only deal with the fraction of the thin filament in the blocked state. They do not address the issue of the size of the unit that switches on or off or the nature of the cooperativity. Information on the cooperativity can be gained from considering the calcium dependence of the equilibrium defined by K_B.

Figure 10.6A shows the experiment of Figure 10.4 repeated for a series of calcium concentrations between pCa 9 and 4.6. In all cases a single exponential transient was observed of similar amplitude (the data have been normalised to eliminate minor variations in amplitude). A plot of k_{obs} vs. pCa is shown in Figure 10.6B with the data fitted

to the hill equation for cooperative binding. This shows a cooperative transition with a mid-point at pCa 6.0 and a hill coefficient of 1.7 for skTn and ααTm. Once again the data were little affected by the Tm isoform, both the mid-points and the hill coefficient were within experimental error (within 0.05 for both values). In contrast the use of cardiac Tn resulted in left shift of the pCa curve to a mid-point of 5.70 with a hill coefficient of 1.1.

If cTn is used in which TnI is either bisphosphorylated or fully dephosphorylated then the pCa curves have similar hill coefficients but the mid point of the shows 0.2–0.3 unit shift to higher pCa values on phosphorylation.[30]

The conclusion of these calcium sensitivity experiments shows that addition of calcium removes the B-state, that the calcium required to switch between B and C-states is compatible with measurements of calcium binding to isolated Tn or actinTmTn. The hill coefficients give no indication of interactions between TmTn units on the actin filaments. The data are simply compatible with one calcium ion being required to switch on a cardiac TmTn unit and two calcium ions being required for a skeletal TmTn unit. These experiments only report on the calcium switch. They give no information on how this B to C switch affects myosin binding except the extent of availability of actin sites. Some indication of the cooperativity in myosin binding is provided by a similar kinetic experiment in which myosin binds to every actin site.

Figure 10.7 shows the result when and excess of S1 is mixed with a limiting amount of actinTmTn. In this case 2.5 μM S1 was mixed with 0.25 μM actinTmTn. As shown in the figure the fluorescence transients in the presence of calcium is an exponential and the k_{obs} was similar to that of Figure 10.4 or 10.6. In the absence of calcium the transient was not exponential but was markedly sigmoid. An initial slow rate of binding goes through an acceleration phase before becoming exponential in character for the last 30% of the amplitude. Analysis of such curves is not straight forward and requires a detailed kinetic model that incorporates both the rate of S1 binding to the on and off states of the filament, the rate at which the filament turns on and the size of the cooperative unit that switches. The number of significant states is very large and the model cannot be reduced to a simple set of equations. We are currently attempting to model this complete reaction system. But a simple inspection of the data shows that there is a different type of cooperativity taking place as a single S1 binding induces the binding of further S1 molecules.

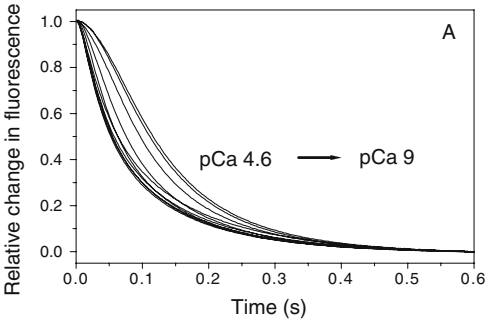

Figure 10.7. Cooperativity in myosin binding to the blocked state of the thin filament. (A) A repeat of the experiment in Figure 10.6 but with excess S1 (2.5 μM) binding to A.Tm.Tn (0.25 μM) at pCa values between 9.0 and 4.6. The transients are sigmoid and cannot be fitted to a simple equation.

10.5. CONCLUSION

What we have attempted to show here is that cooperativity in the thin filament can be probed in various experimental protocols but the degree of cooperativity observed is dependant upon what is being measured. This is not a limitation of the methods but demonstrates that cooperativity of the thin filament is complex and each structural transition is cooperative to a different extent. Thus calcium binding to TnC whether isolated or in the filament appears to bind calcium with a cooperativity that reflects the number of calcium binding sites, i.e. a cooperativity of 1–2 for skeletal Tn and no cooperativity for cardiac Tn. This is the same cooperativity observed for the Blocked to Closed transition in response to calcium binding as illustrated in Figure 10.6. However from a myosin binding perspective the cooperativity is 7, i.e. groups of 7 actins switch from Blocked to Closed at a time whether in response to calcium binding or to myosin binding. For the C-to-M switch the cooperativity can be longer range and typically shows 10–14 actins being switched to the M-state at a time by a single myosin-binding event.

10.6. ACKNOWLEDGEMENTS

This work was supported by grants from the British Heart Foundation (SEB, FS/2000014) the Wellcome Trust (MAG, 070021) and the National Institute of Health (MAG, AR048776)

10.7. REFERENCES

1. S. Ebashi, and A. Kodama, A new protein factor promoting aggregation of tropomyosin, *J. Biochem. (Tokyo)* **58**, 107–108 (1965).
2. S. Ebashi, and A. Kodama, Interaction of troponin with F-actin in the presence of tropomyosin, *J. Biochem. (Tokyo)* **59**, 425–426 (1966).
3. Z. Grabarek, J. Grabarek, P. C. Leavis, and J. Gergely, Cooperative binding to the Ca2+-specific sites of troponin C in regulated actin and actomyosin, *J. Biol. Chem.* **258**, 14098–14102 (1983).
4. M. X. Li, S. M. Gagne, S. Tsuda, C. M. Kay, L. B. Smillie, and B. D. Sykes, Calcium binding to the regulatory N-domain of skeletal muscle troponin C occurs in a stepwise manner, *Biochemistry* **34**, 8330–8340 (1995).
5. P. W. Brandt, R. N. Cox, and M. Kawai, Can the binding of Ca2+ to two regulatory sites on troponin C determine the steep pCa/tension relationship of skeletal muscle? *Proc. Natl. Acad. Sci. USA* **77**, 4717–4720 (1980).
6. R. L. Moss, Ca2+ regulation of mechanical properties of striated muscle. Mechanistic studies using extraction and replacement of regulatory proteins, *Circ. Res.* **70**, 865–884 (1992).
7. S. Takeda, A. Yamashita, K. Maeda, and Y. Maeda, Structure of the core domain of human cardiac troponin in the Ca(2+)-saturated form, Nature **424**, 35–41 (2003).
8. M. V. Vinogradova, D. B. Stone, G. G. Malanina, C. Karatzaferi, R. Cooke, R. A. Mendelson, and R. J. Fletterick, Ca(2+)-regulated structural changes in troponin, *Proc. Natl. Acad. Sci. USA* **102**, 5038–5043 (2005).
9. R. Craig, and W. Lehman, Crossbridge and tropomyosin positions observed in native, interacting thick and thin filaments, *J. Mol. Biol.* **311**, 1027–1036 (2001).
10. Y. Ishii, and S. S. Lehrer, Excimer fluorescence of pyrenyliodoacetamide-labeled tropomyosin: a probe of the state of tropomyosin in reconstituted muscle thin filaments, *Biochemistry* **29**, 1160–1166 (1990).

11. C. Bacchiocchi, P. Graceffa, and S. S. Lehrer, Myosin-induced movement of alphaalpha, alphabeta, and betabeta smooth muscle tropomyosin on actin observed by multisite FRET, *Biophys. J.* **86**, 2295–2307 (2004).
12. M. Miki, H. Hai, K. Saeki, Y. Shitaka, K. Sano, Y. Maeda, and T. Wakabayashi, Fluorescence resonance energy transfer between points on actin and the C-terminal region of tropomyosin in skeletal muscle thin filaments, *J. Biochem. (Tokyo)* **136**, 39–47 (2004).
13. T. L. Hill, E. Eisenberg, and J. M. Chalovich, Theoretical models for cooperative steady-state ATPase activity of myosin subfragment-1 on regulated actin, *Biophys. J.* **35**, 99–112 (1981).
14. A. V. Gomes, J. Liang, and J. D. Potter, Mutations in human cardiac troponin I that are associated with restrictive cardiomyopathy affect basal ATPase activity and the calcium sensitivity of force development, *J. Biol. Chem.* **280**, 30909–30915 (2005).
15. E. Homsher, B. Kim, A. Bobkova, and L. S. Tobacman, Calcium regulation of thin filament movement in an in vitro motility assay, *Biophys. J.* **70**, 1881–1892 (1996).
16. I. D. Fraser, and S. B. Marston, In vitro motility analysis of actin-tropomyosin regulation by troponin and calcium. The thin filament is switched as a single cooperative unit, *J. Biol. Chem.* **270**, 7836–7841 (1995).
17. W. Lehman, V. Hatch, V. Korman, M. Rosol, L. Thomas, R. Maytum, M. A. Geeves, J. E. Van Eyk, L. S. Tobacman, and R. Craig, Tropomyosin and actin isoforms modulate the localization of tropomyosin strands on actin filaments, *J. Mol. Biol.* **302**, 593–606 (2000).
18. T. L. Hill, E. Eisenberg, and L. Greene, Theoretical model for the cooperative equilibrium binding of myosin subfragment 1 to the actin-troponin-tropomyosin complex, *Proc. Natl. Acad. Sci. USA* **77**, 3186–3190 (1980).
19. Y. Chen, B. Yan, J. M. Chalovich, and B. Brenner, Theoretical kinetic studies of models for binding myosin subfragment-1 to regulated actin: hill model versus Geeves model, *Biophys. J.* **80**, 2338–2349 (2001).
20. D. F. McKillop, and M. A. Geeves, Regulation of the interaction between actin and myosin subfragment 1: evidence for three states of the thin filament, *Biophys. J.* **65**, 693–701 (1993).
21. D. A. Smith, and M. A. Geeves, Cooperative regulation of myosin-actin interactions by a continuous flexible chain II: actin-tropomyosin-troponin and regulation by calcium, *Biophys. J.* **84**, 3168–3180 (2003).
22. R. Maytum, S. S. Lehrer, and M. A. Geeves, Cooperativity and switching within the three-state model of muscle regulation, *Biochemistry* **38**, 1102–1110 (1999).
23. S. S. Lehrer, N. L. Golitsina, and M. A. Geeves, Actin-tropomyosin activation of myosin subfragment 1 ATPase and thin filament cooperativity. The role of tropomyosin flexibility and end-to-end interactions, *Biochemistry* **36**, 13449–13454 (1997).
24. L. S. Tobacman, and C. A. Butters, A new model of cooperative myosin-thin filament binding, *J. Biol. Chem.* **275**, 27587–27593 (2000).
25. R. Maytum, B. Westerdorf, K. Jaquet, and M. A. Geeves, Differential regulation of the actomyosin interaction by skeletal and cardiac troponin isoforms, *J. Biol. Chem.* **278**, 6696–6701 (2003).
26. M. A. Geeves, and S. S. Lehrer, Dynamics of the muscle thin filament regulatory switch: the size of the cooperative unit, *Biophys. J.* **67**, 273–282 (1994).
27. S. Schaertl, S. S. Lehrer, and M. A. Geeves, Separation and characterization of the two functional regions of troponin involved in muscle thin filament regulation, *Biochemistry* **34**, 15890–15894 (1995).
28. S. E. Boussouf, *PhD Thesis* (Department of Biosciences, University of Kent, Canterbury, 2004).
29. M. A. Geeves, M. Chai, and S. S. Lehrer, Inhibition of actin-myosin subfragment 1 ATPase activity by troponin I and IC: relationship to the thin filament states of muscle, *Biochemistry* **39**, 9345–9350 (2000).
30. S. U. Reiffert, K. Jaquet, L. M. Heilmeyer Jr, M. D. Ritchie, and M. A. Geeves, Bisphosphorylation of cardiac troponin I modulates the Ca(2+)-dependent binding of myosin subfragment S1 to reconstituted thin filaments, *FEBS Lett.* **384**, 43–47 (1996).

11

CONFORMATIONAL CHANGES IN RECONSTITUTED SKELETAL MUSCLE THIN FILAMENTS OBSERVED BY FLUORESCENCE SPECTROSCOPY

Masao Miki[1,2]

11.1. INTRODUCTION

The cyclic interaction of myosin and actin coupled ATP hydrolysis generates the mechanical force of muscle contraction. During this process, the system passes through several steps. One of these is thought to be identical to the stable rigor complex formed by myosin and actin in the absence of ATP. This cyclic interaction is regulated by changes in tropomyosin (Tm) and troponin (Tn) located on the actin filament in response alterations in intracellular Ca^{2+} concentration (Ebashi et al., 1969). Tm contains seven quasi-equivalent regions, each of which has a pair of putative actin-binding motifs. Tn comprises three different subunits, TnC, TnI, and TnT. TnI alone inhibits actomyosin ATPase activity which is removed on adding TnC, irrespective of Ca^{2+} concentration. TnT is required for full Ca^{2+}-regulation of the ATPase activity of a reconstituted system (Ohtsuki et al., 1986). The globular part of the Tn complex (TnC, TnI and the C-terminal region of TnT) is located on residues 150–180 of Tm (White et al., 1987), and the elongated part, composed of the N-terminal region, covers an extensive region of the C-terminal half of Tm. The binding of Ca^{2+} to TnC induces a series of conformational changes in the other components of the thin filament. This allows the effective association of myosin with actin, thus producing force. Although numerous studies have characterized the interaction between these thin filament proteins, the molecular mechanism whereby the Ca^{2+}-trigger is propagated from TnC to the rest of the thin filament is still not well understood.

X-ray diffraction studies of muscle fibers showed a significant change in the layer line intensities depending on whether the muscle was in a relaxed or contracted state (Haselgrove 1972; Huxley 1972). These intensity changes were interpreted as an azimuthal shift of the Tm strands in the grooves of the actin helix. Thus, the steric blocking

[1] Department of Applied Chemistry and Biotechnology, and [2]Research and Education Program for Life Science, Fukui University, 3-9-1 Bunkyo, Fukui 910-8507, Japan, TEL: +61-776-27-8786 FAX: +61-776-27-8747, e-mail: masao@acbio2.acbio.fukui-u.ac.jp

Regulatory Mechanisms of Striated Muscle Contraction
Edited by Ebashi and Ohtsuki, Springer, 2007

theory was proposed in which Tm physically blocks the myosin-binding site on actin during relaxation. However, instead of a two-state model based on Ca^{2+}-induced on-off switching, kinetic measurements have proposed a three-state model (McKillop and Geeves, 1993). In this model, thin filaments exist in rapid equilibrium between three states (blocked or relaxed, closed, and open). The equilibrium between the relaxed and closed states is calcium-sensitive, and strong myosin binding stabilizes the open state. Recent X-ray diffraction and three-dimensional image reconstructions of electron micrographs (3D-EM) have led to a new model in which Tm moves between three distinct states (Holmes, 1995; Vibert et al., 1997). However, the Ca^{2+}-induced conformational change of the thin filament clearly cannot be assigned to the movement of Tm, since this interpretation assumes that the mass of the Tn/Tm complex is distributed evenly and smoothly along the continuous Tm strands. Squire and Morris (1998) suggested that conformational changes observed from X-ray diffraction (and 3D-EM) data could be explained as movement of Tn instead of Tm. Narita et al. (2001) reconstructed three-dimensional images of thin filaments from cryo-electron micrographs without imposing helical symmetry and showed that the major change due to Ca^{2+} is a shift of Tn head (the main body of Tn). They suggested that while the N-terminal half of Tm does not undergo a major shift, the C-terminal one-third of Tm and/or Tn tail shifts significantly.

Fluorescence resonance energy transfer (FRET) has been used as a spectroscopic ruler in the range of several tens angstroms (Stryer, 1978). This method is especially valuable for detecting small structural changes (several Å), because the FRET efficiency is a function of the inverse sixth power of the distance between probes. Furthermore, fluorescence donor and acceptor molecules can be specifically attached to proteins thus assigning a vector to the conformational change. Here we use FRET to detect conformational changes in skeletal muscle thin filament proteins in both relaxed and active states, and we review the recent research on the structural changes of the skeletal muscle thin filament induced by Ca^{2+}- and/or myosin-binding.

11.2. STRUCTURAL CHANGES IN THIN FILAMENTS MEASURED BY FRET

FRET measurements require that the energy donor and acceptor probes be attached to specific positions on proteins. The requirement for specific labeling limits the application of FRET method. However, recent progress in genetic engineering facilitated the selective labeling of protein and made it easier to introduce reactive amino acid side chains by introducing single cysteine at the required locations in proteins.

11.2.1. Probe Sites on Actin, Tm, and Tn

Actin was labeled with an energy acceptor probe at: (1) Gln-41 using fluorescein cadaverine (FLC); (2) Lys-61 using fluorescein 5-isothiocyanate (FITC); (3) Cys-374 using 4-dimethylaminophenyl 4′-maleimide (DABMI); or (4) the nucleotide-binding site using 2′ (or 3′)-O-(2,4,6-trinitrophenyl) adenosine 5′-diphosphate (TNP-ADP). Figure 11.1A shows the locations of these labeling sites on a cross section of the atomic model

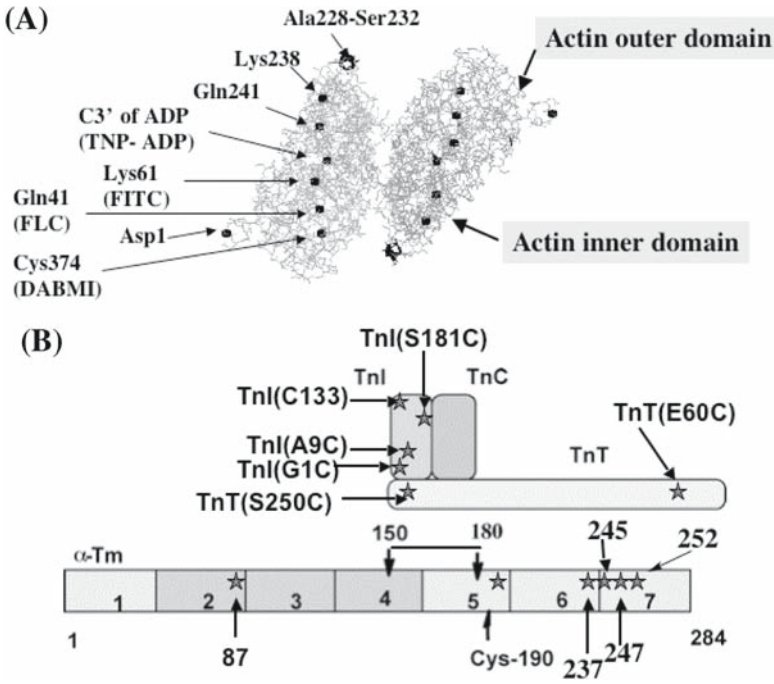

Figure 11.1. Locations of energy acceptor- and donor-labeling sites on a cross-section of an atomic model of F-actin (A) and a schematic model of the Tm-Tn complex (B). F-actin was constructed with two monomers using the atomic coordinates of Lorenz et al. (1993). The globular part of Tn binds Tm near residues 150–180 (White et al., 1987), and the elongated part of TnT extends to the N-terminal region of the next Tm molecule.

of F-actin. Single cysteine αTm mutants were expressed in *Escherichia* coli in which additional residues A-A-S- or A-S- were added at the N-terminus in order to restore their binding ability to F-actin (Monteiro et al., 1994). These αTm mutants (Cys-87, 237, 245, 247 or 252) and native αTm (Cys-190) were labeled with the energy donor probe, 5-(2-iodoacetylaminoethyl)-amnonaphtalene-1-sulfonic acid (IAEDANS). Single cysteine mutants of TnI and TnT25 k were also expressed in *E. coli.* TnT25 k, the 25-kDa fragment (residues: 59–266) of TnT, is functionally identical to native TnT and is soluble at low ionic strength, unlike the native TnT. These TnI mutants (Cys-1, 9, or 181), native TnI (Cys-133) and TnT25 k (Cys-60 or 250) were labeled with the energy donor probe, IAEDANS. The labeled Tn subunits were incorporated into the Tn complex with other unlabeled subunits prepared from rabbit skeletal muscle. Figure 11.1B shows the locations of the FRET energy donor probes on a schematic model of the Tm-Tn complex.

11.2.2. FRET between Tm and Actin

FRET between probes attached to Cys-190 of Tm and Cys-374 of actin showed almost no change in the transfer efficiency in response to a Ca^{2+}-induced structural change of the

thin filament, indicating that Tm does not change its position relative to the actin filament (Miki and Mihashi, 1979; Lin and Dowben, 1983; Tao et al., 1983). However, Tao et al. (1983) proposed a case where a Tm-bound donor and actin-bound acceptors can be positioned so that a movement of Tm in the grooves of F-actin produces no net change in the FRET efficiency. Acceptor probes were selectively attached to several specific points on actin (Cys-374, Lys-61, Gln-41 and the nucleotide-binding site), and a donor probe was selectively attached to Tm at positions 87 or 190. FRET between the probes on actin and Tm showed there was no significant change in transfer efficiency upon the addition of Ca^{2+} (Miki, 1990; Miki et al., 1998b). Since measurement of more than three distances between points on Tm and actin uniquely position Tm on the actin filament, we can exclude the case where the movement of Tm relative to actin produces no net change in FRET efficiency. FRET also showed that the S1-induced structural change in thin filaments did not accompany Tm movement relative to the actin filament (Miki et al., 1998b). In accord with these FRET measurements, polarized fluorescence measurements have suggested there is little or no changes in the position of Tm relative to actin upon binding of Ca^{2+} or upon additional binding of S1 using "ghost" fibers (Borovikov et al., 1993). On the other hand, analysis of frequency-domain FRET between Cys-190 of Tm and the phalloidin-binding site of actin (Bacchiocchi and Lehrer, 2001) suggests that significant movement of Tm relative to actin produces no appreciable change in the FRET efficiency when the two donor positions on Tm in the homodimer structure of Tm are taken into account. Finding these two positions of Tm on actin ($\pm Ca^{2+}$) requires that the two donor probes project in definitive directions from the Tm molecule on the actin filament. Accordingly, a donor probe was selectively attached to residues 237, 245, 247, or 252 of single-cysteine Tm mutants (Miki et al., 2004). FRET between these points on Tm and Cys-374 or Gln-41 of actin did not reveal any appreciable change in the energy transfer efficiency upon binding of Ca^{2+} or when S1 binds to regulated actin (Table 11.1).

Residues 87, 190, 237, 245, 247, and 252 of Tm are located at positions c, a, f, g, b, and g, respectively along this seven repeat α-helical coiled-coil structure. Donor probes at these sites project at different angles to each other on the Tm surface. Therefore we can exclude the case where movement of Tm does not accompany a net change in the transfer efficiency. An alternative and simpler analysis of the FRET data by Bacchiocchi and Lehrer (2001) suggests that Tm does not significantly change its position on actin because there is only a small change in the transfer efficiency in Ca^{2+} regulated actin.

Table 11.1. Distances between probes attached to αTm and actin in reconstituted thin filament in the presence and absence of Ca^{2+} ions. Data are from Miki et al. (2004)

Acceptor (actin)	Donor (Tm)	Efficiency (+Ca/−Ca)	R (2/3) (Å) (+Ca/−Ca)
Cys-374	252	0.54 ± 0.02/0.51 ± 0.03	38.2 ± 0.5/38.9 ± 0.8
	247	0.58 ± 0.03/0.58 ± 0.02	35.7 ± 0.7/35.7 ± 0.5
	245	0.57 ± 0.01/0.58 ± 0.02	36.1 ± 0.2/35.8 ± 0.5
	237	0.68 ± 0.01/0.65 ± 0.02	33.9 ± 0.3/34.6 ± 0.5
Gln-41	252	0.73 ± 0.03/0.62 ± 0.04	38.7 ± 1.0/42.1 ± 1.2
	247	0.75 ± 0.05/0.75 ± 0.05	36.6 ± 1.7/36.6 ± 1.7
	245	0.76 ± 0.05/0.73 ± 0.02	36.3 ± 1.8/37.3 ± 0.6
	237	0.88 ± 0.01/0.85 ± 0.01	32.0 ± 0.5/33.4 ± 0.4

11.2.3. FRET between Tn and Actin

FRET between probes attached to Cys-133 of TnI and Lys-61 or Cys-374 of actin showed that TnI changes its position on F-actin when Ca^{2+} binds to the regulated thin filament (Miki, 1990; Tao et al., 1990). Later, using more labeling sites on TnI (Cys-9, Cys-133), TnC (Cys-98) and actin (Gln-41, Lys-61, Cys-374, and the nucleotide binding site), FRET showed that the C-terminal and inhibitory domains of TnI move towards the outer domain of actin something like a lever arm, and that the C-terminal region of TnC is located at the "hinge" region during this inhibition (Miki et al., 1998a).

According to the three-state model (relaxed, closed and open), Ca^{2+} regulates the equilibrium between the relaxed and closed states and the strong S1 binding stabilizes the open state. FRET showed that rigor S1 binding induces a positional change of TnI on F-actin (Kobayashi et al., 2001; Hai et al., 2002). The deletion mutant Tm (D234Tm) in which internal actin-binding pseudo-repeats 2, 3, and 4 are missing, retains its ability to bind to actin and Tn, but it inhibits actomyosin MgATPase and filament sliding *in vitro*, which is not reversed by Ca^{2+} and Tn (Landis et al., 1997). FRET has demonstrated that the positional change of TnI corresponds well to the three states of the thin filament. However, on thin filaments reconstituted with D234Tm, TnI movement from the closed to open states was impaired, although it was normal from the relaxed to closed states. Plots of the extent of S1-induced conformational change *vs.* molar ratio of S1 to actin showed that the curve is hyperbolic in the presence of Ca^{2+} but sigmoidal in the absence of Ca^{2+}. When the thin filament was reconstituted with D234Tm, the curve was sigmoidal whether or not Ca^{2+} was present (Figure 11.2) (Hai et al., 2002).

Ca^{2+}- and S1-induced movements of TnT on the reconstituted thin filament were also detected. FRET between probes attached to residues 60 or 250 of TnT and Cys-374 or Gln-41 of actin showed significant Ca^{2+}-dependent and S1-dependent changes in the position of TnT on actin (Kimura et al., 2002a). When Ca^{2+} binds to regulated thin filaments, TnT moves away from the outer domain of actin as seen in the case of TnI. Plots of the extent of S1-induced conformational change *vs.* molar ratio of S1 to actin showed that the curve is hyperbolic in the presence of Ca^{2+} but sigmoidal in the absence of Ca^{2+}. However, on the thin filament reconstituted with D234Tm, the N-terminal domain of TnT

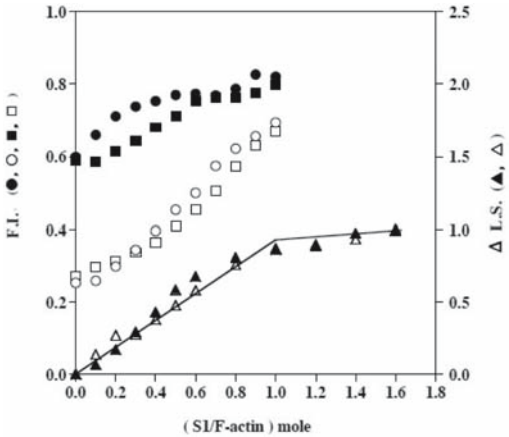

Figure 11.2. Relative Fluorescence Intensities (F.I.) of AEDANS bound to Cys-133 of TnI in the reconstituted thin filaments with Tm (● for $+Ca^{2+}$ and ○ for $-Ca^{2+}$ state) or D234eTm (■ for $+Ca^{2+}$ and □ for $-Ca^{2+}$ state) *vs.* molar ratios of S1 to actin. The binding of S1 to the thin filament was monitored as light scattering intensity (L.S.) of the thin filament reconstituted with Tm (▲) or D234Tm (△) *vs.* molar ratios of S1 to actin. This figure is from Hai et al. (2002).

did not change position upon Ca^{2+} binding, and the C-terminal domain exhibited only a small movement. Plots of the extent of S1-induced conformational change *vs.* molar ratio of S1 to actin revealed that the curve is sigmoidal whether or not Ca^{2+} is present (Figure 11.3). TnT movement on the functionally deficient thin filament is strongly impaired, suggesting that it is closely related to the physiological states of the thin filament.

Thus far, the TnI and TnT subunits in the Tn complex change their position relative to actin corresponding to three states of the thin filament. However, when sufficient ATP is present, the S1-induced movement of TnI or TnT on the thin filament cannot be detected by FRET. This is because the population in the rigor binding state of S1 is extremely small in the presence of excess ATP. While, by addition of ATP under the condition where the transition curve to open state *vs.* molar ratios of S1 to actin shows hyperbolic, the actomyosin ATPase cycle turns actively, but under conditions where the transition curve was sigmoidal, the ATPase cycle is inhibited.

Now let us consider the meaning of the hyperbolic and sigmoidal curves. A hyperbolic transition curve means that a single S1 molecule on a unit length of actin filament can induce the open state. Although the population of the rigor S1 on the unit length of actin filament is very small, one S1 molecule can turn the cycle of actomyosin ATPase. The open state is one of sequential steps during the actomyosin ATPase cycle. In this case, there is no barrier for advancing to the next step. On the other hand, a sigmoidal transition curve means that cooperative binding of several S1 heads along a unit length of an actin filament is required to induce the open state. In the presence of sufficient ATP, the probability of more than two strongly bound S1s along a unit length of actin filament is very small. Thus, the system cannot pass through the open step, and consequently the actomyosin ATPase cycle does not turn on.

NEM-treated S1 binds strongly to actin even in the presence of ATP and releases the inhibition of Tm-Tn even in the absence of Ca^{2+} (Nagashima and Asakura, 1982; Greene et al., 1987). This phenomenon can be explained as follows. When NEM-S1 is added, the probability of several S1 molecules binding simultaneously on a unit length of actin filament becomes substantial even in the presence of ATP, enabling the ATPase cycle of the

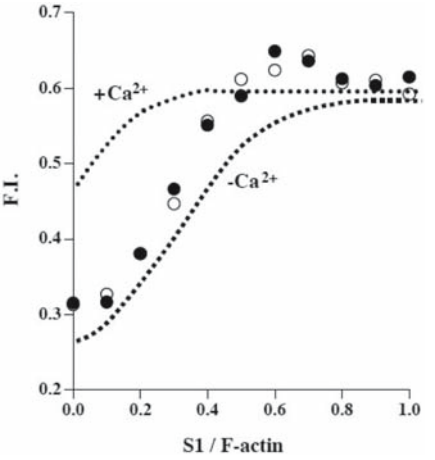

Figure 11.3. Relative fluorescence intensities F. I. of AEDANS bound to Cys-60 of TnT on thin filaments reconstituted with native Tm (broken lines) or D234Tm (○ for $+Ca^{2+}$, • for $-Ca^{2+}$) *vs.* molar ratios of S1 to actin. This figure is from Kimura et al. (2002b).

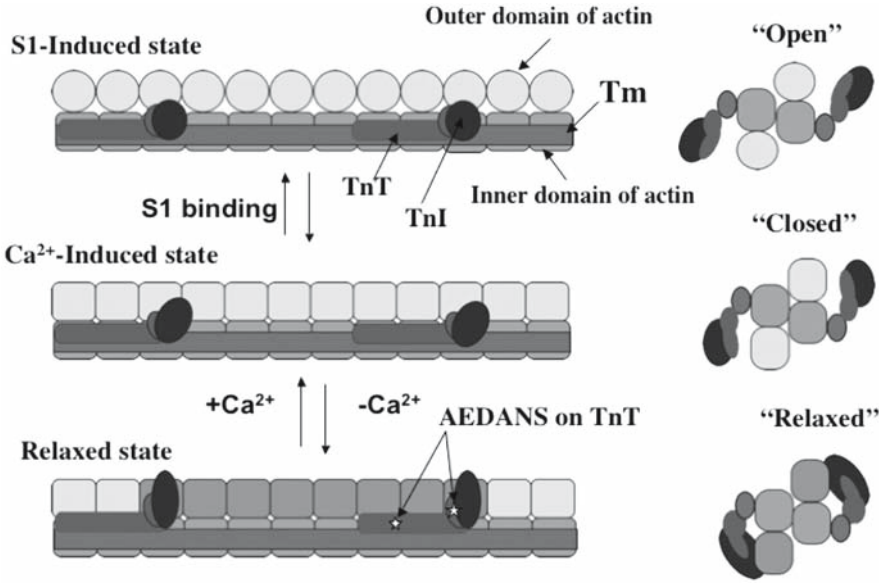

Figure 11.4. A schematic model of Tn and Tm along the long-pitch helix of an actin filament in three states of thin filaments (left side) and a cross section of the thin filament (right side). One actin molecule is illustrated with two frames that represent its outer and inner domains. This figure is from Kimura et al. (2002a).

native S1 to turn actively. The three positions of Tn on thin filament correspond well to three states of thin filaments, and the transition movement of Tn can explain the regulation mechanism of muscle contraction.

Here, we illustrate the three states of thin filaments observed by FRET measurements (Figure 11.4). Although they clearly showed a significant extent of Tn movement relative to actin corresponding to three states of the thin filament, they did not detect any significant movement of Tm relative to actin. This model is in contrast to the steric blocking model where, intra- and/or inter-monomer flexibility of actin play an essential role in regulation. Instead of Tm blocking the myosin-binding site, Tn-Tm regulates this flexibility of actin filament. Cross-linking between the inner and outer domains of actin molecules by two neighboring Tn-Tm complexes along the long-pitch helix of actin filament would reduce the flexibility of the unit length of the thin filament. In an alternative model, two Tn-Tm complexes located on the opposite sides of the long-pitch helix of actin filaments control the flexibility of the thin filament.

11.3. RATES OF TRANSITION BETWEEN THREE STATES OF THIN FILAMENT MEASURED BY FRET

Using time-resolved X-ray diffraction, Kress et al. (1986) detected a rapid structural change in the thin filament before the change derived from cross-bridge movements. This structural change occurs after the stimulus with a half time of 8.5 ms at 14°C and reached a maximum in 15–20 ms. This rapid structural change after Ca^{2+} binding (several ms)

was presumed to be an azimuthal Tm movement on the actin filament. Using FRET in combination with the stopped-flow method, the rate of the TnI movement upon Ca^{2+} binding was determined (Miki and Iio, 1993), although no Tm movement was detected (Miki et al., 2004). The time scale of this TnI movement after Ca^{2+} binding was 530 ± 170 s^{-1} at 20°C in good agreement with the X-ray diffraction data. Thus, it is possible that the changes in X-ray diffraction pattern interpreted as Tm movement are in fact caused by Ca^{2+}-induced changes in Tn-actin interaction.

Numerous stopped-flow measurements have been carried out to study the transition rates between three states of the thin filament (Geeves and Lehrer, 1994; Maytum et al., 2002; Resetar et al., 2002). In these experiments, fluorescent probes were attached to Tm or actin, and the time course of the fluorescence intensity change was traced for kinetic studies of the conformational changes of Tm and actin in response to three states of thin filaments. However, fluorescence intensities of probes on Tm or actin respond primarily to S1 binding but not to changes in Ca^{2+} concentration. In general, the fluorescence intensity change measured in these experiments indicates there is an environmental change around the probe, but it does not necessary mean there is a spatial rearrangement of thin filaments. On the other hand, the change in the transfer efficiency of FRET does indicate a spatial rearrangement in thin filaments. FRET between probes attached to TnI or TnT and actin on the reconstituted thin filament showed significant changes in the transfer efficiencies between three states of the thin filament. This enabled us to directly determine the transition rates between three states of the thin filament.

11.3.1. The Rates of Ca^{2+}-induced Changes of The Thin Filament

Using FRET in combination with the stopped-flow method by rapidly changing the free Ca^{2+} concentration, the rate of the TnT movement between relaxed and closed states was measured as shown in Figure 11.5 (Shitaka et al., 2005). A FRET donor probe was attached at Cys-60 or 250 of TnT, and an acceptor was positioned at Cys-374 of actin. In both Cys-60 and 250 of TnT, the time scale of this TnT movement was ~450 and ~85 s^{-1} at 20°C on Ca^{2+} up and down respectively. This result correlates well with the TnI movement determined previously (Miki and Iio, 1993).

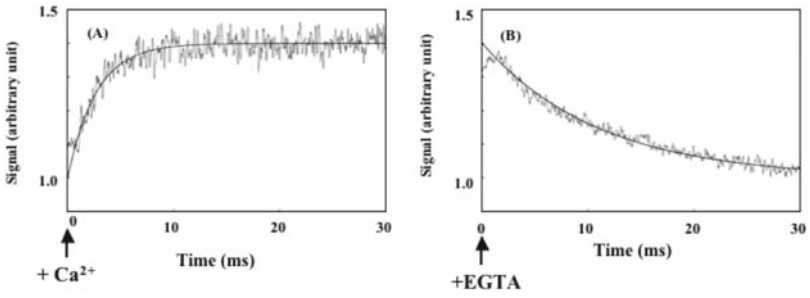

Figure 11.5. Stopped-flow traces of donor fluorescence intensity after rapidly changing the free Ca^{2+} concentrations: Ca^{2+} up (A) or down (B). This figure is from Shitaka et al., 2005.

11.3.2. The Rates of S1-induced Changes in the Thin Filament

After rapidly changing the concentration of rigor bound S1 by mixing the protein solutions with ATP solutions, the transition rates of TnI movement from the open to the closed or relaxed state were measured by monitoring the donor-fluorescence intensity (Shitaka et al., 2004). An energy donor probe was attached at Cys-133 of TnI, and the energy acceptor probe was attached at Cys-374 of actin. S1 binding was monitored from the scattered light under the same experimental conditions. Bound S1 was abruptly dissociated from regulated thin filaments in the presence of Ca^{2+} by mixing with ATP to achieve the transition from the open to closed state. The rate of dissociation increased as the concentration of ATP increased. Under these conditions S1 dissociates with a rate constant of ~900 s^{-1} at 0.5 mM ATP. FRET showed that TnI movement from the open to closed states occurs with a rate constant of ~300 s^{-1} (Figure 11.6A). When regulated thin filaments were rapidly mixed with S1 in the presence of Ca^{2+}, there is a putative a transition from the closed to open states when S1 binds. Light scattering reveals that S1 binding occurs with a rate constant of ~9 s^{-1}, and FRET showed that TnI movement occurs with almost the same rate constant as S1 binding. The result suggests that the transition from closed to open states occurs within several ms after S1 binding. A putative transition from the open to relaxed states occurs when bound S1 abruptly dissociates from regulated thin filaments in the absence of Ca^{2+}. Light scattering measurements show that S1 dissociates with a rate constant of ~900 s^{-1} while FRET shows that TnI movement occurs with two rate constants of ~400 s^{-1} and ~80 s^{-1}. The faster rate constant (k_{FL1}) is comparable to that for transition from the open to closed states observed in the presence of Ca^{2+}. On the other hand, the slower rate constant (k_{FL2}) is similar to that for the transition from the closed to relaxed states.

These results indicate that the transition occurs in two steps, from the open to closed states, and then from the closed to relaxed state. On the other hand, when regulated thin filaments are rapidly mixed with S1 in the absence of Ca^{2+}, a transition from the relaxed to open states after S1 binding has been proposed. Light scattering measurements showed that S1 binding occurs with a rate constant of ~5 s^{-1}. The rate constant of S1 binding to regulated thin filaments in the absence of Ca^{2+} is slower than that in the presence of Ca^{2+}.

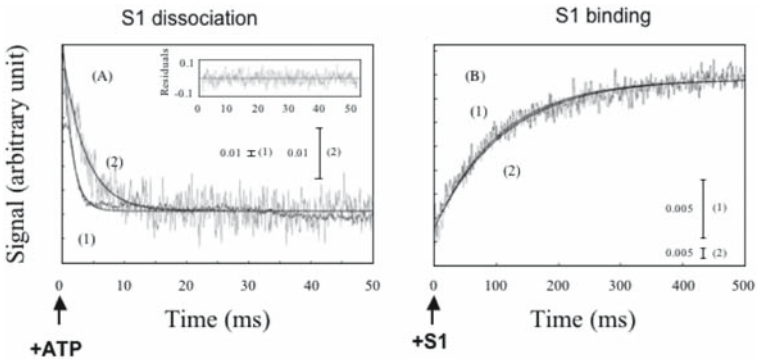

Figure 11.6. TnI-movement after dissociation or binding of S1 from thin filaments. Curve 1: light scattering change, Curve 2: FRET change. This figure is from Shitaka et al., 2004.

Table 11.2. The rate constants of TnI movement between states of thin filaments induced by S1 binding/dissociation. Parentheses indicate the amplitude of the two rate constants. Data are from Shitaka et al. (2004)

Donor site	S1 dissociation			S1 binding	
(TnI) (+Ca^{2+})	k_{LS} (s^{-1}) (L.S.)	k_{FL} (s^{-1}) (F.I.)		k_{LS} (s^{-1}) (L.S.)	k_{FL} (s^{-1}) (F.I.)
TnIG1C	942 ± 75	330 ± 39		8.94 ± 1.16	8.75 ± 1.14
TnICys133	868 ± 76	216 ± 42		9.53 ± 1.24	9.04 ± 1.18
TnIS181C	825 ± 68	384 ± 67		8.91 ± 1.16	8.36 ± 1.09
	k_{LS} (s^{-1})	k_{FL1} (s^{-1})	k_{FL2} (s^{-1})	k_{LS} (s^{-1})	k_{FL} (s^{-1})
(−Ca^{2+})	(L.S.)	(F.I.)	(F.I.)	(L.S.)	(F.I.)
TnIG1C	991 ± 89	549 ± 27 (0.79)	134 ± 6.2 (0.21)	4.74 ± 0.62	4.52 ± 0.59
TnICys133	997 ± 83	360 ± 44 (0.75)	44.9 ± 5.7 (0.25)	6.05 ± 0.79	4.50 ± 0.59
TnIS181C	836 ± 62	388 ± 93 (0.69)	43.9 ± 3.6 (0.31)	5.96 ± 0.77	6.09 ± 0.79

The rate constants for TnI movement between three states of thin filaments induced by S1 binding or dissociation are summarized in Table 11.2.

TnT movement following dissociation or binding of S1 was measured by monitoring the donor-fluorescence intensity and light scattering (Shitaka et al., 2005). When strongly bound S1 is abruptly dissociated from the thin filament by mixing with ATP, the transition from the open to closed and relaxed states would occur in the presence and absence of Ca^{2+}, respectively. A change in the light-scattering intensity indicates the dissociation of S1 from the regulated thin filament and the rate of dissociation increases as the concentration of ATP increased. At 0.5 mM ATP, it was >800 s^{-1}. The change in the fluorescence intensity (TnT movement) was analyzed by a single-exponential curve with a rate constant of ~400 s^{-1} both in the presence and absence of Ca^{2+}. These data indicate that the transition of TnT from the open to relaxed states occurs directly in contrast to the movement of TnI through an intermediate state (the closed state). That is TnT moves differentially with TnI. This differential movement suggests there is a flexible "joint" between TnI and TnT subunits in the Tn complex.

When S1 binds to the thin filament, the transition to the open state from the closed and relaxed states occurs in the presence and absence of Ca^{2+}, respectively. Light-scattering measurements have shown that the S1 binding occurs with the rate constant of ~10 and ~5 s^{-1} in the presence and absence of Ca^{2+}, respectively. The rate constants for the transitions between three states of thin filaments determined by stopped-flow measurements are summarized in Table 11.3.

11.4. CONCLUSIONS

The structural changes of the thin filament between three states and their transition rates are illustrated in Figure 11.7. FRET has demonstrated that Tn has three positions on thin filaments corresponding to three states of the thin filament. However, FRET does not detect movement of Tm on thin filaments. The transition rates of Tn movement

Table 11.3. Comparison of the rate constants of S1-induced movement of TnT. Data are from Shitaka et al. (2005)

Donor site (TnT)	S1 dissociation		S1 binding	
	k_{LS} (s^{-1}) (L.S.)	k_{FL} (s^{-1}) (F.I.)	k_{LS} (s^{-1}) (L.S.)	k_{FL} (s^{-1}) (F.I.)
(+Ca^{2+})				
TnT E60C	975 ± 107	372 ± 48	10.3 ± 1.3	12.2 ± 1.6
TnT S250C	939 ± 103	391 ± 51	11.1 ± 1.3	11.1 ± 1.4
(−Ca^{2+})				
TnT E60C	888 ± 98	407 ± 53	4.5 ± 0.6	5.9 ± 0.7
TnT S250C	828 ± 98	440 ± 57	5.7 ± 0.7	4.9 ± 0.6

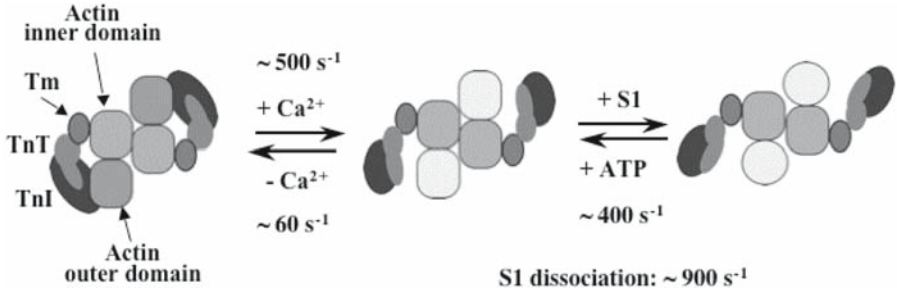

Figure 11.7. The rates of the transition between three states of thin filaments determined from Time-resolved FRET measurements.

between three states are sufficient to explain the movements involved in the regulation mechanism of muscle contraction. Tn movement appears to be critical for the regulation of muscle contraction. Rather than physically blocking the myosin-binding site on the actin filament, Tm appears to regulate the flexibility of the thin and thus controls the regulation of actin-myosin interaction.

11.5. ACKNOWLEDGEMENTS

The author thanks many colleagues for their helpful comments and discussion including: Drs. Y. Maéda, K. Maeda, K. Sano, T. Iio, C. Kimura, H. Hai, and Y. Shitaka. The author also thanks Dr. C. dos Remedios for critical reading of this manuscript. This work was supported in part by grant from the Special Coordination Funds of the Ministry of Education, Culture, Sports, Science and Technology, the Japanese Government.

11.6. REFERENCES

Bacchiocchi, C., and Lehrer, S. S., 2001, Ca^{2+}-induced movement of tropomyosin in skeletal muscle thin filaments observed by multi-site FRET. *Biophys. J.* **82**:1524–1536.

Borovikov, Y. S., Nowak, E., Khoroshev, M. I., and Dabrowska, R., 1993, The effect of Ca^{2+} on the conformation of tropomyosin and actin in regulated actin filaments with or without bound myosin subfragment 1. *Biochim. Biophys. Acta*. **1163**:280–286.

Ebashi, S., Endo, M., and Ohtsuki, I., 1969, Control of muscle contraction, *Q. Rev. Biophys.* **2**:351–384.

Geeves, M. A., and Lehrer, S. S., 1994, Dynamics of the muscle thin filament regulatory switch: the size of the cooperative unit. *Biophys. J.* **67**:273–282.

Greene, L. E., Williams, D. L., Jr., and Eisenberg, E., 1987, Regulation of actomyosin ATPase activity by troponin-tropomyosin: Effect of the binding of the myosin subfragment 1 (S-1), ATP complex. *Proc. Natl. Acad. Sci. USA* **84**:3102–3106.

Hai, H., Sano, K., Maeda, K., Maéda, Y., and Miki, M., 2002, Ca^{2+}-induced conformational change of reconstituted skeletal muscle thin filaments with an internal deletion mutant d234-tropomyosin observed by fluorescence energy transfer spectroscopy: Structural evidence for three states of thin filament. *J. Biochem*. **131**:407–418.

Haselgrove, J., 1972, X-ray evidence for a conformational change in the actin containing filaments of vertebrate striated muscle. *Cold Spring Harb. Symp. Quant. Biol.* **37**:341–352.

Holmes, K. C., 1995, The actomyosin interaction and its control by tropomyosin. *Biophys. J.* **68**:2s–7s.

Huxley, H. E., 1972, Structural changes in the actin- and myosin-containing filaments during contraction. *Cold Spring Harb. Symp. Quant. Biol.* **37**:361–376.

Kimura, C., Maeda, K., Hai, H., and Miki, M., 2002b, Ca^{2+}- and S1-induced movement of troponin T on mutant thin filaments reconstituted with functionally deficient mutant tropomyosin. *J. Biochem*. **132**:345–352.

Kimura, C., Maeda, K., Maéda, Y., and Miki, M., 2002a, Ca^{2+}- and S1-induced movement of troponin T on reconstituted skeletal muscle thin filaments observed by fluorescence energy transfer spectroscopy. *J. Biochem*. **132**:93–102.

Kobayashi, T., Kobayashi, M., and Collins, J. H., 2001, Ca^{2+}-dependent, myosin subfragment 1-induced proximity changes between actin and the inhibitory region of troponin I. *Biochim. Biophys. Acta*. **1549**:148–154.

Kress, M., Huxley, H. E., Faruqi, A. R., and Hendrix, J., 1986, Structural changes during activation of frog muscle studied by time-resolved x-ray diffraction, *J. Mol. Biol*. **188**:325–342.

Landis, C. A., Bobkova, A., Homsher, E., and Tobacman, L. S., 1997, The active state of the thin filament is destabilized by an internal deletion in tropomyosin. *J. Biol. Chem*. **272**:14051–14056.

Lin, T -I., and Dowben, R. M., 1983, Studies on the spatial arrangement of muscle thin filament proteins using fluorescence energy transfer. *J. Biol. Chem*. **258**:5142–5150.

Lorenz, M., Popp, D., and Holmes, K. C., 1993, Refinement of the F-actin model against x-ray fiber diffraction data by the use of a directed mutation algorithm. *J. Mol. Biol.* **234**:826–836.

McKillop, D. F., and Geeves, M. A., 1993, Regulation of the interaction between actin and myosin subfragment 1: evidence for three states of the thin filament. *Biophys. J.* **65**:693–701.

Maytum, R., Geeves, M. A., and Lehrer, S. S., 2002, A modulatory role for the troponin T tail domain in thin filament regulation. *J. Biol. Chem.* **277**:29774–29780.

Miki, M., 1990, Resonance energy transfer between points in a reconstituted skeletal muscle thin filament: A conformational change of the thin filament in response to a change in Ca^{2+} concentration. *Eur. J. Biochem*. **187**:155–162.

Miki, M., Hai, H., Saeki, K., Shitaka, Y., Sano, K-I., Maéda, Y., and Wakabayashi, T., 2004, Fluorescence energy transfer between points on actin and the C-terminal region of tropomyosin in skeletal muscle thin filaments. *J. Biochem.* **136**:39–47.

Miki, M., and Iio, T., 1993, Kinetics of structural changes of reconstituted skeletal muscle thin filaments observed by fluorescence resonance energy transfer. *J. Biol. Chem*. **268**:7101–7106.

Miki, M., Kobayashi, T., Kimura, H., Hagiwara, A., Hai, H., and Maéda, Y., 1998a, Ca^{2+}-induced distance change between points on actin and troponin in skeletal muscle thin filaments estimated by fluorescence resonance energy transfer spectroscopy. *J. Biochem.* **123**:324–331.

Miki, M., and Mihashi, K., 1979, Conformational change of the reconstituted thin filament – fluorescence energy transfer and fluorescence polarization measurements. *Seibutsu-Butsuri* **19**:135–140 (in Japanese).

Miki, M., Miura, T., Sano, K., Kimura, H., Kondo, H., Ishida, H., and Maéda, Y., 1998b, Fluorescence resonance energy transfer between points on tropomyosin and actin in skeletal muscle thin filaments: Does tropomyosin move? *J. Biochem*. **123**:1104–1111.

Monteiro, P. B., Lataro, C., Ferro, J. A., and Reinach, F. C., 1994, Functional a-tropomyosin produced in *Escherichia coli*. *J. Biol. Chem*. **269**:10461–10466.

Nagashima, H., and Asakura, S., 1982, Studies on co-operative properties of tropomyosin-actin and tropomyosin-troponin-actin complexes by the use of N-ethylmaleimide-treated and untreated species of myosin subfragment 1. *J. Mol. Biol*. **155**:409–428.

Narita, A., Yasunaga, T., Ishikawa, T., Mayanagi, K., and Wakabayashi, T., 2001, Ca^{2+}-induced switching of troponin and tropomyosin on actin filaments as revealed by electron cryo-microscopy. *J. Mol. Biol*. **308**: 241–261.

Ohtsuki, I., Maruyama, K., and Ebashi, S., 1986, Regulatory and cytoskeletal proteins of vertebrate skeletal muscle, *Adv. Protein Chem.* **38**:1–67.

Resetar, A. M., Stephens, J. M., and Chalovich, J. M., 2002, Troponin-tropomyosin: An allosteric switch or a steric blocker? *Biophys. J.* **83**:1039–1049.

Squire, J. M., and Morris, E. P., 1998, A new look at thin filament regulation in vertebrate skeletal muscle. *FASEB J.* **12**:761–771.

Shitaka, Y., Kimura, C., Iio, T., and Miki, M., 2004, Kinetics of the structural transition of muscle thin filaments observed by fluorescence resonance energy transfer. *Biochemistry* **46**:10739–10747.

Shitaka, Y., Kimura, C., and Miki, M., 2005, The rates of switching movement of troponin-T between three states of skeletal muscle thin filaments determined by fluorescence resonance energy transfer. *J. Biol. Chem*. **280**:2613–2619.

Stryer, L., 1978, Fluorescence energy transfer as a spectroscopic ruler, *Annu. Rev. Biochem.* **47**:819–846.

Tao, T., Gong, B. J., and Leavis, P. C., 1990, Calcium-induced movement of troponin-I relative to actin in skeletal muscle thin filaments. *Science* **247**:1339–1341.

Tao, T., Lamkin, M., and Lehrer, S. S., 1983, Excitation energy transfer studies of the proximity between tropomyosin and actin in reconstituted skeletal muscle thin filaments. *Biochemistry* **22**:3059–3066.

Vibert, P., Craig, R., and Lehman, W., 1997, Steric-model for activation of muscle thin filaments. *J. Mol. Biol.* **266**:8–14.

White, S. P., Cohen, C., and Phillips, G. N., Jr, 1987, Structure of co-crystals of tropomyosin and troponin. *Nature* **325**:826–828.

12

CALCIUM STRUCTURAL TRANSITION OF TROPONIN IN THE COMPLEXES, ON THE THIN FILAMENT, AND IN MUSCLE FIBRES, AS STUDIED BY SITE-DIRECTED SPIN-LABELLING EPR

Toshiaki Arata, Tomoki Aihara*, Keisuke Ueda, Motoyoshi Nakamura* and Shoji Ueki

12.1. ABSTRACT

We have measured the intersite distance, side-chain mobility and orientation of specific site(s) of troponin (Tn) complex on the thin filaments or in muscle fibres as well as in solution by means of site-directed spin labeling electron paramagnetic resonance (SDSL-EPR). We have examined the Ca^{2+}-induced movement of the B and C helices relative to the D helix in a human cardiac (hc)TnC monomer state and hcTnC-hcTnI binary complex. An interspin distance between G42C (B helix) and C84 (D helix) was 18.4 Å in the absence of Ca^{2+}. The distance between Q58C (C helix) and C84 (D helix) was 18.3 Å. Distance changes were observed by the addition of $Ca^{2+}$and by the formation of a complex with TnI. Both Ca^{2+} and TnI are essential for the full opening ~3 Å of the N-domain in cardiac TnC.

We have determined the *in situ* distances between C35 and C84 by measuring pulsed electron–electron double resonance (PELDOR) spectroscopy. The distances were 26.0 and 27.2 Å in the monomer state and in reconstituted fibres, respectively. The addition of Ca^{2+} decreased the distance to 23.2 Å in fibres but only slightly in the monomer state, indicating that Ca^{2+} binding to the N-lobe of hcTnC induced a larger structural change in muscle fibres than in the monomer state.

We also succeeded in synthesizing a new bifunctional spin labels that is firmly fixed on a central E-helix (94C–101C) of skeletal(sk)TnC to examine its orientation in reconstituted muscle fibres. EPR spectrum showed that this helix is disordered with respect to the filament axis.

We have studied the calcium structural transition in skTnI and tropomyosin on the filament by SDSL-EPR. The spin label at a TnI switch segment (C133) showed three

Department of Biological Sciences, Graduate School of Science, Osaka University and CREST/JST, Toyonaka, Osaka 560-0043, Japan
*Present address: Maeda ERATO/JST, Harima, Hyogo, Japan

Regulatory Mechanisms of Striated Muscle Contraction
Edited by Ebashi and Ohtsuki, Springer, 2007

motional states depending on Ca^{2+} and actin. The data suggested that the TnI switch segment binds to TnC N-lobe in $+Ca^{2+}$ state, and that in $-Ca^{2+}$ state it is free in TnC-I-T complex alone while fixed to actin in the reconstituted thin filaments. In contrast, the side chain spin labels along the entire tropomyosin molecule showed no Ca^{2+}-induced mobility changes.

12.2. INTRODUCTION

Troponin and tropomyosin play a role in Ca^{2+}-sensitive molecular switches that regulate interactions between actin and myosin S1 and these interactions are responsible for the contraction of muscle tissue. Troponin is a hetero-trimeric complex composed of three subunits: TnC, TnI and TnT. TnC binds Ca^{2+}, TnI is the inhibitory subunit that binds to actin and inhibits actomyosin ATPase by preventing strong contacts between myosin and actin in the absence of Ca^{2+}, and TnT anchors the troponin complex to the thin filament and transmits the Ca^{2+} signal along the actin filament.[1–6] X-ray crystal structure showed that TnC was a dumbbell-shaped molecule with separate amino- and carboxy-terminal globular domains (N- and C-domains, respectively) connected by a central linker.[7,8]

The initial activation step consists of the binding of Ca^{2+} to specific binding sites located in the N-domain of skeletal TnC. This binding induces reorientations of the helices in the N-domain, resulting in an open tertiary structure, and exposure of a hydrophobic patch.[9,10] The regulatory and inhibitory regions of TnI are involved in the activation. The regulatory region of TnI moves into the N-domain of TnC activated by Ca^{2+} and interacts with the exposed hydrophobic patch of TnC with a high affinity. This strong interaction facilitates weakening of interactions between the inhibitory region of TnI and actin, thus removing the inhibitory effect of TnI in the presence of Ca^{2+}.[5]

Unlike skeletal TnC which has four competent Ca^{2+} binding sites (site I–IV), cardiac TnC (cTnC) has an inactive Ca^{2+} binding site (site I) in the N-domain. Ca^{2+} binding to the N-domain of cTnC induces little structural change but sets the stage for hcTnI binding. A large "closed" to "open" conformational transition occurs in the N-domain only upon binding cTnI147–163.[11–15] This view was also supported by distance measurements between labeled sites assessed using fluorescence resonance energy transfer (FRET) method and some difference between cardiac and skeletal TnC have been reported.[16]

Recently the X-ray crystal structure of the ternary complex of human cardiac troponin was determined by Takeda et al. (2003) and Vinogradova et al. (2005).[17,18] The troponin complex appears to be divided into subdomains, including the regulatory head, the IT arm, TnT1, C-TnT and TnI_{reg}. The subdomains are connected with the flexible linker conferring the flexibility to the entire molecule. It is thought that during Ca^{2+} activation a middle portion (switch segment) of the regulatory region in TnI associates with the N-domain of TnC and pulls out the inhibitory region from actin. The movements of the regulatory region of TnI were also suggested from FRET analysis within TnI[19] and between TnI and actin.[5,20] It is still unclear whether Ca^{2+} binding to TnC causes an movement of tropomyosin on the thin filament and it facilitates the contraction of muscle tissue.[21–24]

Although *in vitro* structures are available for most of the troponin components and their complexes by X-ray, NMR and FRET methods, it is important to observe dynamic interactions in the complexes *in situ*. Electron paramagnetic resonance (EPR) is a powerful tool for measuring the mobility of spin labels attached to a domain in a protein,[24–30] the angle of attached spin label relative to the applied magnetic field[32–36] and the distance between two spin labels (~25 Å).[37,38] The methods for exchange of TnC andmyosin light chain in muscle fibers[39–41] have made it possible to follow the conformational changes of TnC or myosin neck in permeabilized muscle fiber systems.[33,35,36,42,43] Pioneered EPR[35,36] and fluorescence[43] spectroscopic studies were done to measure the orientation of TnC in muscle fibers. We have investigated Ca^{2+}-induced structural changes of hcTnC reconstituted into muscle fibers, taking advantage of EPR for turbid specimen such as tissues or their homogenates.

In this study, we have employed site-directed mutagenesis to attain specific labeling and positional scanning (i.e. site-directed spin labelling (SDSL)-EPR). We found the Ca^{2+}-induced movement of the B and C helices relative to the D helix both in a human cardiac (hc)TnC monomer state and in hcTnC-hcTnI binary complex.[44] Distance changes between two spin labels at each of the helices were observed by the addition of Ca^{2+} ions and by the formation of a complex with TnI. Both Ca^{2+} and TnI are essential for the full opening ~3 Å of the N-domain in cardiac TnC. We succeeded in measuring the distances between two spin centers in the fibers where the two native cysteine residues (35C and 84C) of hcTnC were both spin-labeled and concluded that Ca^{2+} addition induced structural changes in the N-domain of hcTnC in muscle fibers but only slightly in the monomer state.[45] This work is the first report of pulsed electron-electron double resonance (PELDOR) measurement of the inter-site distance of hcTnC in muscle fibers. We also succeeded in synthesizing a new bifunctional spin label[46] that is firmly fixed on a central E-helix of skTnC to examine its orientation in reconstituted muscle fibres. EPR spectrum showed that this helix is disordered with respect to the filament axis. We have studied the calcium structural transition in skTnI or in tropomyosin on the filament by SDSL-EPR. The spin label at a TnI switch segment (C133) showed three motional states depending on Ca^{2+} and actin.[47] The data suggested that the TnI switch segment binds to TnC N-lobe in $+Ca^{2+}$ state, and that in $-Ca^{2+}$ state it is free in TnC-I-T complex alone while fixed to actin in the reconstituted thin filaments.

12.3. MATERIALS AND METHODS

12.3.1. Spin Labeling of Troponin

Human cardiac troponin C (TnC) and skeletal troponin complex were purified from *E. coli*. expressing TnC with mutational substitution to cysteine (Cys or C) residue or from rabbit skeletal muscle.[44–47] TnC and TnI were labeled with mono-(MSL and MTSL) or bifunctional (BSL) spin labels at excess molar ratio. BSL was synthesized as will be described elsewhere.[46]

12.3.2. Preparation of Reconstituted Muscle Fibres

Skinned fiber bundles, approximately 0.5 mm in diameter, were prepared from rabbit *psoas* muscle fibers and were extracted removing the native TnC and replaced with a spin-labeled TnC while the temperature was kept at 4°C.[45]

12.3.3. EPR Measurements

High-resolution X-band detection from spin labeled troponin in solution and reconstituted muscle fibers was made by Bruker ELEXSYS E500 EPR equipment. Spectral broadening of the double labeled samples, compared with the two single labeled composite spectra, was analyzed using the Fourier deconvolution and the distance distribution was finally obtained.[44] Pulsed ELDOR was performed and analyzed as will be described elsewhere.[45]

12.4. RESULTS AND DISCUSSION

12.4.1. Interspin Distances in Troponin C of the Complex

The EPR spectra of spin-labeled TnC(G42C/C84) and TnC(Q58C/C84) at −100°C are shown in Figure 12.1a. The noninteracting singly labeled TnC(C84) spectrum is also shown by the dotted lines. All spectra were normalized to the same number of spins. A decreased intensity relative to the noninteracting spectrum was observed in all spectra, indicating the existence of dipolar interaction. The spin-spin distances were estimated by

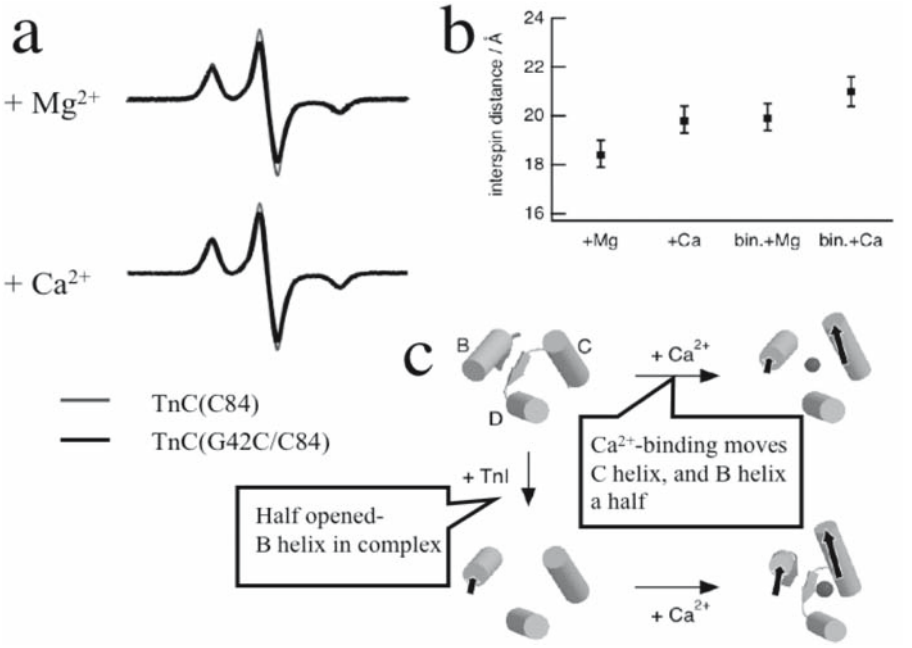

Figure 12.1. EPR distance measurement of Ca^{2+}-induced movement of the B and C helices relative to the D helix in a human cardiac (hc)TnC monomer state and hcTnC-hcTnI binary complex. (a) Comparison between EPR spectra of TnC(C84) and TnC(G42C/C84) in the presence and absence of Ca^{2+}. (b) Ca^{2+}-induced distance changes between G42C and C84 in monomer and binary complex. (c) Closed-open model of B and C helices relative to helix D.

the Fourier deconvolution method. In these estimations, we used one Gaussian function to fit the broadening function in the Fourier space; this means that the mean distances were determined without considering the distance distribution. Figure 12.1b shows the mean spin-spin distances of the binary complex with Mg^{2+}. A further increase was observed by the addition of Ca^{2+} ions in the binary complex. Figure 12.1b shows the distances observed in both the monomer and binary complex. Formation of a complex with TnI had little effect on the spin-spin distance in this spin-labeled mutant. Our data indicated that the C helix moved away from the D helix in a distinct Ca^{2+}-dependent manner, while the B helix did not. A movement of the B helix by interaction with TnI was observed. Both Ca^{2+} and TnI were also shown to be essential for the full opening of the N-domain in cardiac TnC (Figure 12.1c).

12.4.2. Interspin Distances in the Reconstituted Fibers Determined by Pulse EPR

In order to detect the size change of hcTnC induced by Ca^{2+}, we measured the distances between two spin labels (MTSSL) attached to 35C and 84C residues in the monomer state and in fibers using PELDOR analysis. The PELDOR spectra of the monomer states were almost the same and the interspin distances in the monomer state were estimated to be 25.5 Å and 26.0 Å in the presence and absence of Ca^{2+}, respectively. In reconstituted fibers, the spectrum of $-Ca^{2+}$ was different from that of $+Ca^{2+}$ showing that the modulation periodicities were different. If the distance is short, the periodicity of the observed spectrum is short. The period is in proportion to the third power of the distance. The interspin distances were 27.2 Å and 23.2 Å at low and high Ca^{2+} concentrations, respectively (Figure 12.2) and Ca^{2+} addition increased the deviation from 2.1 Å to 5.8 Å. Thus, Ca^{2+} binding to the N-domain induced 4 Å decrease in the distance between 35C and 84C in reconstituted muscle fibers but not in the monomer state. This is the first

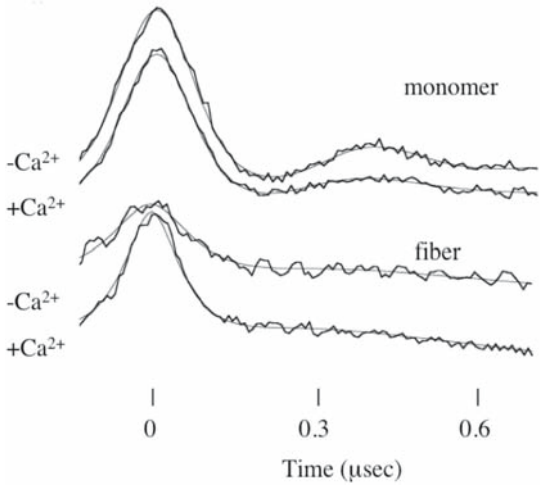

Figure 12.2. Pulsed ELDOR distance measurements of doubly spin-labeled TnC (35C and 84C) in the presence and absence of Ca^{2+} in monomer and in fibers. Ca^{2+} induces changes in periodicity of echo modulation, showing changes in interspin distance.

report that successfully measured the distance between two native cysteine residues (35 and 84) of hcTnC in muscle fibers using PELDOR. Furthermore, we could find that the distance of hcTnC in the monomer state was different from that in the fiber state and that the distance of hcTnC in muscle fibers state became shorter in $+Ca^{2+}$ state than in $-Ca^{2+}$ state.

12.4.3. Bifunctional Spin Label on Troponin C

We have succeeded in synthesizing a new bifunctional spin labels that is firmly fixed on a central E-helix (94C–101C) of skTnC. An enatiomeric pair of C_2-chiral bifunctional spin labels having pyrrolidine nitroxide moiety whose configurations were determined by X-ray crystal diffraction analysis were prepared and applied to troponin C whose binding mode of double disulphide linkagewas proved by EPR spectroscopy.

EPR spectra showed that (S,S)-1 and (R,R)-1 were largely immobilized when they were labelled on the TnC protein (Figure 12.3, second spectrum). Small sharp peaks were completely removed by passing through the thiol resin column. Final spectra from (S,S)-1 and (R,R)-1 (Figure 12.3, third and fourth spectra) showed a high immobilization as compared to monofunctional label. According to Stoke's hydrodynamic theory, the rotational correlation time for TnC (molecular weight of 18,000) at 25°C is 7 ns. The rotational correlation time of 5 ns was calculated for (S,S)-1 and (R,R)-1. The observed spectra were

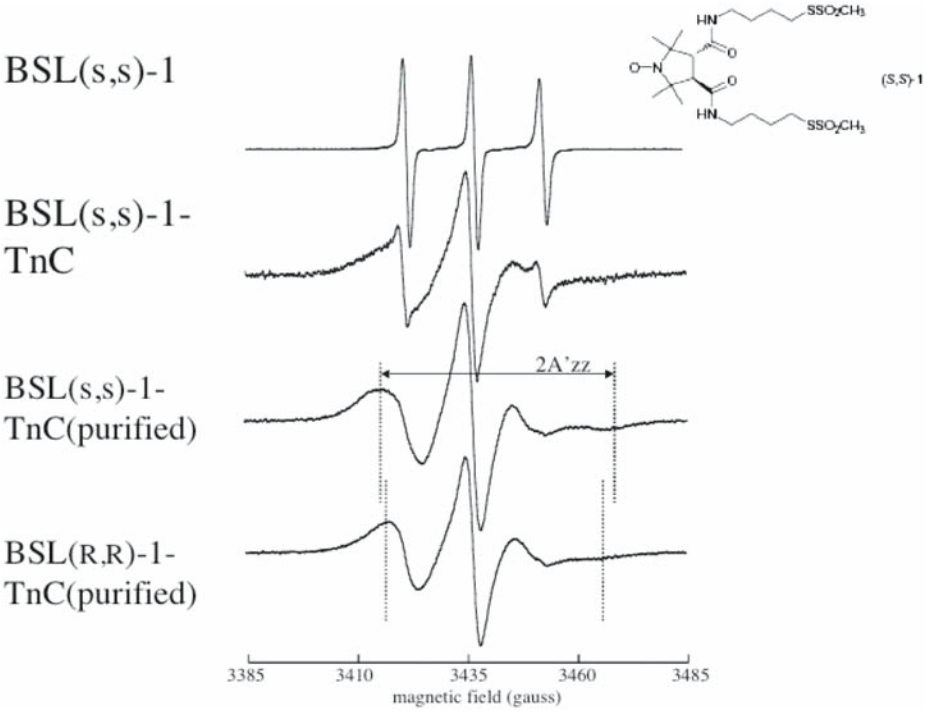

Figure 12.3. Bifunctional spin labels (BSL) and their application to troponin C. EPR spectra show large immobilization of BSL on protein surface as indicated by $2A'_{zz}$.

similar to one simulated with a single motional component according to stochastic Liouville approach by Freed and colleagues for Brownian diffusion. A good agreement in rotational correlation time suggests that spin label motion reflects the motion of the whole protein molecule. However, a small spectral difference in (S,S)-1 and (R,R)-1 arise from diastereomeric interaction between chiral spin labels and protein: (1) the anisotropic motion is characterized by different orientation of spin labels relative to the main rotational axis of protein molecule; (2) the molecular shapes of TnC are slightly different by modification with (S,S)-1 and (R,R)-1; and (3) slight segmental motion of spin label relative to a whole protein molecule is different in (S,S)-1 and (R,R)-1 attached sites.

We have examined the orientation of bifunctional spin label in reconstituted muscle fibres. EPR spectrum showed that this helix is disordered with respect to the filament axis (data not shown).

12.4.4. Spin-label Mobility of Troponin I and Tropomyosin Reconstituted with Actin

We measured EPR spectra from the spin label (MSL) of C133 of TnI in ternary TnC-I-T complexes to investigate conformational changes of the switch segment in TnI, induced by Ca^{2+}. In the $+Ca^{2+}$ state, absorption line shapes were broad, and the two extremes at the low- and high-field were small relative to the central peak. We deduced a slow motion of rotational correlation time of 4.80 ns (Table 12.1). In the $-Ca^{2+}$ state (1 mM EGTA), sharp peaks appeared and corresponded to the correlation time of 1.93 ns (Table 12.1).

To examine how spin label mobility of C133 in TnI changes in response to Ca^{2+} on thin filaments, we reconstituted them with MSL-Tn-tropomyosin, and actin. In the $+Ca^{2+}$ state, spectrum shape mimicked that of troponinC-I-T complexes alone. The rotational correlation time was 4.72 ns (Table 12.1). On the other hand, in the $-Ca^{2+}$ state, a marked shoulder appeared at the lower field. Similar corresponding changes were seen at a higher magnetic field. The shoulder indicates a component of slow motion. The rotational correlation time was calculated as ~45.2 ns from the spectrum produced by spectral subtraction of the spectrum of $+Ca^{2+}$ state containing 72% of the total spins from that of the

Table 12.1. Summary of the rotational correlation time (τ) of spin label in TnI

		τ (ns)	
Proteins	State	Fast	Slow
			–
TnC-I	$-Ca^{2+}$	1.67	
	$+Ca^{2+}$	3.26	–
TnC-I-T	$-Ca^{2+}$	1.93 ± 0.57[a]	–
	$+Ca^{2+}$	4.80 ± 1.57[a]	–
TnC-I-T-Tropomyosin-Actin	$-Ca^{2+}$	4.76 (72%)	45.2 (28%)
	$+Ca^{2+}$	4.76	–
TnI-Actin		2.61(55%)	45.2 (45%)
TnI-Tropomyosin-Actin		2.61 (33%)	43.0 (67%)

[a] Data are taken from three preparations and shown by mean ± SD.

$-Ca^{2+}$ state. We could not observe any enhancement of the fast motional component by adding EGTA, unlike MSL-Tn alone. To examine whether Ca^{2+}-removal induced immobilization of the spin label on C133 of TnI in thin filaments, and that it was due to the binding of the side chain of C133 to actin or TnT/C, we reconstituted isolated MSL-TnI with actin with or without tropomyosin. No Ca^{2+} effect was observed, unlike in the thin filaments (TnC-I-T-tropomyosin-actin). Both spectra, especially from TnI-tropomyosin-actin, were very similar to that from thin filaments reconstituted in the $-Ca^{2+}$ state. Both spectra consisted of two distinct components, i.e, fast and slow motions. The slow component was close to the motion observed in thin filaments in the $-Ca^{2+}$ state (t = ~45 ns). Therefore, the fast component of TnI-actin was easily produced by subtracting 45% of the total spins of the slow component obtained by decomposition of the two spectra of TnC-I-T-tropomyosin-actin. From the spectral parameters, we deduced a rotational correlation time to be 2.6 ns, for the fast component (Table 12.1). This fast component containing 33% of the total spins was subtracted from the spectrum of TnI-tropomyosin-actin to produce the same slow component again (43 ns). These results were a strong indication that C133 in TnI interacted directly with actin in thin filaments in the $-Ca^{2+}$ state, because it could interact with actin in the same way, irrespective of troponin or tropomyosin.

We therefore postulated regarding the mechanism for the switch action of TnI. In troponin complexes in the $-Ca^{2+}$ state, the C-terminal region of TnI is away from TnC, and flexible without interactions with other proteins, leading to the flexible structure of C133 that is like a loop or an independently-tumbling helical segment. When Ca^{2+} is present, the C133 region of TnI folds into a helix or is stabilized by binding with the N-lobe of Ca^{2+}-saturated TnC. These observations are consistent with the crystal structure of chicken skeletal troponin complexes as recently revealed by Vinogradova et al.[18] Although the C-terminal region including Asn(N)133 in TnI has been resolved to a loop in the $+Ca^{2+}$ state, the switch segment (amino acids 113–131) very close to N133 forms an α-helix, and interacts with the N-lobe of TnC. In the $-Ca^{2+}$ state, the switch segment and C-terminus including N133 in TnI are not resolved due to the low density. A recent NMR study[48] showed that 132–140 residues in the α-helix of TnI were flexible and mobile in solution. In reconstituted thin filaments, the C-terminal second actin binding site including C133 binds to actin, and the attached spin label is involved in tertiary contact. Recently, Murakami et al.[48] showed that the C-terminal domain including N133 next to the switch segment bound to an outer domain of the actin subunit at low Ca^{2+} conditions.

To examine whether Ca^{2+} induces mobility changes of the spin label at the amino acid side chain of tropomyosin on the thin filaments, we spin-labeled tropomyosin using cysteine scanning. The binding of tropomyosin with actin and Tn immobilized the spin labels at C-terminal portion (Figure 12.4). The binding with myosin S1 immobilized a spin label at a middle portion. No Ca^{2+} effect was observed when Tn and actin were present. This result suggested that upon Ca^{2+} activation tropomyosin did not undergo a large translocation or conformational changes on the actin filament surface.

We are now undertaking site-directed distance measurements using dipolar EPR methods to identify the detailed mechanisms involved in interactions between the C-terminal region of TnI, the N-lobe of TnC and the entire length of tropomyosin on the surface of actin filament in the $-Ca^{2+}$ and $+Ca^{2+}$ state.

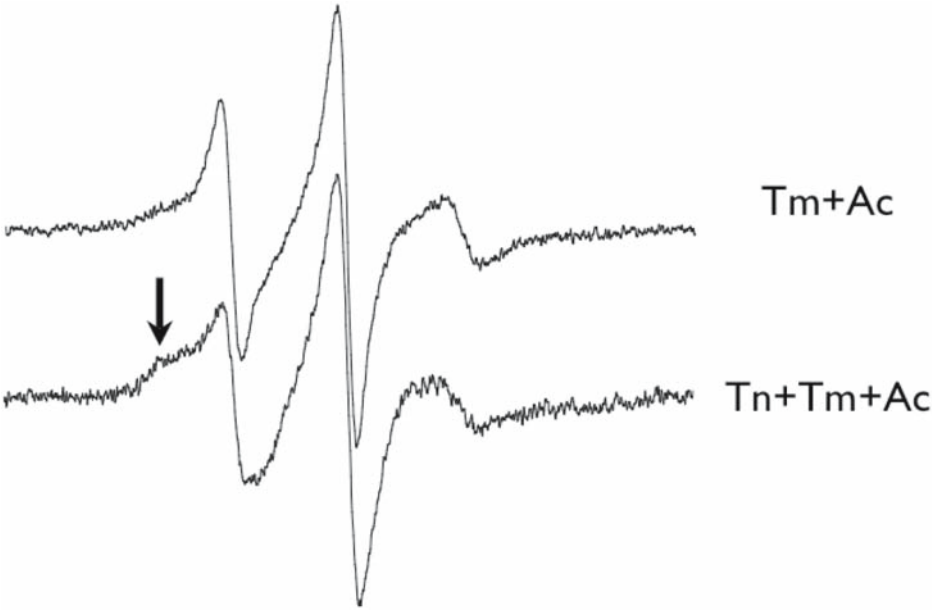

Figure 12.4. EPR spectra of tropomyosin (Tm) spin labeled at S271C complexed with actin (Tm + Ac) and on the thin filament (Tn + Tm + Ac). Troponin (Tn) binding immobilized spin labels as indicated by an arrow.

12.5. ACKNOWLEDGEMENTS

We are grateful to Prof. Yuichiro Maeda and Dr. Soichi Takeda for generously giving us TnC genes and to Drs. Masao Miki and Chieko Kimura for giving us tropomyosin mutants and their valuable discussions. We also thank Dr. Hideyuki Hara for measuring pulse ELDOR in Bruker BioSpin Japan, Tukuba and Prof. Yukio Yamamoto for synthesizing BSL in Kyoto Univesity. We are supported by Special Coordination Funds for promoting Science and Technology and by Grants-in-Aid for Scientific Research, from Ministry of Education, Science, Technology, Culture and Sports of Japanese Government.

12.6. REFERENCES

1. J. Gergely, Molecular switches in troponin, *Adv. Exp. Med. Biol.* **453**, 169–176 (1998).
2. S. Ebashi, and M. Endo, Calcium ion and muscle contraction, *Prog. Biophys. Mol. Biol.* **18**, 123–183 (1968).
3. S. S. Lehrer, and M. A. Geeves, The muscle thin filament as a classical cooperative/allosteric regulatory system, *J. Mol. Biol.* **277**, 1081–1089 (1998).
4. A. S. Zot, and J. D. Potter, Reciprocal coupling between troponin C and myosin crossbridge attachment, *Annu. Rev. Biophys. Biophys. Chem.* **16**, 535–559 (1987).
5. T. Tao, B. J. Gong, and P. C. Leavis, Calcium-induced movement of troponin-I relative to actin in skeletal muscle thin filaments, *Science* **247**, 1339–1341 (1990).
6. S. V. Perry, Troponin I: inhibitor or facilitator, *Mol. Cell. Biochem*. **190**, 9–32 (1999).

7. O. Herzberg, and M. N. James, Refined crystal structure of troponin C from turkey skeletal muscle at 2.0 A resolution, *J. Mol. Biol.* **203**, 761–779 (1988).
8. D. G. Vassylyev, S. Takeda, S. Wakatsuki, K. Maeda, and Y. Maeda, Crystal structure of troponin C in complex with troponin I fragment at 2.3 Å-resolution, *Proc. Natl. Acad. Sci. USA* **95**, 4849–4852 (1998).
9. S. M. Gagne, S. Tsuda, M. X. Li, L. B. Smillie, and B. D. Sykes, Structures of the troponin C regulatory domains in the apo and calcium-saturated states, *Nat. Struct. Biol.* **2**, 784–789 (1995).
10. C. M. Slupsky, and B. D. Sykes, Solution secondary structure of calcium-saturated troponin C monomer determined by multidimensional heteronuclear NMR spectroscopy, *Biochemistry* **34**, 15953–15964 (1995).
11. L. Spyracopoulos, M. X. Li, S. K. Sia, S. M. Gagne, M. Chandra, R. J. Solaro, and B. D. Sykes, Calcium-induced structural transition in the regulatory domain of human cardiac troponin C, *Biochemistry* **36**, 12138–12146 (1997).
12. R. T. McKay, J. R. Pearlstone, D. C. Corson, S. M. Gagne, L. B. Smillie, and B. D. Sykes, Structure and interaction site of the regulatory domain of troponin C when complexed with the 96–148 region of troponin-I, *Biochemistry* **37**, 12419–12130 (1998).
13. M. X. Li, L. Spyracopoulos, and B. D. Sykes, Binding of cardiac troponin-I 147–163 induces a structural opening in human cardiac troponin C, *Biochemistry* **38**, 8289–8298 (1999).
14. X. Wang, M. X. Li, and B. D. Sykes, Structure of the regulatory N-domain of human cardiac troponin C in complex with human cardiac troponin I 147–163 and bepridil, *J. Biol. Chem.* **277**, 31124–31133 (2002).
15. S. K. Sia, M. X. Li, L. Spyracopoulos, S. M. Gagne, W. Liu, J. A. Putkey, and B. D. Sykes, Structure of cardiac muscle troponin C unexpectedly reveals a closed regulatory domain, *J. Biol. Chem.* **272**, 18216–18221 (1997).
16. W. J. Dong, J. Xing, M. Villain, M. Hellinger, J. M. Robinson, M. Chandra, R. J. Solaro, P. K. Umeda, and H. C. Cheung, Conformation of the regulatory domain of cardiac muscle troponin C in its complex with cardiac troponin I, *J. Biol. Chem.* **274**, 31382–31390 (1999).
17. S. Takeda, A. Yamashita, K. Maeda, and Y. Maeda, Structure of the core domain of human cardiac troponin in the Ca^{2+}-saturated form, *Nature* **424**, 35–41 (2003).
18. M. V. Vinogradova, D. B. Stone, G. G. Malanina, C. Karatzaferi, R. Cooke, R. A. Mendelson, R. J. Fletterick, Ca^{2+}-regulated structural chanS. ges in troponin, *Proc. Natl. Acad. Sci. USA* **102**, 5038–5043 (2005).
19. W. J. Dong, J. M. Robinson, S. Stagg, J. Xing, and H. C. Cheung, Ca^{2+}-induced conformational transition in the inhibitory and regulatory regions of cardiac troponin I, *J. Biol. Chem.* **278**, 8686–8692 (2003).
20. M. Miki, T. Kobayashi, H. Kimura, A. Hagiwara, H. Hai, and Y. Maeda, Ca^{2+}-induced distance change between points on actin and troponin in skeletal muscle in filaments estimated by fluorescence energy transfer spectroscopy, *J. Biochem.* **123**, 324–331 (1998).
21. R. Craig, and W. Lehman, Crossbridge and tropomyosin positions observed in native, interacting thick and thin filaments, *J. Mol. Biol.* **311**, 1027–1036 (2001).
22. A. Narita, T. Yasunaga, T. Ishikawa, K. Mayanagi, and T. Wakabayashi, Ca^{2+}-induced switching of troponin and tropomyosin on actin filaments as revealed by electron cryo-microscopy, *J. Mol. Biol.* **308**, 241–261 (2001).
23. C. Bacchiocchi, and S. S. Lehrer, Ca^{2+}-induced movement of tropomyosin in skeletal muscle thin filaments observed by multi-site FRET, *Biophys. J.* **82**, 1524–1536 (2002).
24. M. Miki, H. Hai, K. Saeki, Y. Shitaka, K. Sano, Y. Maeda, and T. Wakabayashi, Fluorescence resonance energy transfer between points on actin and the C-Terminal region of tropomyosin in skeletal muscle thin filaments, *J. Biochem.* **136**, 39–47 (2004).
25. Y. Tonomura, S. Watanabe, and M. Morales, Conformational changes in the molecular control of muscle contraction, *Biochemistry* **8**, 2171–2176 (1969).
26. S. Ebashi, S. Onishi, S. Abe, and K. Maruyama, A spin-label study on calcium-induced conformational changes of troponin components, *J. Biochem.* **75**, 211–213 (1974).
27. T. Arata, and H. Shimizu, Spin-label study of actin-myosin-nucleotide interactions in contracting glycerinated muscle fibers. *J. Mol. Biol.* **151**, 411–437 (1981).
28. V. A. Barnett, and D. D. Thomas, Resolution of conformational states of spin-labeled myosin during steady-state ATP hydrolysis. *Biochemistry* **26**, 314–323 (1987).

29. K. Sugata, M. Nakamura, S. Ueki, P. G. Fajer, and T. Arata, ESR reveals the mobility of the neck linker in dimeric kinesin, *Biochem. Biophys. Res. Commun.* **314**, 447–451 (2004).
30. J. D. Potter, J. C. Seidel, P. Leavis, S. S. Lehrer, and J. Gergely, Effect of Ca^{2+} binding on troponin C. Changes in spin label mobility, extrinsic fluorescence, and sulfhydryl reactivity, *J. Biol. Chem.* **251**, 7551–7556 (1976).
31. H. C. Li, K. Hideg, and P. G. Fajer, The mobility of troponin C and troponin I in muscle, *J. Mol. Recognit.* **10**, 194–201 (1997).
32. D. D. Thomas, and R. Cooke, Orientation of spin-labeled myosin heads in glycerinated muscle fibers, *Biophys. J.* **32**, 891–906 (1980).
33. T. Arata, Orientation of spin-labeled light chain 2 of myosin heads in muscle fibers, *J. Mol. Biol.* **214**, 471–478 (1990).
34. D. Szczesna, and P. G. Fajer, The tropomyosin domain is flexible and disordered in reconstituted thin filaments, *Biochemistry* **34**, 3614–3620 (1995).
35. H. C. Li, and P. G. Fajer, Orientational changes of troponin C associated with thin filament activation, *Biochemistry* **33**, 14324–14332 (1994).
36. H. C. Li, and P. G. Fajer, Structural coupling of troponin C and actomyosin in muscle fibers, *Biochemistry* **37**, 6628–6635 (1998).
37. L. J. Brown, K. L. Sale, R. Hills, C. Rouviere, L. Song, X. Zhang, and P. G. Fajer, Structure of the inhibitory region of troponin by site directed spin labeling electron paramagnetic resonance, *Proc. Natl. Acad. Sci. USA* **99**, 12765–12770 (2002).
38. P. P. Borbat, H. S. McHaourab, and J. H. Freed, *J. Am. Chem. Soc.* **124**, 5304–5314 (2002).
39. R. L. Moss, G. G. Giulian, and M. L. Greaser, Physiological effects accompanying the removal of myosin LC2 from skinned skeletal muscle fibers, *J. Biol. Chem.* **257**, 8588–8591 (1982).
40. S. Morimoto, and I. Ohtsuki, Ca^{2+}- and Sr^{2+}-sensitivity of the ATPase activity of rabbit skeletal myofibrils: effect of the complete substitution of troponin C with cardiac troponin C, calmodulin, and parvalbumins, *J. Biochem.* **101**, 291–301 (1987).
41. R. L. Moss, Ca^{2+} regulation of mechanical properties of striated muscle. Mechanistic studies using extraction and replacement of regulatory proteins, *Circulation Research* **70**, 865–884 (1992).
42. M. Irving, T. St. Claire Allen, C. Sabido-David, J. S. Craik, B. Brandmeier, J. Kendrick-Jones, J. E. Corrie, D. R. Trentham, and Y. E. Goldman, Tilting of the light-chain region of myosin during step length changes and active force generation in skeletal muscle, *Nature* **375**, 688–691 (1995).
43. R. E. Ferguson, Y. B. Sun, P. Mercier, A. S. Brack, B. D. Sykes, J. E. Corrie, D. R. Trentham, and M. Irving, In situ orientations of protein domains: troponin C in skeletal muscle fibers, *Mol. Cell.* **11**, 865–874 (2003).
44. S. Ueki, M. Nakamura, T. Komori, T. Arata, Site-directed spin labeling electron paramagnetic resonance study of the calcium-induced structural transition in the N-domain of human cardiac troponin C complexed with troponin I, *Biochemistry* **44**, 411–416 (2005).
45. M. Nakamura, S. Ueki, H. Hara, and T. Arata, Calcium structural transition of human cardiac troponin C in reconstituted muscle fibres as studied by site-directed spin labelling, *J. Mol. Biol.* **348**, 127–137 (2005).
46. S. Chatani, M. Nakamura, H. Akahane, N. Kohyama, M. Taki, T. Arata, and Y. Yamamoto, Synthesis of C_2-chiral bifunctional spin labels and their application to troponin C, *Chem. Commun.* 1880–1882 (2005).
47. T. Aihara, S. Ueki, M. Nakamura, and T. Arata, Calcium-dependent movement of troponin I between troponin C and actin as revealed by spin-labeling EPR, *Biochem. Biophys. Res. Commun.* **349**, 449–456 (2006).
48. K. Murakami, F. Yumoto, S. Y. Ohki, T. Yasunaga, M. Tanokura, and T. Wakabayashi, Structural basis for Ca^{2+}-regulated muscle relaxation at interaction sites of troponin with actin and tropomyosin, *J. Mol. Biol.* **352**, 178–201 (2005).

13

CRYSTAL STRUCTURES OF TROPOMYOSIN: FLEXIBLE COILED-COIL

Yasushi Nitanai[1,2], Shiho Minakata[1], Kayo Maeda[1], Naoko Oda[1] and Yuichiro Maéda [1,2,3]

13.1. ABSTRUCT

Tropomyosin (Tm) is a 400 Å long coiled coil protein, and with troponin it regulates contraction in skeletal and cardiac muscles in a [Ca^{2+}]-dependent manner. Tm consists of multiple domains with diverse stabilities in the coiled coil form, thus providing Tm with dynamic flexibility. This flexibility must play important roles in the actin binding and the cooperative transition between the calcium regulated states of the entire muscle thin filament. In order to understand the flexibility of Tm in its entirety, the atomic coordinates of Tm are needed. Here we report the two crystal structures of Tm segments. One is rabbit skeletal muscle α-Tm encompassing residues 176–284 with an N-terminal extension of 25 residues from the leucine zipper sequence of GCN4, which includes the region that interacts with the troponin core domain. The other is α-Tm encompassing residues 176–273 with N- and C-terminal extensions of the leucine zipper sequences. These two crystal structures imply that this molecule is a flexible coiled coil. First, Tm's are not homogeneous and smooth coiled coils, but instead they undulate, with highly fluctuating local parameters specifying the coiled coil. Independent fluctuating showed by two crystal structures is important. Second, in the first crystal, the coiled coil is bent by 9 degrees in the region centered about Y214-E218-Y221, where the inter-helical distance has its maximum. On the other hand, no bend is observed at the same region in the second crystal even if its inter-helical distance has also its maximum. E218, an unusual negatively charged residue at the *a* position in the heptad repeat, seems to play the key role in destabilizing the coiled coil with alanine destabilizing clusters.

13.2. INTRODUCTION

Tropomyosin (Tm) was originally discovered by Bailey in the muscle cell as a protein of unknown function.[1] Subsequently, Ebashi and his colleagues established that Tm binds along the length of the actin filament and, together with troponin, plays an important role

[1] ERATO Actin Filament Dynamics Project, JST, Sayo, Hyogo 679-5148, Japan, [2]Laboratory for Structural Biochemistry, RIKEN SPring-8 Center, Sayo, Hyogo 679-5148, Japan, [3]Division of Biological Science, Graduate School of Science, Nagoya University, Nagoya 464-8602, Japan

Regulatory Mechanisms of Striated Muscle Contraction
Edited by Ebashi and Ohtsuki, Springer, 2007

in the [Ca^{2+}]-regulation of muscle contraction.[2,3] In non-muscle cells, many isoforms of Tm are known to be expressed.[4,5] It is believed that, the interactions of Tm with the actin filament not only stabilize the filament but also regulate its conformation and mechanical properties. The muscle Tm molecule is a parallel α-helical coiled coil with a length of about 400 Å, consisting of identical or highly homologous peptides of 284 residues. It is generally accepted that in the cardiac and skeletal muscle thin filaments, the core domain of troponin (Tn) (including TnC, the main part of TnI and TnT_2) interacts with the region of Tm roughly spanning residues 160 to 220,[6] although details of the sites and the manner of the interaction remain unknown.

Each peptide that forms a parallel α-helical coiled coil has heptapeptide repeats (*a-b-c-d-e-f-g*). The residues at positions *a* and *d* are usually hydrophobic and packed in a regular "knobs-into-holes" pattern,[7,8] along the dimerization interface, to form the hydrophobic core. In the core, each side chain *a* (*d*) is surrounded by four side chains of the opposite helix, with two at the *d′* (*a′*) positions, and one each at *a′* (d′) and *g′* (e′).[9] This regular pattern of interactions is facilitated by the formation of the coiled coil, in which two right-handed α-helices wind around each other to form a left-handed coiled coil, with a quasi repeat of 7 residues per 2 turns of each α-helix with respect to the coiled coil axis. The dimer stabilizing energy is contributed mostly by the hydrophobic interactions in the core, as well as by inter-helical hydrogen bonds such as those between the side chains *e – g'* or *g - e'*.[10] Systematic studies[11,12] revealed that the dimer stabilizing effect of different types of residues in the *a* and *d* positions is in the following order: hydrophobic residues of appropriate sizes, bulky hydrophobic residues, alanine residues, neutral hydrophilic residues, basic residues, acidic residues, Gly, and Pro, although there are minor variations between positions *a* and *d*. Thus, the coiled coil domain (the leucine zipper motif) of the yeast transcription factor GCN4 has many Val residues at position *a* and Leu residues at position *d*.[9] The leucine zipper sequence of GCN4 forms the canonical α-helical coiled coil structure.[13]

The entire sequence of Tm consists of uninterrupted heptapeptide repeats that are characteristic of the coiled coil structural motif. However, the Tm sequences are far from the canonical coiled coil sequence. Tm has many alanine residues at positions *a* and *d*, which form clusters and destabilize the coiled coil.[12,14–16] In addition, the remarkable is occurrences of the acidic residues Asp-137(*d*) and Glu-218(*a*) also destabilize the dimer.

The characteristic Tm sequences that are atypical for coiled coil proteins must be associated with its flexibility, which plays a crucial role in regulating the conformation and properties of the actin filament. The concept of flexibility is based on four lines of considerations and observations. First, on the actin filament, Tm cannot be a rigid rod, but rather should follow the helical groove of the actin filament, which rotates by 180 degrees around the filament axis in every axial rise of 385 Å. Second, a perturbation of one part of Tm alters the properties of remote region of the molecule. Thus, between two isomers of lobster skeletal muscle Tm, amino acid replacements within exon-2 (residues 39–81) cause prominent changes in the head-to-tail interaction between the N- and C-terminal regions.[17] Third, in the actin-Tm-Tn complex, where the Tm molecules interact with each other in a head-to-tail fashion, forming a Tm strand, the [Ca^{2+}]-dependent regulation of the actomyosin interaction is cooperative, so that the state of one Tm influences that of the next Tm along the strand. Fourth, upon an increase in temperature or of guanidine hydrochloride concentration, Tm unfolds in two distinct steps.[18,19] In the first step, the pre-transition, Tm unfolds to a partially unfolded stable intermediate in which

the two chains are associated. This is followed by the main transition to a completely unfolded state, where the two chains are separated. Lehrer and his colleagues found that Cys-190 is located in the unstable region of the intermediate,[20] and by measuring the excimer fluorescence from pyrene maleimide-labeled Tm at Cys-190, they concluded that the localized chain separation is associated with the pre-transition.[21,22] Further studies of the fluorescence of probes attached to Cys-190[23] and the electron spin resonance (ESR) spectra of spin-labels attached to Cys-190[24] indicated that, at 30–40°C, Tm is in a dynamic equilibrium between two conformational states. Moreover, NMR studies of His-153[25] and differential calorimetry analyses of Tm[26,27] indicated that, at physiological temperatures, Tm exists in an equilibrium between multiple conformations. This implies that there may be several unstable segments that are separated by more stable segments, and that each unstable segment has distinct instability. In spite of these results, our present understanding of the flexibility of Tm is far from complete. In order to determine the dynamic properties of Tm in their entirety, the atomic coordinates of Tm is needed. Although, in principle, an atomic structure obtained by X-ray crystallography is static in nature, it could provide important clues about the flexibility.

Tm is readily crystallized to form the "Bailey-type" crystals, which were reported as early as in 1948.[24] The Bailey-type crystal, however, poorly diffracts X-ray, due to its extraordinarily high solvent content (>90%). This crystal form, prepared from porcine and rabbit cardiac muscle Tm, was used to obtain information about the overall shape and the packing mode of the entire molecule at 7 Åresolution. [28] The atomic structures at higher resolution were obtained from an 81-residue N-terminal fragment of chicken skeletal muscle α-Tm (Tm81) at 2.0 Åresolution [29] and from a 31-residue C-terminal fragment of rat skeletal muscle α-Tm preceded by a 24-residue fragment of the GCN4 leucine-zipper at 2.7 Åresolution. [30] A solution NMR structure has also been obtained from a 34-residue C-terminal fragment of vertebrate skeletal α-Tm.[31]

In the present study, we have obtained two crystal structures at atomic resolution of two α-Tm segments including the region interacting with the troponin core domain (TnC, TnI and TnT_2). The first crystal structure is obtained from ZrsTm176 composed of the rabbit skeletal muscle α-Tm segment encompassing residues 176–284 (the C-terminus) with an N-terminal extension of 25 residues of the leucine-zipper sequence of GCN4. The second crystal structure is obtained from NZrsTm176NZ composed of α-Tm segment encompassing residues 176–273 with N- and C- terminal extensions of 28 residues of the leucine-zipper sequence.

13.3. METHODS AND MATERIALS

13.3.1. Expression and Purification of ZrsTm176 and NZrsTm176NZ

First, we made six constructs of the C-terminal segment of rabbit skeletal muscle α-Tm. They span from residue 141, 148, 155, 162, 169, or 176 to 284, which is the original C-terminus of Tm. Each construct has the 25-residues leucine-zipper sequence of GCN4 as an N-terminal extension. For simplicity, the procedures described below are only those for ZrsTm176 (*Z* and *rs* stand for leucine *z*ipper sequence and for *r*abbit *s*keletal muscle, respectively), for which structure was successfully obtained, as essentially the same procedures were also used for the other constructs.

To construct the expression vector pETZrsTm176, the DNA fragment ZrsTm176 was amplified by PCR using rabbit skeletal muscle α-Tm cDNA.[37] The amplified fragment was digested by the restriction enzymes NcoI and BamHI. The fragment was ligated to pET3d, which had been digested by the restriction enzymes NcoI and BamHI.

The recombinant protein was expressed in BL21(DE3) cells, and was purified as described previously[29] with some minor modifications. NZrsTm176NZ (*NZ* stands for new leucine *z*ipper sequence) was produced by fundamentally same protocols. It will be described elsewhere in detail.

13.3.2. Crystallization, Data Collection and Structure Determination

Initial screening of the crystallization conditions for each of the six constructs of ZrsTm's was performed by use of the crystallization robot TERA,[38] in combination with large scale manual screenings with high throughput techniques. The best crystallization conditions were as follows: a drop containing 5 µl of ~20 mg/ml protein solution and 5 µl of 40% MPD, 5 mM DTT, 0.2 M ammonium acetate, 0.1 M sodium citrate, pH 5.2–5.6 was set against 500 µl of a reservoir containing 20–40% MPD, 5 mM DTT, 0.2 M ammonium acetate and 0.1 M sodium citrate pH 5.2–5.6, using the sitting drop vapor diffusion method. To grow crystals, we used an unusual annealing technique, in which an entire crystallization plate containing thin crystals was heated in an air gel dryer for 30 min to dissolve the small crystals, followed by slow cooling down to room temperature to grow the crystals.

The diffraction data sets were collected at RIKEN Structural Biology Beamline II (BL44B2) at SPring-8,[39] under a dry nitrogen stream at 100 K. The diffraction patterns from the ZrsTm176 crystals were anisotropic, giving rise to many weak spots. To gain a sufficient S/N ratio, we collected and merged diffractions of 1620 degrees with an average redundancy as high as 16.5, in spite of the fact that the crystal belonged to the space group *P1*. These properties of the crystal must originate from both the properties of the individual Tm molecules and the crystal packing (see the results section). These data were processed with the program *Crystal Clear*.[40]

The structure was determined by the molecular replacement method using *AMoRe*[41] in the of *CCP4* program suit.[42,43] The poly alanine model of an N-terminal tropomyosin fragment[29] gave the best solutions. Refinement and model building were carried out by *CNS*[29] and *Xtalview,*[44] and *MI-fit,* [45] respectively. Due to a lack of electron densities, two residues at both the N-terminus and the C-terminus of each polypeptide, as well as the side chains for a total of 32 residues, could not be modeled. A Ramachandran plot showed that 91.7% of the residues belong to the most favored regions and 8.3% are in the additionally allowed regions, with none in the generously allowed and disallowed regions.

In the case of the crystal of NZrsTm176NZ, the crystals were obtained by the reservoir solution of 40% MPD, 0.4 M Mg Acerate and 0.1 M Tris-HCl, pH8.5. The structure was solved by the molecular replacement method using ZrsTm176 structure as the search model. The good quality of the crystals giving 2.0 Å resolution data can allow a conventional process of the protein crystallography. It will be described in detail elsewhere. The data collection and refinement statistics are summarized in Table 13.1.

Table 13.1. Data collection and refinement statistics

Crystal	ZrsTm176		NZrsTm176NZ	
Diffraction data collection				
Space group	*P*1		*P*1	
Unit cell dimensions (Å, deg.)	*a* = 39.08, *b* = 46.86, *c* = 95.26 α = 101.49, β = 101.66, γ = 90.13		*a* = 43.20, *b* = 63.72, *c* = 73.26 α = 66.64, β = 89.99, γ = 90.30	
Spacing (Å)	45.66 – 2.60	2.69 – 2.60	29.25 – 2.00	2.07 – 2.00
No. of measured reflections	320 783		182 859	
No. of unique reflections	19 366		47 224	
Average redundancy	16.56	17.00	3.87	3.66
Completeness (%)	97.4	97.4	97.4	93.6
$R_{merge}(I)$	0.060	0.184	0.038	0.110
Average $I/\sigma(I)$	29.0	9.0	21.0	4.8
Calculated M.W. in asym. (Da)	62 440 (= 15 610 × 4)		72 600 (= 18 150 × 4)	
Solvent content (%)/V_M	54.1/2.68		51.8/2.55	
Refinement				
Spacing (Å)	45.66 – 2.60	2.76 – 2.60	29.25 – 2.00	2.13 – 2.00
No. of reflections (%)	19 366 (97.3)	3226 (97.2)	47 222 (97.2)	7729 (95.0)
No. of ref in working set (%)	18 380 (92.2)	3056 (91.9)	44 823 (92.1)	7343 (90.0)
No. of ref in test set (%)	986 (5.1)	170 (5.3)	2 399 (5.1)	386 (5.0)
R	0.249	0.346	0.251	0.284
Free *R* (5% excluded)	0.321	0.421	0.306	0.337
No. of peptide chains	4		4	
No. of protein/water atoms	4142/146		5096/295	
No. of modeled/theoretical residues	520/536		616/616	
No. of missing residues (%)	16 (2.98)		0 (0.00)	
No. of missing side chain res. (%)	32 (5.97)		0 (0.00)	
RMSD from ideal values				
Bond length (Å)	0.005		0.005	
Bond angle (degree)	0.9		0.8	
Average B factor of main chain (Å^2)				
Whole	80.9 (153–282)		45.9 (148–301)	
High B region	118.0 (180–218)			
Low B region	64.0 (153–179 and 219–282)			
Leu-Zipper	57.2 (153–175)		50.1 (148–175), 45.6 (274–301)	
C-term. Tm	86.0 (176–282)		45.3 (176–273)	

13.3.3. Analysis of Coiled Coil Geometry

The geometrical parameters of the α-helical coiled coil structures were calculated by use of the program *TWISTER*.[46] The center of each α-helix, $C_{helix}(n)$, at the position of residue n were calculated from the positions of the C_α atoms of residues from $n - 2$ to $n + 2$. The center of the coiled coil, $C_{CC}(n)$, was calculated as the mid-point between two centers of the constituent helices. The position of the C_α atom, the center of each helix $C_{helix}(n)$, and the center of the coiled coil $C_{CC}(n)$ provide parameters such as the inter-helical distance (***HD***), the local pitch (***LP***) of each α-helix around the axis of the coiled coil, the local bend angle (***LBA***), and the local tilt angle (***LTA***). The definitions of the ***LBA*** and the ***LTA*** are described in Figure 13.1.

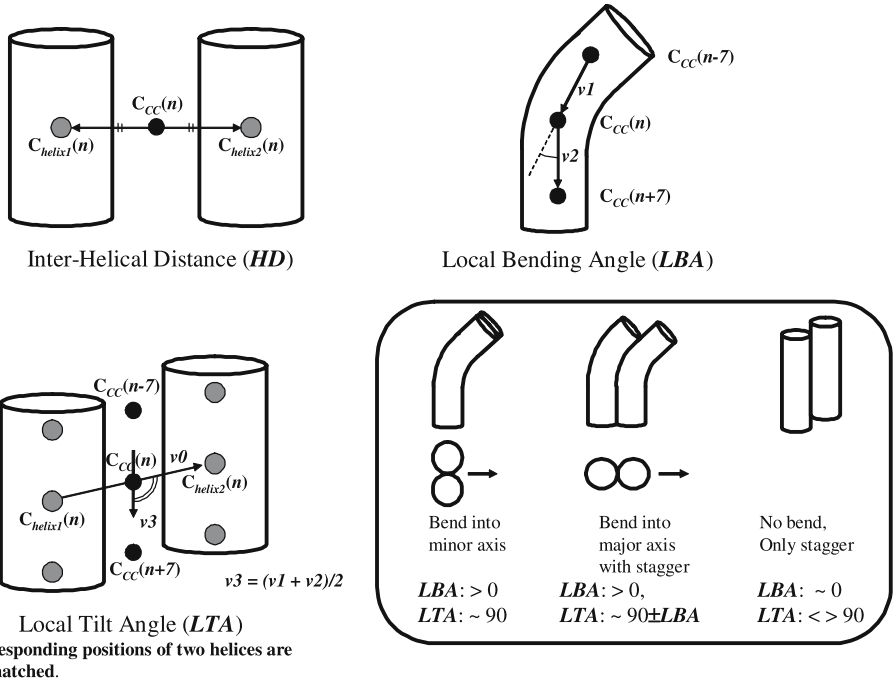

Figure 13.1. Graphic representations of geometrical parameters of a coiled coil structure.

13.4. RESULTS

13.4.1. Crystal Packing

In the crystal lattice of ZrsTm176 (Figure 13.2a–d), the building block is a continuous elongated 360 Åong fi lament, in which two dimers interact with each other at the C-terminus in an anti-parallel fashion. The two dimers are related to each other by non-crystallographic two-fold rotational symmetry about the axis passing though the tail-to-tail contacts. At the tail-to-tail contacts, the two dimers form a four-stranded coiled coil, as previously reported for the crystal structure of the 31-residue C-terminal fragment of rat skeletal muscle α-Tm preceded by a 25-residue fragment of the GCN4 leucine-zipper.[30]

In the crystal, the building blocks lie side by side with a fixed amount of stagger between each block. The key for the side-by-side molecular contacts seems to be the stacking interaction between two aromatic rings of tyrosine, Tyr-261 of Tm and Tyr-163 of the leucine zipper in a neighboring molecule, although the interaction must be weak, due to the long distance (3.8~4.3 Å between the two rings. It is highly likely that, with molecules of different lengths, this type of interaction may not occur without inserting extra solvent spaces in the crystal lattice, which should inhibit crystal formation. This might account for the fact that, among the six constructs tried, only ZrsTm176 gave rise to crystals suited for structural analysis.

On the other hand, the crystal packing of NZrsTm176NZ is completely different from ZrsTm176 (Figure 13.2e,f). A dimer in the lower layer and a dimer in the upper layer in Figure 13.2e make an asymmetric unit. Even if there are two dimers in the *P1* unit cell, these two dimers are not located parallel, but located about 20 degree. One dimer contacts 5 dimers of the lower layer.

13.4.2. Overview of the Electron Density Map

The electron density map of an individual ZrsTm176 molecule may be divided into three parts. The N-terminal segment (D153-A179, consisting of the leucine zipper residues D153-L175 and the Tm residues L176-A179) as well as the C-terminal segment (D219-T282) yielded relatively clear and prominent electron densities, and almost all of the side chains could be identified, with an average B-factor of 64.0 $Å^2$. In contrast, the middle segment, consisting of residues E180-E218 of Tm, showed blurred and low densities with an average B-factor of 118.0 $Å^2$. As many as 22 out of 156 residues within this segment lacked clear electron densities for the side chains, in contrast to the remainder of the molecule (D153-A179, D219-T282), in which 10 out of 372 residues lacked clear side chain densities. In the middle segment, even the residues located at positions *a* and *d* in the heptad repeat showed poor densities. It is remarkable that the electron densities of the side chains of Tyr-214 at position *d* are hard to identify in this crystal structure, in contrast to the usual cases where a tyrosine side chain plays a landmark role in modeling protein structures.

In the case of NZrsTm176NZ, higher resolution map can allow to build all side chains of the fragment in the model. However, main chain B-factor plots of 4 peptide chains clearly shows the peaks on E212-D219, corresponding to the weaker electron density around this region, especially electron density of side chains. The side chains of Tyr-214 at position *d* show only poor electron density again.

13.4.3. Local Conformation of the Coiled Coil

ZrsTm176 forms a two stranded parallel α-helical coiled coil, from the N-terminus (Leu-176) to Tyr-267, except for 15 residues at the C-terminal end that form a 4-stranded coiled coil at the tail-to-tail contacts. NZrsTm176NZ has a complete two stranded parallel coiled-coil except few resides on N- and C-terminus. Figure 13.2 shows the variations of the helical parameters along the coiled coils mentioned above. The averaged values of the chain separation ***HD*** are 9.59 Å for ZrsTm176 (residues 176–267) and 9.60 Å for NZrsTm176NZ (residues 176–273), respectively, compared with 9.74 Å (STD = 0.26 Å) for GCN4 alone (PDB code 2ZTA, residues 1–31). As far as the average

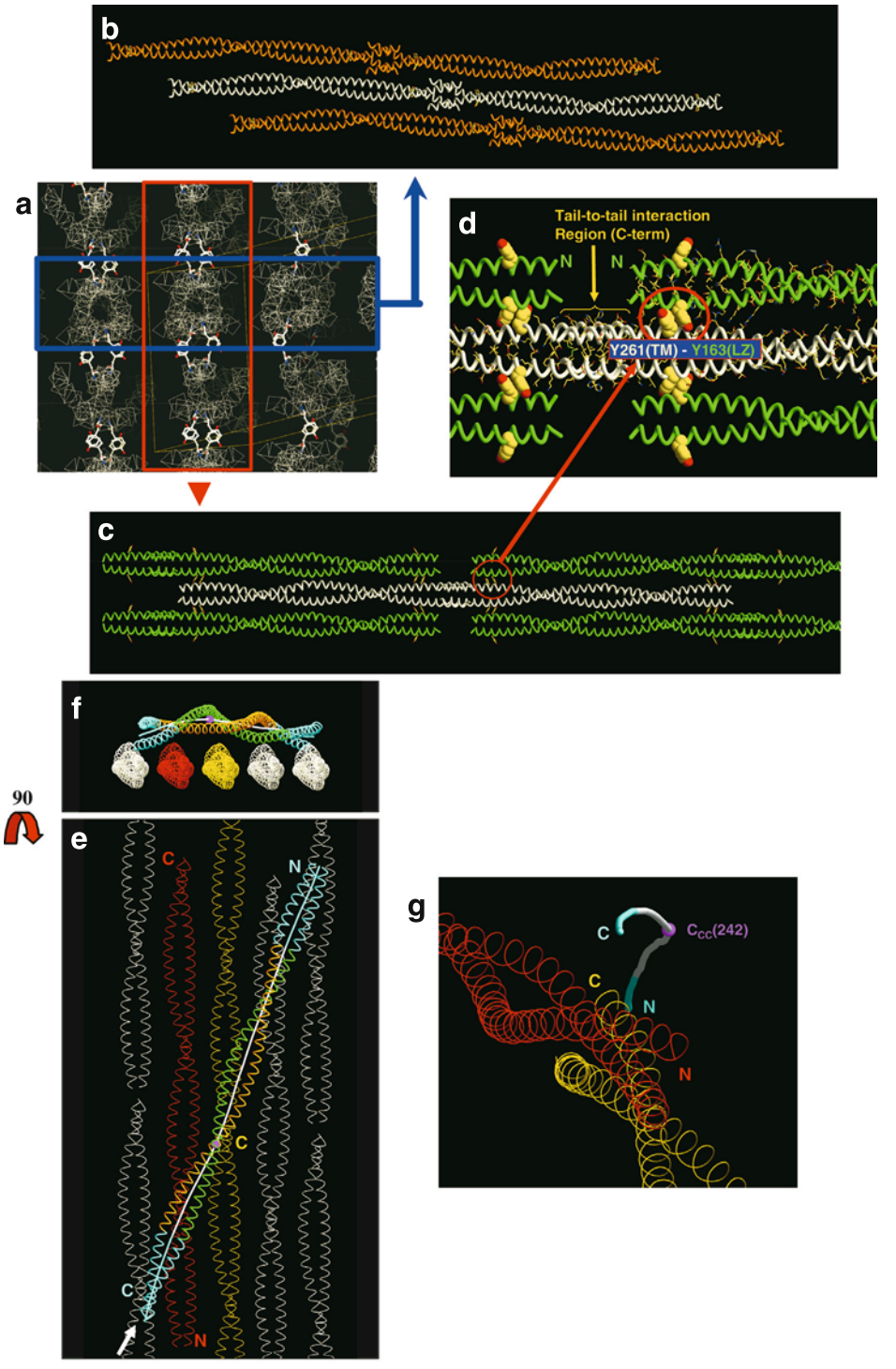
b
a
d
Tail-to-tail interaction
Region (C-term)
N
N
Y261(TM) - Y163(LZ)
c
f
90
e
C
N
C
N
C
N
g
C
Ccc(242)
C
N
N

values are concerned, the Tm segments do not appear to be different from the canonical coiled coils.

A closer inspection, however, revealed that the two stranded coiled coil of this molecule is distinct from the canonical one in three aspects. First, the parameters of the coiled coil vary along the length, which makes the molecule undulating and non-uniform (Figure 13.2). ***HD*** ranges from 8.1 Åto 11.3 Ån both Tm fragments (see below). ***LP***, ***LBA*** and

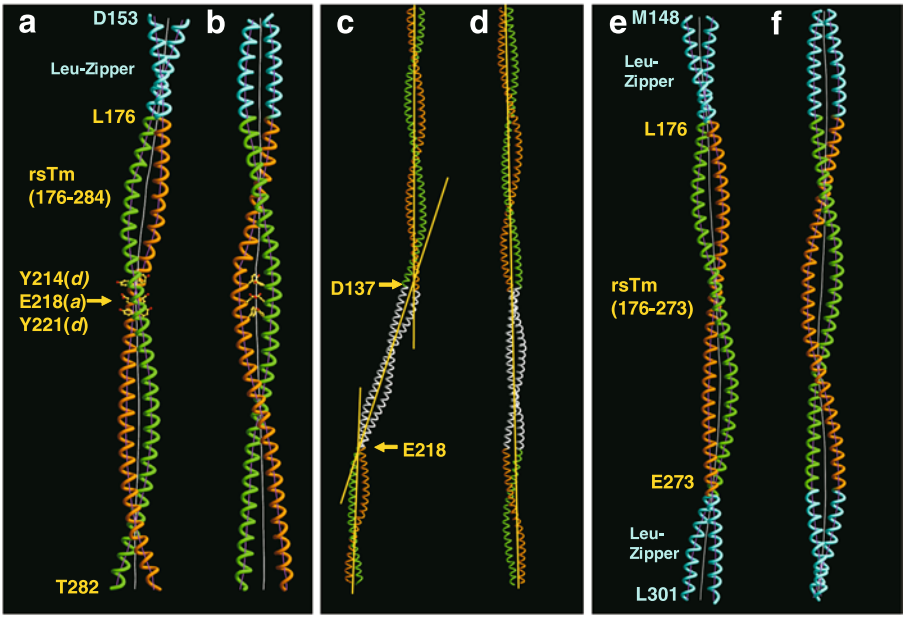

Figure 13.3. (a) A ribbon model of the crystal structure of ZrsTm176, indicating a global bend by about 9 degrees in the axis of the coiled coil centered at about Tyr-214, Glu-218 and Tyr-221, whose side chains are indicated in a ball-and-stick representation. The residues of the leucine zipper sequence, from 153 to 175, are colored in cyan. (b) As in (a), viewed from 90°relative to (a). (c) Ribbon model of the entire tropomyosin structure at 7 Åresolution, indicating the bends around Asp-137 and Glu-218. (d) As in (c), viewed from 90° relative to (c). (e) Ribbon model of the crystal structure of NZrsTm176NZ. The leucine zipper sequences, from 148 to 175 and from 274 to 301, are colored in cyan. (f) As in (e), viewed from 90°relative to (e). The graphics were prepared by using the *CueMol* program (http://www.cuemol.org/).

Figure 13.2. The molecular arrangement of ZrsTm176 and NZrsTm176NZ in the crystals. (a) ZrsTm176 molecules aligned in the crystal viewed from the plane perpendicular to the axis of the molecules. (b) A layer of molecules indicated by a blue box in (a). (c) A layer of molecules indicated by a red box in (a). (d) A magnified view of (c). In (b) to (d), each building block (color coded) consists of two dimers, which interact with each other in a tail-to-tail manner, as indicated by an arrow in (d). The residues Tyr-214 (of Tm) and Tyr-163 (of the leucine zipper sequence) are indicated in ball-and-stick model in (a) and (c), or as space-filling model in (d). The circles in (c) and (d) indicate inter-molecular interaction sites through stacked Tyr-163 and Tyr-214 residues. (e) Two layers composed of NZrsTm176NZ molecules. The molecules of white, yellow and red coil representations are involved in a lower layer and a colored molecule belongs to an upper layer. (f) Two layers viewed from the position of 90°rotation of (e). (g) The trace of the coiled coil center of a colored dimer viewed from the direction of a white allow in (e). All of the graphics were prepared by using the CueMol program (http://www.cuemol.org/).

LTA also substantially undulate. These mean that two chemically identical polypeptide chains forming a coiled coil can clearly differ in their conformation, making the molecule asymmetric. Second, the most prominent feature of ZrsTm176 is the global bend around Y214-E218-Y221, by about 9 degrees (Figure 13.3a,b) with an ***LBA*** peak at about 8.5 degrees (Figure 13.4c). The bend coincides with a peak in the local ***HD***, as well as a prominent peak in ***LP***. On the other hand, there is no global bend on the same region in NZrsTm176NZ, even if ***HD*** and ***LP*** have peaks at the same region (Figure 13.4d). Third, each waist point, a minimum (~8.0 Å in ***HD***, coincides with a cluster of alanine (or serine) residues at three consecutive core positions (position *a* or *d*), either A179(*d*)-A183(*a*)-S186(*d*) or A235(*d*)-A239(*a*)-A242(*d*). This is reminiscent of the crystal structure of the N-terminal 81 residues of chicken skeletal muscle α-Tm (Tm81), in which the sequence A18(*d*)-A22(*a*)-A25(*d*) was associated with the waist with an ***HD*** of ~8.0 Å

13.5. DISCUSSION

Previous studies indicated that Tm may consist of segments with differing stabilities in the inter-helical interactions of the coiled coil. At physiological temperatures, in some segments, the coiled coil is marginally formed, partially unfolded or even separated, while in the others the coiled coil is stable and maintained. Due to this non-uniform character, Tm exists in equilibrium between multiple conformations that are energetically similar to each other, making Tm flexible. As we will discuss below, structural aspects of the present crystal structure of ZrsTm176 and NZrsTm176NZ may support the previous notion that Tm is a flexible coiled coil.

13.5.1. Undulating Coiled Coil

The coiled coils of ZrsTm176 and NZrsTm176NZ undulate; the local parameters of the coiled coil geometry undulate over the length of the molecule, indicating that its physical and dynamic properties vary along its length. The most remarkable properties are these undulations are not shared with two structures, even if these fragments have a long common sequence (residue 176–273). Judging from ***LBA*** and ***LTA***, bending manners and staggering manners of two fragments are completely different from each other. This fact indicates that the entire molecule may be more or less flexible, although we argue that some parts should be more flexible than others in the discussions below.

13.5.2. Global Bend Centered at Y214-E218-Y221

ZrsTm176 is bent by about 9 degrees, in the region centered around Y214-E218-Y221. The position of the bend agrees well with the position of the bend in the whole Tm molecule, by 15 degrees in the crystal structure at 7 Å resolution. [28] The extents of the bends, however, in the two crystals are different, indicating that Tm must be flexible at this point. This bend could be caused by, or at least associated with, the local widening of the coiled coil to the ***HD*** of 11.3 Å This widening may be associated with two factors. First, the negative net charge of Glu-218 on either chain does not apparently form a hydrogen bond with a neighboring residue, and therefore the repulsive force pulls the Glu-218 side chains

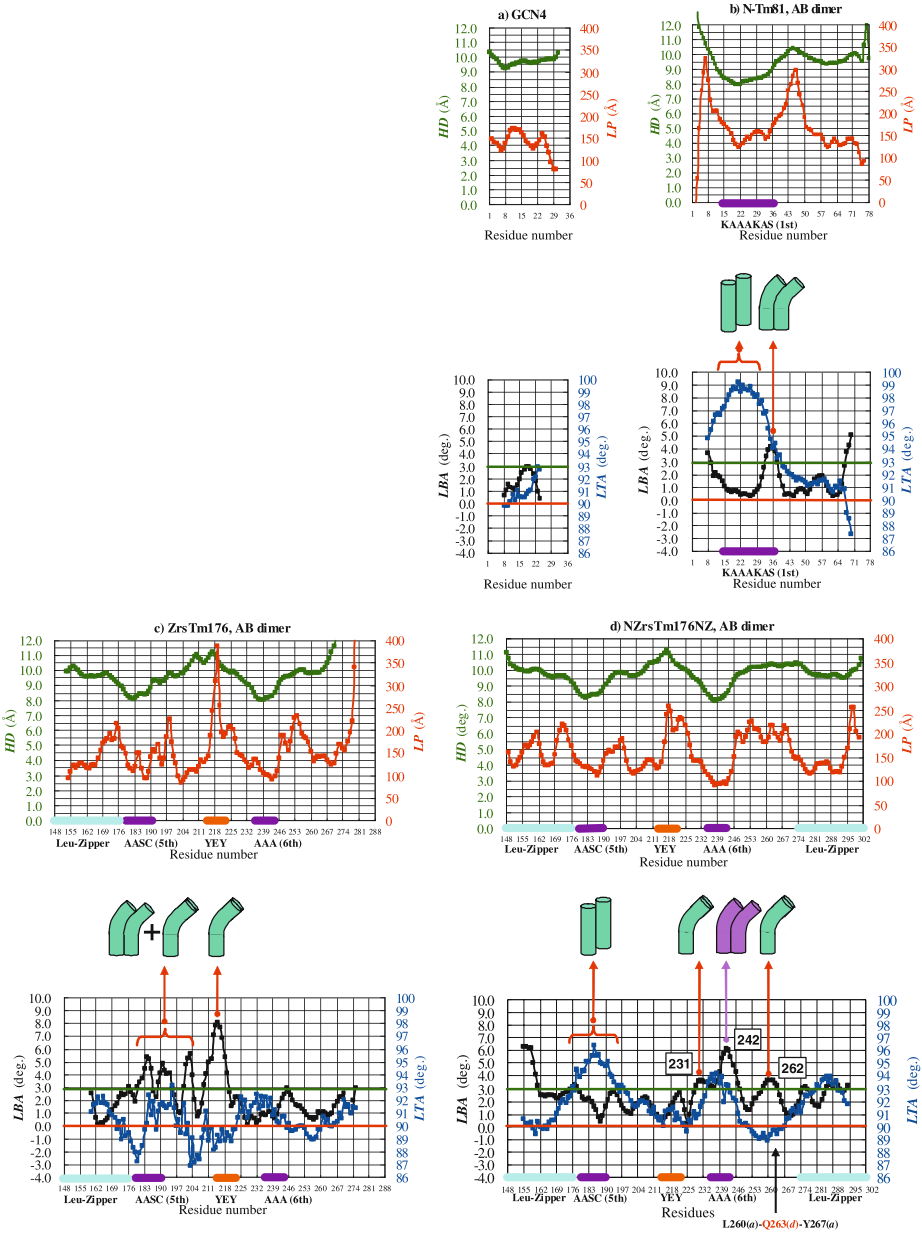

Figure 13.4. Distributions of the local parameters of the coiled coil geometry along the length of the molecules in crystal (a) of the leucine zipper of GCN4 alone (2ZTA), (b) of Tm81 (1IC2), the segment of 81 residues at the N-terminus of chicken skeletal muscle α-Tm, (c) of the Zrs176Tm, and (d) of the NZrsTm176NZ. The local inter-helical distance (***HD***, the points in green with the ordinate on the left side), the local pitch of the coiled coil about the axis (***LP***, the points in red with the ordinate on the right side), the local bending angle (***LBA***, plots in black with the ordinate on the left side) and the local tilt angle (***LTA***, plots in blue with the ordinate on the right side). The definition of these parameters is described in the METHODS AND MATERIANLS. The destabilizing clusters defined by KowK and et al.,[15] the Leu zipper sequences and the region of Y214(*d*)-E218(*a*)-Y221(*d*) are indicated by purple, cyan and orange bars, respectively (see text).

apart from the core. This destabilizes the dimeric interaction and increases the ***HD***, leaving a cavity in the inter-helical space. Second, the pair of Glu-218 residues is located between two pairs of bulky and hydrophobic tyrosine residues, Tyr-214 and Tyr-221, which seem to be mobile, as judged from the low electron densities.

In the case of NZrsTm176NZ, ***HD***, ***LP*** and main chain B-factor plots have peaks around this region, however, the region does not show clear bend judging from ***LBA*** and ***LTA***. This difference would mean that the bending manner of Tm is not only defined by its sequence but also outer environment of Tm. In other words, Tm can be bent as the induced-fit manner.

Interestingly, the 7 Åresolution structure has another prominent bend in the region around Asp-137(*d*). Among all of the residues of rabbit skeletal α-Tm, Glu-218 and Asp-137 are the sole acidic residues at the core positions *a* and *d*, which may destabilize the coiled coil formation. Moreover, these anomalous core residues are well conserved from the *C. elegans* to *Homo sapiens*. Finally, the neighboring Tyr-214 and Tyr-221 are also highly conserved. This implies that the region around Glu-218, and possibly the region around Asp-137, should play important roles in the Tm function by implementing a bending mechanism.

The possible roles of the acidic residues in the coiled coil core merit discussion. An acidic residue at the *a* or *d* position may cause either a widening or narrowing of the coiled coil, depending on whether the side chain of the acidic residue forms hydrogen bonds with the neighboring basic residues. A typical example of both cases is found in the crystal structure of the RhoA-binding domain in Rho-kinase.[33] On one hand, Glu-1010 at position *a* does not form a hydrogen bond with any neighboring residue, and the repulsive force increases the ***HD*** to an abnormally large value (>12 Å This co uld account for the loss of side-chain packing in its neighboring region, the loss of the electron densities of the Glu-1010 side-chain, and the bend of the coiled coil centered at this residue. On the other hand, Glu-1027(*d*) forms an inter-chain hydrogen bond with Lys-1013(*a*) of the opposite chain. This reduces the repulsive force, and gives rise to an ***HD*** of 8.8 Å which is smaller than that for the leucine-zipper of GCN4 (9.6 Å It is not known if this kind of structure, "a pair of dyads" formed on either side of the core, stabilizes or destabilizes the coiled coil. The presence of a cavity in the core would destabilize the structure, while a pair of inter-helical hydrogen bonds would stabilize it.

13.5.3. Alanine Destabilizing Clusters

In the crystal structure of Tm81, Brown *et al*. found that a region with a cluster of Ala residues in the core positions is associated with a reduced ***HD***, as well as with the staggered C_α positions of the residues on one chain relative to those on the opposite chain. They further proposed that the coiled coil of Tm may bend at each boundary between a staggered region and a non-staggered region. Since there are 6 (or 7) alanine clusters along the length of Tm, with a quasi constant period that roughly corresponds to the axial repeat of actin subunits, they proposed that the alanine stagger could be the mechanism that makes Tm flexible enough to wind around the helical tracks on the actin filament.[29] It has also been indicated that alanine residues at three consecutive core positions substantially destabilize the coiled coil.[15]

In the present two crystal structures, we confirmed that each of the two regions with Ala or Ser in three consecutive core positions, A179(*d*)-A183(*a*)-S186(*d*) and A235(*d*)-A239(*a*)-A242(*d*), clearly coincides with the minimal positions of ***HD***. These two clusters

are accord with the 5th and the 6th destabilizing cluster defined by KwoK and *et al.,* respectively.[15] In the case of NZrsTm176NZ, it shows the clear alanine stagger on the 5th destabilizing cluster, but does not show on the 6th cluster. On the other hand, ZrsTm176 did not confirm the alanine stagger; over its entire length, no significant stagger was identified. Therefore, as the case of the region of Y214-E218-Y221, the structural difference exists between two Tm structures of C-terminus, or among known Tm structures. We believe that the multiformity above described would be exactly the nature of Tm, and it would be directly linked to the function of Tm.

13.5.4. Summary

The summary of individual crystal structure of two Tm fragments is below.
First crystal, ZrsTm176

1. The Tm fragment is undulating all along the molecule.
2. The YEY cluster bends into the minor axis. It would be due to the crystal packing.
3. The 5th destabilizing cluster seems to have a complex undulation.

The 6th destabilizing cluster does not show clear stagger, or local bend.
Second crystal, NZrsTm176NZ

1. The Tm fragment is undulating all along the molecule, again.
2. The YEY cluster does not bend.
3. The 5th destabilizing cluster shows clear stagger.
4. The 6th destabilizing cluster associates with two bends of deferent directions. Bends must be due to the crystal packing.
5. The Q263(*d*)-Y267(*a*) seems to be another short destabilizing cluster, bending into the minor axis.

From these two structures, and according to known Tm structures, possible Tm properties are below.

1. The conformation of a Tm molecule can be changeable. It would be induced by an external environment as “the Induced-fit manner”.
2. The property of the destabilizing clusters including Ala’s and one of the destabilizing cluster including bulky residues are different from each other.

The destabilizing clusters including continuous Ala’s would allow stagger, bend into the major axis, or and bend into the minor axis. On the other hand, the destabilizing clusters including bulky residues such as the YEY cluster or the QY cluster would only arrow bend into the major axis. The difference would come from steric hindrance among side chains at the core region of a coiled coil.

13.6. ACKNOWLEDGEMENTS

We are grateful to staffs of Highthroughput Factory, RIKEN Harima Institute for operations of TERA, and staffs of Division of Synchrotron Radiation Instrumentation, RIKEN Harima Institute for assistance of data collections. This work was supported partly by the Special Coordination Funds from the Ministry Mext of the Japanese

Government, and partly by the ERATO fund from the Japan Science and Technology Agency (JST).

13.7. REFERENCES

1. K. Bailey, Tropomyosin: a new asymmetric protein component of muscle, *Nature* **157**, 368–369 (1946).
2. S. Ebashi, Calcium ions and muscle contraction, *Nature* **240**(5378), 217–218 (1972).
3. S. Ebashi, and M. Endo, Calcium ion and muscle contraction, *Prog. Biophys. Mol. Biol.* **18**, 123–183 (1968).
4. S. V. Perry, Vertebrate tropomyosin: distribution, properties and function, *J. Muscle Res. Cell Motil.* **22**(1), 5–49 (2001).
5. J. P. Lees-Miller, and D. M. Helfman, The molecular basis for tropomyosin isoform diversity, *Bioessays* **13**(9), 429–437 (1991).
6. I. Ohtsuki, K. Maruyama, and S. Ebashi, Regulatory and cytoskeletal proteins of vertebrate skeletal muscle, *Adv. Protein. Chem.* **38**, 1–67 (1986).
7. A. N. Lupas, and M. Gruber, The structure of alpha-helical coiled coils, *Adv. Protein. Chem.* **70**, 37–78 (2005).
8. F. H. Crick, Is alpha-keratin a coiled coil?, *Nature* **170**(4334), 882–883 (1952).
9. T. Alber, Structure of the leucine zipper, *Curr. Opin. Genet. Dev.* **2**(2), 205–210 (1992).
10. D. N. Marti, and H. R. Bosshard, Electrostatic interactions in leucine zippers: thermodynamic analysis of the contributions of Glu and His residues and the effect of mutating salt bridges, *J. Mol. Biol.* **330**(3), 621–637 (2003).
11. B. Tripet, K. Wagschal, P. Lavigne, C. T. Mant, and R. S. Hodges, Effects of side-chain characteristics on stability and oligomerization state of a de novo-designed model coiled-coil: 20 amino acid substitutions in position "d", *J. Mol. Biol.* **300**(2), 377–402 (2000).
12. K. Wagschal, B. Tripet, P. Lavigne, C. Mant, and R. S. Hodges, The role of position a in determining the stability and oligomerization state of alpha-helical coiled coils: 20 amino acid stability coefficients in the hydrophobic core of proteins, *Protein Sci.* **8**(11), 2312–2329 (1999).
13. E. K. O'Shea, J. D. Klemm, P. S. Kim, and T. Alber, X-ray structure of the GCN4 leucine zipper, a two-stranded, parallel coiled coil, *Science* **254**(5031), 539–544 (1991).
14. S. M. Lu, and R. S. Hodges, Defining the minimum size of a hydrophobic cluster in two-stranded alpha-helical coiled-coils: effects on protein stability, *Protein Sci.* **13**(3), 714–726 (2004).
15. S. C. Kwok, and R. S. Hodges, Stabilizing and destabilizing clusters in the hydrophobic core of long two-stranded alpha-helical coiled-coils, *J. Biol. Chem.* **279**(20), 21576–21588 (2004).
16. A. Singh, and S. E. Hitchcock-DeGregori, Local destabilization of the tropomyosin coiled coil gives the molecular flexibility required for actin binding, *Biochemistry* **42**(48), 14114–14121 (2003).
17. K. I. Sano, K. Maeda, H. Taniguchi, and Y. Maeda, Amino-acid replacements in an internal region of tropomyosin alter the properties of the entire molecule, *Eur. J. Biochem.* **267**(15), 4870–4877 (2000).
18. E. F. Woods, The conformational stabilities of tropomyosins, *Aust. J. Biol. Sci.* **29**(5–6), 405–418 (1976).
19. A. Sato, and K. Mihashi, Thermal modification of structure of tropomyosin. I. Changes in the intensity and polarization of the intrinsic fluorescence (tyrosine), *J. Biochem. (Tokyo)* **71**(4), 597–605 (1972).
20. S. S. Lehrer, Effects of an interchain disulfide bond on tropomyosin structure: intrinsic fluorescence and circular dichroism studies, *J. Mol. Biol.* **118**(2), 209–226 (1978).
21. P. Graceffa, and S. S. Lehrer, The excimer fluorescence of pyrene-labeled tropomyosin. A probe of conformational dynamics, *J. Biol. Chem.* **255**(23), 11296–11300 (1980).
22. S. L. Betcher-Lange, and S. S. Lehrer, Pyrene excimer fluorescence in rabbit skeletal alphaalphatropomyosin labeled with N-(1-pyrene)maleimide. A probe of sulfhydryl proximity and local chain separation, *J. Biol. Chem.* **253**(11), 3757–3760 (1978).
23. D. R. Betteridge, and S. S. Lehrer, Two conformational states of didansylcystine-labeled rabbit cardiac tropomyosin, *J. Mol. Biol.* **167**(2), 481–496 (1983).
24. P. Graceffa, and S. S. Lehrer, Dynamic equilibrium between the two conformational states of spin-labeled tropomyosin., *Biochemistry* **23**(12), 2606–2612 (1984).

25. B. F. Edwards, and B. D. Sykes, Nuclear magnetic resonance evidence for the coexistence of several conformational states of rabbit cardiac and skeletal tropomyosins, *Biochemistry* **19**(12), 2577–2583 (1980).
26. S. A. Potekhin, and P. L. Privalov, Co-operative blocks in tropomyosin, *J. Mol. Biol.* **159**(3), 519–535 (1982).
27. D. L. Williams Jr., and C. A. Swenson, Tropomyosin stability: assignment of thermally induced conformational transitions to separate regions of the molecule, *Biochemistry* **20**(13), 3856–3864 (1981).
28. F. G. Whitby, and G. N. Phillips Jr., Crystal structure of tropomyosin at 7 Angstroms resolution, *Proteins* **38**(1), 49–59 (2000).
29. J. H. Brown, K. H. Kim, G. Jun, N. J. Greenfield, R. Dominguez, N. Volkmann, S. E. Hitchcock-DeGregori, and C. Cohen, Deciphering the design of the tropomyosin molecule, *Proc. Natl. Acad. Sci. USA* **98**(15), 8496–8501 (2001).
30. Li, Y., S. Mui, J. H. Brown, J. Strand, L. Reshetnikova, L. S. Tobacman, and C. Cohen, The crystal structure of the C-terminal fragment of striated-muscle alpha-tropomyosin reveals a key troponin T recognition site, *Proc. Natl. Acad. Sci. USA* **99**(11), 7378–7383 (2002).
31. N. J. Greenfield, G. V. Swapna, Y. Huang, T. Palm, S. Graboski, G. T. Montelione, and S. E. Hitchcock-DeGregori, The structure of the carboxyl terminus of striated alpha-tropomyosin in solution reveals an unusual parallel arrangement of interacting alpha-helices, *Biochemistry* **42**(3), 614–619 (2003).
32. N. Ookubo, Intramolecular disulfide linked alphabeta and alphaalpha in oxidized tropomyosin: separation, identification, and process of formation, *J. Biochem. (Tokyo)* **81**(4), 923–931 (1977).
33. T. Shimizu, K. Ihara, R. Maesaki, M. Amano, K. Kaibuchi, and T. Hakoshima, Parallel coiled-coil association of the RhoA-binding domain in Rho-kinase, *J. Biol. Chem.* **278**(46), 46046–46051 (2003).
34. M. V. Vinogradova, D. B. Stone, G. G. Malanina, C. Karatzaferi, R. Cooke, R. A. Mendelson, and R. J. Fletterick, Ca(2+)-regulated structural changes in troponin, *Proc. Natl. Acad. Sci. USA* **102**(14), 5038–5043 (2005).
35. S. Takeda, A. Yamashita, K. Maeda, and Y. Maeda, Structure of the core domain of human cardiac troponin in the Ca(2+)-saturated form, *Nature* **424**(6944), 35–41 (2003).
36. R. Maytum, F. Bathe, M. Konrad, and M. A. Geeves, Tropomyosin exon 6b is troponin-specific and required for correct acto-myosin regulation, *J. Biol. Chem.* **279**(18), 18203–18209 (2004).
37. L. Kluwe, K. Maeda, A. Miegel, S. Fujita-Becker, Y. Maeda, G. Talbo, T. Houthaeve, and R. Kellner, Rabbit skeletal muscle alpha alpha-tropomyosin expressed in baculovirus-infected insect cells possesses the authentic N-terminus structure and functions, *J. Muscle Res. Cell Motil.* **16**(2), 103–110 (1995).
38. M. Sugahara, and M. Miyano, Development of high-throughput automatic protein crystallization and observation system, *Tanpakushitsu Kakusan Koso* **47**(8 Suppl), 1026–1032 (2002).
39. S. Adachi, T. Oguchi, H. Tanida, S.-Y. Park, H. Shimizu, H. Miyatake, N. Kamiya, Y. Shiro, Y. Inoue, T. Ueki, and T. Iizuka, The RIKEN Structural Biology Beamline II (BL44B2) at the SPring-8, *Nucl. Instrum. Methods Phys. Res.* **A 467**, 711–714 (2001).
40. J. W. Pflugrath, The finer things in X-ray diffraction data collection, *Acta Crystallogr. D Biol. Crystallogr.* **55**(Pt 10), 1718–1725 (1999).
41. J. Navaza, Implementation of molecular replacement in AMoRe, *Acta Crystallogr. D Biol. Crystallogr.* **57**(Pt 10), 1367–1372 (2001).
42. E. Potterton, P. Briggs, M. Turkenburg, and E. Dodson, A graphical user interface to the CCP4 program suite, *Acta Crystallogr. D Biol. Crystallogr.* **59**(Pt 7), 1131–1137 (2003).
43. Collaborative Computational Project, Number 4, The CCP4 suite: programs for protein crystallography, *Acta Crystallogr. D Biol. Crystallogr.* **50**(Pt 5), 760–763 (1994).
44. D. E. McRee, XtalView/Xfit – A versatile program for manipulating atomic coordinates and electron density, *J. Struct. Biol.* **125**(2–5), 156–165 (1999).
45. D. E. McRee, Differential evolution for protein crystallographic optimizations, *Acta Crystallogr. D Biol. Crystallogr.* **60**(Pt 12, No 1), 2276–2279 (2004).
46. S. V. Strelkov, and P. Burkhard, Analysis of alpha-helical coiled coils with the program TWISTER reveals a structural mechanism for stutter compensation, *J. Struct. Biol.* **137**(1–2), 54–64 (2002).

14

C. ELEGANS MODEL FOR STUDYING TROPOMYOSIN AND TROPONIN REGULATIONS OF MUSCLE CONTRACTION AND ANIMAL BEHAVIOR

Hiroaki Kagawa, Tomohide Takaya, Razia Ruksana,
Frederick Anokye-Danso, Md. Ziaul Amin and Hiromi Terami

14.1. BACKGROUND

There are two muscle tissues in the nematode *Caenorhabditis elegans*: the pharynx for feeding and the body wall for locomotion. These correspond to cardiac and skeletal muscles in vertebrates, respectively. Study of the muscle genes of *C. elegans* can be classified into three stages; first, mutant isolation and gene mapping, second, cloning and sequencing of the gene, and third, complete sequences of all genes. Many uncoordinated mutant animals have been isolated (Brenner, 1974; Waterston, 1988; Moerman and Fire, 1997) and the complete amino acid sequence of myosin heavy chain, twitchin, and paramyosin, (invertebrate specific core protein of thick filament), and were the first determined in any animals by analyzing the *unc-54, unc-22,* and *unc-15* mutants, respectively (Karn et al., 1983; Benian et al., 1989; Kagawa et al., 1989). Tropomyosin and troponin components are also present but as with actin and myosin heavy chain in the worm, there are some differences in gene structure and sequence compared to those in other animals (Kagawa et al., 1995; Myers et al., 1996; Moerman and Fire, 1997). Deficiencies of body wall troponin C or tropomyosin in *C. elegans* cause the Pat (paralyzed arrest at embryonic two-fold stage) phenotype (Williams and Waterston, 1994; Terami et al., 1999) and those of troponin T cause Mup (muscle position abnormal) phenotype (Myers et al., 1996). After determining the complete genome sequences of the nematode (The *C. elegans* Sequence Consortium, 1998), we can find out how isoforms are related to each other. Only one troponin C gene, *pat-10/tnc-1,* is expressed in the body wall muscles and the gene defect causes a developmental arrest of the animals (Terami et al., 1999). This is the first report analyzing a troponin C mutant. Recently we analyzed the tissue expression patterns of the four troponin I genes and their interaction with two troponin C isoforms (Ruksana et al., 2005). It is now possible to compare how the troponin complex works in muscle contraction in invertebrates since Ebashi, Ohtsuki and their school had described these systems in vertebrates (Ohtsuki et al., 1986). In this paper we review how the mutant

Division of Bioscience, Graduate School of Science and Technology, Okayama University, Japan

Regulatory Mechanisms of Striated Muscle Contraction
Edited by Ebashi and Ohtsuki, Springer, 2007

Table 14.1. Summary of gene, tissue expression and phenotype of tropomyosin and troponin isoforms in *C. elegans*

Gene/isoform	Cosmid (LG)	Tissue or Organ	Mutation[a]	RNAi[a]
Tropmyosin[b]				
lev-11/tmy-1/TM-I,-II	Y105E8B.1 (I)	BW[b]	Lev[c]	Unc[d]
lev-11/tmy-1/TM-III,-IV	Y105E8B.1 (I)	Pharynx[b,f]	Pat[e]	Emb[f], Ste[g]
Troponin C				
pat-10/tnc-1	F54C1.7 (I)	BW[h]	Pat[e]	Ste[g]
tnc-2	ZK673.7 (II)	Pharynx[h]	ND	Lva[g,i]
Troponin I				
tni-1	F42E11.4 (X)	BW[j,k]	ND	Unc[j]
unc-27/tni-2	ZK721.2 (X)	BW[j,k]	Unc[j,k,l]	Unc[j]
tni-3	T20B3.2 (V)	BW[j,k], Vulva[j]	ND	Con, Egl, Pvl[j]
tni-4	VO3F8.1 (IV)	Pharynx[j,k]	ND	Gro[i], Emb[j]
Tropnin T				
mup-2/tnt-1	T22E5.5 (X)	BW[m]	Mup, Ste[m]	WT[i], Mup[n]
tnt-2	F53A9.10 (X)	ND	ND	WT[i], Lva[n]
tnt-3	C14F5.3 (X)	ND	ND	WT[i]
tnt-4	T08B1.2 (V)	Pharynx[n]	ND	WT[i], Lva[n],

[a] Designations for phenotypes: Lev, levamisole-resistant; Unc, uncoordinated; Pat, paralyzed arrest at embryonic two-fold stage; Emb, embryonic lethal; Ste, sterile; Con, constipated; Egl, egg laying-defective; Pvl, protruding vulva; Mup, muscle positioning; WT, wild type; ND, not determined.
[b] The tropomyosin gene, *lev-11/tmy-1* encodes four isoforms (Kagawa et al., 1995). [c] Lewis et al., 1980; [d] Ono and Ono, 2002; [e] Williams and Waterston, 1994; [f] Anyanful et al., 2001; [g] Ono and Ono, 2004; [h] Terami et al., 1999; [i] Kamath et al., 2003; [j] Ruksana et al., 2005; [k] Burkeen et al., 2004; [l] Brenner, 1974; [m] Myers et al., 1996; [n] Wormbase (on TnT by Allen et al.).

genes for tropomyosin and the troponin components of *C. elegans* affect animal behavior. A summary of expression, mutation and RNA interference results on these isoforms are provided in Table 14.1.

14.1.1. Tropomyosin Mutant Shows Lethal or Ca^{2+} Signaling Defect

In contrast to one gene encoding one protein in most other muscle genes in *C. elegans* the tropomyosin gene, *tmy-1/lev-11,* encodes four isoforms, which are two each for the pharynx and body wall muscles produced under the control of external and internal promoters and splicing choice, respectively (Kagawa et al., 1995; Anyanful et al., 2001). The *lev-11(st557)* mutant animal, which was isolated as a Pat animal (Williams and Waterston, 1994) produces no tropomyosin due to a mutation at the splice donor site of exon 1 (Kagawa et al., 1997). Another mutant *lev-11(x12)* animal, which was isolated as a levamisol-resistant animal (Lewis et al., 1980) has an amino acid substitution of glutamic acid to lysine at position 234 of tropomyosin (Kagawa et al., 1997).

Exon 1 encodes the N-terminal part of CeTMI and CeTMII isoforms that are only expressed in body wall muscles. Mutant animals lacking CeTMI and CeTMII show a Pat

phenotype suggesting that tropomyosin in body wall muscle is essential for the late development of *C. elegans*. As levamisole is a potent agonist of acetylcholine *lev-11(x12)* mutant animals cannot transmit the Ca^{2+} signal from the post-synaptic membrane to cause actin-myosin sliding step due to the position of the mutant tropomyosin. The mutation site of *lev-11(x12)* is in exon 7 a constitutive exon for all isoforms and causes the Glu-234Lys substitution in tropomyosin (Kagawa et al., 1997). How this mutation affects interactions between troponin and tropomyosin or tropomyosin and actin is not currently known. This mutant will be useful in solving how tropomyosin functions in Ca^{2+} signal transduction.

14.1.2. A Pat Animal has Missed Ca^{2+} Binding to Site II and Troponin I Binding to the H-helix of the Body Wall Troponin C

Two different genes; *pat-10*/*tnc-1* and *tnc-2,* encode the two troponin C isoforms that are expressed in body wall and pharyngeal muscles, respectively (Terami et al., 1999). Comparisons to other troponin C sequences show that body wall troponin C, TnC-1, has the potential for Ca^{2+} binding at sites II and IV. Using TnC-1 produced in bacteria, the apparent Ca^{2+} binding constants, Kapp, of both sites have been confirmed by fluorescence titration method to be $7.9 \times 10^5\,M^{-1}$ and $1.2 \times 10^6\,M^{-1}$, respectively (Ueda et al., 2001). Study of the Mg^{2+}-dependence of the Kapp showed that both Ca^{2+}-binding sites II and IV do not bind Mg^{2+} competitively. This means that the Ca^{2+} binding of nematode TnC-1 is low affinity, fast dissociation and Ca^{2+}-specific.

A troponin C mutant animal was isolated as one of the Pat mutants. These show paralyzed arrest phenotype at embryonic two-fold stage (Williams and Waterston, 1994). We report that the *pat-10(st575)* animal has two mutations in the body wall troponin C; an Asp64Asn (D64N) substitution at site II and a deletion of the H-helix of the C-terminus (Terami et al., 1999). Recombinant mutant troponin C proteins produced in bacteria were assayed by SDS-Page to determine the molecular size and by Western blot analysis to assay their interactions with troponin I.

TnC-1m1: D64N showed no change in mobility with or without Ca^{2+} suggesting that site II has lost Ca^{2+} binding. TnC-1m2: W153stop exhibited a mobility shift dependent on the presence or absence of Ca^{2+}, but did not bind troponin I due to missing H-helix.

A series of amino acid substitution experiments destroying and shortening the H-helix in the C-terminal region of TnC-1 suggest that the length and direction of the H-helix are important for troponin I binding. Especially two residues F152 and W153 were found to be essential for Ca^{2+} binding and troponin I binding (Takaya and Kagawa, unpublished). These results confirm that the H-helix of TnC-1 is essential for Ca^{2+} binding at site IV and troponin I binding. The topographical position of the C-terminal of troponin C close to troponin I is consistent with the crystal structure of the troponin complex (Vassylyev et al., 1998; Takeda et al., 2003).

We have also analyzed transgenic animals to study how troponin C mutants affect the animal phenotype by injecting recombinant mutant genes with the marker plasmid, pTG96 (*sur-5::gfp*) (Figure 14.1) and found that development of mutant animals of m1: D64N (Ca^{2+} binding site II of TnC-1) was almost to the same as wild type, but that adult transgenic animals dramatically lose their motility and show an egg-laying defect phenotype (Takaya, Terami and Kagawa, unpublished). This mutation is the first example of the missense mutant worm that is homozygous for a mutant troponin C gene; the

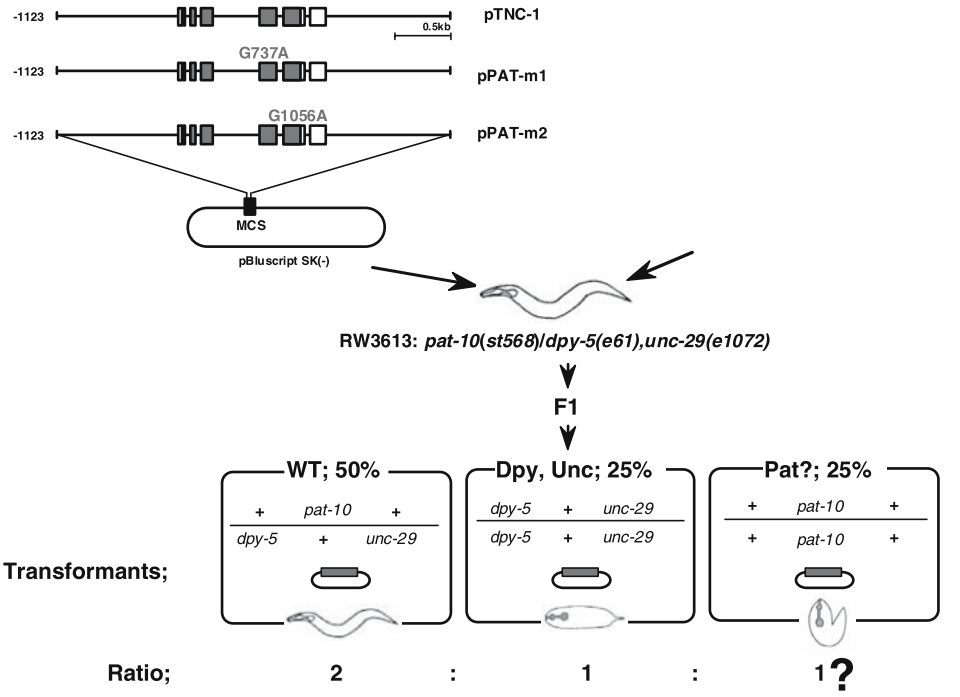

Figure 14.1. Experimental strategy of transgenic worms by injecting mutant gene of the troponin C. How designed mutant gene (top) affects on the animal is analyzed the phenotypic ratio by counting F2 animals (bottom). (Terami, PhD thesis, 2002)

pat-10(st575) animal has two mutations in TnC-1 and is only kept in the heterozygous state (Williams and Waterston, 1994; Terami et al., 1999). On the other hand the mutation of m2: W153stop in TnC-1 caused the Pat phenotype in transgenic animals. Both *in vitro* and *in vivo* experiments indicate that the Pat phenotype of the worm comes from a loss of Ca^{2+} binding to site IV or of troponin I binding to the H-helix.

14.1.3. Pharynx and Body Wall Muscles Express One- and Three-troponin I isoforms, Respectively

Four troponin I isoforms of the worm were characterized and compared to those of other animals (Figure 14.2). It is interesting that the three body wall troponin I isoforms have unique glutamate- rich C-terminal extensions. The C-termini of troponin T in *Drosophila* and crayfish *Astacus* also show conserved glutamate-rich extensions (Fyrberg et al., 1990; Benoist et al., 1998; Domingo et al., 1998). It has been proposed that the C-terminal extension might enhance cooperation of troponin-tropomyosin complexes within thin filaments (White et al., 1987). The *C. elegans* troponin I extensions may have a homologous function. Glutamate has a negative charge, which may contribute to protein-protein interactions under different Ca^{2+} concentrations. The C-terminal hydrophilic regions of the three body wall type troponin I isoforms could be important for interactions with TnC-1 or TnT in the worm body wall muscles.

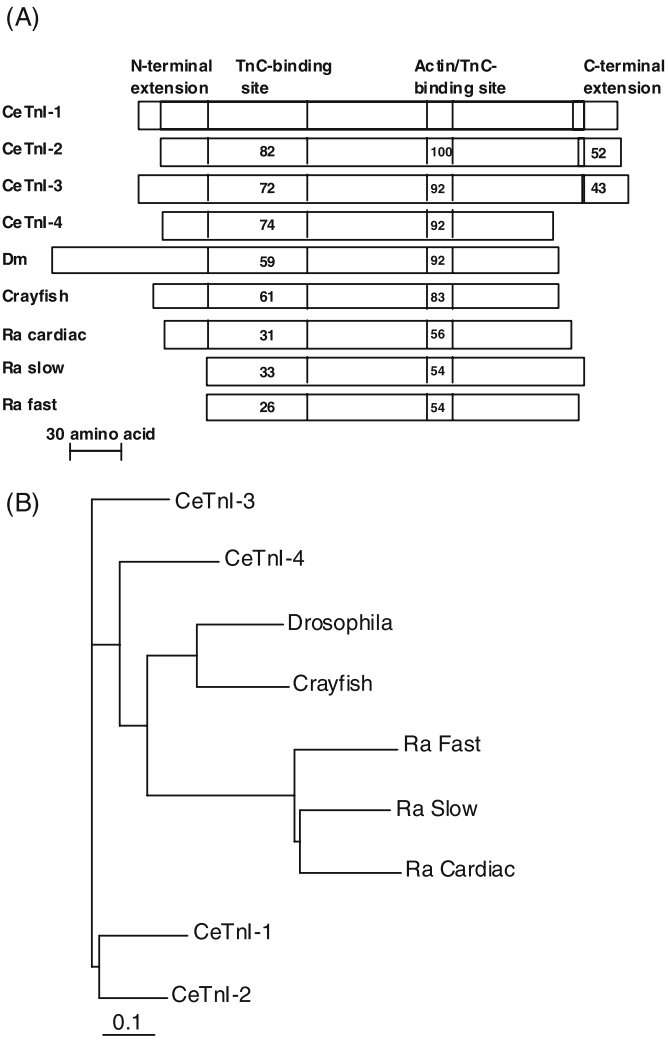

Figure 14.2. Structural homology of troponin I isoforms of invertebrates and vertebrates. (A) The two regulatory regions, TnC-binding and actin/TnC-binding sites showed conserved homology among invertebrates. Numbers represent percentage homology. TnI-1, TnI-2 and TnI-3 of *C. elegans* had unique C-terminal extensions. (B) Phylogenic alignment of four TNI isoforms of *C. elegans*; CeTNI-1, CeTNI-2, CeTNI-3 and CeTNI-4 and TNIs of *Drosophila*, crayfish, *Ciona* body wall, *Ciona* heart, rabbit cardiac (Ra cardiac), rabbit slow (Ra slow) and rabbit fast (Ra fast). The tree was derived using CLUSTALW and TreeView software (from Ruksana et al., 2005).

Tissue expression patterns were determined using *lacZ/gfp/rfp* reporter gene assays. The *tni-1*, *tni-2/unc-27* and *tni-3* genes, each encoding one troponin I isoform, are expressed in body wall, vulval and anal muscles at different intensities, but *tni-4* was expressed solely in the pharynx. Knock down of *tni-1* or *tni-2* gene by RNA interference caused motility defects similar to the *unc-27* (*e155*) mutant, which is a *tni-2/unc-27* null allele. An RNAi experiment for *tni-3* produced egg-laying defects, while similar

experiment with *tni-4* RNAi caused arrest at gastrulation (Table 14.1). These show that body wall troponin I isoforms are important for animal motility and egg-laying and that the pharynx troponin I is essential for animal development (Ruksana et al., 2005).

14.1.4. Body Wall Troponin I Isoforms Interact with Both Tissues Troponin C Isoforms

In vitro overlay assays have been used to analyse interactions between the four troponin I isoforms to the two troponin C isoforms. The three body wall troponin I isoforms interact with the body wall and pharyngeal troponin C isoforms, reciprocally, but the pharyngeal TnI-4 interacts only with the pharyngeal TnC-2. Our results suggest that body wall TnI genes have evolved following duplication of the pharynx gene and provide important data about gene duplication and functional differentiation of nematode troponin I isoforms (Ruksana et al., 2005). Recently we confirmed that the N-terminal part of troponin I interacts with troponin C of the worm (Amin and Kagawa, unpublished). This molecular nature is similar to the molluscan troponin I that interacts with the troponin C of the Akazara scallop (Tanaka et al., 2005). The importance of the N-terminal function of troponin I could be common throughout the invertebrates.

14.1.5. Troponin T Mutant Shows Abnormal Muscle Positioning

Mutants for a troponin T heat-sensitive allele, *mup-2(e2346ts)* and for a putative null, *mup-2(up1)* are defective in embryonic body wall muscle cell contraction and sarcomere organization (Myers et al., 1996). The troponin T gene abundantly expresses in body-wall muscles. The *mup-2(up1)* mutation causes a termination codon near the NH_2 terminus (Glu94) and *mup-2(e2346ts)* is a termination codon in the C-terminal invertebrate specific tail (Trp342) (Myers et al., 1996). These results indicate that the body-wall troponin T is also essential for muscle formation. At least three troponin T genes are expressed in the body wall and one is in the pharynx of the worm (WormBase, from a report of Allen et al.). This expression profile is similar to that of the troponin I isoforms. How isoforms function in muscle cells and interact with other troponin components will be known in future.

14.2. DISCUSSION

Mutants of tropomyosin and three troponin components of *C. elegans* have been isolated and characterized (Table 14.1). The isolated mutants can be divided into two groups; one group are missense alleles having single amino acid substitutions in the protein, the other groups are nulls producing no product. The null mutant phenotypes are consistent with the results obtained in gene knock down experiments using RNAi. Recently we have been able to use the experimental data of the total genome sequence together with the mutant genes, and phenotypes of RNAi animals (WormBase, RNAi). In combination with biochemical and biophysical approaches on tropomyosin and troponin mutants, we have been able to determine the relationships between the molecular nature of the proteins and the behavior of the animals. Interestingly, the mutants isolated map to one of the genes expressed in body wall muscles. Body wall troponin I and troponin T of the worm are encoded by three different genes, but by only one troponin C

gene. This is the reason that troponin C mutant animal is isolated under control of genetic skills, analyzing the F2 ratio of the mutant animals that are kept in the heterozygous state (Williams and Waterston, 1994; Terami et al., 1999). This is also applicable to isolating null mutants of the pharynx type isoform because only one gene encodes one isoform. There are three muscle tissues of the body wall type; body wall for locomotion, vulva for egg-laying and anus for defecation. Isolated mutants of troponin I and troponin T are found only in the abundant body wall isoform genes of *tni-2/unc-27* and *mup-2/tnt-1*, which are expressed in body wall muscles, respectively (Table 14.1). Some differences of expression control and tissue localization of the three troponin I genes are detected between these three muscle groups, but functional differences have not been found in comparisons of the amino acid sequences (Ruksana et al., 2005). It is of interest to know how three isoforms of troponin I and troponin T interact each other and are utilized in different tissues. How minor isoforms can function and interact to other components in different tissues is also of interest in understanding the molecular interactions and evolutionary relationships.

Sequence comparisons between the different isoforms and with other animals indicate that tropomyosin and troponin components have common interaction sites to other proteins and additional unique sequences in their molecules. The binding sites for troponin C and actin/troponin C are common for all isoforms of troponin I (Figure 14.2). The N-terminal extension is found in vertebrate cardiac and all invertebrate troponin I isoforms. There is a C-terminal hydrophilic regions in the three troponin I isoforms of *C. elegans* (Ruksana et al., 2005). This may be important for interactions with other proteins. Recently the crystal structure of the core troponin complex has been determined. The authors stated that the interaction sites between troponin and tropomyosin/actin might be unique to each molecule of the complex in different tissues and animals (Takeda et al., 2003). Ohtsuki and Morimoto and their colleagues have established an *in vitro* physiological testing system for studying interactions between exchanged troponin components in myofibrils (Shiraishi et al., 1992). Using our system, a reverse genetic approach in which a designed gene can be introduced into the animal is possible (Figure 14.2). With this we can determine which part of the molecule functions in muscle and subsequently contributes to animal behavior. These experiments offer two approaches to troponin function; one is to compare proteins from different species and another is related to mutant proteins. The former is useful in studying how molecules are changed during evolution. The later is applicable to understanding how mutations disturb tissue functions of animals or even humans. As we have mentioned, troponin mutants that cause functional defects of these proteins in the nematode will only be apparent in animals homozygous for the mutants. Even in some human disorders in human symptoms will be detected by a combination of genome or gene sequencing approaches of the gene and phenotypic analysis of the transgenic model animal.

14.3. ACKNOWLEDGEMENT

This article will dedicate to Profs Setsuro Ebashi, Iwao Ohtsuki and their school for the fortieth anniversary of their seminal discoveries relating to the troponin system. This study originated the time when one of the authors, H. K. had learned biophysics from Profs. Fumio Oosawa and Sho Asakura, and molecular biology of the worm from Profs.

Sydney Brenner and Jon Karn. Some information on the troponin C and tropomyosin mutants was owed from Profs. Robert Waterston and Benjamin Williams. We acknowledge Prof. Takayoshi Iio for analyzing Ca^{2+} binding constant of the troponin C and Prof. John C. Sparrow for his generous help in critically reading the manuscript.

14.4. REFERENCES

Anyanful, A., Sakube, Y., Takuwa, K., and Kagawa, H., 2001, The third and fourth tropomyosin isoforms of *Caenorhabditis elegans* are expressed in the pharynx and intestines and are essential for development and morphology, *J. Mol. Biol*. **313**:525–537.

Benian, G. M., Kiff, J. E., Neckelmann, N., Moerman, D. G., and Waterston, W. H., 1989, Sequence of unusually large protein implicated in regulation of myosin activity in C. elegans, *Nature* **342**:45–50.

Benoist, P., Mas, J. A., Marco, R., and Cervera, M., 1998, Different muscle-type expression of the *Drosophila* troponin T gene, *J. Biol. Chem*. **273**:7538–7546.

Brenner, S., 1974, The genetics of *Caenorhabditis elegans*, *Genetics* **77**:71–94.

Burkeen, A. K., Maday, S. L., Rybicka, K. K., Sulcove, J. A., Ward, J., Huang, M. M., Barstead, R., Franzini-Armstrong, Allen, T.Stc., 2004, Disruption of *Caenorhabditis elegans* muscle structure and function caused by mutation troponin I, *Biophys. J.* **86**:991–1001.

Domingo, A., Gonzalez-Jurado, J., Maroto, M., Diaz, C., Vinòs, J., Carrasco, C., Cervera, M., and Marco, R., 1998, Troponin T is a calcium-binding protein in insect muscle *in vivo* phosphorylation, muscle-specific isoforms and developmental profile in *Drosophila melanogaster*, *J. Muscle Res. Cell Motil*. **19**:393–403.

Fyrberg, E., Fyrberg, C. C., Beall, C., and Saville, D. L., 1990, *Drosophila melanogaster* troponin T mutations engender three distinct syndromes of myofibrillar abnormalities, *J. Mol. Biol*. **216**:657–675.

Kagawa, H., Gengyo, K, McLachlan, A. D., Brenner, S., and Karn, J., 1989, Paramyosin gene (*unc-15*) of *Caenorhabditis elegans*- Molecular cloning, nucleotide sequence and models for thick filament structure, *J. Mol. Biol.* **207**:311–333.

Kagawa, H., Sugimoto, K., Matsumoto, S., Inoue, T., Imadzu, H., Takuwa, K., and Sakube, Y., 1995, Genome structure, mapping and expression of the tropomyosin gene *tmy-1* of *Caenorhabditis elegans*, *J. Mol. Biol.* **251**:603–613.

Kagawa, H., Takuwa, K., and Sakube, Y., 1997, Mutations and expressions of the tropomyosin gene and the troponin C gene of *Caenorhabditis elegans*, *Cell Struct. Funct.* **22**:213–218.

Kamath, R. S., Fraser, A. G., Dong, Y., Poulin, G., Durbin, R., Gotta, M., Kanapin, A., Le Bot, N., Moreno, S., Sohrmann, M., Welchman, D. P., Zipperlen, P., and Ahringer, J., 2003, Systematical functional analysis of the *Caenorhabditis elegans* genome using RNAi, *Nature* **421**:231–237.

Karn, J., Brenner, S., and Barnett, L., 1983, Protein structural domains in the *Caenorhabditis elegans unc-54* myosin heavy chain gene are not separated by introns, *Proc. Natl. Acad. Sci., USA* **80**:4253–4257.

Lewis, J. A., Wu, C.-H., Berg, H., and Levin, J. H., 1980, The genetics study levamisole resistance in the nematode Caenorhabditis elegans, *Genetics* **95**:905–928.

Moerman, D. G., and Fire, A., 1997, Muscle: Structure, function and development, in: *C. elegans II*, D. L. Riddle, T. Blumenthal, B. J. Meyer, and J. R. Priess, eds, Cold Spring Harbor Laboratory Press, New York, pp. 417–470.

Myers, C. D., Goh, P. Y., Allen, T. S., Bucher, E. A., and Bogaert, T., 1996, Developmental genetics analysis of troponin T mutations in striated and nonstriated muscle cells of *Caenorhabditis elegans*, *J. Cell Biol.* **132**:1061–1077.

Ohtsuki, I., Maruyama, K., and Ebashi, S., 1986, Regulatory and cytoskeletal proteins of vertebrate skeletal muscle, *Adv. Protein Chem*. **38**:1–67.

Ono, S., and Ono, K., 2002, Tropomyosin inhibits ADF/cofilin-dependent actin filament dynamics, *J. Cell Biol.* **156**:1065–1076.

Ono, K., and Ono, S., 2004, Tropomyosin and troponit are required for ovarian contraction in the *Caenorhabditis elegans* reproductive system, *Mol. Biol. Cell* **15**:2782–2793.

Ruksana, R., Kuroda, K., Terami, H., Bando, T., Kitaoka, S., Takaya, T., Sakube, Y., and Kagawa, H., 2005, Tissue expression of four troponin I genes and their molecular interactions with two troponin C isoforms in *Caenorhabditis elegans*, *Genes Cells* **10**:261–276.

Shiraishi, F., Kambara, M., and Ohtsuki, I., 1992, Replacement of troponin components in myofibrils, *J. Biochem. (Tokyo)* **111**:61–65.

Takeda, S., Yamashita, A., Maeda, K., and Maeda, Y., 2003, Structure of the core domain of human cardiac troponin in the Ca2+-saturated form, *Nature* **424**:35–41.

Tanaka, H., Takeya, Y., Doi, T., Yumoto, F., Tanokura, M., Ohtsuki, I., Nishita, K., and Ojima, T., 2005, Comparative studies on the functional roles of N- and C-terminal regions of molluskan and vertebrate troponin I, *FEBS J.* **272**:4475–4486.

Terami, H., Williams, B. D., Kitamura, S., Sakube, Y., Matsumoto, S., Doi, S., Obinata, T., and Kagawa, H., 1999, Genomic organization, expression and analysis of the Troponin C gene *pat-10* of *Caenorhabditis elegans*, *J. Cell Biol.* **146**:93–202.

Terami, H. 2002 Molecular studies on body wall-and pharyngeal troponin C isoforms in *Caenorhabditis elegans* Ph. D thesis, Okayama University

The C. elegans Sequence Consortium, 1998, Genome sequence of the nematode *C. elegans*: A platform for investigating biology, *Science* **282**:2012–2018.

Ueda, T, Katsuzaki, H., Terami, H., Ohtsuka, H., Kagawa, H., Murase, T., Kajiwara, Y., Yoshioka, O., and Iio, T., 2001, Calcium-binding of wild type and mutant troponin Cs of Caenorhabditis elegans, *Biochim. Biophys. Acta* **1548**:220–228.

Vassylyev, D. G., Takeda, S., Wakatsuki, S., Maeda, K., and Maeda, Y., 1998, Crystal structure of troponin C in complex with troponin I fragment at 2.3-A° resolution, *Proc. Natl. Acad. Sci. USA* **95**:4847–4852.

Waterston, R. H., 1988, Muscle, in: *The nematode Caenorhabditis elegans*, W. B. Wood, ed., Cold Spring Harbor Laboratory Press, New York, pp. 281–335.

White, S. P., Cohen, C., and Phillips, G. N. Jr, 1987, Structure of co-crystals of tropomyosin and troponin, *Nature* **325**:826–828.

Williams, B. D., and Waterston, R. H., 1994, Genes critical for muscle development and function in *Caenorhabditis elegans* identified through lethal mutations, *J. Cell Biol.* **124**:475–490.

WormBase; http://www.wormbase.org/ or WormBase, RNAi; http://www.wormbase.org/db/searches/rnai_search TNT; http://www.wormbase.org/db/misc/paper?name=WBPaper00010575;class=Paper

15

STRUCTURAL AND FUNCTIONAL ANALYSIS OF TROPONINS FROM SCALLOP STRIATED AND HUMAN CARDIAC MUSCLES

Fumiaki Yumoto[1,2] and Masaru Tanokura[1]

15.1. INTRODUCTION

The Ca^{2+}-regulation of scallop striated muscle contraction, a Ca^{2+}-regulation mechanism that is linked to myosin, was first discovered by A. G. Szent-Györgyi and his colleagues.[1,2] In myosin-linked Ca^{2+}-regulation, the Ca^{2+}-receptive site is the essential light chain of myosin, and the ATPase of the scallop myofibrils has been found to be desensitized to Ca^{2+} by removal of the regulatory light chain (RLC) of myosin in response to treatment with a divalent cation chelator (EDTA). At the same time, three components of troponin and tropomyosin have also been isolated from scallop striated muscle, and several of their biochemical properties have been investigated.[3–5] In this troponin-linked Ca^{2+}-regulation, the concurrent presence of all three components of troponin (troponins C, I, and T; TnC, TnI, and TnT) and tropomyosin are necessary for the regulation of actomyosin ATPase activity.[6–10] The action of Ca^{2+} on TnC ultimately induces actomyosin ATPase activity. Troponin-linked Ca^{2+}-regulation is also desensitized by the removal of TnC in response to treatment with divalent cation chelators such as EDTA or CDTA. The mutual relation of these two types of Ca^{2+}-regulations in scallop myofibrils was then investigated as follows.[11] Desensitized scallop myofibrils were prepared by removing both RLC and TnC by treatment with a divalent cation chelator, CDTA, and the effects of reconstitution with RLC and/or TnC on the ATPase activity of the desensitized myofibrils were examined. It was then demonstrated that reconstitution with TnC does not inhibit ATPase in the absence of Ca^{2+} but instead induces ATPase activity only in the presence of Ca^{2+}, while reconstitution with RLC inhibits ATPase in the absence of Ca^{2+} and this inhibition is eliminated with increasing Ca^{2+} concentrations. These results indicate that scallop troponin has a predominantly activating effect on the contractile system. This finding is in sharp contrast to vertebrate troponin, which primarily exhibits inhibition-deinhibition type Ca^{2+}-regulating ability with slight activating action. In this article, we will discuss several biochemical properties of scallop troponin components with particu-

[1] Department of Applied Biological Chemistry, Graduate School of Agricultural and Life Sciences, University of Tokyo, Tokyo 113-8657, and [2]Department of Physiology II, The Jikei University School of Medicine, Tokyo 105-8641, Japan

Regulatory Mechanisms of Striated Muscle Contraction
Edited by Ebashi and Ohtsuki, Springer, 2007

lar reference to the Ca^{2+}-bound structure of the TnC C-lobe. In addition, we also present some findings from ongoing studies of the functional as well as structural consequences of mutations of human cardiac troponin I associated with restrictive cardiomyopathy (RCM).

15.2. SCALLOP TROPONIN

Scallop TnC binds only one Ca^{2+} ion at its C-terminal EF-hand motif (site IV) in C-the terminal lobe (C-lobe) due to the amino acid replacement that is critical to Ca^{2+}-binding, while vertebrate fast skeletal muscle TnC has four Ca^{2+}-binding sites: two regulatory low-affinity sites in the N-terminal lobe (N-lobe) and two high-affinity sites in the C-lobe[3–5,12,13] (Figure 15.1). Therefore, scallop TnC is a curious TnC that binds only Ca^{2+} at the C-lobe. In addition, Doi et al. have reported that the N-lobe of scallop TnC also plays a role in Ca^{2+} regulation, though the N-lobe itself has no Ca^{2+}-binding activity.[14] A chimeric protein containing the rabbit fast skeletal TnC N-lobe and scallop TnC C-lobe shows virtually no Ca^{2+} sensitivity with regard to Mg^{2+}-ATPase activity of a troponin and tropomyosin-reconstituted actomyosin. These results support the the hypothesis that the N-lobe of scallop TnC also plays an important role in the regulatory function of the TnC.

The followings are some unique characteristics of the scallop striated muscle TnI. The TnI is a polypeptide containing 292 amino acid residues (M.W. 34 678) and its molecular weight is greater by approximately 14 000 than that of the vertebrate skeletal muscle polypeptide.[15–18] The homologous sequence to vertebrate TnIs is found in the C-terminal portion. The sequence of the inhibitory region is essential to the inhibitory function, which is achieved by binding to actin or TnC, and this inhibitory region is highly conserved. On the other hand, scallop TnI has 100–133 extra residues at the N-terminus of the vertebrate TnI. This extra region has a unique sequence and contains many Glu and Arg residues. Moreover, there is no similarity between the second TnC binding

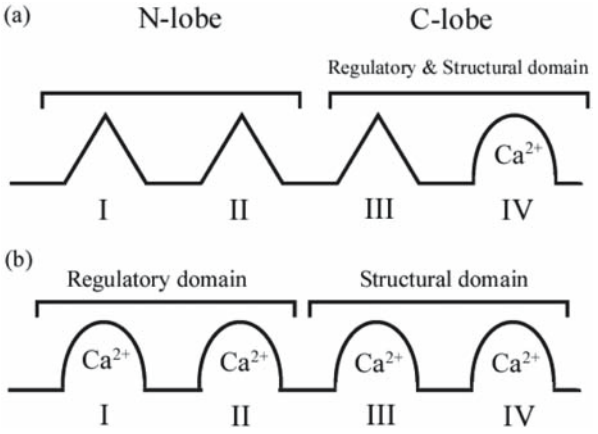

Figure 15.1. Ca^{2+}-binding sites of TnCs. (a) Ca^{2+}-binding site of Akazara scallop TnC (b) Ca^{2+}-binding sites of vertebrate fast skeletal muscle TnC.

region of the vertebrate fast skeletal muscle TnI and the corresponding region of scallop TnI. Since there are some differences between vertebrate fast skeletal muscle troponin components and those of scallop, it is possible that the molecular mechanism of Ca^{2+}-regulation by scallop troponin may be distinct from that of vertebrate striated muscle.

Many structural investigations of the structures of vertebrate cardiac and fast skeletal muscle TnCs have been carried out to increase our understanding of the molecular regulatory mechanism of Ca^{2+} and troponin.[19–23] A recent remarkable achievement was determination of the core domain crystal structures of human cardiac and chicken fast skeletal muscle troponins.[24,25] The structural information regarding invertebrate TnC, however, was limited. For instance, the coordination structures of Ca^{2+} and Mg^{2+} in scallop TnC have been investigated.[26] In Site IV of scallop TnC, the COO^- group in Glu142 has been found to bind Ca^{2+} in the bidentate coordination mode, while COO^- groups in Asp131 and Asp133 bind Mg^{2+} via the pseudo-bridging mode with low affinity (Figure 15.2). Through the use of mutagenesis, functional and structural studies of the scallop TnC E142Q mutant have demonstrated that the mutation from Glu to Gln results in a loss of Ca^{2+} binding ability and Ca^{2+}-dependent regulatory function of TnC.[13,27] These results indicate that Site IV of scallop TnC has both regulatory and structural function by through the exchange of Mg^{2+} with Ca^{2+}. Circular dichroism (CD) spectra and the gel-filtration profiles of scallop TnC have shown that the secondary structure is conserved among the three states (apo, Mg^{2+}-bound, and Ca^{2+}-bound), and the tertiary structure is in fact altered upon Ca^{2+}-binding.[26] TnC shows a more compact conformation when it binds Ca^{2+}. The concrete tertiary structural changes, however, have not been clarified.

To analyze the precise Ca^{2+}-dependent regulatory mechanism of scallop TnC, we conducted an NMR structural analysis of the scallop TnC C-lobe, which contains two EF-hand motifs (Sites III and IV) complexed with $TnI_{129–183}$.[28] Scallop $TnI_{129–183}$ is a peptide that corresponds to the N-terminal region of vertebrate fast skeletal muscle TnIs, which bind to the TnC C-lobe in the presence and absence of Ca^{2+}. Scallop TnC, TnC C-lobe, and $TnI_{129–183}$ were prepared using an *E. coli* expression system. Both TnC and the C-lobe of TnC tend to form oligomers at concentrations in the millimolar range (Figure 15.3a). On the other hand, the formation of the $TnI_{129–183}$ complex with the C-lobe of TnC suppresses the aggregation process (Figure 15.3b). We were therefore able to completely assign the backbone amide signals of the C-lobe of scallop TnC[28] (Figure 15.4). For the assignment of the NMR signals from the side-chains, HCCH-TOCSY, HCCH-COSY, 3D ^{15}N-edited NOESY, and ^{13}C-edited NOESY spectra were used. The constraints for the distances and angles were identified using the two 3D NOESY spectra and HNHA spectrum, respectively. The structure of the C-lobe of TnC in the complex with $TnI_{129–183}$, was then calculated using DYANA ver. 1.4.[29] The solution structure of Ca^{2+}-bound TnC C-lobe binding to $TnI_{129–183}$ was determined. The 3D structure showed that the C-lobe contained four

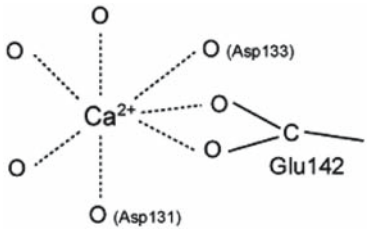

Figure 15.2. Ca^{2+}-coordination structure of scallop TnC.

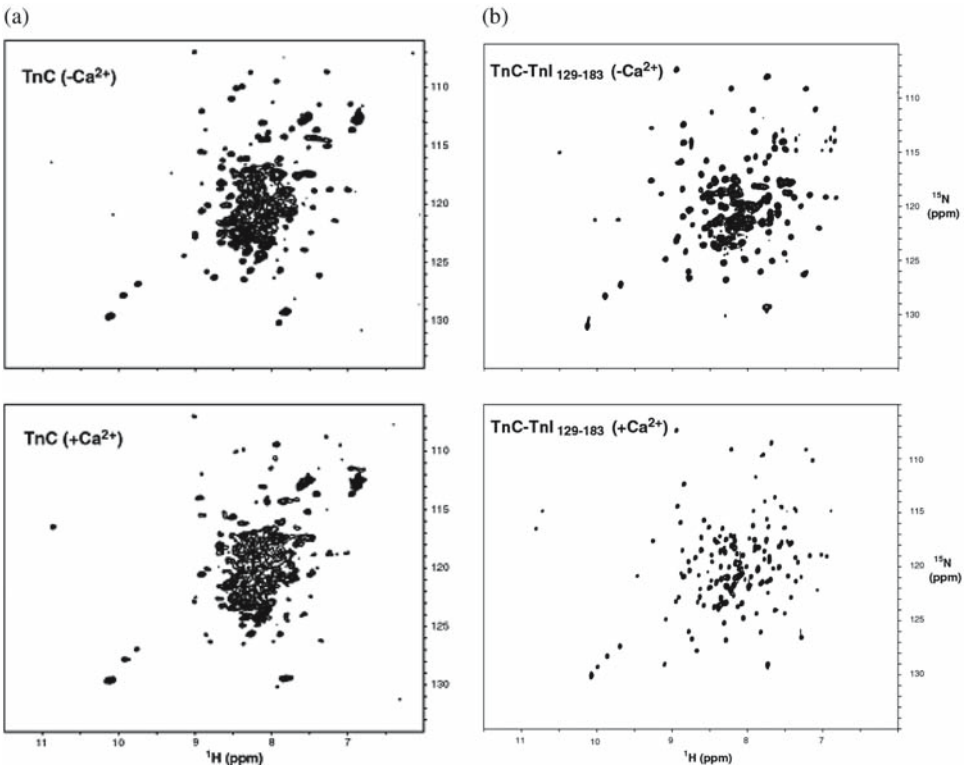

Figure 15.3. (a) ^{15}N—^{1}H HSQC spectra of scallop TnC ($-Ca^{2+}$: upper panel, $+Ca^{2+}$: lower panel) and (b) TROSY-type ^{15}N—^{1}H HSQC spectra of scallop TnC binding to $TnI_{129–183}$ ($-Ca^{2+}$: upper panel, $+Ca^{2+}$: lower panel).

α-helices and two short anti-parallel β-sheets (Figure 15.5). In general, the conformational change in the EF-hand motif due to Ca^{2+}-binding is regarded as the transition from the closed- to the open-state, which correspond to the approximately anti-parallel orientation and almost perpendicular orientation, respectively, between the two helices that are a part of the helix-loop-helix.[30] The structures of both EF-hand motifs have the open conformation. Therefore, the C-lobe of TnC is in the activated form when it binds Ca^{2+}. The conformational change to the open-state must be one of the triggers of striated muscle contraction of the scallop. However, it is not clear whether Site III, which does not bind Ca^{2+}, has a closed- or an open-conformation in the resting state in a cell (Figure 15.6). Determining the structure of the scallop TnC C-lobe in the apo state will help to clarify these details.

With regard to the biological significance of the structural transition, an interesting study was carried out by Tanaka et al.[31] They performed a comparative study of the functional roles of N- and C-terminal regions of molluscan and vertebrate TnIs (Figure 15.7). The results suggested that scallop troponin regulates muscle contraction via activating mechanisms that involve the region spanning from the TnC C-lobe binding site to the inhibitory region of TnI, and that there is no alternative binding of the TnI C-terminal region to TnC. The research also revealed that the TnI N-terminal region (from the TnC C-lobe-binding region to the inhibitory region) participates in Ca^{2+}-dependent activation. In addition, similar activation is observed for the vertebrate troponin, which contains a

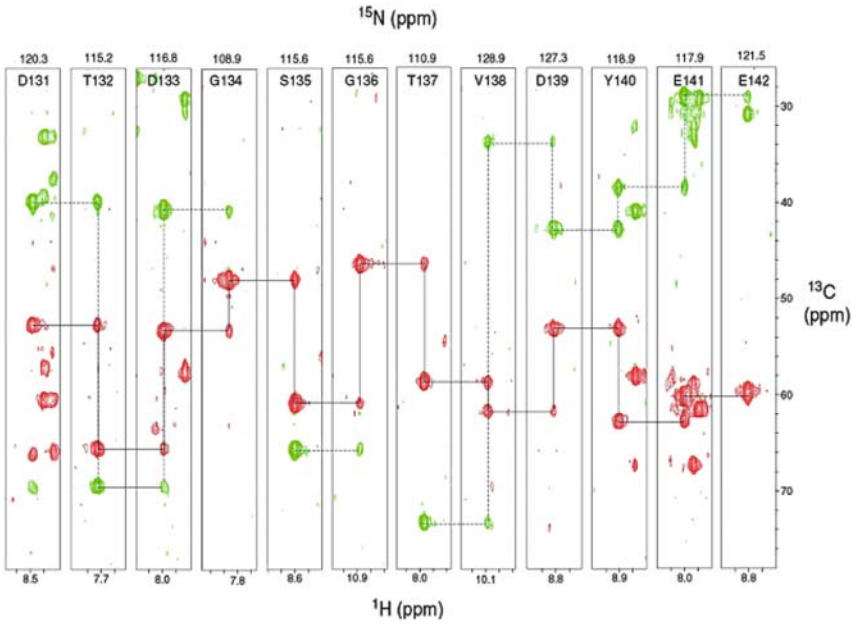

Figure 15.4. Strip-plots of the HNCACB spectrum of the Akazara scallop TnC C-lobe that binds $TnI_{129–183}$.

Figure 15.5. Amino acid sequence and the secondary structure of the Akazara scallop TnC C-lobe that binds $TnI_{129–183}$.

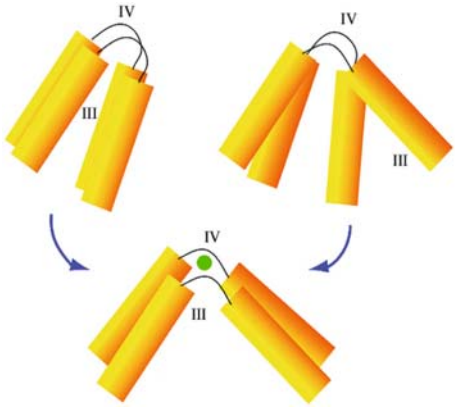

Figure 15.6. Schematic representation of the conformational changes from the closed (III)–closed (IV) state or the open (III)–closed (IV) state to the open (III)–open (IV) state.

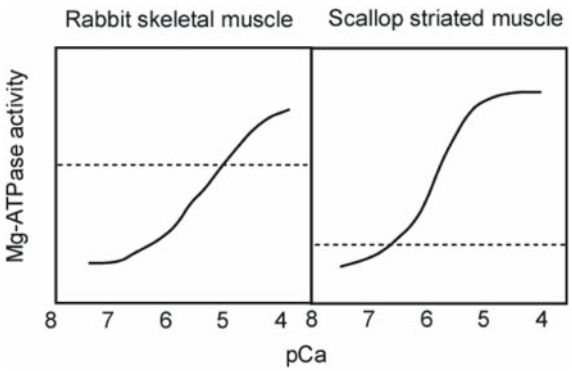

Figure 15.7. Schematic representation of the Ca^{2+}-regulation of actomyosin-tropomyosin Mg^{2+}-ATPase by rabbit and Akazara scallop reconstituted troponins at 15°C (Tanaka et al. (2005).) The activities in the absence of troponin are indicated by dashed line.

TnI-fragment. It was therefore concluded that there is a common activating mechanism between vertebrates and scallops. The activation of the scallop striated muscle might be induced by strengthening of the interaction between the TnC C-lobe and the TnC-binding region of TnI.

Based on the molecular mechanism of vertebrate striated muscle contraction, which is regulated by troponin-tropomyosin and is generally classified as the inhibition-deinhibition type, we assume that the activation effects of scallop troponin occur via the common mechanism of Ca^{2+}-regulation by mutant human cardiac troponin. The functional analyses of gene mutations for human cardiac TnT associated with hypertrophic cardiomyopathy (HCM) have revealed that Ca^{2+}-sensitization of the force generation of skinned fibers is a major functional consequence of these mutations as much as the 15 mutations causing HCM.[32–34] However, one HCM-causing mutation (F110I) does not show Ca^{2+}-sensitization but instead enhances force generation, and another mutation (E244D) shows both enhanced force generation and Ca^{2+}-sensitization.[35] This finding strongly suggests that the activating action plays some role in the genetic disorder of cardiac troponin, although the activating action of vertebrate troponin is a minor mechanism under physiological conditions. Therefore, detailed studies of scallop troponin should contribute to clarifying the pathogenic mechanism of the two TnT mutants for which the activating effect has been potentiated.

It has been demonstrated that conformational change occurs in scallop TnC when it binds Ca^{2+} at Site IV, and that it changes to an open-state that triggers muscle contraction. Therefore, further investigation of scallop troponin is essential to understanding the mechanism of the activation effect and the actin-linked Ca^{2+} regulation of invertebrate striated muscles.

15.3. CARDIAC TROPONIN

We also present herein our recent research on human cardiac troponin related to cardiomyopathy. It has been demonstrated that mutations in the genes that code for two human cardiac Tn components, cTnI and cTnT, are often responsible for cardio-

myopathy.[34,36] Cardiac TnC is a Ca^{2+}-binding component, and mutation in the gene encoding this component is also responsible for cardiomyopathy.[37] The functional consequences of cTnI and cTnT mutations linked to HCM and/or DCM have been investigated by Morimoto et al. and Ohtsuki.[31–34,38] They have shown that these mutations alter the regulatory properties of the troponin ternary complex, thereby resulting in an increase and a decrease in the Ca^{2+} sensitivity of force generation that may primarily contribute to the pathogeneses of HCM and DCM, respectively.

In addition to the two cardiomyopathies, six missense mutations (L144Q, R145W, A171T, K178E, D190G, and R192H) occurring in the human cTnI gene have been found to be associated with restrictive cardiomyopathy (RCM).[39] RCM, the least common form of the three cardiomyopathies, is characterized by restrictive diastolic dysfunction (restrictive filling and reduced diastolic volume of either or both ventricles) with normal or near-normal systolic function and wall thickness.[40] The prognosis of RCM is very poor, particularly in the young with heart failure, and patients affected by this condition often require heart transplantation. The RCM-causing mutations in cTnI occur in residues that are highly conserved among different animal species and tissues;[41–46] as such, these mutations would perturb an important physiological function of cTnI (Figure 15.1). With regard to the positions of the mutations, these mutations occur in distinct functional regions of cTnI. L144Q and R145W are positioned in the inhibitory region that binds to actin and TnC to inhibit and activate muscle contraction, respectively. HCM-causing mutations R141Q, R145G, and R145Q have also been reported to occur in the same region.[47] A171T and K178E are located near and within the second actin-tropomyosin binding region, respectively, which is necessary for the complete inhibitory activity of the inhibitory region.[48] D190G and R192H are positioned in the C-terminal region, which is also required for the complete inhibitory action of cTnI.[49]

We have shown the functional and structural consequences of RCM-causing cTnI mutations through the use of recombinant proteins.[50] In order to explore the functional consequences of cTnI mutations on force generation, each of the purified human cTnI mutants was incorporated into a skinned fiber with recombinant human cTnT and cTnC by using the troponin-exchanging method developed by Hatakenaka and Ohtsuki with a slight modification.[51–53] All six mutations shifted the force-pCa relationship curve to lower Ca^{2+} concentrations and exerted Ca^{2+}-sensitizing effects on force generation. Moreover, RCM-causing mutations were found to have considerably greater Ca^{2+}-sensitizing effects than the HCM-causing mutations. Gomes et al. have recently reported the same result by using porcine skinned cardiac muscle fibers into which human cTnIs with five RCM-causing mutations, except D190G, were incorporated.[54] With regard to ATPase activity, the six mutations also exerted Ca^{2+}-sensitizing effects, which were evident from the leftward shifts in the pCa-ATPase activity relationships. The K178E mutation exerted the most prominent Ca^{2+}-sensitizing effect on ATPase activity. These results were similar to those from the experiments on force generation. These experiments revealed that RCM-causing mutations show considerably greater Ca^{2+} sensitivity of the cardiac myofilament than HCM-causing mutations. As such, the amplitude of the Ca^{2+} sensitization might be a determinant for the phenotypic expression of RCM or HCM.

To clarify the molecular mechanisms of such drastic Ca^{2+} sensitization of cardiac myofilaments, we examined the K178E mutation from a structural perspective using CD and NMR spectroscopy. Because the full-length cTnI polypeptide tends to aggregate

easily and become insoluble at physiological ionic strength, we prepared a C-terminal cTnI fragment, $cTnI_{129–210}$. This peptide inhibits the actomyosin Mg^{2+}-ATPase activity. The CD analysis of wild-type and K178E $cTnI_{129–210}$ peptides revealed that the K178E mutation causes only a small change in the secondary structure of $cTnI_{129–210}$. To determine the component involved in the structural change following K178E substitution, wild-type and K178E $cTnI_{129–210}$ peptides were analyzed by 2D NMR. Most signals in the $^{15}N—^{1}H$ HSQC spectrum were found to be unaffected by the K178E mutation, and only a small number of peaks in the $^{15}N—^{1}H$ HSQC spectrum were found to be perturbed by the mutation. The residues changed by the mutation were K177, K(E)178, E179, and T181. These findings indicate that the structural change occurs in a restricted region surrounding the K178E mutation site. A recent NMR study of the structure of a chicken fast skeletal muscle TnI, which is complexed with the chicken skeletal muscle TnC and TnT_2, indicates that this region forms part of an anti-parallel β-sheet[55] (Figure 15.8a). This structure suggests that the K178E mutation destabilizes the β-structure critical to the physiological function of the second actin-Tm binding region in cTnI (Figure 15.8b). Therefore, the mutation caused drastic Ca^{2+} sensitization of cardiac myofilaments by inducing a subtle structural change in an unexpectedly restricted region within the cTnI molecule. We also recently found that the L144Q, A171T, D190G, and R192H mutations lead to subtle structural perturbations (Yumoto et al., unpublished results)

On the basis of these results, small molecules that desensitize the Ca^{2+}-sensitivities of force generation of cardiac muscle would likely be effective in therapy for cardiomyopathies such as HCM and RCM. Accordingly, we have screened some chemical compounds and have identified the materials that modify the Ca^{2+}-sensitivity. We have discussed the functional and structural basis of the modifier of Ca^{2+}-sensitivity in this symposium.

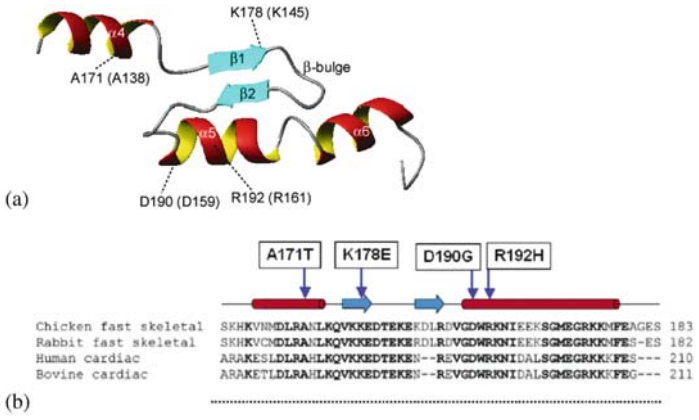

Figure 15.8. (a) The positions of RCM-causing mutations in cTnI mapped on a solution structure model of chicken fast skeletal muscle TnI C-terminal region[24] (PDB 1VDJ). The Figures are generated by MOLMOL[56]. (b) The secondary structure elements are drawn above the sequence alignments of TnIs. The common amino acids are indicated with bold characters.

15.4. ACKNOWLEDGEMENTS

This research was supported in part by Grants-in-Aid for Scientific Research from the Ministry of Education, Culture, Sports, Science, and Technology of Japan. We would like to express our sincere thanks to Dr. I. Ohtsuki for his constant encouragement. We thank Drs. T. Ojima, K. Nishita and H. Tanaka for cooperative collaboration on the scallop and cardiac troponin research, and for Drs. S. Morimoto, Q. W. Lu, and N. Tadano for their collaboration on human cardiac troponin related to cardiomyopathy. We would also like to thank Drs. K. Nagata, N. Nemoto, and K. Adachi for their advice regarding NMR measurements and structure determination, Drs. M. Nara and H. Kagi for their help in FT-IR studies of scallop troponin, and Drs. Y. Kato and Y. Sawano for their advice regarding protein sample preparations.

15.5. REFERENCES

1. A. G. Szent-Györgyi, E. M. Szentkiralyi, and J. Kendrick-Jonas, The light chains of scallop myosin as regulatory subunits, *J. Mol. Biol.* **74**, 179–203 (1973).
2. A. G. Szent-Györgyi, V. N. Kalabokis, and C. L. Perreault-Micale, Regulation by molluscan myosins. *Mol. Cell. Biochem.* **190**, 55–62 (1999).
3. T. Ojima, and K. Nishita, Isolation of troponins from striated and smooth adductor muscles of Akazara scallop. *J. Biochem.* **100**, 821–824 (1986).
4. T. Ojima, and K. Nishita, Troponin from Akazara scallop striated adductor muscles. *J. Biol. Chem.* **261**, 16749–16754 (1986).
5. K. Nishita, H. Tanaka, and T. Ojima, T. Amino acid sequence of troponin C from scallop striated adductor muscle. *J. Biol. Chem.* **269**, 3464–3468 (1994).
6. S. Ebashi, and M. Endo, Calcium ion and muscle contraction. *Prog. Biophys. Mol. Biol.* **18**, 123–183 (1968).
7. I. Ohtsuki, K. Maruyama, and S. Ebashi, Regulatory and cytoskeletal proteins of vertebrate skeletal muscle, *Adv. Protein Chem.* **38**, 1–67 (1986).
8. C. S. Farah, and F. C. Reinach, The troponin complex and regulation of muscle contraction. *FASEB, J.* **9**, 755–767 (1995).
9. L. S. Tobacman, Thin filament-mediated regulation of cardiac contraction. *Ann. Rev. Physiol.* **58**, 447–481 (1996).
10. T. Kobayashi, and R. J. Solaro, Calcium, thin filaments, and the integrative biology of cardiac contractility. *Annu. Rev. Physiol.* **67**, 39–67 (2005).
11. F. Shiraishi, S. Morimoto, K. Nishita, T. Ojima, and I. Ohtsuki, Effects of removal and reconstitution of myosin regulatory light chain and troponin C on the Ca^{2+}-sensitive ATPase activity of myofibrils from scallop striated muscle. *J. Biochem.* **126**, 1020–1024 (1999).
12. A. S. Zot, J. D. Potter, and W. L. Strauss, Isolation and sequence of a cDNA clone for rabbit fast skeletal muscle troponin C. Homology with calmodulin and parvalbumin. *J. Biol. Chem.* **262**, 15418–15421 (1987).
13. T. Ojima, N. Koizumi, K. Ueyama, A. Inoue, and K. Nishita, Functional role of Ca^{2+}-binding site IV of scallop troponin C. *J. Biochem.* **128**, 803–809 (2000).
14. T. Doi, A. Satoh, H. Tanaka, A. Inoue, F. Yumoto, M. Tanokura, I. Ohtsuki, K. Nishita, and T. Ojima, Functional importance of Ca^{2+}-deficient N-terminal lobe of molluscan troponin C in troponin regulation. *Arch. Biochem. Biophys.* **436**, 83–90 (2005).
15. J. M. Wilkinson, and R. J. Grand, The amino-acid sequence of chicken fast-skeletal-muscle troponin I. *Eur. J. Biochem.* **82**, 493–501 (1978).
16. T. Ojima, and K. Nishita, Biochemical characteristics of the Mr 52 000 component of Akazara scallop troponin. *J. Biochem.* **104**, 207–210 (1988).
17. T. Ojima, H. Tanaka, and K. Nishita, Cyanogen bromide fragments of Akazara scallop Mr 52 000 troponin-I. *J. Biochem.* **108**, 519–521 (1990).

18. H. Tanaka, T. Ojima, and K. Nishita, Amino acid sequence of troponin-I from Akazara scallop striated adductor muscle. *J. Biochem.* **124**, 304–310 (1998).
19. O. Herzberg, and M. N. G. James, Structure of the calcium regulatory muscle protein troponin-C at 2.8 Å resolution. *Nature* **313**, 653–659 (1985).
20. M. Sundaralingam, R. Bergstrom, G. Strasburg, S. T. Rao, P. Roychowdhury, M. Greaser, and B. C. Wang, Molecular structure of troponin C from chicken skeletal muscle at 3-angstrom resolution. *Science* **227**, 945–948 (1985).
21. S. M. Gagné, S. Tsuda, M. X. Li, L. B. Smillie, and B. D. Sykes, Structures of the troponin C regulatory domains in the apo and calcium-saturated states. *Nat. Struct. Biol.* **2**, 784–789 (1995).
22. C. M. Slupsky, and B. D. Sykes, NMR solution structure of calcium-saturated skeletal muscle troponin C. *Biochemistry* **12**, 15953–15964 (1995).
23. D. G. Vassylyev, S. Takeda, S. Wakatsuki, K. Maeda, and Y. Maéda, Crystal structure of troponin C in complex with troponin I fragment at 2.3 Å – resolution. *Proc. Natl. Acad. Sci. USA* **95**, 4847–4852 (1998).
24. S. Takeda, A. Yamashita, K. Maeda, and Y. Maéda, Structure of the core domain of human cardiac troponin in the Ca^{2+}-saturated form. *Nature* **424**, 35–41 (2003).
25. M. V. Vinogradova, D. B. Stone, G. G. Malanina, C. Karatzaferi, R. Cooke, R. A. Mendelson, and R. J. Fletterick, Ca^{2+}-regulated structural changes in troponin. *Proc. Natl. Acad. Sci. USA* **102**, 5038–5043 (2005).
26. F. Yumoto, M. Nara, H, Kagi, W. Iwasaki, T. Ojima, K. Nishita, K. Nagata, and M. Tanokura, Coordination structures of Ca^{2+} and Mg^{2+} in Akazara scallop troponin C in solution. FTIR spectroscopy of side-chain COO^- groups. *Eur. J. Biochem.* **268**, 6284–6290 (2001).
27. M. Nara, F. Yumoto, K. Nagata, M. Tanokura, H. Kagi, T. Ojima, and K. Nishita, Fourier transform infrared spectroscopic study on the binding of Mg^{2+} to a mutant Akazara scallop troponin C (E142Q). *Biopolymers* **74**, 77–81 (2004).
28. F. Yumoto, K. Nagata, K. Adachi, N. Nemoto, T. Ojima, K. Nishita, I. Ohtsuki, and M. Tanokura, NMR structural study of troponin C C-terminal domain complexed with troponin I fragment from Akazara scallop. *Adv. Exp. Med. Biol.* **538**, 195–201 (2003).
29. P. Güntert, C. Mumenthaler, and K. Wüthrich, Torsion angle dynamics for NMR structure calculation with the new program DYANA. *J. Mol. Biol.* **273**, 283–298 (1997).
30. M. R. Nelson and W. J. Chazin, Structures of EF-hand Ca^{2+}-binding poroteins: Diversity in the organization, packing and response to Ca^{2+} binding, *Biometals* **11**, 297–318 (1998).
31. H. Tanaka, Y. Takeya, T. Doi, F. Yumoto, M. Tanokura, I. Ohtsuki, K. Nishita, and T. Ojima, Comparative studies on the functional roles of N- and C-terminal regions of molluskan and vertebrate troponin-I, *FEBS J.* **17**, 4475–4486 (2005).
32. S. Morimoto, F. Yanaga, R. Minakami, and I. Ohtsuki, Ca^{2+}-sensitizing effects of the mutations at Ile-79 and Arg-92 of troponin T in hypertrophic cardiomyopathy, *Am. J. Physiol.* 275, C200–C207 (1998).
33. F. Takahashi-Yanaga, S. Morimoto, K. Harada, R. Minakami, F. Shiraishi, M. Ohta, Q.-W. Lu, T. Sasaguri, and I. Ohtsuki, Functional consequences of the mutations in human cardiac troponin I gene found in familial hypertrophic cardiomyopathy, *J. Mol. Cell. Cardiol.* **3**, 2095–2107 (2001).
34. I. Ohtsuki, Molecular basis of calcium regulation of striated muscle contraction, *Adv. Exp. Med. Biol.* **565**, 223–231 (2005).
35. H. Nakaura, F. Yanaga, I, Ohtsuki, and S. Morimoto, Effects of missense mutations Phe110Ile and Glu-244Asp in human cardiac troponin T on force generation in skinned cardiac muscle fibers. *J. Biochem.* **126**, 457–460 (1999).
36. A. V. Gomes, and J. D. Potter, Molecular and cellular aspects of troponin cardiomyopathies, *Ann. N. Y. Acad. Sci.* **1015**, 214–224 (2004).
37. B. Hoffmann, H. Schmidt-Traub, A. Perrot, K. J. Osterziel, and R. Gessner, First mutation in cardiac troponin C, L29Q, in a patient with hypertrophic cardiomyopathy. *Hum. Mutat.* **17**, 524 (2001).
38. S. Morimoto, Q.-W. Lu, K. Harada, F. Takahashi-Yanaga, R. Minakami, M. Ohta, T. Sasaguri, and I. Ohtsuki, Ca^{2+}-desensitizing effect of a deletion mutation ΔK210 in cardiac troponin T that causes familial dilated cardiomyopathy, *Proc. Natl. Acad. Sci. USA* **99**, 913–918 (2002).
39. J. Mogensen, T. Kubo, M. Duque, W. Uribe, A. Shaw, R. Murphy, J. R. Gimeno, P. Elliott, and W. J. McKenna, Idiopathic restrictive cardiomyopathy is part of the clinical expression of cardiac troponin I mutations, *J. Clin. Invest.* **111**, 209–216 (2003).

40. S. S. Kushwaha, J. T. Fallon, and V. Fuster, Restrictive cardiomyopathy, *N. Engl. J. Med.* **336**, 267–276 (1997).
41. W. J. Vallins, N. J. Brand, N. Dabhade, G. Butler-Brown, M. H. Yacoub, and P. J. Barton, Molecular cloning of human cardiac troponin I using polymerase chain reaction, *FEBS Lett.* **270**, 57–61 (1990).
42. S. Ausoni, M. Campione, A. Picard, P. Moretti, M. Vitadello, C. De Nardi, and S. Schiaffino, Structure and regulation of the mouse cardiac troponin I gene, *J. Biol. Chem.* **269**, 339–346 (1994).
43. AJ842179 NCBI, *Bos taurus* tnni3 gene for cardiac troponin I, exons 1–8.
44. J. M. Wilkinson, and R. J. Grand, The amino acid sequence of troponin I from rabbit skeletal muscle, *Biochem. J.* **149**, 493–496 (1975).
45. R. B. Quaggio, J. A. Ferro, P. B. Monteiro, and F. C. Reinach, Cloning and expression of chicken skeletal muscle troponin I in *Escherichia coli*: the role of rare codons on the expression level, *Protein Sci.* **2**, 1053–1056 (1993).
46. H. Syska, J. M. Wilkinson, R. J. Grand, and S. V. Perry, The relationship between biological activity and primary structure of troponin I from white skeletal muscle of the rabbit, *Biochem. J.* **153**, 375–387 (1976).
47. C. Seidman et al., CardioGenomics, Mutation Database, Cardiac troponin I URL: http://genetics.med.harvard.edu/~seidman/cg3/muts/TNNI3_mutations_TOC.html.
48. H. M. Rarick, X.-H. Tu, R. J. Solaro, and A. F. Martin, The C terminus of cardiac troponin I is essential for full inhibitory activity and Ca^{2+} sensitivity of rat myofibrils, *J. Biol. Chem.* **272**, 26887–26892 (1997).
49. D. B. Foster, T. Noguchi, P. VanBuren, A. M. Murphy, and J. E. Van Eyk, C-terminal truncation of cardiac troponin I causes divergent effects on ATPase and force: implications for the pathophysiology of myocardial stunning, *Circ. Res.* **93**, 917–924 (2003).
50. F. Yumoto, Q. W. Lu, S. Morimoto, H. Tanaka, N. Kono, K. Nagata, T. Ojima, F. Takahashi-Yanaga, Y. Miwa, T. Sasaguri, K. Nishita, M. Tanokura, I. Ohtsuki. Drastic Ca^{2+} sensitization of myofilament associated with a small structural change in troponin I in inherited restrictive cardiomyopathy, *Biochem. Biophys. Res. Commun.* **338**, 1519–1526 (2005).
51. S. Morimoto, and I. Ohtsuki, Ca^{2+}- and Sr^{2+}-sensitivity of the ATPase activity of rabbit skeletal muscle myofibrils: effect of the complete substitution of troponin C with cardiac troponin C, calmodulin, and parvalbumins, *J. Biochem.* **101**, 230–291 (1987).
52. M. Hatakenaka, and I. Ohtsuki, Replacement of three troponin components with cardiac troponin components within single glycerinated skeletal muscle fibers, *Biochem. Biophys. Res. Commun.* **181**, 1022–1027 (1991).
53. M. Hatakenaka and I. Ohtsuki, Effect of removal and reconstitution of troponins C and I on the Ca^{2+}-activated tension development of single glycerinated rabbit skeletal muscle fibers, *Eur. J. Biochem.* **205**, 985–993 (1992).
54. A. V. Gomes, J. Liang, and J. D. Potter, Mutations in human cardiac troponin I that are associated with restrictive cardiomyopathy affect basal ATPase activity and the calcium sensitivity of force development, *J. Biol. Chem.* **280**, 30909–30915 (2005).
55. K. Murakami, F. Yumoto, S. Ohki, T. Yasunaga, M. Tanokura, and T. Wakabayashi, Structural basis for Ca^{2+}-regulated muscle relaxation at interaction sites of troponin with actin and tropomyosin, *J. Mol. Biol.* **352**, 178–201 (2005).
56. R. Koradi, M. Billeter, and K. Wüthrich, MOLMOL: a program for display and analysis of macromolecular structures, *J. Mol. Graph.* **14**, 51–55 (1996).

III

REGULATION IN CARDIAC MUSCLE AND DISORDERS

16

COOPERATIVITY IN THE REGULATION OF FORCE AND THE KINETICS OF FORCE DEVELOPMENT IN HEART AND SKELETAL MUSCLES

Cross-bridge activation of force

Daniel P. Fitzsimons and Richard L. Moss

16.1. INTRODUCTION

Twitches are the unitary contractile events in both heart and skeletal muscles, but twitch plasticity in terms of force and the kinetics of force development differs considerably in the two muscle types. In skeletal muscle, twitch contractions are relatively invariant as long as temperature is constant and the muscle is well rested. In contrast, twitches in heart muscle exhibit much greater dynamic range, such that both force and the kinetics of force development can vary tremendously on a beat-to-beat basis. These differences are in part due to muscle-specific differences in the delivery of Ca^{2+} to the myoplasm during excitation-contraction coupling. In skeletal muscle, a single action potential elicits a transient increase in intracellular Ca^{2+} sufficient to saturate thin filament regulatory sites on troponin-C. Because of this, force development and the ability to do work depend upon the duration of the Ca^{2+} transient and therefore the time available for cross-bridge binding to actin, which in skeletal muscles can be prolonged by tetanic stimulation. In heart muscle, the increase in intracellular Ca^{2+} during a twitch is typically insufficient to saturate thin filament sites, so that twitch force and work production are sub-maximal. In contrast to skeletal muscle, cardiac muscle cannot be tetanized under physiological conditions, but twitch force and power can be varied by regulating the delivery of Ca^{2+} to the myoplasm and also by agonist-induced regulation of cross-bridge cycling kinetics.

Twitch kinetics in heart and skeletal muscles are also determined by the turnover kinetics of the contractile protein myosin[1] and by the responsiveness of the thin filaments to the activating effects of Ca^{2+} and cross-bridge binding.[2] While thin filaments are activated by either Ca^{2+} or cross-bridge binding,[2–5] the relative contributions of these binding events differ in cardiac and skeletal muscles. In all vertebrate striated muscles, Ca^{2+} binding to TnC initiates cross-bridge binding, which cooperatively induces additional cross-bridge binding. In fast-twitch skeletal muscle, the near saturation of thin filaments

Department of Physiology and the Cardiovascular Research Center, University of Wisconsin School of Medicine and Public Health, Madison, WI, USA

Regulatory Mechanisms of Striated Muscle Contraction
Edited by Ebashi and Ohtsuki, Springer, 2007

with Ca^{2+} during a twitch results in near maximal activation, and consequently the kinetics of force development are fast. In cardiac muscle, the thin filaments are rarely saturated with Ca^{2+} during a twitch, so that neither Ca^{2+} nor cross-bridge binding is saturated and the kinetics of force development are relatively slow. However, interventions such as β-adrenergic stimulation increase the amount of Ca^{2+} released to the myoplasm and also accelerate cross-bridge cycling kinetics,[4] thereby accelerating myocardial twitch kinetics. In this way, it is possible to grade the myocardial twitch on a beat-to-beat basis and thereby scale force and power output to the load on the heart when venous return changes.

The present work investigated the mechanisms of cross-bridge regulation of force in both heart and skeletal muscles in an attempt to account for differences in the kinetics of force development in the two muscles and the much greater plasticity that is evident in the regulation of the kinetics of force development in heart muscle.

16.2. Ca^{2+} REGULATION OF FORCE IN HEART AND SKELETAL MUSCLES

Activation of muscle contraction requires Ca^{2+} binding to the TnC subunit of the thin filament regulatory protein troponin.[2,6,7] In skinned muscles, isometric force increases as the concentration of Ca^{2+} in the bathing solution is increased, i.e., the relationship between force and pCa (i.e., $-\log[Ca^{2+}]$) is sigmoidal (Figure 16.1) and is well fit with the Hill equation:[8]

$$P/P_o = [Ca^{2+}]^n / (k^n + [Ca^{2+}]^n) \quad (1)$$

where P is force, P_o is maximum force, n is the Hill coefficient or slope of the relationship, and k is the pCa required for half-maximal activation (i.e., pCa_{50}). The Hill coefficient is typically greater in fast skeletal muscle than in cardiac muscle, which is evident from the data in Figure 16.1, which is consistent with the observation that skeletal TnC has two

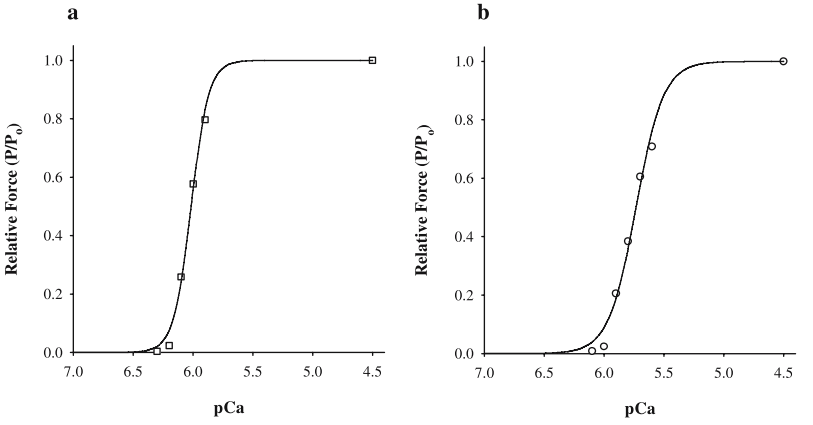

Figure 16.1. Tension-pCa relationships from a rat skinned skeletal muscle fiber (a) and from rat skinned myocardium (b) activated at 15°C. Hill coefficients and pCa_{50}'s were 5.94 and 6.02 for the skeletal muscle fiber and 3.79 and 5.73 for the myocardial preparation. Forces at submaximal pCa were scaled to maximum force at pCa 4.5 in the same preparation.

Ca^{2+}-specific binding sites and cardiac TnC has just one.[7] However, the Hill coefficient is greater than 3 in both muscles, which has been taken to mean that there is significant cooperativity in the regulation of force.[2,5,7] The larger Hill coefficient in skeletal muscle implies that the cooperativity of thin filament activation is greater than in cardiac muscle. Possible mechanisms include positive cooperativity in Ca^{2+} binding to TnC[9,10] and/or cross-bridge binding to the thin filament. The latter mechanism is the primary focus of the present work.

16.3. COOPERATIVITY IN CROSS-BRIDGE BINDING TO ACTIN

Cooperativity in cross-bridge binding was first shown in experiments in which myosin binding to regulated actin was facilitated by the presence of rigor complexes.[11] The importance of this process in force development in striated muscles is evident from experiments in which variations in MgADP or inorganic phosphate concentrations were used to manipulate the number of strongly bound cross-bridges and thereby change the Ca^{2+}-sensitivity of force. For example, increased [MgADP] increases the Ca^{2+} sensitivity of force,[12–14] presumably by increasing the number of strongly-bound cross-bridges at each [Ca^{2+}] and thereby cooperatively recruiting additional cross-bridges to force generating states.[15] Conversely, increased [P_i] reduces the Ca^{2+}-sensitivity of force by reversing the power-stroke and thereby decreasing the number of strongly-bound cross-bridges.[16,17]

While interventions such as altered [MgADP] or [P_i] have yielded important insights into the activating effects of strongly-bound cross-bridges on force, they do not provide quantitative information because these interventions also have direct effects on force. One experimental tool that has overcome this complication is N-ethylmaleimide-modified myosin subfragment-1, NEM-S1, which can be applied to skinned fibers[18] where it binds strongly to the thin filament but does not develop force. In biochemical experiments, NEM-S1 facilitates cross-bridge binding to regulated thin filaments[19] and potentiates ATPase activity in the presence of Ca^{2+},[20] consistent with the idea that cross-bridge binding cooperatively activates the thin filament. Studies with NEM-S1 provide convincing evidence in support of cross-bridge-induced cross-bridge binding to actin, but also show that there are pronounced differences between heart and skeletal muscles in the responsiveness of their thin filaments to the activating effects of strong cross-bridge binding.

16.3.1. Skeletal Muscle

In skeletal muscle, NEM-S1 increases isometric force at sub-maximal [Ca^{2+}] but has no effect on maximum force,[18,21] i.e., cross-bridges increase the Ca^{2+}-sensitivity of force (Figure 16.2). Since Fuchs and colleagues[22–24] have shown that there is no change in the Ca^{2+}-binding affinity of troponin-C in skeletal muscle thin filaments as force increases, the increase in Ca^{2+}-sensitivity of force is presumably a manifestation of positive cooperativity in cross-bridge binding, i.e., as predicted in the models proposed by Geeves[25] and Campbell.[26]

The mechanism of this cooperation is not known in detail but the results of various studies[2,7] have suggested that cross-bridge binding has allosteric effects on the regulatory

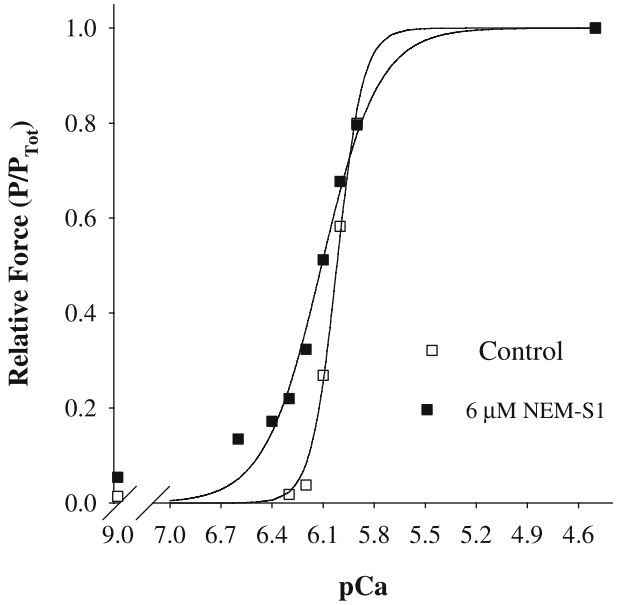

Figure 16.2. Effects of 6μM NEM-S1 on force and the Ca^{2+} sensitivity of force in a rat skinned skeletal muscle fiber. NEM-S1 increased the Ca^{2+} sensitivity of force (seen as an increased pCa_{50}) and increased the Ca^{2+}-independent force at pCa 9.0. Maximum force at pCa 4.5 was unaffected by NEM-S1. Forces at sub-maximal pCa were expressed as a fraction of maximum force developed under the same conditions at pCa 4.5.

strand, i.e., tropomyosin plus troponin, such that there is a spread of activation within and between functional groups, i.e., 7 actins plus the associated tropomyosin and troponin molecules.[27,28] Importantly, NEM-S1 has virtually no effect on the maximum force developed in the presence of saturating [Ca^{2+}], which implies that the combined activating effects of Ca^{2+} and strong-binding cross-bridges are maximal under these conditions.

NEM-S1 also activates force at Ca^{2+} concentrations where virtually no Ca^{2+} is bound to the regulatory sites of TnC, which is evident as active tension at pCa 9.0 (Figure 16.2). If activation of contraction is indeed a synergistic process involving both Ca^{2+} and cross-bridge binding,[3] this result indicates that it is possible to activate the thin filament in the absence of Ca^{2+} if the number of strong-binding cross-bridges is sufficiently high. Such a phenomenon is non-physiological since the number of strongly bound cross-bridges is never this high *in vivo*. However, the fact that contraction can be activated by strong-binding cross-bridges in the absence of Ca^{2+} implies that the skeletal muscle thin filament is not completely switched off in the absence of Ca^{2+}. In the activation model proposed by Geeves and colleagues,[25] the thin filament without Ca^{2+} bound is in a "blocked" state in which it cannot bind cross-bridges, but Ca^{2+} binding converts the filament to a "closed" state in which it can bind cross-bridges. In the context of this model, the present results suggest that the skeletal muscle thin filament is not fully blocked in the absence of Ca^{2+}.

16.3.2. Cardiac Muscle

In skinned cardiac muscle, NEM-S1 increases force at each sub-maximal [Ca^{2+}] (Figure 16.3) and thereby the Ca^{2+}-sensitivity of force.[29] While this effect is qualitatively similar to the response in skeletal muscle, the increase in Ca^{2+} sensitivity due to a given amount of NEM-S1 is much greater in cardiac muscle. While both muscles exhibit positive cooperativity in cross-bridge binding, skeletal muscle is more cooperative since a greater number of strongly-bound cross-bridges is required to achieve similar potentiation of force. Viewed another way, cardiac thin filaments are much more responsive to the activating effects of even a small number of cross-bridges, which presumably contributes to fine gradations in twitch force observed on a beat-to-beat basis in living myocardium. Just as in skeletal muscle, there is no effect of NEM-S1 on maximum force at pCa 4.5, implying that activation of force is saturated by cross-bridge and Ca^{2+} binding under these conditions.

NEM-S1 also increases force in the absence of Ca^{2+} in skinned myocardium (Figure 16.3), but the effects are much greater than in skeletal muscle. For example, at 6 μM NEM-S1 the force developed in skinned myocardium was ~20% of the maximum active force at pCa 4.5, while in skeletal muscle under the same conditions force was ~5% of maximum. This difference in cross-bridge activation of force is consistent with the greater responsiveness of myocardium to strong-binding cross-bridges observed at sub-maximal Ca^{2+} concentrations and also leads to the conclusion that the cardiac thin filament is not completely switched off, or blocked, in the absence of Ca^{2+}.

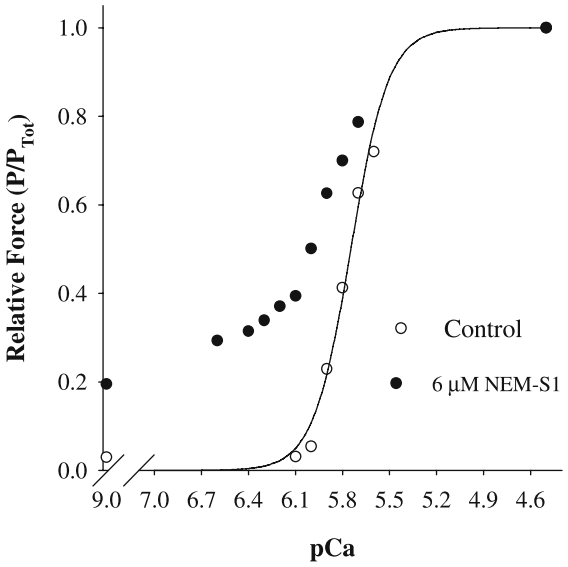

Figure 16.3. Effects of 6 μM NEM-S1 on force and the Ca^{2+} sensitivity of force in a rat skinned heart muscle preparation. NEM-S1 increased the Ca^{2+} sensitivity of force (i.e., increased pCa_{50}) and increased the Ca^{2+}-independent force at pCa 9.0. Maximum force at pCa 4.5 was unaffected by NEM-S1. Forces at sub-maximal pCa were expressed as a fraction of maximum force developed under the same conditions at pCa 4.5.

16.4. REGULATION OF THE KINETICS OF FORCE DEVELOPMENT

16.4.1. Activation-Dependence of the Kinetics of Force Development

The rate of force development in skinned cardiac and skeletal muscles varies with Ca^{2+} activation.[2] The rate constant of tension redevelopment (k_{tr}), measured in active muscle following a release/re-stretch maneuver to reduce force near to zero,[30] increases approximately 10-fold when $[Ca^{2+}]$ is increased from threshold for force development to maximal. While the maximum k_{tr} is greater in rat skinned skeletal muscle (~15 s^{-1}) than in rat skinned myocardium (~10 s^{-1}), the rate of cross-bridge cycling increases by an order of magnitude in both muscles when activation is increased from threshold to maximal levels (Figure 16.4).

The activation dependence of k_{tr} is potentially important in determining the rate of rise of force in living muscles, but the underlying mechanism is not know for certain. One possibility is that $[Ca^{2+}]$ *per se* mediates the activation dependence of k_{tr}, as suggested by Brenner[31] and modeled by Landesberg and Sideman.[32] Another possibility is that cycling kinetics are regulated by strong binding of cross-bridges to the thin filament, such that cycling is cooperatively accelerated by cross-bridge binding. In the latter case, the activation dependence of k_{tr} would be an indirect consequence of alterations in the amount of activator Ca^{2+} delivered to the myoplasm. We have done experiments to explore this possibility.

16.4.2. Cross-Bridge Regulation of Cycling Kinetics

Increasing evidence suggests that strong-binding of myosin cross-bridges to the thin filament accelerates the rate of force development in both skeletal and cardiac muscles,

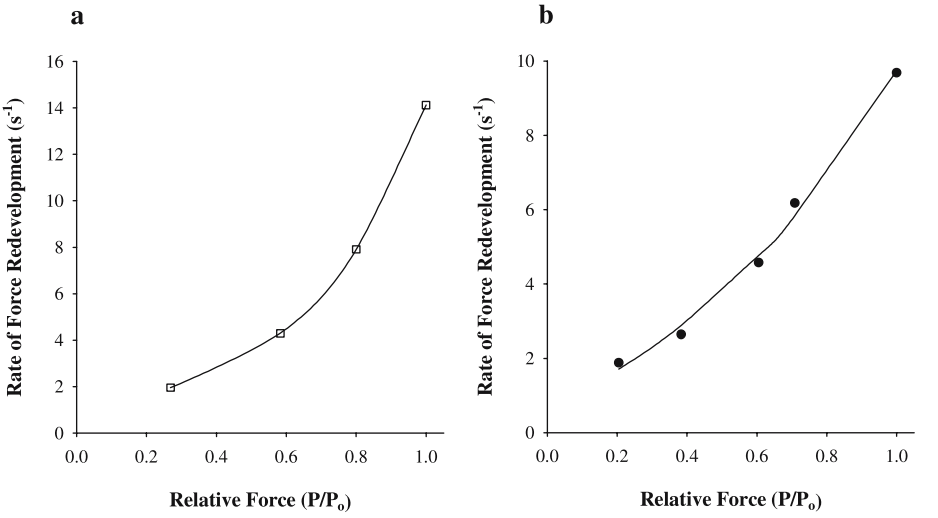

Figure 16.4. Activation-dependence of k_{tr} at 15°C in (a) a rat skinned skeletal muscle fiber and in (b) rat skinned myocardium. k_{tr} was estimated by fitting a single exponential equation to the time course of force recovery following release and re-stretch of the activated muscle, as described previously by Brenner and Eisenberg.[30]

even when the changes in force due to increased cross-bridge binding are taken into account. For example, increased [MgADP] in skinned skeletal muscle increases k_{tr} during submaximal Ca^{2+}-activations,[12,13] presumably by increasing the number of strongly-bound cross-bridges. Furthermore, reducing the number of strongly bound cross-bridges with vanadate[33] slows k_{tr} at submaximal Ca^{2+} concentrations (Lu, Moss and Walker, unpublished). As might be expected from results such as these, cross-bridge effects on the rate of force development comprise a key element of current models of muscle contraction.[25,26,34,35]

We have used NEM-S1, a strong binding derivative of myosin sub-fragment-1, to assess possible cooperative activating effects of strong-binding cross-bridges on the rate constant of force development, k_{tr}, in both heart and skeletal muscles. These results are presented in the following sections.

16.4.2.1. Skeletal Muscle

In skinned skeletal muscle (Figure 16.5), NEM-S1 increased k_{tr} at all submaximal Ca^{2+} concentrations.[18,21] At very low concentrations of Ca^{2+}, NEM-S1 increased k_{tr} to values equal to those measured at maximal [Ca^{2+}] in the absence of NEM-S1, while at intermediate [Ca^{2+}] k_{tr} was less than maximal but greater than the value measured at the same Ca^{2+} concentrations before adding NEM-S1.

We have also done experiments to see whether k_{tr} can be increased to values greater than the value measured at saturating concentrations of Ca^{2+}. Previous experiments by Regnier and colleagues[36] showed that it is possible to increase k_{tr} at all levels of activation using an ATP derivative, de-oxy ATP, which accelerates the maximum rate of cross-

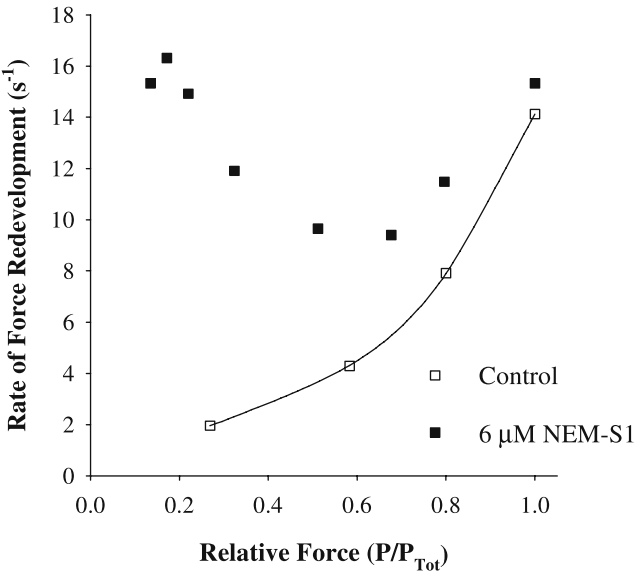

Figure 16.5. Effects of 6 μM NEM-S1 on the rate constant of force redevelopment (k_{tr}) in rat skinned skeletal muscle fibers at 15°C.

bridge cycling. k_{tr} can also be increased, at least at low [Ca^{2+}], by adding NEM-S1 to the bathing solution.[18,21] At the very lowest levels of activation, NEM-S1 increased k_{tr} to values greater than the maximum at saturating [Ca^{2+}] (Figure 16.5). This ability to increase k_{tr} to supramaximal values leads to the conclusion that in terms of the kinetics of force development the thin filaments of skeletal muscles are not completely activated during a twitch, or even in a tetanus in which the intracellular [Ca^{2+}] is at saturating levels.

Several models might account for the activation dependence of k_{tr} and the changes in this relationship caused by adding NEM-S1. Brenner[31] explained the activation dependence of k_{tr} with a model in which increases in Ca^{2+} increase the rate constant of cross-bridge attachment to actin, f_{app}. Such a mechanism could certainly be operative in skeletal muscle but does not account for the effect of strong-binding cross-bridges (NEM-S1) to accelerate k_{tr}. Because of this we favor a model developed by Campbell,[26,35] which is a variation on the model developed earlier by McKillop and Geeves.[25] According to Campbell, the Ca^{2+}-dependence of k_{tr} is due to cooperativity-induced slowing of force development during submaximal activation.[26] In active muscle, cross-bridges are either in cycling or non-cycling pools: cycling cross-bridges undergo transitions between non-force-bearing and force-bearing states, under the influence of the rate constants f_{app} and g_{app}, while non-cycling cross-bridges are recruited to the cycling pool as a result of Ca^{2+} binding to troponin or thin filament activating effects due to strong binding of cross-bridges. At low [Ca^{2+}], a small fraction of cross-bridges is initially recruited into the cycling pool as a direct result of Ca^{2+} binding to the thin filament, so that most cross-bridges are in the non-cycling pool and are thus available for recruitment to the cycling pool. Progressive recruitment of cross-bridges from the non-cycling pool would then slow the rate of force development. In contrast, at high [Ca^{2+}], the rate of force development is much greater because most cross-bridges are recruited to the cycling pool when Ca^{2+} first binds to troponin, which leaves few non-cycling cross-bridges available for cooperative recruitment. At saturating [Ca^{2+}], k_{tr} would thus approach the sum of the forward and reverse rate constants for the force-generating transition, i.e., $f_{app} + g_{app}$.

Using this model, the effects of NEM-S1 to accelerate k_{tr} can be explained as a cooperative activation of the thin filament by an increased number of strong-binding cross-bridges. The finding that k_{tr} in the absence of NEM-S1 is near maximal at the very lowest levels of activation implies that there is little cooperativity in cross-bridge binding in this activation range, perhaps due to reduced interactions between neighboring functional groups.[34] The decrease in k_{tr} as [Ca^{2+}] is increased would then be explained on the basis of an increase in cooperativity in cross-bridge binding, and the increase in k_{tr} at the highest Ca^{2+} concentrations would be due to reduced cooperativity due to saturation of Ca^{2+} and cross-bridge binding to the thin filaments.

While NEM-S1 dramatically accelerates k_{tr}, strong-binding cross-bridges do not entirely account for the activation of cross-bridge kinetics, since NEM-S1 alone was insufficient at intermediate levels of activation to increase k_{tr} to maximal or to completely eliminate the activation dependence of k_{tr}. Instead, elimination of activation dependence required *both* NEM-S1 and partial extraction of TnC from the thin filament.[21] Since partial extraction of TnC disrupts near-neighbor communication between functional groups in the thin filament,[37,38] the activation dependence of k_{tr} involves effects of strongly-bound cross-bridges to cooperatively recruit additional cross-bridges within the same and neighboring regions of the thin filament. A modification of Campbell's[26] model to include

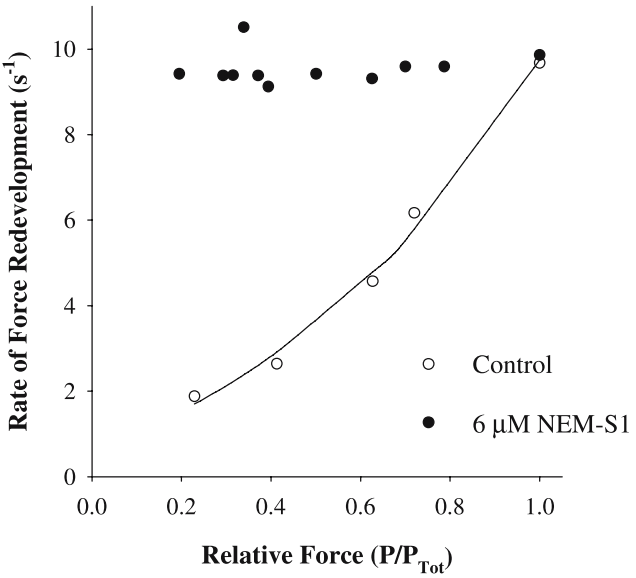

Figure 16.6. Effects of 6μM NEM-S1 on the rate constant of force redevelopment (k_{tr}) in rat skinned myocardium at 15°C.

near-neighbor interactions that cooperatively recruit cross-bridges to strongly-bound states predicts these results.[34] By extracting TnC, these interactions were presumably disrupted and cooperative recruitment of cross-bridges from neighboring functional groups was reduced or eliminated, thereby speeding k_{tr}.

16.4.2.2. Heart Muscle

k_{tr} is also Ca^{2+}-dependent in heart muscle,[29,39–41] increasing ~10-fold as Ca^{2+} is increased from threshold to saturating concentrations (Figure 16.4b). Similar to skeletal muscle, NEM-S1 accelerated k_{tr} at submaximal Ca^{2+} concentrations but had no effect on maximal k_{tr} (Figure 16.6). Unlike skeletal muscles, partial extraction of TnC did not further increase maximal k_{tr}, implying that in cardiac muscle the kinetics of force development are fully activated at saturating [Ca^{2+}]. From these observations, we conclude that cardiac muscle is less cooperative than skeletal muscle in the sense that fewer cross-bridges are required to cooperatively activate the cardiac thin filament.

16.5. IMPLICATIONS OF COOPERATIVITY FOR MUSCLE FUNCTION

The results presented here indicate that the regulation of contraction in heart and skeletal muscles is a highly cooperative process involving the activating effects of Ca^{2+} binding to TnC and cross-bridge binding to the thin filament. However, the two muscles differ in their sensitivity to the activating effects of strong binding cross-bridges. The activation state of cardiac thin filaments is exquisitely sensitive to strong binding cross-bridges in that a given number of such cross-bridges will yield greater increases in the

Ca^{2+} sensitivities of force and the kinetics of force development. In contrast, skeletal muscle thin filaments require a greater number of strongly bound cross-bridges to achieve maximal activation, making it the more cooperative of the two muscles. Consistent with these conclusions, both force and the kinetics of force development are maximal in cardiac muscle at saturating Ca^{2+}, but this is not the case in skeletal muscle.

16.6. COOPERATIVITY IN THE ACTIVATION OF FORCE DEVELOPMENT

While NEM-S1 has significant effects on force development in heart and skeletal muscles, the muscles differ dramatically in their responsiveness to the activating effects of strong-binding cross-bridges. In cardiac muscle, NEM-S1 increases the rate constant of force development (k_{tr}) to its maximum but no greater, implying that cross-bridge activation of the thin filament becomes saturated over the physiological range of Ca^{2+} concentrations. In skeletal muscle, application of NEM-S1 in sufficient amounts actually increases k_{tr} at low [Ca^{2+}] to values greater than the maximum at saturating Ca^{2+}. Thus, cross-bridges accelerate the kinetics of force development in skeletal muscle, but the effect is not saturated under physiological conditions. Still, strong-binding cross-bridges contribute to the activation of k_{tr} in fast-twitch skeletal muscle since reducing the number of strong binding cross-bridges with vanadate significantly reduces k_{tr} throughout the entire range of Ca^{2+} activation (Lu, Moss and Walker, unpublished).

These differences in the responsiveness of skeletal and cardiac muscles to the activating effects of strong-binding cross-bridges contribute to the *in vivo* function of these muscles. In the skeletal muscle twitch, the increase in myoplasmic Ca^{2+} saturates the thin filament, or nearly so, resulting in a rate of rise of force that is near maximal and a twitch force that is relatively invariant as long as the muscle is well rested. Increases in twitch force are observed following periods of activity as exemplified in post-tetanic potentiation.[42] Otherwise, increases in the force developed by single muscle fibers are achieved by increasing the frequency of action potentials along the motor nerve in order to prolong the Ca^{2+} transient and thereby increase the time available for cross-bridge attachment.

In cardiac muscle, the increase in myoplasmic Ca^{2+} during the twitch does not saturate the thin filament, so that cross-bridge activation of the thin filament is sub-maximal and the rate of force development is submaximal. Variations in the amount of Ca^{2+} released from the sarcoplasmic reticulum would be expected to either speed (increased Ca^{2+}) or slow the rate of rise of force (decreased Ca^{2+}). This variability in the rate of rise of force makes it possible to scale twitch kinetics and twitch force on a beat-to-beat basis and thereby scale work production to the load on the heart. Phosphorylation of thin filament[4] and other myofibrillar proteins[43] would presumably provide further modulation of twitch force through changes in Ca^{2+} sensitivity of force and in cross-bridge cycling kinetics.

16.7. EFFECTS OF COOPERATIVITY ON MUSCLE RELAXATION

The activating effects of cross-bridges on thin filaments in both skeletal and cardiac muscles could play important roles in controlling the rate of relaxation in both muscle types. To test this idea, we have done experiments (Patel, Fitzsimons and Moss, unpub-

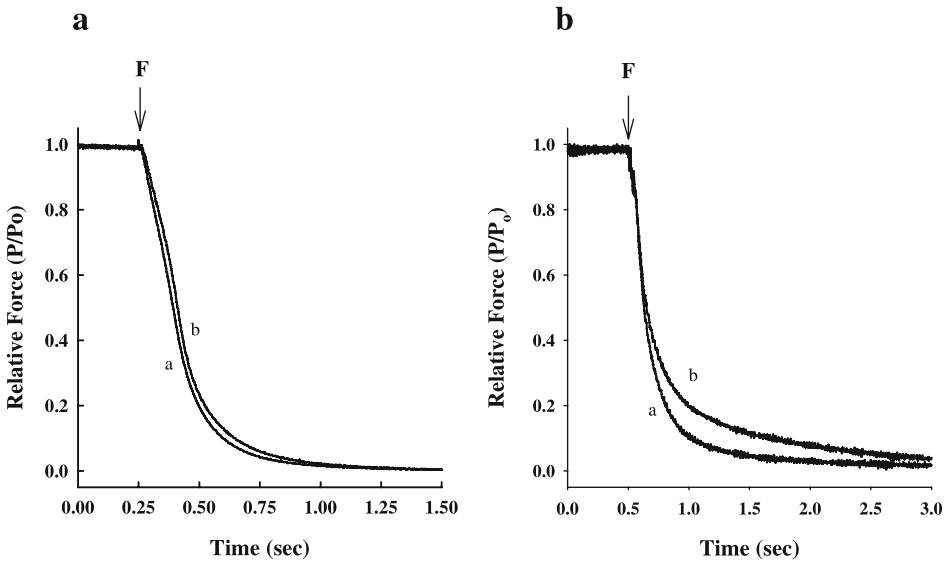

Figure 16.7. Rate of force relaxation following flash photolysis of diazo-2 from a rat skinned skeletal muscle fiber (a) and from rat skinned myocardium (b) activated at 15°C in the absence (trace a) and presence (trace b) of NEM-S1. The rat skinned skeletal muscle fiber was incubated with 6 μM NEM-S1, while the rat skinned myocardium was incubated with 0.25 μM NEM-S1. Each preparation generated ~0.70P_o in the loading solution prior to photolysis of diazo-2.

lished) in which we assessed the effects of NEM-S1 on relaxation of skinned muscle preparations elicited by photorelease of the caged Ca^{2+} chelator, diazo-2. Even at NEM-S1 concentrations of 6.0 μM, neither the rate nor extent of relaxation was affected in skeletal muscle (Figure 16.7a). One interpretation of this result is that both Ca^{2+} and strong binding cross-bridges are needed to maintain activation of thin filaments in skeletal muscle, and once Ca^{2+} is removed, cross-bridges alone are insufficient to sustain activation. Consistent with this idea, a similar concentration of NEM-S1 increased Ca^{2+}-independent force by approximately 5% (Figure 16.2).

In contrast, NEM-S1 has dramatic effects on relaxation in skinned myocardium: NEM-S1 greatly slowed the extent and rate of force relaxation following photolysis of diazo-2. In the absence of NEM-S1, steady-state force declined to near-zero active force with an apparent rate constant (k_{rel}) of 6.9 s^{-1}, whereas force decreased by ~20% with a k_{rel} of 0.9 s^{-1} in the presence of NEM-S1.[29] Even at an NEM-S1 concentration of 0.25 μM, the rate of relaxation was slowed by more than 20% (Figure 16.7b). These results support that idea that cross-bridges strongly activate cardiac thin filaments even in the absence of Ca^{2+}, which was also evident in the development of active force at pCa 9.0 when NEM-S1 was added to the solution bathing skinned myocardium (Figure 16.3).

These activating effects of strong binding cross-bridges could modulate the rate of relaxation in healthy myocardium but might also have important implications for the contractile dysfunction that is observed in some diseases of the myocardium. For example, human heart failure is often associated with a slowing of relaxation during the initial stages of diastole, which leads to impairment of filling and thereby depresses systolic ejection.[44]

This slowing of relaxation in failing myocardium might be a consequence of sustained cooperative activation of the thin filament even after myoplasmic Ca^{2+} concentration is reduced to diastolic levels. The observation[44] that there is increased expression of slower isoforms of myosin in human heart failure would provide a basis for such an effect.

16.8. REFERENCES

1. S. Schiaffino, and C. Reggiani, Molecular diversity of myofibrillar proteins: gene regulation and functional significance, *Physiol. Rev.* **76**(2), 371–423 (1996).
2. A. M. Gordon, E. Homsher, and M. Regnier, Regulation of contraction in striated muscle, *Physiol. Rev.* **80**(2), 853–924 (2000).
3. S. S. Lehrer, The regulatory switch of the muscle thin filament: Ca^{2+} or myosin heads, *J. Muscle Res. Cell Motil.* **15**(3), 232–236 (1994).
4. R. J. Solaro, and H. M. Rarick, Troponin and tropomyosin: proteins that switch on and tune in the activity of cardiac myofilaments, *Circ. Res.* **83**(5), 471–480 (1998).
5. R. L. Moss, M. Razumova, and D. P. Fitzsimons, Myosin cross-bridge activation of cardiac thin filaments: implications for myocardial function in health and disease, *Circ. Res.* **94**(10), 1290–1300 (2004).
6. S. Ebashi, and M. Endo, Calcium ion and muscle contraction, *Prog. Biophys. Mol. Biol.* **18**, 123–183 (1968).
7. L. S. Tobacman, Thin filament-mediated regulation of cardiac contraction, *Ann. Rev. Physiol.* **58**, 447–481 (1996).
8. J. S. Shiner, and R. J. Solaro, The Hill coefficient for the Ca^{2+}-activation of striated muscle contraction, *Biophys. J.* **46**(3), 541–543 (1984).
9. Z. Grabarek, J. Grabarek, P. C. Leavis, and J. Gergely, Cooperative binding to the Ca^{2+} specific sites of troponin C in regulated actin and actomyosin, *J. Biol. Chem.* **258**(23), 14098–14102 (1983).
10. K. Guth, and J. D. Potter, Effect of rigor and cycling cross-bridges on the structure of troponin C and on the Ca^{2+} affinity of the Ca^{2+} specific regulatory sites in skinned rabbit psoas fibers, *J. Biol. Chem.* **262**(28), 13627–13635 (1987).
11. R. D. Bremel, and A. Weber, Cooperation within actin filament in vertebrate skeletal muscle, *Nature* **238**(5359), 97–101 (1972).
12. Z. Lu, R. L. Moss, and J. W. Walker, Tension transients initiated by photogeneration of MgADP in skinned skeletal muscle fibers, *J. Gen. Physiol.* **101**(6), 867–888 (1993).
13. Z. Lu, D. R. Swartz, J. M. Metzger, R. L. Moss, and J. W. Walker, Regulation of force development studied by photolysis of caged ADP in rabbit skinned psoas fibers, *Biophys. J.* **81**(1), 334–344 (2001).
14. H. Thirlwell, J. E. T. Corrie, G. P. Reid, D. R. Trentham, and M. A. Ferenczi, Kinetics of relaxation from rigor of permeabilized fast-twitch skeletal fibers from rabbit using a novel caged ATP and apyrase, *Biophys. J.* **67**(6), 2346–2447 (1994).
15. J. A. Dantzig, M. G. Hibberd, D. R. Trentham, and Y. E. Goldman, Cross-bridge kinetics in the presence of MgADP investigated by photolysis of caged ATP in rabbit psoas muscle fibers, *J. Physiol.* **432**(1), 639–680 (1991).
16. J. A. Dantzig, Y. E. Goldman, N. C. Millar, J. Lacktis, and E. Homsher, Reversal of the cross-bridge force-generating transition by photogeneration of phosphate in rabbit psoas muscle fibres, *J. Physiol.* **451**(1), 247–278 (1992).
17. J. W. Walker, Z. Lu, and R. L. Moss. Effects of Ca^{2+} on the kinetics of phosphate release in skeletal muscle, *J. Biol. Chem.* **267**(4), 2459–2466 (1992).
18. D. R. Swartz, and R. L. Moss, Influence of a strong-binding myosin analogue on calcium-sensitive mechanical properties of skinned skeletal muscle fibers, *J. Biol. Chem.* **267**(28), 20497–20506 (1992).
19. H. Nagashima, and S. Asakura, Studies on cooperative properties of tropomyosin-actin and tropomyosin-troponin-actin comples by the use of N-ethylmaleimide-treated and untreated species of myosin subfragment 1, *J. Mol. Biol.* **155**(4), 409–428 (1982).
20. D. L. Williams, L. E. Greene, and E. Eisenberg, Cooperative turning on of myosin subfragment 1 adenosinetriphosphatase activity by the troponin-tropomyosin-actin complex, *Biochemistry* **27**(18), 6987–6993 (1988).

21. D. P. Fitzsimons, J. R. Patel, K. S. Campbell, and R. L. Moss, Cooperative mechanisms in the activation dependence of the rate of force development in rabbit skinned skeletal muscle fibers, *J. Gen. Physiol.* **117**(2), 133–148 (2001).
22. P. A. Hofmann, and F. Fuchs, Effect of length and cross-bridge attachment on Ca^{2+} binding to troponin C, *Am. J. Physiol.* **253**(1), C90–C96 (1987).
23. F. Fuchs, and Y.-P. Wang, Force, length, and Ca^{2+}-troponin C affinity in skeletal muscle, *Am. J. Physiol.* **261**(5), C787–C792 (1991).
24. F. Fuchs, Mechanical modulation of the Ca^{2+} regulatory protein complex in cardiac muscle, *NIPS* **10**, 6–12 (1995).
25. D. F. A. McKillop, and M. A. Geeves, Regulation of the interaction between actin and myosin subfragment 1: evidence for three states of the thin filament, *Biophys. J.* **65**(2), 693–701 (1993).
26. K. Campbell, Rate constant of muscle force redevelopment reflects cooperative activation as well as cross-bridge kinetics, *Biophys. J.* **72**(1), 254–262 (1997).
27. C. A. Butters, J. B. Tobacman, and L. S. Tobacman, Cooperative effect of calcium binding to adjacent troponin molecules on the thin filament-myosin subfragment 1 MgATPase rate, *J. Biol. Chem.* **272**(20), 13196–13202 (1997).
28. S. S. Lehrer, and M. A. Geeves, The muscle thin filament as a classical cooperative/allosteric regulatory System, *J. Mol. Biol.* **277**(5), 1081–1089 (1998).
29. D. P. Fitzsimons, J. R. Patel, and R. L. Moss, Cross-bridge interaction kinetics in rat myocardium are accelerated by strong binding of myosin to the thin filament, *J. Physiol.* **530**(2), 263–272 (2001).
30. B. Brenner, and E. Eisenberg, Rate of force generation in muscle: correlation with actomyosin ATPase activity in solution, *Proc. Natl. Acad. Sci. USA* **83**(10), 3542–3546 (1986).
31. B. Brenner, Effect of Ca^{2+} on cross-bridge turnover kinetics in skinned single rabbit psoas fibers: implications for regulation of muscle contraction, *Proc. Natl. Acad. Sci. USA* **85**(9), 3265–3269 (1988).
32. A. Landesberg, and S. Sideman, Coupling calcium binding to troponin C and cross-bridge cycling in skinned cardiac cells, *Am. J. Physiol.* **266**(3), H1260–H1271 (1994).
33. J. A. Dantzig, and Y. E. Goldman, Suppression of muscle contraction by vanadate, *J. Gen. Physiol.* **86**(3), 305–327 (1985).
34. M. V. Razumova, A. E. Bukatina, and K. B. Campbell, Different myofilament nearest-neighbor interactions have distinctive effects on contractile behavior, *Biophys. J.* **78**(6), 3120–3137 (2000).
35. K. Campbell, M. Chandra, R. D. Kirkpatrick, B. K. Slinker, and W. C. Hunter, Interpreting cardiac muscle force-length dynamics using a novel functional tool, *Am. J. Physiol.* **286**(4), H1535–H1545 (2004).
36. M. Regnier, D. A. Martyn, and P. B. Chase, Calcium regulation of tension redevelopment kinetics with 2-deoxy-ATP or low [ATP] in skinned rabbit psoas fibers, *Biophys. J.* **74**(4), 2005–2015 (1998).
37. P. W. Brandt, M. S. Diamond, and F. H. Schachat, The thin filament of vertebrate skeletal muscle co-operatively activates as a unit, *J. Mol. Biol.* **180**(2), 379–384 (1984).
38. R. L. Moss, G. G. Giulian, and M. L. Greaser, The effects of partial extraction of TnC upon the tension-pCa relationship in rabbit skinned skeletal muscle fibers, *J. Gen. Physiol.* **86**(4), 585–600 (1985).
39. M. R. Wolff, K. S. McDonald, and R. L. Moss, Rate of tension development in cardiac muscle varies with level of activator calcium, *Circ. Res.* **76**(1), 154–160 (1995).
40. S. Palmer, and J. C. Kentish, Roles of Ca^{2+} and crossbridge kinetics in determining the maximum rates of Ca^{2+} activation and relaxation in rat and guinea pig skinned trabeculae, *Circ. Res.* **83**(2), 179–186 (1998).
41. M. Regnier, H. Martin, R. J. Barsotti, A. J. Rivera, D. A. Martyn, and E. Clemmens, Cross-bridge versus thin filament contributions to the level and rate of force redevelopment in cardiac muscle, *Biophys. J.* **87**(2), 1815–1824 (2004).
42. D. R. Manning, and J. T. Stull, Myosin light chain phosphorylation-dephosphorylation in mammalian skeletal muscle, *Am. J. Physiol.* **242**(3), C234–C241 (1982).
43. W. G. Pyle, and R. J. Solaro, At the cross-roads of myocardial signaling: the role of Z-discs in intracellular signaling and cardiac function, *Circ. Res.* **94**(3), 296–305 (2004).
44. S. Miyata, W. Minobe, M. R. Bristow, and L. A. Leinwand, Myosin heavy chain isoform expression in the failing and nonfailing human heart, *Circ. Res.* **86**(4), 386–390 (2000).

17

HEART FAILURE, ISCHEMIA/REPERFUSION INJURY AND CARDIAC TROPONIN

R. John Solaro[1] and Grace M. Arteaga[1,2]

17.1. SUMMARY

Over the forty years since its discovery, there has been a profound transition in thinking with regard to the role of troponin in the control of cardiac function. This transition involved a change in perception of troponin as a passive molecular switch responding to membrane controlled fluctuations in cytoplasmic Ca^{2+} to a perception of troponin as a critical element in signaling cascades that actively engage in control of cardiac function. Evidence demonstrating functionally significant developmental and mutant isoform switches and post-translational modifications of cardiac troponin complex proteins, troponin I (cTnI) and troponin T (cTnT) provided convincing evidence for a more complicated role of troponin in control of cardiac function and dynamics. The physiological role of these modifications of troponin is reviewed in this monograph and has also been reviewed elsewhere (Solaro and Rarick, 1998; Gordon et al., 2000; Solaro et al., 2002a; Kobayashi and Solaro, 2005). Our focus here is on studies related to modifications in troponin that appear important in the processes leading from compensated hypertrophy to heart failure. These studies reveal the potentially significant role of post-translational modifications of troponin in these processes. Another focus is on troponin as a target for inotropic agents. Pharmacological manipulation of troponin by small molecules remains an important avenue of approach for the treatment of acute and chronic heart failure (Kass and Solaro, 2006).

17.2. INTRODUCTION: TROPONIN AND STRESS RESPONSES IN THE HEART

Figure 17.1 illustrates a minimal view of the cascade of reactions triggered by stresses on the myocardium that may lead to cardiac dysfunction and failure. Extrinsic stresses such as hypertension, myocardial infarction (MI), and ischemia as well as ischemia

[1] Department of Physiology and Biophysics (M/C 901), and [2]Department of Pediatrics University of Illinois at Chicago, College of Medicine, Chicago, IL 60612, USA

Regulatory Mechanisms of Striated Muscle Contraction
Edited by Ebashi and Ohtsuki, Springer, 2007

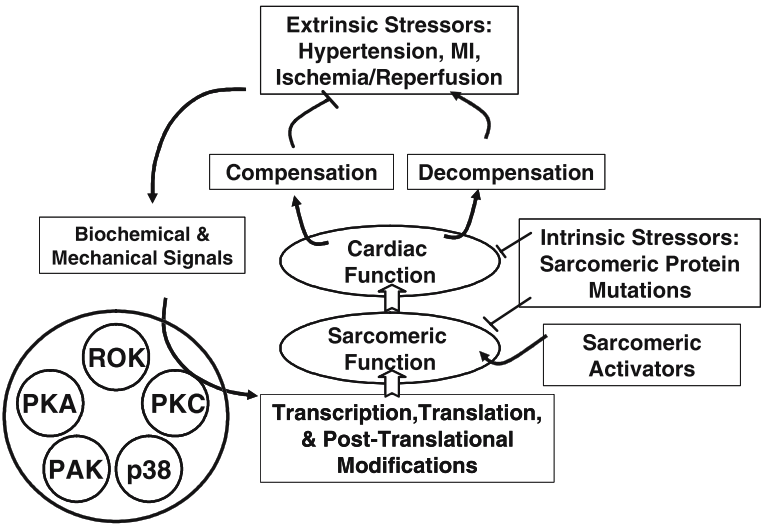

Figure 17.1. Scheme summarizing cardiac response to extrinsic and intrinsic stressors. See text for details.

followed by reperfusion induce biochemical and mechanical signals that activate kinases, phosphatases, and proteases. In turn these kinase/phosphatase cascades induce altered phosphorylation of transcriptional factors that move into the nucleus to increase protein synthesis (Frey and Olson, 2003; Dorn and Force, 2005). Effects on translation also occur (Crozier et al., 2005). The increase in protein synthesis enlarges cell and heart size and remodels the heart both in gross structure and in the relative proportions and isoform populations of cardiac proteins. The mechanical signaling is attributed largely to stretch of the myocardium that occurs with the elevated end diastolic volumes in response to the external stresses (Samarel, 2005). Stretch induces an elaboration of biochemical signals through an induction of the release of ligands such as angiotensin and endothelin. Thus, one response to stress is that the heart makes more sarcomeres, which, for a time, is a compensatory response. For example, in the case of hypertension an increased number of sarcomeres and cardiac remodeling would permit cardiac output to occur at a lower end-diastolic volume and normal stretch despite the increased afterload. This phase of compensation is indicated in Figure 17.1 as blunting the stressor. However, in time with continued stresses on the myocardium the adaptation fails and decompensation occurs. We discuss here the evidence that a critical factor in this decompensation is altered troponin function.

Our hypothesis is that together with the cascade of signaling through large and small G proteins, which increases sarcomere number and remodels the myocardium, there is also a modification of phosphorylation of cTnI and cTnT that alters sarcomeric function. We think this alteration in sarcomeric activity may lead to a malignant vicious cycle in which heart cells are stimulated to grow in the face of depressed function (Solaro et al., 2002a; de Tombe and Solaro, 2000). Linkage of mutations in genes controlling expression of sarcomeric proteins to hypertrophic and dilated cardiomyopathies support this idea (Mogensen et al., 2003; Gomes and Potter, 2004). This is depicted in Figure 17.1 as an "instrinsic stressor." In this case the hypertrophy, failure, and sudden death begin with a

primary defect in sarcomeric proteins, including all the proteins in the troponin heterotrimer. In most cases, the genetic defect involves a mis-sense mutation involving a charge modification. It is likely to be significant that charge modifications are also induced by protein phosphorylation. The charge modification induced by point mutations linked to familial hypertrophic cardiomyopathy (Gomes and Potter, 2004) and restrictive cardiomyopathy (Yumoto et al., 2005) is often associated with an enhanced myofilament response to Ca^{2+}. On the other hand there is emerging evidence that the sarcomeric mutations leading to a depressed myofilament response to Ca^{2+} are linked to dilated cardiomyopathies (Mirza et al., 2005). While these theories on the relation between sarcomeric function and cardiomyopathies remain speculative, there is evidence, which we summarize here, that a maladaptive altered phosphorylation of the myofilaments increases and decreases myofilament response to Ca^{2+} in a way similar to that occurring with mutations in sarcomeric proteins linked to cardiomyopathies.

17.3. KINASES, PHOSPHATASES, AND REGULATION BY CARDIAC TROPONIN

The kinases depicted in the scheme in Figure 17.1 are most of those for which there is evidence of an altered phosphorylation of thin filament proteins proteins. These include protein kinase A (PKA) (Metzger and Westfall, 2001; Solaro, 2001), rho-dependent kinase (ROK) (Vahebi et al., 2005), protein kinase C (PKC) (Burkart et al., 2003; Sumandea et al., 2003), p38 MAP kinase (p38) (Vahebi et al., 2003), and p21 activated kinase (Pak) (Buscemi et al., 2002; Ke et al., 2004). In the case of PKA and Pak (Pak1 isoform), it is apparent that the maladaptive alteration may be a depression in phosphorylation. Down-regulation of adrenergic signal transduction in heart failure is well-known (Wang and Dhalla, 2000), and there is evidence that myofilaments isolated from hearts at end-stage heart failure contain cTnI with a reduced level of phosphorylation at the PKA sites (Wolff et al., 1996). These sites exist at Ser 23, Ser 24 in an N-terminal extension unique to the cardiac isoform (Solaro, 2001). There is compelling evidence that phosphorylation of these sites is an important mechanism for increased cross-bridge kinetics during beta-adrenergic signaling and maintenance of power and frequency response in ejecting ventricles (Herron et al., 2001; Kentish et al., 2001; Pi et al., 2002; Layland et al., 2004, Takimoto et al., 2004). Thus, an inability to phoshorylate Ser 23, Ser 24 would be expected to be maladaptive.

We have also reported that adenoviral transfer of cDNA encoding an active form of Pak1 promotes the activity of protein phosphatase 2a (PP2a) and enhances myofilament response to Ca^{2+} (Ke et al., 2004) The p21-activated kinases (PAKs) 1–3 are serine/threonine protein kinases with activities stimulated by the binding of active Rac and Cdc42 GTPases (Bokoch, 2003). This myofilament Ca^{2+}-sensitizing effect of active Pak1 is associated with a reduced phosphorylation of cTnI, most likely at Ser 23, Ser 24 by activation of PP2a (Ke et al., 2004) There is also the potential for direct phosphorylation of cTnI at Ser 149 which is an *in vitro* substrate for p21 activated kinase (Pak 3 isoform), and located in a second actin binding region or switch peptide of cTnI. Buscemi et al. (2002) reported that *in vitro* phosphorylation of this site increases myofilament sensitivity to Ca^{2+} with no effect on maximum or basal tension of the myofilaments. They also reported an *in vitro* phosphorylation of cTnT at both its N- and C-terminal domains by

Pak3. In view of our finding that increases in active Pak1, the predominant isoform in heart activates phosphatase activity, the physiological relevance of Pak3 dependent phosphorylations of cTnI and cTnT remains unclear.

Signaling of hypertrophy involving the low molecular GTPase RhoA may also alter troponin phosphorylation (Sah et al., 1996). Phenylephrine has been demonstrated to induce myofibrillar formation and organization and expression of ANF by a mechanism involving activation of Rho-dependent kinases (ROCK) in neonatal heart cells (Hoshijima et al., 1998). Stressors such as rapid pacing and pressure overload induced heart failure in animal models also involve Rho/ROCK activation (Suematsu et al., 2001; Torsoni et al., 2003). Inhibitors of ROCK are also known to induce an improved cardiac function and blunting of hypertrophy associated with the hypertension in the Dahl salt sensitive rat (Kobayashi et al., 2002). Two types of altered myofilament function have been shown to occur with activation of Rho signaling and ROCK. One (Kimura et al., 1996) involved increases in myosin light chain phosphorylation associated with a ROCK-induced depression of myosin light chain phosphatase (MLCP) activity. MLCP was the first substrate identified for ROCK (Kimura et al., 1996). Targeting of MLCP to myosin light chains occurs through a 110–130 kDa sub-unit designated as the MBS (myosin binding site) or MYPT (myosin phosphatase targeting peptide). MYPT contains Ser/Thr residues that are substrates for ROCK. With ROCK phosphorylation, there is a depression of MYPT-enhanced activity of the 37 kDa catalytic sub-unit of MLCP. Thus, there is a phosphorylation of myosin light chain independent of changes in Ca^{2+} concentration and an increase in tension. Such an increase in myofilament sensitivity to Ca^{2+} associated with increased RhoA levels was reported by Suematsu et al. (2001) in dog hearts stressed by rapid pacing. The second potential mechanism for altered myofilament activity with Rho-signaling involves direct phosphorylation of sites on cTnT as report in the studies of Vahebi et al. (2005). These studies employed a variety of transgenic models and mass spectrometry in demonstrating that specific phosphorylation of cTnT at Ser 278 and Thr 287 by ROCK induced a depression in myofilament sensitivity to Ca^{2+} and maximum tension. The *in situ* role of activation of the RhoA/ROCK pathway of Tn phosphorylation requires further investigation.

Evidence for a role of protein kinase C (PKC) in the scheme presented in Figure 17.1 is most well-developed. We have previously discussed the hypothesis that PKC pathway as a downstream effector of both cardiac remodeling and altered myofilament response to Ca^{2+} (de Tombe and Solaro, 2000; Solaro et al., 2002b). The evidence demonstrated that PKC-dependent sarcomeric phosphorylations, depress cross-bridge cycling and power as well as maximum tension. Indeed there is evidence for up-regulation of beta- and alpha-PKC isoforms in end-stage human heart failure (Bowling et al., 1999). We have tested the role of up-regulation of these PKC isforms in studies with transgenic mouse models (Huang et al., 2001; Goldspink et al., 2004; Scruggs et al., 2006). Hearts of these mice demonstrate progressive depressions in cardiac function correlated with altered sarcomeric protein phosphorylation. Moreover, *in vitro* investigation of sarcomeric activity employing skinned fiber bundles or the motility assay demonstrated significant effects of site specific phosphorylation of troponin I on tension development and sliding velocity (Burkart et al., 2003). Maximum tension, Ca^{2+} sensitivity, and sliding velocity were significantly depressed by phosphorylation of Ser 43, Ser 45, and Thr 144 of cTnI. We have also reported evidence for depression of tension and tension cost by site specific phosphorylation of cTnT at Thr 210 (Sumandea et al., 2003). In view of this depressive effect

of phosphorylation of sites on cTnI and cTnT, we would expect that hearts missing these phosphorylation sites may be less susceptible to activation of the PKC dependent pathways. Studies employing transgenic mouse models with complete replacement of cTnI with cTnI(S43A,S45A,T144A) also support the idea that phosphorylation of these sites slows down velocity of shortening (Pi et al., 2003). Following treatment of heart preparations with activators of the PKC pathway, myofilament response to Ca^{2+} was depressed in control non-transgenic hearts, but to a significantly less extent in the transgenic mice. We (Scruggs et al., 2006) have investigated a double transgenic mouse model in which a mouse expressing a cardiac directed cTnI mutant (cTnIS43A,S45A) that replaced about 40% of the native cTnI was cross-bred with a mouse expressing at low levels active epsilon PKC. Comparison of hemodynamic and biochemical properties in double TG mice, NTG mice, and single TG mice demonstrated that at 12 months of age there was significant amelioration of the progressive heart failure in the double TG hearts. Associated with this improved function and decrease in markers of heart failure there was a redistribution of sites of phosphorylation on cTnI. More work needs to be done in follow up to these findings in order to identify site specific changes in cTnI.

17.4. ACIDOSIS, ISCHEMIA, REPERFUSION AND CARDIAC TROPONIN

There is substantial evidence that troponin isoform population is a significant factor in the deactivation of the heart and the myofilaments by acidic pH. Neonatal heart muscle is known to be less sensitive to deactivation by acidosis and ischemia, and early studies demonstrated that this resistance is likely to be due to differences in thin filament components between adult and neonatal hearts (Solaro et al., 1986). Transgenic studies have provided strong evidence that embryonic/neonatal isoforms of both TnI and TnT play a prominent role in this resistance. In the case of TnT, there is evidence that compared to wild-type controls, expression fast skeletal TnT in the hearts of transgenic mice induces a greater decrease in contractility as determined by dF/dt max in intact fiber bundles under conditions of acidosis (Nosek et al., 2004). The expression of mutant forms of TnT in transgenic mouse hearts also induces an altered response of the myofilaments to deactivation by acidosis. We (Solaro et al., 2002b) reported that skinned fiber bundles containing cTnT-R92Q, which is linked to familial hypertrophic cardiomyopathy, demonstrated an increased Ca^{2+} sensitivity compared to controls at pH 7.0. However, when the pH was dropped to pH 6.5, this relative increase in Ca^{2+} sensitivity was enhanced. We have focused also on the role of slow skeletal TnI in the response to acidosis based on early observations that neonatal hearts express this isoform (Saggin et al., 1989; Martin et al., 1991). These studies (Solaro et al., 1988; Wolska et al., 2001) demonstrated a significant protection of intact fiber bundles and cardiac myofilaments from the depression of tension and Ca^{2+} sensitivity that occurs with acidosis. Most recently, we (Urboniene et al., 2005) have tested this hypothesis in the intact mouse expressing either cTnI or ssTnI in place of cTnI in the cardiac compartment by assessing left ventricular function by trans-thoracic two-dimensional targeted M-mode and pulsed Doppler echocardiography. Controls and transgenic mice breathing 35% CO_2 demonstrated the same decrease arterial pH, but the hearts of the ssTnI-mice were significantly protected from depression in cardiac function that occurred in the controls.

The relative insensitivity of myofilaments regulated by ssTnI to acidic pH led us to test whether this specific change in the thin filament would protect hearts against injury and depressed function associated with ischemia and reperfusion (Arteaga et al., 2005). We were also motivated to do these experiments as a proof of concept relating to the use of inotropic agents that sensitize the myofilaments to Ca^{2+}. In particular, Levosimendan (Vardax®) had been reported to improve cardiac function following ischemia and reperfusion in both animal studies (Du Toit et al., 1999) employing isolated perfused hearts, and in patients after percutaneous trans-luminal coronary angioplasty in acute myocardial ischemia (Sonntag et al., 2004). Whether these effects of Levosimendan are due to its binding to cTnC or its "off target" effects as a phospho-diesterase inhibitor or opener of K-channels remains unclear (Kass and Solaro, 2006). Hearts of mice expressing ssTnI in place of cTnI provide a preparation with constitutive sensitization to Ca^{2+} and with essentially no alterations in other aspects of cardiac regulation. Figure 17.2 illustrates the ability of cardiac expression of ssTnI to protect against the depression in cardiac function associated with ischemia/reperfusion.

In the experiments depicted in Figure 17.2, we also added EMD 57033 to the reperfusion media. EMD afforded significant protection, which at the 30 min time point was indistinguishable from that obtained in the TG-ssTnI hearts. EMD 57033 is a sarcomeric activator that increases the myofilament response to Ca^{2+}. EMD 57033 is a very weak inhibitor of phospho-diesterase activity and has no known activity in affecting K channel open state. Although there is evidence relatively high concentrations of EMD 57033 are

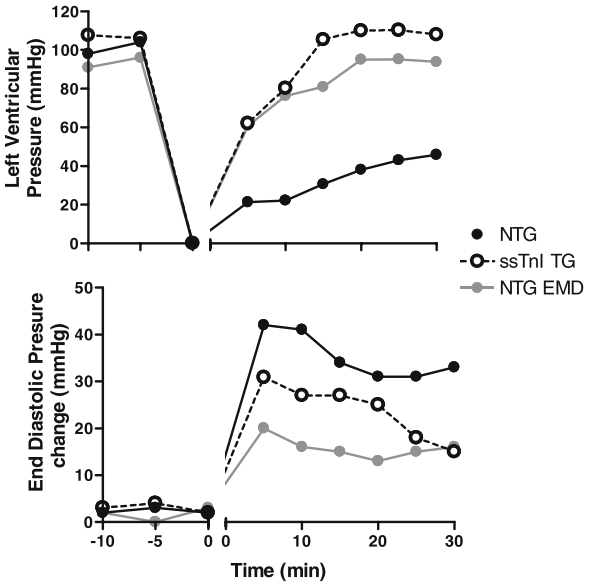

Figure 17.2. Comparison of recovery of function after a 20 min period of global ischemia followed by 30 min or reperfusion in isolated, perfused non-transgenic mouse hearts (NTG), transgenic hearts expressing ssTnI in place of cTnI (TG-ssTnI), and in NTG hearts treated with 3 μM EMD-57033 during the reperfusion. See text for discussion.

able to promote actin-myosin interactions in the absence of Tn-tropomyosin, sensitization to Ca^{2+} occurs over a lower concentration range in preparations containing Tn-tropomyosin (Solaro et al., 1993). Moreover, EMD docks at the interface between the C-lobe of cTnC and the near N-terminus of cTnI. This docking site was resolved in NMR structural studies of a 1 : 1 complex of EMD 57033 and the C-lobe of cTnC (Wang et al., 2001). In these studies, a peptide of cTnI comprised of amino acids 34–71 completely displaced EMD. Ca^{2+}-sensitization is expected to slow cardiac relaxation and this has been noted in unloaded myocyte preparations (Solaro et al., 1993). However Senszaki et al. (2000) reported that EMD 57033 improved contractility and mechano-energetics in a dog model of heart failure with no deleterious effects of diastolic function. These data emphasize the importance of testing effects of sarcomeric activators on heart beating against an afterload. It is also noteworthy that data reported in the bottom panel of Figure 17.2 indicate that EMD 57033 is able to improve diastolic function in hearts stressed by ischemia/reperfusion. In summary, the data shown in Figure 17.2 support the hypothesis that interactions of TnI with its neighbors in the thin filament are important determinants of the extent of depression of cardiac function elicited by ischemia/reperfusion. Modification of these interactions using small molecules remains an important potential avenue for drug discovery research.

17.5. ACKNOWLEDGEMENTS

This chapter is dedicated to Professor Setsuro Ebashi and to Professor F. N. Briggs and Professor S. V. Perry, who got RJS interested in troponin. We are grateful to our many colleagues for collaborations permitting the study of troponin at many levels of organization in the heart. The work described in this review was supported in part by grants from the NIH NHLBI and AHA.

17.6. REFERENCES

Arteaga, G. M., Warren, C. M., Milutinovic, S., Martin, A. F., and Solaro, R. J., 2005, Specific enhancement of sarcomeric response to Ca^{2+} protects murine myocardium against ischemia/reperfusion dysfunction, *Am. J. Physiol. Heart Circ. Physiol.* **289**:H2183–H2192.

Bokoch, G. M., 2003, Biology of the p21-activated kinases, *Annu Rev Biochem.* **72**:743–781.

Bowling, N., Walsh, R. A., Song, G., Estridge, T., Sandusky, G. E., Fouts, R. L., Mintze, K., Pickard, T., Roden, R., Bristow, M. R., Sabbah, H. N., Mizrahi, J. L., Gromo, G., King, G. L., and Vlahos, C. J., 1999, Increased protein kinase C activity and expression of Ca2+-sensitive isoforms in the failing human heart, *Circulation* **99**:384–391.

Burkart, E. M., Sumandea, M. P., Kobayashi, T., Nili, M., Martin, A. F., Homsher, E., and Solaro, R. J., 2003, Phosphorylation or glutamic acid substitution at protein kinase C sites on cardiac troponin I differentially depress myofilament tension and shortening velocity, *J. Biol. Chem.* **278**:11265–11272.

Buscemi, N., Foster, D. B., Neverova, I., and Van Eyk, J. E., 2002, p21-activated kinase increases the calcium sensitivity of rat triton-skinned cardiac muscle fiber bundles via a mechanism potentially involving novel phosphorylation of troponin I, *Circ. Res.* **91**:509–516.

Crozier, S. J., Vary, T. C., Kimball, S. R., and Jefferson, L. S., 2005, Cellular energy status modulates translational control mechanisms in ischemic-reperfused rat hearts, *Am. J. Physiol. Heart Circ. Physiol.* **289**: H1242–H1250.

Dorn, G. W., 2nd, and Force, T., 2005, Protein kinase cascades in the regulation of cardiac hypertrophy, *J. Clin. Invest.* **115**:527–537.

Du Toit, E. F., Muller, C. A., McCarthy, J., and Opie, L. H. 1999, Levosimendan: effects of a calcium sensitizer on function and arrhythmias and cyclic nucleotide levels during ischemia/reperfusion in the Langendorff-perfused guinea pig heart, *J. Pharmacol. Exp. Ther.* **290**:505–514.

Frey, N., and Olson, E. N., 2003, Cardiac hypertrophy: the good, the bad, and the ugly, *Annu. Rev. Physiol.* **65**:45–79.

Goldspink, P. H., Montgomery, D. E., Walker, L. A., Urboniene, D., McKinney, R. D., Geenen, D. L., Solaro, R. J., and Buttrick, P. M., 2004, Protein kinase C-epsilon overexpression alters myofilament properties and composition during the progression of heart failure, *Circ. Res.* **95**:424–432.

Gomes, A. V., and Potter, J. D., 2004, Molecular and cellular aspects of troponin cardiomyopathies, *Ann. N. Y. Acad. Sci.* **1015**:214–224.

Gordon, A. M., Homsher, E., and Regnier, M., 2000, Regulation of contraction in striated muscle, *Physio. Rev.* **80**:853–924.

Herron, T. J., Korte, F. S., and McDonald, K. S., 2001, Power output is increased after phosphorylation of myofibrillar proteins in rat skinned cardiac myocytes, *Circ. Res.* **89**:1184–1190.

Hoshijima, M., Sah, V. P., Wang, Y., Chien, K. R., and Brown, J. H., 1998, The low molecular weight GTPase Rho regulates myofibril formation and organization in neonatal rat ventricular myocytes. Involvement of Rho kinase, *J. Biol. Chem.* **273**:7725–7730.

Huang, L., Wolska, B. M., Montgomery, D. E., Burkart, E., Buttrick, P. M., and Solaro, R. J., 2001, Increased contractility and altered Ca^{2+}-transients of mouse heart myocytes conditionally expressing PKC-beta II, *Am. J. Physiol. (Cell).* **280**:C1114–C1120.

Kass, D., and Solaro, R. J., 2006, Mechanisms and use of calcium sensitizing agents, *Circulation* 113:305–315.

Ke, Y., Huang, L., and Solaro, R. J., 2004, Intracellular localization and functional effects of P21-activated kinase-1 (Pak1) in cardiac myocytes, *Circ. Res.* **94**:194–200.

Kentish, J. C., McCloskey, D. T., Layland, J., Palmer, S., Leiden, J. M., Martin, A. F., and Solaro, R. J., 2001, Phosphorylation of troponin I by protein kinase A accelerates relaxation and cross-bridge cycle kinetics in mouse ventricular muscle, *Circ. Res.* **88**:1059–1065.

Kimura, K., Ito, M., Amano, M., Chihara, K., Fukata, Y., Nakafuku, M., Yamamori, B., Feng, J., Nakano, T., Okawa, K., Iwamatsu, A., and Kaibuchi K., 1996, Regulation of myosin phosphatase by Rho and Rho-associated kinase (Rho-kinase). *Science* **273**:245–248.

Kobayashi, N., Horinaka, S., Mita, S., Nakano, S., Honda, T., Yoshida, K., Kobayashi, T., and Matsuoka, H., 2002, Critical role of Rho-kinase pathway for cardiac performance and remodeling in failing rat. *Cardiovasc. Res.* **55**:757–767.

Kobayashi, T., and Solaro, R. J., 2005, Calcium, thin filaments, and integrative biology of cardiac contractility, *Annu. Rev. Physiol.* **67**:39–67.

Layland, J., Grieve, D. J., Cave, A. C., Sparks, E., Solaro, R. J., and Shah, A. M., 2004, Essential role of troponin I in the positive inotropic response to isoprenaline in mouse hearts contracting auxotonically, *J. Physiol.* **556**:835–847.

Martin, A. M., Ball, K., Gao, L., Kumar, P. K., and Solaro, R. J., 1991, Identification and functional significance of troponin I isoforms in neonatal rat heart myofibrils, *Circ. Res.* **69**:1244–1252.

Metzger, J. M., and Westfall, M. V. 2001, Covalent and noncovalent modification of thin filament action: the essential role of troponin in cardiac muscle regulation, *Circ. Res.* **94**:146–158.

Mirza, M., Marston, S., Willott, R., Ashley, C., Mogensen, J., McKenna, W., Robinson, P., Redwood, C., and Watkins, H., 2005, Dilated cardiomyopathy mutations in three thin filament regulatory proteins result in a common functional phenotype, *J. Biol. Chem.* **280**:28498–28506.

Mogensen, J., Kubo, T., Duque, M., Uribe, W., Shaw, A., Murphy, R., Gimeno, J. R., Elliott, P., and McKenna, W. J., 2003, Idiopathic restrictive cardiomyopathy is part of the clinical expression of cardiac troponin I mutations, *J. Clin. Invest.* **111**:209–216.

Nosek, T. M., Brotto, M. A., and Jin, J. P., 2004, Troponin T isoforms alter the tolerance of transgenic mouse cardiac muscle to acidosis, *Arch. Biochem. Biophys.* **430**:178–184.

Pi, Y., Kemnitz, K. R., Zhang, D., Kranias, E. G., and Walker, J. W., 2002, Phosphorylation of troponin I controls cardiac twitch dynamics: evidence from phosphorylation site mutants expressed on a troponin I-null background in mice, *Circ. Res.* **90**:649–656.

Pi, Y., Zhang, D., Kemnitz, K. R., Wang, H., and Walker, J. W., 2003, Protein kinase C and A sites on troponin I regulate myofilament Ca^{2+} sensitivity and ATPase activity in the mouse myocardium, *J. Physiol.* **552**:845–857.

Saggin, L., Gorza, L., Ausoni, S., and Schiaffino, S., 1989, Troponin I switching in the developing heart, *J. Biol. Chem.* **264**:16299–16302.

Sah, V. P., Hoshijima, M., Chien, K. R., and Brown, J. H., 1996, Rho is required for Galphaq and alpha1-adrenergic receptor signaling in cardiomyocytes. Dissociation of Ras and Rho pathways, *J. Biol. Chem.* **271**:31185–31190.

Samarel, A. M., 2005, Costameres, focal adhesions, and cardiomyocyte mechanotransduction, *Am. J. Physiol. Heart Circ. Physiol*. **289**:H2291–H2301.

Scruggs, S. B., Walker, L. A., Lyu, T., Geenen, D. L., Solaro, R. J., Buttrick, P. M., and Goldspink, P. H., 2006, Partial replacement of cardiac troponin I with a non-phosphorylatable mutant at serines 43/45 attenuates the contractile dysfunction associated with PKC epsilon phosphorylation, *J. Mol. Cell Cardiol.* 40:465–473.

Senszaki, H., Isoda, T., Paolocci, N., Ekelund, U., Hare, J. M., and Kass, D. A., 2000, Improved mechanoenergetics and cardiac rest and reserve function of an in vivo failing heart by calcium sensitizer EMD-57033, *Circulation* **101**:1040–1048.

Sonntag, S., Sundberg, S., Lehtonen, L. A., and Kleber, F. X., 2004, The calcium sensitizer levosimendan improves the function of stunned myocardium after percutaneous transluminal coronary angioplasty in acute myocardial ischemia, *J. Am. Coll. Cardiol.* **43**:2177–2182.

Solaro, R. J., 2001, Modulation of cardiac myofilament activity by protein phosphorylation, in: *Handbook of Physiology: Section 2. The Cardiovascular System. Vol 1. The Heart*, E. Page, H. Fozzard, R. J. Solaro, eds., Oxford University Press, New York, pp. 264–300.

Solaro, R. J., Gambassi, G., Warshaw, D. M., Keller, M. R., Spurgeon, H. A., Beier, N., and Lakatta, E. G., 1993, Steroselective actions of thiadiazinones on dog cardiac myocytes and myofilaments, *Circ. Res.* **73**:981–990.

Solaro, R. J., Kumar, P., Blanchard, E. M., and Martin, A. M., 1986, Differential effects of pH on Ca^{2+} activation of myofilaments of adult and perinatal dog hearts: evidence for developmental differences in thin filament regulation, *Circ. Res.* **58:**721–729.

Solaro, R. J., Lee, J., Kentish, J., and Allen, D. A., 1988, Differences in the response of adult and neonatal heart muscle to acidosis, *Circ. Res.* **63**:779–787.

Solaro, R. J., and Rarick, H. M., 1998, Troponin and tropomyosin: proteins that switch on and tune in the activity of cardiac myofilaments, *Circ. Res.* **83**:471–480.

Solaro, R. J., Varghese, J., Marian, A. J., and Chandra, M., 2002a, Molecular mechanisms of cardiac myofilament activation: Modulation by pH and a troponin T mutant R92Q, *Basic Res. Cardiol.* **97**: I102–I110.

Solaro, R. J., Wolska,, B. M., Arteaga, G., Martin, A. F., Buttrick, P., and de Tombe, P., 2002b, Modulation of Thin Filament Activity in Long and Short Term Regulation of Cardiac Function, in: *Molecular Control Mechanisms in Striated Muscle Contraction,* R. J. Solaro, R. L. Moss, eds, Kluwer Academic Publishers, Netherlands, pp. 291–327.

Suematsu, N., Satoh, S., Kinugawa, S., Tsutsui, H., Hayashidani, S., Nakamura, R., Egashira, K., Makino, N., and Takeshita, A., 2001, Alpha1-adrenoceptor-Gq-RhoA signaling is upregulated to increase myofibrillar $Ca2^{+}$ sensitivity in failing hearts, *Am. J. Physiol. Heart Circ. Physiol.* **281**:H637–H646.

Sumandea, M. P., Pyle, W. G., Kobayashi, T., de Tombe, P. P., and Solaro, R. J., 2003, Identification of a functionally critical protein kinase C phosphorylation residue of cardiac troponin T, *J. Biol. Chem.* **278**:35135–35144.

Takimoto, E., Soergel, D. G., Janssen, P. M., Stull, L. B., Kass, D. A., and Murphy, A. M., 2004, Frequency- and afterload-dependent cardiac modulation in vivo by troponin I with constitutively active protein kinase A phosphorylation sites, *Circ. Res.* **94**:496–504.

de Tombe, P. P., and Solaro, R. J., 2000, Integration of Cardiac Myofilament Activity and Regulation with Pathways Signaling Hypertrophy and Failure, *Ann. Biomed. Eng.* **28**:991–1001.

Torsoni, A. S., Fonseca, P. M., Crosara-Alberto, D. P., and Franchini, K. G., 2003, Early activation of p160ROCK by pressure overload in rat heart, *Am. J. Physiol. Cell Physiol.* **284**:C1411–C1419.

Urboniene, D., Dias, F., Peña, J. R., Walker, L. A., Solaro, R. J., and Wolska, B. M., 2005, Expression of slow skeletal troponin I in adult mouse heart helps to maintain the left ventricular systolic function during Respiratory Hypercapnia, *Circ. Res.* **97**:70–77.

Vahebi, S., Kobayashi, T., Warren, C. M., de Tombe, P. P., and Solaro, R. J., 2005, Functional effects of rho-kinase (ROCK-II)-dependent phosphorylation of specific sites on cardiac troponin, *Circ. Res.* **96**:740–747.

Vahebi, S., Manxiang, L., de Tombe, P. P., Wang, Y., and Solaro, R. J., 2003, Activation of p38 MAP Kinase in transgenic mouse hearts depresses cardiac myofilament tension and ATPase rate, *J. Mol. Cell Cardiol.* **35**:A43.

Wang, X., and Dhalla, N. S., 2000, Modification of beta-adrenoceptor signal transduction pathway by genetic manipulation and heart failure, *Mol. Cell. Biochem.* **214**:131–155.

Wang, X., Li, M., Spyracopoulos, L., Beier, N., Chandra, M., Solaro, R. J., and Sykes, B. D., 2001, Structure of the C-domain of human cardiac troponin C in complex with the Ca^{2+}-sensitizing drug EMD 57003, *J. Biol. Chem.* **276**:25456–25466.

Wolff, M. R., Buck, S. H., Stoker, S. W., Greaser, M. L., and Mentzer, R. M., 1996, Myofibrillar calcium sensitivity of isometric tension is increased in human dilated cardiomyopathies: role of altered beta-adrenergically mediated protein phosphorylation, *J. Clin. Invest.* **98**:167–176.

Wolska, B. M., Vijayan, K., Arteaga, G. M., Konhilas, J. P., Phillips, R. M., Kim, R., Naya, T., Leiden, J. M., Martin, A. F., de Tombe, P. P., and Solaro, R. J., 2001, Expression of slow skeletal troponin I in adult transgenic mouse heart muscle reduces the force decline observed during acidic conditions, *J. Physiol.* **536**:863–870.

Yumoto, F., Lu, Q. W., Morimoto, S., Tanaka, H., Kono, N., Nagata, K., Ojima, T., Takahashi-Yanaga, F., Miwa, Y., Sasaguri, T., Nishita, K., Tanokura, M., and Ohtsuki, I., 2005, Drastic Ca^{2+} sensitization of myofilament associated with a small structural change in troponin I in inherited restrictive cardiomyopathy. *Biochem. Biophys. Res. Commun*. **338**:1519–1526.

18

TROPONIN MUTATIONS IN CARDIOMYOPATHIES

Jens Mogensen

18.1. INTRODUCTION

Cardiomyopathies are a group of cardiac disorders characterized by structural and functional abnormalities of the myocardium of unexplained aetiology. By convention idiopathic cardiomyopathies are divided into 4 different diagnostic entities: *Hypertrophic cardiomyopathy (HCM)*, *dilated cardiomyopathy (DCM)*, *restrictive cardiomyopathy (RCM)* and *arrythmogenic right ventricle cardiomyopathy (ARVC)* (Figure 18.1).[1] Recent investigations have revealed that the conditions in many cases are hereditary.[2–4]

HCM is the most studied of the conditions and considered to be the commonest hereditary cardiac disease with a prevalence in young adults of about 1 : 500.[5] The diagnosis relies on demonstration of unexplained thickening of the left ventricle.[1] The majority of patients have asymmetric septal hypertrophy, involving the anterior and posterior septum. However, the hypertrophy may be concentric or isolated to segments other than the anterior and posterior septum. Systolic function is variable, with hyperdynamic, normal and impaired indices of contractile performance. About 25% of patients have left ventricular outflow tract obstruction at rest or a pressure gradient precipitated by pharmacological or physiological stress.[6–9] Disease manifestations typically develop during adolescence although clinical presentation may occur at any age. The clinical expression is heterogeneous and varies even between related individuals.[10–12] The major clinical problems are reduced exercise capacity, risk of arrhythmia, and thrombo-embolic events. Sudden cardiac death may occur as the initial disease manifestation and is believed to be the most frequent cause of cardio-vascular related death in young individuals. Available data largely based on recorded arrhythmic events from implantable defibrillators (ICD) suggest that ventricular arrhythmia is the most common cause of sudden death. Several studies have proposed specific risk factors for sudden death as outlined in Table 18.1.[13–17]

HCM is inherited by autosomal dominant transmission implying that disease carriers have a 50% risk of passing the disease gene on to each of their children. Molecular genetic studies have suggested that HCM is a disease of the contractile unit of the heart with the identification of disease-causing mutations in eight different sarcomeric protein genes

Departments of Cardiology, Skejby University Hospital Aarhus, Denmark, and The Heart Hospital, University College London, UK

Regulatory Mechanisms of Striated Muscle Contraction
Edited by Ebashi and Ohtsuki, Springer, 2007

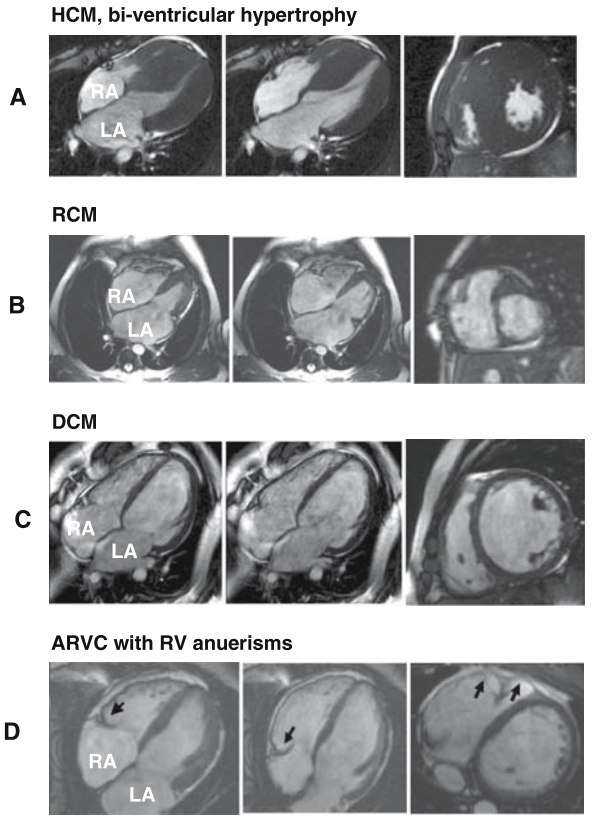

Figure 18.1. Cine Cardiac Magnetic Resonance (CMR) images of patients with HCM, RCM, DCM and ARVC. (A) HCM: Extreme bi-ventricular hypertrophy in a patient 21 years of age.[12] (B) RCM: Severe bi-atrial dilatation and restrictive filling in a child 6 years of age[100]. (C) DCM: Severe ventricle dilatation and impaired LV function in a 40 year old patient. (D) ARVC: Severe right ventricle dilatation and wall thinning with aneurisms indicated by arrows in a patient 24 years of age. RA: right atrium; LA: left atrium. CMR images: from left to right: 4 chamber systole, 4 chamber diastole, cross-sectional view at papillary muscle level diastole.

Table 18.1. Risk factors for sudden death in HCM

Previous cardiac arrest
Sustained ventricular tachycardia
Family history of sudden death
Unexplained syncope
LV thickness greater ≥30 mm
Abnormal exercise blood pressure
Non-sustained ventricular tachycardia

(Table 18.2).[18–23] Sequence variations in 3 additional sarcomeric genes have been reported but only in 3 single individuals and further evidence is needed to establish if these variations are disease causing mutations or merely rare normal variations within the human genome.[24–26] Recently, 3 HCM families were reported with mutations in the gene for muscle LIM protein (MLP) which has diverse regulatory and cytoskeletal functions.[27]

RCM is a rare condition defined by impaired ventricular filling in the presence of normal systolic function and normal or near normal myocardial thickness. The disease is characterised by symptoms of progressive left- and right-sided heart failure. The overall prognosis is poor especially when onset is in childhood, and patients often require cardiac transplantation. RCM usually results from increased stiffness of the myocardium which may be caused by a variety of local or systemic diseases.[1,28,29] In the Western hemisphere amyloidosis is probably the most frequent and most studied cause of non-idiopathic RCM. Other secondary causes of amyloidosis include rare hereditary forms of defects in the gene encoding plasma protein transthyretin and amyloid deposition secondary to chronic inflammatory diseases.[30] In equatorial Africa endomyocardial fibrosis is a common cause of RCM and is believed to be the same disease as Loeffler's eosinophilic endocarditis. The aetiology is unknown but eosinophils in the myocardium are believed to degranulate and cause fibrosis particularly of the endocardium.

DCM is a condition characterised by unexplained left ventricle dilatation, impaired systolic function and non-specific histological abnormalities dominated by myocardial fibrosis.[1,31,32] The condition has an estimated prevalence of 36.5/100.000 in a US-population and is the commonest cause of heart failure and cardiac transplantation in the young.[33,34] Patients may experience severe disease complications including arrhythmia, thrombo-embolic events and sudden death due to ventricular arrhythmia. Recent developments in medical treatment has diminished symptoms and improved prognosis considerably.[35–39] In addition novel bi-ventricular pacing modalities seems promising in treatment

Table 18.2. Disease genes in HCM

	Gene symbol
Confirmed disease genes	
β-myosin heavy chain (18)	*MYH7*
α-tropomyosin (19)	*TPM1*
Troponin T (19)	*TNNT2*
Myosin binding protein C (20,21)	*MYBPC3*
Regulatory myosin light chain (22)	*MYL2*
Essential myosin light chain (22)	*MYL3*
Troponin I (23)	*TNNI3*
α-cardiac actin (81)	*ACTC*
Muscle LIM protein (27)	*MLP*
Potential disease genes with sequence variations identified in probands only	
Troponin C (24)	*TNNC1*
Titin (25)	*TTN*
α-myosin heavy chain (26)	*MYH6*

of patients with severe heart failure.[40–43] The aetiology of DCM is poorly understood and appears to be very heterogeneous (Figure 18.2). Viral infections, autoimmune disease and toxic substances are believed to be causative in a proportion of DCM although definitive proof has often been difficult to obtain (for review see[31,44]). Recent studies have suggested that genetic factors may account for as many as 30–50% of cases.[3,45,46] A large number of disease genes have been identified encoding proteins involved in a variety of cell functions ranging from force generation within the sarcomere to regulation of myocyte ion-channels (Table 18.3).[47–64] Most affected families present with a "pure" cardiac phenotype and in these families autosomal dominant transmission is most frequent followed by recessive and X-linked inheritance. In addition to impaired cardiac function variable degrees of skeletal muscle dystrophy and cardiac conduction disease has been reported with mutations in genes such as dystrophin, desmin and emerin. Less frequent affected individuals present with involvement of other organ systems as in Barth syndrome which is characterised by DCM, neutropenia, abnormal mithochondrial function as well as skeletal myopathy.[65,66] Disease responsible mutations for this condition have been identified in the gene *G4.5* encoding the protein taffazin in which mutations may also lead to "pure" DCM, endocardial fibrosis or left ventricle non compaction without any features of Barth syndrome. Mitochondrial mutations may be suspected in DCM patients with neurological deficits, skeletal muscle involvement in addition to symptoms from other organ systems.[67]

It is a challenge to manage patients with cardiomyopathies not the least because the clinical presentation is diverse. This makes assessment of individual risk profile for sudden death and adverse disease complications difficult. Since the conditions are hereditary it is an important task of the physician to counsel affected families and offer clinical screening of individuals at risk of having inherited the condition. The results of a dedi-

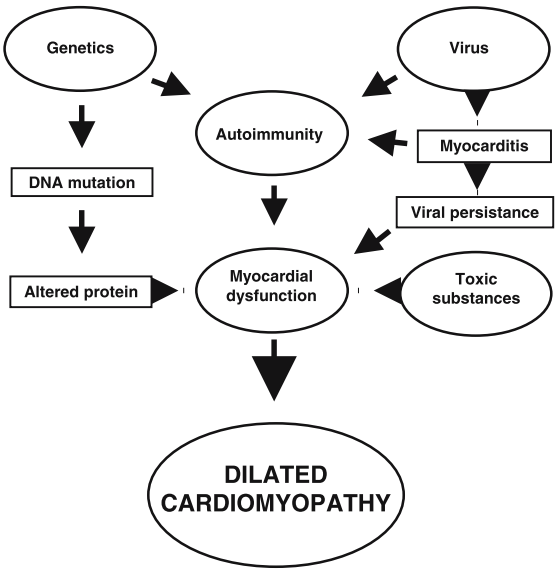

Figure 18.2. Causes of dilated cardiomyopathy.

Table 18.3. Disease genes in DCM

Protein	Disease gene	Inheritance	Phenotype
Sarcomeric	α-cardiac actin (47)	Autosomal dominant	DCM
	α-tropomyosin (48)	Autosomal dominant	DCM
	β-myosin heavy chain (49)	Autosomal dominant	DCM
	Troponin T (49)	Autosomal dominant	DCM
	Troponin I (45)	Autosomal recessive	DCM
	Troponin C (46)	Autosomal dominant	DCM
	Titin (50,51)	Autosomal dominant	DCM
	Myosin binding protein C (52)	Autosomal dominant	DCM
	Telethonin (53)	Autosomal dominant	DCM
Nuclear envelope	Lamin A/C (54)	Autosomal dominant	DCM +/− muscle dystrophy and +/− conduction disease
	Emerin (55)	X-linked	
Cytoskeletal/ sarcolemma	Desmin (56)	Autosomal dominant	DCM +/− muscle dystrophy and +/− cardiac conduction disease
	δ-sarcoglycan (57)	Autosomal dominant	DCM
	Dystrophin (58)	X-linked	DCM +/− muscle dystrophy
	Desmoplakin (59)	Autosomal recessive	DCM, Carvajal syndrome
	Metavinculin (60)	Autosomal dominant	DCM
Z-disc associated	MLP (53)	Autosomal dominant	DCM
	α-actinin-2 (61)	Autosomal dominant	DCM
	Cypher/ZASP (62)	Autosomal dominant	DCM and LV non-compaction
Ion channels	Phosphlamban (63)	Autosomal dominant	DCM
	ABBC9 (K^+-channel) (64)	Autosomal dominant	DCM

cated research effort in HCM through the past 10–15 years has revealed that the condition is a disease of the cardiac sarcomere and initial reports have suggested that a specific genotype may be correlated to the clinical expression of the disease (phenotype).[11,68,69,80] If such a correlation is present information about the genotype would be a valuable tool for individual risk stratification. However, most of the available knowledge has been obtained by investigations of individual patients (probands) or families selected for gene identification studies. Proband studies have provided information about disease expression in single individuals but have not contained information of disease presentation in families. Gene identification studies require large families with many affected individuals which are rare and may not resemble the disease expression in the much smaller families most frequently seen in a clinical setting. The use of genetic diagnosis in clinical management of cardiomyopathy families is dependent on investigations of unselected consecutive cohorts of patients. The results obtained should carry information about the

prevalence of mutations, genotype-phenotype correlation in relation to age of onset, penetrance, characteristics of disease expression, and risk of sudden death.

18.2. GENETIC INVESTIGATIONS OF CARDIOMYOPATHIES

Within the past few decades the number of disease causing genes identified in various hereditary conditions has increased dramatically not the least due to results achieved by the human genome project. This has generated a basis for mutation screening in many hereditary disorders and increased the need for reliable and cost-effective methods for mutation detection with high sensitivity and specificity. Tremendous developments in technology have made it feasible to investigate large genes in many patients over a short period of time and identify sequence variations with high accuracy. However, most genes within the human genome harbour sequence variations that occur with a variable prevalence in healthy control populations. These normal variations are know as polymorphisms and may lead to variations in amino acid composition of proteins. Whereas mutation screening has become less demanding within the past few years it remains a challenge to determine whether a given sequence variation identified in a clinically affected individual is a true disease causing mutation or merely a benign polymorphism. Various information is needed about the sequence variation to elucidate if it might be a disease causing mutation: (1) documentation that the sequence variation segregates with the disease in the family; (2) absence of the sequence variation in ethnically matched control individuals; (3) information about presence of the same sequence variation in other affected families; (4) information about prevalence of amino acid polymorphisms in the gene; (5) information about evolutionary conservation of the amino acid change by comparison to similar proteins in other species; and (6) potential functional impact of the sequence variation based on in vivo/vitro protein expression studies. However, it is rarely possible to obtain exhaustive information about all aspects of the sequence variation and the investigator will have to make a decision about the nature of the sequence variation based on integration of available data. For instance if the sequence variation segregate with the disease in the family, is absent in healthy controls and mutations in the same domain of the gene has been identified in other families it would be reasonable to assume that it is a disease causing mutation. In contrast if a novel sequence variation was identified in a gene with recognised amino acid polymorphisms in a single patient without segregation data it would not be possible to determine if it is a rare polymorphism or a disease causing mutation. No definitive rules in making this decision can be given and the investigator would have to weigh the quality of the data available against the potential clinical consequences for an affected family following genetic counselling based on the genetic findings. If the data are solid genotype negative individuals may terminate clinical follow-up since they would not be at risk of disease development while mutation carriers would be recommended sustained clinical screening.

18.2.1. In Vitro Protein-protein Interaction Studies of Troponin Mutations

As pointed out in the previous paragraph it is often difficult to determine if novel sequence variations identified in small families with limited number of affected individuals are disease associated or rare polymorphisms. To substantiate if a sequence variation

is a disease causing mutation it would be relevant to further characterise the effect of the mutation at protein level. It would be ideal to investigate cardiac tissue from affected individuals but this would require a substantial amount of myocardium which is rarely obtainable except when HCM patients with outflow tract obstruction undergo myectomi or patients receive a cardiac transplant. Within recent years a substantial number of studies have investigated the potential impact of various sarcomeric gene mutations in different expression systems. A new scientific discipline has developed studying transgenic animals with sarcomeric gene mutations.[63,70–72] Clinical methods have been developed to study disease development in small rodents including echocardiography, ECG-recording and Holter-monitoring. Several mutations have successfully been expressed in animals developing a phenotype similar to the clinical disease expression seen in HCM and DCM patients. Much has been learnt about mechanisms involved in disease development by investigations of genetically modified myocardium in relation to changes in Ca^{++}-sensitivity, energy metabolism, impact on protein-protein interaction and consequences for force generation within the sarcomere.

Most expression studies of specific sarcomeric mutations in transgenic animals have reported development of a homogeneous phenotype and a uniform effect on various muscle parameters investigated. Similarly, studies of specific mutations in myotube test systems have lead to unambiguous results.[73–77] However, these results do not readily explain the extreme heterogeneous clinical disease expression observed in humans indicating that the human phenotype is a product of more than one single amino acid sub-stitution in a sarcomeric gene. From a clinical stand point expression studies are particularly useful to investigate if a sequence variation identified in an affected family has the potential to initiate disease development. However, transgenic animal studies and myotube experiments are expensive, time consuming and requires specially trained staff making them inapplicable in a clinical setting to elucidate whether a given sequence variation might be disease causing. It would be of great value if cheaper, faster, and more simple test systems were available that would indicate if a sequence variation had the potential of changing protein-protein interaction. Recently, a mammalian two-hybrid system has become available to conduct studies of this kind (Figure 18.3) (Promega, Madison, WI, USA). We used the system to investigate the effect of Troponin I, C, and T mutations identified in studies of patients with DCM on inter-troponin interaction.[45,46] There was a significant impairment of mutated $cTnI_{A2V} - cTnT_{wildtype}$ protein interaction compared to wildtype control, (t-test: $P < 0.001$), while no change was observed in mutated $cTnI_{A2V} - cTnC_{wildtype}$ interaction ($P = 0.6$). Further experiments showed a significant impairment of mutated $cTnT_{R131W,R205L,\Delta K210,D270N} - cTnI_{wildtype}$ and $cTnT_{R131W,R205L,\Delta K210,D270N} - cTnC_{wildtype}$ protein interactions compared to wildtype controls (t-test: $P < 0.001$) (Figure 18.4). Likewise a significant impairment of mutated $cTnC_{G159D} - cTnT_{wildtype}$protein interaction was observed while the interaction between $cTnC_{G159D} - cTnI_{wildtype}$ was significantly enhanced (P-values for both experiments <0.001). No significant change was observed following similar inter-troponin protein interaction studies of a recognized cTnT amino acid polymorphism, (K253R), which appeared with a frequency of 2.3% in controls and served as negative control in the test system. The test system has been used in several protein-protein interaction studies but has not previously been used to investigate sarcomeric contractile proteins.[78,79] The current results indicate that the assay may be helpful in providing supporting evidence to determine if an amino acid change identified in an affected individual is a disease causing mutation. The assay is

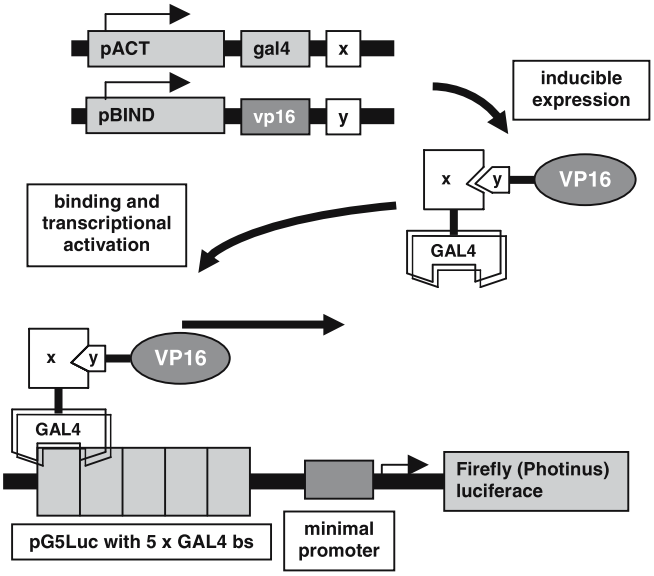

Figure 18.3. Schematic diagram of a mammalian two hybrid system for imaging the interaction of proteins X and Y adapted from Ray et al.[108] The first step involves the vectors pACT-gal4-x and pBIND-vp16-y, which are used to drive transcription of gal4-x and vp16-y through use of promoters ACT and BIND. In the second step, the two fusion proteins GAL4-X and VP16-Y interact because of the specificity of protein X for protein Y. Subsequently, GAL4-X-Y-VP16 binds to GAL4-binding sites on a pG5Luc reporter plasmid. This leads to VP16-mediated transactivation of firefly luciferase reporter gene expression under the control of GAL4 response promoter elements. Transcription of the firefly luciferase reporter gene generates firefly luciferase protein, which, in turn, leads to a detectable visible light signal (Photinus luciferase) in the presence of an appropriate substrate (D-luciferin). The pBIND vector expresses Renilla luciferase which allows normalizing the transfection efficiency when assaying Photinus luciferase activity by use of a dual–luciferase assay. It is important to conduct control experiments and investigate every combination of empty vector (X) versus fusion (Y) +/− mutation and the reverse to ensure trustworthy results.

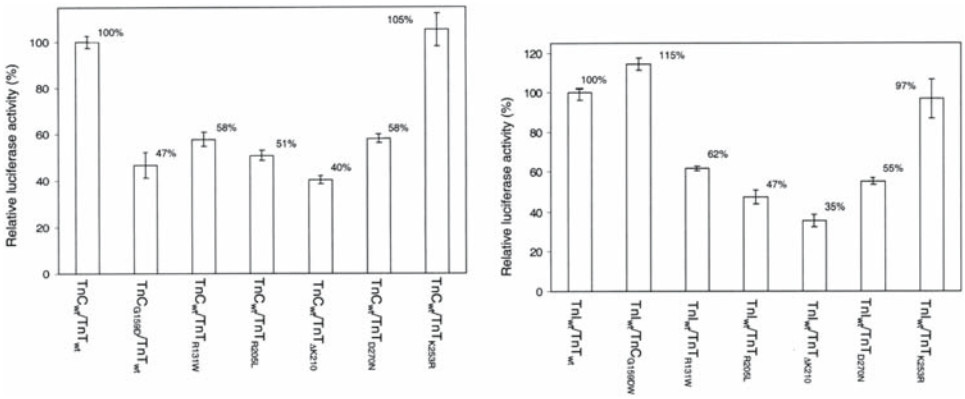

Figure 18.4. Effect of Troponin C ($cTnC_{G159D}$) and Troponin T ($cTnT_{R131W}$, $cTnT_{R205L}$, $cTnT_{\Delta K210}$, $cTnT_{D270N}$) mutations on inter-troponin interactions assessed by a mammalian two-hybrid assay.[46] All mutations impaired cTnT-cTnC and cTnT-cTnI interaction significantly (t-test: $P < 0.001$) compared to wildtype protein interaction ($cTnT_{WT}$, $cTnC_{WT}$, $cTnI_{WT}$). A recognized Troponin T polymorphism ($cTnT_{K253R}$) did not change inter-troponin interaction significantly compared to wildtype troponin interaction. Vertical bars indicate standard deviation.

qualitative in nature and can be used to observe changes in protein-protein interaction only. More sophisticated expression systems are needed to characterize the specific changes introduced by the mutation such as Ca^{++}-sensitivity, force generation, and energy metabolism.

18.3. HYPERTROPHIC CARDIOMYOPATHY

18.3.1. Diagnosis

The diagnosis of HCM relies on demonstration of unexplained myocardial hypertrophy by echocardiography.[1] Charron et al. investigated the ability of various diagnostic criteria to predict disease carriers in genotyped HCM families.[82] The authors concluded that the presence of one major echocardiographic criterion or one major ECG criterion was sufficient to diagnose HCM except for the presence of negative T waves on precordial leads in women. McKenna et al. suggested similar major diagnostic criteria based on many years of clinical experience working with HCM families and not the least by conducting several successful gene identification studies where the suggested diagnostic criteria proved their value.[18,83–85] These studies were undertaken by linkage analysis in which the basis for appointing a disease gene is correct phenotypic assessment. Only one individual falsely defined as being affected would invalidate the analysis and make it impossible to identify the disease causing gene.

18.3.2. Cardiac Troponin I Mutations in HCM

Cardiac Troponin I was identified as a disease gene in HCM by Kimura and co-workers in 1997.[23] They investigated 184 HCM families and identified 6 *TNNI3* mutations in 6 small families. The study focused on the genetic aspects of their findings and the clinical information referring to mutation carriers was spares (Table 18.4). The total number of affected individuals was 13 of whom 5 presented with apical hypertrophy and 8 had "hypertrophy characteristic of HCM". Three individuals carrying a Gly203Ser amino acid substitution also had an accessory conduction pathway known as the Wolf-Parkinson-White syndrome (WPW). Mörner et al. investigated 46 Caucasian HCM families and identified a 33 base-pair deletion (Gly203del) in a small pedigree with 3 affected individuals without significant symptoms except for a woman 78 years of age who suffered from dyspnoea (Table 18.4).[86,87] Kokado and co-workers investigated exon 7 of *TNNI3* in 130 HCM families and identified the same Lysine deletion (Lys183del) in 7 families including 25 mutation carriers.[88] The penetrance was high since 21 had echo abnormalities dominated by septal hypertrophy while 7 had impaired systolic function. Twenty-three had major ECG abnormalities. Seven individuals were reported to have died suddenly based on information obtained from relatives. No documentation was presented in relation to genotypic status, autopsy reports, death certificates, histological evaluation of myocardial specimens or any clinical data (ECG, echocardiogram) of the deceased. The finding of a significant number of families with the same mutation is unusual and it would be reasonable to consider if there was a common founder of the mutation. However, it was not reported if the affected families lived or originated from the same geographical area nor was haplotype analysis performed to reveal if the families were related. Niimura

Table 18.4. Clinical profile associated with *TNNI3* mutations in HCM and **RCM (in bold)**

Mutation	Individuals fulfilling diagnostic criteria/all mutation carriers	Echocardiography	Abnormal ECG	Ventricular arrhythmia	SCD
Arg141Gln (12)	2/6	2:1 ASH;1 BIV	2	1	–
Arg141Gln (90)	1/1	1:ASH	No data	No data	–
Arg141Gln (2)	No data*	No data	No data	No data	No data
Leu144Gln (100)	**1/1**	**1:RCM**	**1**	**–**	**–**
Arg145Trp (100)	**8/20**	**6:3 ASH;1 BIV;2 RCM**	**8**	**–**	**–**
Arg145Trp (100)	**1/1**	**1:RCM**	**1**	**–**	**–**
Arg145Gln (12)	1/5	1:Apical	1	–	–
Arg145Gln (23)	1/1	1:ASH	No data	No data	No data
Arg145Gly (23)	4/4	4:ASH	No data	No data	No data
Ala157Val (12)	5/12	2:2 ASH;2 ESD	5	2	1
Ala157Val (2)	No data*	No data	No data	No data	No data
Arg162Gln (12)	7/15	1:1 ASH;1 Apical	6	–	1
Arg162Gln (90)	2/2	2:2 ASH	No data	No data	No data
Arg162Trp (23)	2/2	2:Apical	No data	No data	No data
Arg162Pro (2)	No data*	No data	No data	No data	No data
Ser166Phe (12)	1/2	1:1 ASH	1	–	–
Ser166Phe (102)	3/3	3:3 ASH	No data	No data	–
Ser166Phe (89)	1/1	1:1 ASH	No data	No data	–
Ala171Thr (100)	**1/1**	**1:RCM**	**1**	**–**	**–**
Lys177Del (2)	No data*	No data	No data	No data	No data

Lys178Glu (100)	**1/1, de novo**	**1 : RCM**	**1**	**1**	**1**
Lys183Glu (12)	3/3	3 : 1 ASH;2 Apical	3	–	–
Lys183del (23)	2/2	1 Apical;1 without data	No data	No data	No data
Lys183del (88)	23/25	21 : 13 ASH,1 Apical,7 ESD	23	–	Uncertain
Arg186Gln (12)	5/11	3 : 2 ASH;1 ESD	4	1	2
Arg186Gln (2)	No data*	No data	No data	No data	No data
Asp190Gly (100)	**12/13**	**9 : 4 ASH;2 Apical;3 RCM**	**12**	**–**	**12**
Arg192His (100)	**1/1, de novo**	**1 : RCM**	**1**	**–**	**–**
Asp196Asn (12)	4/7	3 : 2ASH;1 Apical	4	–	–
Asp196Asn (26)	1/1	1 : 1ASH	1	–	–
Asp196Asn (2)	No data*	No data	No data	No data	No data
Ser199Asn (12)	8/13	4 : 4 Apical	7	–	2
Ser199Gly (12)	1/1	1 : 1 Apical	1	–	–
Glu202Gly (12)	1/1	1 : 1 ASH	1	–	–
Gly203Arg (12)	2/4	1 : 1 Apical	2	1	–
Gly203Ser (26)	3/3	3 : 3 Apical	3 WPW	No data	No data
Gly203del (86)	3/4	2 : 2 ASH	3	–	–
Lys206Gln (23)	1/1, De Novo	No data	No data	No data	No data

* Richard et al. identified 7 *TNNI3* mutations in 17 individuals and reported an average LVWT of 16.6 mm ± 3.3 mm following echocardiography. No further clinical data was available.

ASH, asymmetrical septal hypertrophy; BIV, bi-ventricular hypertrophy; ESD, end-stage dilatation; LV, left ventricle; NSVT, non sustained ventricular tachycardia; RCM, restrictive cardiomyopathy; SCD, sudden cardiac death; VF, ventricular fibrillation; – indicates absence of event.

investigated 31 HCM probands ≥40 years of age and identified 2 amino acid substitutions in 2 individuals (Table 18.4).[26] One of these substitutions (Pro82Ser) has in subsequent studies been identified in healthy control individuals of Afro-Caribbean origin and is therefore likely to be a polymorphism.[12] Erdman and colleagues investigated 108 HCM families of various ethnicities and identified one mutation (Ser166Phe) in a proband diagnosed at the age of 39 with septal hypertrophy of 14 mm.[89] The patient was also shown to carry an amino acid substitution in *MYH7* (C905F) which has not been identified in other HCM families. No segregation data was available and the impact of the *MYH7* amino acid substitution remained unknown. Richard and co-workers investigated 197 HCM patients and identified 7 mutations in 8 families with a total number of 17 affected individuals (Table 18.4).[2] The clinical information available was restricted to the average LV wall thickness estimated by echocardiography (16.2 mm ± 3.3 mm). The prognosis of the families was assessed based on information from relatives. Each family was allocated to one of three groups with malignant, intermediate, or benign prognosis dependent on the number of major cardiac events in the family defined as the number of sudden deaths, cardiac transplants, heart failure deaths, or stroke deaths before the age of 60. Based on this score system 3 of 6 families had a malignant and 3 of 6 families had a benign prognosis. Neither documentation of the cardiac events in the families leading to the applied prognostic grouping nor discussion of the validity of the score system in predicting prognosis of individual mutation carriers was presented. Van Driest and colleagues investigated 389 HCM probands and identified 6 mutations in 6 unrelated individuals (Table 18.4).[90] Investigations in relatives of affected probands were not performed except for recording a family history of sudden death. The majority of probands with *TNNI3* mutations had left ventricle outflow tract obstruction with a significant gradient which may reflect that the study was conducted at the Mayo clinic which is a major centre for surgical myectomi of patients with left ventricle outflow obstruction.

The clinical information available in previous studies was limited and based on observations in single patients or small numbers of HCM families with few affected individuals. Only limited information was available of the clinical disease expression in affected families. To evaluate familial disease expression we performed systematic clinical and genetic investigations of *TNNI3* in 748 HCM patients and their relatives.[12] In addition, we investigated the potential utility of genetic diagnosis in management and counselling of affected families. One hundred mutation carriers were identified in 23 families with 13 different mutations. All mutations were identified in exon 7 and 8 in consistency with previous findings investigating a total of 1.081 HCM patients in all protein encoding exons of *TNNI3*. Thus, the probability of identifying a mutation outside these exons would be less than 1 in 1.081 (<0.09%) and therefore it seems reasonable to limit mutation analysis of *TNNI3* to exon 7 and 8. Patients were diagnosed continuously from the second to eighth decade of life. The cardiac morphology observed in affected individuals ranged from mild ASH, apical and bi-ventricular hypertrophy to "end-stage" dilated HCM, and HCM with restrictive physiology. A similar degree of heterogeneity was observed in ECG abnormalities and the prevalence of arrhythmias. Four individuals died suddenly and 2 offspring of unaffected mutation carriers were resuscitated from cardiac arrest. Six individuals experienced other disease related deaths. The severity of disease in parents or siblings did not reflect disease expression of individual patients. Disease penetrance was 48% including probands and 33% when probands were omitted from the equation.

The extreme clinical heterogeneity of *TNNI3* mutations in relation to age of diagnosis, penetrance, morphology and prognosis indicate that follow-up of unaffected mutation carriers is warranted to decrease disease complications and sudden death. Knowledge of the genetic status enhances the ability to provide accurate counselling of clinically unaffected relatives. Individuals who are shown to carry the mutation can be informed that disease penetrance is 48%, that age of diagnosis is variable, and that clinically unaffected carriers are at risk of having affected offspring who may experience disease related complications. Finally, it is important to emphasise that individuals without the mutation have no risk of developing or passing the disease on to their offspring and that ongoing cardiovascular evaluation is unnecessary. Genetic diagnosis of *TNNI3* is technically feasible by investigation of 2 exons only and valuable in identifying individuals at risk of disease development and enhances the ability to provide accurate counselling of unaffected relatives.

The results of our study demonstrate that the clinical expression of *TNNI3* mutations is extremely heterogeneous within and between families with no apparent mutation or gene-specific disease pattern. Other genotype-phenotype studies have suggested that mutations in different HCM genes may be associated with a specific phenotype. Watkins and co-workers identified 8 families with *TNNT2* mutations following genetic investigations of 52 families, (prevalence 15%), and suggested that *TNNT2* mutations were associated with absent or mild cardiac hypertrophy and an adverse prognosis.[69] Subsequent studies have reported a more diverse phenotypic expression and a significant lower prevalence (2–4%) following investigations of much larger study populations.[2,89–91] Niimura and co-workers investigated a large number of HCM families recruited from many different referral centres worldwide for mutations in *MYBPC3*.[11] A total number of 212 genotype positive individuals were identified. No clinical data was available but it was reported that: "the extent and distribution of clinical symptoms and signs of cardiac hypertrophy in these patients appeared similar to those observed in patients with other mutations causing hypertrophy". The study was cross-sectional and no follow-up data of mutation carriers were available. Disease penetrance was defined by echocardiography only and reported as a percentage for various age groups and compared with similar penetrance percentages associated with unspecified mutations in *MYH7* and *TNNT2*. The age distribution of the study populations was not reported nor the absolute number of patients with *MYH7* and *TNNT2* mutations participating in the studies. The authors concluded that *MYBPC3* mutations were associated with a late onset of disease and a more favourable outcome when compared to unspecified mutations in *MYH7* and *TNNT2* although the data presented to support this hypothesis were modest. Specific mutations in *MYH7* have been reported with malignant or benign prognosis based on findings in highly selected families while subsequent studies of the same mutations in other patient populations have shown different results.[2,68,92–94] Evidence from growing numbers of genotype-phenotype studies suggest that the disease expression associated with specific mutations and specific disease genes is highly variable both within and between families. No specific genotype-phenotype correlation is apparent. The conclusions in previous studies suggesting a gene and mutation specific disease expression were based on investigations of relatively few families often with many affected individuals selected for gene identification studies. These families frequently originated from relatively isolated areas and did have a more uniform phenotype in relation to penetrance and sudden death (personal communication, Professor McKenna).[11,18,69,84] This led the investigators to suggest

that specific mutations did carry prognostic information and it was thought that knowledge of the specific mutation in an affected family would help in risk assessment for sudden death. As emphasized above subsequent studies have revealed that the disease course is independent of the specific mutation present in the family. It seems likely that the entire genetic constitution of an affected individual determines the severity of the disease expression and that families originating from isolated areas with a small gene pool tend to have a more uniform disease expression compared to families from urbanised areas with a much larger and diverse gene pool. In other words it is the entire genetic constitution of the family and of each individual that determines the disease expression and not the specific mutation itself.

There is no doubt that clinical investigations of families with hereditary conditions are demanding and interpretation of data is often difficult. A variety of selection bias will inevitably influence the results of the clinical investigations. For instance it may well be that families with many sudden deaths are more willing to participate in clinical screening than families with a more benign clinical appearance. Also it is often difficult to obtain complete data sets of deceased individuals and determine if they died of the condition or of other causes. In addition most studies are cross sectional in nature which makes it difficult to determine the age of disease onset and penetrance which ideally would require prospective evaluation of clinically unaffected mutation carriers.

The lack of precise information about death causes and the fact that it is impossible to obtain clinical data of all individuals in a family should lead to caution in using Kaplan-Meier survival curves to illustrate the prognosis of a specific mutation. Furthermore the value of comparing clinical disease expression of mutations identified in selected families from various patient populations seems limited. However, the results of our current investigation suggest that genetic diagnosis of *TNNI3* will aid clinical management and counselling of HCM patients and their families which justifies mutation analysis in clinical practice. The study reflects the challenges facing cardiologists in applying genetic advances to patient care and indicates that comprehensive genotype-phenotype studies of affected families are necessary before genetic diagnosis can be implemented.

18.4. RESTRICTIVE CARDIOMYOPATHY

18.4.1. Diagnosis

According to the diagnostic criteria proposed by WHO in 1995 idiopathic RCM is characterised by a restrictive filling pattern and reduced diastolic volume in the presence of normal to near-normal systolic function and wall thickness.[1]

18.4.2. Cardiac Troponin I Mutations in RCM

Familial RCM has been reported previously and histological examination of cardiac- or skeletal-muscle has in some cases revealed deposits of desmin-immuno-reactive material believed to be the disease causing agent.[95,96] However, mutations in specific disease genes have not been identified in these families. Other reports have identified mutations in the gene for desmin and desmin-deposits in patients with varying degrees of skeletal muscle myopathy, dilated cardiomyopathy and cardiac conduction defects. Interestingly,

several independent studies have identified the same desmin missense mutation in patients with pure DCM or isolated skeletal myopathy.[56,97,98] In 1992 Feld and Caspi reported a family with a mixed appearance of RCM and HCM.[99] The cardiac morphology of a deceased individual with RCM showed typical features of HCM with myocyte disarray. Angelina et al. reported similar morphological features of cardiac tissue following investigations of several patients with a clinical diagnosis of idiopathic RCM and suggested that RCM and HCM may represent 2 different phenotypes of the same basic sarcomeric disease.[29] We investigated a large family in which the proband and 2 additional individuals were diagnosed with idiopathic RCM, 9 individuals had clinical features of HCM and 12 individuals died suddenly.[100] Linkage analysis to selected sarcomeric contractile protein genes identified *TNNI3* as the likely disease gene. Subsequent mutation analysis revealed a missense mutation, which segregated with the disease in the family (lod score: 4.8). To elucidate if *TNNI3* mutations were common in RCM, mutation analysis was performed in 9 unrelated RCM patients with unexplained restrictive filling patterns, gross atrial dilatation, normal systolic function, and normal wall thickness. *TNNI3* mutations were identified in 7 of 10 patients including the index family of the study (Table 18.4). Two of the mutations identified in young individuals were de novo mutations. All mutations were novel missense mutations and appeared in conserved and functionally important domains of the gene. We concluded that mutations in cardiac Troponin I were responsible for the development of RCM in a significant proportion of patients diagnosed with idiopathic RCM. The findings imply that RCM is part of the clinical expression of hereditary sarcomeric contractile protein disease and familial evaluation should be considered when a diagnosis of RCM has been made.

18.5. DILATED CARDIOMYOPATHY

18.5.1. Diagnosis

A diagnosis of DCM should be reserved to patients with unexplained LV dilatation and impaired systolic function. However, the clinical disease expression is broad and includes arrhythmia, sudden death, stroke, and conduction disease which imply, like the scenario in HCM, that the chance of being affected in the presence of isolated mild dilatation, arrhythmia, or conduction disease is high in a family with relatives having a diagnosis of DCM.[3,101]

18.5.2. Sarcomeric Gene Mutations in DCM

Recently mutations in sarcomeric contractile protein genes were identified in DCM (Table 18.5). Olson and co-workers reported the finding of 2 *ACTC* mutations in two small DCM families with a total number of 6 affected individuals who were diagnosed at ages varying from 1–41 years.[47] No information about the total number of families investigated for mutations was available but subsequent studies did not identify any *ACTC* mutations in 225 DCM patients of various ethnic origins from Finland, Japan, and South African.[102–104] This indicated a low frequency of *ACTC* mutations in DCM. Olson et al. also identified 2 *TPM1* mutations in 2 DCM families with a total number of 3 affected individuals following investigation of the gene in 350 individuals.[48] Likewise, the affected

Table 18.5. Sarcomeric gene mutations in DCM with dominant inheritance

Disease gene	Mutations	Genotype positive individuals fulfilling DCM criteria/all mutation carriers	Presumed affected relatives without genotype	Number of probands screened for mutations
A–Cardiac	Arg312His (47)	3/4	–	No data
Actin	Glu361Gly (47)	3/4	–	No data
β–Myosin Heavy	Ala223Thr (52)	1/1	–	46
Chain	Ser642Leu (52)	1/1	1	
	Pro523Lys (49)	17/19	–	21
	Phe764Leu (49)	3/3	1	
Troponin T	Arg131Trp (46)	1/1	2	235
	Arg205Leu (46)	3/3	1	
	Del210Lys (46)	3/3	1	
	Arg141Trp (106)	15/20	17	1
	Del210Lys (49)	7/7	3	21
	Del210Lys (107)	1/2	5	114
Troponin C	Gly159Asp (46)	7/7	1	235
Myosin Binding Protein C	Asn948Thr (52)	1/1	–	46
α–Tropomyosin	Glu40Lys (48)	2/2	–	350
	Glu54Lys (48)	1/1	2	–
Titin	InsAG326 Stop330 (50)	12/15	4	2
	Trp930Arg (50)	9/9	3	–
	Val54Met (51)	1/1	–	120
	Ala743Val (51)	1/1	–	
	Glu4053ter (51)	1/1	–	
	Ser4465Asn (51)	1/1	–	
Troponin I	Ala2Val (45)	2/2	–	235

individuals with *TPM1* mutations were relatively young at diagnosis (1–33 years). Subsequent studies have not identified *TPM1* mutations in 67 DCM patients.[49,52] In 1999 Siu et al. identified a novel disease locus on chromosome 2q31 following linkage analysis in a large DCM family with 12 affected individuals.[105] The clinical data suggested an early-disease onset with a rapidly progressive course although some mutation carriers were clinically unaffected at the time of the investigation. Later, this family was identified with a disease causing mutation in the gene for titin (*TTN*) by Gerull and co-workers who in the same paper reported one additional *TTN* mutation in a large DCM family without accompanying clinical information.[50] Satoh et al. also reported 4 different *TTN* mutations in 4 DCM probands without information about other affected relatives.[51] Kamisago et al. identified two *MYH7*- and two *TNNT2*-mutations in four unrelated families following investigation of 21 DCM families.[49] They reported a severe and early disease onset and suggested that DCM mutations in genes encoding sarcomere proteins are prevalent as causes of cardiac dilatation and dysfunction in young people. However, no information

was available in relation to the criteria used to select families for genetic investigations. Li et al. identified a *TNNT2* mutation in a large family in which clinical data was available in 21 mutation carriers.[106] The authors reported that the mutation was associated with premature cardiac death, onset of cardiac symptoms predominant in the second decade of life, and a penetrance of about 75%. Two other studies have identified 2 *MYH7*-, 1 *MYBPC3*-, and 1 *TNNT2*- mutations in 3 probands and 1 small family with limited clinical information.[52,107]

We investigated the genes *TNNT2*, *TNNC1* and *TNNI3* encoding proteins of the troponin complex for mutations in 235 consecutive DCM patients.[45,46] Within the study cohort 43% (102/235) had one or more relatives with DCM identified by clinical investigation or a family history of premature cardiac death <40 years. Eighty-five percent of these families (87/102) exhibited an autosomal dominant mode of inheritance while the remaining 15% (15/102) transmitted the condition consistent with autosomal recessive inheritance. In families with dominant inheritance we identified one *TNNC1* mutation in one family and 4 *TNNT2* mutations in 4 families. In families with recessive inheritance we identified one *TNNI3* mutation. The frequency of Troponin mutations among patients with hereditary DCM was 6% (6/102). Twenty-three mutation carriers were identified of which 7 had transplants, 4 died form heart failure, 5 experienced sudden death, 6 remained stable on medication and 1 was unaffected. The penetrance of mutations in *TNNC1*, *TNNT2* and *TNNI3* was 100%. The average age of diagnosis was 29 (range: 16–52). Cardiac tissue was available in 9 patients for histological evaluation and showed typical features of DCM without significant myocyte disarray characteristic of hypertrophic cardiomyopathy. No patients had skeletal myopathy or cardiac conduction abnormalities. To substantiate that the sequence variations identified were disease associated mutations we performed functional protein-protein interaction studies by use of a qualitative mammalian expression system as mentioned previously. The results of these studies suggested that mutated protein interaction was altered compared to wildtype controls which may indicate in vivo dysfunction and lead to impaired myocardial contractility.

We identified *TNNC1* as a novel dominant DCM gene while *TNNI3* was revealed as the first recessive disease gene in DCM. The disease expression appeared malignant since 70% (16/23) of mutation carriers experienced premature cardiac death or received a cardiac transplant mostly by the fourth decade with an average duration of 6 months from diagnosis to event. Overall the clinical findings in these studies were comparable to the disease expression reported in other studies and left the impression that sarcomeric gene mutations in DCM are associated with a relatively early onset and adverse prognosis. However, this and other studies have reported the clinical findings in patients diagnosed over decades in which advances in pharmacological treatment have substantially improved the prognosis of heart failure patients. Although a limited number of DCM patients in our studies are currently alive with a relatively short observation period it is of note that their condition appears stable on modern pharmacological therapy with ACE-inhibitors and beta-blockers. The results of previous drug trials of heart failure patients have indicated a beneficial effect of prophylactic pharmacological therapy in asymptomatic individuals with impaired systolic function.[35,38] Therefore, it is reasonable to assume that early diagnosis and treatment of asymptomatic patients with hereditary DCM may also improve their prognosis.[37] The many premature cardiac deaths observed suggest that regular clinical investigation of relatives at risk of disease development is warranted to ensure early diagnosis. Genetic diagnosis would be helpful in identifying unaffected mutation carriers

who require follow-up and would enable termination of clinical screening of relatives with a normal genotype. In addition, knowledge of the specific disease gene and mutation present in a family may allow risk stratification although limited data are available in relation to sarcomeric gene mutations. So far, few families have been identified and only the genes for *ACTC*, *TPM1* and *TNNI3* have been fully investigated in large cohorts of DCM families with a frequency of mutations that account for less than 3% of all cases.[45–48] Most other patient populations studied were small in number with limited clinical information available and our findings re-emphasize the importance of designing genetic studies in larger DCM populations to describe the prevalence and associated clinical disease expression of these mutations.

18.6. CLINICAL UTILITY OF GENETIC DIAGNOSIS IN CARDIOMYOPATHIES

With advances in diagnostic molecular genetic techniques it is now feasible to perform high-throughput mutation analysis for use in clinical practice. Genetic investigation of recognised HCM genes is practical within a reasonable timeframe and will result in a genetic diagnosis in about 50–60% of unselected HCM probands.[2,90] The results of our investigations have shown that mutations in *TNNI3* are associated with an extreme heterogeneous disease expression and have emphasized that no specific genotype-phenotype correlation is apparent. Similar findings are emerging from investigations of other HCM genes. The fact that identical mutations in the same gene are associated with a diverse clinical expression in related as well as unrelated individuals underscores that HCM mutations in general do not carry prognostic information. This is in contrast to the conclusions of previous reports in which specific disease genes and mutations were found to be associated with a specific prognosis. However, the conclusions presented in papers from the early era of genetic investigations in HCM were largely based on findings in families with many affected individuals selected for gene identification studies. These families often originated from small and isolated communities with a limited gene pool and did have a more uniform clinical appearance than families living in urbanised areas with larger gene pools. Thus it is likely that the entire genetic constitution is an important determinant of the clinical disease expression implying that a uniform genetic background results in a uniform phenotype of the family and vice versa. The clinical lesson should be that information about the disease course of affected individuals in specific families may carry important information in relation to risk of sudden death and prognosis. This reflect that the disease expression is related to the integrated genetic constitution of the family and not restricted to a single mutation in a sarcomeric disease gene as anticipated previously. Recent studies of DCM patients have suggested a genetic predisposition in 30–50% of cases.[3] Numerous disease genes have been identified encoding proteins with a variety of different functions in the myocyte. Only few studies have investigated the prevalence of mutations and the associated disease expression in large cohorts of DCM patients to clarify the clinical relevance of gene testing. The results of our investigations suggest that the prevalence of troponin disease in familial DCM is about 6% and that investigation of these genes may be helpful to identify a subset of patients with severe disease expression and prognosis.[45,46] Clinical features of cardio-myopathies may be subtle even in individuals who develop severe disease related complications. Current routine clinical methods for cardiac evaluation including, 12 lead ECG, Holter monitoring, echocardiography, and

MRI may not identify all such individuals. The most definitive way to reveal individuals at risk of developing a cardiomyopathy is the identification of a disease causing mutation by genetic investigation of recognised disease genes. Establishment of a genetic diagnosis enables the physician to discharge non-carriers of the mutation since they are not at risk of developing the disease and to focus clinical resources on mutation carriers. The knowledge of an individuals carrier status help the physician to interpret symptoms and to choose appropriate investigations such as long term monitoring for arrhythmia. In addition to the clinical advantages of genetic diagnosis affected families often find it relieving to obtain an accurate answer to whether they do or do not carry a mutation. They are usually aware of the hereditary nature of the disease from other relatives and prefer clarification to the uncertainty of not knowing their carrier status. It is recommended clinical practice that cardiologists should inform their patients that cardiomyopathies may well be hereditary and that cardiac evaluation of relatives "at risk" is warranted to ensure early diagnosis and treatment to avoid severe complications and sudden death in otherwise undiagnosed individuals. However, the logistics of offering and performing family evaluation are not inconsiderable within the context of a routine cardiology clinic and ideally should involve a joint clinic with clinical geneticists. It is desirable to hand out written information about the disease to index patients at their first clinical visit including an offer of clinical investigation addressed to relatives at risk of having inherited the disease. In accordance with established ethical guidelines index patients should distribute the information and relatives return a reply slip to the department, which subsequently arrange clinical investigation if wanted. Relatives do often have questions following receipt of written information and it is important to have a contact person available who has knowledge of the disease. A specially trained and experienced nurse may serve as co-ordinator of the investigations and as contact person for the family. The follow-up scheme for healthy individuals is individualised and depends on the age of the person, the family history with respect to age of onset of disease and severity of disease expression including the number of sudden deaths.

It remains to be clarified if the costs of genetic investigations outweigh the savings of the health care system by termination of clinical screening of non-carriers. However, the fact that genetic investigations have become cheaper and less labour intensive within recent years make it likely that genetic diagnosis will be increasingly cost-effective for the health care system. Physicians with knowledge of both genetic and clinical aspects of the disease are needed to inform patients about the results and implication of the genetic investigations in close collaboration with clinical geneticists to ensure adequate counselling of patients. There is no doubt that the number of diseases in which genetic diagnosis will have clinical consequences for patients will continue to increase and training of physicians in the aspects of genetics and counselling is important. The implementation of genetic diagnosis into clinical practice is challenging but once in place has the potential to benefit clinical diagnosis and management.

18.7. REFERENCES

1. P. Richardson, W. McKenna, M. Bristow, B. Maisch, B. Mautner, J. O'Connell, E. Olsen, G. Thiene, J. Goodwin, I. Gyarfas, I. Martin, and P. Nordet, Report of the 1995 World Health Organization/International Society and Federation of Cardiology Task Force on the Definition and Classification of cardiomyopathies, *Circulation* **93**, 841–842 (1996).

2. P. Richard, P. Charron, L. Carrier, C. Ledeuil, T. Cheav, C. Pichereau, A. Benaiche, R. Isnard, O. Dubourg, M. Burban, J. P. Gueffet, A. Millaire, M. Desnos, K. Schwartz, B. Hainque, and M. Komajda, Hypertrophic cardiomyopathy: distribution of disease genes, spectrum of mutations, and implications for a molecular diagnosis strategy, *Circulation* **107**(17), 2227–2232.
3. L. Mestroni, C. Rocco, D. Gregori, G. Sinagra, L. A. Di, S. Miocic, M. Vatta, B. Pinamonti, F. Muntoni, A. L. Caforio, W. J. Mckenna, A. Falaschi, and M. Giacca, Familial dilated cardiomyopathy: evidence for genetic and phenotypic heterogeneity. Heart Muscle Disease Study Group, *J. Am. Coll. Cardiol.* **34**, 181–190 (1897).
4. M. S. Hamid, M. Norman, A. Quraishi, S. Firoozi, R. Thaman, J. R. Gimeno, B. Sachdev, E. Rowland, P. M. Elliott, and W. J. McKenna, Prospective evaluation of relatives for familial arrhythmogenic right ventricular cardiomyopathy/dysplasia reveals a need to broaden diagnostic criteria, *J. Am. Coll. Cardiol.* **40**, 1445–1450 (2002).
5. B. J. Maron, J. M. Gardin, J. M. Flack, S. S. Gidding, T. T. Kurosaki, and D. E. Bild, Prevalence of hypertrophic cardiomyopathy in a general population of young adults. Echocardiographic analysis of 4111 subjects in the CARDIA Study. Coronary Artery Risk Development in (Young) Adults, *Circulation* **92**, 785–789 (1995).
6. B. J. Maron, J. S. Gottdiener, and S. E. Epstein, Patterns and significance of distribution of left ventricular hypertrophy in hypertrophic cardiomyopathy. A wide angle, two dimensional echocardiographic study of 125 patients, *Am. J. Cardiol.* **48**, 418–428 (1981).
7. H. G. Klues, A. Schiffers, and B. J. Maron, Phenotypic spectrum and patterns of left ventricular hypertrophy in hypertrophic cardiomyopathy: morphologic observations and significance as assessed by two-dimensional echocardiography in 600 patients, *J. Am. Coll. Cardiol.* **26**, 1699–1708 (1995).
8. B. J. Maron, R. O. Bonow, R. O. Cannon 3rd, M. B. Leon, and S. E. Epstein, Hypertrophic cardiomyopathy. Interrelations of clinical manifestations, pathophysiology, and therapy (2), *N. Engl. J. Med.* **316**, 844–852 (1987).
9. P. Spirito, and B. J. Maron, Patterns of systolic anterior motion of the mitral valve in hypertrophic cardiomyopathy: assessment by two-dimensional echocardiography, *Am. J. Cardiol.* **54**, 1039–1046 (1984).
10. B. J. Maron, P. Spirito, Y. Wesley, and J. Arce, Development and progression of left ventricular hypertrophy in children with hypertrophic cardiomyopathy, *N. Engl. J. Med.* **315**, 610–614 (1986).
11. H. Niimura, L. L. Bachinski, S. Sangwatanaroj, H. Watkins, A. E. Chudley, W. McKenna, A. Kristinsson, R. Roberts, M. Sole, B. J. Maron, J. G. Seidman, and C. E. Seidman, Mutations in the gene for cardiac myosin-binding protein C and late- onset familial hypertrophic cardiomyopathy [see comments], *N. Engl. J. Med.* **338**, 1248–1257 (1998).
12. J. Mogensen, R. T. Murphy, T. Kubo, A. Bahl, J. C. Moon, I. C. Klausen, P. M. Elliott, and W. J. McKenna, Frequency and clinical expression of cardiac troponin I mutations in 748 consecutive families with hypertrophic cardiomyopathy, *J. Am. Coll. Cardiol.* **44**, 2315–2325 (2004).
13. P. M. Elliott, J. Poloniecki, S. Dickie, S. Sharma, L. Monserrat, A. Varnava, N. G. Mahon, and W. J. McKenna, Sudden death in hypertrophic cardiomyopathy: identification of high risk patients, *J. Am. Coll. Cardiol.* **36**(7), 2212–2218 (2000).
14. B. J. Maron, J. Shirani, L. C. Poliac, R. Mathenge, W. C. Roberts, and F. O. Mueller, Sudden death in young competitive athletes. Clinical, demographic, and pathological profiles [see comments], *JAMA* **276**, 199–204 (1996).
15. B. J. Maron, W. K. Shen, M. S. Link, A. E. Epstein, A. K. Almquist, J. P. Daubert, G. H. Bardy, S. Favale, R. F. Rea, G. Boriani, N. A. Estes, and P. Spirito, Efficacy of implantable cardioverter-defibrillators for the prevention of sudden death in patients with hypertrophic cardiomyopathy, *N. Engl. J. Med.* **342**(6), 365–373 (2000).
16. P. M. Elliott, S. Sharma, A. Varnava, J. Poloniecki, E. Rowland, and W. J. McKenna, Survival after cardiac arrest or sustained ventricular tachycardia in patients with hypertrophic cardiomyopathy, *J. Am. Coll. Cardiol.* **33**, 1596–1601 (1999).
17. B. J. Maron, W. J. McKenna, G. K. Danielson, L. J. Kappenberger, H. J. Kuhn, C. E. Seidman, P. M. Shah, W. H. Spencer III, P. Spirito, F. J. TenCate, E. D. Wigle, R. A. Vogel, J. Abrams, E. R. Bates, B. R. Brodie, P. G. Danias, G. Gregoratos, M. A. Hlatky, J. S. Hochman, S. Kaul, R. C. Lichtenberg, J. R. Lindner, R. A. O'Rourke, G. M. Pohost, R. S. Schofield, C. M. Tracy, W. L. Winters, Jr., W. W. Klein, S. G. Priori, A. Alonso-Garcia, C. Blimstrom-Lundqvist, G. De Backer, J. Deckers, M. Flather, J. Hradec, A. Oto, A. Parkhomenko, S. Silber, and A. Torbicki, American College of Cardiology/European Society

of Cardiology Clinical Expert Consensus Document on Hypertrophic Cardiomyopathy. A report of the American College of Cardiology Foundation Task Force on Clinical Expert Consensus Documents and the European Society of Cardiology Committee for Practice Guidelines, *Eur. Heart J.* **24**, 1965–1991 (2003).

18. A. A. Geisterfer-Lowrance, S. Kass, G. Tanigawa, H. P. Vosberg, W. McKenna, C. E. Seidman, and J. G. Seidman, A molecular basis for familial hypertrophic cardiomyopathy: a beta cardiac myosin heavy chain gene missense mutation, *Cell* **62**, 999–1006 (1990).
19. L. Thierfelder, H. Watkins, C. MacRae, R. Lamas, W. McKenna, H. P. Vosberg, J. G. Seidman, and C. E. Seidman, Alpha-tropomyosin and cardiac troponin T mutations cause familial hypertrophic cardiomyopathy: a disease of the sarcomere, *Cell* **77**, 701–712 (1994).
20. G. Bonne, L. Carrier, J. Bercovici, C. Cruaud, P. Richard, B. Hainque, M. Gautel, S. Labeit, M. James, J. Beckmann, J. Weissenbach, H. P. Vosberg, M. Fiszman, M. Komajda, and K. Schwartz, Cardiac myosin binding protein-C gene splice acceptor site mutation is associated with familial hypertrophic cardiomyopathy, *Nat. Genet*. **11**, 438–440 (1995).
21. H. Watkins, D. Conner, L. Thierfelder, J. A. Jarcho, C. MacRae, W. J. McKenna, B. J. Maron, J. G. Seidman, and C. E. Seidman, Mutations in the cardiac myosin binding protein-C gene on chromosome 11 cause familial hypertrophic cardiomyopathy, *Nat. Genet*. **11**, 434–437 (1995).
22. K. Poetter, H. Jiang, S. Hassanzadeh, S. R. Master, A. Chang, M. C. Dalakas, I. Rayment, J. R. Sellers, L. Fananapazir, and N. D. Epstein, Mutations in either the essential or regulatory light chains of myosin are associated with a rare myopathy in human heart and skeletal muscle, *Nat. Genet.* **13**, 63–69 (1996).
23. A. Kimura, H. Harada, J. E. Park, H. Nishi, M. Satoh, M. Takahashi, S. Hiroi, T. Sasaoka, N. Ohbuchi, T. Nakamura, T. Koyanagi, T. H. Hwang, J. A. Choo, K. S. Chung, A. Hasegawa, R. Nagai, O. Okazaki, H. Nakamura, M. Matsuzaki, T. Sakamoto, H. Toshima, Y. Koga, T. Imaizumi, and T. Sasazuki, Mutations in the cardiac troponin I gene associated with hypertrophic cardiomyo-pathy, *Nat. Genet*. **16**, 379–382 (1997).
24. B. Hoffmann, H. Schmidt-Traub, A. Perrot, K. J. Osterziel, and R. Gessner, First mutation in cardiac troponin C, L29Q, in a patient with hypertrophic cardiomyopathy, *Hum. Mutat*. **17**(6), 524 (2001).
25. M. Satoh, M. Takahashi, T. Sakamoto, M. Hiroe, F. Marumo, and A. Kimura, Structural analysis of the titin gene in hypertrophic cardiomyopathy: identification of a novel disease gene, *Biochem. Biophys. Res. Commun.* **262**, 411–417 (1999).
26. H. Niimura, K. K. Patton, W. J. McKenna, J. Soults, B. J. Maron, J. G. Seidman, and C. E. Seidman, Sarcomere protein gene mutations in hypertrophic cardiomyopathy of the elderly, *Circulation* **105**(4), 446–451 (2002).
27. C. Geier, A. Perrot, C. Ozcelik, P. Binner, D. Counsell, K. Hoffmann, B. Pilz, Y. Martiniak, K. Gehmlich, P. F. van der Ven, D. O. Furst, A. Vornwald, E. von Hodenberg, P. Nurnberg, T. Scheffold, R. Dietz, and K. J. Osterziel, Mutations in the human muscle LIM protein gene in families with hypertrophic cardiomyopathy, *Circulation* **107**(10), 1390–1395 (2003).
28. A. Keren, and R. L. Popp, Assignment of patients into the classification of cardiomyopathies, *Circulation* **86**, 1622–1633 (1992).
29. A. Angelini, V. Calzolari, G. Thiene, G. M. Boffa, M. Valente, L. Daliento, C. Basso, F. Calabrese, R. Razzolini, U. Livi, and R. Chioin, Morphologic spectrum of primary restrictive cardiomyopathy, *Am. J. Cardiol.* **80**, 1046–1050 (1997).
30. M. J. Saraiva, Hereditary transthyretin amyloidosis: molecular basis and therapeutical strategies, *Expert Rev. Mol. Med.* **2002**, 1–11 (2002).
31. J. A. Towbin, and N. E. Bowles, The failing heart, *Nature* **415**(6868), 227–233 (2002).
32. L. Mestroni, B. Maisch, W. J. McKenna, K. Schwartz, P. Charron, C. Rocco, F. Tesson, A. Richter, A. Wilke, and M. Komajda, Guidelines for the study of familial dilated cardiomyopathies. Collaborative Research Group of the European Human and Capital Mobility Project on Familial Dilated Cardiomyopathy, *Eur. Heart J.* **20**, 93–102 (1999).
33. M. B. Codd, D. D. Sugrue, B. J. Gersh, and L. J. Melton, Epidemiology of idiopathic dilated and hypertrophic cardiomyopathy. A population-based study in Olmsted County, Minnesota, 1975–1984. *Circulation* **80**, 564–572 (1989).
34. J. N. Cohn, M. R. Bristow, K. R. Chien, W. S. Colucci, O. H. Frazier, L. A. Leinwand, B. H. Lorell, A. J. Moss, E. H. Sonnenblick, R. A. Walsh, S. C. Mockrin, and L. Reinlib, Report of the national heart,

lung, and blood institute special emphasis panel on heart failure research, *Circulation* **95**, 766–770 (1997).
35. Effect of enalapril on mortality and the development of heart failure in asymptomatic patients with reduced left ventricular ejection fractions. The SOLVD Investigattors, *N. Engl. J. Med.* **327**, 685–691 (1992).
36. M. A. Pfeffer, E. Braunwald, L. A. Moye, L. Basta, E. J. J. Brown, T. E. Cuddy, B. R. Davis, E. M. Geltman, S. Goldman, and G. C. Flaker, Effect of captopril on mortality and morbidity in patients with left ventricular dysfunction after myocardial infarction. Results of the survival and ventricular enlargement trial. The SAVE Investigators, *N. Engl. J. Med.* **327**, 669–677 (1992).
37. F. Waagstein, M. R. Bristow, K. Swedberg, F. Camerini, M. B. Fowler, M. A. Silver, E. M. Gilbert, M. R. Johnson, F. G. Goss, and A. Hjalmarson, Beneficial effects of metoprolol in idiopathic dilated cardiomyopathy. Metoprolol in Dilated Cardiomyopathy (MDC) Trial Study Group, *Lancet* **342**, 1441–1446 (1993).
38. P. A. Poole-Wilson, K. Swedberg, J. G. Cleland, L. A. Di, P. Hanrath, M. Komajda, J. Lubsen, B. Lutiger, M. Metra, W. J. Remme, C. Torp-Pedersen, A. Scherhag, and A. Skene, Comparison of carvedilol and metoprolol on clinical outcomes in patients with chronic heart failure in the Carvedilol Or Metoprolol European Trial (COMET): randomised controlled trial, *Lancet* **362**(9377), 7–13 (2003).
39. J. G. Cleland, D. J. Pennell, S. G. Ray, A. J. Coats, P. W. Macfarlane, G. D. Murray, J. D. Mule, Z. Vered, and A. Lahiri, Myocardial viability as a determinant of the ejection fraction response to carvedilol in patients with heart failure (CHRISTMAS trial): randomised controlled trial, *Lancet* **362**(9377), 14–21 (2003).
40. S. G. Molhoek, J. J. Bax, L. van Erven, M. Bootsma, E. Boersma, P. Steendijk, E. E. Van der Wall, and M. J. Schalij, Comparison of benefits from cardiac resynchronization therapy in patients with ischemic cardiomyopathy versus idiopathic dilated cardiomyopathy, *Am. J. Cardiol.* **93**, 860–863 (2004).
41. P. T. Mortensen, P. Sogaard, H. Mansour, J. Ponsonaille, D. Gras, A. Lazarus, W. Reiser, C. Alonso, C. M. Linde, M. Lunati, B. Kramm, and E. M. Harrison, Sequential biventricular pacing: evaluation of safety and efficacy, *Pacing Clin. Electrophysiol.* **27**, 339–345 (2004).
42. J. J. Blanc, V. Bertault-Valls, M. Fatemi, M. Gilard, P. Y. Pennec, and Y. Etienne, Midterm benefits of left univentricular pacing in patients with congestive heart failure, *Circulation* **109**, 1741–1744 (2004).
43. A. Auricchio, C. Stellbrink, C. Butter, S. Sack, J. Vogt, A. R. Misier, D. Bocker, M. Block, J. H. Kirkels, A. Kramer, and E. Huvelle, Clinical efficacy of cardiac resynchronization therapy using left ventricular pacing in heart failure patients stratified by severity of ventricular conduction delay, *J. Am. Coll. Cardiol.* **42**, 2109–2116 (2003).
44. J. G. Seidman, and C. Seidman, The genetic basis for cardiomyopathy: from mutation identification to mechanistic paradigms, *Cell* **104**(4), 557–567 (2001).
45. R. T. Murphy, J. Mogensen, A. Shaw, T. Kubo, S. Hughes, and W. J. McKenna, Novel mutation in cardiac troponin I in recessive idiopathic dilated cardiomyopathy, *Lancet* **363**, 371–372 (2004).
46. J. Mogensen, R. T. Murphy, T. Shaw, A. Bahl, C. Redwood, H. Watkins, M. Burke, P. M. Elliott, and W. J. McKenna, Severe disease expression of cardiac troponin C and T mutations in patients with idiopathic dilated cardiomyopathy, *J. Am. Coll. Cardiol.* **44**, 2033–2040 (2004).
47. T. M. Olson, V. V. Michels, S. N. Thibodeau, Y. S. Tai, and M. T. Keating, Actin mutations in dilated cardiomyopathy, a heritable form of heart failure, *Science* **280**, 750–752 (1998).
48. T. M. Olson, N. Y. Kishimoto, F. G. Whitby, and V. V. Michels, Mutations that alter the surface charge of alpha-tropomyosin are associated with dilated cardiomyopathy, *J. Mol. Cell Cardiol.* **33**(4), 723–732 (2001).
49. M. Kamisago, S. D. Sharma, S. R. DePalma, S. Solomon, P. Sharma, B. McDonough, L. Smoot, M. P. Mullen, P. K. Woolf, E. D. Wigle, J. G. Seidman, and C. E. Seidman, Mutations in sarcomere protein genes as a cause of dilated cardiomyopathy, *N. Engl. J. Med.* **343**(23), 1688–1696 (2000).
50. B. Gerull, M. Gramlich, J. Atherton, M. McNabb, K. Trombitas, S. Sasse-Klaassen, J. G. Seidman, C. Seidman, H. Granzier, S. Labeit, M. Frenneaux, and L. Thierfelder, Mutations of TTN, encoding the giant muscle filament titin, cause familial dilated cardiomyopathy, *Nat. Genet.* **30**(2), 201–204 (2002).
51. M. Itoh-Satoh, T. Hayashi, H. Nishi, Y. Koga, T. Arimura, T. Koyanagi, M. Takahashi, S. Hohda, K. Ueda, T. Nouchi, M. Hiroe, F. Marumo, T. Imaizumi, M. Yasunami, and A. Kimura, Titin mutations as the molecular basis for dilated cardiomyopathy, *Biochem. Biophys. Res. Commun.* **291**, 385–393 (2002).

52. S. Daehmlow, J. Erdmann, T. Knueppel, C. Gille, C. Froemmel, M. Hummel, R. Hetzer, and V. Regitz-Zagrosek, Novel mutations in sarcomeric protein genes in dilated cardiomyopathy, *Biochem. Biophys. Res. Commun.* **298**(1), 116–120 (2002).
53. R. Knoll, M. Hoshijima, H. M. Hoffman, V. Person, I. Lorenzen-Schmidt, M. L. Bang, T. Hayashi, N. Shiga, H. Yasukawa, W. Schaper, W. McKenna, M. Yokoyama, N. J. Schork, J. H. Omens, A. D. McCulloch, A. Kimura, C. C. Gregorio, W. Poller, J. Schaper, H. P. Schultheiss, and K. R. Chien, The cardiac mechanical stretch sensor machinery involves a Z disc complex that is defective in a subset of human dilated cardiomyopathy, *Cell* **111**(7), 943–955 (2002).
54. D. Fatkin, C. MacRae, T. Sasaki, M. R. Wolff, M. Porcu, M. Frenneaux, J. Atherton, H. J. J. Vidaillet, S. Spudich, G. U. De, et al., Missense mutations in the rod domain of the lamin A/C gene as causes of dilated cardiomyopathy and conduction-system disease, *N. Engl. J. Med.* **341**, 1715–1724 (1897).
55. S. Bione, E. Maestrini, S. Rivella, M. Mancini, S. Regis, G. Romeo, and D. Toniolo, Identification of a novel X-linked gene responsible for Emery-Dreifuss muscular dystrophy, *Nat. Genet.* **8**, 323–327 (1994).
56. D. Li, T. Tapscoft, O. Gonzalez, P. E. Burch, M. A. Quinones, W. A. Zoghbi, R. Hill, L. L. Bachinski, D. L. Mann, and R. Roberts, Desmin mutation responsible for idiopathic dilated cardiomyopathy, *Circulation* **100**, 461–464 (1897).
57. S. Tsubata, K. R. Bowles, M. Vatta, C. Zintz, J. Titus, L. Muhonen, N. E. Bowles, and J. A. Towbin, Mutations in the human delta-sarcoglycan gene in familial and sporadic dilated cardiomyopathy, *J. Clin. Invest.* **106**(5), 655–662 (2000).
58. F. Muntoni, M. Cau, A. Ganau, R. Congiu, G. Arvedi, A. Mateddu, M. G. Marrosu, C. Cianchetti, G. Realdi, and A. Cao, Brief report: deletion of the dystrophin muscle-promoter region associated with X-linked dilated cardiomyopathy, *N. Engl. J. Med.* **329**, 921–925 (1993).
59. E. E. Norgett, S. J. Hatsell, L. Carvajal-Huerta, J. C. Cabezas, J. Common, P. E. Purkis, N. Whittock, I. M. Leigh, H. P. Stevens, and D. P. Kelsell, Recessive mutation in desmoplakin disrupts desmoplakin-intermediate filament interactions and causes dilated cardiomyopathy, woolly hair and keratoderma, *Hum. Mol. Genet.* **9**, 2761–2766 (2000).
60. T. M. Olson, S. Illenberger, N. Y. Kishimoto, S. Huttelmaier, M. T. Keating, and B. M. Jockusch, Metavinculin mutations alter actin interaction in dilated cardiomyopathy, *Circulation* **105**(4), 431–437 (2002).
61. B. Mohapatra, S. Jimenez, J. H. Lin, K. R. Bowles, K. J. Coveler, J. G. Marx, M. A. Chrisco, R. T. Murphy, P. R. Lurie, R. J. Schwartz, P. M. Elliott, M. Vatta, W. McKenna, J. A. Towbin, and N. E. Bowles, Mutations in the muscle LIM protein and alpha-actinin-2 genes in dilated cardiomyopathy and endocardial fibroelastosis, *Mol. Genet. Metab.* **80**, 207–215 (2003).
62. M. Vatta, B. Mohapatra, S. Jimenez, X. Sanchez, G. Faulkner, Z. Perles, G. Sinagra, J. H. Lin, T. M. Vu, Q. Zhou, K. R. Bowles, A. Di Lenarda, L. Schimmenti, M. Fox, M. A. Chrisco, R. T. Murphy, W. McKenna, P. Elliott, N. E. Bowles, J. Chen, G. Valle, and J. A. Towbin, Mutations in Cypher/ZASP in patients with dilated cardiomyopathy and left ventricular non-compaction, *J. Am. Coll. Cardiol.* **42**, 2014–2027 (2003).
63. J. P. Schmitt, M. Kamisago, M. Asahi, G. H. Li, F. Ahmad, U. Mende, E. G. Kranias, D. H. MacLennan, J. G. Seidman, and C. E. Seidman, Dilated cardiomyopathy and heart failure caused by a mutation in phospholamban, *Science* **299**(5611), 1410–1413 (2003).
64. M. Bienengraeber, T. M. Olson, V. A. Selivanov, E. C. Kathmann, F. O'Cochlain, F. Gao, A. B. Karger, J. D. Ballew, D. M. Hodgson, L. V. Zingman, Y. P. Pang, A. E. Alekseev, and A. Terzic, ABCC9 mutations identified in human dilated cardiomyopathy disrupt catalytic KATP channel gating, *Nat. Genet.* **36**, 382–387 (2004).
65. F. Ichida, S. Tsubata, K. R. Bowles, N. Haneda, K. Uese, T. Miyawaki, W. J. Dreyer, J. Messina, H. Li, N. E. Bowles, and J. A. Towbin, Novel gene mutations in patients with left ventricular noncompaction or Barth syndrome, *Circulation* **103**(9), 1256–1263 (2001).
66. R. Chen, T. Tsuji, F. Ichida, K. R. Bowles, X. Yu, S. Watanabe, K. Hirono, S. Tsubata, Y. Hamamichi, J. Ohta, Y. Imai, N. E. Bowles, T. Miyawaki, and J. A. Towbin, Mutation analysis of the G4.5 gene in patients with isolated left ventricular noncompaction, *Mol. Genet. Metab.* **77**(4), 319–325 (2002).
67. A. Suomalainen, A. Paetau, H. Leinonen, A. Majander, L. Peltonen, and H. Somer, Inherited idiopathic dilated cardiomyopathy with multiple deletions of mitochondrial DNA, *Lancet* **340**, 1319–1320 (1992).

68. H. Watkins, A. Rosenzweig, D. S. Hwang, T. Levi, W. McKenna, C. E. Seidman, and J. G. Seidman, Characteristics and prognostic implications of myosin missense mutations in familial hypertrophic cardiomyopathy, *N. Engl. J. Med.* **326**, 1108–1114 (1992).
69. H. Watkins, W. J. McKenna, L. Thierfelder, H. J. Suk, R. Anan, A. O'Donoghue, P. Spirito, A. Matsumori, C. S. Moravec, C. Seidman, and J. G. Seidman, Mutations in the genes for cardiac troponin T and alpha-tropomyosin in hypertrophic cardiomyopathy, *N. Engl. J. Med.* **332**, 1058–1064 (1995).
70. A. Kumar, K. Crawford, L. Close, M. Madison, J. Lorenz, T. Doetschman, S. Pawlowski, J. Duffy, J. Neumann, J. Robbins, G. P. Boivin, B. A. O'Toole, and J. L. Lessard, Rescue of cardiac alpha-actin-deficient mice by enteric smooth muscle gamma-actin, *Proc. Natl. Acad. Sci. USA* **94**, 4406–4411 (1997).
71. J. James, Y. Zhang, H. Osinska, A. Sanbe, R. Klevitsky, T. E. Hewett, and J. Robbins, Transgenic modeling of a cardiac troponin I mutation linked to familial hypertrophic cardiomyopathy, *Circ. Res.* **87**(9), 805–811 (2000).
72. M. Muthuchamy, K. Pieples, P. Rethinasamy, B. Hoit, I. L. Grupp, G. P. Boivin, B. Wolska, C. Evans, R. J. Solaro, and D. F. Wieczorek, Mouse model of a familial hypertrophic cardiomyopathy mutation in alpha- tropomyosin manifests cardiac dysfunction, *Circ. Res.* **85**, 47–56 (1999).
73. D. Burton, H. Abdulrazzak, A. Knott, K. Elliott, C. Redwood, H. Watkins, S. Marston, and C. Ashley, Two mutations in troponin I that cause hypertrophic cardiomyopathy have contrasting effects on cardiac muscle contractility, *Biochem. J.* **362**(Pt2), 443–451 (2002).
74. K. Elliott, H. Watkins, and C. S. Redwood, Altered regulatory properties of human cardiac troponin I mutants that cause hypertrophic cardiomyopathy, *J. Biol. Chem.* **275**(29), 22069–22074 (2000).
75. A. Hinkle, and L. S. Tobacman, Folding and function of the troponin tail domain. Effects of cardiomyopathic troponin T mutations, *J. Biol. Chem.* **278**, 506–513 (2003).
76. R. Lang, A. V. Gomes, J. Zhao, P. R. Housmans, T. Miller, and J. D. Potter, Functional analysis of a troponin I (R145G) mutation associated with familial hypertrophic cardiomyopathy, *J. Biol. Chem.* **277**(14), 11670–11678 (2002).
77. S. Morimoto, Q. W. Lu, K. Harada, F. Takahashi-Yanaga, R. Minakami, M. Ohta, T. Sasaguri, and I. Ohtsuki, Ca(2+)-desensitizing effect of a deletion mutation Delta K210 in cardiac troponin T that causes familial dilated cardiomyopathy, *Proc. Natl. Acad. Sci. USA* **99**(2), 913–918 (2002).
78. Y. Nakamura, H. Suzuki, M. Sakaguchi, and K. Mihara, Targeting and assembly of rat mitochondrial translocase of outer membrane 22 (TOM22) into the TOM complex, *J. Biol. Chem.* **279**, 21223–21232 (2004).
79. C. Y. Hong, J. H. Park, R. S. Ahn, S. Y. Im, H. S. Choi, J. Soh, S. H. Mellon, and K. Lee, Molecular mechanism of suppression of testicular steroidogenesis by proinflammatory cytokine tumor necrosis factor alpha, *Mol. Cell. Biol.* **24**, 2593–2604 (2004).
80. A. A. Hagege, O. Dubourg, M. Desnos, R. Mirochnik, G. Isnard, G. Bonne, L. Carrier, P. Guicheney, J. B. Bouhour, K. Schwartz, and M. Komajda, Familial hypertrophic cardiomyopathy. Cardiac ultrasonic abnormalities in genetically affected subjects without echocardiographic evidence of left ventricular hypertrophy, *Eur. Heart J.* **19**, 490–499 (1998).
81. J. Mogensen, I. C. Klausen, A. K. Pedersen, H. Egeblad, P. Bross, T. A. Kruse, N. Gregersen, P. S. Hansen, U. Baandrup, and A. D. Borglum, Alpha-cardiac actin is a novel disease gene in familial hypertrophic cardiomyopathy, *J. Clin. Invest.* **103**, R39–R43 (1999).
82. P. Charron, O. Dubourg, M. Desnos, R. Isnard, A. Hagege, A. Millaire, L. Carrier, G. Bonne, F. Tesson, P. Richard, J. B. Bouhour, K. Schwartz, and M. Komajda, Diagnostic value of electrocardiography and echocardiography for familial hypertrophic cardiomyopathy in a genotyped adult population, *Circulation* **96**, 214–219 (1997).
83. L. Thierfelder, C. MacRae, H. Watkins, J. Tomfohrde, M. Williams, W. McKenna, K. Bohm, G. Noeske, M. Schlepper, A. Bowcock, H. Vosberg, J. G. Seidman, and C. Seidman, A familial hypertrophic cardiomyopathy locus maps to chromosome 15q2, *Proc. Natl. Acad. Sci. USA* **90**, 6270–6274 (1993).
84. H. Watkins, C. MacRae, L. Thierfelder, Y. H. Chou, M. Frenneaux, W. McKenna, J. G. Seidman, and C. E. Seidman, A disease locus for familial hypertrophic cardiomyopathy maps to chromosome 1q3, *Nat. Genet.* **3**, 333–337 (1993).
85. W. J. McKenna, P. Spirito, M. Desnos, O. Dubourg, and M. Komajda, Experience from clinical genetics in hypertrophic cardiomyopathy: proposal for new diagnostic criteria in adult members of affected families, *Heart* **77**, 130–132 (1997).

86. S. Morner, P. Richard, E. Kazzam, B. Hainque, K. Schwartz, and A. Waldenstrom, Deletion in the cardiac troponin I gene in a family from northern Sweden with hypertrophic cardiomyopathy, *J. Mol. Cell Cardiol.* **32**(3), 521–525 (2000).
87. S. Morner, P. Richard, E. Kazzam, U. Hellman, B. Hainque, K. Schwartz, and A. Waldenstrom, Identification of the genotypes causing hypertrophic cardiomyopathy in northern Sweden, *J. Mol. Cell. Cardiol.* **35**, 841–849 (2003).
88. H. Kokado, M. Shimizu, H. Yoshio, H. Ino, K. Okeie, Y. Emoto, T. Matsuyama, M. Yamaguchi, T. Yasuda, N. Fujino, H. Ito, and H. Mabuchi, Clinical features of hypertrophic cardiomyopathy caused by a Lys183 deletion mutation in the cardiac troponin I gene, *Circulation* **102**(6), 663–669 (2000).
89. J. Erdmann, S. Daehmlow, S. Wischke, M. Senyuva, U. Werner, J. Raible, N. Tanis, S. Dyachenko, M. Hummel, R. Hetzer, and V. Regitz-Zagrosek, Mutation spectrum in a large cohort of unrelated consecutive patients with hypertrophic cardiomyopathy, *Clin. Genet.* **64**(4), 339–349 (2003).
90. S. L. Van Driest, E. G. Ellsworth, S. R. Ommen, A. J. Tajik, B. J. Gersh, and M. J. Ackerman, Prevalence and spectrum of thin filament mutations in an outpatient referral population with hypertrophic cardiomyopathy, *Circulation* **108**, 445–451 (2003).
91. F. Torricelli, F. Girolami, I. Olivotto, I. Passerini, S. Frusconi, D. Vargiu, P. Richard, and F. Cecchi, Prevalence and clinical profile of troponin T mutations among patients with hypertrophic cardiomyopathy in Tuscany, *Am. J. Cardiol.* **92**, 1358–1362 (2003).
92. M. J. Ackerman, S. L. VanDriest, S. R. Ommen, M. L. Will, R. A. Nishimura, A. J. Tajik, and B. J. Gersh, Prevalence and age-dependence of malignant mutations in the beta-myosin heavy chain and troponin T genes in hypertrophic cardiomyopathy: a comprehensive outpatient perspective, *J. Am. Coll. Cardiol.* **39**, 2042–2048 (2002).
93. D. S. Van, M. J. Ackerman, S. R. Ommen, R. Shakur, M. L. Will, R. A. Nishimura, A. J. Tajik, and B. J. Gersh, Prevalence and severity of "benign" mutations in the beta-myosin heavy chain, cardiac troponin T, and alpha-tropomyosin genes in hypertrophic cardiomyopathy, *Circulation* **106**(24), 3085–3090 (2002).
94. O. Havndrup, H. Bundgaard, P. S. Andersen, L. A. Larsen, J. Vuust, K. Kjeldsen, and M. Christiansen, The Val606Met mutation in the cardiac beta-myosin heavy chain gene in patients with familial hypertrophic cardiomyopathy is associated with a high risk of sudden death at young age, *Am. J. Cardiol.* **87**, 1315–1317 (2001).
95. J. Zhang, A. Kumar, H. J. Stalker, G. Virdi, V. J. Ferrans, K. Horiba, F. J. Fricker, and M. R. Wallace, Clinical and molecular studies of a large family with desmin-associated restrictive cardiomyopathy, *Clin. Genet.* **59**, 248–256 (2001).
96. E. Arbustini, P. Morbini, M. Grasso, R. Fasani, L. Verga, O. Bellini, B. Dal Bello, C. Campana, G. Piccolo, O. Febo, C. Opasich, A. Gavazzi, and V. J. Ferrans, Restrictive cardiomyopathy, atrioventricular block and mild to subclinical myopathy in patients with desmin-immunoreactive material deposits, *J. Am. Coll. Cardiol.* **31**, 645–653 (1998).
97. Y. Miyamoto, H. Akita, N. Shiga, E. Takai, C. Iwai, K. Mizutani, H. Kawai, A. Takarada, and M. Yokoyama, Frequency and clinical characteristics of dilated cardiomyopathy caused by desmin gene mutation in a Japanese population, *Eur. Heart J.* **22**, 2284–2289 (2001).
98. A. Kaminska, S. V. Strelkov, B. Goudeau, M. Olive, A. Dagvadorj, A. Fidzianska, M. Simon-Casteras, A. Shatunov, M. C. Dalakas, I. Ferrer, H. Kwiecinski, P. Vicart, and L. G. Goldfarb, Small deletions disturb desmin architecture leading to breakdown of muscle cells and development of skeletal or cardioskeletal myopathy, *Hum. Genet.* **114**, 306–313 (2004).
99. S. Feld, and A. Caspi, Familial cardiomyopathy with variable hypertrophic and restrictive features and common HLA haplotype, *Isr. J. Med. Sci.* **28**, 277–280 (1992).
100. J. Mogensen, T. Kubo, M. Duque, W. Uribe, A. Shaw, R. Murphy, J. R. Gimeno, P. Elliott, and W. J. McKenna, Idiopathic restrictive cardiomyopathy is part of the clinical expression of cardiac troponin I mutations, *J. Clin. Invest.* **111**, 209–216 (2003).
101. M. K. Baig, J. H. Goldman, A. L. Caforio, A. S. Coonar, P. J. Keeling, and W. J. McKenna, Familial dilated cardiomyopathy: cardiac abnormalities are common in asymptomatic relatives and may represent early disease, *J. Am. Coll. Cardiol.* **31**, 195–201 (1897).
102. B. M. Mayosi, S. Khogali, B. Zhang, and H. Watkins, Cardiac and skeletal actin gene mutations are not a common cause of dilated cardiomyopathy [letter], *J. Med. Genet.* **36**, 796–797 (1999).
103. S. Karkkainen, K. Peuhkurinen, P. Jaaskelainen, R. Miettinen, P. Karkkainen, J. Kuusisto, and M. Laakso, No variants in the cardiac actin gene in Finnish patients with dilated or hypertrophic cardiomyopathy, *Am. Heart J.* **143**(6), E6 (2002).

104. E. Takai, H. Akita, N. Shiga, K. Kanazawa, S. Yamada, M. Terashima, Y. Matsuda, C. Iwai, K. Kawai, Y. Yokota, and M. Yokoyama, Mutational analysis of the cardiac actin gene in familial and sporadic dilated cardiomyopathy, *Am. J. Med. Genet.* **86**, 325–327 (1999).
105. B. L. Siu, H. Niimura, J. A. Osborne, D. Fatkin, C. MacRae, S. Solomon, D. W. Benson, J. G. Seidman, and C. E. Seidman, Familial dilated cardiomyopathy locus maps to chromosome 2q31, *Circulation* **99**, 1022–1026 (1897).
106. D. Li, G. Z. Czernuszewicz, O. Gonzalez, T. Tapscott, A. Karibe, J. B. Durand, R. Brugada, R. Hill, J. M. Gregoritch, J. L. Anderson, M. Quinones, L. L. Bachinski, R. Roberts, Novel cardiac troponin T mutation as a cause of familial dilated cardiomyopathy, *Circulation* **104**(18), 2188–2193 (2001).
107. E. L. Hanson, P. M. Jakobs, H. Keegan, K. Coates, S. Bousman, N. H. Dienel, M. Litt, and R. E. Hershberger, Cardiac troponin T lysine 210 deletion in a family with dilated cardiomyopathy, *J. Card. Fail.* **8**(1), 28–32 (2002).
108. P. Ray, H. Pimenta, R. Paulmurugan, F. Berger, M. E. Phelps, M. Iyer, and S. S. Gambhir, Noninvasive quantitative imaging of protein-protein interactions in living subjects, *Proc. Natl. Acad. Sci. USA* **99**, 3105–3110 (2002).

19

MOLECULAR PATHOGENIC MECHANISMS OF CARDIOMYOPATHIES CAUSED BY MUTATIONS IN CARDIAC TROPONIN T

Sachio Morimoto

19.1. INTRODUCTION

Troponin plays a central role in the Ca^{2+} regulation of contraction in vertebrate skeletal and cardiac muscles. It consists of three subunits with distinct structure and function, troponin T (TnT), troponin I (TnI), and troponin C (TnC), and their accurate and complex intermolecular interaction in response to the rapid rise and fall of Ca^{2+} in cardiac and skeletal myocytes plays a key role in maintaining the normal cardiac pump function and body movement. Over past decade, a great number of mutations in human genes for the troponin subunits have been shown to cause striated muscle disorders.

Since 1990, a large number of mutations in the cardiac sarcomeric proteins, including human cardiac troponin subunits, have been found to cause various types of cardiomyopathy in human.[1] On the other hand, three mutations in human fast skeletal troponin subunits (TnI and TnT) and one mutation in human slow skeletal TnT have recently been found to cause distal arthrogryposis and nemaline myopathy, respectively.[2–4] Since the discovery of troponin complex by Dr. Setsuro Ebashi in 1963,[5] a great many studies have been made to elucidate the molecular mechanisms by which troponin subunits regulate the striated muscle contraction. Nevertheless, it is still difficult to predict the functional consequences responsible for the pathogenesis of the disease only from the position and kind of mutations found in troponin subunits. To explore the effects of the mutations on the physiological function of troponin subunits and their contribution to the pathogenesis, functional studies are now extensively being made by using recombinant proteins and gene-manipulated animal models. This section focused on the mutations found in the genes for human cardiac troponin T (cTnT) and possible molecular mechanisms for the pathogenesis of cardiomyopathies associated with these mutations.

Department of Clinical Pharmacology, Kyushu University Graduate School of Medicine, 3-1-1 Maidashi, Higashi-ku, Fukuoka 812-8582, Japan

Regulatory Mechanisms of Striated Muscle Contraction
Edited by Ebashi and Ohtsuki, Springer, 2007

19.2. CARDIOMYOPATY

Cardiomyopathy, a disease of cardiac muscle, can be classified into three main forms, hypertrophic cardiomyopathy (HCM), dilated cardiomyopathy (DCM), and restrictive cardiomyopathy (RCM). HCM and DCM increase myocardial mass with distinct patterns of ventricular remodeling.[6,7] HCM produces ventricular wall thickening (i.e., hypertrophy), especially in the interventricular septum, with decrease in ventricular chamber volumes. DCM produces a prominent increase in chamber volumes as well as ventricular wall thickening. In HCM, systolic function is increased or at least preserved, while diastolic function is impaired in part because of the hypertrophy itself, interstitial fibrosis, and/or myocyte disarrays. Diastolic dysfunction is thought to be responsible for symptoms of heart failure and premature sudden cardiac death of HCM patients. In contrast, DCM is characterized by systolic dysfunction, which leads to congestive heart failure requiring cardiac transplantation. RCM, the least common form of the three cardiomyopathies, is characterized by restrictive diastolic dysfunction (restrictive filling and reduced diastolic volume of either or both ventricles) with normal or near normal systolic function and wall thickness.[8] Prognosis of RCM is poor, especially in the young with heart failure, and patients often require heart transplantation.

19.2.1. Hypertrophic Cardiomyopathy

HCM is a primary disease of the muscle of the heart with approximate prevalence of 1 : 500,[9] which is characterized by left ventricular hypertrophy in the absence of an apparent cause such as hypertension, hyperthyroidism, and acromegaly. HCM is the most common cause of sudden death in the young competitive athletes.[10] Recent genetic investigations of the gene in patients have revealed that HCM is a genetically heterogeneous "sarcomere disease" caused by the numerous mutations in 10 genes for myofibrillar proteins, myosin heavy chains, myosin regulatory and essential light chains, myosin-binding protein C, troponin subunits (cTnT, cTnI, and cTnC), tropomyosin, actin, and titin/connectin. Genetic epidemiological studies indicate that approximately 80% of the genes responsible for HCM have already been identified. HCM is also a clinically heterogeneous disease with most patients being asymptomatic or marginally symptomatic, and sudden death is often the first clinical manifestation in apparently healthy young individuals.[10,11]

19.2.1.1. Troponin T Mutations in HCM

Three years after the discovery of the first causal mutation in β-myosin heavy chain gene for HCM by Seidman group in 1990,[12] several mutations in other loci were found to be associated with HCM.[13] Those loci were then identified as the genes for cTnT and α-tropomyosin. Since then, 32 different mutations in the human cTnT gene have been found to cause HCM.[14] Mutations in the gene for cTnT accounts for 5–15% of all HCM cases,[15–17] and HCM patients harboring cTnT mutations have generally been described to show moderate or no significant cardiac hypertrophy in spite of their malignant prognosis.

19.2.1.2. I79N, R92Q, ΔE160 and Intron 16G1 → A Mutations of Troponin T in HCM

HCM-causing missense mutations I79N and R92Q, a deletion mutation ΔE160, and a splice donor site mutation intron $16G_1 \rightarrow A$ in cTnT have been reported to develop a

similar malignant clinical phenotype.[15] The life expectancy of patients with these mutations is approximately 35 years, which is comparable to that of patients with a malignant β-myosin heavy chain mutation R403Q and significantly shorter than that with a benign myosin mutation V606M. The survival analyses also indicated that these cTnT mutations are associated with a higher incidence of death before 30 yr of age and a significant higher proportion of sudden death compared with the myosin mutation R403Q. The degree of hypertrophy was similar in these cTnT mutations (mean maximal left-ventricular-wall thickness, 15.9 ± 5 mm), and was significantly less than that produced by β-myosin heavy chain mutation (mean maximal left-ventricular-wall thickness, 23.7 ± 7.7 mm). Approximately 25% of the surviving subjects with these cTnT mutations were asymptomatic; thus the penetrance of HCM caused by these mutations in the cTnT gene is estimated to be 75%, in contrast to the high penetrance of approximately 95% estimated for the mutations in the β-myosin heavy chain gene with a comparable malignant phenotype.[18–20]

The similarity between the phenotypic expressions of these four cTnT mutations suggested a common functional defect of cTnT involved in the pathogenesis of HCM in spite of the differences in the position and nature of these mutations. A great number of studies have been made on the functional aspects of these cTnT mutant proteins expressed in HCM, and rapidly clarified functional consequences primarily involving the molecular pathogenic mechanisms.

Physiological studies using cultured myocytes transected or infected with mutant cTnT cDNA construct indicate that these cTnT mutations impair the cardiac muscle contractility and thus might cause a compensatory hypertrophy.[21–24] In other functional studies,[25,26] however, the I79N and R92Q mutant human cTnTs, when incorporated into the rabbit cardiac skinned muscle fibers or myofibrils, both confer the higher Ca^{2+} sensitivity compared to the wild-type human cTnT, without impairing the maximum force-generating capability and ATPase activity (Figure 19.1). Szczesna et al.[27] and Harada and

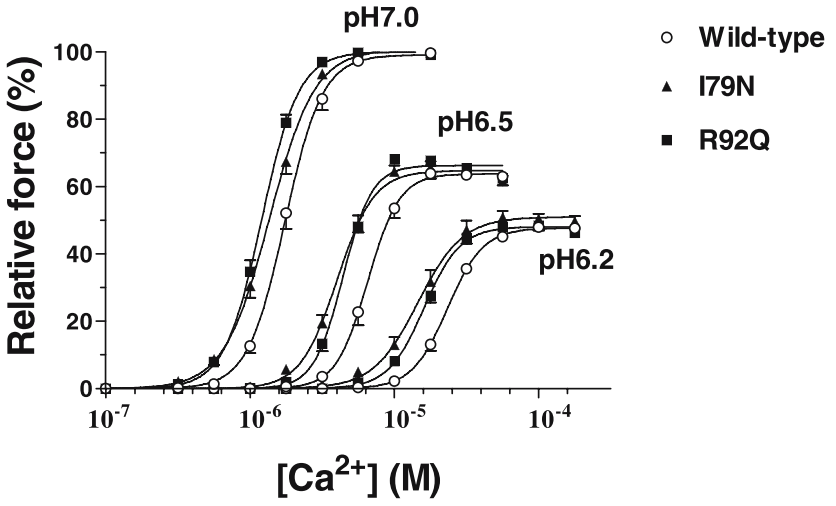

Figure 19.1. Effects of HCM-causing mutations in cTnT on the force-[Ca^{2+}] relationships of cardiac muscle. Recombinant wild-type, I79N, or R92Q human cTnT was exchanged into rabbit cardiac skinned muscle fibers, and force-[Ca^{2+}] relationships were determined at pHs 7.0, 6.5, and 6.2. Note that force developed by individual fiber was normalized to the maximum force at pH 7.0. The data are expressed as means ± SE.

Potter[14] reported similar results concerning the cTnT mutations I79N R92Q, R92W, and R92L by using almost the same experimental system.

Miller et al.[28] created a transgenic mouse model expressing I79N mutant human cTnT and confirmed that the skinned cardiac muscle fibers prepared from transgenic mice did show an increase in the Ca^{2+} sensitivity of force generation and ATPase activity. Tardiff et al.[29] created a transgenic mouse model expressing R92Q mutant human cTnT. Isolated working hearts of the mutant mice show hypercontractility and diastolic dysfunction, both of which are common findings in patients with HCM. Isolated cardiac myocytes from these mice have increased basal sarcomeric activation, impaired relaxation, and shorter sarcomere lengths, which are indicative of increased Ca^{2+} sensitivity of myofilaments.

Chandra et al.[30] demonstrated that Ca^{2+} sensitivity of myofilaments was indeed increased in skinned cardiac muscle fibers from these transgenic mice expressing R92Q cTnT. They also reported that maximum force or ATPase activity and the force-ATPase relations (economy of force maintenance) of skinned cardiac muscle fibers was the same in non-transgenic and R92Q mutant mice.

The HCM-causing deletion mutation ΔE160 also increases the Ca^{2+} sensitivity of cardiac muscle contraction without affecting the maximum force or ATPase activity and cooperativity, and the magnitude of Ca^{2+}-sensitization is almost the same as those in the I79N and R92Q missense mutations when mutant human proteins are exchanged into rabbit cardiac skinned muscle fibers by approximately 50%.[25,31] Transgenic mouse models expressing the ΔE160 human or mouse mutant cTnT have been shown to exhibit an increased Ca^{2+} sensitivity of contraction in skinned muscle fiber preparations from their hearts.[32,33]

The splice donor site mutation in intron 16 of the cTnT gene (intron $16G_1 \rightarrow A$) is expected to produce two truncated cTnT mutants lacking COOH-terminal 21 amino acids due to replacement of 28 amino acids with seven novel residues ($cTnT_{\Delta 28(+7)}$) and simply lacking COOH-terminal 14 amino acids ($cTnT_{\Delta 14}$). We have demonstrated that both the two truncated cTnT mutants increase the Ca^{2+} sensitivity and decrease the cooperativity in the force generation of cardiac muscle and that the mutant $cTnT_{\Delta 28(+7)}$ but not $cTnT_{\Delta 14}$ decreases the maximum force when mutant human proteins are exchanged into rabbit cardiac skinned muscle fibers by approximately 50%.[34] The magnitude of Ca^{2+}-sensitizating action of this mutation is significantly larger than the missense mutations I79N, R92Q, and ΔE160. Another characteristic consequence of this splice donor site mutation in the cTnT gene is an impairment of the cooperative Ca^{2+} regulation of cardiac muscle contraction (a decrease in the slope of the force-pCa relationships).[34]

The functional studies so far made strongly suggest that an increased Ca^{2+} sensitivity of cardiac muscle contraction is involved in the pathogenesis of HCM associated with these cTnT mutations, and also support the idea that the intracellular mechanisms by which mutations in the cTnT and β-myosin heavy chain gene cause HCM may be quite different. Most of the mutations in β-myosin heavy chain gene were shown to impair the contractility of myofilament,[35–38] suggesting that these mutations cause a compensatory cardiac hypertrophy. In contrast, the cTnT mutations are expected to enhance the contractility of cardiac myofilament by increasing its response to Ca^{2+}, so that it is not easy to anticipate that the cTnT mutations cause a compensatory hypertrophic response in agreement with the fact that cardiac hypertrophy produced by cTnT mutations is mild or not significant.

19.2.2. Dilated Cardiomyopathy

DCM represents a heterogeneous group of inherited and acquired disorders characterized by cardiac dilation and systolic dysfunction. Idiopathic DCM is a relatively common disorder (~50% of DCM) that accounts for more than 10 000 deaths annually by heart failure and sudden death in the United States (5 year mortality = 40~80%), being the primary indication for cardiac transplantation.[6,39,40]

Recent genetic studies of large families with DCM have revealed that inherited gene defects in cytoskeletal (dystrophin, desmin, tafazzin, lamin A/C, and Δ-sarcoglycan) and sarcomeric (actin, β-myosin heavy chain, α-tropomyosin, myosin-binding protein C, titin, troponin T, troponin I, and troponin C) proteins are an important cause of idiopathic DCM.[41] The overall frequency of mutations in troponin subunits in familial DCM was estimated to be approximately 6%.[42] Mutations in troponin subunits appear to be associated with a malignant phenotype with a high incidence of premature cardiac death/heart transplantation.

Mutations in cytoskeletal proteins imply that deficits in transmission of force generated by sarcomere may be one mechanism for the pathogenesis of DCM. On the other hand, emerging evidence from functional studies on mutations in sarcomeric proteins indicates that Ca^{2+} desensitization of cardiac muscle contraction is involved in the pathogenesis of DCM caused by mutations in these proteins.

19.2.2.1. Troponin T Mutations in DCM

Kamisago et al.[43] reported a deletion mutation in the cTnT gene, ΔK210, in two independent families, which is the first cTnT mutation responsible for familial primary DCM that is clearly distinguished from an end-stage dilated phase of HCM. The same mutation has been identified in other DCM patients in two families independent from those studied by Kamisago et al.,[43] suggesting that the K210 residue in cTnT is a mutation "hot spot."[42,44] Since then, at least six different mutations in cTnT (R131W, R141W, A172S, R205L, ΔK210 and D270N) associated with DCM have been reported. All these mutations have not been found in HCM, clearly indicating that the specific mutation in the same gene determines the distinct phenotypes of HCM and DCM.

19.2.2.2. ΔK210 Mutation in Cardiac Troponin T

In a family reported by Kamisago et al.,[43] the deletion mutation ΔK210 in cTnT causes frequent sudden deaths in infants and young adults (<30 years) with marked dilation of both ventricles and increased interstitial fibrosis. In another family, this mutation causes frequent deaths due to congestive heart failure in individuals less than 20 years of age with marked dilation of both ventricles and increased interstitial fibrosis. A marked enlargement of the heart (cardiomegaly; heart weight, 400 g) was observed in a 15-year-old boy who died of congestive heart failure.

Early-onset phenotype of this mutation with a high incidence of sudden death and/or heart failure was also seen in a different family reported by Hanson et al.[44] All family members showed characteristic features of DCM, i.e., significant cardiac dilation and marked systolic dysfunction, and two members were found to have left ventricular wall thickness greater than normal (14 and 18 mm).

In a family reported by Mogensen et al.,[42] a significant number of affected individuals experienced sudden cardiac death, heart failure death, and/or heart transplantation in the second or third decade of life. Examination of explanted heart showed cardiomegaly (heart weight, 450–540 g).

The functional consequences of the mutations in cTnT associated with DCM are clearly different from those of the mutations associated with HCM. In a study we made, the deletion mutation ΔK210 had a Ca^{2+}-desensitizing effect on the force generation in skinned cardiac muscle fibers and the ATPase activity in isolated cardiac myofibrils[31] (Figure 19.2). Other groups have reported basically the same finding.[45,46] On the other hand, three mutations R92W, E163R, and K273E that cause a dilated form of HCM (i.e., secondary DCM) have been reported to have Ca^{2+}-sensitizing effects on the cardiac muscle contraction.[14,46]

These findings strongly suggest that the decrease in the Ca^{2+} sensitivity of force generation in sarcomere might be a primary mechanism for the pathogenesis of DCM in the patients with the deletion mutation ΔK210 in cTnT. This mutation does not affect the maximum force generating capability of sarcomere. However, even a small decrease in Ca^{2+} sensitivity is expected to cause a significant reduction in the force generation of cardiac muscle in the heart, given that intact cardiac muscle is never activated beyond half-maximal level.[47] The reduction in the force generation by sarcomere with the deletion mutation ΔK210 in cTnT and the deficits of force-transmission in cytoskeletal proteins might go through the same process of pathogenesis, leading to a ventricular dilation as a compensatory mechanism for the decrease in the stroke volume due to the reduction in the contractile force of the heart.

The lysine residue 210 in cTnT is in a domain that is involved in the Ca^{2+}-sensitive strong TnC binding and in the very weak tropomyosin and TnI binding.[48] Thus, the deletion mutation ΔK210 might impair the Ca^{2+}-induced interaction of cTnC with this region on cTnT. However, most recent structural information on human cardiac troponin complex

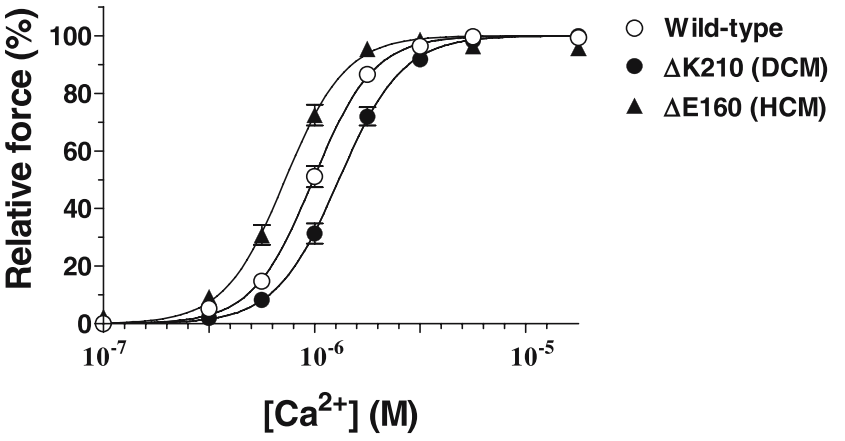

Figure 19.2. Effects of DCM-causing mutations in cTnT on the force-[Ca^{2+}] relationships of cardiac muscle. Recombinant human wild-type, DCM-causing ΔK210 mutant, or HCM-causing ΔE160 mutant cTnT was exchanged into rabbit cardiac skinned muscle fibers, and force-[Ca^{2+}] relationships were determined at pH 7.0. Note that forces were normalized to the averaged maximum force, and are expressed as means ± SE.

from X-ray crystallography indicates that the lysine residue 210 in cTnT interacts with neither cTnC nor cTnI,[49] and the molecular mechanism by which the ΔK210 mutation in cTnT causes the depression of Ca^{2+}-sensitivity of force generation remains to be elucidated.

Mutant mice developed enlarged hearts and showed a high incidence of sudden death[50] (Figure 19.3); approximately 50% of heterozygous $cTnT^{+/\Delta K210}$ mice and all homozygous $cTnT^{\Delta K210/\Delta K210}$ mice died within 6 months of age mostly without evidence of overt heart failure. Histological examination of cardiac sections from mutant mice showed a significant dilation of both ventricles and fibrosis. Echocardiography showed that the systolic function of left ventricle was significantly reduced in mutant mice, with homozygous $cTnT^{\Delta K210/\Delta K210}$ mice being more severely affected than heterozygous cTnT $cTnT^{+/\Delta K210}$ mice. Isolated working heart preparations from mutant mice, however, showed no significant changes in left ventricular dP/dt_{max} and dP/dt_{min} and in cardiac output, suggesting that the impaired systolic function in mutant mice is fully compensated probably through cardiac enlargement.

Consistent with our previous *in vitro* studies using ΔK210 mutant cTnT-exchanged skinned muscle fibers, skinned cardiac muscle fibers prepared from mutant mice showed a significant decrease in the Ca^{2+} sensitivity of force generation, with the change being greater in $cTnT^{\Delta K210/\Delta K210}$ mice than in $cTnT^{+/\Delta K210}$ mice. Surprisingly, however, intact cardiac muscle fibers from heterozygous and homozygous mutant mice showed no significant reduction in isometric force generated per cross-sectional area. Fluorescent analyses of cardiac myocytes isolated from mutant mice revealed that this was due to an increase in the peak amplitude of intracellular Ca^{2+} transient. DNA microarray and immunoblot analyses demonstrated that expression of phosphodiesterase 4B (PDE4B) was down-regulated in the heart of mutant mice, and an enzyme-immuno assay confirmed the resultant increase in the intracellular cAMP level in cardiac myocytes. These results strongly suggest that a decrease in the Ca^{2+} sensitivity of cardiac myofilament

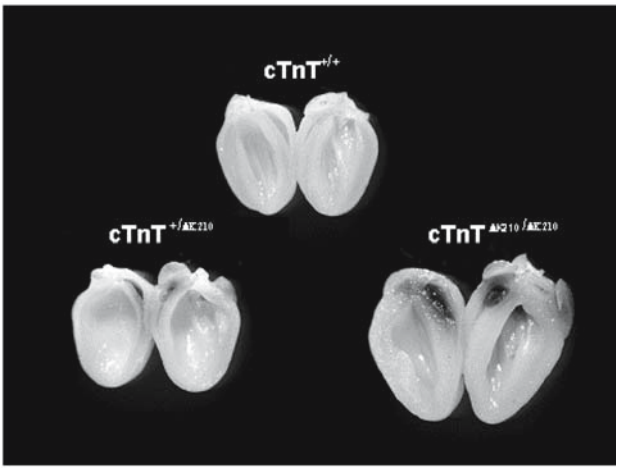

Figure 19.3. Gross morphology of hearts from wild-type ($cTnT^{+/+}$), heterozygous ($cTnT^{+/\Delta K210}$) and homozygous ($cTnT^{\Delta K210/\Delta K210}$) mice. Mutant mice hearts are enlarged and have markedly dilated right and left ventricular chambers.

induces a down-regulation of PDE4B expression in a compensatory manner to maintain contractile function of cardiac muscle by increasing the intracellular cAMP level and thus the intracellular Ca^{2+} transient through phosphorylation of L-type Ca^{2+} channels and phospholamban by cAMP-dependent protein kinase. A resultant increase in the intracellular Ca^{2+}, however, would increase the risk for arrhythmia at the same time, which might be responsible for the high incidence of sudden death. Studies using a telemetry system for ECG recording confirmed that the mutant mice suffered from sudden death due to a cardiac electrophysiological abnormality despite well-compensated mechanical performance of the heart.

19.2.2.3. R141W Mutations in Cardiac Troponin T

The second mutation, R141W, in the cTnT gene that causes DCM was found in a large family spanning 5 generations.[51] Clinical features of this missense mutation appear to be different from the deletion mutation ΔK210.DCM in this family has a phenotype primarily of heart failure that is variable in age of onset and severity with moderate to high penetrance. The majority of the deceased persons developed a cardiac condition in the second decade of life and had severe congestive heart failure in the third to fifth decade. There was no documented case of sudden cardiac death in contrast to the ΔK210 mutation associated with a high frequency of sudden death, suggesting that there exists some difference in the functional consequences of these two mutations.

We found that the missense mutation R141W in cTnT decreases the Ca^{2+} sensitivity of force generation without changing maximum force-generating capability and cooperativity in skinned cardiac muscle fibers.[52] The magnitude of Ca^{2+}-desensitization seems to be almost the same as those in the ΔK210 deletion mutation ΔK210. Venkatraman et al.[48] reported that this mutation did not significantly decrease the Ca^{2+} sensitivity of force generation in an experimental system similar to ours and that it reduced the maximum actomyosin ATPase activity. However, they also found that a Ca^{2+}-desensitization of force generation does occur when this mutation is introduced into the fetal isoform of human cTnT.[53]

The R141W mutation does not change the unloaded shortening velocity of skinned cardiac muscle, suggesting that this mutation have no effects on the myosin cross-bridge kinetics.[52] The mutation R141W lies in the strong tropomyosin-binding region. An assay using a quarts-crystal microbalance (a very sensitive mass measuring device) revealed that R141W mutation increased the affinity of cTnT for α-tropomyosin by approximately three-times.[52] In cardiac muscle cells, the binding of cTnI to actin in the thin filaments inhibits cardiac muscle contraction, and Ca^{2+}-induced interaction of cTnI with cTnC releases this inhibition, allowing myosin cross-bridges to generate force through interacting with actin. However, this Ca^{2+}-dependent regulation cannot occur and cardiac muscle contracts independently of Ca^{2+} concentrations unless cTnT anchors cTnI to the thin filament via its two-way bindings to cTnI and tropomyosin and forces cTnI to inhibit the thin filament only at low $[Ca^{2+}]i$.[47,54] The increase in the affinity of cTnT for tropomyosin caused by the mutation R141W is, therefore, expected to further strengthen the structural integrity of cTnI in the thin filament and probably its inhibitory action on the thin filament. Although further investigation should be required to clarify this hypothesis, the resulting increase in the inhibition exerted by cTnI on the thin filaments might lead to an increase in the Ca^{2+} concentration required for cTnC to release it (i.e., a

Ca^{2+}-desensitization). This study provides direct evidence that changes in the interaction between cTnT and tropomyosin may alter the Ca^{2+} sensitivity of cardiac muscle contraction. However, another DCM-causing mutation ΔK210 and an HCM-causing mutation R94L lying outside the strong tropomyosin-binding region in cTnT had no effects on the affinity of cTnT for tropomyosin. The HCM-causing mutation ΔE160, which lies just inside the strong tropomyosin-binding region, also had no effect on the affinity of cTnT for tropomyosin in spite of its Ca^{2+}-sensitizing effect on the cardiac muscle contraction.[52] These findings indicate that molecular mechanisms by which these cTnT mutations in DCM and HCM alter the Ca^{2+} sensitivity of cardiac muscle contraction are quite different from the molecular mechanism involving the mutation R141W.

19.3. CONCLUSION

Functional studies have been made to elucidate the molecular mechanisms by which HCM is developed in patients harboring mutations in sarcomeric proteins since the discovery of a mutation in the gene for β-myosin heavy chain by Geisterfer-Lowrance et al.[12] Especially, the functional consequences of cTnT mutations were intensively examined at different levels from molecules to animal models, revealing a heterogeneity in the functional and structural consequences of a variety of mutations spreading over the entire molecule. For instance, Palm et al.[55] have demonstrated that mutations within a region including residues 92–110 (R92L/Q/W, R94L, A104V, and F110I) impair the tropomyosin-dependent function of cTnT, but mutations outside the region (I79N, ΔE160, and E163K) do not. Nevertheless, a wide variety of mutations including these mutations are responsible for a similar heart disease diagnosed as HCM, implying that there may be a common mechanism for the pathogenesis of HCM associated with cTnT mutations. In 1998, we provided the first evidence that the two HCM-linked cTnT mutations (I79N and R92Q) increased the Ca^{2+} sensitivity of force generation in cardiac muscle.[25] Since then it has been shown that most mutations of cTnT and cTnI associated with HCM and RCM have a Ca^{2+}-sensitizing effect on the force generation of cardiac muscle and the ATPase activity of cardiac myofibrils. Moreover, it has been demonstrated that the skinned cardiac muscle fibers from transgenic mice expressing HCM mutant of cTnT or cTnI show an increased Ca^{2+} sensitivity of force generation.[28,30,56,57] These studies strongly suggest that Ca^{2+}-sensitization is a common primary mechanism for the pathogenesis of HCM and RCM with mutations in the gene for cTnT and cTnI. An increased Ca^{2+} sensitivity would involve an increase in the utilization of ATP by actomyosin ATPase at submaximal intracellular Ca^{2+} concentrations, which facilitates the rapid exhaustion of the intracellular ATP under severe stress and leads to an imbalance in energy supply and demand in the heart that might be responsible for sudden death. A recent study has revealed that cardiac energetics is altered in transgenic mice harboring the cTnT mutation R92Q,[58] as is the case of HCM patients with sarcomeric protein mutations, including cTnT.[59]

Troponin mutations so far identified in DCM are much less than those identified in HCM, and their functional consequences have just begun to be investigated. In a few studies, five cTnT mutations found in DCM (R131W, R141W, R205L, ΔK210 and D270N) have been shown to have an effect directly opposite to that seen in the HCM-causing mutations, i.e., Ca^{2+}-desensitization of the force generation and/or myofibrillar ATPase activity in cardiac muscle.[31,52,53,60] DCM-causing mutations in α-tropomyosin (E40K and

E54K) and cTnC (G159D) have also been demonstrated to decrease the Ca^{2+} sensitivity of cardiac myofilament in vitro.[60,61] Because intact cardiac muscle is known to never be activated beyond a half-maximal level, a decrease in Ca^{2+} sensitivity is expected to cause a significant reduction in the force generation of cardiac muscle. These in vitro studies, therefore, led to a rather simple hypothesis that ventricular dilation is just a compensatory mechanism for a reduced contractility of cardiac muscle due to decreased myofilament Ca^{2+} sensitivity. However, a mouse knockin model we have created recently,[50] in which ΔK210 mutation is directly introduced into the cTnT gene of mouse genome using embryonic stem cell technology, reveals an ingenious compensatory mechanism for the decreased myofilament response to Ca^{2+} involving cellular and molecular pathogenic events that ultimately leads to DCM. This mice model strongly suggest that a decreased myofilament Ca^{2+} sensitivity caused by ΔK210 mutation induces a down-regulation of PDE4B expression in a compensatory manner to maintain the contractile function of myocardium by increasing the cAMP level and thus the intracellular Ca^{2+} transient amplitude. The increase in cAMP, however, would also increase the ATP consumption by SR Ca^{2+} pump and trigger the isoform shift from α- to β-MyHC with lower ATPase activity and power output, which in turn might trigger the structural remodeling involving cardiac enlargement with chamber dilation. Functional and structural remodeling of the heart in these manners well compensates for a reduction in the cardiac output due to the decreased myofilament Ca^{2+} sensitivity. Unfortunately, however, the functional remodeling involving the enhancement of SR Ca^{2+} pump activity would decrease the electrophysiological stability of myocardium and increase the risk for arrhythmia and sudden death.

19.4. ACKNOWLEDGEMENTS

This work was supported by Special Coordination Funds from the Ministry of Education, Culture, Sports, Science and Technology of Japan and Grants-in-Aid (15300136 and 17300129) for Science Research from the Japan Society for the Promotion of Science.

19.5. REFERENCES

1. F. Ahmad, J. G. Seidman, and C. E. Seidman, The genetic basis for cardiac remodeling. *Annu. Rev. Genomics Hum. Genet.* **6**, 185–216 (2005).
2. S. S. Sung, A. E. Brassington, K. Grannatt, A. Tutherford, F. G. Whitby, P. A. Krakowiad, L. B. Jorde, J. C. Carey, and M. Bamshad, Mutations in genes encoding fast-twitch contractile proteins cause distal arthrogryposis syndromes. *Am. J. Hum. Genet.* **72**(3), 681–690 (2003).
3. S. S. Sung, A. E. Brassington, P. A. Krakowiak, J. C. Carey, L. B. Jorde, and M. Bamshad, Mutations in *TNNT3* cause multiple congenital contractures: a second locus for distal arthrogryposis type 2B. *Am. J. Hum. Genet.* **73**(1), 212–214 (2003).
4. J. J. Johnston, R. I. Kelley, T. O. Crawford, D. H. Morton, R. Agarwala, T. Koch, A. A. Schaffer, C. A. Francomano, and L. G. Biesecker, A novel nemaline myopathy in the amish caused by a mutation in troponin T. *Am. J. Hum. Genet.* **67**(4), 814–821 (2000).
5. S. Ebashi, Third component participating in the superprecipitation of "natural actomyosin". *Nature* **200**, 1010 (1963).

6. G. W. Dec, and V. Fuster, Idiopathic dilated cardiomyopathy. *N. Engl. J. Med.* **331**(23), 1564–1575 (1994).
7. B. J. Maron, Hypertrophic cardiomyopathy: a systematic review. *JAMA* **287**(10), 1308–1320 (2002).
8. S. S. Kushwaha, J. T. Fallon, and V. Fuster, Restrictive cardiomyopathy. *N. Engl. J. Med.* **336**(4), 267–276 (1997).
9. B. J. Maron, J. M. Gardin, J. M. Flack, et al., Prevalence of hypertrophic cardiomyopathy in a general population of young adults. Echocardiographic analysis of 4111 subjects in the CARDIA Study. Coronary Artery Risk Development in (Young) Adults. *Circulation* **92**(4), 785–789 (1995).
10. B. J. Maron, J. Shirani, L. C. Poliac, R. Mathenge, W. C. Roberts, and F. O. Mueller, Sudden death in young competitive athletes. Clinical, demographic, and pathological profiles. *JAMA* **276**(3), 199–204 (1996).
11. W. McKenna, J. Deanfield, A. Faruqui, D. England, C. Oakley, and J. Goodwin, Prognosis in hypertrophic cardiomyopathy: role of age and clinical, electrocardiographic and hemodynamic features. *Am. J. Cardiol.* **47**(3), 532–538 (1981).
12. A. A. Geisterfer-Lowrance, S. Kass, G. Tanigawa, H. P. Vosberg, W. McKenna, C. E. Seidman, and J. G. Seidman, A molecular basis for familial hypertrophic cardiomyopathy: a beta cardiac myosin heavy chain gene missense mutation. *Cell* **62**(5), 999–1006 (1990).
13. H. Watkins, C. MacRae, L. Thierfelder, Y. H. Chou, M. Frenneaux, W. McKenna, J. G. Seidman, and C. E. Seidman, A disease locus for familial hypertrophic cardiomyopathy maps to chromosome 1q3. *Nat. Genet.* **3**(4), 333–337 (1993).
14. K. Harada, and J. D. Potter, Familial hypertrophic cardiomyopathy mutations from different functional regions of troponin T result in different effects on the pH- and Ca^{2+}-sensitivity of cardiac muscle contraction. *J. Biol. Chem.* **279**(15), 14488–14495 (2004).
15. H. Watkins, W. J. McKenna, L. Thierfelder, Wat, Mutations in the genes for cardiac troponin T and alpha-tropomyosin in hypertrophic cardiomyopathy. *N. Engl. J. Med.* **332**(16), 1058–1064 (1995).
16. P. Richard, P. Charron, L. Carrier,, C. Ledeuil, T. Cheav, C. Pichereau, A. Benaiche, R. Isnard, O. Dubourg, M. Burban, J. P. Gueffet, A. Millaire, M. Desnos, K. Schwartz, B. Hainque, and M. Komajda, Hypertrophic cardiomyopathy distribution of disease genes, spectrum of mutations, and implications for a molecular diagnosis strategy. *Circulation* **107**(17), 2227–2232 (2003).
17. F. Torricelli, F. Girolami, I. Olivotto, I. Passerini, S. Frusconi, D. Vargiu, P. Richard, and F. Cecchi, Prevalence and clinical profile of troponin T mutations among patients with hypertrophic cardiomyopathy in tuscany. *Am. J. Cardiol.* **92**(11), 1358–1362 (2003).
18. N. D. Epstein, G. M. Cohn, F. Cyran, and L. Fananapazir, Differences in clinical expression of hypertrophic cardio-myopathy associated with two distinct mutations in the β-myosin heavy chain gene: a 908Leu → Val mutation and a 403Arg → Gln mutation. *Circulation* **86**(2), 345–352 (1992).
19. H. Watkins, A. Rosenzweig, D.-S. Hwang, T. Levi, W. McKenna, C. E. Seidman, and J. G. Seidman, Characteristics and prognostic implications of myosin missense mutations in familial hypertrophic cardiomyopathy. *N. Engl. J. Med.* **326**(17), 1108–1114 (1992).
20. R. Anan, G. Greve, L. Thierfelder, H. Watkins, W. J. McKenna, S. Solomon, C. Vecchio, H. Shono, S. Nakao, H. Tanaka, A. Mares, Jr., J. A. Towbin, P. Spirito, R. Roberts, J. G. Seidman, and C. E. Seidman, Prognostic implications of novel cardiac myosin heavy chain gene mutations that cause familial hypertrophic cardiomyopathy. *J. Clin. Invest.* **93**(1), 280–285 (1994).
21. H. Watkins, C. E. Seidman, J. G. Seidman. H. S. Feng, and H. L. Sweeney, Expression and functional assessment of a truncated cardiac troponin T that causes hypertrophic cardiomyopathy. *J. Clin. Invest.* **98**(11), 2456–2461 (1996).
22. H. L. Sweeney, H. S. Feng, Z. Yang, and H. Watkins, Functional analyses of troponin T mutations that cause hypertrophic cardiomyopathy: insights into disease pathogenesis and troponin function. *Proc. Natl. Acad. Sci. USA* **95**(24), 14406–14410 (1998).
23. A. J. Marian, G. Zhao, Y. Seta, R. Roberts, and Q. Yu, Expression of a mutant (Arg92Gln) human cardiac troponin T, known to cause hypertrophic cardiomyopathy, impairs adult cardiac myocyte contractility. *Circ. Res.* **81**(1), 76–85 (1997).
24. E. M. Rust, F. P. Albayya, and J. M. Metzger, Identification of a contractile deficit in adult cardiac myocytes expressing hypertrophic cardiomyopathy–associated mutant troponin T proteins. *J. Clin. Invest.* **103**(10), 1459–1467 (1999).
25. S. Morimoto, F. Yanaga, R. Minakami, and I. Ohtsuki, Ca^{2+}-sensitizing effects of the mutations at Ile-79 and Arg-92 of troponin T in hypertrophic cardiomyopathy. *Am. J. Physiol. Cell Physiol.* **275**(1 Pt 1), C200–C207 (1998).

26. F. Yanaga, S. Morimoto, and I. Ohtsuki, Ca^{2+} sensitization and potentiation of the maximum level of myofibrillar ATPase activity caused by mutations of troponin T found in familial hypertrophic cardiomyopathy. *J. Biol. Chem.* **274**(13), 8806–8812 (1999).
27. D. Szczesna, R. Zhang, J. Zhao, M. Jones, G. Guzman, and J. D. Potter, Altered regulation of cardiac muscle contraction by troponin T mutations that cause familial hypertrophic cardiomyopathy. *J. Biol. Chem.* **275**(1), 624–630 (2000).
28. T. Miller, D. Szczesna, P. R. Housmans, J. Zhao, F. de Freitas, A. V. Gomes, L. Culbreath, J. McCue, Y. Wang, Y. Xu, W. G. Kerrick, and J. D. Potter, Abnormal contractile function in transgenic mice expressing a familial hypertrophic cardiomyopathy-linked troponin T (I79N) mutation. *J. Biol. Chem.* **276**(6), 3743–3755 (2001).
29. J. C. Tardiff, T. E. Hewett, B. M. Palmer, C. Olsson, S. M. Factor, R. L. Moore, J. Robbins, and L. A. Leinwand, Cardiac troponin T mutations result in allele-specific phenotypes in a mouse model for hypertrophic cardiomyopathy. *J. Clin. Invest.* **104**(4), 469–481 (1999).
30. M. Chandra, V. L. M. Rundell, J. C. Tardiff, L. A. Leinwand, P. P. De Tombe, and R. J. Solaro, Ca^{2+} activation of myofilaments from transgenic mouse hearts expressing R92Q mutant cardiac troponin T. *Am. J. Physiol. Heart. Circ. Physiol.* **280**(2), H705–H713 (2001).
31. S. Morimoto, Q.-W. Lu, K. Harada, F. Takahashi-Yanaga, R. Minakami, M. Ohta, T. Sasaguri, and I. Ohtsuki, Ca^{2+}-desensitizing effect of a deletion mutation ΔK210 in cardiac troponin T that causes familial dilated cardiomyopathy. *Proc. Natl. Acad. Sci. USA* **99**(2), 913–918 (2002).
32. S. Morimoto, C.-K. Du, K. Harada, M. Ohta, N. Oka, Q.-W. Lu, R. Minakami, M. Suzuki, T. Sasaguri, K. Yamamura, and I. Ohtsuki, Cardiac function of a transgenic mouse model of ΔGlu160 troponin T mutation-linked familial hypertrophic cardiomyopathy. *Biophys. J.* **86**, 386A (2004).
33. T. E. Haim, C. Dowell, T. Dhjamanti, J. Scheuer, and J. C. Tardiff, Independent mutations in Cardiac Troponin T lead to impairments in calcium handling that relate to alterations in myocellular function. *Biophys. J.* **86**, 47A–48A (2004).
34. H. Nakaura, S. Morimoto, F. Yanaga, M. Nakata, H. Nishi, T. Imaizumi, and I. Ohtsuki, Functional changes in troponin T by a splice donor site mutation that causes hypertrophic cardiomyopathy. *Am. J. Physiol. Cell Physiol.* **277**(2 Pt 1), C225–C232 (1999).
35. G. Cuda, L. Fananapazir, W.-S. Zhu, J. R. Sellers, and N. D. Epstein, Skeletal muscle expression and abnormal function of β-myosin in hypertrophic cardiomyopathy. *J. Clin. Invest.* **91**(6), 2861–2865 (1993).
36. H. L. Sweeney, A. J. Straceski, L. A. Leinwand, B. A. Tikunov, and L. Faust, Heterologous expression of a cardiomyopathic myosin that is defective in its actin interaction. *J. Biol. Chem.* **269**(3), 1603–1605 (1994).
37. E. B. Lankford, N. D. Epstein, L. Fananapazir, and H. L. Sweeney, Abnormal contractile properties of muscle fibers expressing β-myosin heavy chain gene mutations in patients with hypertrophic cardiomyopathy. *J. Clin. Invest.* **95**(3), 1409–1414 (1995).
38. H. Fujita, S. Sugiura, S. Momomura, M. Omata, H. Sugi, and K. Sutoh, Characterization of mutant myosins of dictyostelium discoideum equivalent to human familial hypertrophic cardiomyopathy mutants – molecular force level of mutant myosins may have a prognostic implication. *J. Clin. Invest.* **99**(5), 1010–1015 (1997).
39. E. K. Kasper, W. R. Agema, G. M. Hutchins, J. W. Deckers, J. M. Hare, and K. L. Baughman, The causes of dilated cardiomyopathy: a clinicopathologic review of 673 consecutive patients. *J. Am. Coll. Cardiol.* **23**(3), 586–590 (1994).
40. E. M. Gilbert, and M. R. Bristow, Idiopathic dilated cardiomyopathy. In: *The Heart*, edited by J. W. Hurst (MacGraw-Hill, New York, 1994), pp. 1609–1619.
41. D. Fatkin, and R. M. Graham, Molecular mechanisms of inherited cardiomyopathies. *Physiol. Rev.* **82**(4), 945–980 (2002).
42. J. Mogensen, R. T. Murphy, T. Shaw, A. Bahl, C. Redwood, H. Watkins, M. Burke, P. M. Elliott, and W. J. McKenna, Severe disease expression of cardiac troponin C and T mutations in patients with idiopathic dilated cardiomyopathy. *J. Am. Coll. Cardiol.* **44**(10), 2033–2040 (2004).
43. M. Kamisago, S. D. Sharma, S. R. DePalma, S. Solomon, P. Sharma, B. McDonough, L. Smoot, M. P. Mullen, P. K. Woolf, E. D. Wigle, J. G. Seidman, and C. E. Seidman, Mutations in sarcomere protein genes as a cause of dilated cardiomyopathy. *N. Engl. J. Med.* **343**(23), 1688–1696 (2000).
44. E. L. Hanson, P. M. Jakobs, H. Keegan, K. Coates, S. Bousman, N. H. Dienel, M. Litt, and R. E. Hershberger, Cardiac troponin T lysine 210 deletion in a family with dilated cardiomyopathy. *J. Card. Fail.* **8**(1), 28–32 (2002).

45. P. Robinson, M. Mirza, A. Knott, H. Abdulrazzak, R. Willott, S. Marston, H. Watkins, and C. Redwood, Alterations in thin filament regulation induced by a human cardiac troponin T mutant that causes dilated cardiomyopathy are distinct from those induced by troponin T mutants that cause hypertrophic cardiomyopathy. *J. Biol. Chem.* **277**(43), 40710–40716 (2002).
46. G. Venkatraman, K. Harada, A. V. Gomes, W. G. Kerrick, and J. D. Potter, Different functional properties of troponin T mutants that cause dilated cardiomyopathy. *J. Biol. Chem.* **278**(43), 41670–41676 (2003).
47. J. C. Ruegg, *Calcium in Muscle Activation* (Springer-Verlag, Berlin; Tokyo, 1986).
48. M. Tanokura, Y. Tawada, A. Ono, and I. Ohtsuki, Chymotryptic subfragments of troponin T from rabbit skeletal muscle. Interaction with tropomyosin, troponin I and troponin C. *J. Biochem. (Tokyo)* **93**(2), 331–337 (1983).
49. S. Takeda, A. Yamashita, K. Maeda, and Y. Maeda, Structure of the core domain of human cardiac troponin in the Ca^{2+}-saturated form. *Nature* **424**, 35–41 (2003).
50. S. Morimoto, C.-K. Du, M. Ohta, Q.-W. Lu, K. Harada, K. Nishii, R. Minakami, N. Oka, N. Tadano, J. Miyazaki, K. Yamamura, and I. Ohtsuki, A knock-in mouse model for familial dilated cardiomyopathy caused by the mutation ΔK210 in cardiac troponin T. *Biophys. J.* **88**(1), 480A (2005).
51. D. Li, G. Z. Czernuszewicz, O. Gonzalez, T. Tapscott, A. Karibe, J. B. Durand, R. Brugada, R. Hill, J. M. Gregoritch, J. L. Anderson, M. Quinones, L. L. Bachinski, and R. Roberts, Novel cardiac troponin T mutation as a cause of familial dilated cardiomyopathy. *Circulation* **104**(8), 2188–2193 (2001).
52. Q.-W. Lu, S. Morimoto, K. Harada, C. K. Du, F. Takahashi-Yanaga, Y. Miwa, T. Sasaguri, and I. Ohtsuki, Cardiac troponin T mutation R141W found in dilated cardiomyopathy stabilizes the troponin T-tropomyosin interaction and causes a Ca^{2+} desensitization. *J. Mol. Cell. Cardiol.* **35**(12), 1421–1427 (2003).
53. G. Venkatraman, A. V. Gomes, W. G. L. Kerrick, and J. D. Potter, Characterization of troponin T dilated cardiomyopathy mutations in the fetal troponin isoform. *J. Biol. Chem.* **280**(18), 17584–17592 (2005).
54. I. Ohtsuki, K. Maruyama, and S. Ebashi, Regulatory and cytoskeletal proteins of vertebrate skeletal muscle. *Adv. Protein Chem.* **38**, 1–67 (1986).
55. T. Palm, S. Graboski, S. E. Hitchcock-DeGregori, and N. J. Greenfield, Disease-causing mutations in cardiac troponin T: identification of a critical tropomyosin-binding region. *Biophys. J.* **81**(5), 2827–2837 (2001).
56. J. James, Y. Zhang, H. Osinska, A. Sanbe, R. Klevitsky, T. E. Hewett, and J. Robbins, Transgenic modeling of a cardiac troponin I mutation linked to familial hypertrophic cardiomyopathy. *Circ. Res.* **87**(9), 805–811 (2000).
57. D. E. Montgomery, J. C. Tardiff, and M. Chandra, Cardiac troponin T mutations: correlation between the type of mutation and the nature of myofilament dysfunction in transgenic mice. *J. Physiol.* **536**(Pt 2), 583–592 (2001).
58. M. M. Javadpour, J. C. Tardiff, I. Pinz, and J. S. Ingwall, Decreased energetics in murine hearts bearing the R92Q mutation in cardiac troponin T. *J. Clin. Invest.* **112**(5), 768–775 (2003).
59. J. G. Crilley, E. A. Boehm, E. Blair, B. Rajagopalan, A. M. Blamire, P. Styles, W. J. McKenna, I. Ostman-Smith, K. Clarke, and H. Watkins, Hypertrophic cardiomyopathy due to sarcomeric gene mutations is characterized by impaired energy metabolism irrespective of the degree of hypertrophy. *J. Am. Coll. Cardiol.* **41**(10), 1776–1782 (2003).
60. M. Mirza, S. Marston, R. Willott, C. Ashley, J. Mogensen, W. McKenna, P. Robinson, C. Redwood, and H. Watkins, Dilated cardiomyopathy mutations in three thin filament regulatory proteins result in a common functional phenotype. *J. Biol. Chem.* **280**(31), 28498–28506 (2005).
61. A. N. Chang, K. Harada, M. J. Ackerman, and J. D. Potter, Functional consequences of hypertrophic and dilated cardiomyopathy-causing mutations in alpha-tropomyosin. *J. Biol. Chem.* **280**(40), 34343–34349 (2005).

20

CARDIAC TROPONIN LEVELS AS A PREFERABLE BIOMARKER OF MYOCARDIAL CELL DEGRADATION

Teruhiko Toyo-oka and Hiroyuki Kumagai

Abbreviations in the article,
A, actin; ACS, acute coronary syndromes; AMI, acute myocardial infarction; CCU, coronary care unit; CK, creatine kinase; CK-MB, creatine kinase-MB isoenzyme; cTnI, cardiac troponin-I subunit; cTnT, cardiac troponin-T subunit.; HC, myosin heavy chain; LC_1, light chain 1 of myosin; LC_2 light chain 2 of myosin; P_1 and P_2 degraded products; NAM, natural actomyosin; SDS-PAGE, sodium dodecylsulfate-polyacrylamide gel electrophoresis; Tm, tropomyosin; sTn, troponin.

20.1. PREFACE

The enzymatic assay of creatine kinase (CK) activity in serum was established in 1959 by Okinaka's group including Dr. Ebashi. As a biomarker of muscle cell injury,[1] the activity assay has been a main procedure to make the precise diagnosis among most markers. It is my honor and privilege to appreciate Dr. Setsuro Ebashi and his wife, Dr. Fumiko Ebashi, for their discovery of troponin (Tn) in skeletal muscle and cardiac muscle and their contribution to the clinical research of a variety of skeletal and cardiac muscle diseases or syndromes, as well as the biological significance.[2]

In addition to the original World Health Organization criteria,[3] the European Society of Cardiology (ESC, ref. 4) and joint committee of the American College of Cardiology and American Heart Association have discussed refinements of not only diagnosis, but also risk stratification and decision-makings for the treatment of several cardiac diseases that accompany myocardial injury.[5] The cTn assay is now a golden standard in marker testing for the management of patients with suspected acute myocardial infarction (AMI), acute coronary syndromes (ACS), myocarditis of several origins and cardiac trauma or surgery. This monograph was not intended to make a review but mainly addressed to a

Department of Molecular Cardiology, Tohoku University Bioengineering Research Organization (TUBERO); Department of Pathophysiology and Internal Medicine, Tokyo University Hospital, University of Tokyo, Tokyo, Japan

Regulatory Mechanisms of Striated Muscle Contraction
Edited by Ebashi and Ohtsuki, Springer, 2007

short overview of the current state of cTn measurement, emphasizing (1) biomarkers of necrosis and/or ischemia; (2) their roles in precise diagnosis; and (3) triage and selection of the treatment of patients with suspected acute AMI or ACS.[6]

20.2. BIOMARKER INCREMENT IN PLASMA OR SERUM IN CORONARY DISEASES

It is necessary to establish both the high specificity and high sensitivity that may vary with time after the onset of symptoms. The spectrum of ischemic heart disease is not fixed in a single stage but includes acute (sudden death, non-Q- and Q-wave infarctions), subacute and chronic (stable, unstable, and variant angina) phases. Both cTnI and cTnT are now the most valuable in the diagnosis of ACS, and some of these markers are increasingly found to have a predictive value in ischemic heart disease or heart failure in general.

Improved plasma biomarkers with better sensitivity and specificity have been examined in preference to other classic markers, such as total CK activity, its MB isoform (CK-MB), lactate dehydrogenase, and/or aspartate aminotransferase. Rapid assays helpful for the early detection of infarction will be delineated, and the cTnI and/or cTnT will be recommended to serve for the risk stratification of patients with ACS. Katus et al. found that an unbound cytosolic troponin T pool was detected in ultracentrifuged homogenates of myocardial tissue of different species ranging from 0.013 to 0.036 mg/g wet weight. The soluble troponin T molecule had electrophoretic properties identical to troponin T compartmented in the myofibrils.[7]

In human patients with AMI, cTnI starts to be detected early after the onset of chest pain (4.3 ± 2.1 h, mean ± SD) peaked at 12.2 ± 4.6 h in a population undergoing fibrinolysis therapy, which is now one of the most beneficial treatments except emergency coronary angioplasty or coronary percutaneous intervention. The cTnI disappearance was generally observed between 5 and 9 days after. When reperfusion therapy was not undertaken, both the peak and the washout time are delayed, probably reflecting gradual release to systemic circulation *via*. lymphatic flow within AMI region. No cTnI was detected in healthy subjects or in a control group of patients with skeletal damage or rhabdomyolysis. This assay allows a specific diagnosis of AMI in an acute phase with extremely high diagnostic meaning (ref. 5). Plasma increment of these biomarkers in cardiac muscle cells is indicative of myocardial injury, but the elevations do not simply approve the diagnosis of AMI. Both cTnI and cTnT are the preferable markers for the diagnosis of myocardial injury, compared with CK-MB or other conventional markers.[8,9]

20.3. SPECIFICITY OF cTn AS THE CARDIAC MARKER

Antibodies of the first generation had made the specificity of cTnT questionable, through the epitope similarity between skeletal and cardiac Tn, especially in patients with renal failure.[10] Introduction of the second generation of specific antibody improved the diagnostic significance of cTn.[11] Immunohistochemical and molecular studies on the skeletal muscle has established that the isoforms of TnT expressed in response to skeletal muscle injury has not been detected with the newer assays.[11] When conjoint skeletal and

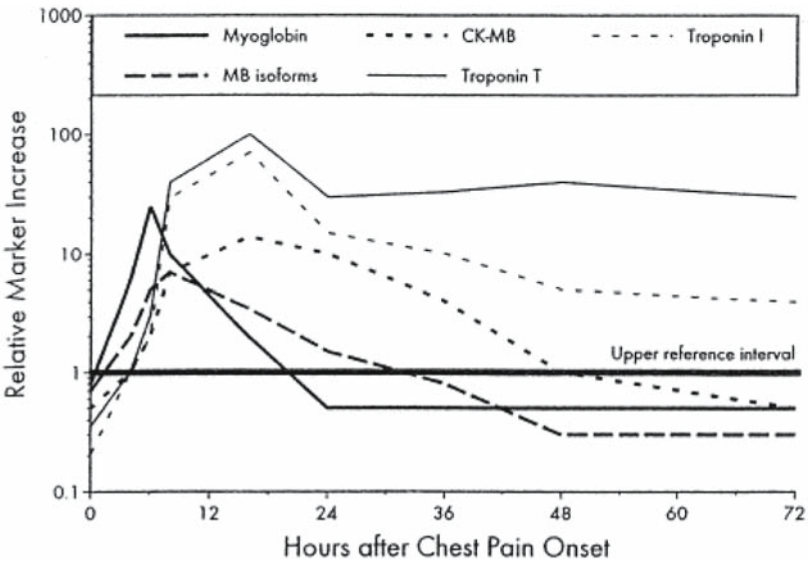

Figure 20.1. Time course after the cardiac symptom onset for various biochemical markers of myocardial necrosis. CK-MB, creatine kinase-MB isoenzyme.

cardiac injury is present, the improved specificity of both cTnT and cTnI reduces the number of false-positive results while maintaining high sensitivity.[11]

These results along with the prolonged time window during which Tn markers are elevated allows detection of a larger number of patients at risk of subsequent adverse cardiac events.[5,6] For these reasons, cTn was more valuable for the accurate diagnosis than classic CK-MB activities.[7,11] Classic markers other than cTn have shown poor specificity for the detection of cardiac injury secondary to their wide tissue distribution. Because increases of cTn are persistent (Figure 20.1), timing of myocardial events can be unclear (e.g., if the cTn values are increased in the first sample on presentation or in situations where re-infarction is suspected). In these settings, myoglobin or CK-MB values may be useful in estimating whether the event is recent (within 48 h).

20.4. TnI OR TnT FOR ACTUAL DIGNOSIS?

Tn complex in striated muscles would be expressed in 4 different isoforms, two in skeletal muscle (slow-twitch and fast-twitch fibers), and two in cardiac muscle (ventricular, ref. 2, and probably atrial fibers, ref. 12). Either cTnI or cTnT is available for clinical diagnosis of myocardial cell injury. The direct evidence for the diagnostic value of cTnT and cTnI was derived from an experimental dog model.[13] In 1981, Toyo-oka and Ross analyzed the Ca^{2+} sensitivity of natural actomyosin (NAM) isolated from both the intact left ventricular muscle and an area of AMI by use of superprecipitation response from 2 to 48 h after the coronary artery ligation. NAM contains regulatory proteins, *i.e.* tropomyosin and three components of Tn (TnT, TnI and TnC) in addition to actomyosin.[2] NAM from the intact tissue showed normal superprecipitation and normal Ca^{2+} sensitivity. Four

hours after the coronary ligation, Ca^{2+} sensitivity was lowered only in the endocardial AMI region; it was markedly decreased both in the epicardial and endocardial halves at 6 h and completely lost at 24 and 48 h.

A superprecipitation response was, however, demonstrated in all samples, indicating that both myosin and actin preserved their functions in the course of MI. With SDS-PAGE, NAM from the AMI region revealed moderate decrease of cTnT and cTnC and drastic reduction of cTnI and resulted in the formation of extra bands of low molecular weights (Figure 20.2). The degradation and release of cTn subunits from NAM occurs early and from the endocardial half of MI region.[13]

Later, the cTnI degradation was shown to accompany covalent bond formation with cTnT.[14] The cTnI products in rat hearts after a brief ischemia followed by reperfusion that occurs naturally or intentionally after coronary intervention therapy. cTnI was progressively degraded from 210 amino acid residues to fragments 1–193, 63–193, and 73–193 with increased severity of injury.[14]

McDonough et al. have proposed a model in which the extent of proteolytic and transglutaminase activities to make a complex of cTnI with the counterpart, cTnT, ultimately determines whether apoptosis or necrosis is achieved.[14] The diagnostic performance of cTnT assay in the differential diagnosis of suspected patients were studied in coronary care unit (CCU). At a cutoff value of 0.2 μg/L, cTnT measurements at 12–24 h after admission or 12–48 h from the onset of chest pain showed an overall efficiency of 97.6% for diagnosis of proven AMI. It was not detectable when ischemic heart disease was excluded but was present in a few patients with angina. Detectable cTnT in the last group patients was associated with subsequent cardiac events.[8] Both cTnI and cTnT are found to be useful for determining triage of patients in CCU, when rapid and accurate testing is employed.[15] In contrast, cardiac troponin-C subunit has less valuable for the

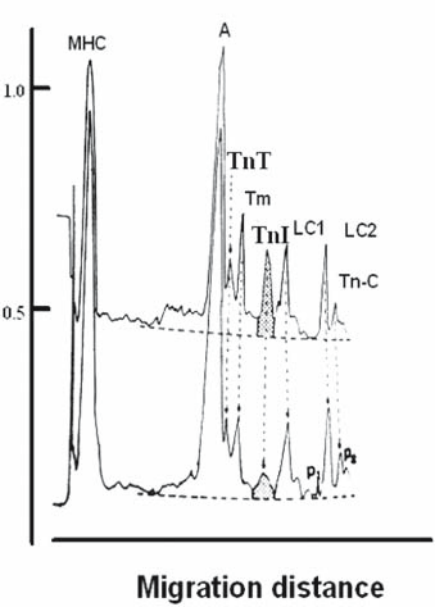

Figure 20.2. Densitometry of SDS-PAGE of natural actomyosin prepared from control region (upper trace) or ischemic site (lower trace) of dog heart. Because the amount of protein applied on gel was adjusted to 20 μg, the amount of myosin heavy chain (HC) or actin (A) looked to be increased. Note the marked reduction of TnI and moderate decrease of TnT even at these modified conditions. *Other abbreviations*: LC_1, light chain 1 of myosin; LC_2 light chain 2 of myosin; P_1 and P_2 degraded products and Tm, tropomyosin.

accurate diagnosis of myocardial injury, because specific antibody for cardiac, but not for skeletal, troponin is difficult to prepare, possessing high titer.

20.5. IRREVERSIBLE OR REVERSIBLE INJURY TO HESRT?

Moderate increases in cTnI and cTnT have raised a question whether all such increments represent an irreversible injury. Morphologically, it is difficult to recognize the reversible injury. Though each Tn component is smaller than CK-MB, cTnI, is chemically modified and released as complexes with a similar molecular weight to that of CK-MB.[14] In addition, because 97% of cTnI and 95% of cTnT are tightly complexed to thin filaments,[2] the Tn fragments degraded from the contractile machinery would have higher specificity for the irreversible injury, than other markers released from the cytosol.[9,10]

A relationship was observed between the amount of cTn released and the amount depleted from the myocardium.[16] Cardiac pacing to temporally induce myocardial ischemia together with coronary sinus blood sampling has failed to detect increase in cTn.[17] These data suggest that temporary ischemia does not cause of leakage of macromolecules from cardiomyocytes, unlike an increased permeability in advanced heart failure.[18]

Experimental models or human cases in which cTn increases have been observed to be associated with histological evidence of myocardial injury.[16,17] Furthermore, there will likely be a continuum from reversible to irreversible release, and it may be hard to determine which type elevates these biomarker levels. Regardless of the mechanism of cellular injury, it may not be important in clinical situations to discriminate the precise mechanisms of the injury.

20.6. STANDARDIZATION FOR Tn ASSAYS

To exactly compare clinical reports from different clinics, a high level of consistency is critical across manufacturers' lots. Differential antibody recognition of degraded products may reflect hydrolysis of the epitopes on cTnI or cTnT by endogenous protease(s), such as calcium-activated neutral proteases (CANP, calpains, ref. 18–22), lysosomal proteases[23] or the ubiquitin-proteasome system.[24] Some degradation can also occur in other compartments, and the sites of reaction for many of the cleavage products are still being defined.[25,26]

Thus, it appears that central region epitope-based assays will be preferred. For the cTnI and cTnT assay and for CK-MB activity measurements, the upper limit should be set to the 99th percentile. This corresponds to 3SDs, but not to 2SD as is the case in other assays, above the mean for the normal range and serial determinations are required to clarify Tn increases when values are near the reference limit.[9]

20.7. DEFINITION OF ACUTE MYOCALDIAL INFARCTION (AMI)

The term AMI should provide evidence of cardiac damages, as detected not only by biomarkers indicative of myocardial ischemia but also by the documentations of other clinical symptoms with chest pain, echocardiography and ECG recordings. However, if

it is unclear whether the ischemia is truly etiologic, additional information may be added to determine mechanism of the biomarker increase. Subendocardial injury due to the increased wall stress occurs in patients with congestive heart failure, hypertension with left ventricular hypertrophy, response to tachycardia and hemodynamic compromise (*ex*, in patients with shock) or to right ventricular injury in patients with pulmonary embolism.[27]

20.8. STRATIFICATION OF RISK AMONG PATIENTS WITH ACUTE CORONARY SYNDROME (ACS)

For patients with an ischemic injury, the prognosis is related in part to the extent of increase in levels of cTnI and cTnT. This contention has been reported for patients with unstable angina and overt AMI.[28–30] Therapy should be predicated on the extent of the increases, the type of infarction (i.e., Q-wave or non–Q-wave), and the other clinical factors that lead to high or low risk. Isolated elevations in the absence of other criteria do not mandate a similarly aggressive approach (Figure 20.3).

20.9. cTn LEVELS IN MISCELLANEOUS PATHOLOGICAL PROCESSES

This chapter is not intended to declare the non-specificity or non-accuracy of the diagnosis of ischemic myocardial diseases. Because both cTnT and cTnI leak from injured myocardial cells, the increments are often detected under several pathological conditions. The increments occur secondary to direct trauma or injury to the heart,[31] as a result of myocardial toxins such as adriamycin or 5-fluorouracil that is of great use for the chemotherapy of several malignant tumors,[32] or in response to endogenous substances released in critically ill patients with septic shock.[33,34] It would be very attractive to assume that levels of cTnT or cTnI predict the appropriate dose not to cause an irreversible injury to cardiac muscle cells.

Mechanical ablation,[35] electrical discharges of implantable cardioverter defibrillator and cardioversion[36,37] induce cardiac injury. Furthermore, a variety of transitory abnor malities can cause minor degrees of myocardial injury that may occur with cardiotrophic

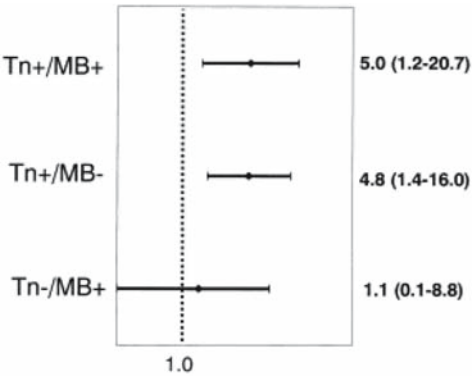

Figure 20.3. Adjusted OR and 95% CI for 30-day death or MI by marker status in the CHECKMATE population (patients with negative results for CK-MB and Tn [Tn−/MB−] are the reference group. +, positive; −, negative; CI, confidence interval; CK-MB, creatine kinase-MB isoenzyme; MI, myocardial infarction; OR, odds ratio; Tn, troponin.

infections with bacteria[38] or virus,[39] with only a small subset of patients progressing to overt myocarditis.[40]

20.10. DECISION-MAKING FOR TREATMENT FOLLOWING cTn LEVEL MEASUREMENTS

Abe et al. measured cTn and CK-MB levels in patients with AMI whose infarct-related artery was totally occluded before reperfusion therapy and sequentially calculated the increase in cTnT (ΔcTnT) and CK-MB (ΔCK-MB). Mean ΔcTnT and ΔCK-MB levels were 20 to 50 and 12 to 15 folds higher in a successful angioplasty group and in a successful fibrinolytic group, respectively, than those in an unsuccessful reperfusion group 60 min after treatment. The predictive accuracy for detecting reperfusion was 100% in the first group and 92% in the second group 60 min after treatment.[41]

Combination of a rapidly appearing marker (CK-activity or myoglobin) and a marker that rises later (cTn or CK-MB) is recommended for patients in need of urgent diagnosis. This approach should be used when the results will lead to changes in therapy. Blood sampling time should be set at admission, at 2 to 4 hours, at 6 to 9 hours, and at 12 to 24 hour as an optional sampling. A similar protocol is advocated for patients undergoing interventional procedures. However, in this situation, the initial sample should be taken before the procedure.[42]

Riou et al. prospectively measured both circulating cTnT and the left ventricular ejection fraction area (LVEFa) in brain-dead patients to determine the candidate for the donor in cardiac transplantation. They found that 61% patients showed normal LVEFa, 25% demonstrated moderate decrease (30% to 50%), and the rest had severe decrease (less than 30%).[43] Circulating cTn levels were significantly higher in patients with a severe reduction in LVEFa than in other groups, and they found a significant correlation between LVEFa and cTnT concentration. Furthermore, cTnT level is more accurate in predicting a severe decrease in LVEFa than an elevated CK-MB activity. Since the quality of the donor's heart may determine the prognosis in heart transplantation, the assay of circulating cTnT level could be useful.

20.11. CONCLUSION

Measurement of either cTnI or cTnT is the most reliable index so far not only to evaluate ischemia in myocardial tissue but also to estimate the prognosis of patients with a variety of cardiac diseases. Therefore, the quantification of the cTn level is the most valuable for establishing triage and/or a decision of the treatment option in a patient's care, e.g. conventional or aggressive.

20.12. ACKNOWLEDGEMENTS

A part of this study was financially supported by the Ministry of Education, Science and Culture and the Ministry of Health, Welfare and Labor, Vehicle Foundation and Uehara Memorial Foundation, Japan. The authors appreciate Ms. Asao and Ms. Goto for their collaboration in preparing the manuscript.

20.13. REFERENCES

1. S. Okinaka, H. Sugita, H. Momoi, and S. Ebashi, et al., Serum creatine phosphokinase and aldolase activity in neuromuscular disorders. *Trans. Am. Neurol. Assoc.* **84**, 62–64 (1959).
2. S. Ebashi, Y. Nonomura, and T. Toyo-oka, et al., Regulation of muscle contraction by the calcium-troponin- tropomyosin system, *Symp. Soc. Exp. Biol.* (Cambridge Univ. Press) **30**, 349–360 (1976).
3. Hypertension and coronary heart disease: classification and criteria for epidemiological studies, *WHO Tech. Support. Ser.* **168**, 3–28 (1959).
4. H. A. Katus, A. Remppis, and F. J. Neumann, et al., Diagnostic efficiency of troponin T measurements in acute myocardial infarction, *Circulation* **83**, 902–912 (1991).
5. A. S. Jaffe, J. Ravkilde, and R. Roberts, et al., It's time for a change to a troponin standard, *Circulation* **102**, 1216 (2000).
6. O. Bazzino, J. J. Fuselli, and F. Botto, et al., PACS group of investigators. Relative value of N-terminal probrain natriuretic peptide, TIMI risk score, ACC/AHA prognostic classification and other risk markers in patients with non-ST-elevation acute coronary syndromes, *Eur. Heart J.* **25**, 859–866 (2004).
7. H. A. Katus, A. Remppis, Sheffold, et al., Intracellular compartmentation of cardiac troponin T and its release kinetics in patients with reperfused and nonreperfused myocardial infarction, *J. Am. Coll. Cardiol.* **67**, 1360–1367 (1991).
8. H. A. Katus, A. Remppis, and F. J. Neumann, et al., Diagnostic efficiency of troponin T measurements in acute myocardial infarction, *Circulation* **83**, 902–912 (1991).
9. J. E. Adams 3rd, G. A. Sicard, and B. T. Allen, et al., Diagnosis of perioperative myocardial infarction with measurement of cardiac troponin I, *N. Engl. J. Med.* **330**, 670–674 (1994).
10. M. D. McLaurin, F. S. Apple, and E. M. Voss, et al., Cardiac troponin I, cardiac troponin T, and creatine kinase MB in dialysis patients without ischemic heart disease: evidence of cardiac troponin T expression in skeletal muscle, *Clin. Chem.* **43**, 976–982 (1997).
11. V. Ricchiuti, E. M. Voss, and A. Ney, et al., Cardiac troponin T isoforms expressed in renal diseased skeletal muscle will not cause false-positive results by the second generation cardiac troponin T assay by Boehringer Mannheim, *Clin. Chem.* **44**, 1919–1924 (1998).
12. T. Katsuki, T. Toyo-oka, and T. Takayasu, et al., Differences in regulatory mechanisms of atrial and ventricular muscle contraction in bovine heart, *Jpn Circ. J.* **52**, 376–384 (1988).
13. T. Toyo-oka, J. Ross Jr, Ca^{2+} sensitivity change and troponin loss in cardiac natural actomyosin after coronary occlusion, *Am. J. Physiol.* **240**, H704–H708 (1981).
14. J. L. McDonough, D. K. Arrell, and J. E. Van Eyk, et al., Troponin I degradation and covalent complex formation accompanies myocardial ischemia/reperfusion injury, *Circ. Res.* **84**, 9–20 (1999).
15. C. W. Hamm, C. Heeschen, and B. Goldmann, et al., Benefit of abciximab in patients with refractory unstable angina in relation to serum troponin T levels: c7E3 Fab Antiplatelet Therapy in Unstable Refractory Angina (CAPTURE) study investigators, *N. Engl. J. Med.* **340**, 1623–1629 (1999).
16. E. M. Voss, S. W. Sharkey, and A. E. Gernert, et al., Human and canine cardiac troponin T and creatine kinase-MB distribution in normal and diseased myocardium: infarct sizing using serum profiles, *Arch. Pathol. Lab. Med.* **119**, 799–806 (1995).
17. V. Ricchiuti, S. W. Sharkey, and M. M. Murakami, et al., Cardiac troponin I and T alterations in dog hearts with myocardial infarction: correlation with infarct size, *Am. J. Clin. Pathol.* **110**, 241–247 (1998).
18. T. Toyo-oka, T. Kawada, and J. Nakata, et al., Translocation and cleavage of myocardial dystrophin as a common pathway to advanced heart failure: a scheme for the progression of cardiac dysfunction, *Proc. Natl. Acad. Sci. USA* **101**, 7381–7385 (2004).
19. T. Toyo-oka, T. Shimizu, and T. Masaki, Inhibition of proteolytic activity of calcium activated neutral protease by leupeptin and antipain, *Biochem. Biophys. Res. Commun.* **82**, 484–491 (1978).
20. T. Toyo-oka, and T. Masaki, Calcium-activated neutral protease from bovine ventricular muscle: isolation and some of its properties, *J. Mol. Cell. Cardiol.* **11**, 769–786 (1979).
21. H. Yoshida, M. Takahashi, and M. Koshimizu, et al., Decrease in sarcoglycans and dystrophin in failing heart following acute myocardial infarction, *Cardiovasc. Res.* **59**, 419–427 (2003).
22. M. Takahashi, K. Tanonaka, and H. Yoshida, et al., Effects of ACE inhibitor and AT(1) blocker on dystrophin-related proteins and calpain in failing heart, *Cardiovasc. Res.* **65**, 356–365 (2005).
23. K. Wildenthal, J. S. Crie, J. M. Ord, and J. R. Wakeland, The role of lysosomes and microtubules in cardiac protein degradation, *Adv. Myocardiol.* **5**, 137–144 (1985).

24. M. H. Glickman, A. Ciechanover, The ubiquitin-proteasome proteolytic pathway: destruction for the sake of construction, *Physiol. Rev.* **82**, 373–428 (2002).
25. A. G. Katrukha, A. V. Bereznikova, and V. L. Filatov, et al., Degradation of cardiac troponin I: implication for reliable immunodetection, *Clin. Chem.* **44**, 2433–2440 (1998).
26. Q. Shi, M. Ling, and X. Zhang, et al., Degradation of cardiac troponin I in serum complicates comparisons of cardiac troponin I assays, *Clin. Chem.* **45**, 1018–1025 (1999).
27. E. Missov, C. Calzolari, and B. Pau, Circulating cardiac troponin I in severe congestive heart failure, *Circulation* **96**, 2953–2958 (1997).
28. M. Galvani, F. Ottani, and D. Ferrini, et al., Prognostic influence of elevated values of cardiac troponin I in patients with unstable angina, *Circulation* **95**, 2053–2059 (1997).
29. C. W. Hamm, C. Heeschen, and B. Goldmann, et al., Benefit of abciximab in patients with refractory unstable angina in relation to serum troponin T levels: c7E3 Fab Antiplatelet Therapy in Unstable Refractory Angina (CAPTURE) study investigators, *N. Engl. J. Med.* **340**, 1623–1629 (1999).
30. P. Stubbs, P. Collinson, and D. Moseley, et al., Prognostic significance of admission troponin T concentrations in patients with myocardial infarction, *Circulation* **94**, 1291–1297 (1996).
31. J. E. D. Adams, G. S. Bodor, and V. G. Davila-Roman, et al., Cardiac troponin I: a marker with high specificity for cardiac injury, *Circulation* **88**, 101–106 (1993).
32. F. M. Fink, N. Genser, and C. Fink, et al., Cardiac troponin T and creatine kinase MB mass concentrations in children receiving anthracycline chemotherapy, *Med. Pediatr. Oncol.* **25**, 185–189 (1995).
33. C. Spies, V. Haude, and R. Fitzner, et al., Serum cardiac troponin T as a prognostic marker in early sepsis, *Chest* **113**, 1055–1063 (1998).
34. T. M. Guest, A. V. Ramanathan, and P. G. Tuteur, et al., Myocardial injury in critically ill patients: a frequently unrecognized complication, *JAMA* **273**, 1945–1949 (1995).
35. S. P. Rao, S. Miller, and R. Rosenbaum, et al., Cardiac troponin I and cardiac enzymes after electrophysiologic studies, ablations, and defibrillator implantations, *Am. J. Cardiol.* **84**(4), **470**, A9 (1999).
36. J. J. Allan, R. D. Feld, and A. A. Russell, et al., Cardiac troponin I levels are normal or minimally elevated after transthoracic cardioversion, *J. Am. Coll. Cardiol.* **30**, 1052–1056 (1997).
37. J. Zimmerman, R. Fromm, and D. Meyer, et al., Diagnostic marker cooperative study for the diagnosis of myocardial infarction, *Circulation* **99**, 1671–1677 (1999).
38. J. Kamblock, L. Payot, and B. Iung, et al., Does rheumatic myocarditis really exists? Systematic study with echocardiography and cardiac troponin I blood levels, *Eur. Heart J.* **24**, 855–862 (2003).
39. B. Lauer, C. Niederau, and U. Kuhl, et al., Cardiac troponin T in the diagnosis and follow up of suspected myocarditis, *Dtsch. Med. Wochenschr.* **123**, 409–417 (1998).
40. J. Soongswang, K. Durongpisitkul, and S. Ratanarapee, et al., Cardiac troponin T: its role in the diagnosis of clinically suspected acute myocarditis and chronic in children, *Pediatr. Cardiol.* **23**, 531–535 (2002).
41. S. Abe, S. Arima, and T. Yamashita, et al., Early assessment of reperfusion therapy using cardiac troponin T, *J. Am. Coll. Cardiol.* **23**, 1382–1389 (1994).
42. M. A. Karim, M. S. Shinn, and H. Oskarsson, et al., Significance of cardiac troponin T release after percutaneous transluminal coronary angioplasty, *Am. J. Cardiol.* **76**, 521–523 (1995).
43. B. Riou, S. Dreux, and S. Roche, et al., Circulating cardiac troponin T in potential heart transplant donors, *Circulation* **92**, 409–414 (1995).
44. R. J. Aviles, A. T. Askari, and B. Lindahl, et al., Troponin T levels in patients with acute coronary syndromes, with or without renal dysfunction, *N. Engl. J. Med.* **346**, 2047–2052 (2002).

IV

REGULATION BY MYOSIN

21

REGULATION BY MYOSIN: HOW CALCIUM REGULATES SOME MYOSINS, PAST AND PRESENT

Andrew G. Szent-Györgyi

21.1. INTRODUCTION

This symposium celebrates the seminal discovery of troponin by Professor Ebashi. In the 1960s we knew quite a bit about how muscle functions. It was established that contraction was the result of the interaction of ATP with the complex formed from actin and myosin.[1] The filamentous structure[2] and the constancy of the A-band of striated muscle led to the sliding filament theory.[3,4] A detailed model relating muscle mechanics with the cross bridge cycle was produced.[5] A change in orientation of the cross bridge between rest and rigor in insect muscle was also demonstrated.[6] However, we were ignorant regarding how muscles stay relaxed.

The discovery reported in the paper by Kumagai, Ebashi and Takeda (alias Mrs. Ebashi) that the "Marsh factor" is not a soluble enzyme[7] and the demonstration that it serves as a calcium-pump[7a,8,9] opened the way to our present understanding of calcium activation of contraction in heart and skeletal muscles and its role in excitation-contraction coupling. Ebashi's discovery of troponin, and the role of tropomyosin 40 years ago,[10,11] followed by studies with his colleagues, opened our understanding of the molecular basis of regulation. These works continue to provide the foundation of present day research on how contraction of these muscles is inhibited by the action of troponin and tropomyosin on actin in the absence of calcium, and how calcium reverses this inhibition.[12] I am deeply honored to participate in this celebration and to pay homage to the insights and originality of Professor Ebashi. I am eager to listen to the great advances arising from the seeds Professor Ebashi with his collaborators have planted and so carefully nurtured.

I will concentrate on describing some of the history and main features of regulation of molluscan myosins, since these are activated directly by binding calcium and therefore are simpler to study. Much of the information was obtained by *in vitro* experiments on scallop myosin, which turned out to be particularly suitable both for transient kinetic studies and also for structural studies at the atomic level. Smooth muscle myosin is regulated by phosphorylation, which in turn requires calcium-dependent activation of myosin

Brandeis University, Waltham, USA

Regulatory Mechanisms of Striated Muscle Contraction
Edited by Ebashi and Ohtsuki, Springer, 2007

light chain kinase. Nevertheless, in spite of differences in the path of activation, many of the features of regulation of these myosins are similar.

21.2. EVIDENCE FOR MYOSIN LINKED REGULATION

Myosin-linked regulation was discovered some six years after Ebashi's epochal studies. We wanted to check whether all troponin components were associated with thin filaments Native thin filaments could be readily obtained from molluscan muscles without exposure to organic solvents or concentrated salt solutions.[13] Thin filaments obtained from *Mercenaria mercenaria* muscles activated the ATPase activity of rabbit myosin but the activation did not require calcium, indicating that the filament preparation did not contain active regulatory proteins that were functional[13] (Figure 21.1). In contrast, when different molluscan myosins were combined with pure rabbit actin lacking tropomyosin and troponin, calcium was needed for ATPase activity. Molluscan thin filaments did not bind calcium unless combined with regulatory proteins prepared from rabbit muscle (Figure 21.2). The myosin of several molluscan muscles contained a high affinity specific calcium binding site that bound Ca^{2+} even in the presence of several millimolar concentrations of magnesium[14] (Figure 21.3). Therefore, molluscan myosins were directly regulated by calcium.

Tropomyosin is present in all molluscan thin filaments so far studied.[15] Several different thin filament preparations also contained troponin components, and troponin could be obtained from several molluscan muscles.[16,17] Nevertheless, striated scallop myosin ATPase is significantly activated by calcium in the absence of actin,[18,19] and regulation of tension generation by skinned fiber bundles of *Placopecten magellanicus* (the sea scallop) requires scallop regulatory light chains.[20]

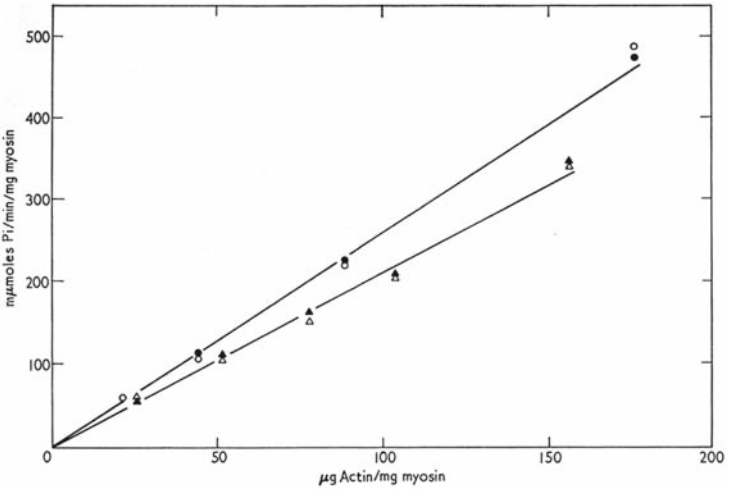

Figure 21.1. ATPase activation of rabbit myosin by pure rabbit actin (circles) and by the thin filaments of *Mercenaria mercenaria* (triangles). *Empty* symbols: in the presence of 10 μM $CaCl_2$. Filled symbols: in the presence of 100 μM EGTA. Conditions: 30 mM KCl, 1 mM $MgCl_2$ and 0.5 mM ATP at pH 7.6. Note the lack of calcium effect. Reproduced by permission [Szent-Györgyi et al. *J. Mol. Biol.* **56**, 239–258 (1971)].

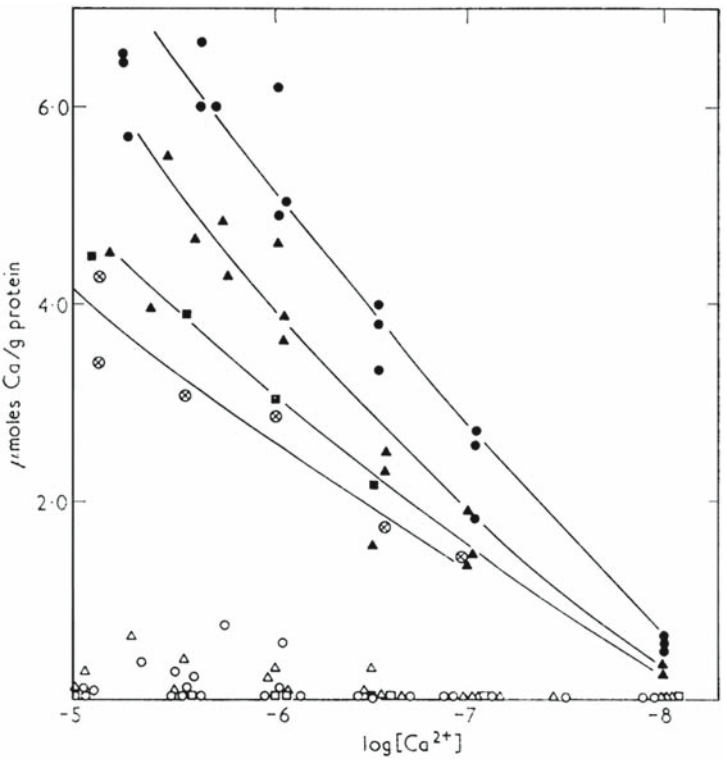

Figure 21.2. Calcium binding by thin filaments: Empty symbols: native thin filaments, filled symbols: filaments with added regulatory proteins…Circles with x: rabbit thin filaments. Circles: *Mercenaria* thin filaments. Squares: striated *Aquipecten* thin filaments. Triangles: purified rabbit actin. Conditions: 50 mM KCl, 5 mM $MgCl_2$, 5 mM imidazole (pH 7). Note that the molluscan thin filaments bind calcium only if regulatory proteins are added. Reproduced by permission [Kendrick-Jones et al. *J. Mol. Biol.* **54**, 313–326 (1970)].

21.3. THE ROLE OF THE LIGHT CHAINS IN REGULATION

The light chains are regulatory subunits. To clarify their roles, the studies concentrated on the striated scallop adductor muscles. This was a lucky choice since it was particularly suitable to demonstrate the different roles of the regulatory light chain (RLC) and the essential light chain (ELC), and also was suitable for determination of atomic structures. The role of the RLC is to inhibit contraction, while the ELC binds calcium and thereby induces contraction.

The light chains occupy the neck region of the myosin head, known as subfragment-1 (S1). Along with this neck region, they form the "regulatory domain," which is also called the lever arm. The light chains and this short region of the heavy chains mutually stabilize each other so that the whole regulatory domain is protected from proteolysis.[21]

The RLC can be partially removed in the cold by addition of EDTA[22] that binds the magnesium of the N-terminal EF hand.[23] The removal of the RLC from myosin is complete at room temperature.[24] Evidently, both hydrophobic interactions and salt links play a role in RLC binding. It is noteworthy that there is a cluster of hydrophobic residues in

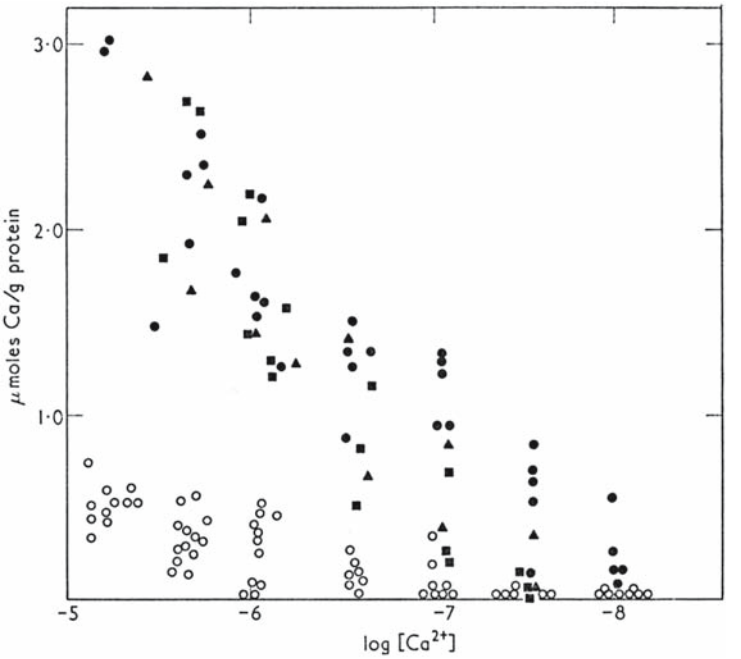

Figure 21.3. Calcium binding by myosins. Empty symbols: rabbit myosin. Filled symbols: molluscan myosins. Circles: *Mercenaria*, squares: *Aquipecten* striated triangles: *Aquipecten* smooth muscle myosins. Reproduced by permission [Kendrick-Jones et al. *J. Mol. Biol.* **54**, 313–326 (1970)].

the heavy chain where the RLC binds.[25] In addition scallop RLC binds relatively weakly to the heavy chain, since it has a methionine in place of glutamate, present in other RLCs.[26] Loss of the RLC removes the inhibition of ATPase activity or tension development. In the absence of the RLC, the myosin does not bind calcium. Foreign RLCs obtained from regulated myosins restore regulation and calcium binding.[27,28] Hybrids formed with RLCs obtained from skeletal and cardiac myosins are not regulated.[28]

The ELC activates ATPase activity by binding calcium. Since the exchange of the ELC on myosin is limited, calcium binding is best studied on the regulatory domain. In 4 M urea the light chains detach from the heavy chain and the components can be isolated in the presence of urea by gel filtration. Upon removal of urea the heavy chain fragment spontaneously recombines with the light chains. However, calcium binding is restored to the recombined regulatory domain only if the source of ELC is molluscan myosin.[29]

21.4. THE CALCIUM BINDING SITE

Scallop ELC has four EF hands, but only domain 3 has a conventional EF hand; this was proposed to be the calcium binding site.[30] However, mutations of aspartate to alanine at the +X position or serine to methionine at the –X position did not affect calcium binding. Chimeras between the domains containing EF hands of rat cardiac ELC with scallop ELC domains established that the unusual EF hand is located in domain 1 of

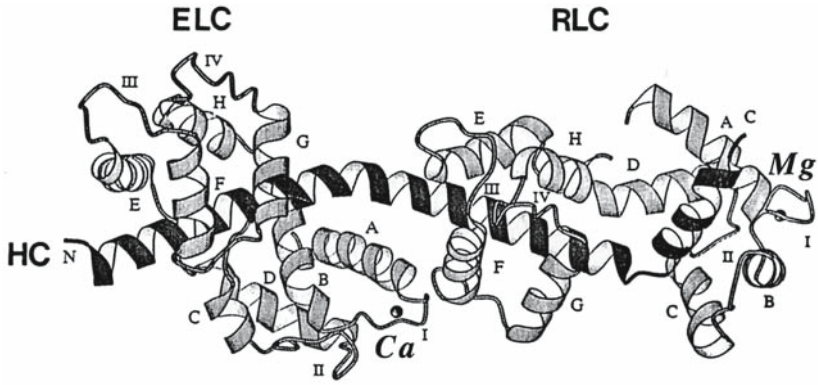

Figure 21.4. Structure of the scallop regulatory domain. Note: Mg^{2+} is bound by the N-terminal lobe of the RLC, Ca^{2+} is located in the first EF hand of ELC. Reproduced by permission [Xie et al. *Nature* **368**, 306–312 (1994)].

scallop ELC.[31] The loop of this domain contains a five residue sequence present only in molluscan ELC. Mutation of aspartate 19 to alanine of the loop of domain 1 abolishes specific calcium binding.[31]

The isolated light chains alone or together fail to bind calcium in the absence of the heavy chain of the regulatory domain. Atomic structure of the regulatory domain shows that although the ELC contains all the ligands for calcium binding, the calcium binding loop needs to be stabilized by the RLC and the heavy chain fragment (Figure 21.4).[32] There is a network of interactions between the light chains and the heavy chain fragments that positions glycine 117 of the RLC close to glycine 23 of the ELC, and the carbonyl bond of the latter provides important ligand for calcium (Figure 21.5). The calcium binding loop is an unusual one and the calcium is bound in a closed conformation of the loop.[33]

The presence of glycine 117 in the RLC is crucial for regulation. RLC from gizzard myosin contains glycine in this crucial position, and even though it activates smooth muscle by phosphorylation, it can replace scallop RLCs without loss of calcium sensitivity.[27] In contrast, hybrids with skeletal RLC, which have methionine in the corresponding position, are not regulated. Mutation of methionine to glycine confers calcium sensitivity to the hybrids and is a "gain in function" mutation.[34]

21.5. KINETICS AND COOPERATIVITY

Regulation requires two headed molecules, such as myosin or HMM. Although S1 can bind calcium and contains both light chains it is fully active in the absence of calcium. Therefore, there is communication between the two heads of myosin which is required for regulation.[22] Regulation can be studied in the absence of actin since soluble HMM alone is activated significantly by calcium and is particularly suitable for kinetic studies.[19] Transient kinetics of HMM ATPase has been extensively investigated using formycine substituted nucleotides whose fluorescence is altered when bound to proteins.[35–37] In the absence of calcium, i.e. in the "off" state, the pathway of ATPase leading to the release of ADP is extremely slow, in the range of several minutes. In the presence of calcium the

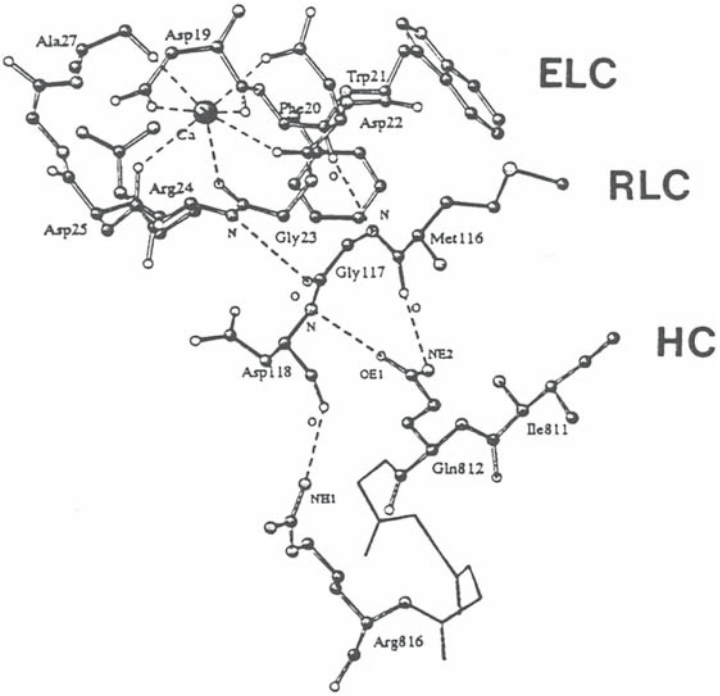

Figure 21.5. Structure of the calcium binding site of domain 1 of the ELC showing some of the critical linkages to the RLC and the heavy chain. Note the link between Gly-117 of the RLC to Gly-23 of the ELC. Reproduced by permission [Xie et al. *Nature* **368**, 306–312 (1994).

slow bypath is eliminated and ADP release is fast. The "off" state is tightly controlled. Single turnover studies that separate the unregulated fraction from the regulated species indicate that calcium activates about 100-fold and activation by actin amounts to an additional 7–10-fold acceleration.[37]

Transient kinetic studies were later expanded for two reasons. It was shown that there is one single gene for the muscle myosins of the bay-scallop, *Argopecten irradians* and the differences between the striated and smooth muscle myosins are due to alternative RNA splicing.[38] The sequence differences between the two muscles are few and concentrated almost exclusively on a 20 residue long segment in surface loop 1 (17 residues out of 20). The same is true for the sea scallop (*Placopecten magellanicus*).[39] It is noteworthy that kinetic analysis of the *Placopecten* catch and striated S1 indicates that the only significant difference between the two is a slower ADP release rate and slower motility in the catch muscle.[40]

A second reason for expanding studies was the observation of cooperativity in the steady state ATPase activity[41] and calcium binding[42] of *Argopecten* HMM. In the absence of nucleotides, calcium binding (obtained by equilibrium dialysis) showed normal binding to S1, HMM, and myosin. Nucleotides did not alter the normal calcium binding by S1; however, in the presence of ADP or other ATP analogs, calcium binding became cooperative with HMM and myosin (Figure 21.6). The cooperativity had a Hill coefficient of 1.8

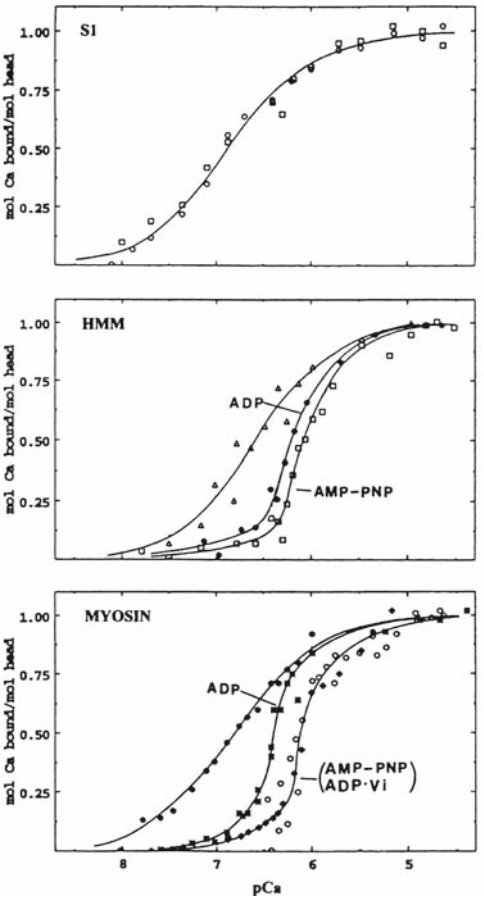

Figure 21.6. Calcium binding by scallop S1, HMM and myosin. Note binding by S1 is hyperbolic unaffected by presence (square) or absence (circles) of nucleotide…Binding by HMM and myosin is normal in the absence of nucleotides and cooperative in their presence. Reproduced by permission [Kalabokis, and Szent-Györgyi, *Biochemistry* **36**, 15834–15840 (1994)].

for HMM and was higher for myosin. The results indicated a communication between the calcium and nucleotide binding sites in double headed constructs but not in S1. The various ATP analogs and ADP had similar effects.[42] This is in sharp contrast with the cross bridge cycle where particular nucleotides occupying the active site define the different structural states. Similar results were obtained in sedimentation studies of the calcium induced asymmetry change of the HMM molecule in the presence of different ATP analogs and ADP,[43] and also in the calcium dependent rate change of ADP dissociation, obtained by transient kinetics.[44] The values of calcium affinity and the Hill coefficients of cooperativity agreed closely using these different techniques. A simple model was developed assuming that scallop HMM can exist in two conformations which are in rapid equilibrium: ADP favoring the "off" state, calcium the "on" state.[44] Without nucleotides, both heads bind strongly to actin even in the absence of calcium. However, ADP dissociates actin from HMM and affinity for actin is very week and exceeds 20 μM.[45] The "off" state is sensitive to ionic strength and is completely abolished at 500 mM KCl, indicating the importance of ionic interactions between the two heads.[19,46]

21.6. STRUCTURAL ASPECTS OF REGULATION

Muscles regulated by myosin need to be tightly controlled in the resting state to avoid wasting excessive amounts of energy at rest. In principle there are two ways to achieve the "off" state. One way is to block a particular step in the cross-bridge cycle by freezing the system at a particular structure of the cycle. Another possibility is that regulated myosins assume a unique structure, different from the ones responsible for the cross-bridge cycle, which is stable enough in the absence of calcium and does not require energy for maintaining the resting state. In skeletal and cardiac muscles, myosin in the pre-power stroke state can interact only weakly with actin in the "off" state. This condition is achieved by the help of the regulatory proteins, which block myosin binding sites on actin, preventing myosin from entering the cross-bridge cycle. However, regulatory myosins must be in the "off" state even in the absence of actin. They accomplish this by having a structure that is not part of the cross-bridge cycle, and are stabilized in the absence of calcium by different ATP analogs and ADP unless activated directly or indirectly by calcium.

The heads of unphosphorylated smooth muscle HMM[47] and scallop HMM[43] in the "off" state bend towards the tail of HMM. This appears to be a stable structure. Upon addition of calcium to scallop HMM the heads become mobile and can enter the cross bridge-cycle.[43] The structure of unphosphorylated smooth muscle HMM has been solved at low resolution obtained by electron microscopy of crystals formed over lipid monolayers[48,49] (Figure 21.7). The important results of this study show that the arrangement of the two heads is asymmetric. The 50 kDa domain of one of the heads (blocked head) interacts with the converter region of the other head (free head). Thus the ATPase activity of both heads is inhibited, while the actin binding ability of the free head may be retained.[48] The structure readily explains why two heads are required for regulation. Such structures are not seen in S1 although three crystal structures of the whole S1 have been obtained from scallop.[50]

It is noteworthy that kinetic studies give support to the asymmetric arrangement of the heads of HMM in the "off" state although there may be differences in some details. Only one head can bind ADP in the absence of calcium[44] and in the case of scallops neither of the two heads binds to actin.[45] Single particle analysis using cryo-electron

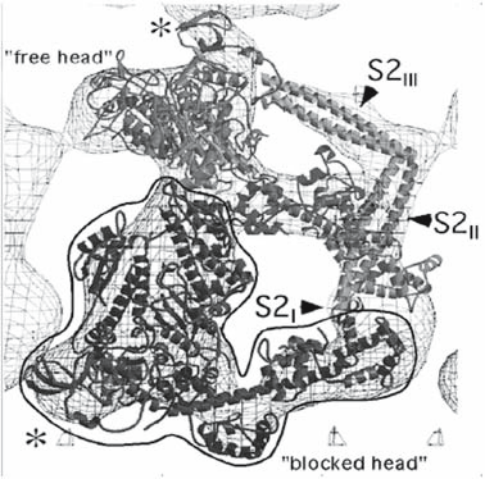

Figure 21.7. Head-head interactions in the "off" state of smooth muscle HMM. Note the asymmetric position of the two heads: the free head is available for actin, ATPase activity of both heads is inhibited. Reproduced by permission [Wendt et al. *J. Cell. Biol.* **147**, 1385–1389 (1999).

microscopy indicates that at low resolution the scallop myosin and smooth muscle myosins form very similar compact structures in the "off" state.[51] In addition, recent studies of tarantula myosin filaments indicate that the unphosphorylated myosin heads lying on the surface of the filament cores also have a similar structure with asymmetrically arranged heads like those found in HMM of smooth muscle.[52] It is possible that regulated muscle myosin II-s in general take up similar structures to maintain the "off" state. Nevertheless, more detailed understanding of possible differences requires the determination of high resolution atomic structures of HMMs in the "off" state.

21.7. PHYSIOLOGICAL IMPLICATIONS

The twitch of the intact striated sea scallop muscle is completed in about 100 milliseconds.[53] The structural change needed for activation needs to be considerably faster. In the absence of calcium and the presence of ADP, isolated myosin filaments exhibit an oblique periodicity arising from the orderly helical arrangement of myosin heads on the surface of the filaments which is readily seen by electron microscopy.[54] Addition of calcium abolishes the periodicity within 10 milliseconds followed by dispersion of the myosin heads away from the core of the filament which is completed within 30 milliseconds.[55] It is noteworthy that the *in vitro* kinetics of the calcium induced conformational change is also very fast and occurs in about 10 milliseconds.[44] It may be that members of other myosin families that alternate between activity and rest solve the problem of saving energy similarly to regulated myosins of muscles, i.e. they can have an "off" state structure that does not consume energy. For instance, myosins involved in transporting organelles (such as myosin V), will use ATP for delivering the load to its destination, then return to its loading platform by diffusion. The "off" state will be different from that of muscle and would include the particular load and the load bearing structures that are coupled to the active site and are involved regulating movement. Such appears to be the case of myosin V.[56] It will be lots of fun to determine the various "off" state structures that satisfy the functional requirements and specificity of the members of the 37 myosin families involved in cellular functions. It would not be surprising if the general principle announced by Prof. Ebashi that regulation by calcium is a reversal of inhibition will turn out to be true not only for muscles but for all the 37 families of myosin.

21.8. ACKNOWLEDGEMENTS

The work described in this review is the result of contributions by students, postdoctoral associates and collaboration with other laboratories. In particularly I am grateful for the 50 years long collaboration with Dr. Carolyn Cohen. The current work is supported by her NIH grant (AR17346).

21.9. REFERENCES

1. A. Szent-Györgyi, Studies on muscle, *Acta Physiol. Scand.* **9**(Suppl. 25), 25 (1945).
2. H. E. Huxley, The double array of filaments in cross-striated muscle, *J. Biophys. Biochem. Cytol.* **3**, 631–648 (1957).

3. A. F. Huxley and A. F. Niedergerke, Structural changes in muscle during contraction. Interference microscopy of living muscle fibers, *Nature* **173**, 971–978 (1954).
4. H. E. Huxley and J. Hanson, Changes in the cross-striations of muscle during contraction and stretch and their structural interpretation, *Nature* **173**, 979–978 (1954).
5. A. F. Huxley, Muscle structure and theories of contraction, *Progr. Biophys. Biophys. Chem.* **7**, 255–318 (1957).
6. M. K. Reedy, K. C. Holmes, and R. T. Tregear, Induced changes in orientation of the cross bridges of glycerinated insect flight muscle, *Nature* **207**, 1276–1280 (1965).
7. S. Kumagai, S. Ebashi, and F. Takeda, Essential relaxing factor in muscle other than myokinase and creatine-phosphokinase, *Nature* **176**, 166 (1955).
7a. A. Weber, R. Herz, and I. Reiss, Study of the kinetics of calcium transport by isolated fragmented sarcoplasmic reticulum, *Biochem. Z.* **345**, 329–369 (1966).
8. W. Hasselbach and N. Makinose, Die calciumpumpe der "erschlaffungsgrana" des muskels und ihre abhangigkeit von der ATP-spaltung, *Biochem. Z.* **333**, 94–111 (1961).
9. S. Ebashi and F. Lippman, Adenosine triphosphate-linked concentration of calcium ions in a particular fraction of rabbit muscle, *J. Cell. Biol.* **14**, 389–400 (1962).
10. S. Ebashi, Third component participating in the superprecipitation of "natural actomyosin", *Nature* **200**, 1010 (1963).
11. S. Ebashi and F. Ebashi, A new protein component participating in the superprecipitation of myosin B, *J. Biochem.* **55**, 604–613 (1964).
12. S. Ebashi and M. Endo, Calcium ion and muscle contraction, *Progr. Biophys. Mol. Biol.* **18**, 123–183 (1968).
13. A. G. Szent-Györgyi, C. Cohen, and J. Kendrick-Jones. Paramyosin and the filaments of molluscan "catch" muscles II. Native filaments: isolation and characterization, *J. Mol. Biol.* **56**, 239–258 (1971).
14. J. Kendrick-Jones, W. Lehman, and A. G. Szent-Györgyi, Regulation in molluscan muscles, *J. Mol. Biol.* **54**, 313–326 (1970).
15. W. Lehman and A. G. Szent-Györgyi, Regulation of muscular contraction: Distribution of actin control and myosin control in the animal kingdom, *J. Gen. Physiol.* **66**, 1–30 (1975).
16. A. Goldberg and W. Lehman, Troponin-like proteins from muscles of the scallop, *Aequipecten irradians. Biochem. J.* **171**, 413–418 (1978).
17. T. Ojima and K. Mishita, Troponin from Akazara scallop striated adductor muscles, *J. Biol. Chem.* **261**, 16749–16754 (1986).
18. G. Ashiba, T. Asada, and S. Watanabe, Calcium regulation in clam foot muscle. Calcium sensitivity of clam foot myosin, *J. Biochem.* **58**, 837–846 (1980).
19. C. Wells and C. R. Bagshaw, Calcium regulation of molluscan myosin ATPase in the absence of actin, *Nature* **313**, 696–697 (1985).
20. R. N. Simmons and A. G. Szent-Györgyi, Reversible loss of calcium control of tension in scallop striated muscle associated with the removal of regulatory light chains, *Nature* **273**, 62–64 (1978).
21. E. M. Szentkiralyi, Tryptic digestion of scallop S1: evidence for a complex between the two light chains and a heavy-chain peptide, *J. Muscle Res. Cell. Motil.* **5**, 147–164 (1987).
22. A. G. Szent-Györgyi, E. M. Szentkiralyi, and J. Kendrick-Jones, The light chains of scallop myosin as regulatory subunits, *J. Mol. Biol.* **74**, 179–203 (1973).
23. C. R. Bagshaw and J. Kendrick-Jones, Characterization of homologous divalent metal ion binding sites of vertebrate myosins using paramagnetic resonance spectroscopy, *J. Mol Biol.* **130**, 317–336 (1979).
24. P. D. Chantler and A. G. Szent-Györgyi, Regulatory light chains and scallop myosin: full dissociation and cooperative effects, *J. Mol. Biol.* **138**, 473–499 (1980).
25. L. Nyitray, E. B. Goodwin, and A. G. Szent-Györgyi, Complete primary structure of a scallop striated muscle myosin heavy chain, *J. Biol. Chem.* **266**, 18469–18476 (1991).
26. J. H. Collins, Myosin light chains and troponin C: structural and evolutionary relationships revealed by amino acid sequence comparisons, *J. Muscle Res. Cell Motil.* **12**, 3–25 (1991).
27. J. R. Sellers, P. D. Chantler, and A. G. Szent-Györgyi, Hybrid formation between scallop myofibrils and foreign regulatory light-chains, *J. Mol. Biol.* **144**, 223–245 (1980).
28. J. M. Scholey, K. A. Taylor, and J. Kendrick-Jones, The role of myosin light chains in regulating actin-myosin interaction, *Biochimie* **63**, 255–271 (1981).

29. H. Kwon, E. B. Goodwin, L. Nyitray, E. Berliner, E. O'Neall-Hennessey, F. D. Melandri, and A. G. Szent-Györgyi, Isolation of the regulatory domain of scallop myosin. Role of the essential light chain in calcium binding, *Proc. Natl. Acad. Sci. USA* **87**, 4771–4775 (1990).
30. J. H. Collins, J. R. Jakes, J. Kendrick-Jones, J. Leszyk, W. Baruch, J. L. Theibert, J. Spiegel, and A. G. Szent-Györgyi, Amino acid sequence of myosin essential light chain from the scallop *Aequipecten irradians, Biochemistry* **25**, 7651–7656 (1986).
31. S. Fromherz and A. G. Szent-Györgyi, Role of essential light chain EF hand domain in calcium binding and regulation of scallop myosin, *Proc. Natl. Acad. Sci. USA* **92**, 7652–7656 (1995).
32. X. Xie, D. H. Harrison, I. Schlichting, R. M. Sweet, V. N. Kalabokis, A. G. Szent-Györgyi, and C. Cohen, Structure of the regulatory domain of scallop myosin at 2.8 Å resolution, *Nature* **368**, 316–394 (1994).
33. A. Houdusse and C. Cohen, Structure of the regulatory domain of scallop myosin at 2 Å resolution; implications for regulation, *Structure (London)* **4**, 21–32 (1996).
34. A. Jancso and A. G. Szent-Györgyi, Regulation of scallop myosin by the regulatory light chain depends on a single glycine residue, *Proc. Natl. Acad. Sci. USA* **91**, 8762–8766 (1994).
35. C. Wells, K. E. Warriner, and C. R. Bagshaw, Fluorescence studies on the nucleotide and Ca^{2+} binding domains of molluscan myosin, *Biochem. J.* **231**, 31–38 (1985).
36. A. P. Jackson and C. R. Bagshaw, Transient-kinetic studies of the adenosine triphosphate activity of scallop heavy meronyosin, *Biochem. J.* **251**, 515–526 (1988).
37. A. P. Jackson. and C. R. Bagshaw, Kinetic trapping of intermediates of the scallop heavy meromyosin adenosine triphosphatase reaction revealed by formycin nucleotides, *Biochem. J.* **251**, 527–540 (1988).
38. L. Nyitray, A. Jancso, Y. Ochiai, L. Graf, and A. G. Szent-Györgyi, Scallop striated and smooth muscle myosin heavy chain isoforms are produced by alternative RNA splicing from a single gene, *Proc. Natl. Acad. Sci. USA* **91**, 12686–12690 (1994).
39. C. L. Perreault-Micale, V. N. Kalabokis, L. Nyitray, and A. G. Szent-Györgyi, Sequence variations in the surface loop near the nucleotide binding site modulate the ATP turnover rates of molluscan myosins, *J. Muscle. Res. Cell Motil.* **14**, 543–553 (1996).
40. S. E. Kurzawa-Goertz, C. L. Perreault-Micale, K. M. Trybus, A. G. Szent-Györgyi, and M. A. Geeves, Loop I can modulate ADP affinity, ATPase activity, and motility of different scallop myosins. Transient kinetic analysis of S1 isoforms, *Biochemistry* **37**, 7517–7525 (1998).
41. P. D. Chantler, J. R. Sellers, and A. G. Szent-Györgyi, Cooperativity in scallop myosin, *Biochemistry* **20**, 210–216 (1981).
42. V. N. Kalabokis and A. G. Szent-Györgyi, Cooperativity and regulation of scallop myosin and myosin fragments, *Biochemistry* **36**, 15834–15840 (1997).
43. W. F. Stafford, M. P. Jacobsen, J. Woodhead, R. Craig, E. O'Neall-Hennessey, and A. G. Szent-Györgyi, Calcium-dependent structural changes in scallop heavy meromyosin, *J. Mol. Biol.* **307**, 137–147 (2001).
44. M. Nyitrai, A. G. Szent-Györgyi, and M. A. Geeves, A kinetic model of the co-operative binding of calcium and ADP to scallop *(Argo-pecten irradians)* heavy meromyosin, *Biochem. J.* **365**, 19–30 (2002).
45. M. Nyitrai, A. G. Szent-Györgyi, and M. A. Geeves, Interactions of the two heads of scallop *(Argo-pecten irradians)* heavy meromyosin with actin: influence of calcium and nucleotides, *Biochem. J.* **370**, 839–848 (2003).
46. M. Nyitray, W. F. Stafford, A. G. Szent-Györgyi, and M. A. Geeves, Ionic interactions play a role in the regulatory mechanism of scallop heavy meromyosin, *Biophys. J.* **85**, 1053–1562 (2003).
47. H. Suzuki, W. F. Stafford, H. S. Slayter, and J. C. Seidel, A conformational transition in gizzard heavy meromyosin involving the head tail junction, resulting in changes in sedimentation coefficient, ATPase activity, and orientation of heads, *J. Biol. Chem.* **260**, 4810–14817 (1985).
48. D. Wendt, D. Taylor, T. Messier, K. M. Trybus, and K. A. Taylor, Visualization of head-interactions in the inhibited state of smooth muscle myosin, *J. Cell. Biol.* **147**, 1385–1389 (1999).
49. J. Liu, T. Wendt, D. Taylor, and K. Taylor, Refined model of the 10S conformation of smooth muscle by cryo-electron microscopy 3D image reconstruction, *J. Mol. Biol.* **329**, 963–972 (2003).
50. A. Houdusse, A. G. Szent-Györgyi, and C. Cohen, Three conformational state of scallop myosin S1, *Proc. Natl. Acad. Sci. USA* **97**, 11238–11243 (2000).
51. H. S. Jung, S. A. Burggess, M. Colegrave, H. Patel, P. D. Chantler, J. M. Chalovich, J. Trinick, and P. J. Knight, Comparative studies of the folded structures of scallop striated and vertebrate smooth muscle myosins, *Biophys. J.* **86**, 406a (2004).

52. J. Woodhead, F.-Q. Zhao, R. Craig, E. H. Egelman, L. Alamo, and R. Padron, Atomic model of a myosin filament in the relaxed state, *Nature* **436**, 1195–1199 (2005).
53. J. A. Rall, Mechanics and energetics of contraction in striated muscle of the sea scallop, *Placopecten magellanicus*, *J. Physiol.* **321**, 287–295 (1981).
54. P. Vibert and R. Craig, Structural changes that occur in scallop myosin filaments upon activation, *J. Cell. Biol.* **101**, 830–837 (1985).
55. F.-Q. Zhao and R. Craig, Ca^{2+} causes release of myosin heads from the thick filament surface on the milliseconds time scale, *J. Mol. Biol.* **327**, 145–158 (2003).
56. F. Wang, K. Thirumurugan, W. F. Stafford, J. A. Hammer, P. J. Knight, and J. R. Sellers, Regulated conformation of myosin V, *J. Biol. Chem.* **279**, 2333–2336 (2003).

22

CALCIUM INHIBITION OF PHYSARUM MYOSIN AS EXAMINED BY THE RECOMBINANT HEAVY MERO-MYOSIN

Hozumi Kawamichi[1,4], Ying Zhang[1], Mizuki Hino[1], Akio Nakamura[1], Hideyuki Tanaka[2], László Farkas[3], László Nyitray[3] and Kazuhiro Kohama[1]

22.1. INTRODUCTION

Plasmodia of Physarum polycephalum shows vigorous cytoplasmic streaming by changing direction every few minutes. This oscillatory streaming is regulated by Ca^{2+} and is thought to be driven by a conventional myosin, i.e., by a myosin II isoform.[1,2] While working as an assistant professor in Professor Ebashi's laboratory at the University of Tokyo, one of the present authors (K.K.) induced the superprecipitation of actomyosin preparation or myosin B from the plasmodia to examine the effect of Ca^{2+}. It superprecipitated without requiring Ca^{2+}. When Ca^{2+} at μM level was present, the superprecipitation was inhibited.[3] This calcium inhibition was quite the opposite of the superprecipitation of actomyosin from vertebrate muscles,[4] and we expected that the inhibitory mode could be involved in the plant cytoplasmic streaming.[2] With the finding of the diverse classes of unconventional myosin such as myosin I and V[5] in vertebrate muscles, the inhibitory mode was shown to play a role in cell motility in both animal and plant kingdoms. In this case the myosins have calmodulin (CaM) as the light chains and are regulated by interaction of Ca^{2+} with CaM, which exerts an inhibitory effect on activity.[5]

Since of the findings of calcium inhibition in the plasmodia, efforts have been made to define the way in which Ca^{2+} regulates the actomyosin system, leading to the discovery that, while that Physarum myosin is the major site of action of Ca^{2+},[6] actin-linked regulation through actin-binding protein is involved in the inhibition.[7] Further biochemical studies on the myosin-linked regulation showed that Ca^{2+} binding to the Ca-binding light chain (CaLC) inhibits the activity of Physarum myosin[8] (Figure 22.1). Similar to Physarum myosin, mollusk scallop myosin belongs to the myosinII isoform family and the

[1] Department of Molecular and Cellular Pharmacology, Gunma University Graduate School of Medicine, [2]Department of Research Sciences, Gunma University School of Health Science, Maebashi, Gunma 371-8511, [3]Department of Biochemistry, Eötvös-Loránd University, Budapest, H-1117 Hungary, and [4]Department of Molecular Physiology, Yamaguchi University School of Medicine, Ube 755-8505, Japan

Regulatory Mechanisms of Striated Muscle Contraction
Edited by Ebashi and Ohtsuki, Springer, 2007

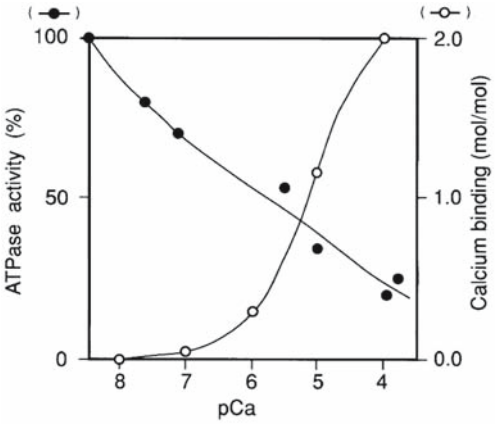

Figure 22.1. Calcium-binding to Physarum myosin and calcium inhibition of its ATPase activity. Physarum myosin was purified from plasmodia and then was allowed to bind $^{45}CaCl_2$, which was detected by the centrifugation method.[6] ATPase activity of the same myosin preparation was measured in the presence of actin by the pH-stat method.[6]

activity of scallop myosin is regulated by Ca^{2+}.[9] However, the effect of Ca^{2+} on this myosin is in an opposite to the regulation of Physarum myosin; Ca^{2+} activates the activity. Because structure and function in relation to the regulation by Ca^{2+} are known better for scallop myosin than that of Physarum myosin,[10] we adopted a strategy to compare the two myosins for a better understanding of Ca^{2+} regulation. As the first step to analyze how Ca^{2+} exerts a regulatory role on Physarum myosin through binding to CaLc, we tried to obtain recombinant heavy mero-myosin of Physarum myosin (HMM). In this article, we report the successful expression and preliminary characterization of the HMM.

22.2. EXPRESSION OF HMM AS A RECOMBINANT PROTEIN

We cloned full length Physarum myosin heavy chain (GenBank™ accession number AF335500), CaLC of essential light chain class (GenBank™ accession number J03499), and phosphorylatable light chain of regulatory light chain class (GenBank™ accession number AB076705) from plasmodia and then constructed baculovirus vectors with the heavy chain of Met1-Lys1181, and full length light chains of CaLC and PLC. The Sf-9 cells cultured in Grace's insect culture medium were co-infected by three constructs at once to allowed to express HMM as a recombinant protein. Utilizing His-tag of the vectors, we purified HMM by the Ni-NTA Superflow column chromatography. As shown in Figure 22.2, the purified HMM consisted of 135 kDa HMM-heavy chain 18 kDa PLC, and 16 kDa. The electron micrograph of HMM in Figure 22.2 showed the structure consisting of two globular hands and a short tail, confirming the expression of HMM.

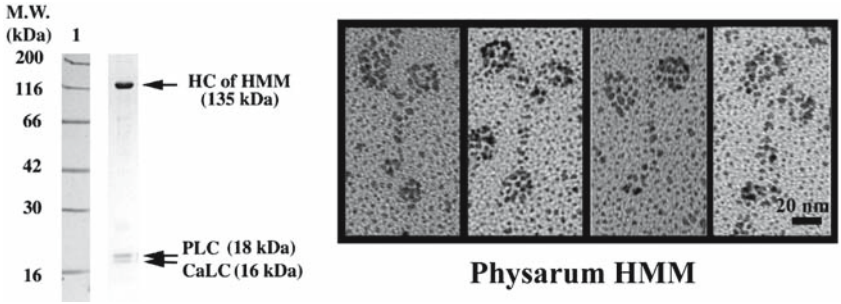

Figure 22.2. Composition and shape of the recombinant HMM. HMM of Physarum myosin was expressed in Sf-9 cells by CO-imfecting with recombinant baculovirus with cDNAs coding CaLC, PLC and myosin heavy chain fragment of HMM as described in the text. Then, HMM was purified by the His-tag affinity column. The composition of HMM is shown in the left panel. HMM was visualized by the rotary shadow electron microscope method followed by the electron microscope. Typical examples of the head and tail structure were shown in the right panel.

Table 22.1. Amino acid sequences of the EF-hand loops of CaLC

EF-1(15–26)	D*	K	D*	N	D	G	K	V	S	I	E	E*
EF-1(15–26)	A	E	L	N	A	K	E	F	D	L	A	T
EF-1(15–26)	D	K	E	G	N	G	T	I	Q	E	A	E
EF-1(15–26)	S	V	S	G	D	G	A	I	N	Y	E	S
Consensus	D	X	O	X	O	G	X	#	O	X	X	E
	x		Y		z		−y		−x			−z

The amino acids substituted for alanine in the mutant CaLC3A marked with asterisk (*). Consensus sequence of the canonical Ca2+ binding loop together with the six coordinating residues (x, y, z, −y, −x, −z) is shown below. O, oxygen-containing side group; #, hydrophobic residue; X, any amino acid residue.

22.3. CALCIUM-BINDING TO CaLC AND ITS MUTANTS

The amino acid sequence deduced from cDNA of CaLC was highly homologous with CaM,[11] which enabled us to assign 4 loops of canonical EF-hands (Table 22.1). We expressed full length CaLC, its N-terminal lobe of 1–77 residues, and its C-terminal lobe of 73–144 residues by the use of pET15b expression vector with His-tag sequence, followed by the expression in E. coli of BL21(DE3) strain. Calcium-binding experiments to CaLC, N-lobe, and C-lobe by the flow dialysis method indicated that only N-lobe was furnished with Ca-binding activity as measured and that calcium-binding activity is localized in the loop of EF-hand 1 which consisted of residues 15–26. We also produced the mutant CaLC-3A by mutating 3 acidic residues of EF-hand 1 of CaLC at D15A, D17A, and E26A and confirmed the complete loss of calcium-binding activity in CaLC-3A[12] (Figure 22.3).

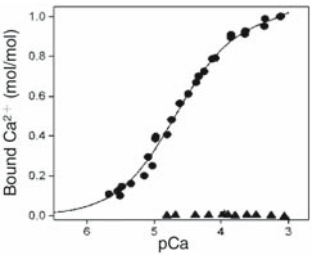

Figure 22.3. Calcium binding to CaLC and its mutant. cDNA of CaLC was mutated at D15, D17 and E26 to Ala as shown in Table 22.1. Wild type CaLC (●) and mutant CaLC-3A (▲) were expressed in E. coli and were purified. The $^{45}CaCl_2$ binding activity of Ca LC and CaLC-3A was examined by the flow dialysis method.[12] Note that Ca-binding ability of CaLC-3A was totally lost.

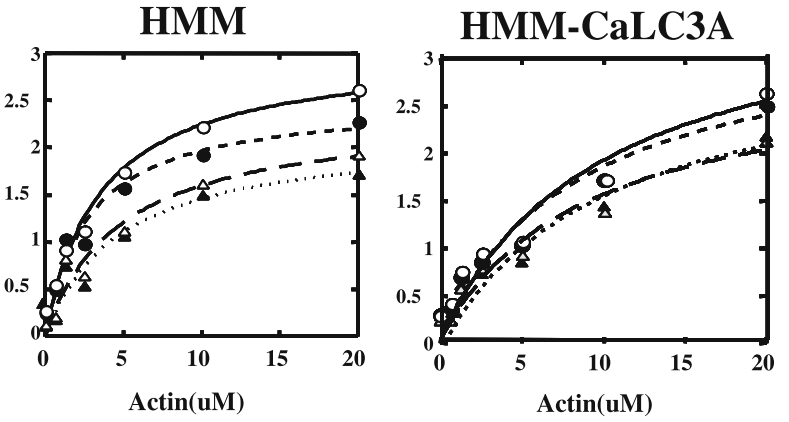

Figure 22.4. Effect of actin and Ca^{2+} on the ATPase activity of HMM and HMM-CaLC-3A. Wild type HMM and mutant HMM-CaLC-3A (Figure 22.5) were purified from Sf-9 cells and used as unphosphorylated samples. To phosphorylated PLC of both HMMs they were incubated with ATP in the presence of Ca^{2+}, CaM and the recombinant CaM-dependent protein kinase.[14] The dephosphoprylate and phosphorylated HMM and its mutant were subjected to the ATPase activity assay in the presence of various concentrations of actin. Note that actin and phosphorylation enhanced ATPase activities of the both wild type and mutant HMM-CaLC-3A. A slight inhibitory effect of Ca^{2+} was detectable with HMM, but not with HMM-CaLC-3A.

22.4. ATPase ACTIVITIES OF HMM

The ATPase activity of HMM without phosphorylation was measured by the use of HPLC, which enabled the quantification with much smaller amounts of HMM.[13] It showed basal Mg^{2+}-ATPase activity of 0.13 s^{-1} in the presence of 0.1 mM EGTA. Actin at 20 μM increased the activity to 1.93 s^{-1} with $K_{1/2} = 3.4$ μM, indicating that HMM is activated by actin about 15-fold (Figure 22.4, left, open triangles). In the presence of Ca^{2+} at 0.1 mM the effect of actin on the ATPase activity of HMM was also examined in the presence of various concentrations of actin. The activities in the absence and presence of 20 μM actin were 0.12 s^{-1} and 1.73 s^{-1}, respectively. Thus, an effect of Ca^{2+} could not be detected. Experiments with a similar protocol were carried out using mutant HMM in which CaLC was replaced by CaLC-3A (Figure 22.5). This mutant HMM also did not show calcium inhibition, although its ATPase activity was activated by actin to a similar extent to that of wild type HMM.

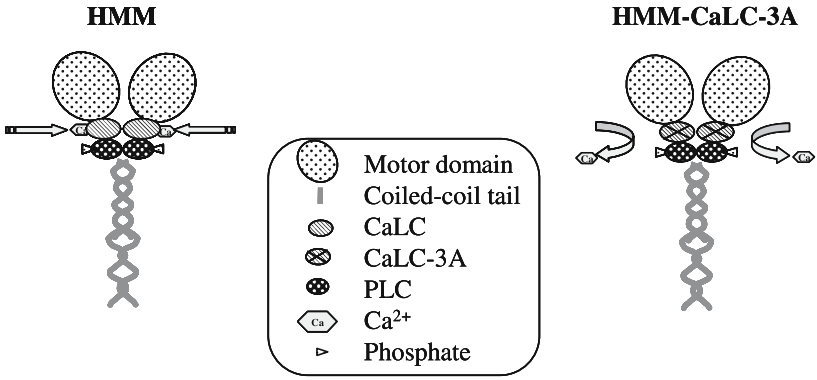

Figure 22.5. Schematic representation of wild type HMM and mutant HMM-CaLC-3A. Wild type HMM, which contains CaLC of calcium-binding activity, was expressed in Sf-9 cells. Mutant HMM-CaLC3A containing CaLC3A, whose Ca-binding activity was totally lost. Both HMMs contain PLC which could be phosphorylated at Ser1814 (see the legend to Figure 22.4). Note that Ca-binding activity of HMM-CaLC-3A was expected to be lost (see Table 22.2).

We obtained a Physarum CaM-dependent protein kinase as a recombinant protein and phosphorylated PLC at Ser18.[14] The HMM with phosphorylated PLC showed basal Mg-ATPase activity of 0.27 s^{-1}, and the activating effect of 20 μM actin was 2.62 s^{-1}. When 0.1 mM Ca^{2+} was present, the activities in the absence and presence of 20 μM actin were 0.25 s^{-1} and 2.28 s^{-1}, respectively. Thus, a slight inhibitory effect of Ca^{2+} could be detected in the presence of actin (Figure 22.4 left, open circles). We also examined the effects of actin and PLC phosphorylation with mutant HMM-CaLC-3A. In this experiment we detected the enhancement of ATPase activity by actin and phosphorylation (Figure 22.5). But, we could not detect any effect of Ca^{2+}.

22.5. CALCIUM INHIBITION AS MEASURED BY THE IN VITRO MOTILITY ASSAY

Actin filaments were allowed to move on a surface coated with phosphorylated HMM in an ATP-dependent manner (Table 22.2). With the motility assay carried out in the presence of 0.1 mM EGTA, the mean velocity was 1.02 ± 0.185 μm/s; whereas, in the presence of 0.1 mM Ca^{2+}, the mean velocity was reduced to 0.565 ± 0.105 μm/s. Return to 0.1 mM EGTA resulted in recovery of velocity to 1.30 ± 0.569 μm/s. The effect of Ca^{2+} was confirmed in corollary experiments in which Ca^{2+} was added first and then EGTA followed by Ca^{2+}. When velocity was measured with untreated HMM, the velocity was low, i.e., 0.33 ± 0.128 μm/s in EGTA. However, the inhibit effect of Ca^{2+} and recovery by EGTA were evident.

When we used the glass surface coated with the phosphorylated HMM where CaLC was replaced by the mutant CaLC-3A, the velocity of actin movement in EGTA was 0.871 ± 0.188 μm/s, a value that is comparable to HMM with wild type CaLC. In contrast to this wild type, the mutant HMM-CaLC-3A in Ca^{2+} resulted in actin no change in velocity (0.979 ± 0.259 μm/s). The failure to detect calcium inhibition with HMM-CaLC-3A with

Table 22.2. Calcium inhibition as monitored by the in vitro motility assay

Sample	HMM with phosphorylated PLC		
Test	1st	2nd	3rd
Buffer	EGTA	Ca^{2+}	EGTA
Velocity (μm/sec)	1.02 ± 0.186	0.565 ± 0.105	1.30 ± 0.569
Test	1st	2nd	3rd
Buffer	Ca^{2+}	EGTA	Ca^{2+}
Velocity (μm/sec)	0.543 ± 0.167	1.08 ± 0.254	0.614 ± 0.139
Sample	HMM with unphosphorylated PLC		
Test	1st	2nd	3rd
Buffer	EGTA	Ca^{2+}	EGTA
Velocity (μm/sec)	0.334 ± 0.128	0.287 ± 0.069	0.435 ± 0.096
Test	1st	2nd	3rd
Buffer	Ca^{2+}	EGTA	Ca^{2+}
Velocity (μm/sec)	0.239 ± 0.084	0.428 ± 0.082	0.308 ± 0.105
Sample	HMM-CaLC3A with phosphorylated PLC		
Test	1st	2nd	3rd
Buffer	EGTA	Ca^{2+}	EGTA
Velocity (μm/s)	0.871 ± 0.188	0.979 ± 0.259	0.866 ± 0.255
Test	1st	2nd	3rd
Buffer	Ca^{2+}	EGTA	Ca^{2+}
Velocity (μm/sec)	0.839 ± 0.202	0.814 ± 0.225	0.845 ± 0.11
Sample	HMM-CaLC3A with unphosphorylated PLC		
Test	1st	2nd	3rd
Buffer	EGTA	Ca^{2+}	EGTA
Velocity (μm/sec)	0.326 ± 0.100	0.353 ± 0.074	0.302 ± 0.103
Test	1st	2nd	3rd
Buffer	Ca^{2+}	EGTA	Ca^{2+}
Velocity (μm/sec)	0.361 ± 0.112	0.362 ± 0.094	0.397 ± 0.103

Actin filaments labeled with rhodamine phalloidin were mounted on a glass surface coated with recombinant HMM or HMM-CaLC-3A. The ATP-dependent movement of the actin filaments in 0.1 mM EGTA or 0.1 mM Ca^{2+} was observed under a fluorescent microscope and recorded with a video camera. The velocities of movement of actin filaments ($n = 25$) was calculated from the distance moved. For phosphorylation, see the legend to Figure 22.4 and for mutant HMM-CaLC-3A, see the legend to Figure 22.5. The inhibitory effect of Ca^{2+} on HMM is significant whether PLC was phosphorylated or not ($P < 0.01$). However, the effect of Ca^{2+} on HMM-CaLC-3A is not significant.

the phosphorylated PLC was confirmed not only by changing the order of Ca^{2+} and EGTA addition but also by the use of HMM with unphosphorylated PLC.

22.6. PERSPECTIVE

The crystal structure of scallop myosin subfragment 1 and the activation mechanism of Ca^{2+} has been resolved.[10] However, the expression of regulated scallop myosin and its fragments has not been successful so far. Therefore, we expressed a hybrid HMM where Physarum LCs are replaced by scallop LCs (Figure 22.6). Unfortunately, the hybrid HMM

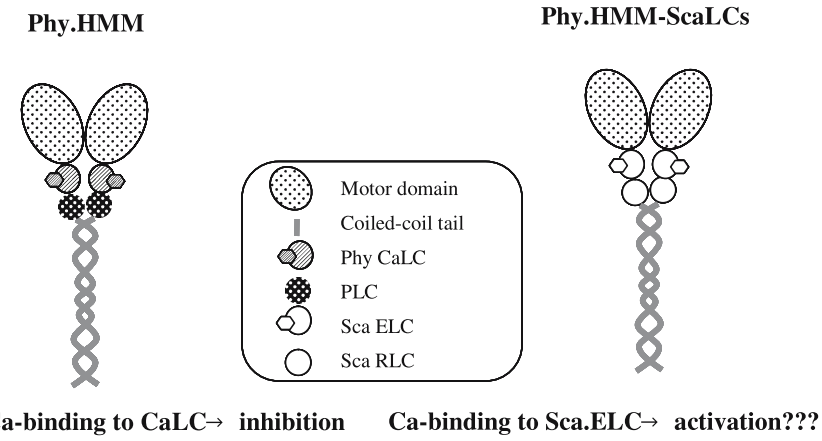

Figure 22.6. Schematic representation of the components of hybrid HMM. Phy HMM is the wild type of HMM that was shown in Figure 22.5. By expressing heavy chain consisting of HMM together with the essential light chain (Sca ELC) and the regulatory light chain (Sca RLC) of scallop, the hybrid HMM (Phy HMM-ScaLCs) could be expressed.

failed to move actin filaments. We are now expressing the chimeric HMM where the regulatory domain of Physarum HC is replaced by the scallop HC sequence, expecting the functional hybrid HMM. To understand regulation of myosin II isoforms by Ca^{2+} comprehensively, i.e., including both activation and inhibition modes, producing hybrids and/or chimeras of HMMs of scallop and Physarum myosins would be promising approach.

22.7. ACKNOWLEDGEMENTS

Two of the authors (L. N. and K. K.) met in the laboratory of Prof. Andrew G. Szent-Gyorgyi at Brandeis University in the summer of 1996. This encounter is the start of the expression of Physarum HMM. We thank him for giving us the opportunity for collaboration and for his continuous encouragment. Our thanks are also to Prof. Gary L. Wright at Marshall University for reading the manuscript with valuable comments.

22.8. REFERENCES

1. N. Kamiya, Physical and chemical basis of cytoplasmic streaming, *Annu. Rev. Plant Physiol.* **32**, 205–236 (1981).
2. A. Nakamura, K. Kohama, Calcium regulation of the actin-myosin interaction of *Physarum polycephalum, Int. Rev. Cytol.* **191**, 53–98 (1999).
3. K. Kohama, K. Kobayashi, and S. Mitani, Effects of Ca ion and ADP on superprecipitation of myosin B from slime mold, *Physarum polycephalum*, *Proc. Jpn Acad.* **56B**, 591–596 (1980).
4. S. Ebashi and M. Endo, Calcium ion and muscle contraction, *Prog. Biophys. Mol. Biol.* **18**, 123–183 (1968).
5. J. S. Wolenski, Regulation of calmodulin-binding myosins, *Trends Cell Biol.* **5**, 310–316 (1995).
6. K. Kohama and J. Kendrick-Jones, The inhibitory Ca^{2+}-regulation of the actin-activated Mg-ATPase activity of myosin from *Physarum polycephalum* plasmodia, *J. Biochem.* **99**, 1433–1446 (1986).

7. R. Ishikawa, T. Okagaki, S. Higashi-Fujime, and K. Kohama, Stimulation of the interaction between actin and myosin by *Physarum* caldesmon-like protein and smooth muscle caldesmon, *J. Biol. Chem.* **266**, 21784–21790 (1991).
8. K. Kohama, T. Okagaki, H. Takano-Ohmuro, and R. Ishikawa, Characterization of calcium-binding light chain as a Ca^{2+}-receptive subunit of *Physarum* myosin, *J. Biochem.* **110**, 566–570 (1991).
9. A. G. Szent-Gyorgyi, V. N. Kalabokis, and C. L. Perreault-Micale, Regulation by molluscan myosins, *Mol. Cell. Biochem.* **190**, 55–62 (1999).
10. S. Xie, D. H. Harrison, I. Schlichting, R. M. Sweet, V. N. Kalabokis, A. G. Szent-Gyorgyi, and C. Cohen, Structure of the regulatory domain of scallop myosin at 2.8 Å resolution, *Nature* **368**, 306–312 (1994).
11. T. Kobayashi, K. Tkagi, K. Konishi, Y. Hamada, M. Kawaguchi, and K. Kohama, Amino acid sequence of the calcium-binding light chain of myosin from the lower eukaryote, *Physarum polycephalum*, *J. Biol. Chem.* **263**, 305–313 (1988).
12. L. Farkas, A. Malnasi-Csizmadia, A. Nakamura, K. Kohama, and L. Nyitray, Localization and characterization of the inhibitory Ca^{2+}-binding site of *Physarum polycephalum* myosinII, *J. Biol. Chem.* **278**, 27399–27405 (2003).
13. K. Samizo, R. Ishikawa, A. Nakamura, and K. Kohama, A highly sensitive method for measurement of myosin ATPase activity by reversed-phase high-performance liquid chromatography, *Anal. Biochem.* **293**, 212–215 (2001).
14. A. Nakamura, Y. Hanyuda, T. Okagaki, and K. Kohama, A calmodulin-dependent protein kinase from lower eukaryote *Physarum polycephamum*, *Biochem. Biophys. Res. Commun.* **328**, 838–844 (2005).

V

EXCITATION-CONTRACTION COUPLING AND DISORDER

23

CALCIUM-INDUCED RELEASE OF CALCIUM FROM THE SARCOPLASMIC RETICULUM

Makoto Endo

23.1. INTRODUCTION

In early 1960s clear evidence was presented by Professor S. Ebashi for the fact that contraction-relaxation cycle of living muscle is regulated by calcium ion (Ca^{2+}) (cf. Ebashi and Endo, 1968). He then inquired into the mechanism of the action of Ca^{2+} and disclosed that the regulation of contractile reaction by Ca^{2+} requires the presence of a protein component other than myosin and actin (Ebashi, 1963). A few years later, he showed that the protein component is a complex of a known protein, tropomyosin, and a new protein, troponin (Ebashi and Kodama, 1965).

I was in Professor Ebashi's Laboratory at that time, and closely witnessed his discovery of troponin. Shortly after his discovery, we showed that troponin is distributed along the entire thin filament together with tropomyosin, by using FITC-labeled anti-troponin antibody (Endo et al., 1966). This is my only work on troponin, because my main interest moved toward earlier stages of EC-coupling, especially the mechanism of Ca^{2+} release from the sarcoplasmic reticulum (SR). In this symposium commemorating 40^{th} anniversary of the discovery of troponin by Professor Ebashi, I was given an opportunity of presenting my own work, which was my great pleasure especially as one of the pupils of Professor Ebashi.

23.2. DISCOVERY OF Ca^{2+}-INDUCED RELEASE OF Ca^{2+} FROM THE SR

In 1966 we started working on Natori's skinned fiber (Natori, 1954) originally to examine the effect of Ca^{2+} on its contractile responses quantitatively. However, we also tried to examine the effect of Ca^{2+}-releasing action of caffeine in skinned skeletal muscle fibers immersed in a relaxing solution containing a low concentration of EGTA. Caffeine was known to cause Ca^{2+} release from the SR (Weber and Herz, 1968), and, therefore, we expected that it would cause concentration-dependent contraction of skinned fiber, which would last as far as the agent is present. Unexpectedly, a low concentration of caffeine caused after a pretty long latency a large contraction that spontaneously relaxed

Faculty of Medical Care and Health, Saitama Medical University, Kawagoe Building, 21-7 Wakitahoncho, Kawagoe 350-1123, Japan

Regulatory Mechanisms of Striated Muscle Contraction
Edited by Ebashi and Ohtsuki, Springer, 2007

while caffeine was still present. To our further surprise similar transient contractions repeated with more-or-less constant interval of several minutes over and over again. Figure 23.1 demonstrates an example of initial two transient contractions at such a low frequency under low concentration of caffeine. Higher concentrations of caffeine caused recurrent contractions with higher frequencies.

The fact that peak tension of repeated transient contractions under a low concentration of caffeine is nearly maximal suggests that the characteristics of Ca^{2+} release from the SR in this condition follows an essentially all-or-none pattern (albeit not genuine) along the entire length of the fiber. Indeed microscopic observation revealed that sometimes during the rising phase of tension, a region of about 20–30 μm in which sarcomeres were highly shortened moved slowly from one end of the fiber to the other. If part of the effect of Ca^{2+} release or its underlying processes were the induction of further release of Ca^{2+}, a positive feedback loop would be formed and release of Ca^{2+} would be according to an all-or-none pattern. We, therefore, looked for the mechanism of the positive feedback.

We first examined whether chemical or physical consequences of contraction, the main effect of Ca^{2+} release, could cause further release of Ca^{2+}. However, ADP, inorganic phosphate or stretching the fiber did not cause Ca^{2+} release at all. Then we found that Ca^{2+} itself can cause Ca^{2+} release (Ca^{2+}-induced Ca^{2+} release [CICR]). A typical experiment is shown in Figure 23.2 where 10^{-6} M Ca^{2+}, which is below the threshold of contraction under the experimental condition (therefore, the fiber developed no tension at the steady state), evoked a transient contraction due to Ca^{2+} release if the SR had been preloaded (Endo et al., 1970). Further evidence for CICR was presented in detail in the report.

Ford and Podolsky (1970) also discovered CICR entirely independently. They demonstrated that the rate of tension development of a skinned fiber immersed in a solution containing 10^{-4} M Ca^{2+} was very slow if the SR was unloaded, but it was very fast if the SR had been loaded. Although the rapid tension development could be interpreted simply as the result of absence of effective Ca^{2+} sink, the fact that the initial contraction was

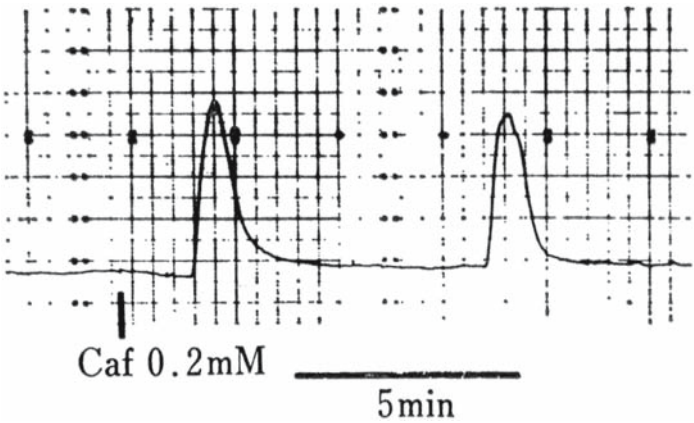

Figure 23.1. Repeated transient contractions of a skinned fiber under the influence of 0.2 mM caffeine. Caffeine was applied at the time indicated by the vertical bar (Endo et al., 1970).

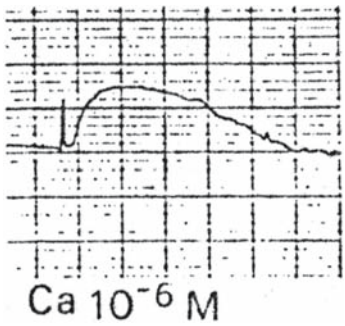

Figure 23.2. Contraction of a skinned fiber evoked by a release of Ca^{2+} from SR induced by Ca^{2+} 10^{-6} M, of which time of application was indicated by the vertical artifact (Endo et al., 1970).

transient and partial relaxation occurred after 20–30 s suggested that unloading of Ca^{2+} in the SR occurred during initial contraction. By using ^{45}Ca they later demonstrated that net efflux of Ca^{2+} from the SR actually occurred under such an experimental condition (Ford and Podolsky, 1972).

It is interesting to note that although Ca^{2+}-releasing action of Ca^{2+} was not very strong in skeletal muscle under physiological conditions, both groups mentioned above could discover CICR because they unintentionally conducted experiments under conditions facilitating CICR; the presence of caffeine in our case and lower than physiological concentration of free Mg^{2+} in the case of Ford and Podolsky.

23.3. PROPERTIES OF CICR

In order to examine properties of CICR quantitatively, simple monitoring of Ca^{2+} concentration is inappropriate because the increase of Ca^{2+} concentration as a result of Ca^{2+} release stimulates further release of Ca^{2+} to amplify the rise of Ca^{2+} concentration, and also stimulates Ca^{2+} pump of the SR to diminish the increase in Ca^{2+} concentration. In order to avoid the interference by these secondary processes, the rate of Ca^{2+} release was determined in the presence of a high concentration of Ca^{2+} buffer to keep free Ca^{2+} concentration practically unchanged even when Ca^{2+} was released, and in the absence of ATP to stop Ca^{2+} pump activity (Endo and Iino, 1988).

Figure 23.3 is a result of CICR experiments with the care mentioned above, and shows that Ca^{2+} in the SR decreased exponentially during continuous stimuli of fixed concentrations of Ca^{2+}. As is seen, the higher the Ca^{2+} concentration, the larger the rate constant. An example of the Ca^{2+} concentration dependence of rate constants of SR Ca^{2+} release is shown in Figure 23.4. At the foot of the curve, the rate constant increases with the square of Ca^{2+} concentration, suggesting that two Ca^{2+} ions are necessary to activate the Ca^{2+} release channel. At higher Ca^{2+} concentrations the rate decreases with Ca^{2+} concentration, indicating inhibitory action of Ca^{2+} in this concentration range.

CICR is modified by various agents (cf. Endo, 1985). All the adenine compounds enhance CICR without altering its dependence on Ca^{2+} concentration; the effect of AMP as an example is shown in Figure 23.5. ATP and its non-hydrolyzable analogue such as AMPOPCP are strongest in its action, and ADP, AMP, adenosine and adenine follow in this order. It is interesting to note that adenine inhibits CICR in the presence of ATP

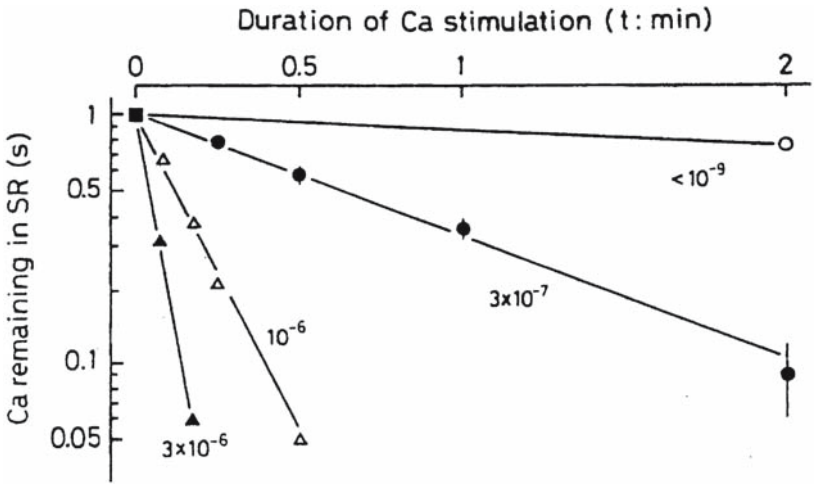

Figure 23.3. Relation between duration of Ca^{2+} stimulation and relative amount of Ca^{2+} remaining in SR. Note that the scale in the ordinate is logarithmic (Ohta et al., 1989).

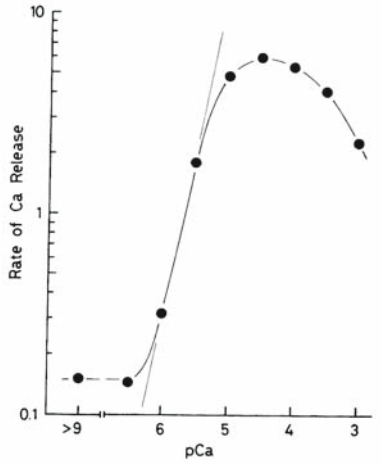

Figure 23.4. Dependence of the rate of Ca^{2+} release from the SR on Ca^{2+}($pCa = -\log[Ca^{2+}]$). The slope of the straight line is two (Modified from Endo et al., 1983).

although it enhances CICR by itself. This is because the strong potentiating action of ATP is replaced by a much weaker action of adenine.

Caffeine and other xanthine derivatives also strongly potentiate CICR. In contrast to adenine compounds, caffeine increases Ca^{2+} sensitivity of CICR as well as maximal Ca^{2+} release rate at the optimal Ca^{2+} concentration as also shown in Figure 23.5. The well-known contracture-producing effect of caffeine can be explained by this enhancement of CICR. Under the action of a high concentration of caffeine, Ca^{2+} sensitivity and maximum rate of Ca^{2+} release of CICR are so much enhanced that the resting Ca^{2+} concentration could start an explosive Ca^{2+} release.

Mg^{2+} inhibits Ca^{2+}-releasing action of Ca^{2+} competetively. Therefore, in the presence of Mg^{2+} Ca^{2+}-activation curve of CICR shifts to the right, but at the same time maximum rate of release is suppressed (Figure 23.6), indicating a further inhibitory action of Mg^{2+}

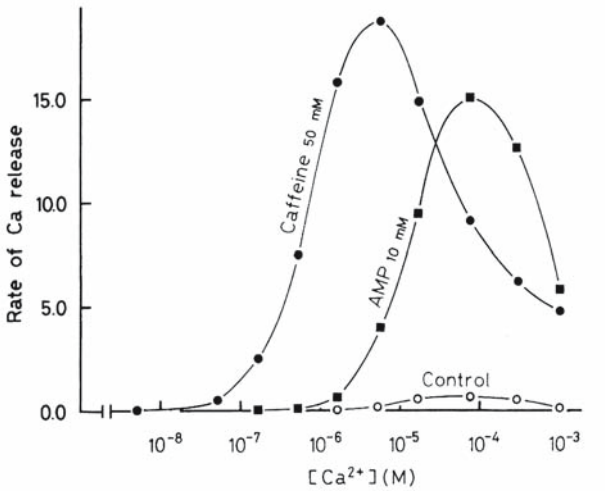

Figure 23.5. Effects of caffeine and AMP on CICR in skinned fibers of Xenopus skeletal muscle (Endo, 1981).

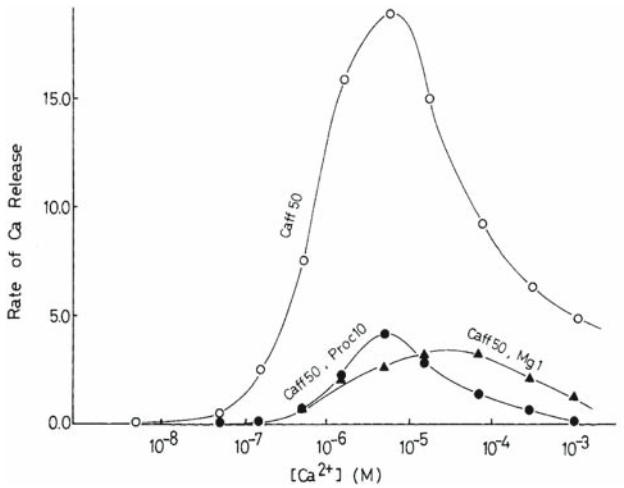

Figure 23.6. Inhibitory effects of Mg^{2+} and procaine on CICR in skinned fibers of Xenopus muscle. Experiments were done in the presence of caffeine to show the inhibition clearly (Endo, 1981).

probably in common with that of high concentrations of Ca^{2+}. Procaine inhibits CICR essentially without changing its Ca^{2+} sensitivity as is also shown in Figure 23.6.

In late 1980s, biochemists succeeded in isolating and purifying the Ca^{2+} release channel protein of the SR by utilizing specific binding of a plant alkaloid ryanodine (Fleischer et al., 1985; Imagawa et al., 1987; Inui et al., 1987; Lai et al., 1988). Therefore, the channel protein is called ryanodine receptor (RyR). It was then sequenced by Takeshima et al. (1989), and at present three types of RyR are known in mammals (Sorrentino and Volpe, 1993); RyR1, RyR2 and RyR3, which are called skeletal muscle

type, cardiac type and brain type, respectively, although their distribution is not confined to the respective tissue mentioned.

All types of RyRs show the properties of CICR. Namely, if purified RyRs are incorporated into lipid bilayer membrane, the channels are open if Ca^{2+} is applied from the sarcoplasmic surface of the channel and the channel opening is enhanced by ATP and inhibited by Mg^{2+} (Lai et al., 1988). Thus, RyRs show the properties as CICR channel.

23.4. CICR AND PHYSIOLOGICAL Ca^{2+} RELEASE

In the skeletal myocyte from mutant mice that lack RyR1, neither electrical stimulation nor potassium depolarization could induce contraction (Takeshima et al., 1994). However, EC-coupling of the myocyte recovered if RyR1, but not RyR2, is expressed (Yamazawa et al., 1996). These experiments clearly show that RyR1 is the physiological Ca^{2+} release channel in skeletal muscle.

Since RyR1 is CICR channel as described in the previous section, it is conceivable that action potential or depolarization of the cell membrane of skeletal myocyte would somehow raise Ca^{2+} concentration in the vicinity of RyR1, and Ca^{2+} in turn would open RyR1 channel to lead to contraction. If so, inhibitors of CICR should inhibit physiological contraction. However, adenine, an inhibitor of CICR in the presence of ATP, did not inhibit twitch contraction at all (Ishizuka et al., 1983), whereas it potently inhibited caffeine contracture that was induced through the strong enhancement of CICR by the agent (Ishizuka and Endo, 1983). Similarly, procaine strongly inhibited caffeine-induced contracture, but it did not inhibit potassium depolarization-induced contractions of the same fiber as shown in Figure 23.7 (Thorens and Endo, 1975). These results clearly indicate that physiological Ca^{2+} release is not mediated by CICR. It is generally considered that physiological Ca^{2+} release in skeletal muscle is the result of protein-protein interaction

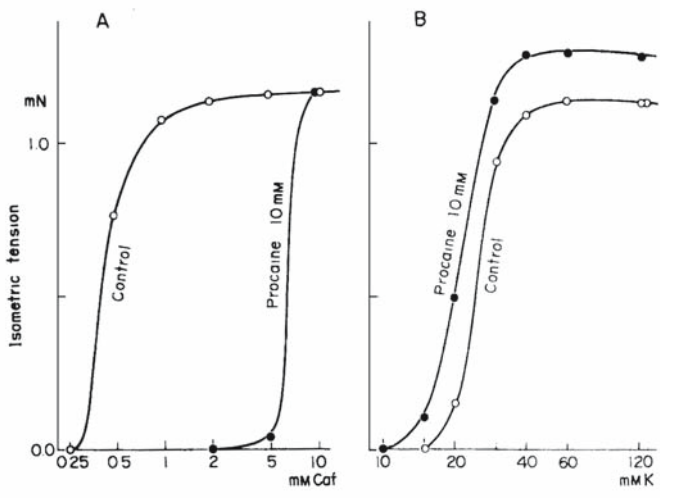

Figure 23.7. Effects of procaine on caffeine-induced contraction (A) and potassium-induced contraction (B) of a single finer of Xenopus skeletal muscle (Thorens and Endo, 1975).

Table 23.1. Comparison of clofibric acid-induced Ca^{2+} release with Physiological Ca^{2+} release and CICR

Mode of opening	Ca^{2+} required	Adenine compounds Potentiation	Procaine inhibition	Dantrolene inhibition at room temperature
Physiological	–	–?	–?	+
Clof-induced*	–	Inhibition	–	+
Ca^{2+}-induced	+	+	+	–

+, positive; –, negative; *Clofibric acid-induced Ca^{2+} release: properties confined to those at very low Ca^{2+} concentrations. For further explanation, see Ikemoto and Endo, 2001.

between the voltage sensor, dihydropyridine receptor, in the T-tubule membrane and RyR1 in the SR membrane.

From the fact that although RyR1 is the physiological Ca^{2+} release channel and also CICR channel, yet physiological Ca^{2+} release is not mediated by CICR, we must conclude that RyR1 could open in two different modes depending on the kind of stimulation, through T-tubule voltage sensor or by Ca^{2+}.

Almost all the substances reported so far to enhance opening of RyR channels are enhancers of CICR, but not of opening in the physiological mode. However, we have found that clofibric acid opens RyR channels in a mode quite different from CICR (Ikemoto and Endo, 2001). Contrary to CICR or caffeine-induced Ca^{2+} release, clofibric acid-induced Ca^{2+} release is quite effective in the practical absence of Ca^{2+}, not enhanced but rather inhibited by AMP, not inhibited by procaine, but inhibited by dantrolene at room temperature. [Dantrolene, which is known to inhibit physiological Ca^{2+} release at any temperature, inhibits CICR only at 37°C, but not at room temperature (Ohta and Endo, 1986].) Such a mode of clofibric acid-induced Ca^{2+} release is somewhat similar to the physiological Ca^{2+} release as shown in Table 23.1. Therefore, clofibric acid might be the first example of an enhancer of physiological Ca^{2+} release, and, therefore, further investigation into the action of this agent might throw some light into the mechanism of physiological mode of opening of RyR1.

23.5. PATHOPHYSIOLOGICAL SIGNIFICANCE OF CICR

Although the role of CICR is not essential in physiological Ca^{2+} release, it plays a major role in some pathophysiological conditions. Under inhalation anesthesia a serious syndrome called malignant hyperthermia (MH) could happen, though rarely (Denborough and Lovell, 1960). MH is characterized by a very high fever, over 40°C, and if not properly treated, metabolic vicious cycle secondary to the high temperature would lead the patients into danger of death with a high probability. Muscles of patients suffering MH are rigid, i.e., contracted, and the abnormal heat production by the generalized muscle contraction is considered to be the cause of high fever. The muscle rigidity cannot be removed by neuromuscular blocking agents, and, therefore, the cause of contraction should be within muscle cells, not in the nervous system. Similar disease is known to be present in pigs and some other animals.

The abnormality in muscles of MH patients is first demonstrated by Kalow et al. (1970). Muscles of MH patients showed higher caffeine sensitivity; namely, lower concentrations of caffeine cause contracture in patient muscles than in normal ones both with simple caffeine application and in the presence of halothane that enhances caffeine effect. These results suggested to us that CICR in patient muscles might be accelerated in comparison with normal subjects, and we demonstrated that it is actually so (Endo et al., 1983). CICR of muscles of MH patients shows higher Ca^{2+} sensitivity and greater maximum rate of Ca^{2+} release than in normal muscle. The same is true in skeletal muscle of a malignant hyperthermia-susceptible (MHS) pig (Figure 23.8).

Halothane and all the other inhalation anesthetics are found to enhance CICR (Matsui et al., 1991). If the hereditary accelerated CICR of MH patients is further enhanced by inhalation anesthetics such as halothane, CICR overwhelms Ca^{2+} pump activity in most concentration range of Ca^{2+}, which leads to spontaneous and explosive Ca^{2+} release that induces contraction. We have calculated rates of CICR and Ca^{2+} uptake by Ca^{2+} pump with reasonable assumptions based on values obtained in skinned fiber experiments. In both normal muscle under halothane and muscle of MH patient without halothane rate of Ca^{2+} pump is still considerably higher than rate of Ca^{2+} release, so that no hazard would occur. However, if MH patients are treated with halothane, rate of Ca^{2+} release of their muscle now exceeds that of Ca^{2+} uptake, resulting an explosive Ca^{2+} release (Endo et al., 1983).

Whether the acceleration of CICR correlates with the occurrence of high fever in MH suspected patients were examined, and the result is shown in Table 23.2 (Kawana et al., 1992). The correlation is high but not perfect. However, among the false positive cases, fever may have been produced by an event unrelated to MH, for example by the central nervous system disorders. Furthermore, among false negative cases, early treatment may have prevented the development of high fever. Therefore, the real correlation may well be higher than indicated by the figures in Table 23.2.

The inhibitors of CICR were reported to be effective in treating MH. Especially, dantrolene is known as a specific drug to remedy MH.

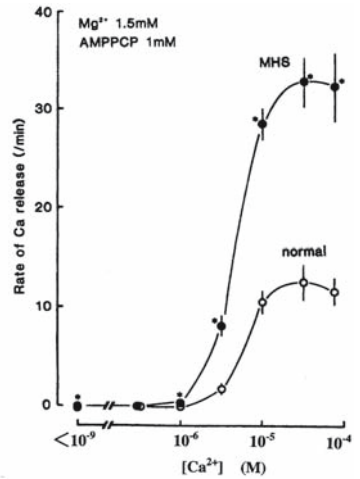

Figure 23.8. Relationship between Ca^{2+} concentration and the rate of Ca^{2+} release in MHS and normal porcine fibers in physiological ionic conditions (Ohta et al., 1989).

Table 23.2. Comparison of CICR acceleration and fever during anesthesia

	CICR accelerated	CICR normal
Fever (+)	18 + 1 CNS	2 + 3 CNS
Fever (−)	2	18

Fever (+): Cases with maximum temperature ≧40°C and/or rate of rise in temperature ≧0.5°C/15 min during anesthesia. CNS: Patient with central nervous system disorders.

From all the facts mentioned above, we could convincingly conclude that the major cause of MH is the abnormally accelerated CICR in skeletal muscles of MH patients and MHS pigs.

23.6. CICR IN CARDIAC MUSCLE

The way in which the contractile strength of cardiac muscle is regulated is quite different from that of skeletal muscles. In skeletal muscle, regulation is basically accomplished by the nervous system; number of muscle cells or motor units excited is adjusted while each muscle cell responds to command of the nerve with essentially fixed magnitude of contraction for each action potential. In cardiac muscle, however, all cells contract at every beat and, therefore, regulation of the contractile strength of the heart must be made by altering the strength of contraction of each cardiac cell.

In contrast to skeletal muscle, it is generally believed that CICR plays an essential role in evoking physiological contraction in mammalian cardiac muscle; namely, Ca^{2+} that flows into cardiac cells during action potential activates CICR channels of the SR to cause physiological Ca^{2+} release. Regulation of cardiac contraction is made basically by altering the amount of Ca^{2+} acting on the CICR channel, typically by modulating the activity of voltage-dependent Ca^{2+} channel of the surface membrane.

The presence of CICR in cardiac muscle was demonstrated by Fabiato and Fabiato (1972) soon after its discovery in skeletal muscle.

At one time I was rather skeptical about CICR theory of cardiac EC-coupling; one of the reasons was the fact that CICR in cardiac skinned fiber under physiological condition appeared not sensitive enough, EC_{50} being about 2×10^{-6} M (Endo, 1985). However, this and other difficulties now appear to have been reasonably eliminated essentially by theories of local control (Stern, 1992) and adaptation (Gyorke and Fill, 1993).

It is interesting and rather ironical that CICR with its inherently regenerative nature is not used in skeletal muscle where Ca^{2+} release occurs in a quasi-all-or-none manner, but used in cardiac muscle that must release Ca^{2+} in a finely graded manner.

23.7. REFERENCES

Denborough, M. A., and Lovell, R. R. H., 1960, Anesthetic deaths in a family. *Lancet* **II**:45.

Ebashi S., 1963, Third component participating in the superprecipitation of "natural actomyosin." *Nature* **200**:1010.

Ebashi, S., and Endo, M., 1968, Calcium ion and muscle contraction, in: *Progr. in Biophys. and Mol. Biol.* **Vol. 18**, J. A. V. Butler, and D. Noble, eds, Pergamon Press, Oxford, pp. 123–183.

Ebashi, S., and Kodama, A., 1965, A new protein factor promoting aggregation of tropomyosin. *J. Biochem.* **58**:107–108.

Endo, M., 1981, Mechanism of calcium-induced calcium release in the SR membrane, in: *The Mechanism of Gated Calcium Transport across Biological Membranes*, S. T. Ohnishi, and M. Endo, eds, Academic Press, New York, pp. 257–264.

Endo M., 1985, Calcium release from sarcoplasmic reticulum. *Curr. Top. Membr. Transp.* **25**:181–230.

Endo, M., and Iino, M., 1988, Measurement of Ca^{2+} release in skinned fibers from skeletal muscle. *Methods Enzymol.* **157**:12–26.

Endo, M., Nonomura, Y., Masaki, T., Ohtsuki, I., and Ebashi, S., 1966, Localization of native tropomyosin in relation to striation patterns. *J. Biochem.* **60**:605–608.

Endo, M., Tanaka, M., and Ogawa, Y., 1970, Calcium-induced release of calcium from the sarcoplasmic reticulum of skinned skeletal muscle fibres. *Nature* **228**:34–36.

Endo, M., Yagi, S., Ishizuka, T., Horiuti, K., Koga, Y., and Amaha, K., 1983, Changes in the Ca-induced Ca release mechanism in the sarcoplasmic reticulum of the muscle from a patient with malignant hyperthermia. *Biomed. Res.* **4**:83–92.

Fabiato, A., and Fabiato, F., 1972, Excitation-contraction coupling of isolated cardiac fibers with disrupted or closed sarcolemmas. Calcium-dependent cyclic and tonic contractions. *Circ. Res.* **31**:293–307.

Fleischer, S. E., Ogunbunmi, E. M., Dixon, M. C., and Fleer, E. A., 1985, Localization of Ca^{2+} channels with ryanodine in junctional terminal cisternae of sarcoplasmic reticulum of fast skeletal muscle. *Proc. Natl. Acad. Sci. USA* **82**:7256–7259.

Ford, L. E., and Podolsky, R. D., 1970, Regenerative calcium release within muscle cells. *Science* **167**:58–59.

Ford, L. E., and Podolsky, R. D., 1972, Intracellular calcium movements in skinned muscle fibres. *J. Physiol.* **223**:21–33.

Gyorke, S., and Fill M., 1993, Ryanodine receptor adaptation: control mechanism of Ca^{2+}-induced Ca^{2+} release in heart. *Science* **260**:807–809.

Ikemoto, T., and Endo, M., 2001, Properties of Ca^{2+} release induced by clofibric acid from sarcoplasmic reticulum of mouse skeletal muscle fibres. *Br. J. Pharmacol.* **134**:719–728.

Imagawa, T., Smith, J. S., Coronado, R., and Campbell, K. P., 1987, Purified ryanodine receptor from skeletal muscle sarcoplasmic reticulum is the Ca^{2+} permeable pore of the calcium release channel. *J. Biol. Chem.* **262**:16636–16643.

Inui, M., Saito, A., and Fleischer, S., 1987, Purification of the ryanodine receptor and identity with feet structures of junctional terminal cisternae of sarcoplasmic reticulum from fast skeletal muscle. *J. Biol. Chem.* **262**:1740–1747.

Ishizuka, T., and Endo, M., 1983, Effects of adenine on skinned fibers of amphibian fast skeletal muscle. *Proc. Jpn Acad.* **59**:93–96.

Ishizuka, T., Iijima, T., and Endo, M., 1983, Effect of adenine on twitch and other contractile responses of single fibers of amphibian fast skeletal muscle. *Proc. Jpn Acad.* **59**:97–100.

Kalow, W., Britt, B. A., Terreau, M. E., and Haist C., 1970, Metabolic error of muscle metabolism after recovery from malignant hyperthermia. *Lancet* **II**:895–898.

Kawana, Y., Iino, M., Horiuti, K., Matsumura, N., Ohta, T., Matsui, K., and Endo, M., 1992, Accerelation in calcium-induced calcium release in the biopsied muscle fibers from patients with malignant hyperthermia. *Biomed. Res.* **13**:287–297.

Lai, F. A., Erickson, H. P., Rousseau, E., Liu, Q.-Y., and Meissner, G., 1988, Purification and reconstitution of the calcium release channel from skeletal muscle. *Nature* **331**:315–319.

Matsui, K., Fujioka, Y., Kikuchi, H., Yuge, O., Fujii, K., Morio, M., Endo, M., 1991, Effects of several volatile anesthetics on the Ca^{2+}-related functions of skinned skeletal muscle fibers from the guinea pig. *Hiroshima J. Med. Sci.* **40**:9–13.

Natori, R., 1954, The property and contraction process of isolated myofibrils. *Jikeikai Med. J.* **1**:119–126.

Ohta, T., and Endo, M., 1986, Inhibition of calcium-induced calcium release by dantrolene at mammalian body temperature. *Proc. Jpn Acad.* **62**:329–332.

Ohta, T., Endo, M., Nakano, T., Morohoshi, Y., Wanikawa, K., and Ohga, A., 1989, Ca-induced Ca release in malignant hyperthermia-susceptible pig skeletal muscle. *Am. J. Physiol.* **256**:C358-C367.

Sorrentino, V., and Volpe, P., 1993, Ryanodine receptors: how many, where and why? *Trends Pharmacol. Sci.* **14**:98–103.

Stern, M., 1992, Theory of excitation-contraction coupling in cardiac muscle. *Biophys. J.* **79**:3353–3354.

Takeshima, H., Iino, M., Takekura, H., Nishi, M., Kuno, J., Minowa, O., Takano, H., and Noda, T., 1994, Excitation-contraction uncoupling and muscular degeneration in mice lacking functional skeletal muscle ryanodine receptor gene. *Nature* **369**:556–559.

Takeshima H, Nishimura S, Matsumoto T, Ishida H, Kangawa K, Minamino N, Matsuo, H., Ueda, M., Hanaoka, M., Hirose, T., and Numa, S., 1989, Primary structure and expression from complementary DNA of skeletal muscle of ryanodine receptor. *Nature* **339**:439–445.

Thorens, S., and Endo, M., 1975, Calcium-induced calcium release and "depolarization"-induced calcium release: their physiological significance. *Proc. Jpn Acad.* **51**:473–478.

Weber, A., and Herz, R., 1968, The relationship between caffeine contracture of intact muscle and the effect of caffeine on reticulum. *J. Gen. Physiol.* **52**:750–759.

Yamazawa, T., Takeshima, H., Sakurai, T., Endo, M., and Iino, M., 1996, Subtype specificity of the ryanodine receptor for Ca^{2+} signal amplification in excitation-contraction coupling. *EMBO J.* **15**:6172–6177.

24

DYSREGULATION OF THE GAIN OF CICR THROUGH RYANODINE RECEPTOR1 (RYR1): THE PUTATIVE MECHANISM UNDERLYING MALIGNANT HYPERTHERMIA

Yasuo Ogawa

24.1. INTRODUCTION

Ca^{2+} released through the Ca^{2+} release channel triggers muscle contraction. The Ca^{2+} release channel in the sarcoplasmic reticulum (SR) of the striated muscles is referred to as the ryanodine receptor (RyR), and is so named because of its binding ability of the open state with a high affinity to ryanodine.[1–6] Three genetically distinct isoforms (RyR1–3) are identified in mammals: RyR1 is the primary isoform in the skeletal muscle, RyR2 in the cardiac muscle, and RyR3 is ubiquitously expressed, although in a minuscule amount. In non-mammalian vertebrate skeletal muscles, e.g., chicken, frog, and fish, two isoforms referred to as α- and β-RyR are expressed in almost equal amounts. Further studies show that α- and β-RyR are homologs of RyR1 and RyR3, respectively, and that RyR3 is much degenerated and almost disappears in adult mammalian skeletal muscles except diaphragm and soleus.[2,5,6]

RyR is a protein composed of about 5000 amino acid residues with a MW of about 560 kDa. The tetramer (usually homotetramer) is the active Ca^{2+} release channel, and the channel activity can be modulated by such accessory proteins as calmodulin (CaM), FKBP12 and others.[1]

The gate of the channel is opened by Ca^{2+}, i.e., Ca^{2+} induced Ca^{2+} release (CICR).[7] Only RyR1 isoform can also open the gate upon conformation change of the voltage sensor, dihydropyridine receptor (DHPR), which is induced by change in the membrane potential. This mode of Ca^{2+} release is called depolarization-induced Ca^{2+} release (DICR).[8]

CICR is modulated by many endogenous agents: Ca^{2+}, Mg^{2+}, adenine nucleotides, modification of –SH by the redox state or NO, pH, the concentrations of the solutes, accessory proteins, the loading level of the Ca^{2+} store and others. CICR is also stimulated or inhibited by many kinds of drugs: caffeine, halothane, procaine, dantrolene and so on.[1–4]

Department of Pharmacology, Juntendo University School of Medicine, Tokyo 113-8421, Japan

Regulatory Mechanisms of Striated Muscle Contraction
Edited by Ebashi and Ohtsuki, Springer, 2007

We recently found that α-RyR from frog skeletal muscle[9,10] and RyR1 from rabbit and bovine skeletal muscles[11] have CICR activity selectively suppressed in the SR membrane (about 4–15% of the activity of RyR3) without obvious changes in sensitivity to many of the endogenous modulators mentioned above. A detergent, CHAPS (3-[(3-chol amidopropyl)dimethylammonio]-1-propanesulfonate), relieved the suppression of RyR1, whereas it exerted no obvious effect on RyR3. These findings suggest that intermolecular or interdomain interactions may be critically involved in the gain regulation of CICR activity.[9–11]

Ikemoto and his colleagues[12,13] proposed an interdomain interaction hypothesis for the mechanism underlying malignant hyperthermia (MH), showing the activating effect of DP4 (corresponding to L2442-P2477 of RyR1) on CICR activity of RyR1, but no effect of DP4-mut (replacement of R with C in DP4, mimicking R2458C in MH).

MH has been recognized to have unusual metabolic reactions to certain anesthetic agents that are often inherited, including a rapid and sustained rise in body temperature, tachycardia, elevated arterial CO_2 and lactic acid, and skeletal muscle contracture.[4,13–20] Characteristically high sensitivity to caffeine and halothane of skeletal muscle is used for diagnosis. A missense mutation of RyR1 is the basis for the disorder in major cases, although other distinct and heterogeneous changes have been proposed. Missense mutations in RyR1 have been found clustered into three regions: region 1 (36–615), region 2 (2100–2500), and region 3 (4100–4900). MH is mainly related to a mutation in regions 1 and 2. How mutation results in an increased Ca^{2+} release, however, still remains controversial.[4,13–25]

We have clarified that DP4 and CHAPS share a common mechanism for activating CICR activity.[26] This is probably due to interference of the interdomain interaction between region 1 and region 2. In the next step to confirm this hypothesis, we investigated RyR1 with R615C mutation from pig skeletal muscle (MH susceptible porcine) and compared it with the isoform from a wild type animal. Ca^{2+} dependent [^{3}H]ryanodine binding of the mutated RyR1 on the SR was enhanced to over 8 times greater than the wild type, being comparable to the unsuppressed one. These findings support our hypothesis that the affected interdomain interaction between the two regions increases the gain of CICR, resulting in enhanced Ca^{2+} release.

24.2. SUPPRESSION OF CICR ACTIVITY IS CHARACTERISTIC OF RYR1

Ca^{2+} dependent [^{3}H]ryanodine binding was used as the biochemical measure for CICR activity, because they were parallel to each other under various conditions.[5] The open state of the CICR channel showed a greatly increased affinity for [^{3}H]ryanodine and the affinity for the ligand was found to follow the degree of activation of the Ca^{2+} release channels, RyR.

Frog skeletal muscle SR contains almost equal amounts of RyR1 and RyR3 homologs. The precise ratio of the contents of the two isoforms was found to be 45 : 55 on the basis of the density of the two bands on SDS-PAGE. The ratio was also supported by the maximum capacity for [^{3}H]ryanodine binding (Bmax). Purified isoforms showed very similar Ca^{2+} dependent [^{3}H]ryanodine binding. RyR1 homolog in the SR, however, showed only 4% of RyR3 homolog in [^{3}H]ryanodine binding without obvious change in the sensitivity to Ca^{2+}, Mg^{2+} or AMPPCP (a nonhydrolyzable analog of ATP). The pos-

sibile involvement of FKBP12 or CaM was excluded, because treatment with FK506 or with CaM-binding peptide showed no effect.[10]

Bovine diaphragm contained a detectable amount of RyR3. The ratio of RyR1 and RyR3 was determined to be 96 : 4 on the basis of their respective Bmax values in the bovine diaphragm SR. When the [^{3}H]ryanodine binding (B) to RyR1 and RyR3 were calibrated by the respective Bmax values, the ratio B/Bmax would represent an averaged specific activity of a single channel of each isoform. Then, RyR1 was about 1/6 to 1/7 of RyR3 in terms of B/Bmax. The value of RyR3 in the SR was comparable to that of purified RyR3. It can be concluded, therefore, that RyR1 is selectively suppressed in the SR membrane in CICR activity, whereas RyR3 is not suppressed.[11] As shown in Table 24.1, RyR2 does not appear to be much suppressed in the SR. We can conclude, therefore, that it is characteristic of RyR1 to have CICR activity suppressed in the SR membrane.

RyR1 in the SR showed an affinity for the ligand (Kd = 10–20 nM) in the 1 M NaCl-medium, whereas RyR3 showed Kd = 1–3 nM. Purified RyR1 and RyR3, on the other hand, showed Kd = 1–3 nM.[10,11] These findings show that the suppression of RyR1 in the SR membrane is due to a decreased affinity for the ligand, but not due to a decreased number of RyR channels, i.e., Bmax.

After further purification steps including processing by French Press to dissociate the T-tubule from the SR in the triad and fractionation by sucrose density gradient ultracentrifugation, we obtained a fraction where DHPR was selectively reduced to less than 10% of control in reference to the amount of RyR1 and RyR3. Suppression remained unchanged with this preparation. The possible interaction with DHPR cannot be the cause of suppression.[11] The SR vesicles from the epicranial muscle, on the other hand, contained RyR1 alone, but no RyR3. The magnitude of suppression with RyR1 in this SR was similar to the case with the SR from diaphragm where the two isoforms coexist as mentioned above. This finding indicates that the coexisting RyR3 cannot be the explanation for the suppression.[11]

Selective suppression of RyR1 in the SR may be intrinsic of the isoform. Responses to Ca^{2+}, Mg^{2+} and AMPPCP were not substantially different between in situ and purified isoforms. RyR1 of the SR vesicles which had CaM reduced to 1/10 by the treatment with CaM binding peptide maintained low [^{3}H]ryanodine binding activity. This excludes CaM from the list of candidates. Addition of 10 μM FK506 which dissociates FKBP12 from RyR increased B/Bmax for RyR1 in the SR from 0.025 to 0.040, whereas 1% CHAPS increased it to 0.12. The combination of the two reagents further increased it to 0.18 which was comparable to the value of RyR3 (0.19–0.22). The ratio of enhancement by FK506

Table 24.1. B/Bmax values for RyR isoforms in the SR

RyR1	RyR2	RyR3
0.009 (frog) 0.025–0.037 (bovine)	0.2–0.3 (rabbit)	0.13–0.25 (frog, bovine)

[^{3}H]Ryanodine binding (B) in terms of pmol/mg protein of SR was determined in 0.17 M NaCl-medium according to the routine method in our laboratory. The maximum binding sites (Bmax) in terms of pmol/mg protein in SR were obtained from the Scatchard plot for B in the 1 M NaCl-medium. B/Bmax, then, reflects the averaged relative activity of the single active channel, which was evaluated in the presence of about 9 nM [^{3}H]ryanodine. The B/Bmax values for purified RyR1 and RyR3 were 0.25 and 0.29, respectively, under similar conditions. With purified RyR2, the corresponding B/Bmax would be not less than these values.

or CHAPS was not affected by the presence or absence of the counterpart, therefore the two reagents work independently of each other. RyR3 was not affected by either of them. Similar results were also obtained in the 1 M NaCl-medium where RyR1 and RyR3 were markedly stimulated. These results indicate that the suppression of RyR1 in the SR can be relieved largely by CHAPS, although FKBP12, to a lesser extent, independently contributes to the suppression. FKBP12, by the way, cannot be detected on the immunoprecipitation of RyR3, although it could bind to RyR3 without an apparent stabilizing effect on the isoform. The stimulating effect of CHAPS was observed selectively with RyR1, but not with RyR3.

Reversal of suppression of RyR1 by CHAPS may be due to its more or less specific effect in view of the fact that RyR3 was not affected by the detergent, whereas both were markedly stimulated in the 1 M NaCl-medium.[11] It should be pointed out that β-RyR of frog skeletal muscle was stimulated by CHAPS.[10]

24.3. A DOMAIN PEPTIDE, DP4, IS VERY SIMILAR TO CHAPS IN ITS STIMULATING EFFECTS

Ikemoto and his colleagues[12,13] proposed an interdomain interaction hypothesis for the underlying mechanism of malignant hyperthermia (MH). As shown in Figure 24.1, the mutated sites of RyR1 in MH are clustered into 3 regions of which region 1 (N-terminal region) and region 2 (central region) are dominant in the typical form of MH.[4,13,16,18] They examined synthetic peptides that corresponded to these two regions. One of these peptides, designated as DP4 (L2442-P2477 of RyR1), was found to be a potent activator of [^{3}H]ryanodine binding and CICR activity. Interestingly, DP4-mut (replacement of R with C in DP4, mimicking the R2458C in MH) totally abolished these

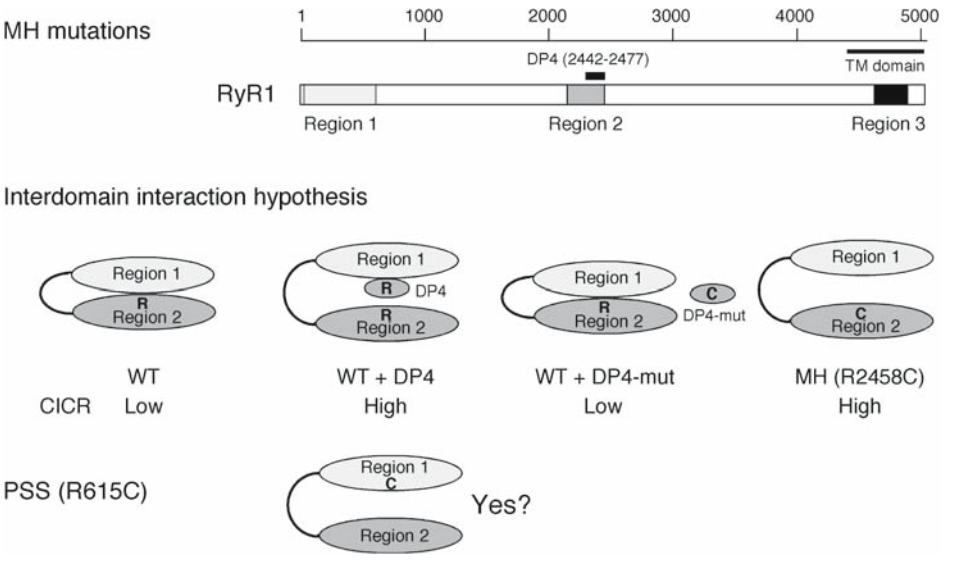

Figure 24.1. Interdomain interaction hypothesis for MH.

effects. Furthermore, cross-linking studies showed that DP4 bound to the N-terminal region of RyR1.[27] They proposed that the two domains in region 1 and region 2 within RyR1 interact with each other to stabilize the closed state of the channel. A missense mutation in either domain would weaken the domain-domain interaction, resulting in channel destabilization and enhanced channel activity. The primary effect of DP4 is to interfere with the domain-domain interaction by competing with the corresponding domain for the mating domain, leading to destabilization of the RyR channel.

We hypothesized that the stimulating effect of CHAPS would be primarily similar to that of DP4.[26] DP4 stimulated selectively RyR1 but not RyR3. DP4-mut, in contrast, showed only a weak effect on RyR1 or RyR3. Responses to Ca^{2+}, Mg^{2+} and AMPPCP were hardly affected by DP4. DP4 stimulated [^{3}H]ryanodine binding in a dose-dependent manner, and the effect was saturated around 300 μM (Figure 24.2A). The stimulating effect of CHAPS alone was also dose-dependent and reached the maximum at 2%. In the presence of 2% CHAPS, further stimulation on addition of DP4 was not observed. In the presence of an intermediate concentration of CHAPS, say 1%, DP4 showed a dose dependent stimulation, but the maximum effect did not exceed the upper limit caused by 2% CHAPS, 300 μM DP4 or their combination (Figure 24.2A). This highest value is not due to the limitation of the assay system, because even much larger values were obtained with FK506 or at a higher ionic strength. These findings support the notion that DP4 and CHAPS act on RyR1 through a common activation mechanism. To confirm this further, we examined the inhibitory effect of dantrolene, which is a well-known antidote to MH[14,15,17,28] (Figure 24.2B). Recent investigations showed that the dantrolene-binding sequence in RyR1 was identified within region 1[29] and that the agent stabilized the inter-domain interactions.[30] Because it was more effective at a high temperature and at a low concentration of Ca^{2+}, determinations were carried out at 37°C.[31,32] As shown in Figure 24.2B, dantrolene inhibited [^{3}H]ryanodine binding to RyR1 in the presence of 100 μM DP4 or 1% CHAPS, and showed the identical concentration dependent inhibition, irrespective of stimulating reagent, DP4 or CHAPS. Consistent with reported results on its antagonistic effect, the extent of inhibition by dantrolene was greater at 1 μM Ca^{2+} than at 30 μM Ca^{2+}. Similar results were obtained with azumolene, a more water soluble

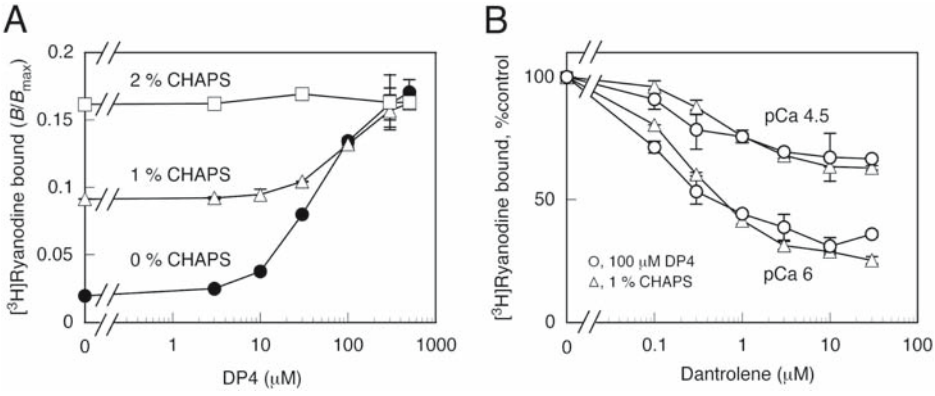

Figure 24.2. CHAPS and DP4 act on RyR1 through a common activation mechanism. Reproduced from ref. 26 with permission of The American Physiological Society.

analog of dantrolene. These findings support that DP4 and CHAPS share a common underlying mechanism for stimulation: prevention of interdomain interaction between regions 1 and 2.

24.4. [^{3}H]RYANODINE BINDING IN PORCINE STRESS SYNDROME (PSS) PIG

PSS pig with R615C mutation in RyR1 is a good animal model for human MH. Despite having been well studied to elucidate the underlying mechanism for MH, it still remains unclear.[14–25] In the view of the findings described above, study of the mutated RyR1 will facilitate our understanding about the selective suppression mechanism of RyR 1 and the mechanism of MH, because PSS has mutation in region 1, complementary to the case of mutation in region 2.

The bands of RyR1 from wild type (WT) and PSS skeletal muscle (MHS) were not different in their density or mobility on the SDS-PAGE. The Ca^{2+} dependences of the [^{3}H]ryanodine binding were well overlapped when the curves were calibrated by the respective peak activities at about 30 μM Ca^{2+}. The peak activities, however, were different: the B/Bmax was 0.024 with WT, and 0.21 with MHS, more than 8-fold of WT. Responses to Mg^{2+} and AMPPCP as well as to Ca^{2+} were very similar. Interestingly, the stimulating effect of DP4 on WT was similar to the case shown in Figure 24.2A, and DP4-mut showed a minor effect. Dose-dependent stimulation by DP4 in MHS which showed an enhanced basal activity, however, was much weaker in magnitude than in WT, and DP4-mut showed similar stimulation. FK506 treatment caused slight stimulation, but there was no significant difference between WT and MHS; and the relative extents of inhibition by dantrolene were similar between them. The SR vesicles from MHS showed apparently increased sensitivity to caffeine (about 5-fold) than those from WT in its Ca^{2+} releasing action. These results strongly indicate that MH mutation weakens the interdomain interaction and reduces the suppression in RyR1. The increased sensitivity to caffeine would be apparent in the presence of the Ca^{2+} uptake activity.

The three dimensional structure of RyR looks very similar, regardless of the isoforms. Region 1 and region 2 are believed to be located in the corners of the square- or rhombic-shaped cytoplasmic part.[33–35] The channel pore or gate would be in the C-terminal region and is thought to be located in the central portion in the transmembrane part. Therefore, how the interdomain interaction between region 1 and region 2 modulates the pore or gate is indeed a challenging problem. Alternatively, the function as the pore or gate might be localized around the each corner of the cytoplasmic part, although this is less likely to be the case.

24.5. ACKNOWLEDGEMENTS

The experimental results cited in this paper are owed to the following collaborators: Takashi Murayama, Akito Chugun, and Nagomi Kurebayashi (Juntendo Univ. Sch. Med., Tokyo); Toshiharu Oba (Nagoya City Univ. Grad. Sch. Med., Nagoya); Shigeki Kobayashi and Noriaki Ikemoto (BBRI, Boston); and Hiroshi Haga and Kikuo Wakabe (NLBC, Miyazaki).

24.6. REFERENCES

1. G. Meissner, Ryanodine receptor/Ca^{2+} release channels and their regulation by endogenous effectors, *Ann. Rev. Physiol.* **56**, 485–508 (1994).
2. J. A. Sutko, and J. A. Airey, Ryanodine receptor Ca^{2+} release channels: does diversity in form equal diversity in function? *Physiol. Rev.* **76**, 1027–1071 (1996).
3. C. Franzini-Armstrong, and F. Protasi, Ryanodine receptors of striated muscles: a complex channel capable of multiple interactions, *Physiol. Rev.* **77**, 699–729 (1997).
4. D. H. MacLennan, Ca^{2+} signaling and muscle disease, *Eur. J. Biochem.* **267**, 5291–5297 (2000).
5. Y. Ogawa, Role of ryanodine receptors, *Crit. Rev. Biochem. Mol. Biol.* **29**, 229–274 (1994).
6. V. Sorrentino, and C. Reggiani, Expression of the ryanodine receptor type 3 in skeletal muscle. A new partner in excitation-contraction coupling? *Trends Cardiovasc. Med.* **9**, 54–61 (1999).
7. M. Endo, Calcium release from the sarcoplasmic reticulum, *Physiol. Rev.* **57**, 71–108 (1977).
8. M. F. Schneider, and W. K. Chandler, Voltage dependent charge movement in skeletal muscle: a possible step in excitation-contraction coupling, *Nature* **242**, 244–246 (1973).
9. T. Murayama, and Y. Ogawa, Roles of two ryanodine receptor isoform coexisting in skeletal muscle, *Trends Cardiovasc. Med.* **12**, 305–311 (2002).
10. T. Murayama, and Y. Ogawa, Selectively suppressed Ca^{2+}-induced Ca^{2+} release activity of α-ryanodine receptor (α-RyR) in frog skeletal muscle sarcoplasmic reticulum: potential distinct modes in Ca^{2+} release between α- and β-RyR, *J. Biol. Chem.* **276**, 2953–2960 (2001).
11. T. Murayama, and Y. Ogawa, RyR1 exhibits lower gain of CICR activity than RyR3 in the SR: evidence for selective stabilization of RyR1 channel, *Am. J. Physiol. Cell. Physiol.* **287**, C36–C45 (2004).
12. T. Yamamoto, R. El-Hayek, and N. Ikemoto, Postulated role of interdomain interaction within the ryanodine receptor in Ca^{2+} channel regulation, *J. Biol. Chem.* **275**, 11618–11625 (2000).
13. N. Ikemoto, and T. Yamamoto, Regulation of Ca^{2+} release by interdomain interaction within ryanodine receptors, *Front. Biosci.* **7**, d671–d683 (2002).
14. J. R. Mickelson, and C. F. Louis, Malignant hyperthermia: excitation-contraction coupling, Ca^{2+} release channel and cell regulation defects, *Physiol. Rev.* **76**, 537–592 (1996).
15. M. Denborough, Malignant hyperthermia, *Lancet* **352**(9134), 1131–1136 (1998).
16. K. Jurkat-Rott, T. McCarthy, and F. Lehmann-Horn, Genetic and pathogenesis of malignant hyperthermia, *Muscle Nerve* **23**, 4–17 (2000).
17. T. E. Nelson, Malignant hyperthermia: a pharmacogentic disease of Ca^{2+} regulating proteins, *Curr. Mol. Med.* **2**, 347–369 (2002).
18. M. Brini, Ryanodine receptor defects in muscle genetic diseases, *Biochem. Biophys. Res. Commun.* **322**, 1245–1255 (2004).
19. N. A. Benkusky, E. F. Farrell, and H. H. Valdivia, Ryanodine receptor channelopathies, *Biochem. Biophys. Res. Commun.* **322**, 1280–1285 (2004).
20. R. T. Dirksen, and G. Avila, Pathophysiology of muscle disorders linked to mutations in the skeletal muscle ryanodine receptor, in: *Ryanodine Receptors: Structure, Function and Dysfunction in Clinical Disease*, edited by X. H. Wehrens, and A. R. Marks (Springer Science, New York, 2005), pp. 229–242.
21. M. Endo, S. Yagi, T. Ishizuka, K. Horiuti, Y. Koga, and K. Amaha, Changes in the Ca-induced Ca release mechanism in the sarcoplasmic reticulum of the muscle from a patient with malignant hyperthermia, *Biomed. Res.* **4**, 83–92 (1983).
22. D. R. Laver, V. J. Owen, P. R. Junankar, N. L. Taske, A. F. Dulhunty, and G. D. Lamb, Reduced inhibitory effect of Mg^{2+} on the ryanodine receptor-Ca^{2+} release channels in malignant hyperthermia, *Biophys. J.* **73**, 1913–1924 (1997).
23. J. Tong, H. Oyamada, N. Demaurex, S. Grinstein, T. V. McCarthy, and D. H. MacLennann, Caffeine and halothane sensitivity of intracellular Ca^{2+} release is altered by 15 calcium release channel (ryanodine receptor) mutations associated with malignant hyperthermia and/or central core disease, *J. Biol. Chem.* **272**, 26332–26339 (1997).
24. E. M. Balog, B. R. Fruen, N. H. Shomer, and C. F. Louis, Divergent effects of the malignant hyperthermia-susceptible Arg615→Cys mutation on the Ca^{2+} and Mg^{2+} dependence of the RyR1, *Biophys. J.* **81**, 2050–2058 (2001).
25. T. Yang, T. A. Ta, I. N. Pessah, and P. D. Allen, Functional defects in six ryanodine receptor isoform-1 (RyR1) mutations associated with malignant hyperthermia and their impact on skeletal excitation-contraction coupling, *J. Biol. Chem.* **278**, 25722–25730 (2003).

26. T. Murayama, T. Oba, S. Kobayashi, N. Ikemoto, and Y. Ogawa, Postulated role of interdomain interactions within the type 1 ryanodine receptor in the low gain of Ca^{2+}-induced Ca^{2+} release activity of mammalian skeletal muscle sarcoplasmic reticulum, *Am. J. Physiol. Cell. Physiol.* **288**, 1222–1230 (2005).
27. T. Yamamoto, and N. Ikemoto, Spectroscopic monitoring of local conformational changes during the intramolecular domain-domain interaction of the ryanodine receptor, *Biochemistry* **41**, 1492–1501 (2002).
28. T. Krause, M. V. Gerbershagen, M. Fiege, R. Weisshorn, and F. Wrappler, Dantrolene: a review of its pharmacology, therapeutic use and new developments, *Anesthesia* **59**, 364–373 (2004).
29. K. Paul-Pletzer, T. Yamamoto, M. B. Bhat, J. Ma, N. Ikemoto, L.S. Jimenez, H. Morimoto, P. G. Williams, and J. Parness, Identification of a dantrolene-binding sequence on the skeletal muscle ryanodine receptor, *J. Biol. Chem.* **277**, 34918–34923 (2002).
30. S. Kobayashi, M. L. Bannister, J. P. Gangopadhyay, T. Hamada, J. Parness, and N. Ikemoto, Dantrolene stabilizes domain interactions within the ryanodine receptor, *J. Biol. Chem.* **280**, 6580–6587 (2005).
31. T. Ohta, M. Endo, T. Nakano, Y. Morohoshi, K Wanikawa, and A. Ohga, Ca^{2+}-induced Ca^{2+} release in malignant hyperthermia-susceptible pig skeletal muscle, *Am. J. Physiol. Cell. Physiol.* **256**, C358–C367 (1989).
32. B. R. Fruen, J. R. Mickelson, and C. F. Louis, Dantrolene inhibition of sarcoplasmic reticulum Ca^{2+} release by direct and specific action at skeletal muscle ryanodine receptors, *J. Biol. Chem.* **272**, 26965–26971 (1997).
33. T. Murayama, T. Oba, E. Katayama, H. Oyamada, K. Oguchi, M. Kobayashi, K. Otsuka, and Y. Ogawa, Further characterization of type 3 ryanodine receptor (RyR3) purified from rabbit diaphragm, *J. Biol. Chem.* **274**, 17297–17308 (1999).
34. I. I. Serysheva, S. L. Hamilton, W. Chiu, and S. J. Ludtke, Structure of Ca^{2+} release channel at 14 Å resolution, *J. Mol. Biol.* **345**, 427–431 (2005).
35. Z. Liu, R. Wang, J. Zhang, S. R. W. Chen, and T. Wagenknecht, Localization of a disease-associated mutation site in the three-dimensional structure of cardiac ryanodine receptor, *J. Biol. Chem.* **280,** 37941–37947.

25

ION PUMPING BY CALCIUM ATPASE OF SARCOPLASMIC RETICULUM

Chikashi Toyoshima

25.1. INTRODUCTION

Ca^{2+}-ATPase of skeletal muscle sarcoplasmic reticulum (SERCA1a) is an integral membrane protein of 110K and the best characterised member of the P-type (or E1/E2-type) ion translocating ATPases. It was first identified by Ebashi in the "relaxing factor" of muscle contraction and gave rise to the calcium theory that Ca^{2+} is a fundamental and ubiquitous factor in the regulation of intracellular processes.[1] There are several types of Ca^{2+}-ATPases in different tissues; all transfer Ca^{2+} from the cytoplasm to the opposite side of the membrane and countertransport H^+. Stoichiometry of Ca^{2+}: ATP may be variable but it is well established that SERCA1a can transfer two Ca^{2+} per ATP hydrolysed.[2] In the sarcoplasmic reticulum (SR) membrane, Ca^{2+}-ATPase pumps Ca^{2+}, released into muscle cells during muscle contraction, back into SR, thereby relaxes muscle cells. This pump runs as long as ATP and Ca^{2+} are present, and establishes more than 10^4-fold concentration gradient across membranes. According to the classical E1/E2 theory, transmembrane Ca^{2+}-binding sites have high affinity and face the cytoplasm in E1; in E2, the binding sites have low affinity and face the lumen of SR (extracellular side).[2,3] Actual transfer of bound Ca^{2+} is thought to take place between two phosphorylated intermediates, E1P and E2P, in exchange of H^+. Because 2 Ca^{2+} are transferred in the forward direction and 2 to 3 protons in the opposite direction, active transport of Ca^{2+} is an electrogenic process. Although no H^+ gradient is built up across the SR membrane because it is leaky to H^+, this Ca^{2+}/H^+ exchange may cause pathological pH effects with plasma membrane Ca^{2+}-ATPase.[4]

Because Ca^{2+} is so fundamental in regulation of biological processes, malfunctioning of Ca^{2+}-pumps is likely to be deleterious to living organisms. Therefore, human diseases related to Ca^{2+}-ATPases are not many. Conversely Ca^{2+}-ATPases can be utilised for killing cells. For instance, cancer cells may be killed by delivering a potent inhibitor of this pump, such as thapsigargin (TG).[5] Artemisinin, a well-known anti-malarial drug, is reported to be targeted to a malarial Ca^{2+}-ATPase.[6] In cardiac muscles, phospholamban and sarcolipin work as regulators of Ca^{2+}-ATPase and are becoming therapeutic targets.[7]

Institute of Molecular and Cellular Biosciences, The University of Tokyo, 1-1-1 Yayoi, Bunkyo-ku, Tokyo 113-0032, Japan

Regulatory Mechanisms of Striated Muscle Contraction
Edited by Ebashi and Ohtsuki, Springer, 2007

Table 25.1. Current status of the crystallography of SR Ca^{2+}-ATPase in our laboratory

State	Substrate analogues[a]	Other ligands	Resolution (current)	References
E1·2Ca^{2+}	(TNP-AMP)	Ca^{2+}	2.4 (2.3) Å	8
E1·ATP	AMPPCP	Ca^{2+}, Mg^{2+}	2.9 (2.5)	10, *2I*[d]
E1 : P ADP[b]	ADP, AlF_x	Ca^{2+}, Mg^{2+}	2.7 (2.4)	11, *2I*[d]
E2 : Pi[b]	AlF_4^-	Mg^{2+}, TG[c]	*3.0*[d] (2.7)	*22*[d]
E2·Pi[b]	MgF_4^{2-}	Mg^{2+}, TG	2.3	11
E2		TG, TG + BHQ[c]	3.1, 2.4	9, 12

[a] AlF_x and MgF_4^{2-} are stable analogues of phosphate.

[b] The colon denotes here a transition state, where as the dot denotes a product state.

[c] TG (thapsigargin) and BHQ (2,5-di-*tert*-butyl-1,4-dihydroxybenzene) are potent inhibitors of SERCA1, binding to different parts of the transmembrane domain.[12]

[d] Published by a Danish group.[21,22]

We crystallised Ca^{2+}-ATPase from rabbit white skeletal muscle in phospholipid bilayer and solved the first atomic structure in 2000 by X-ray crystallography.[8] We now have determined 7 crystal structures of this ATPase in 6 different states that cover the entire reaction cycle (Table 25.1; Figure 25.1),[8–12] and also carried out all-atom molecular dynamics simulations for native structures and some mutants.[13] As a result, we can now propose a synopsis of ion pumping based on the atomic structures and answer important questions such as (i) what are the roles of ATP[10] and phosphorylation,[11] (ii) why such large domain movements are necessary,[14] and (iii) why H^+ countertransport is necessary despite that SR membrane is leaky to H^+ (ref. 12). An earlier overview of Ca^{2+}-ATPase structures is found in ref. 14, and more general ones on P-type ATPases in refs. 2 and 15.

25.2. ARCHITECTURE OF CA^{2+}-ATPASE

SERCA1a consists of 3 cytoplasmic domains (A, actuator; N, nucleotide binding; P, phosphorylation), 10 transmembrane (M1-M10) helices and small lumenal loops (Figure 25.1). As described below, the A-domain, connected to the M1-M3 helices with rather long linkers, works as the actuator of the transmembrane gating mechanism that regulates Ca^{2+} binding and release. It contains one of the signature sequences ^{181}TGES motif,[2] which plays an important role in dephosphorylation.[16,17] The P-domain contains the phosphorylation residue Asp351, magnesium co-ordinating residue Asp703 and many other critical residues for phosphorylation. This domain has a haloacid dehalogenase fold[18] and shares critical residues for phosphorylation with those of bacterial two-component regulators,[19] which have a different folding pattern. The N-domain, a long insertion between two parts forming the P-domain, contains the residues for adenosine binding (Phe487) and those critical for bridging ATP and P-domains (Arg560).[17,20] These three domains are well separated in E1·2Ca^{2+} but gather to form a compact headpiece in the other states (Figure 25.1).

There are 10 transmembrane helices and some of them (M2-M5) have long cytoplasmic extensions (Figure 25.1). In particular, M5 is 60 Å long and extends from the lumenal surface to the end of the P-domain, working as the spine of the molecule. Two (M4 and M6) helices are partly unwound throughout the whole reaction cycle. M6 and M7 are far

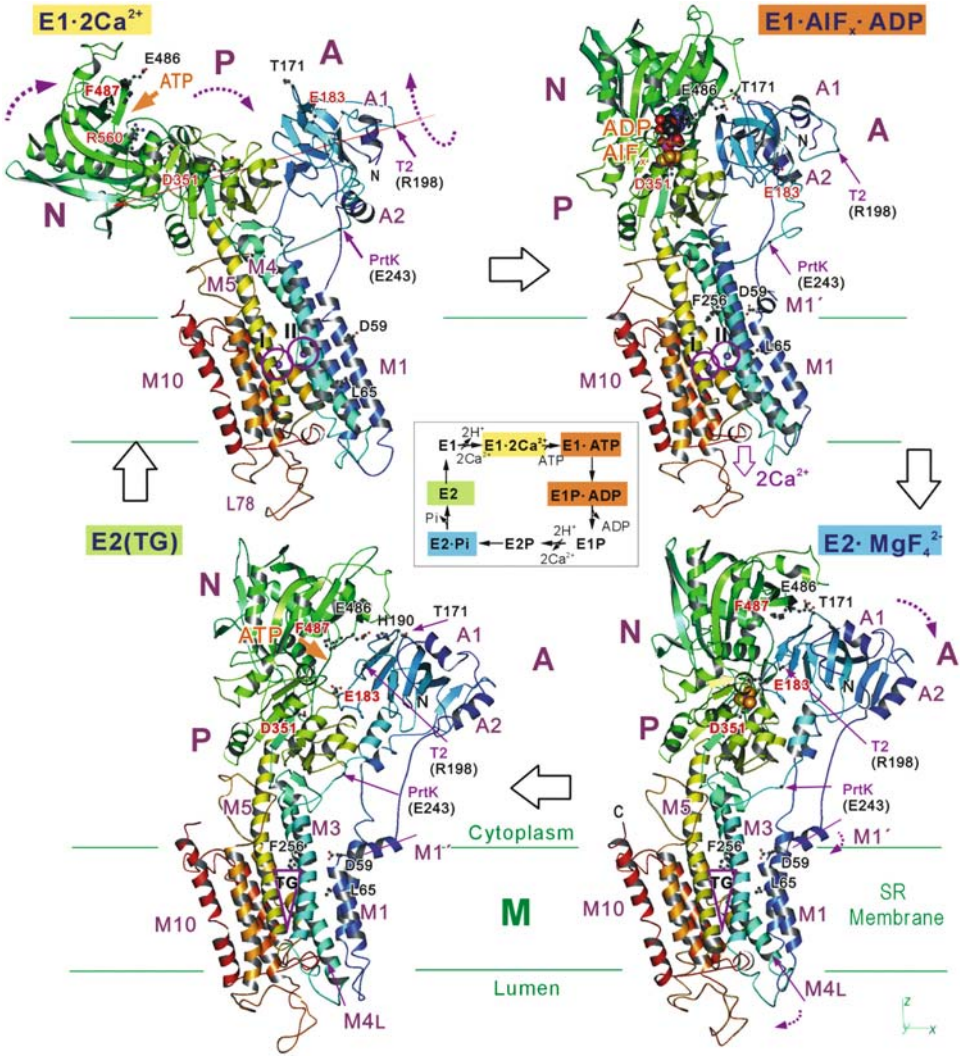

Figure 25.1. Front views (parallel to the membrane ($x - y$) plane) of Ca^{2+}-ATPase in four different states and a simplified reaction scheme (showing only the forward direction), in which different colours correspond to the respective structures presented here. Colours change gradually from the amino terminus (blue) to the carboxy terminus (red). Purple spheres (numbered and circled) represent bound Ca^{2+}. Three cytoplasmic domains (A, N and P), the α -helices in the A-domain (A1 and A2) and those in the transmembrane domain (M1, M4L, M5 and M10) are indicated. M1′ is an amphipathic part of the M1 helix lying on the bilayer surface. PtrK, a proteinase-K digestion site (around Glu243); SR, sarcoplasmic reticulum; T2, a trypsin digestion site at Arg198; ATP, the binding pocket for the adenosine moiety of ATP; TG, thapsigargin. Several key residues – E183 (A), F487 (N, adenine binding), D351 (P, phosphorylation site), D59 and L65 (M1), F256 (M3, TG binding) – and those involved in interdomain hydrogen bonds (including T171, H190 and E486) are shown in ball-and-stick representation. PDB accession codes are 1SU4 ($E1{\cdot}2Ca^{2+}$), 1WPE ($E1{\cdot}AlF_x{\cdot}ADP$), 1WPG ($E2{\cdot}MgF_4^{2-}$) and 1IWO(E2(TG)). Atomic co-ordinates of the aligned models are available at the author's web site (http://www.iam.u-tokyo.ac.jp/StrBiol/resource/res.html).

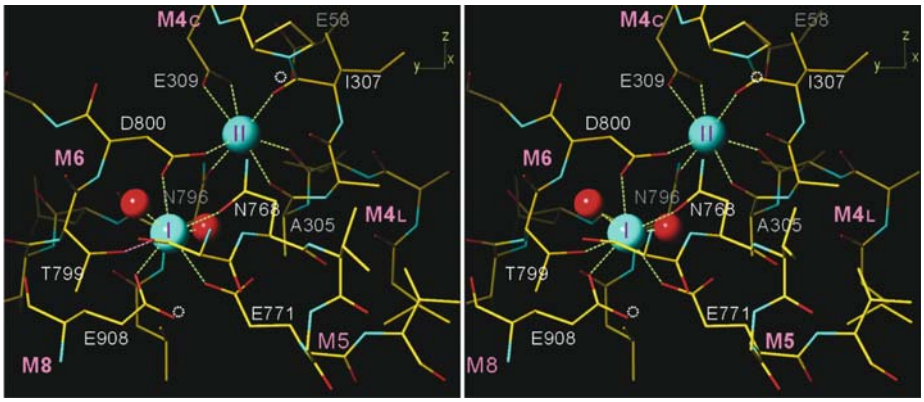

Figure 25.2. Detail of the transmembrane Ca^{2+}-binding sites. Viewed in stereo approximately parallel to the membrane. Two bound Ca^{2+} appear as cyan spheres and two water molecules bound to site I Ca^{2+} as small red spheres. Both Ca^{2+} are co-ordinated by 7 oxygen atoms. White dotted circles indicate predicted protonation sites.[13]

apart and connected by a long cytosolic loop (L67). L67 runs along the bottom of the P-domain and is hydrogen bonded to M5, presumably to restrict the movement of the M5 helix. M4-M6 and M8 contain the residues directly co-ordinating the two Ca^{2+} (Figure 25.2). The amino acid sequence is well conserved for M4 to M6 but not for M8 even within the members of closely related P-type ATPases, such as Na^+K^+- and H^+K^+-ATPases.[2] All helices from M1 to M6 move considerably during the reaction cycle, whereas M7–10 helices keep their positions (Figures 25.1, 25.3), apparently acting as a membrane anchor. M7–M10 are thought to have a specialised function in each subfamily of P-type ATPases, and are in fact absent in bacterial type I P-type ATPases.[2]

25.3. STRUCTURE OF THE CA^{2+}-BINDING SITES

It is well established that SERCA1 has two high affinity transmembrane Ca^{2+}-binding sites and the binding is co-operative.[23] There was much confusion as to their locations, partly because these Ca^{2+} binding sites do not appear to bind lanthanides. Debates still exist as to the presence of low affinity sites, in particular, in the lumenal region. X-ray crystallography of the rabbit SERCA1a in 10 mM Ca^{2+} at pH 6.1 identified two binding sites in the transmembrane region but none outside the membrane.[8]

The two Ca^{2+} binding sites (I and II) are located side by side near the cytoplasmic surface of the lipid bilayer (Figures 25.1, 25.3), even though the binding of two Ca^{2+} is sequential and co-operative. Site I, the binding site for the first Ca^{2+}, is located at the center of the transmembrane domain when viewed normal to the membrane in a space surrounded by M5, M6 and M8 helices. Site I is formed by Asn768, Glu771 (M5), Thr799, Asp 800 (M6) and Glu908 (M8) and two water molecules (Figure 25.2). Thus, no main chain oxygen atoms contribute to this site. Site II is nearly "on" the M4 helix, and located slightly (~3 Å) closer to the cytoplasmic surface than site I (Figure 25.1). Site II is formed

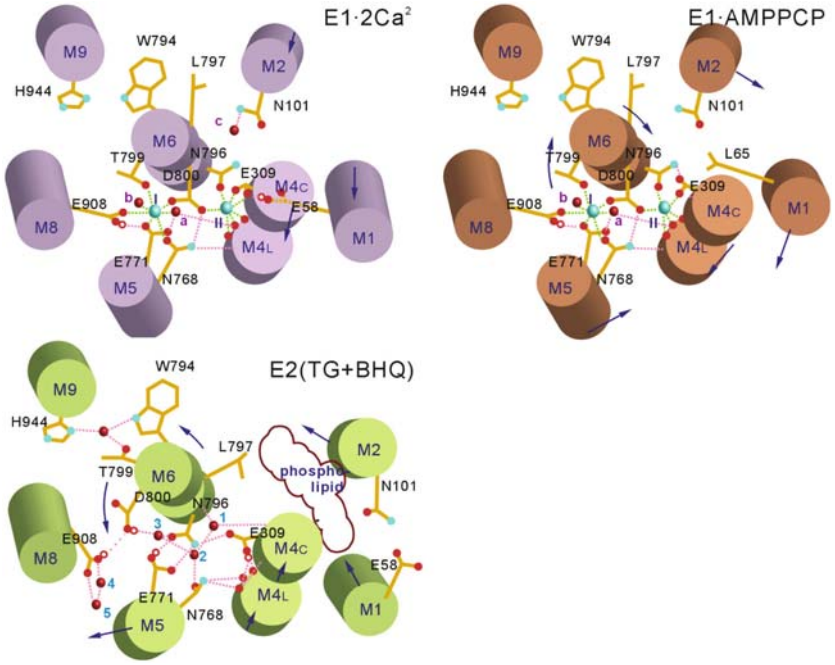

Figure 25.3. A diagram showing the Ca^{2+} binding sites in three states viewed from the cytoplasmic side approximately normal to the membrane. Cyan spheres represent Ca^{2+}, red ones water. Arrows indicate the movements of helices; pink dotted lines show hydrogen bonds and green ones Ca^{2+} co-ordination. Arrows indicate the movements of transmembrane helices in the forward direction. Labelling of the water molecules follows ref. 12.

with the contribution of M4-M6 and no water molecules (Figure 25.2). The M4 helix is partly unwound (between Ile307-Gly310) and provides 3 main chain oxygen atoms to the co-ordination (Figure 25.2). Asn796 and Asp800 (M6) provide one side chain oxygen atom whereas Glu309 provides two to cap the bound Ca^{2+} (Figure 25.2). This arrangement of oxygen atoms is reminiscent of the EF-hand motif.

Thus, both site I and site II have 7 co-ordination but of different characteristics. Asp800, on the unwound part of M6, is the only residue that contributes to both sites (Figures 25.2, 25.3). Any substitutions to site I residues, except one for Glu908, totally abolish the binding of Ca^{2+}. In contrast, even double mutations of Glu309 and Asn796 leave 50% Ca^{2+} binding.[24] Taken together, these mutagenesis experiments show that site II is the binding site for the second Ca^{2+}. Further mutagenesis studies demonstrated that Glu309 is the gating residue.[25] It is well known that the second Ca^{2+} is exchangeable with those in the cytoplasm without affecting the first Ca^{2+}. The Asn796Ala mutant kept such property. In contrast, even the first Ca^{2+} exchanged rapidly with the Glu309Gln mutant, showing that site II Ca^{2+} is the second Ca^{2+} and exchanged with Ca^{2+} in the cytoplasm by conformation change of the Glu309 side chain. Thus, the first Ca^{2+} will enter the binding cavity through improperly formed site II (otherwise it will be trapped there); the binding of the first Ca^{2+} to site I will position Asp800 properly and alter the arrangements of oxygen atoms in site II to form a high affinity binding site.

Thus, the phosphorylation site and Ca^{2+}-binding sites are distant by more than 50 Å. A key question is how these two sites communicate with each other. In this regard, it is important to note that the cytoplasmic end of M5 is integrated into the P-domain near the phosphorylation site and hydrogen bonded to the M4 helix forming a short β-strand at the cytoplasmic end.[9] The P-domain is also connected to M3 with a flexible joint. Thus, the events that occur at either site will be transmitted to the other site mechanically.[9,14]

25.4. SYNOPSIS OF ION PUMPING

Based on 7 crystal structures listed in Table 25.1, we can now propose a fairly detailed description of ion pumping. We do not yet have exact analogues of E1P and E2P. However, as revealed by limited proteolysis,[26,27] domain organisations of E1·AMPPCP and E1·AlF_x·ADP crystal structures are virtually the same[10,21] and expected to be very similar to that of E1P. Also, E2·AlF_4^- and E2·MgF_4^{2-} have also virtually identical domain organisations,[11,22] which will be similar to E2P, except that the lumenal gate is not fully open in either crystal structure to allow access of Ca^{2+} from the lumenal side.[28] Thus, we can describe the entire reaction cycle with 4 principal crystal structures presented in Figure 25.4. They show how the affinity of the transmembrane Ca^{2+} binding sites is altered, and how the lumenal gate is opened and closed by events that occur around the phosphorylation site some 50 Å away (see also movies available at the author's web site (http://www.iam.u-tokyo.ac.jp/StrBiol/resource/res.html).

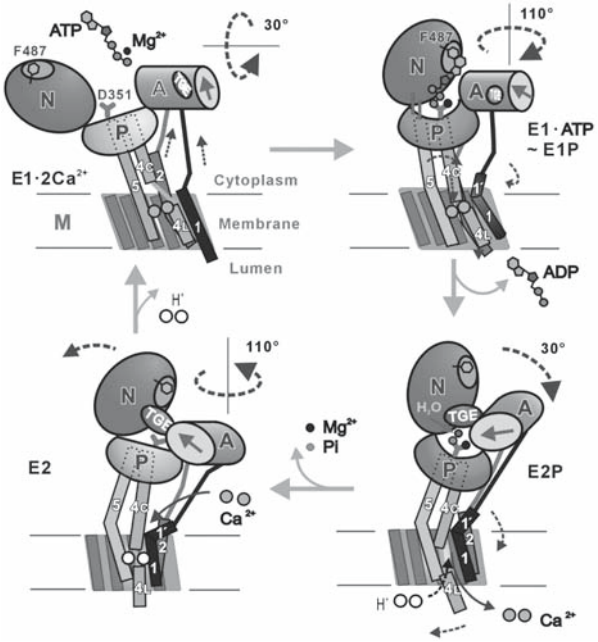

Figure 25.4. A cartoon depicting the structural changes of the Ca^{2+}-ATPase during the reaction cycle based on crystal structures of 5 different states.[11]

(i) Ca^{2+} binding to E2, the ground state, in exchange with H^+, straightens the M5 helix and breaks the closed configuration of the three cytoplasmic domains to allow more inclination of the N-domain. ATP may bind to the N-domain in E2 but cannot reach Asp351, the phosphorylation residue before Ca^{2+}-binding. Two Ca^{2+} enter the high affinity sites formed by transmembrane helices M4, M5, M6 and M8 through the gating residue Glu309 on M4. Because there is enough space around Glu309, the cytoplasmic gate is still open and site II Ca^{2+} can exchange with those in the cytoplasm. The M1 helix is deeply embedded in the lipid bilayer, stabilised indirectly by the bound Ca^{2+}.

(ii) ATP crosslinks the P- and N-domains, so that the γ-phosphate of ATP and a Mg^{2+} bind to the P-domain to bend it. The N-domain is fixed in a highly inclined position and makes contact with the A-domain to form a mechanical couple between them in preparation for the next main event, the rotation of the A-domain. The bending of the P-domain tilts the A-domain by ~30°, placing strain on the link between the A-domain and the M3 helix. This strain appears to be the driving force for the A-domain rotation in the next step. At the same time, the M1 helix is pulled up and bent so that the top of the transmembrane part (in particular Leu65; Figure 25.3) closes the cytoplasmic gate of the Ca^{2+} binding sites, by fixing the conformation of Glu309. Thus, two Ca^{2+} are occluded in the transmembrane binding sites.

(iii) Phosphoryl transfer to Asp351 allows the dissociation of ADP, which triggers the opening of the N- and P-domain interface. The A-domain rotates horizontally by 110° so that the TGES loop of the A-domain wedges into the gap. Thus the TGES loop occupies the space where ADP was to prevent the binding of ADP and to shield the aspartylphosphate from bulk water, and interacts with the phosphorylation site with the help of the Mg^{2+} bound to the P-domain. This A-domain rotation causes a drastic rearrangement of the transmembrane helices M1-M6; large downward movements of M4, sharp bending of M5 towards M1 (Figure 25.1) and rotation of M6 destroy the Ca^{2+}-binding sites.[9] The lower sections of M1 and M2 push against M4L, opening the lumenal gate and releasing the bound Ca^{2+} into the lumen.

(iv) The TGES-loop of the A-domain now fixes a particular water molecule and catalyses its attack on the aspartylphosphate. Glu183 plays a particularly important role here. The release of the phosphate and Mg^{2+} relaxes the P-domain. This in turn releases the M1 and M2 helices so that M4L closes the lumenal gate. The top amphipathic part of M1 (M1′) forms a part of a cytoplasmic access funnel leading to Glu309, the gating residue of the Ca^{2+} binding sites.

25.5. CONCLUSIONS

As described, the P- and N-domains change interfaces and thereby control the orientation of the A-domain, the actuator of transmembrane gates. ATP, phosphate, Mg^{2+} and Ca^{2+} are the modifiers of the interfaces. Energy barriers between the principal intermediate states appear to be comparable to the thermal energy, as the key events, e.g., the rotation of the A-domain, occur when ADP is released and when dephosphorylation takes place. In fact, in the crystal structures, we see devices integrated into Ca^{2+}-ATPase to decrease the chance of back reactions.[11] Presumably the use of large-scale domain rearrangements, rather than small changes in the residues co-ordinating Ca^{2+}, is the means

that Nature has found to convert inherently stochastic thermal motions into concerted sequential movements with the help of ATP and the other modifiers.

We now also understand, to some extent, why the structure of Ca^{2+}-ATPase has to be so. For instance, closed configurations of the cytoplasmic domains are necessary, because Ca^{2+}-ATPase changes domain interfaces to orient the A-domain for regulation of the gating mechanism. In the E2 state, the closed configuration appears to be important in two other aspects: (i) restriction of the delivery of ATP to the phosphorylation site; (ii) restriction of the thermal movements of transmembrane helices. As ATP can bind to the ATPase even in the E2 state and there is no mechanism for regulating the reaction cycle other than Ca^{2+} itself, the delivery of ATP γ-phosphate to the phosphorylation site has to be restricted physically in the E2 state. If the A-domain fluctuates too much by thermal energy, Ca^{2+} transferred into the lumen of SR may leak to the cytoplasm. Therefore, the A-domain has to be fixed by other cytoplasmic domains, unless Ca^{2+} itself directly fixes the transmembrane helices against thermal fluctuations. The link between the A-domain and the M1 helix has to be flexible, to provide tolerance to the gating machinery for thermal fluctuation. Perhaps the most important message from this study is that ion pumps are working in thermally fluctuating world, utilising thermal energy effectively for ion transport.

25.6. ACKNOWLEDGEMENTS

This work was supported in parts by Grant-in-Aid for Creative Scientific Research from the Ministry of Education, Culture, Sports, Science and Technology 14GS0308, and Technology, the Japan New Energy and Industry Technology Development Organization, and the Human Frontier Science Program. I thank my colleagues in Tokyo, Baltimore, Sarclay and Cape Town, and in particular, Hiromi Nomura who prepared nearly all the crystals and Yuji Sugita who gave us new insights by molecular dynamics simulation. I am greatly indebted to Giuseppe Inesi in many aspects of this work.

25.7. REFERENCES

1. S. Ebashi, and F. Lipman, Adenosine triphosphate-linked concentration of calcium ions in a particulate fraction of rabbit muscle, *J. Cell Biol.* **14**, 389–400 (1962).
2. J. V. Møller, B. Juul, and M. le Maire, Structural organization, ion transport, and energy transduction of P-type ATPases, *Biochim. Biophys. Acta* **1286**, 1–51 (1996).
3. L. de Meis, and A. L. Vianna, Energy interconversion by the Ca^{2+}-dependent ATPase of the sarcoplasmic reticulum, *Annu. Rev. Biochem.* **48**, 275–292 (1979).
4. A. M. Mata, and M. R.Sepúlveda, Caclium pumps in the central nervous system, *Brain Res. Rev.* **49**, 398–405 (2005).
5. S. R. Denmeade, and J. T. Isaacs, The SERCA pump as a therapeutic target: making a “smart bomb” for prostate cancer, *Cancer Biol. Ther.* **4**, 14–22 (2005).
6. U. Eckstein-Ludwig, R. J. Webb, I. D. A. van Goethem, J. M. East, A. G. Lee, M. Kimura, P. M. O’Neill, P. G. Bray, S. A. Ward, and S. Krishna, Artemisinins target the SERCA of *Plasmodium falciparum*, *Nature* **424**, 957–960 (2003).
7. D. H. MacLennan, and E. G. Kranias, Phospholamban: a crucial regulator of cardiac contractility, *Nature Rev. Mol. Cell Biol.* **4**, 566–567 (2003).
8. C. Toyoshima, M. Nakasako, H. Nomura, and H. Ogawa,. Crystal structure of the calcium pump of sarcoplasmic reticulum at 2.6 Å resolution, *Nature* **405**, 647–655 (2000).

9. C. Toyoshima, and H. Nomura, Structural changes in the calcium pump accompanying the dissociation of calcium, *Nature* **418**, 605–611 (2002).
10. C. Toyoshima, and T. Mizutani, Crystal structure of the calcium pump with a bound ATP analogue, *Nature* **430**, 529–535 (2004).
11. C. Toyoshima, H. Nomura, and T. Tsuda, Lumenal gating mechanism revealed in calcium pump crystal structures with phosphate analogues, *Nature* **432**, 361–368, 2004.
12. K. Obara, N. Miyashita, C. Xu, I. Toyoshima, Y. Sugita, G. Inesi, and C. Toyoshima, Structural role of countertransport revealed in Ca^{2+}-pump crystal structure in the absence of Ca^{2+}, *Proc. Natl. Acad. Sci. USA* **102**, 14489–14496 (2005).
13. Y. Sugita, N. Miyashita, M. Ikeguchi, A. Kidera, and C. Toyoshima, Protonation of the acidic residues in the transmembrane cation-binding sites of the Ca^{2+}-pump, *J. Am. Chem. Soc.* **127**, 6150–6151 (2005).
14. C. Toyoshima, and G. Inesi, Structural basis of ion pumping by Ca^{2+}-ATPase of the sarcoplasmic reticulum, *Annu. Rev. Biochem* **73**, 269–292 (2004).
15. W. Kühlbrandt, Biology, structure and mechanism of P-type ATPases, *Nat. Rev. Mol. Cell Biol*. **5**, 282–295 (2004).
16. J. D. Clausen, B. Vilsen, D. B. McIntosh, A. P. Einholm, and J. P. Andersen, Glutamate-183 is the conserved TGES motif of domain A of sarcoplasmic reticulum Ca^{2+}-ATPase assists in catalysis of E_2/E_2P partial reactions, *Proc. Natl. Acad. Sci. USA* **101**, 2776–2781 (2004).
17. H. Ma, D. Lewis, C. Xu, G. Inesi, and C. Toyoshima, Functional and structural roles of critical amino acids within the "N," "P" and "A" domains of the Ca^{2+} ATPase (SERCA) headpiece, *Biochemistry* **44**, 8090–8100 (2005).
18. L. Aravind, M. Y. Galperin, and E. V. Koonin, The catalytic domain of the P-type ATPase has the haloacid dehalogenase fold, *Trends Biochem. Sci.* **23**, 127–129 (1998).
19. L. N. Johnson, and R. J. Lewis, Structural basis for control by phosphorylation, *Chem. Rev.* **101**, 2209–2242 (2001).
20. J. D. Clausen, D. B. McIntosh, B. Vilsen, D. G. Woolley, and J. P. Andersen, Importance of conserved N-domain residues Thr^{441}, Glu^{442}, Lys^{515}, Arg^{560}, and Leu^{562} of sarcoplasmic reticulum Ca^{2+}-ATPase for MgATP binding and subsequent catalytic steps, *J. Biol. Chem.* **278**, 20245–20258 (2003).
21. T. L. Sørensen, J. V. Møller, and P. Nissen, Phosphoryl transfer and calcium ion occlusion in the calcium pump, *Science* **304**, 1672–1675 (2004).
22. C. Olesen, T. L. Sørensen, R. C. Nielsen, J. V. Møller, and P. Nissen, Dephosphorylation of the calcium pump coupled to counterion occlusion, *Science* **306**, 2251–2255 (2004).
23. G. Inesi, M. Kurzmack, C. Coan, and D. E. Lewis, Cooperative calcium binding and ATPase activation in sarcoplasmic reticulum vesicles, *J. Biol. Chem.* **255**, 3025–3031 (1980).
24. Z. Zhang, D. Lewis, C. Strock, G. Inesi, M. Nakasako, H. Nomura, and C. Toyoshima, Detailed characterization of the cooperative mechanism of Ca^{2+} binding and catalytic activation in the $Ca2^{+}$ transport (SERCA) ATPase, *Biochemistry* **39**, 8758–8767 (2000).
25. G. Inesi, H. Ma, D. Lewis, and C. Xu, Ca^{2+} Occlusion and gating function of Glu309 in the ADP-Fluoroaluminate analog of the Ca^{2+}-ATPase phosphoenzyme intermediate, *J. Biol. Chem.* **279**, 31629–31637 (2004).
26. S. Danko, T. Daiho, K. Yamasaki, M. Kamidochi, H. Suzuki, and C. Toyoshima, ADP-insensitive phosphoenzyme intermediate of sarcoplasmic reticulum Ca^{2+}-ATPase has a compact conformation resistant to proteinase K, V8 protease and trypsin, *FEBS Lett.* **489**, 277–282 (2001).
27. S. Danko, K. Yamasaki, T. Daiho, H. Suzuki, and C. Toyoshima, Organization of cytoplasmic domains of sarcoplasmic reticulum Ca^{2+}-ATPase in E1P and E1ATP states: a limited proteolysis study, *FEBS Lett.* **505**, 129–135 (2001).
28. M. Picard, C. Toyoshima, and P. Champeil, Effects of inhibitors on luminal opening of $Ca2^{+}$ binding sites in an E2P-like complex of sarcoplasmic reticulum Ca^{2+}-ATPase with Be^{2+}-fluoride, *J. Biol. Chem.* in press.

26

REGULATION OF CELL FUNCTIONS BY Ca^{2+} OSCILLATION

Masamitsu Iino

26.1. INTRODUCTION

Since the initial discovery of the regulatory role of intracellular Ca^{2+} signals in skeletal muscle contraction (Ebashi and Endo, 1968; Ebashi et al., 1969), the list of cellular functions that are regulated by Ca^{2+} signals has expanded. Now, it is recognized that intracellular Ca^{2+} signals are involved in the regulation of various cell functions including fertilization, secretion, transcription, immunity, learning and memory (Berridge et al., 2000). One of the striking features of Ca^{2+} signals is that they display complex spatiotemporal distributions such as Ca^{2+} waves and oscillations. An oscillatory change in Ca^{2+} concentration was first observed in skinned fiber experiments by Endo and collaborators in 1970 (Endo et al., 1970). When skinned skeletal muscle fibers were immersed in a solution mimicking intracellular conditions and caffeine was added to the solution at millimolar concentrations, the skinned fibers underwent periodic contractions because of the periodic release of Ca^{2+} from the sarcoplasmic reticulum, in the absence of membrane potential changes. With the advent of methods of measuring intracellular Ca^{2+} concentration, Ca^{2+} oscillation has been observed in many types of intact cell. In 1986, Cobbold and collaborators (Woods et al., 1986) observed Ca^{2+} oscillation in agonist-stimulated hepatocytes using aequorin, a Ca^{2+}-sensitive luminescent protein. The introduction of fluorescent Ca^{2+} indicators further facilitated the observation of intracellular Ca^{2+} transients (Tsien, 1988). Initially, the physiological significance of Ca^{2+} oscillation was not fully appreciated, because they were observed only in cell lines or in isolated cells. In 1994, we succeeded in imaging intracellular Ca^{2+} concentration in intact arterial walls using a fluorescent Ca^{2+} indicator and observed Ca^{2+} oscillation in sympathetic-nerve-stimulated vascular smooth muscle cells in the arterial wall (Iino et al., 1994). Today, Ca^{2+} oscillation is recognized as a physiological mode of Ca^{2+} signalling.

How and why does intracellular Ca^{2+} concentration oscillate? Although the mechanism underlying the induction of Ca^{2+} oscillation attracted many theoretical studies, the molecular and cellular mechanisms of such oscillation have remained elusive. Further-

Department of Pharmacology, Graduate School of Medicine, The University of Tokyo, Bunkyo-ku, Tokyo 113-0033, Japan

Regulatory Mechanisms of Striated Muscle Contraction
Edited by Ebashi and Ohtsuki, Springer, 2007

more, the physiological significance of Ca^{2+} oscillations is not yet well understood. In this review, I address these issues referring to our recent results.

26.2. HOW IS Ca^{2+} OSCILLATION GENERATED?

Inositol 1,4,5-trisphosphate (IP_3)-induced Ca^{2+} release is involved in Ca^{2+} oscillation in many cell types (Berridge, 1993). Interestingly, Ca^{2+} oscillations are observed in cells even at a constant level of agonist activation. Although a simple signalling cascade comprising receptor activation, phospholipase C-mediated IP_3 generation, and Ca^{2+} release from the endoplasmic reticulum (ER) via the IP_3 receptor (IP_3R) may induce a monophasic Ca^{2+} concentration increase, a more complex mechanism must underlie an oscillatory Ca^{2+} concentration increase. There have been a number of theoretical studies of the mechanism of Ca^{2+} oscillation, and these studies highlight the importance of Ca^{2+}-dependent and time-dependent factors for the generation of Ca^{2+} oscillation (for example Goldbeter et al., 1990). Among various Ca^{2+}- and time-dependent factors, the most important components of the previous models are the Ca^{2+}-induced Ca^{2+} release (CICR) mechanism from the intracellular Ca^{2+} store and the "delay line" mechanism in the replenishment of Ca^{2+} in the Ca^{2+} store. A qualitative explanation of why such a system generates Ca^{2+} oscillation is as follows: The CICR mechanism underlies the regenerative Ca^{2+} release from the Ca^{2+} store during the upstroke of each Ca^{2+} oscillation. The delay line mechanism is a transient movement of Ca^{2+} to an unreleasable compartment, and a slow return of Ca^{2+} from this compartment to the Ca^{2+} store. The time required to replenish the Ca^{2+} store determines the timing of the next Ca^{2+} oscillation. Although the models provide a theoretical framework of the mechanism underlying Ca^{2+} oscillation, the molecular mechanism underlying real Ca^{2+} oscillation remains to be identified.

26.2.1. Ca^{2+} Sensitivity of IP_3-induced Ca^{2+} Release

Working on skinned smooth muscle fibers, I found that IP_3-induced Ca^{2+} release rate is biphasically dependent on the cytoplasmic Ca^{2+} concentration ($[Ca^{2+}]_{cyt}$) with the maximum Ca^{2+} release rate observed at ~300 nM Ca^{2+} (Iino, 1990). That is, IP_3-induced Ca^{2+} release may be regeneratively activated at submicromolar Ca^{2+} concentrations. This mechanism, therefore, is a plausible candidate for the regenerative CICR mechanism underlying Ca^{2+} oscillation. To examine the role of the Ca^{2+} sensitivity of IP_3R in Ca^{2+} oscillation, we designed an experiment to test this hypothesis. We first identified glutamate at position 2100 (E2100) of type 1 IP_3R (IP_3R1) to be the key amino acid that determines Ca^{2+} sensitivity (Miyakawa et al., 2001). When this amino acid was substituted with aspartate (E2100D), the mutant IP_3R1 had an approximately tenfold decrease in Ca^{2+} sensitivity without any change in IP_3 sensitivity (Figure 26.1A,B). If the Ca^{2+} sensitivity of IP_3R is required for the induction of Ca^{2+} oscillation, then cells expressing the E2100D mutant IP_3R1 cannot induce Ca^{2+} oscillation. In IP_3R-deficient DT40 cells expressing E2100D mutant IP_3R1, agonist-evoked Ca^{2+} oscillation was strongly inhibited, whereas, in cells expressing wild-type IP_3R1, vigorous Ca^{2+} oscillation was induced (Figure 26.1C,D) (Miyakawa et al., 2001). This result clearly shows that the Ca^{2+} sensitivity of IP_3R is essential for the generation of Ca^{2+} oscillation.

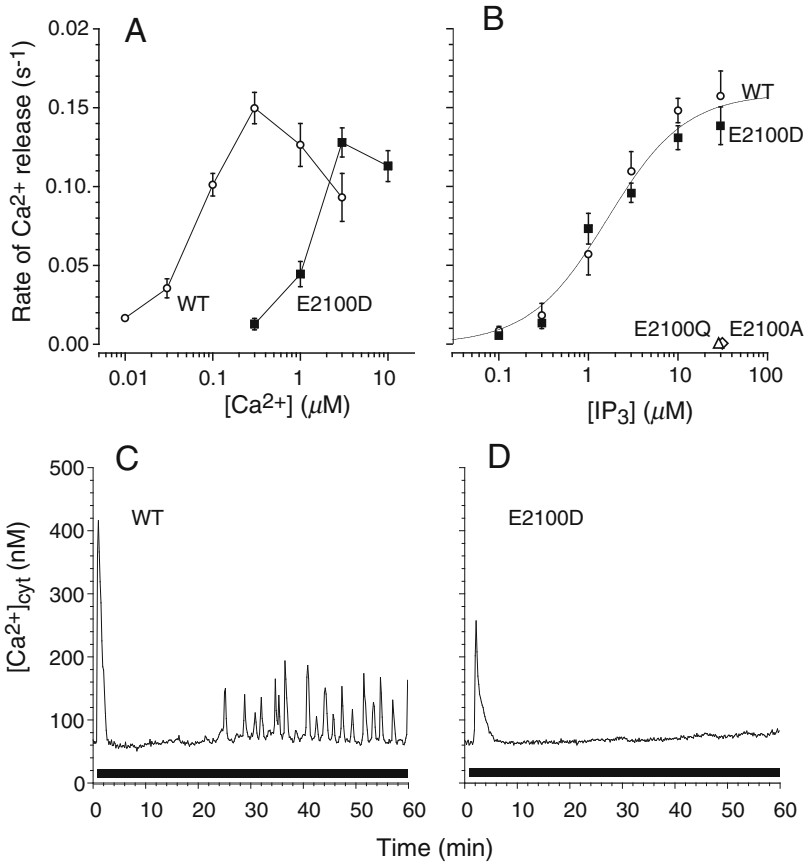

Figure 26.1. Functional importance of Ca^{2+} sensitivity of IP_3R in generation of Ca^{2+} oscillation. (A) Ca^{2+} concentration dependence of Ca^{2+} release via wild-type and E2100D IP_3R1s. The IP_3 concentration was 10 μM. (B) IP_3 concentration dependence of Ca^{2+} release via wild-type and E2100D IP_3R1s. Ca^{2+} release rate at 30 μM IP_3 is also plotted for the E2100A and E2100Q IP_3R1s. The Ca^{2+} concentrations were 0.3 μM for wild-type IP_3R1 and 3 μM for mutant IP_3R1. Mean ± SEM (n = 4–5). Ca^{2+} responses of single DT40 cells expressing wild-type (C), and E2100D (D) IP_3R1s. The anti-BCR antibody (1 μg/ml) was applied as indicated by the horizontal bars below the traces. Representative trace of more than 600 cells in each panel. From Miyakawa et al. (2001), with permission.

26.2.2. Pacemaking Mechanism of Ca^{2+} Oscillation

How is intermittent Ca^{2+} release induced during constant agonist activation? Previous models predict that Ca^{2+} has to be replenished to a certain level before each Ca^{2+} oscillation is initiated. We, therefore, measured luminal Ca^{2+} concentration in the ER ($[Ca^{2+}]_{er}$) using an ER-targeted GFP-based Ca^{2+} indicator (Ishii et al., 2006). $[Ca^{2+}]_{er}$ showed a change opposite to that of $[Ca^{2+}]_{cyt}$. However, there was an important phase difference between the time courses of Ca^{2+} concentrations in the two compartments. Although the initiation of Ca^{2+} release coincided with that of $[Ca^{2+}]_{cyt}$ increase, Ca^{2+} release from the ER continued even after $[Ca^{2+}]_{cyt}$ reached its peak. This implies that ER Ca^{2+} is transferred to either the extracellular space or another intracellular compartment without increasing

$[Ca^{2+}]_{cyt}$. Another important phase difference was observed in the second and subsequent Ca^{2+} oscillations, where $[Ca^{2+}]_{cyt}$ started to increase before $[Ca^{2+}]_{er}$ decreased. This indicates that Ca^{2+} is supplied from a non-ER compartment to generate a "pacemaker" $[Ca^{2+}]_{cyt}$ increase, which then activates the regenerative CICR mechanism from the ER. An intracellular organelle must play a role as the third non-ER Ca^{2+} compartment, because these results were obtained in the presence and absence of extracellular Ca^{2+}. What then is the third compartment?

26.2.3. Mitochondria as Third Player of Ca^{2+} Oscillation

Recent results suggest that mitochondria take up Ca^{2+} released from the ER (Jouaville et al., 1995; Babcock et al., 1997; Rizzuto et al., 1998). Therefore, it is possible that mitochondria are the third intracellular Ca^{2+} compartment. We, therefore, measured intramitochondrial Ca^{2+} concentration ($[Ca^{2+}]_{mt}$) during Ca^{2+} oscillation using a mitochondrion-targeted GFP-based Ca^{2+} indicator (Ishii et al., 2006). $[Ca^{2+}]_{mt}$ rapidly increased upon agonist stimulation and decreased gradually. However, there was also a phase difference between $[Ca^{2+}]_{cyt}$ and $[Ca^{2+}]_{mt}$. Although $[Ca^{2+}]_{mt}$ increased concomitantly with $[Ca^{2+}]_{cyt}$, it continued to increase after $[Ca^{2+}]_{cyt}$ reached its peak. This indicates that Ca^{2+} is supplied to mitochondria from another compartment, most likely the ER. Interestingly, there were sinusoidal changes corresponding to the second and subsequent Ca^{2+} oscillations concomitant with the gradual decrease. Furthermore, a phase difference in oscillatory change between $[Ca^{2+}]_{cyt}$ and $[Ca^{2+}]_{mt}$ was observed, and $[Ca^{2+}]_{mt}$ decreased (i.e., Ca^{2+} was released from mitochondria) before the initiation of Ca^{2+} oscillation. These results suggest that mitochondria supply "pacemaker" Ca^{2+} to initiate Ca^{2+} oscillation.

The important role of mitochondria in Ca^{2+} oscillation was further examined by inhibiting mitochondrial functions. When mitochondrial membrane potential, which drives Ca^{2+} uptake by mitochondria, was disrupted using oligomycin and FCCP, there was no uptake of Ca^{2+} into mitochondria upon the agonist-induced increase in $[Ca^{2+}]_{cyt}$, resulting in a continuous increase in $[Ca^{2+}]_{cyt}$ without Ca^{2+} oscillation. When the mitochondrial Na^+/Ca^{2+} exchanger, which mediates Ca^{2+} release from mitochondria, was inhibited by CGP-37157, Ca^{2+} was transferred to mitochondria during the first Ca^{2+} oscillation, but the release of Ca^{2+} from mitochondria was markedly suppressed and Ca^{2+} oscillation was inhibited.

Taken together, these results indicate that Ca^{2+} shuttles between the ER and mitochondria along with Ca^{2+} oscillation, and suggest that the following sequence of events drives Ca^{2+} oscillation (Figure 26.2) (Ishii et al., 2006). IP_3-induced Ca^{2+} release from the ER is essential for the initiation of the very first Ca^{2+} oscillation, during which mitochondria are loaded with Ca^{2+} released from the ER (Figure 26.2A). During the second and subsequent Ca^{2+} oscillations, Na^+/Ca^{2+} exchanger-mediated Ca^{2+} release from mitochondria supplies the pacemaker Ca^{2+} to generate the foot of each Ca^{2+} oscillation. When the foot reaches a threshold, it then activates IP_3R, causing regenerative Ca^{2+} release from the ER (Figure 26.2B).

26.3. PHYSIOLOGICAL ROLES OF Ca^{2+} OSCILLATION

Questions remain: Why does intracellular Ca^{2+} concentration oscillate? How do cells interpret Ca^{2+} oscillation to regulate their functions? What is the advantage for cells to use Ca^{2+} oscillation in regulating their functions? Ca^{2+}-dependent transcription factors respond to Ca^{2+} oscillation frequencies and direct frequency-dependent transcription

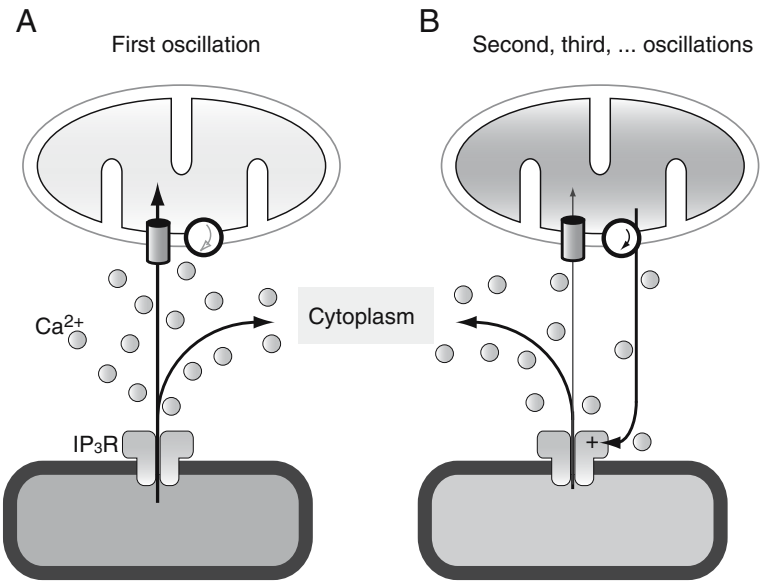

Figure 26.2. Schematic drawings of Ca^{2+} regulation by ER and mitochondria during Ca^{2+} oscillation. (A) The first Ca^{2+} oscillation is generated by Ca^{2+} release from the ER via IP_3R. A considerable amount of Ca^{2+} released from the ER is taken up by mitochondria. (B) The second and subsequent Ca^{2+} oscillations are initiated by Ca^{2+} release from mitochondria, which then triggers regenerative Ca^{2+} release from the ER. Mitochondrial Ca^{2+} is partially reloaded. The sequence is repeated until mitochondrial Ca^{2+} is depleted. In both (A) and (B), the regenerative CICR mechanism underlies the upstroke of each Ca^{2+} oscillation (not shown). From Ishii et al. (2006), with permission.

(Dolmetsch et al., 1998; Li et al., 1998). To examine how Ca^{2+} oscillation frequency is decoded by transcription factors, we studied the Ca^{2+}-dependent nuclear translocation of the nuclear factor of activated T cells (NFAT) in cells where Ca^{2+} concentration was clamped at various concentrations (Tomida et al., 2003).

We expressed GFP-tagged NFAT (NFAT-GFP) in baby hamster kidney (BHK) cells and obtained time-lapse images of NFAT-GFP during Ca^{2+} concentration clamp experiments. NFAT was present in the cytoplasmic region in the resting state, and was slowly translocated from the cytoplasm to the nucleus upon an increase in $[Ca^{2+}]_{cyt}$ (Figure 26.3A). NFAT is phosphorylated in the cytoplasm and is translocated to the nucleus upon dephosphorylation. We, therefore, measured the time course of the dephosphorylation after an increase in $[Ca^{2+}]_{cyt}$ making use of the electrophoretic mobility shift of NFAT upon dephosphorylation. Interestingly, the dephosphorylation of NFAT took place rapidly, within a few minutes, after the increase in Ca^{2+} concentration. Therefore, nuclear translocation, rather than dephosphorylation, is the rate-limiting step of the nuclear translocation of NFAT. On the other hand, the rephosphorylation of NFAT proceeded slowly after the decrease in $[Ca^{2+}]_{cyt}$. A slow rephosphorylation of NFAT implies that dephosphorylated NFAT functions as a working memory of Ca^{2+} signal for about 7 minutes.

We developed a model that describes the dephosphorylation and nuclear translocation of NFAT (Figure 26.3A,B). When the Ca^{2+} concentration increase interval is shorter than the memory time of NFAT, there is a buildup of dephosphorylated (i.e., nuclear-translocation-ready) NFAT. This facilitates nuclear translocation of NFAT (Figure 26.3B, high

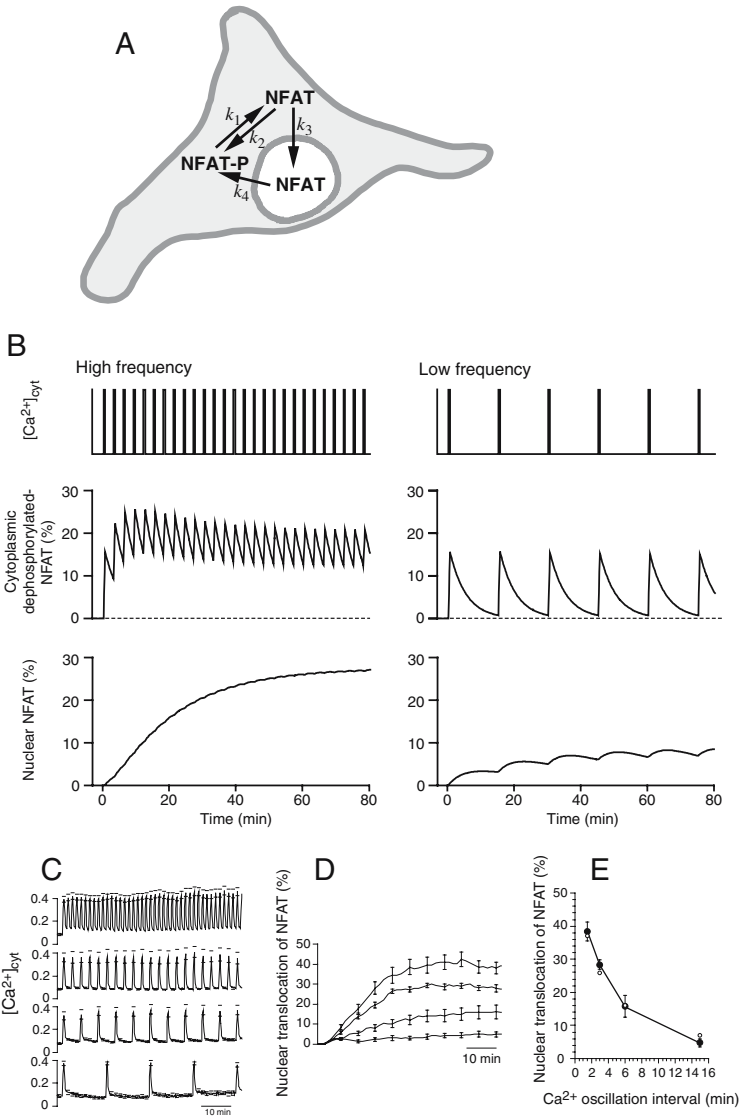

Figure 26.3. Ca^{2+} oscillation frequency dependence of NFAT nuclear translocation in a model and in cells. (A) Schematic illustration of a model of NFAT translocation. NFAT assumes one of three states: cytoplasmic/phosphorylated, cytoplasmic/dephosphorylated, and nucleus-transported. Rate constants are defined as indicated. Dephosphorylation rate constant (k_1) was assumed to be regulated by $[Ca^{2+}]_{cyt}$. (B) Model prediction of NFAT translocation during Ca^{2+} oscillation. High-frequency Ca^{2+} oscillation maintains dephosphorylated NFAT in the cytoplasm and induces significant nuclear translocation. Low-frequency oscillation results in intermittent dephosphorylation and induces only a partial nuclear translocation of NFAT. Model parameters used: k_1, 0.359 min^{-1} (during Ca^{2+} stimulation); k_2, 0.147 min^{-1}; k_3, 0.060 min^{-1}; and k_4, 0.035 min^{-1}. (C) $[Ca^{2+}]_{cyt}$ in GFP-NFAT expressing BHK cells challenged with Ca^{2+} pulses of 0.5-min duration at different intervals (1.5 to 15 min). (D) GFP-NFAT translocation during oscillatory Ca^{2+} stimulation. Increase in GFP fluorescence intensity of nuclear region normalized by that of entire cell region. (E) The extent of steady-state nuclear translocation of GFP-NFAT is plotted against Ca^{2+} oscillation interval. Filled circles, experimental results. Open circles, model predictions. Mean ± SEM (n = 5–10) for all the results. Error ranges are shown only at selected time points for clarity in C and D. From Tomida et al. (2003), with permission.

frequency). On the other hand, when the Ca^{2+} oscillation interval is longer than the memory time, there is no accumulation of nuclear, translocation-ready NFAT and only limited nuclear translocation of NFAT is expected (Figure 26.3B, low frequency).

We then examined the model-predicted frequency dependence of the nuclear translocation of NFAT in intact cells, and indeed found Ca^{2+} oscillation-frequency-dependent nuclear translocation (Figure 26.3C–E). Thus, Ca^{2+} oscillation frequency codes the extent of the nuclear translocation of NFAT, and the working memory mechanism allows the decoding of information encoded by this frequency.

Because the Ca^{2+} oscillation-dependent nuclear translocation of NFAT does not require a continuous increase in $[Ca^{2+}]_{cyt}$, it is a cost-effective means of regulating cell functions. We then analyzed the advantage of the Ca^{2+}-oscillation-mediated regulation of cell functions. The extent of steady-state nuclear translocation of NFAT per unit duration of Ca^{2+} concentration increase was greater with Ca^{2+} oscillation than with a continuous increase in Ca^{2+} concentration. This implies that the efficiency of Ca^{2+} signals is high when Ca^{2+} signals have oscillatory temporal patterns.

The decoding mechanism observed in NFAT may have general significance. Because there are several types of Ca^{2+}-dependent protein kinase, phosphorylated molecules may also function as a working memory in cellular functions. For example, the rate of phosphorylation of myosin light chains by myosin light chain kinase is greater than that of dephosphorylation by myosin light chain phosphatase (Mitsui et al., 1994). The difference becomes greater when myosin light chain phosphatase is inhibited by an agonist-dependent mechanism involving Rho kinase (Somlyo and Somlyo, 2003; Ito et al., 2004). In this scheme, phosphorylated myosin light chains may function as a working memory of Ca^{2+} signals and play a role in decoding Ca^{2+} oscillation.

26.4. CONCLUSIONS

How and why does intracellular Ca^{2+} concentration oscillate in various cell types? The results presented in this review provide important insights into this fundamental question. In many cell types, membrane-potential-independent Ca^{2+} oscillation is observed. In such cells, IP_3-induced Ca^{2+} release plays a key role in Ca^{2+} signalling and Ca^{2+} oscillation requires regenerative Ca^{2+} release from the ER via the Ca^{2+} dependence of IP_3R activity. Ca^{2+} shuttles between the ER and mitochondria at least in certain cell types, and this Ca^{2+} shuttling is important in pacemaking in Ca^{2+} oscillations. The Ca^{2+}-dependent dephosphorylated (or phosphorylated) states of certain molecules may function as a working memory of Ca^{2+} signals. This working memory may underlie decoding of information encoded by Ca^{2+} oscillation frequency. Furthermore, oscillatory changes in Ca^{2+} concentration improve cell signalling efficiency. These findings provide the basis for the understanding of the Ca^{2+}-dependent regulatory mechanism of cell functions.

26.5. REFERENCES

Babcock, D. F., Herrington, J., Goodwin, P. C., Park, Y. B., and Hille, B., 1997, Mitochondrial participation in the intracellular Ca^{2+} network, *J. Cell Biol.* **136**:833–844.

Berridge, M. J., 1993, Inositol trisphosphate and calcium signaling, *Nature* **361**:315–325.

Berridge, M. J., Lipp, P., and Bootman, M. D., 2000, The versatility and universality of calcium signalling, *Nat. Rev. Mol. Cell Biol.* **1**:11–21.

Dolmetsch, R. E., Xu, K., and Lewis, R. S., 1998, Calcium oscillations increase the efficiency and specificity of gene expression, *Nature* **392**:933–936.

Ebashi, S., and Endo, M., 1968, Calcium ion and muscle contraction, *Prog. Biophys. Mol. Biol.* **18**:123–183.

Ebashi, S., Endo, M., and Ohtsuki, I., 1969, Control of muscle contraction, *Q. Rev. Biophys.* **2**:351–384.

Endo, M., Tanaka, M., and Ogawa, Y., 1970, Calcium induced release of calcium from the sarcoplasmic reticulum of skinned skeletal muscle fibres, *Nature* **228**:34–36.

Goldbeter, A., Dupont, G., and Berridge, M. J., 1990, Minimal model for signal-induced Ca^{2+} oscillations and for their frequency encoding through protein phosphorylation, *Proc. Natl. Acad. Sci. USA* **87**:1461–1465.

Iino, M., 1990, Biphasic Ca^{2+} dependence of inositol 1,4,5-trisphosphate-induced Ca release in smooth muscle cells of the guinea pig taenia caeci, *J. Gen. Physiol.* **95**:1103–1122.

Iino, M., Kasai, H., and Yamazawa, T., 1994, Visualization of neural control of intracellular Ca^{2+} concentration in single vascular smooth muscle cells in situ, *EMBO J* **13**:5026–5031.

Ishii, K., Hirose, K., and Iino, M., 2006, Ca^{2+} shuttling between endoplasmic reticulum and mitochondria underlying Ca^{2+} oscillations, *EMBO Rep.* **7**:390–396.

Ito, M., Nakano, T., Erdodi, F., and Hartshorne, D. J., 2004, Myosin phosphatase: structure, regulation and function. *Mol. Cell. Biochem.* **259**:197–209.

Jouaville, L. S., Ichas, F., Holmuhamedov, E. L., Camacho, P., and Lechleiter, J. D., 1995, Synchronization of calcium waves by mitochondrial substrates in Xenopus laevis oocytes, *Nature* **377**:438–441.

Li, W., Llopis, J., Whitney, M., Zlokarnik, G., and Tsien, R. Y., 1998, Cell-permeant caged $InsP_3$ ester shows that Ca^{2+} spike frequency can optimize gene expression, *Nature* **392**:936–941.

Mitsui, T., Kitazawa, T., and Ikebe, M., 1994, Correlation between high temperature dependence of smooth muscle myosin light chain phosphatase activity and muscle relaxation rate, *J. Biol. Chem.* **269**:5842–5848.

Miyakawa, T., Mizushima, A., Hirose, K., Yamazawa, T., Bezprozvanny, I., Kurosaki, T., and Iino, M., 2001, Ca^{2+}-sensor region of IP_3 receptor controls intracellular Ca^{2+} signaling, *EMBO J.* **20**:1674–1680.

Rizzuto, R., Pinton, P., Carrington, W., Fay, F. S., Fogarty, K. E., Lifshitz, L. M., Tuft, R. A., and Pozzan, T. 1998, Close contacts with the endoplasmic reticulum as determinants of mitochondrial Ca^{2+} responses, *Science* **280**:1763–1766.

Somlyo, A. P., and Somlyo, A. V., 2003, Ca^{2+} sensitivity of smooth muscle and nonmuscle myosin II: modulated by G proteins, kinases, and myosin phosphatase, *Physiol. Rev.* **83**:1325–1358.

Tomida, T., Hirose, K., Takizawa, A., Shibasaki, F., and Iino, M., 2003, NFAT functions as a working memory of Ca^{2+} signals in decoding Ca^{2+} oscillation, *EMBO J.* **22**:3825–3832.

Tsien, R. Y., 1988, Fluorescence measurement and photochemical manipulation of cytosolic free calcium, *Trends Neurosci.* **11**:419–424.

Woods, N. M., Cuthbertson, K. S., and Cobbold, P. H., 1986, Repetitive transient rises in cytoplasmic free calcium in hormone-stimulated hepatocytes, *Nature* **319**:600–602.

VI

MOLECULAR MECHANISMS OF MUSCLE CONTRACTION

27

EVIDENCE ABOUT THE STRUCTURAL BEHAVIOUR OF MYOSIN CROSSBRIDGES DURING MUSCLE CONTRACTION

Hugh E. Huxley

It has been a great honor and a particular pleasure to participate in this meeting to celebrate the fortieth anniversary of the discovery of troponin by Professor Ebashi, whom I have been privileged to know for many years of my scientific life. I thought therefore it would be appropriate to described briefly what was happening in studies of another aspect of muscle contraction over somewhat the same time period.

27.1. INTRODUCTION

In this review, I will discuss the successive stages of the development of our understanding of how crossbridges between actin and myosin filaments develop the sliding force that powers muscle contraction and many other forms of cell motility. The experimental evidence at each stage has come from the development of new techniques of structural investigation, and particularly from the harnessing of enormous increases in the available brightness of X-ray beams for diffraction experiments. In recent years, remarkable advances in nanotechnology, and their use in characterizing single molecule interactions between actin and myosin have also played a very important role. A very high degree of consistency now exists between the different types of evidence for a lever arm tilting mechanism in the myosin head as the source of contractile force and movement.

27.2. EARLY X-RAY EVIDENCE ABOUT CROSSBRIDGES (1950–52)

The first indications of the existence of crossbridges came from low angle equatorial X-ray diffraction patterns from surviving frog muscles. These strongly suggested the presence of a double hexagonal array of filaments (Huxley 1951, 1952, 1953a). In relaxed muscles, a primary hexagonal array of filaments spaced about 440 angstroms apart was

Rosenstiel Center, Brandeis University, Waltham, MA 02454, USA

Regulatory Mechanisms of Striated Muscle Contraction
Edited by Ebashi and Ohtsuki, Springer, 2007

the dominant feature, and was assumed to represent the major structural protein, myosin. When the muscles went into rigor (a condition associated with the loss of ATP, which even at that time was believed to allow molecules of actin and myosin to combine together), a large change in the relative intensities of the two main equatorial reflections occurred. This indicated the presence of a secondary array of filaments, presumably actin, now located predominantly at the trigonal positions of the lattice, symmetrically placed within each group of three nearest neighbour myosin filaments. This suggested that the actin filaments were now held in position by crosslinks to the nearby myosin filaments. The center-to-center separation of the two types of filament was about 250 angstroms. There was evidence that the myosin filaments had a diameter of 100 to 150 angstroms (i.e., a radius of up to 75 angstroms), and that the actin filaments would be smaller (i.e., a radius of up to 50 angstroms); thus the surface-to-surface separation would be at least 125 angstroms. Thus the crosslinks would have to bridge this separation, though the distances involved were not explicitly discussed in this context at that time.

While the axial arrangement of actin and myosin filaments was not then understood, it was nevertheless recognized that even if only one type of filament was axially rigid, then crosslinks between the filaments could produce axial rigidity of the composite structure, a characteristic feature of rigor muscle.

It was also observed that relaxed muscles showed a clear pattern of low angle axial reflections which did not change in spacing when the muscle was stretched. This reinforced the picture of separate filaments of actin and myosin, and the idea that crosslinking these filaments could rigidify the structure; and it was also supposed that such crosslinks were involved in some way in force production during contraction (Huxley 1952). However, there was no evidence at that time as to how force development and shortening might occur, and the only speculative suggestion put forward was that it might involve actin depolymerization during actin-activated myosin ATPase activity, an idea rapidly discarded in two years time!

27.3. INITIAL ELECTRON MICROSCOPIC AND PHASE CONTRAST LIGHT MICROSCOPIC EVIDENCE (1952–53)

Early electron-micrographs of cross-sections of striated muscle showed the predicted double hexagonal filament arrays (Huxley 1953b), with larger diameter filaments at the hexagonal lattice points, and smaller diameter ones at the trigonal points. The appearance of crossbridges between the thin and thick filament could be seen in places, but not with sufficient clarity or consistency to be totally convincing to others. However, the fact that the two independent techniques – X-ray diffraction and electron microscopy – both showed strong evidence for the same basic structure was a big step forward, and provided a paradigm for work on many other structural problems. X-ray diffraction can provide evidence about a structure in its completely native, fully hydrated state, but the evidence needs interpretation before it can give a direct structural picture. Electron microscopy can give a direct visual image of a structure, but one which may contain artifacts from the preparative methods; in the case of thin sectioning used here, these methods involved chemical fixations, dehydration, embedding in plastic,sectioning, and staining with heavy metals. However, if the structure seen in the electron microscope would generate an X-ray pattern similar to the one actually seen, and if the observed X-ray pattern can be interpreted in terms of a structure closely similar to the EM images, then the combined evi-

dence is very powerful indeed. However, at the time many observers did not appreciate the strength of this argument, and remained skeptical for a number of years!

Our understanding of the overall nature of the muscle structure was greatly clarified by phase-contrast light microscopy (combined with electron microscopy), in studies of the effect of myosin extraction on the structure of striated myofibrils (Hanson and Huxley, 1953). These experiments showed, quite unambiguously, that the thick filaments contained the protein myosin and were present only in the A-bands and accounted for the high density and birefringence of those regions of the sarcomere. Actin filaments were attached to the Z-lines at the ends of each sarcomere, ran through the I-bands and into the A-bands, where they partially overlapped the myosin filaments, forming the double hexagonal array; they terminated at the edges of the H-zone (in muscles at rest length or stretched) giving rise to the lower density of that zone, which contains only myosin filaments.

This overlapping array of filaments model immediately provided a clear interpretation of the constancy of the periodicity of the axial reflections from live relaxed muscle when it was stretched: namely that stretching was accomplished by a relative sliding process between the arrays of actin and myosin filaments, in which the length of the filaments remained constant (Huxley, 1953b). It was also noted that a similar process, in reverse, might be involved in contraction. Such a mechanism would explain, in a very natural way, why muscles lacking ATP became rigid and inextensible, provided that both the myosin and the actin filaments were themselves inextensible. At that time, it was not known whether the axial reflections, which extended from over 400 angstroms down to 59 angstroms and 51 angstroms, and remained constant during passive stretch, came just from actin filaments or from the myosin filaments as well, but this did not affect the general argument (the latter was indeed the case [Worthington, 1959]).

27.4. FIRST DIRECT EVIDENCE FOR SLIDING FILAMENT MODEL, 1954–55

Subsequent phase contrast observations on isolated myofibrils contracting in ATP showed that both the length of the A-bands, and the distance between the Z-lines and the edges of the H-zone, remained constant during active shortening, within the limits of accuracy of the light microscope measurements (Huxley and Hanson, 1954). These limits were considerably less than the amount of sarcomere shortening, so it seemed certain that the shortening must be associated with active sliding of actin filaments past myosin, and that the lengths of both sets of filaments remained at least approximately constant. Experiments on intact muscle fibers showed that here too, the A-bands remained approximately constant in length (Huxley and Niedergerke, 1954), and were similarly interpreted in terms of the overlapping arrays of filament structure.

These results showed clearly that a sliding force must be generated between the actin and myosin filaments by the action of the crossbridges, since they provided the only physical connection between the filaments. But the observations did not provide any direct evidence as to what that action might be. Two specific possibilities were suggested in a review by Hanson and Huxley in 1954 (published 1955). In one, small decreases in actin periodicity were arranged to add together successively along a filament during each cycle of the process, so that a given myosin crossbridge would transfer from one actin monomer to the adjacent one – a distance of perhaps 50 to 100 angstroms. By combining

this with waves of attachment and detachment, an overall sliding movement might be produced. However, the fact that force and sliding can be produced at very small extents of filament overlap render such a mechanism very problematical, and much recent experimentation makes it totally implausible. The second possibility, however, was very close to the scheme now generally accepted. It supposed that force was produced by branches of the myosin filaments which operated in a cyclical fashion, attaching to actin, then shortening in such a way as to pull the actin along by 50 to 100 angstroms or so, then detaching from actin, re-extending, and attaching again to another actin site, further along the actin filament. But at that time, there was a little evidence about the nature of such branches or crosslinks or crossbridges, and no direct evidence whatsoever that they might change their structure during the actomyosin ATPase cycle. However, it was well recognized that a repetitive cyclical process must be taking place at the crossbridges, in order to account for the known energetics of contracting muscle (loc. cit.).

27.5. BETTER ELECTRON MICROSCOPE EVIDENCE (1955–57)

Initially, several superposed layers of the filament lattice were included in the thinnest longitudinal sections available (about 1000 angstroms or more in thickness), and details of the filament and crossbridge structures were not visible. However, improvements in sectioning and staining techniques made it possible, by 1957, to obtain sections only 100 to 150 angstroms in thickness and containing well ordered arrays of thick and thin filaments, with clearly defined crossbridges between them (Huxley, 1957b). These crossbridges occurred at axial intervals of 300 to 400 angstroms, and were part of the myosin filament structure, since they were still visible in places where an actin filament was absent. The diameter of these projections was about 50 angstroms. Their orientation was somewhat variable, but that could have been an artifact of sectioning or fixation. It was suggested that the projections consisted of the heavy meromyosin component of myosin identified by A.G. Szent-Gyorgyi (1953), which carried the actin binding and ATPase sites, and that the backbone consisted of the more helical light meromyosin component identified by him and shown to have solubility properties similar to the parent myosin.

In 1957, A.F. Huxley put forward a very important kinetic model of how an axially moving cycling crossbridge model (the second type mentioned above) might operate using thermal motion rectified by positional constraints of the enzyme cycle and of the attachment and detachment rate constants (Huxley, 1957a). The model was able to reproduce a number of characteristic physiological properties of striated muscle, and similar kinetic schemes could be applied to other models where force was generated by a structural change in the crossbridge after it had attached to actin, rather than from a pre-existing thermal motion-induced distortion.

27.6. EVIDENCE OF STRUCTURAL POLARITY IN ACTIN AND MYOSIN FILAMENTS (1960–63)

This came from negative stain electron microscopic studies of actin and myosin filaments prepared by controlled mechanical disruption of intact muscle, and by reconstitution from purified proteins (Huxley, 1963). It was shown that the myosin filaments were

bipolar structures. Each myosin molecule had globular, actin-binding regions, at one end only, the rest of the molecule being a linear, helical, tail region about 1500 angstroms in length, which assembled with the tail regions of other molecules to form the backbone of the myosin filament. The tails always pointed inwards towards the central M-region of the myosin filaments, so that the orientation of the molecules was 180° different in the two halves of each filament. Therefore, if a specific structural change could take place in a myosin head attached to actin such that the actin would be pulled towards the center of the sarcomere, then all the other myosin heads in that half-sarcomere would pull in that same direction. In the other half-sarcomere, the directions would all be reversed, and so the actin filaments in the two half sarcomeres would be drawn together towards the center of the A-band. Additionally, it was shown that the actin filaments were also structurally polarized (i.e., every actin monomer in an actin filament was oriented in the same direction). That direction was reversed on either side of the Z-lines, and so was reversed in each half of a sarcomere, so that the relative orientation of the interacting actin and myosin molecules was always the same, as would be required by the specific type of interaction envisaged as producing the structural change. Electron microscopy and X-ray studies on insect oscillatory flight-muscle by Reedy et al. (1965) showed that in rigor, the crossbridges were all attached to actin at an inclined angle, giving an "arrowhead" appearance similar to that seen in the HMM-decorated actin filaments used to establish actin polarity. In resting insect muscle, a more perpendicular orientation of the crossbridges was indicated, suggestive of a mechanism for the oscillation.

27.7. X-RAY DIFFRACTION EVIDENCE ABOUT OTHER IMPORTANT FEATURES OF THE CROSSBRIDGES-ACTIN INTERACTIONS (1965–70)

Major improvements in low-angle X-ray diffraction technology (using fine-focus rotating anode X-ray tubes and focusing mirrors and monochromators) led to a more specific picture of the structural change (Huxley and Brown, 1967; Huxley, 1969). The actin and myosin filaments in resting muscle both contain helically arranged molecules, but the helical parameters are different in each. In a rigor muscle, the myosin helical pattern disappears, but the actin reflections are intensified, showing that the myosin heads have been able to move sufficiently for a high proportion of them to attach to actin, in somewhat specific orientations. This indicates that the actin-binding part of myosin (by now identified by Mueller and Perry (1961, 1962) as myosin S1) is able to move radially and azimuthally from the myosin filament backbone, by swinging on its connecting link to the backbone, myosin subfragment 2 (myosin S1 and S2 together form the larger subfagment identified earlier by Szent-Gyorgyi and called "heavy meromyosin"). This would be possible if the S1-S2 junction, and the S2-LMM junction were both flexible, as indeed hydrodynamic data had indicated was the case.

Similarly, during contraction, myosin S1 heads were presumably able to search, within some limited range, for a suitably positioned actin site to interact with. This would also enable the muscle to accommodate itself to changes in the side spacing between actin and myosin filaments that occur as the sarcomere length changes. A tilting motion of the attached heads, or an equivalent change of shape, would then develop a sliding force between the filaments, as shown in Figure 27.1, providing that the S2 part of the myosin molecule, a 2-chain coiled-coil α-helical structure, was relatively inextensible axially, as

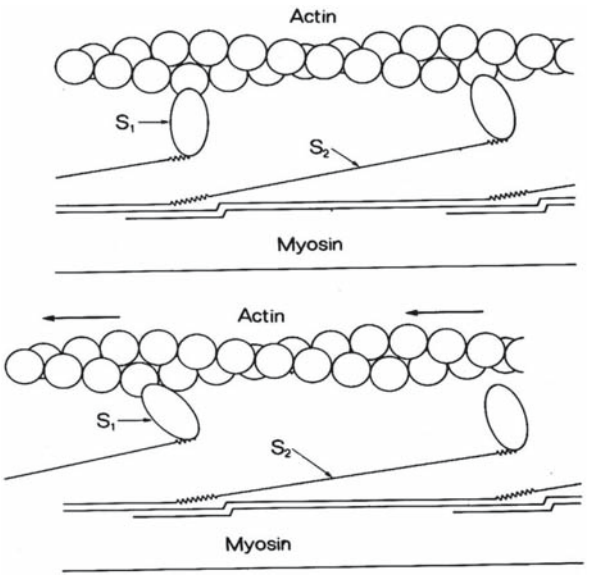

Figure 27.1. In this scheme, myosin S1 can hinge out sideways from the myosin filament backbone, since the junctions at either end of the S2 rod are flexible. This enables S1 to search for a suitably positioned actin monomer to which to attach. Then, an appropriate change in the angle of attachment to actin, or an equivalent change in the shape of S1, would displace the distal end of S1 in an axial direction, and transmit force and movement to the myosin backbone, producing relative sliding between the filaments.

such structures are normally believed to be. This scheme focused attention on the actin-myosin interaction as itself being the seat of the contractile force, rather than an active movement of the crossbridge relative to the backbone of the myosin filament, as in the crawling centipede model.

During contraction, the characteristic accentuation of actin reflections in rigor is not seen, showing that the attached myosin heads are fewer in number, and/or they are more dispersed in their angle of attachment to actin. Nevertheless, the characteristic myosin resting helical pattern virtually disappears (apart from the 14.5 and 7.25 nm meridional reflections (M3 and M6). Presumably, the regular helical arrangement is disrupted as all the heads are involved in the cycling process, even though only a proportion of them are attached to actin at any one time (and are constrained in a dispersion around their original axial positions).

This model appeared very plausible and satisfactory when it was first put forward (and indeed, it approximates very closely to what is now believed to be the case), but it still needed more direct experimental evidence to support it. What was needed was evidence of a major structural change in the myosin S1 head (or a change in orientation) during the attached phase of the actin-activated ATP splitting cycle. Unfortunately, such evidence proved very difficult to obtain for many years, although now it is abundant (see, for example, Geeves and Holmes, 2005).

The problem was that experimental techniques were not yet available for obtaining this type of information from muscle, nor was our knowledge of the myosin head structure adequate to understand what other experiments needed to be done.

27.8. THE BEGINNINGS OF THE MODERN ERA OF SYNCHROTRON RADIATION AND SINGLE MOLECULE STUDIES (1980–95)

X-ray diffraction studies of muscle contraction had been greatly hampered by inadequate X-ray intensity (even using the best rotating anode tubes and focusing cameras). Synchrotron radiation was shown to be a promising source in 1971 (Rosenbaum et al., 1971), but another 10 years passed before suitable X-ray beam-line facilities became available on electron-positron storage rings, very major facilities which had to be developed before this high intensity X-ray source could be put to use. It then became possible to record the X-ray pattern from a contracting muscle during the one millisecond time period when the structural changes associated with force development and shortening can be approximately synchronized in all the crossbridges, by applying a very rapid, very small length change to the muscle (the A.F. Huxley-Simmons maneuver, 1971). It was found that a large drop in the intensity of the 14.5 nm meridional reflection occurred, approximately synchronous with the length change (Huxley et al., 1981, 1983).

This showed that a large structural change took place in the crossbridges when the actin and myosin filaments slid past each other by up to 10–12 nm, in about 1 millisecond. The most straightforward explanation was that the myosin S1 heads were elongated structures, that they tilted over during their working stroke relative to the actin to which they were attached (or changed their shape in an equivalent way). Thus their axial-projected densities became more spread out, which weakened the axial reflection to which they give rise (i.e., the 14.5 nm meridional reflection). This would be exactly what was predicted by the 1969 model. However, it was also possible in principle that the crossbridges merely became disordered when the tension in the muscle decreased substantially. So while the result was consistent with the predictions of the model, it was not conclusive proof of correctness. More evidence about the nature of the system was necessary to overcome the skepticism which had developed during the ten year gap of the 1970s, when the expected evidence had not been forthcoming.

The next very important breakthrough came from a novel direction, when Spudich and his colleagues (Sheetz and Spudich, 1983; Spudich et al., 1985; Kron and Spudich, 1986; Toyashima et al., 1987) and Yanagida and his colleagues (Yanagida et al., 1984, 1985; Kishino and Yanagida, 1988) showed that single fluorescently-labelled actin filaments could be seen to slide unidirectionally, and to develop force, when allowed to interact, in the presence of ATP, with surfaces covered with myosin sub-fragment 1. That is, isolated crossbridges, supported by a surface (rather than a myosin backbone), and presumably present in sufficient numbers that many of them were appropriately oriented to interact with actin, were able to develop a relative sliding force, just as in a muscle. The clear, unambiguous demonstration of sliding was very important, as was the implied absence of any function for the myosin backbones, except as to provide support and orient the heads. Later experiments (Finer et al., 1994) opened the way for detailed studies of force and movement production by single molecules of myosin.

27.9. DETAILED EVIDENCE ABOUT THE STRUCTURAL CHANGES IN CROSSBRIDGES WHICH PRODUCE FORCE AND MOVEMENT (1990–2005)

The most important advance during the period was the publication by Rayment and his colleagues (1993a,b) of the high-resolution crystallographic structure of myosin S1,

and of the positioning of that molecule when attached to actin. The S1 structure was found to consist of two parts: 1) a more globular region, containing the actin binding site and the ATP binding pocket; and 2) an elongated region, formed by a long (9 nm) α-helical region of the myosin heavy chain, projecting out from the globular region, with the myosin light chains wound around it, presumably giving it mechanical stability. When the S1 was "docked" on an actin filament, this elongated region was directed away from actin and towards where the myosin filament backbone would be in a muscle. Thus the heavy chain could join up with the S2 domain of the myosin molecule and thence be attached to the myosin filament backbone, exactly as visualized in the earlier model. The new feature was the obvious possibility that the elongated region of S1 (the light-chain binding region), could function as a lever arm, to amplify smaller structural changes within the "catalytic" domain (which itself would remain relatively fixed on actin) by changing its angle of tilt so that its distal end could move axially by the required amount (a maximum of about 10 nm) (Figure 27.2). Subsequent crystallographic studies (Dominguez et al., 1998; Houdusse et al., 2000) have shown that such changes can in fact occur in the presence of nucleotide analogues mimicking different states of the ATPase cycle.

Thus the myosin head can indeed undergo the type of structural changes that were required of it by the swinging crossbridge model.

There is also now a great deal of evidence that this is indeed what happens in a muscle. Irving, Lombardi, and their colleagues (Irving et al., 1992; Lombardi et al., 1995; Dobbie et al., 1998), were able to obtain excellent X-ray diffraction data from single-muscle fibers, and were able to show that the behaviour of the M3 reflection, in a wide variety of length transient protocols, corresponded exactly with the predictions of the

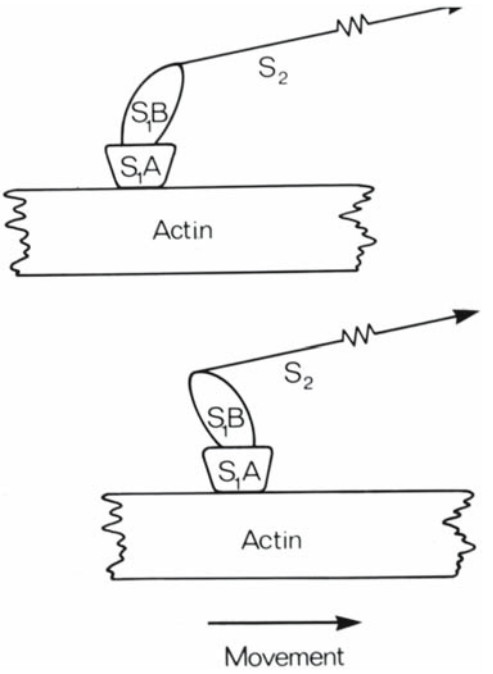

Figure 27.2. Diagrammatic representation of operation of tilting lever arm model. S1A is the catalytic domain of the myosin head (S1), S1B is the light chain binding domain (serving as the lever arm), as identified by Rayment et al. from X-ray crystallographic data (1993a,b). A tilting force developed between S1A and S1B would produce relative sliding movement of actin past myosin, and is strongly supported by X-ray interference data on contracting muscle.

tilting crossbridge model. Moreover, this group discovered that it is possible to make use of X-ray interference effects (which produce fine-structure within the axial profiles of the myosin meridional reflections) to measure, very accurately, small changes in the average axial position of the attached myosin heads, as well as the simultaneous changes in lever arm angle, during length transients. This has enabled them to characterize the tilting behaviour of the lever arms both at the T1 and T2 times during quick releases by various extents and also during steady shortening (Linari et al., 2000; Lombardi et al., 2000; Piazzesi et al., 2002; Reconditi et al., 2004). This evidence is in close accord with the predictions of the tilting lever arm model.

Additional significant details have been provided by analogous X-ray interference studies on whole muscle, where the much greater diffracted intensity facilitates data collection and extends it to higher order meridional reflections, which provide data not accessible from the M3 reflection along (Huxley et al., 2000, 2001, 2002, 2003a,b, 2004, 2005). These experiments enable one to determine the dispersion of lever arm angles about the mean angle, whereas the M3 data alone generally gives information about the mean angle only. In isometric contraction, the mean angle of the lever arms of the actin attached heads lies about 63° away from the rigor position as seen in electron-microscope studies (Holmes et al., 2003) but with considerable angular dispersion, which may be represented by either a uniform dispersion of ±20–25° (i.e., on either side of the mean) or possibly by a Gaussian dispersion of characteristic width of 17°. Following quick releases (which do not allow sufficient time for significant detachment), the mean angle changes towards the rigor position, which it reaches in releases of 10–12 nm, at time T2 (i.e., 1–2 ms after the release). Both sets of studies give results which are in full agreement with the predictions of the tilting lever arm model.

However, some of the detailed findings provide a slightly different picture of the length of the attachment phase of the crossbridge cycle than that which has usually been assumed to occur during muscle shortening. The quick-release experiments of A.F. Huxley and Simmons (1971) indicated that the full working stroke of a crossbridge was 10–12 nm, and similar values were given by the X-ray interference studies mentioned above. There was a tendency, therefore, to assume that, during steady shortening at rates when the muscle's efficiency is high, crossbridges would attach near the beginning of their full working stroke, and that most of them would stay attached until the end, usually presumed to be near the rigor orientation. This tendency may have been reinforced by the success of the A.F. Huxley (1957a) model in predicting correctly some of the energetics of contraction, since the attachment and detachment rate constants (which were chosen in part for mathematical convenience) did lead to an almost uniform distribution of crossbridges throughout the whole working stroke during slow shortening. It was also fostered in the present author's mind by the very low intensity of labeled actin reflection in contracting muscle, attributable to a very wide dispersion of lever arm angles, though it was also believed to be due in part to only a small proportion of myosin heads being attached at any one time.

But when the X-ray interference diagrams are recorded from muscles during slow, steady shortening, one finds that the dispersion of lever arm angles remains much the same as it is during isometric contraction, and that the mean angle has moved only a small way towards the rigor position. Clearly, one is seeing a dynamic equilibrium between attachment and detachment processes, in which the cumulative probability of a head being attached to actin at first increases, in the first part of the full working stroke,

and then, later in the stroke, is overtaken by the increasing probability of detachment. Presumably, Nature has not been able to arrange that such probabilities change as sharply with position as an ideal machine would prefer! The consequence of this is that the average distance over which a head remains attached at lower shortening velocities is somewhat less than half the whole working stroke over which a head can remain attached when it is translated very rapidly through the stroke by quick release. The energetics of this are not clear at present, but it seems possible that energy is released predominantly over a restricted part of the working stroke. It is also interesting to note that the length of the working stroke as determined in many single molecule experiments is also only of the order of 5 nm.

It still remains to be determined how the detailed atomic positioning within the myosin head enables the energy from ATP hydrolysis to be stored in the actomyosin structure and then released in the forceful movement of the lever arm, but there can be little doubt that the main outlines of the mechanism have now been agreed upon, and are in fact closely similar to those previously deduced from less comprehensive evidence. It is gratifying that this tilting model has also been found to provide a successful basis for understanding a great deal of intracellular motility too.

27.10. REFERENCES

Dobbie, I., Linari, M., Piazzesi, G., Reconditi, M., Koubassova, N., Ferenczi, M., Lombardi, V., and Irving, M., 1998, Elastic bending and active tilting of myosin leads during muscle contraction, *Nature* **396**: 383–387.

Dominguez, R., Freyzon, Y., Trybus, K. M., and Cohen, C., 1998, Crystal structure of vertebrate smooth muscle myosin motor domain: visualization of the pre-power stroke state, *Cell* **94**:559–571.

Finer, J. T., Simmons, R. M., and Spudich, J. A., 1994, Single myosin molecule mechanics: piconewton forces and nanometer steps, *Nature* **368**:113–119.

Geeves, M. A., and Holmes, K. C., 2005, The molecular mechanism of muscle contraction, *Adv. Protein. Chem.* **71**:161–193.

Hanson, J., and Huxley, H. E., 1953, The structural basis of the cross-striation in muscle, *Nature Lond.* **172**: 530–532.

Holmes, K. C., Angert, I., Kull, J., Jahn W., and Schroeder, R. R. 2003, Electron cryomicroscopy shows how strong binding of myosin to actin releases nucleotide. *Nature, Lond.* **425**:423–427.

Houdusse, A., Szent-Gyorgyi, A. G., and Cohen C., 2000, Three conformational states of scallop myosin S1, *Proc. Natl. Acad. Sci. USA* **97**:11238–11243.

Huxley, A. F., 1957a, Muscle structure and theories of contraction, *Prog. Biophys. and Biophys. Chem.* **7**:255–318.

Huxley, A. F., and Niedergerke, R., 1954, Structural changes in muscle during contraction. Interference microscopy of living muscle fibres, *Nature Lond.* **173**:971–973.

Huxley, A. F., and Simmons, R. M., 1971, Proposed mechanism of force generation in striated muscle, *Nature, Lond.* **233**:533–538.

Huxley, H. E., 1951, Low-angle X-ray diffraction studies on muscle, *Disc Faraday Soc.* **11**:148–149.

Huxley, H. E., 1952, Investigations in biological structures by X-ray methods. The structure of muscle: Ph.D. Thesis, University of Cambridge.

Huxley, H. E., 1953a, X-ray diffraction and the problem of muscle, *Proc. Roy. Soc. B.* **141**:59.

Huxley, H. E., 1953b, Electron-microscope studies of the organization of the filaments in striated muscle, *Biochem. Biophys. Acta* 12.

Huxley, H. E., 1957b, The double array of filaments in cross-striated muscle, *J. Biophys. Biochem. Ctyol.* **3**:631–648.

Huxley, H. E., 1963, Electron microscope studies on the structure of natural and synthetic protein filaments from striated muscle, *J. Mol. Biol.* **7**:281–308.

Huxley, H. E., 1969, The mechanism of muscle contraction, *Science* ***164***:1356–1366.
Huxley, H. E., and Brown, W., 1967, The low angle x-ray diagram of vertebrate striated muscle and its behaviour during contraction and rigor, *J. Mol. Biol.* **30**:383–434.
Huxley, H. E., and Hanson, J., 1954, Changes in the cross-striations of muscle during contraction and stretch and their structural interpretation, *Nature Lond.* **173**:**4412**:973–976.
Huxley, H. E., Simmons, R. M., Faruqi, A. R., Kress, M., Bordas, J., and Koch, M. H. J., 1981, Millisecond time-resolved changes in x-ray reflections from contracting muscle during rapid mechanical transients, recorded using synchrotron radiation, *Proc. Nat. Acad. Sci. USA* **78**:2297–2301.
Huxley, H. E., Simmons, R. M., Faruqi, A. R., Kress, M., Bordas, J., and Koch, M. H. J., 1983, Changes in the x-ray reflections from contracting muscle during rapid mechanical transients and their structural implications, *J. Mol. Biol.* **169**:469–506.
Huxley, H. E., Reconditi, M., Stewart, A., and Irving, T., 2000, Interference changes on the 14.5 nm reflection during rapid length changes, *Biophys. J.* **78**:134A.
Huxley, H. E., Reconditi, M., Stewart, A., and Irving, T., 2002, Crossbridge and backbone contributions to interference effects on meridional X-ray reflections, *Biophys. J.* **82**:5A.
Huxley, H. E., Reconditi, M., Stewart, A., and Irving, T., 2003b, What the higher order meridional reflections tell us, *Biophys. J.* **84**:139A.
Huxley, H. E., Reconditi, M., Stewart, A., Irving, T., Fischetti, R., 2001, Use of X-ray interferometry to study crossbridge behavior during rapid mechanical transients, *Biophys. J.* **80**:266A.
Huxley, H. E., Reconditi, M., Stewart, A., and Irving, T., 2003a, X-ray interference evidence concerning the range of crossbridge movement and backbone contributions to the meridional pattern, in: *Molecular and Cellular Aspects of Muscle Contraction*, H. Sugi, ed., Klewer/Plenum, New York, pp. 233–241.
Huxley, H. E., Reconditi, M., Stewart, A., and Irving, T., 2004, Implications of the predicted dispersion of lever arm angles in contraction, *Biophys J.* **86**:214A.
Huxley, H. E., Reconditi, M., Stewart, A., and Irving, T., 2005, Crossbridge configurations in frog sartorius muscle during steady shortening, *Biophys. J.* **88**:606A.
Irving, M., Lombardi, V., Piazzesi, G., and Ferenczi, M., 1992, Myosin head movements are synchronous with the elementary force-generating process in muscle, *Nature* **357**:156–158.
Kishino, A., and Yanagida, T., 1988, Force measurements by micromanipulation of a single actin filament by glass needles, *Nature* **334**:74–76.
Kron, S. J., and Spudich, J. A., 1986, Fluorescent actin filaments move on myosin fixed to a glass surface, *Proc. Natl. Acad. Sci. USA* **83**:6272–6276.
Linari, M., Piazzesi, G., Dobbie, I., Koubassova, N., Reconditi, M., Narayanan, T., Diat, O., Irving, M., and Lombardi, V., 2000, Interference fine structure and sarcomere length dependence of the axial X-ray pattern from active single muscle fibers, *Proc. Natl. Acad. Sci. USA* **97**:7226–7231.
Lombardi, V., Piazzesi, G., Ferenczi, M. A., Thirlwell, H., Dobbie, I., and Irving, M., 1995, Elastic distortion of myosin leads and repriming of the working stroke in muscle, *Nature* **357**:553–555.
Lombardi, V., Piazzesi, G., Linari, M., Vannicelli-Casoni, M. E., Lucii, L., Boesecke, P., Narayahan, T., and Irving, M. 2000, X-ray interference studies of the working stroke in single muscle fibres. *Biophys. J.* **78:** 134A.
Mueller, H., and Perry, S. V., 1961, The chromatography of the meromyosins on diethylaminoethylcellulose, *Biochem. J.* **80**:217–223.
Mueller, H., and Perry, S. V., 1962, The degradation of heavy meromyosin by trypsin, *Biochem. J.* **85**: 431–439.
Piazzesi, G., Reconditi, M., Linari, M., Lucii, L., Sun, Y-B., Nagayanan, T., Boesecke, P., Lombardi, V., and Irving, M., 2002, Mechanism of force generation by myosin heads in skeletal muscle, *Nature* **415**:659–662.
Rayment, I., Holden, H. M., Whittaker, M., Yohn, C. B., Lorenz, M., Holmes, K. C., and R.A, M., 1993b, Structure of the actin-myosin complex and its implications for muscle contraction, *Science* **261**:58–65.
Rayment, I., Rypniewski, W., Schmidt-Base, K., Smith, R., Tomchick, D., Benning, M., Winkelmann, D., Wesenberg, G., and Holden, H., 1993a, Three-dimensional structure of myosin subfragment-1: a molecular motor, *Science* **162**:50–58.
Reconditi, M., Linari, M., Lucii, L., Stewart, A., Sun, Y. B., Boesecke, P., Narayanan, T., Fischetti, R. F., Irving, T., Piazzesi, G., Irving, M., and Lombardi V., 2004, The myosin motor in muscle generates a smaller and slower working stroke at higher load, *Nature* **428**:**6982**:578–581.

Reedy, M. K., Holmes, K. C., and Tregear, R. T., 1965, Induced changes in orientation of the crossbridges of glycerinated insect flight muscle, *Nature* **207**:1276–1280.

Rosenbaum, G., Holmes, K. C., and Witz, J., 1971, Synchrotron radiation as a source for X-ray diffraction, *Nature* **230**:434–437.

Sheetz, M. P., and Spudich, J. A., 1983, Movement of myosin-coated fluorescent beads on actin cables in vitro, *Nature* **303**:31–35.

Spudich, J. A., Kron, S. J., and Sheetz, M. P., 1985, Movement of myosin-coated beads on oriented filaments reconstituted from purified actin, *Nature* **315**:584–586.

Szent-Gyorgyi, A. G., 1953, Meromyosins, the subunits of myosin, *Arch. Biochem. Biophys.* **42**:305–320.

Toyoshima, Y. Y., Kron, S. J., McNally, E. M., Niebling, K. R., Toyoshima, C., and Spudich, J. A. 1987, Myosin subfragment-l is sufficient to move actin filaments in vitro. *Nature Lond.* **328**:536–539.

Worthington, C. R., 1959, Large axial spacings in striated muscle, *J. Mol. Biol.* **1:** 398–401.

Yanagida, T., Arata, T., and Oosawa, F., 1985, Sliding distance of actin filament induced by a myosin cross-bridge during one ATP hydrolysis cycle, *Nature* **316**:366–369.

Yanagida, T., Nakase, M., Nishiyama, K., and Oosowa, F., 1984, Direct observation of motion of single F-actin filaments in the presence of myosin, *Nature* **307**:58–60.

28

STRUCTURAL ALTERATIONS OF THIN ACTIN FILAMENTS IN MUSCLE CONTRACTION BY SYNCHROTRON X-RAY FIBER DIFFRACTION

Katsuzo Wakabayashi, Yasunobu Sugimoto, Yasunori Takezawa, Yutaka Ueno*, Shiho Minakata[+], Kanji Oshima, Tatsuhito Matsuo, and Takakazu Kobayashi[#]

28.1. ABSTRACT

Strong evidence has been accumulated that the conformational changes of the thin actin filaments are occurring and playing an important role in the entire process of muscle contraction. The conformational changes and the mechanical properties of the thin actin filaments we have found by X-ray fiber diffraction on skeletal muscle contraction are explored. Recent studies on the conformational changes of regulatory proteins bound to actin filaments upon activation and in the force generation process are also described. Finally, the roles of structural alterations and dynamics of the actin filaments are discussed in conjunction with the regulation mechanism and the force generation mechanism.

28.2. INTRODUCTION

The thin actin filaments are the point of actin-myosin interaction and its regulation in vertebrate striated muscle. The X-ray diffraction patterns from isometrically contracting skeletal muscles reported that the active interaction of myosin and actin occurs in the incommensurate periodicities of thin and thick filaments.[1,2] In this framework, intensity changes of the "principal"* actin-based reflections occur with their magnitude varying

Division of Biophysical Engineering, Graduate School of Engineering Science, Osaka University, Toyonaka, Osaka 560–8531, Japan

* Neuroscience Research Institute, National Institute of Advanced Science and Technology, Tsukuba, Ibaraki 305–8568, Japan

[#] Department of Electronic Engineering, Shibaura Institute of Technology, Minato-ku, Tokyo 108–8531, Japan

[+] Present address, Harima Institute, The Institute of Physical and Chemical Research, Kouto, Sayo, Hyogo 679–5148, Japan

* The term "principal" is used here for the actin-based reflections at the positions that are observed in the X-ray diffraction pattern from resting muscle.

Regulatory Mechanisms of Striated Muscle Contraction
Edited by Ebashi and Ohtsuki, Springer, 2007

from the layer line to the layer line and keeping their radial positions at rest. Such intensity changes of these actin reflections seen in the thin filament X-ray pattern have been assumed to come from the thin actin structure activated by an asynchronous interaction of myosin heads as well as by regulation mechanisms. Distinct evidence has been accumulated that the actin filaments actively participate in force generation mechanism as well as in regulation mechanism.

In this article, we explore the conformational changes of regulatory proteins and actin in the thin filaments by X-ray fiber diffraction using synchrotron radiation, and discuss the roles of structural alterations of the thin actin filaments in the entire process of skeletal muscle contraction.

28.3. STRUCTURAL CHANGES OF THE THIN ACTIN FILAMENTS IN MUSCLE CONTRACTION

28.3.1. Intensity changes of troponin-associated reflections

Skeletal muscle contraction is regulated by Ca^{2+}-binding to and releasing from troponins bound on the thin filaments.[3] The intensity behaviors of the troponin-associated meridional reflections in the X-ray diffraction pattern from skeletal muscles during activation/contraction are first concerned.[4] Figure 28.1(a) shows a comparison of X-ray diffraction patterns between resting and contracting states of muscle at full filament overlap. Figure 28.1(b) shows that between resting and activation states of overstretched muscles.

Figure 28.2(a) shows the time courses of intensity changes of the first (Tn1) to the third order (Tn3) troponin meridional reflections with the basic repeat of 38.4 nm. In Fig. 28.2(b), the data are adjusted to a scale from 0 to 1 where the zero is defined as the

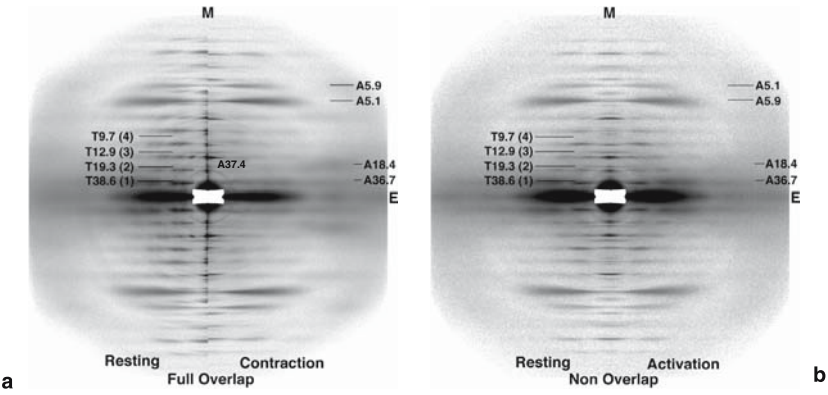

Figure 28.1. X-ray diffraction patterns from frog skeletal muscles. (a) A comparison between resting and contracting states of muscle at full filament overlap and (b) that of resting and activation states of overstretched muscle. The meridional axis (M) is coincided. The fiber axis is vertical. The letter T with numerical values denotes troponin-associated reflections with the basic period of 38.4 nm. The letter A with the numerical values denotes the actin-based reflections. E, the equatorial axis.

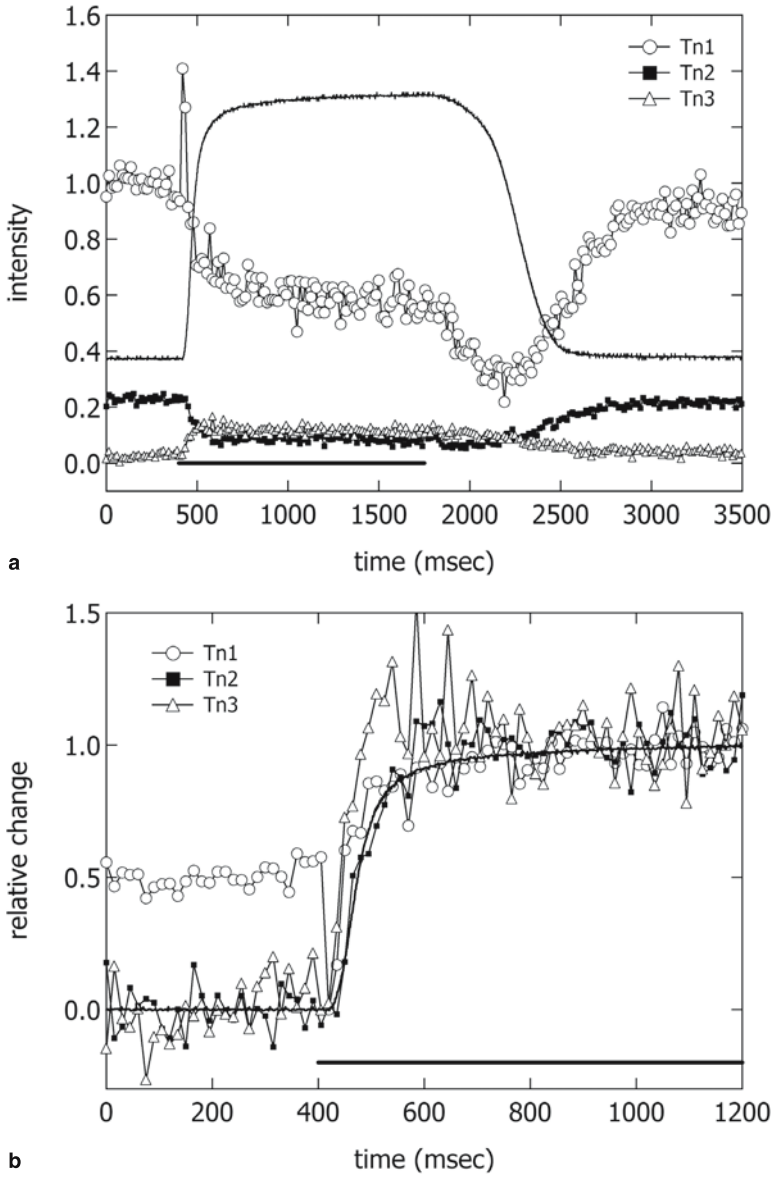

Figure 28.2. (a) Time courses of the intensity changes of troponin meridional reflections. (b) The intensity data are adjusted to a scale from 0 to 1 where the zero is defined as the intensity level at rest and 1 the average intensity level between 400 and 800 ms after stimulation. Tn1-Tn3 are the first order to the third order reflections. The horizontal bar denotes the period of electric pulse stimulation. The solid curve is the tension exerted by muscle.

intensity level at rest and 1 the average intensity level between 400 and 800 ms after stimulation. In the case of Tn1, the initial peak at the onset of stimulation is defined as 0. The intensity of the Tn1 increased promptly at the onset of stimulation before the development of tension, and then decreased to the level below the resting value as the tension developed (Fig. 28. 2(a)). The magnitude of the prompt intensity increase in the first phase was very close to that occurring in the activation of overstretched muscles, and its time course run parallel to that seen in overstretched muscles.[4] The intensity change of the Tn1 was consistent with the observations by Maeda et al.[5] and Yagi.[6] The reflection width along the equator started to widen with the development of tension. Thus the intensity decrease in the second phase is greatly affected by axial disordering between filaments due to the development of tension.[4,6] The intensity change of Tn2 occurred apparently without a substantial initial rise, the intensity decrease running parallel to the development of tension. Although the initial intensity change was not apparently seen, the intensity of Tn2 is also affected by the axial filament arrangement and subjected to disordering during contraction. The intensity of the Tn3 increased. This change run ahead the development of tension and overshot the average level at the initial phase of tension plateau. The lateral width of this reflection changed little during contraction. In overstretched muscles, very small increase in intensity of Tn2 and Tn3 was observed. In the relaxation phase, the Tn1 started to decrease in intensity without an appreciable change of the lateral width just upon the cease of stimulation and then the intensity and the lateral width gradually returned to the resting level with a delay behind the tension recovery.[4] The time-dependent intensity changes reveal that the structural alterations of troponin take place upon Ca^{2+}-binding and in the relaxation phase, and additional changes in the force generation process are much obscured by the filament disordering.

28.3.2. Low-resolution modeling of structural changes of troponins bound to thin filaments

Using the meridional intensities of the first four Tn reflections in the resting state and during activation of overstretched muscles (Fig. 28.3), the low-resolution modeling was made to show the molecular change of troponin bound to the thin actin filaments in the initial state. In overstretched muscles, the lateral widths of the Tn reflections changed little upon activation. Based on the image model in the electron micrographs,[7] the simple box function model consisting of the globular core domain composed of troponin I (TnI), troponin C (TnC) and the long tail domain of troponin T(TnT), was used (Fig. 28.4(a)). The models giving the lowest intensity R-factor were searched by changing those parameters describing the box functions, and the results are shown in Fig. 28.4(b). In the resting state, the core domain and the tail domain of Tn partially overlapped with each other. Upon activation, the density of the core domain becomes higher by a full overlap between two domains together with their own conformational changes, the tail domain passing through the core-domain region. These changes may be caused by the orientational changes of the bridge-like V-shaped core domain of Tn that is anchored by the TnT1 around and/or along the fiber axis, as seen in the structural alteration of free Tn molecules in crystal with and without bound Ca^{2+} (Fig. 28.4(c)).[8,9] Similar modeling for muscles at full filament overlap was hard to perform due to the perplexing changes of the lateral widths of reflections.

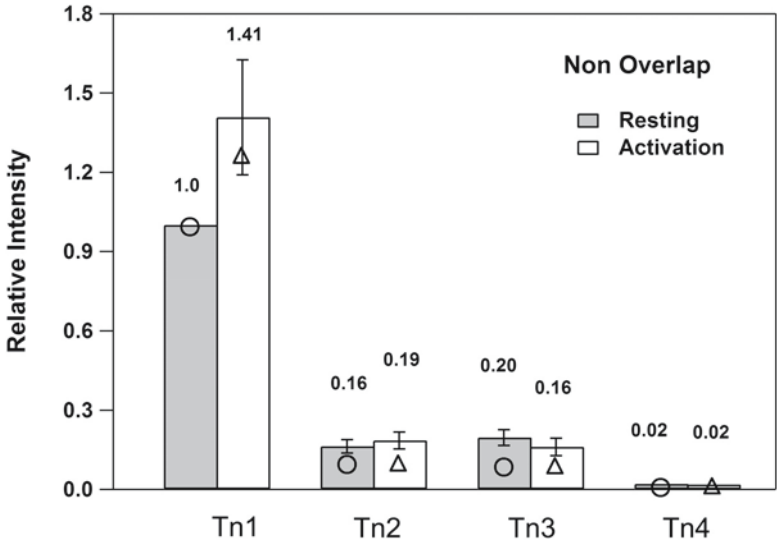

Figure 28.3. The intensity data of the first order (Tn1) to the fourth order (Tn4) troponin meridional reflections from overstretched muscles in the transition of muscle from the resting state to the activation state. The symbols on the bar graphs denote the calculated intensities from the models having the lowest R-factor in Fig. 28.4.

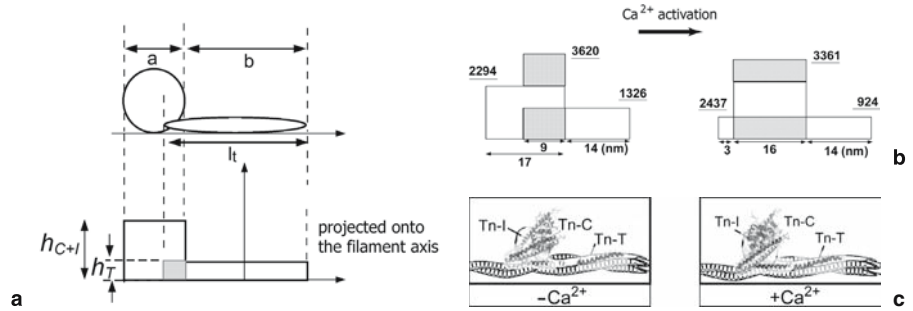

Figure 28.4. (a) The simplified model of troponin molecule on the tropomyosin strands from the electron microscopic image.[7] The box function used for the structure of troponin molecule projected onto the filament axis and the parameters used in the modeling; a, b and lt denote the effective lengths of the core domain, the part of the tail domain except for an overlap part and the tail domain along the fiber axis. h_{c+I} and h_T are the heights of the projected densities of core and tail domains, respectively and the areas are proportional to the respective molecular weights. (b) The box function models giving the lowest R-factor for the resting state (0.03) and the activation state (0.01) of overstretched muscles. The R-factor is defined as $\Sigma_i \mid I_{obs}(Z_i) - sI_{calc}(Z_i) \mid / \Sigma_i I_{obs}(Z_i)$ where s is a scale factor and Z_i is the axial coordinate of the ith order reflection. The numerical values are the relative weights of the respective parts. (c) The crystallographic structures (PDB codes; 1YV0 and 1YTZ) of the core domain of Tn[8] are superimposed on the Flicker et al.'s model.[7]

28.3.3. Enhancement of the fourfold rotational symmetry of thin actin filaments

The thin actin-based first layer-line components were separated from the nearby reflections in the high-angular resolution X-ray diffraction patterns and their intensities in several radial regions were precisely measured. Figure 28.5 shows the intensity changes in some regions during an isometric contraction of muscle at full filament overlap (a) and those upon activation of overstretched muscles (b).[2,10] The principal actin first layer-line component (1st L.L) (contributed by the J_2 Bessel function) denoted by an arrow decreased its intensity during an isometric contraction, much greater than that occurring upon activation of overstretched muscles. This result confirmed our earlier measurement[11] but incompatible with the result of Yagi.[12] While the intensity of the second actin layer line (2nd L.L) (contributed by the J_4 Bessel function) concomitantly increased during contraction and the relative magnitude of its intensity increase was greater by about three-fold than that upon activation of overstretched muscles.[2,10] Thus the full intensity changes of

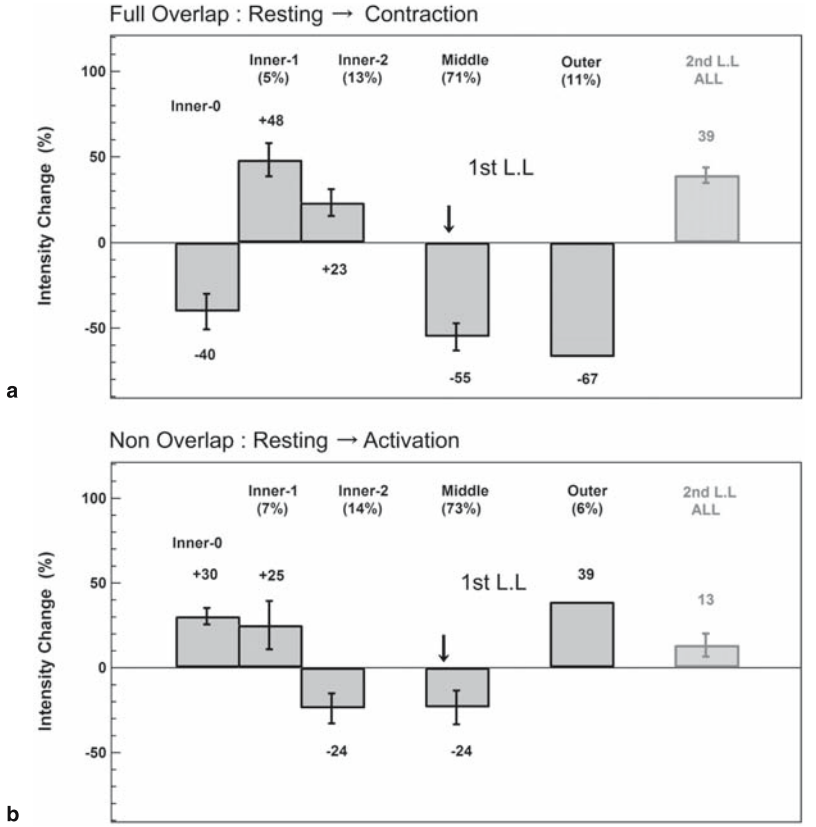

Figure 28.5. The integrated intensities of the first (1st LL) and the second (2nd LL) actin-based layer lines during a contraction of muscles at full filament overlap (a) and upon activation of overstretched muscles (b). The arrow indicates the principal part of the first actin layer line.

these first and second actin-based layer lines require the actin and myosin interaction. Such reciprocal intensity changes of these two principal low-angle layer lines indicate that the four-fold rotational symmetry of the thin actin filament is more enhanced in the force generating process than in the initial activation.

In order to interpret the intensity changes of the principal actin-based X-ray diffraction pattern during contraction, we have performed the modeling studies using the atomic structures of actin and regulatory proteins to show the structural changes occurring in the thin actin filaments. Firstly, the model consisting of the F-actin and TM without Tn was constructed.[13,14] In the simulation, each of four conventional subdomains of the actin monomer was moved as a rigid body and the model giving a better fit between the calculated and observed intensities was searched. At the same time, TM molecules were also moved around the periphery of actin filaments. In this modeling, the mass of Tn is averaged over the actin helical structure. As mentioned previously,[13,14] the relaxing model was consistent with the Holmes et al.'s model[15]; TMs sit in a cleft between subdomains 1 and 3 of actin at the radial position of about 3.6 nm from the filament axis. Modeling during contraction revealed that conformational changes were made by small movements of subdomains and the positional changes of TM around the actin filament. The largest movement within an actin monomer occurred in the subdomain 2; moving in the opposite direction of this figure. The subdomains 3 and 4 changed little, possibly contributing to maintenance of the helical structure. In the modeling without Tn, TM strands were forced to shift toward the subdomains 3 and 4 by about 8° azimuthally with the radial distance remaining mostly unchanged. As seen in the cross-sectional view (Fig. 28.6),[13,14] these changes during contraction were indeed caused by the enhancement of the four-fold rotational symmetry of the thin actin filaments.

As mentioned above, the atomic structure of most of the Tn core domain region was recently determined by X-ray crystallography.[8,9] We have further attempted to incorporate Tn components in the above actin-tropomyosin model. We extended the intensity measurements of X-ray diffraction pattern to the medium-angle region containing the second actin meridional reflection with an axial spacing of 1.35 nm. X-ray data fitting is now in progress to aim at elucidating detailed models of the regulated actin filaments. In the modeling, each of four subdomains of actin monomer was further divided into four subgroups and the better-fit models were searched by moving all subgroups together with

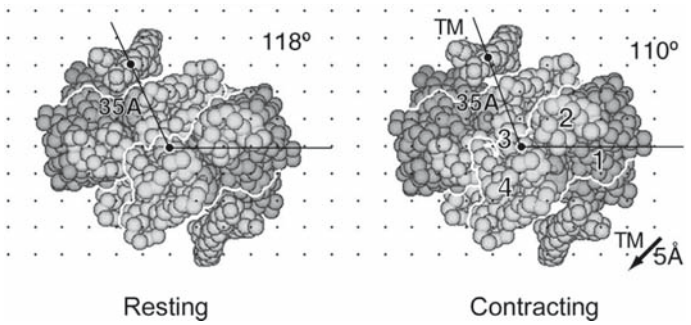

Figure 28.6. The cross-sectional view of the modeling of the thin actin filament using the atomic data of actin and tropomyosin.[13,14] Troponin molecules are omitted in this modeling. The numbers of 1–4 denote four subdomains within an actin monomer in the filament. TM is tropomyosin. A mesh interval, 1 nm.

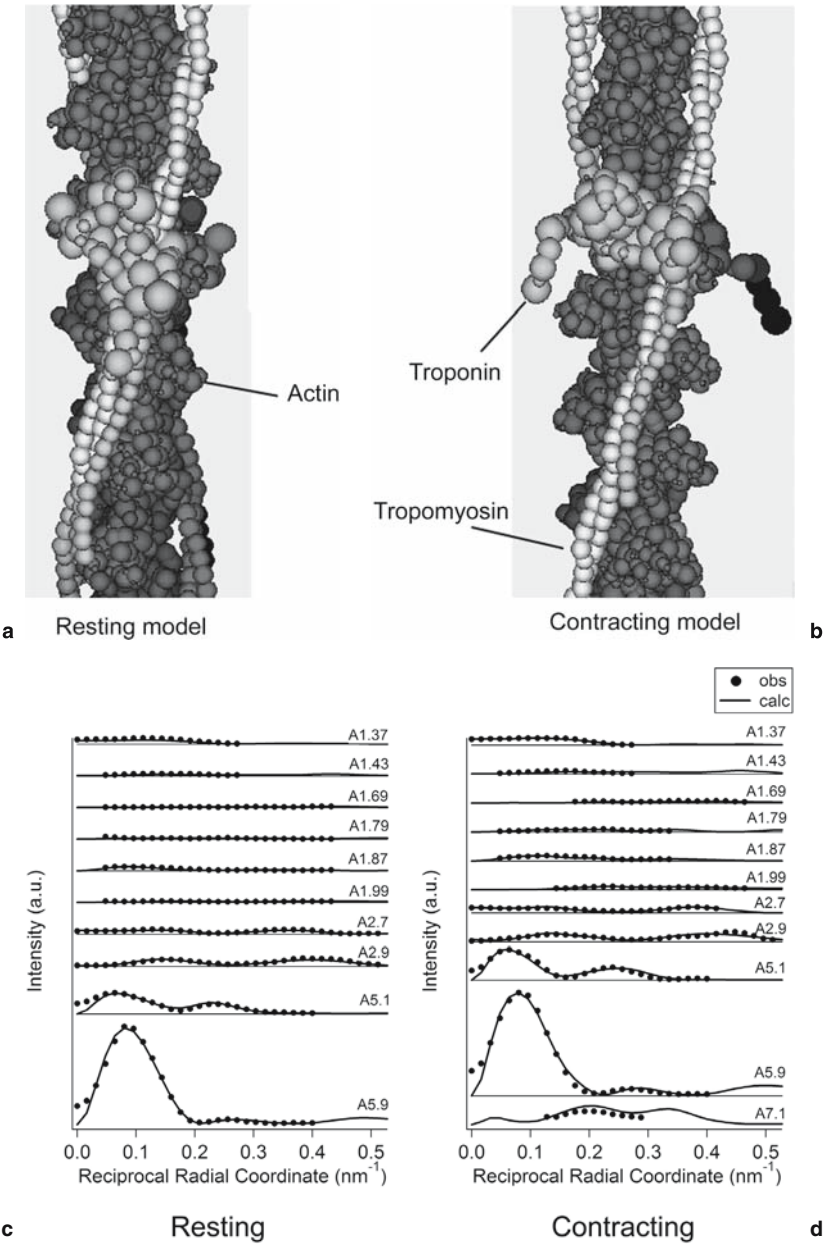

Figure 28.7. Preliminary models of the thin actin filament both with troponin and tropomyosin which explain the observed actin-based layer-line intensities from muscles at full filament overlap. (a) A resting model and (b) a contracting model. A comparison between the calculated and observed layer-line intensities, (c) at rest and (d) during contraction.

the regulatory proteins. The crystallographic shape of the Tn molecule by tentative additions of the missing chains and the TnT1 portion was constructed and was approximated by space-filling of the spheres of 1.5-nm radius. At present we found better models for dispositioning of the Tn core domain region both in the resting and contracting states of muscles at full filament overlap that explain the observed layer-line intensity data. Preliminary models are depicted in Fig. 28.7 (a) and (b). The long axis of a Tn core domain orients nearly parallel to the TM strands in the resting state and becomes crossing the TM strands in the force generation state possibly by the rotation of the core domain toward the actin filament. The disposition of the long TnT1 part, which was moved together with the TM strands in the present modeling, is a bit arbitrary. The calculated and observed layer-line intensities are compared in Fig 28.7 (c) and (d). The movements of TM and TnT in the entire process of contraction should be waited until the structural contribution of the whole Tn molecule is determined.

28.3.4. Elastic properties of the actin filaments

We suggested that the extensibility of the actin filaments accompanied by the twisting changes of the helical filaments.[16,17] In order to obtain firm evidence on this point, we have extensively investigated the spacing changes of the low-angle actin-based layer lines.[18] The fractional spacing change ($\Delta P_{36}/P_{36}$) of the first actin layer line due to the pitch (P_{36}) of the two long-pitch right-handed helical strands is related to those of the pitches of the right- and left-hand genetic helices,

$$\Delta P_{36}/P_{36} = \Delta P_{5.1}/P_{5.1} + 6.2 \times (\Delta P_{5.1}/P_{5.1} - \Delta P_{5.9}/P_{5.9}) \quad (1)$$

where $\Delta P_{5.1}/P_{5.1}$ and $\Delta P_{5.9}/P_{5.9}$ denote the fractional spacing changes of the right- and left-handed genetic helices, respectively. The fractional spacing change of the first layer line is expected to be much larger if the small difference between the fractional spacing changes of the 5.1-nm and 5.9-nm layer-line reflections is positive. We have analyzed the low-angle parts of high-angular resolution X-ray diffraction patterns in the experiments of the rest → contraction → stretch protocol. The spacing change of the first actin layer line was measured in the component denoted by an arrow with A37.4 in Fig. 28.1 (a) which locates in the radial range of $0.039 < R < 0.062\,nm^{-1}$. The result of the fractional spacing changes of this layer-line component obtained by deconvolution of the axial profiles with the overlapping Gaussian functions is shown in Fig. 28.8. We observed a large spacing change (*ca*. 0.9%) of the first layer line during contraction of muscles at full overlap (the shaded bar graphs in Fig. 28.8(a)). The white bar graphs show the values calculated from the spacing changes of the two other reflections. The results upon activation of overstretched muscles are shown in Fig. 28.8(b) where the large change (*ca*. −0.38%) of this layer-line spacing was also observed in the opposite direction.[19] We found that the fractional spacing change of the right-handed genetic helix was always greater than that of the left-handed genetic helix in the absolute value; the magnitude of the fractional spacing changes of three representative actin-based reflections was in the following order both upon activation and in the force generation,

$$|\Delta P_{5.1}/P_{5.1}| > |\Delta h/h| > |\Delta P_{5.9}/P_{5.9}| \quad (2)$$

where $\Delta h/h$ is the fractional spacing change of the axial rise of the subunits (*i.e*., that of the 2.7-nm reflection).[20,21] The differential spacing changes of these three reflections were

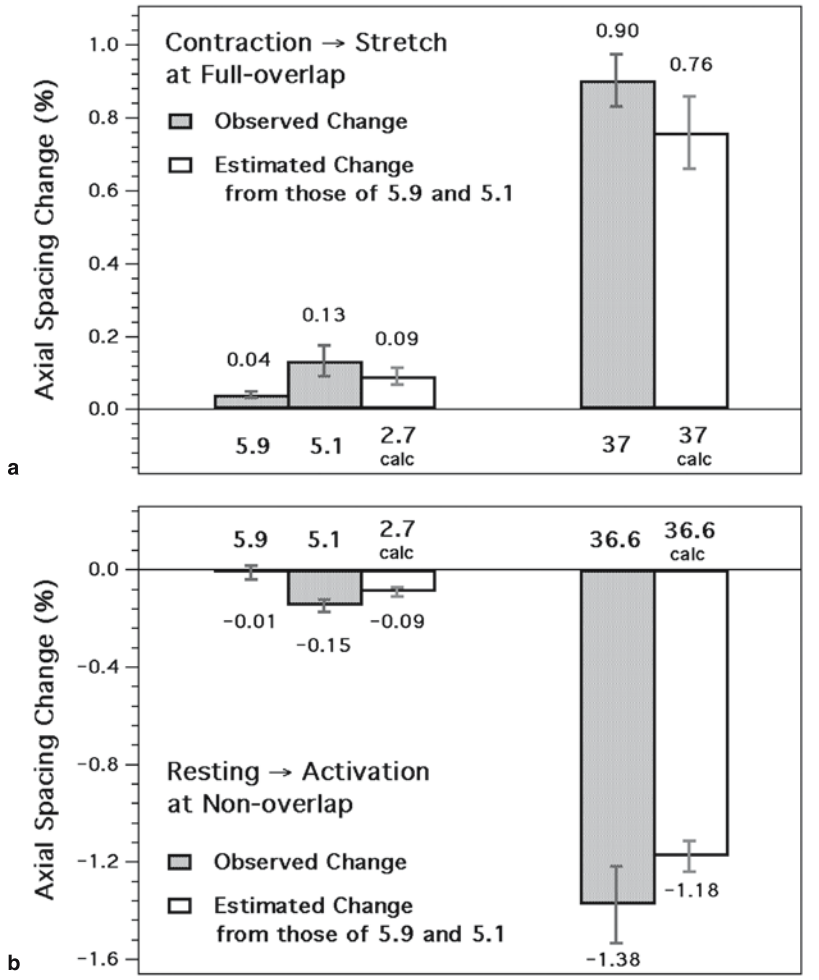

Figure 28.8. Axial spacing changes of the first actin-based layer-line component (denoted by 37). (a) The fractional spacing changes in the transition of muscle from the contracting state (P_0) to the stretched state (~$1.3P_0$) of contracting muscles at full filament overlap and (b) those in the transition of muscle from the resting state to the activation state of overstretched muscles. The white bar graphs denote the fractional spacing changes calculated from those of the 5.1-nm and 5.9-nm genetic reflections. 2.7 denotes the 2.7-nm actin meridional reflection. In (a) the spacing changes are scaled up to a 100% tension increase.

genuine, confirming that the extensibility of the actin filament accompanied by the twisting change of its helical structure. For instance, the change of the unit twist (an azimuthal increment per subunit in the filament) of the right-handed genetic helix is estimated by the equation,

$$\Delta\psi_{5.1} = (2\pi h/P_{5.1})\ (\Delta h/h - \Delta P_{5.1}/P_{5.1}) \tag{3}$$

Shortening of about 0.1% accompanies by a positive change in $\phi_{5.1}$ of about 0.19° in the transition of muscle from the rest to the initial activation, that is, the right-handed helices twist. In the subsequent transition of muscle to the force generation, the net twist of the

actin helical structure amounts to −0.23° (=−0.04°−0.19°), thus the right-handed helices untwist. It is worthwhile mentioning that the axial periodicity of Tn molecules bound to the thin filaments changed in accordance with the actin periodicity both upon activation and in generation of force.[20] Thus, Ca^{2+}-binding to Tn triggers the shortening and twisting changes of the actin filaments. In summary, the actin filaments shorten upon activation by about 1 nm with a twisting of their right-handed helices corresponding to the anti-clockwise rotation of about 60° at their pointed end. As the tension develops, they elongate by about 4 nm with an untwisting of their right-handed helices corresponding to about 90° clockwise rotation at the pointed end. In both activation and force generating processes, the actin subunit moves nearly along the left-handed genetic helical track in the radial projection of the actin helical structure.[17] The result of extensibility shows that the compliance of the thin actin filaments amounts to about 60% of the total compliance of a sarcomere during contraction.

From the twisting changes, the changes of the helical symmetry of the actin filaments can be estimated. In the resting state, the actin filament has an 80 subunits/37 turns symmetry and upon activation, the actin helical symmetry shifts toward the 13 subunits/6 turns symmetry (an 106/49 symmetry), representing a switch-on configuration of the thin actin filaments by Ca^{2+}-binding. This symmetry change upon activation differs in the direction from that derived eariler by Gillis and O'Brien[22] with the optical diffraction of the electron micrographs of the reconstituted thin filaments by addition of Ca^{2+}. As the tension develops, it turns toward the 28 subunits/13 turns symmetry (a 54/25 symmetry), and this symmetry presumably yields an appropriate geometry for active interaction between actin and myosin crossbridges. The twisting changes may alter the exposure of hydrophobic and hydrophilic sites on the actin filaments. Alteration of the extensibility accompanying by twisting changes of the actin filaments relates closely to a force generation mechanism and regulation mechanism as well.

28.3.5. Time courses of the structural changes of the thin actin filaments

The time courses of the intensity changes in the actin-based second and the 5.9 nm layer lines are as fast as that of the troponin-associated reflection (Tn1), much preceding the development of tension.[2,23,24] Structural alteration of troponin occurring in response to Ca^{2+}-binding is essential in the activation of the thin filament and simultaneously induces the changes in actin-tropomyosin structure. Also, actin attachment of the certain number of myosin heads that move much earlier induces the structural changes of actin filaments, the resulting intensity changes running ahead the tension production. The time course of the change of the actin axial repeat (the 2.7-nm meridional reflection) by Huxley et al.[25] revealed that a small initial decrease in spacing occurred very early in contraction and then in parallel to the develpoment of tension. Bordas et al.[26] showed that the axial spacings of the 2.7-nm, 5.1-nm and 5.9-nm reflections rapidly decreased to the levels lower than zero in response to the rapid length changes imposed on a contracting muscle. These observations were such as expected from our stationary data. There were also the differential spacing changes among these three reflections in rapid length change measurements, which satisfied the equation (2). Subsequently these spacings increased closely in parallel to the redevelopment of tension.[25,26] In contrast, the intensity changes of these reflections run ahead the redevelopment of tension.[25,26] Thus, the myosin-actin interaction is a two-step reaction requiring a non-force generating state before force production.

28.3.6. Cooperative property of actin monomers in the thin filaments

The force in muscle is transmitted to the ends of the contractile unit through thin actin filaments. Given that the contractile force is generated in the overlap region between the actin and myosin filaments in the sarcomere, there would be the non-uniform distribution of the tension in the sarcomere in the low compliant myofilament model.[27] Both tension and strain at the free ends of both filaments are zero, whereas the full tension and strain appear at their ends of connection at the Z and M lines. This non-uniform tension distribution should generate the non-uniformity in the periodicity of actin filaments, producing axial asymmetry of the meridional reflection profiles to some extent. A one-dimensional model of the actin subunit array in the filament was constructed, and the axial profiles of the meridional reflections under the assumption of the non-uniform distribution for the subunit spacings were simulated.[28] The calculated profiles were convoluted with the beam profile that was experimentally measured and derived as the function of the extent of extensibility. The simulation indicated that if there was the non-uniform distance distribution, the profiles of the reflections were distorted with increasing the reflection order and the extent of extensibility. In the fourth order actin meridional reflection with an axial spacing of 0.68 nm, a measurable asymmetric effect could be observed at the 0.3–0.4% elongation even if the influence of the axial reflection width was taken into consideration. However, during contraction we observed no appreciable asymmetric effect even in fourth order meridional reflection in the X-ray diffraction pattern from contracting muscle (manuscript in preparation). The observation implicates strongly that the associated variation of distortion along the filaments that is mediated by the interaction of myosin heads, if any, is spread out by some cooperative transition among actin subunits, making a uniform extension over the whole filaments. This observation comes from the highly compliant and elastic properties of the actin filaments. Thus actin filaments are much more than simple force transmitters in the force generation process, and actin filament's internal dynamics is important for muscle contraction.

28.4. SUMMARY

The X-ray diffraction investigations have indicated that structural alteration of troponin in response to Ca^{2+}-binding is essential in the activation of the thin filament and simultaneously induces the changes in actin-tropomyosin structure. In the active state, the actin filaments accept myosin crossbridges having ADP+Pi and undergo an asynchronous cycle of attachment and detachment with crossbridges. During such cycling, the conformation of the actin monomers in the thin filament is further altered in a cooperative manner. The direction of conformational change of the actin monomers mediated by the myosin interaction is different from that of the conformational change induced by the binding of Ca^{2+} to troponin. The time course of the actin axial repeat during contraction revealed a small initial decrease very early in contraction and then increased, running parallel to the time course of tension generation. The spacing changes of the actin meridional reflection and the two genetic reflections quickly decrease respond to rapid length changes imposed on contracting muscle, subsequently following in parallel to the redevelopment of tension, as would be expected if they represented the elastic, mechanical

strain. In contrast, the intensity change of most of the actin reflections runs ahead the tension changes. The helical symmetry of the actin filament changes in the transition of muscle from the resting state to the initial activation state by twisting the right-handed helices toward the 13/6 symmetry. In the subsequent transition to the force generating state, it turns by untwisting them toward the 28/13 symmetry. These changes are caused by the movement of actin monomers along the left-handed genetic track in the actin filament. Twisting changes are a unique property of the actin filaments in muscle. Thus it is now very certain that the conformational changes of actin monomers are involved in the force generating process and in the regulation process as well.

The earlier structural alterations of the actin filaments may be requisite for the formation of the directional potential for the interaction force between myosin heads and the actin for sliding. Most of the sliding mechanisms proposed previously have claimed that a tilting or rotation of the lever-arm portion of myosin heads which stereospecifically bound to thin actin filaments, stretches an elastic structure which is assumed to be resided around myosin heads, and generates a force for sliding. However, a similar mechanism can now be realistic, where the bonds among actin monomers are extended and twisted and a tension is generated by an elastic strain accumulated in the actin filaments through the interaction of energized myosin crossbridges. High compliant actin filament's internal dynamics is important both for regulation mechanism and force generation mechanism.

28.5. REFERENCES

1. Amemiya, Y., Wakabayashi, K., Tanaka, H., Ueno, Y., and Miyahara, J., Laser-stimulated luminescence used to measure X-ray diffraction of a contracting striated muscle, *Science* **237**, 164–168 (1987).
2. Wakabayashi, K., and Amemiya, Y., Progress in X-ray synchrotron diffraction studies of muscle contraction, *Handbook Synchrotron Radiation*, **4**, 597–678 (1991).
3. Ebashi, S., Endo, M., and Ohtsuki, I., Control of muscle contraction, *Quart. Rev. Biophys*., **2**, 351–384 (1969).
4. Sugimoto, Y., Takezawa, Y., Minakata, S., Kobayashi, T., Tanaka, H., and Wakabayashi, K., Time-resolved X-ray diffraction studies on skeletal muscle regulation: Intensity changes of the troponin-associated meridional reflections during activation, *Photon Factory Activity Rep.*, **20B**, 237 (2003), and to be submitted for publication.
5. Maeda, Y., Popp, D., and Stewart, A., Time-resolved X-ray diffraction study of the troponin-associated reflections from the frog muscle, *Biophys. J.*, **63**, 815–882 (1992).
6. Yagi, N., An X-ray diffraction study on early structural changes in skeletal muscle contraction, *Biophys. J.*, **84**, 1093–1102 (2003).
7. Flicker, P. F., Phillips, Jr., G. N., and Cohen, C., Troponin and its interaction with tropomyosin. An electron microscopy study, *J. Mol. Biol.*, **162**, 495–501 (1982).
8. Vinogradova, M. V., Stone, D. B., Malania, G. G., Karatzaferi, C., Cooke, R., Mendelson, R. A., and Flattering, R. J., Ca^{2+}-regulated structural changes in troponin. *Proc. Natl. Acad. Sci. USA* **102**, 5038–5054 (2005).
9. Takeda, S., Yamashita, A., Maeda, K., and Maeda, Y., Structure of the core domain of human cardiac troponin in the Ca(2+)-saturated form, *Nature* **424**, 35–41 (2003).
10. Takezawa, Y., Sugimoto, Y., Kobayashi, T., and Wakabayashi, K., Intensity changes of the first layer-line complex in the X-ray pattern of a frog skeletal during isometric contraction: The intensity of actin-based layer line decreases, *J. Muscle Res. Cell Motil.*, **21**, 197 (2000), and to be submitted for publication.
11. Wakabayashi, K., Saitow, H., Moriwaki, N., Kobayashi, T., and Tanaka, H., The first thin filament layer line decreases in intensity during an isometric contraction of frog skeletal muscle, *Adv. Exp. Med. Biol.*, **332**, 451–460 (1993).
12. Yagi, N., Intensification of the first actin layer-line during contraction of frog skeletal muscle, *Adv. Biophys*., **27**, 35–43 (1991).

13. Ueno, Y., X-ray structure analyses of the thin filaments in relaxed, contracting and rigor states of striated muscles, *Ph.D Thesis*, Engineering Science, Osaka University, Japan (1996).
14. Wakabayashi, K., Ueno, Y., Takezawa, Y., and Sugimoto, Y., Muscle contraction: Use of synchrotron X-ray diffraction, *Encyclopedia of Life Sciences*, Nature Publishing Group, 1–11 (2001). http://www.els.net.
15. Holmes, K. C., Popp, D., Gebhard, W., and Kabsch, W., Atomic model of the actin filament, *Nature* **347**, 44–49 (1990).
16. Wakabayashi, K., Sugimoto, Y., Tanaka, H., Ueno, Y., Takezawa, Y., and Amemiya, Y., X-ray diffraction evidence for the extensibility of actin and myosin filaments during muscle contraction, *Biophys. J.*, **67**, 2422–2435 (1994).
17. Takezawa, Y., Sugimoto, Y., and Wakabayashi, K., Extensibility of actin and myosin filaments in various states of skeletal muscles as studied by X-ray diffraction, *Adv. Exp. Med. Biol.*, **453**, 309–317 (1998).
18. Takezawa, Y., Sugimoto, Y., Kobayashi, T., and Wakabayashi, K., An alteration of the helical twist of the actin filaments accompanied by a force generation as revealed by the spacing change of the actin-based first layer-line component, *J. Muscle Res. Cell Motil.*, **22**, 206 (2001).
19. Takezawa, Y., Sugimoto, Y., Kobayashi, T., Oshima, K., and Wakabayashi, K., Alteration of the helical twist associated with the shortening of the thin actin filaments upon activation of skeletal muscles, *Photon Factory Activity Rep.*, **19B**, 204 (2001).
20. Takezawa, Y., Oshima, K., Sugimoto, Y., Kobayashi, T., and Wakabayashi, K., Alteration of the helical twist associated with the extensibility of the actin and myosin filaments during force generation of skeletal muscles, *Photon Factory Activity Rep.*, **21B**, 243 (2002), and to be submitted for publication.
21. Takezawa, Y., Extensibility and helical twisting of the actin filaments during muscle contraction, *KEK Proc.*, **2001–24**, pp.171–182. (In Japanese)
22. Gillis, J. M., and O'Brien, E. J., The effect of calcium ions on the structure of reconstituted muscle thin filaments, *J. Mol. Biol.*, **99**, 445–459 (1975).
23. Kress, M., Huxley, H. E., Faruqi, A. F., and Hendrix, J., Structural changes during activation of frog muscle studied by time-resolved X-ray diffraction, *J. Mol. Biol.*, **188**, 325–342 (1986).
24. Bordas, J., Diakun, G. P., Harries, J. E., Lewis, R. A., Mant, G. R., Martin-Fernandez, M. L., and Towns-Andrews, E., Two-dimensional time-resolved X-ray diffraction of muscle: Recent studies, *Adv. Biophys.*, **27**, 15–33 (1991).
25. Huxley, H. E., Stewart, A., and Irving, T., Measurements and implications of spacing changes in muscle, *Biophys. J.*, **78**, M-PM-A6 (1998).
26. Bordas, J., Svensson, A., Rothery, M., Lowy, J., Diakun, G. P., and P. Boesecke, P., Extensibility and symmetry of actin filaments in contracting muscles, *Biophys. J.*, **77**, 3197–3207 (1999).
27. White, D. C., and Thorson, J., The kinetics of muscle contraction, *Prog. Biophys. Mol. Biol.*, **27**, 173–255 81973.
28. Takezawa, Y., Satoi, N., Oshima, K., Kobayashi, T., and Wakabayashi, K., Axial profile of the actin-based meridional reflections associated with the actin extensibility during force generation of skeletal muscles, *Photon Factory Activity Rep.*, **22B**, 246 (2004), and to be submitted for publication.

29

REGULATION OF MUSCLE CONTRACTION BY Ca^{2+} AND ADP: FOCUSING ON THE AUTO-OSCILLATION (SPOC)

Shin'ichi Ishiwata[1,2], Yuta Shimamoto[1], Madoka Suzuki[2] and Daisuke Sasaki[1]

29.1. ABSTRACT

A molecular motor in striated muscle, myosin II, is a non-processive motor that is unable to perform physiological functions as a single molecule and acts as an assembly of molecules. It is widely accepted that a myosin II motor is an independent force generator; the force generated at a steady state is usually considered to be a simple sum of those generated by each motor. This is the case at full activation (pCa <5 in the presence of MgATP); however, we found that the myosin II motors show cooperative functions, i.e., non-linear auto-oscillation, named SPOC (SPontaneous Oscillatory Contraction), when the activation level is intermediate between those of contraction and relaxation (that is, at the intermediate level of pCa, 5~6, for cardiac muscle, or at the coexistence of MgATP, MgADP and inorganic phosphate (Pi) at higher pCa (>7) for both skeletal and cardiac muscles). Here, we summarize the characteristics of SPOC phenomena, especially focusing on the physiological significance of SPOC in cardiac muscle. We propose a new concept that the auto-oscillatory property, which is inherent to the contractile system of cardiac muscle, underlies the molecular mechanism of heartbeat. Additionally, we briefly describe the dynamic properties of the thin filaments, i.e., the Ca^{2+}-dependent flexibility change of the thin filaments, which may be the basis for the SPOC phenomena. We also describe a newly developed experimental system named "bio-nanomuscle," in which tension is asserted on a single reconstituted thin filament by interacting with cross-bridges in the A-band composed of the thick filament lattice. This newly devised hybrid system is expected to fill the gap between the single-molecule level and the muscle system.

[1] Department of Physics, Faculty of Science and Engineering, Waseda University, 3-4-1 Okubo, Shinjuku-ku, Tokyo 169-8555, Japan, and [2]Consolidated Research Institute for Advanced Science and Medical Care, Waseda University, 513 Wasedatsurumaki-cho, Shinjuku-ku, Tokyo 162-0041, Japan
E-mail: Ishiwata@waseda.jp Tel/Fax: +81-3-5286-3437.

Regulatory Mechanisms of Striated Muscle Contraction
Edited by Ebashi and Ohtsuki, Springer, 2007

29.2. INTRODUCTION

In the early 1960s, Prof. S. Ebashi found that Ca^{2+} is a regulator of muscle contraction (Ebashi and Endo, 1968; Ebashi et al., 1969; Ebashi, 1972). This finding was the first demonstration of the universal role of Ca^{2+} as a regulator of various kinds of cellular functions. After a while, Prof. Ebashi and his associates (Ebashi et al., 1968) succeeded in isolating a protein named troponin (Tn) that specifically binds Ca^{2+} (troponin was the first protein identified as a Ca^{2+} receptor). It was demonstrated that the tropomyosin(Tm)-troponin(Tn) complex is located on the thin filament approximately every 40 nm along the axis of an actin filament (Ebashi and Endo, 1968; Ebashi et al., 1969; Ohtsuki et al., 1968, 1986). Since then, the most important research subjects on the regulation of muscle contraction have been focused on the Ca^{2+}-dependence of the state and the structure of the thin filaments.

In 1972, we reported that the flexibility of the reconstituted thin filaments (F-actin-Tm-Tn complexes) depends on the concentration of free Ca^{2+} ($pCa = -\log[Ca^{2+}]$), namely, the flexibility decreases upon detachment of Ca^{2+} from Tn (Ishiwata and Fujime, 1972). Our paper was the second reporting that the physico-chemical properties of the thin filaments change depending on the pCa value (following the work by Tonomura et al., 1969). In 1974, we proposed a model, in which the Ca^{2+}-induced changes in the flexibility of thin filaments play a role in the lattice effects on the tension development of striated muscle (Ishiwata and Oosawa, 1974). We would like to mention here that those old experiments and the model might still be of some significance in understanding the dynamic phenomena of *the contractile system of muscle* (being composed of an assembly of sarcomeres without membrane system such as sarcoplasmic reticulum (SR)).

About 20 years ago, we found that the sarcomere length of *skeletal* myofibrils auto-oscillate when the state of the contractile system is intermediate between contraction and relaxation (Okamura and Ishiwata, 1988). We named this auto-oscillatory phenomenon SPOC (Ishiwata and Yasuda, 1993). Particularly, SPOC that occurs at the coexistence of (Mg)ATP, (Mg)ADP and inorganic phosphate (Pi) in the absence of Ca^{2+} was named "ADP-SPOC." The dynamic properties of ADP-SPOC of skeletal muscle have been extensively examined under various conditions (Ishiwata et al., 1991, 1993; Shimizu et al., 1992; Ishiwata and Yasuda, 1993). *Cardiac* myofibrils (fibers) exhibit the auto-oscillation over a wider range of the intermediate activating conditions (Fukuda et al., 1996, 1998; Fujita and Ishiwata, 1998; Fukuda and Ishiwata, 1999). In particular, in cardiac muscle SPOC occurs at the intermediate Ca^{2+} concentrations, at which SPOC is not observed in skeletal muscle (Fabiato and Fabiato, 1978; Sweitzer and Moss, 1990; Linke et al., 1993; Fukuda et al., 1996; Fukuda and Ishiwata, 1999). We named this phenomenon "Ca-SPOC" (Ishiwata and Yasuda, 1993).

Though SPOC may not have direct relevance to physiological functions in skeletal muscle, we considered that it might be significant for the mechanism of heartbeat, because the auto-oscillation itself is the major physiological function of the contractile system of cardiac muscle. Indeed, we recently found that the period of ADP-SPOC observed in a contractile system of cardiac muscle (prepared from a ventricle of several animals, namely, rat, rabbit, dog, pig, and cow) has a linear relationship with the period of resting heartbeat of each animal (Sasaki et al., 2005). Moreover, we finally confirmed, after a long period of trial and error, that such a linear relationship exists in Ca-SPOC as well (Sasaki et al., 2006, and the poster presented at this Troponin Conference). Thus, we

propose here that the contractile system itself is an auto-oscillator that significantly contributes to the efficiency of the myocardial beating. We also discuss the molecular mechanism of SPOC based on the mechanical instability observed in myofibrils, and on the sliding behavior of an actin filament observed in the A-band motility assay, which we developed recently (Suzuki et al., 2005).

29.3. MATERIALS AND METHODS

29.3.1. Proteins and Fibers

The materials used in the present study spread over several levels of hierarchy in the striated muscle, that is, from a thin filament reconstituted by purified actin, Tm and Tn (or a native tropomyosin, i.e., a complex of Tm and Tn; Ebashi and Kodama, 1965), and an assembly of myofilaments (thick and thin filaments), to single myofibrils (Ishiwata and Funatsu, 1985; Anazawa et al., 1992) and muscle fibers (skeletal fibers, Ishiwata et al., 1985; Shimizu et al., 1992; cardiac fibers, Fukuda et al., 1996, 1998; Fujita and Ishiwata, 1998; Fukuda and Ishiwata, 1999; Sasaki et al., 2005, 2006). All the proteins were prepared from rabbit white skeletal muscle (Ishiwata, 1975).

29.3.2. Reconstitution of Thin Filaments

The thin filaments can be reconstituted *in vitro* by simply mixing an actin filament and a native Tm, or an actin filament, Tm and Tn in sequence. However, when the concentration of actin in the reconstituted thin filaments exceeds several μM, the solution undergoes gelation, exhibiting high viscoelasticity (thixotropy) due to the inter-filament interaction (Ebashi and Kodama, 1966; Ebashi and Endo, 1968). Ishiwata (1973) found that this thixotropic structure spontaneously disappears in temperature-dependent manner. The kinetics of this gel-sol transition are characterized by $\exp(-\Delta H^{\ddagger}/k_B T)$, where $\Delta H^{\ddagger}$ is the activation enthalpy, k_B is the Boltzmann constant and T is the absolute temperature; the value of $\Delta H^{\ddagger}$ depends on Ca^{2+} concentration (Ishiwata, 1973, 1978; Ishiwata and Kondo, 1978). We infer that the end-to-end interaction between Tm-Tn complexes bound to different actin filaments occurs due to protrusion of the end of the Tm-Tn complex from the side of an actin filament, namely, the deficiency of the binding sites on actin due to "the parking problem." The rearrangement of the Tm-Tn complexes to approach the most stable manner of binding along an actin filament occurs due to thermal agitation (an annealing effect), so that the kinetics of the irreversible transition from the gel structure to the dispersed filament structure obey the Arrhenius relation as described above. According to this finding, we devised a way to prepare the solution in which the reconstituted thin filaments are dispersed; that is, the standard protocol for the annealing treatment is to incubate the solution at 45°C for 10 min after mixing the proteins in the presence of several micromolar Ca^{2+} (Ishiwata and Fujime, 1972; Ishiwata, 1973).

29.3.3. A-band Motility Assay System

The A-band motility assay system (*Bio-nanomuscle* system) is composed of a single actin filament with a gelsolin-coated bead attached to its B-end (a bead-tailed actin

filament; Nishizaka et al., 1995; Suzuki et al., 1996), and an isolated A-band prepared by treating a single myofibril or a small bundle of myofibrils with gelsolin (Funatsu et al., 1990, 1993; Suzuki et al., 2005). The bead was trapped with the optical tweezers, and the tension developed on a single actin filament inside or at the outer surface of the A-band was estimated as the displacement of the bead from the trap center × the trap stiffness of the optical tweezers (Nishizaka et al., 1995, 2000). To prepare the reconstituted thin filaments, the Tm-Tn complex (prepared as native Tm) was mixed with very diluted solutions of F-actin, so that we need not to care about the entanglement of the filaments.

29.3.4. Myofibrils

Myofibrils were prepared by homogenizing the rabbit psoas (skeletal) glycerinated fibers according to the procedure described previously (Ishiwata and Funatsu, 1985). To measure the tension produced on a single myofibril, the two ends of the myofibril were fixed to a pair of glass micro-needles (one of which is flexible and the other is stiff) under an inverted optical (phase-contrast and fluorescence) microscope. The developed tension was measured by image analysis of the deflection of the flexible glass needle (Anazawa et al., 1992; Yasuda et al., 1996a).

29.3.5. Cardiac Muscle Fibers

Glycerinated cardiac muscle fibers were prepared from live hearts of rat, rabbit, dog, pig, and cow (Sasaki et al., 2005, 2006). The tension development was measured according to the standard technique (Fukuda et al., 1996). The striated pattern was observed under the phase contrast/confocal fluorescence microscope. To observe the oscillation pattern of each sarcomere under the SPOC conditions, the sarcomere length was estimated from the fluorescence image of muscle; here, the muscle was labeled with a fluorescent dye (rhodamine-phalloidin). Without chemical-fixative pretreatment, the thin filaments in cardiac muscle were labeled over the whole length with rhodamine-phalloidin, whereas in skeletal muscle only both ends of the thin filaments, i.e., the free (P-)ends and the Z-line region, were labeled (Yasuda et al., 1994). For the measurement of the period of oscillation, the back and forth movement of a plastic bead adhered to the surface of muscle fiber was recorded under a phase-contrast microscope.

29.4. RESULTS AND DISCUSSION

29.4.1. Characterization of Physical Properties of Thin Filaments

The thin (actin) filaments are usually considered to be a mere track for the molecular motors, namely myosins, to walk on it. In practice, there has been no explicit evidence demonstrating the direct coupling of the structural changes of the thin filaments with the function of molecular motors. However, a lot of experimental data indicates that the structure of the thin (actin) filaments changes as a result of the interaction with myosin II (cf. Oosawa et al., 1972). The bending flexibility of the reconstituted thin (or pure actin) filaments changes with the binding of myosin (HMM) (Fujime and Ishiwata, 1971; Ishiwata and Fujime, 1971, 1972). This has been demonstrated by the measurements of

the relaxation time of the bending Brownian motion in solution using quasielastic light scattering of laser beam (Fujime, 1970) and by direct observation of the bending Brownian motion of a single fluorescent actin filament in solution under a fluorescence microscope (Yanagida et al., 1985; Isambert et al., 1995). Namely, the bending relaxation time of an actin filament (FA) becomes shorter with the binding of Tm, implying that the FA-Tm complex is stiffer than the pure FA. When Tn is further complexed with the FA-Tm complex, the flexibility of the reconstituted thin filaments becomes sensitive to micromolar concentrations of Ca^{2+}. In the presence of higher concentrations of Ca^{2+}, the flexibility of the reconstituted thin filaments is similar to that of the FA-Tm complex, but it becomes least flexible with lowering the Ca^{2+} concentration. On the other hand, when HMM binds in the absence of ATP, FA becomes more flexible, exhibiting the maximum flexibility at a molar ratio of 6 : 1 (actin : HMM). When HMM binds to the reconstituted thin filament, the largest difference in the flexibility of the filament with and without Ca^{2+} is at the molar ratio of 2 : 1 (actin : HMM) (Ishiwata and Fujime, 1971; Ishiwata, 1975). These observations have been schematically depicted in Figure 29.1 (Fujime, 1972; Oosawa et al., 1972; Ishiwata, 1975).

In the traditional theory of muscle contraction (Huxley, 1957), the thin (actin) filaments are assumed to be a rigid body. But, in practice, it is not the case. The Young's modulus of the filament was estimated to be one to two orders magnitude smaller than that of steel from the quasi-elastic light scattering experiments (Fujime, 1970, 1972). This was later confirmed by microscopic analysis of the bending Brownian motion of single

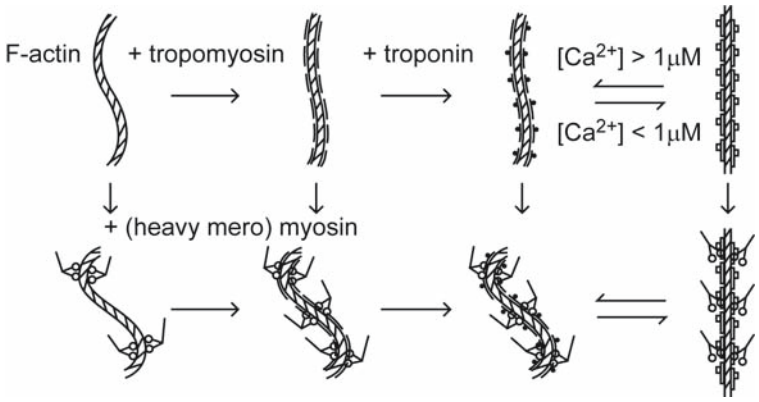

Figure 29.1. Schematic illustration showing the bending flexibility of an actin filament (FA) studied by quasi-elastic scattering of laser light (Oosawa et al., 1972; Ishiwata, 1975). The flexibility of FA (Fujime, 1970) decreased on the addition of Tm (tropomyosin) (Fujime and Ishiwata, 1971), and the flexibility of the FA-Tm complex remained nearly constant with the addition of Tn (troponin) in the presence of Ca^{2+} and decreased when Ca^{2+} was removed by the addition of EGTA (Ishiwata and Fujime, 1972). Additionally, the flexibility of FA increased on the addition of HMM in the absence of ATP (rigor condition) at an appropriate molar ratio (about 6 : 1) (Fujime and Ishiwata, 1971). The most flexible state of the FA-Tm complex was achieved by the addition of HMM in rigor condition at the molar ratio of about 2 : 1. In case of the reconstituted thin filament (an FA-Tm-Tn complex) in rigor, the transition between the most rigid and the most flexible states could be regulated by the concentration of Ca^{2+} in the presence of HMM at the molar ratio of about 2 : 1 (Ishiwata and Fujime, 1971; Ishiwata, 1975). Such a flexibility change was also observed in the presence of ATP (Oosawa et al., 1972; Ishiwata, 1975; Yanagida et al., 1985).

actin filaments (Yanagida et al., 1985; Isambert et al., 1995), and direct measurements of stiffness on muscle fiber (Higuchi et al., 1995) and a single actin filament (Kojima et al., 1994). Besides, the torsional rigidity of single actin filaments was directly measured on single actin filaments (Tsuda et al., 1996; Yasuda et al., 1996b). Thus, it was estimated that the 1 μm-long thin filament in the muscle fiber would elongate by a few nm under maximum tension. In practice, this estimation was experimentally demonstrated on skeletal muscle based on the analysis using a small-angle X-ray diffraction (Huxley et al., 1994; Wakabayashi et al., 1994). Besides, a lot of spectroscopic data showed the dynamic properties of actin filaments (on ESR, Thomas et al., 1975, 1979; on fluorescence data, cf. Ishiwata, 1998). It has also been established that the helical structure of actin filaments changes upon binding of regulatory proteins (cf. Egelman et al., 1982; McGough et al., 1997; Prochniewicz et al., 2005).

The structural changes of thin filaments that occur upon interaction with myosin and the regulatory proteins strongly suggest that the thin filaments are not a mere track (a rigid body) but may function as an active element in the molecular mechanism of tension development and its regulation (Prochniewicz-Nakayama et al., 1983). In fact, as described below, there are several phenomena in muscle, which cannot be explained simply by summing up independent force generators. In other words, there exists non-linearity in the mechanisms of tension generation and its regulation, where a long-range cooperativity along the thin filament is considered to play a role.

First, we would like to mention that tension does not necessarily depend linearly on the overlap between the thick and the thin filaments. As demonstrated by Gordon et al. (1966), tension is developed proportionally to the overlap, but this is the case only when the muscle is fully activated. In fact, Endo was the first to demonstrate that, when the muscle is activated partially at intermediate Ca^{2+} concentrations, the maximum tension is developed at a shorter overlap (longer SL), rather than at the maximum overlap (short SL) (Endo, 1972a,b; Stephenson and Wendt, 1984; cf. Figure 29.2b). This demonstrates that the tension is not necessarily proportional to the overlap between the thick and thin filaments; in other words, tension is not always proportional to the number of available cross-bridges.

The above results have been quantitatively explained according to the model shown in Figure 29.2, in which we assume that (1) the flexibility of the thin filaments increases with an increase in the concentration of free Ca^{2+}. In this model, the lateral position of actin, $P(q)$, is assumed to follow the Gaussian distribution, and the width of the Gaussian distribution, $(\langle q^2 \rangle)^{1/2}$, increases as the flexibility of the filament increases; (2) the interaction probability of myosin cross-bridges depends on the distance between the thick and the thin filaments, d, and the effective length of cross-bridges, a; (3) the volume of the filament lattice is constant irrespectively of the sarcomere length, and (4) the isometric tension is determined by (the length of overlap between the thick and the thin filaments) × (the interaction probability of cross-bridges, which is proportional to the hatched area in Figure 29.2a) (Ishiwata and Oosawa, 1974). The effective distance between the thick and the thin filaments decreases with increasing the flexibility of the thin filaments. In this model there are only two parameters, namely, $(\langle q^2 \rangle)^{1/2}$ and a (Figure 29.2a). With an increase in the sarcomere length, the distance between the thick and the thin filaments decreases due to the constant volume of the filament lattice. Because of this, the probability of cross-bridge formation increases, especially sharply at the intermediate level of activation, whereas the number of available myosin heads decreases only linearly. Thus,

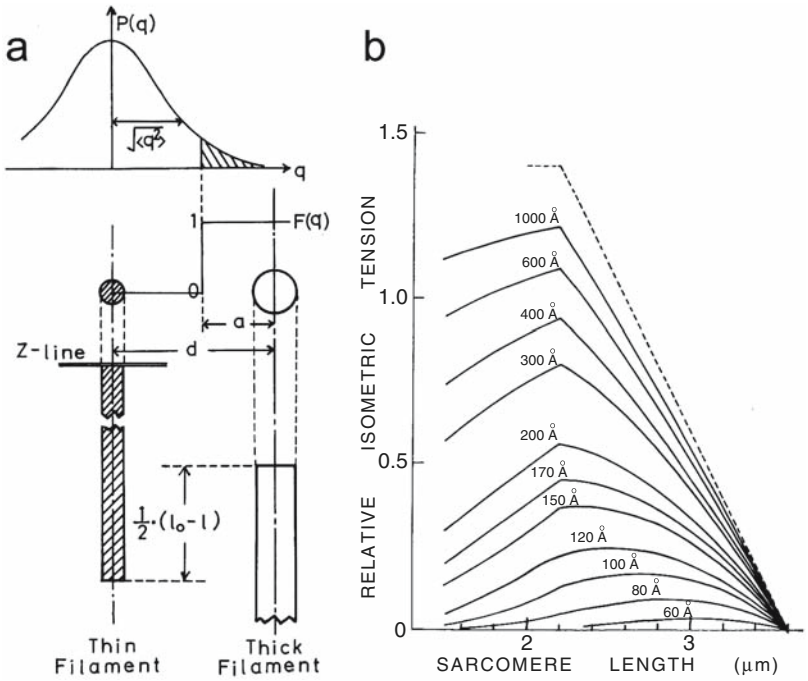

Figure 29.2. Model describing the length vs. tension relationship based on the flexibility change of the thin filaments. (a) Schematic diagram of the model. P(q), the Gaussian distribution showing the existence probability of actin against the lateral coordinate, q; $(\langle q^2 \rangle)^{1/2}$, the width of the Gaussian distribution that represents the bending flexibility of the thin filaments; F(q), the probability of cross-bridge formation; d, the distance between the thick and the thin filaments; a, the length of the region in which cross-bridges are formed (the effective length of cross-bridges) (cf. Kinosita et al., 1984; Ishiwata et al., 1987); l, sarcomere length; l_0, the sarcomere length, at which there is no overlap between the thick and the thin filaments, i.e., 3.6 μm in this model. We assume that the maximum overlap is realized at the sarcomere length of 2.2 μm. (b), Relative isometric tension vs. sarcomere length at various $(\langle q^2 \rangle)^{1/2}$ values as shown in this Figure. Here, the values of d and a were assumed to be 25 nm (at the sarcomere length of 2.5 μm) and 15 nm (independent of the sarcomere length), respectively. The length vs. tension relationship obtained at pCa of about 6 by Endo (1972a,b) approximately corresponds to 10 nm for the value of $(\langle q^2 \rangle)^{1/2}$. Taken from Ishiwata and Oosawa (1974).

at the intermediate level of activation, where the bending flexibility of the thin filaments is also intermediate, the developed tension becomes largest at a smaller overlap between the thick and the thin filaments. This mechanism may be relevant to the stretch activation, which is particularly profound in cardiac muscle, a property known as Frank-Starling law (Fukuda et al., 2001; Fuchs and Martyn, 2005).

29.4.2. A-band Motility Assay System (*Bio-nanomuscle*) with Reconstituted Thin Filaments

The A-band motility assay system is a newly devised hybrid experimental system that fills the gap between a single-molecular assay and a myofibril (Molloy, 2005; Suzuki et al., 2005). In this system, a single actin filament interacts with myosin cross-bridges that are regularly aligned in a thick filament lattice, i.e., an exposed A-band (cf.

Figure 29.3a). We found that the bead-tailed actin filament trapped with optical tweezers moved back and forth, probably due to the fluctuations in the number of interacting cross-bridges. In spite of these large tension fluctuations, the average force developed on a single actin filament was proportional to the overlap between the thick and the thin filaments, at least within ca. 300 nm from the end of the A-band. From this data, the average force developed by each head of myosin was estimated to be about 0.9 pN under a physiological ionic strength (Suzuki et al., 2005).

Here, we found that when the Tm-Tn complex was added to the above system, the Ca^{2+} sensitivity was recovered as shown in Figure 29.3. In the absence of Ca^{2+}, the reconstituted thin filament did not interact with the A-band (Figure 29.3b), whereas in the presence of Ca^{2+} the large tension development occurred (Figure 29.3c), as was the case for a pure actin filament (Suzuki et al., 2005). These data suggested that the average tension developed by each cross-bridge became larger compared with that in a pure actin filament. This result is consistent with that obtained in bovine cardiac muscle fiber, where

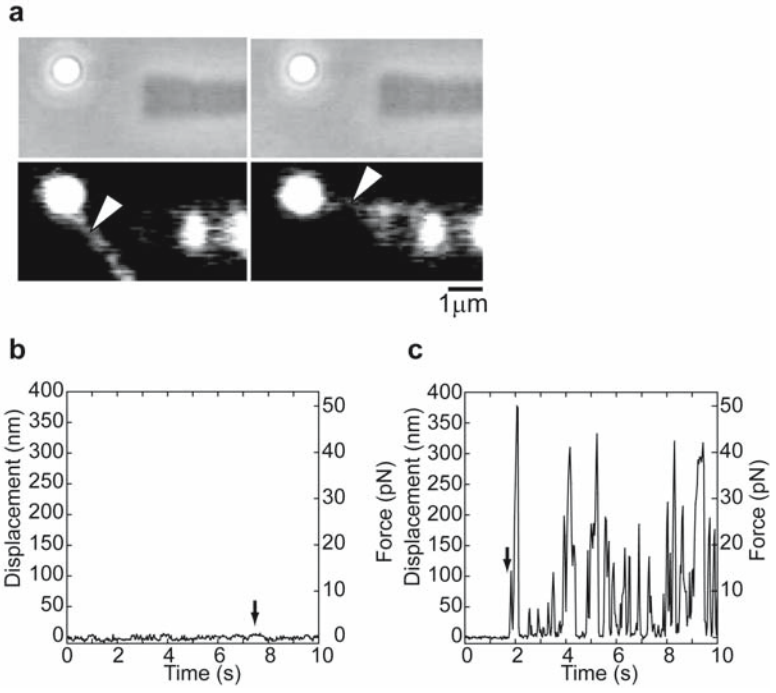

Figure 29.3. A-band motility assay system of muscle (*bio-nanomuscle*) with the reconstituted thin filament. (a) Phase-contrast (top) and fluorescence (bottom) images of the A-band motility assay system. The bead initially remained at the trap center, because the actin filament did not interact with the A-band (left). After the actin filament touched the outer surface of the A-band, the filament was drawn toward the A-band, as a result, the bead deviated from the trap center (right). Here, the arrowheads indicate the reconstituted thin filament bound to a polystyrene bead (1 μmϕ). (b, c) Time course of the bead movement in the absence (b) and the presence (c) of Ca^{2+}. Arrows indicate the moment at which the reconstituted thin filament touched the A-band (see Figure a, right). Solution conditions: 96 mM KCl, 25 mM Imidazole-HCl, pH 7.4, 4.2 mM $MgCl_2$, 2.2 mM ATP, 2 mM EGTA, – (b) or + (c) 2 mM $CaCl_2$, 10 mM DTT, 0.5 mg/ml BSA, 0.1 μM Tm-Tn complex, 4.5 mg/ml D(+)-glucose, 50 units/ml glucose oxidase, 50 units/ml catalase, 15 mM creatine phosphate and 150 units/ml creatine phosphokinase at 28°C.

the thin filaments were replaced with pure actin filaments (prepared from rabbit white muscle) using a technique of reconstitution of actin (thin) filaments after selective removal of the endogenous thin filaments with gelsolin treatment, and the effects of cardiac Tm-Tn complexes on the tension development were examined (Fujita et al., 1996, 2002; Kawai and Ishiwata, 2006, for cardiac muscle; Funatsu et al., 1994, for skeletal muscle).

Using the A-band motility assay system with the reconstituted thin filaments, we examined the ADP-SPOC conditions described below (Suzuki, M., unpublished). The results showed that the time course of the movement of the filament exhibited a saw-tooth waveform similar to that observed in SPOC of myofibrils (see Figure 29.4b), that is, after the filament had rather slowly been drawn inside the A-band, it was abruptly pulled out toward the trap center. However, in this case the saw-tooth waveform was less regular compared to that observed in SPOC. We expect that the detailed study under the SPOC conditions using a high-speed camera (1 ms temporal resolution), which is now underway, will contribute to clarifying the molecular mechanism of SPOC.

29.4.3. State of the Contractile System of Muscle

The previous studies showed that the contractile system of cardiac muscle spontaneously oscillates under the intermediate values of pCa; not only the tension, but the sarcomere lengths oscillate as well (Fabiato and Fabiato, 1978; Sweitzer and Moss, 1990; Linke et al., 1993; Fukuda et al., 1996).

The state exhibiting the auto-oscillation is considered to represent the third state, in addition to contraction and relaxation. The 3D-state diagram constructed against the concentrations of MgADP and Pi and the value of pCa at the fixed concentration of MgATP clearly shows that the SPOC region is located between the contraction and the relaxation regions (Figure 29.4a). The auto-oscillation that occurs in the SPOC region on the y-z plane in Figure 29.4a, the 2D space constructed against the concentrations of Mg-ADP and Pi in the absence of Ca, corresponds to ADP-SPOC, whereas the auto-oscillation that occurs on the x (pCa) axis represents Ca-SPOC.

The 3D state diagram is mostly similar in both skeletal and cardiac muscles. The main differences between skeletal and cardiac muscles are: 1) the SPOC region for cardiac muscle is broader than that for skeletal muscle, namely, the triple point on the z-axis, at which the transition from relaxation to contraction occurs, is lower in cardiac muscle, implying that the relative affinity for ADP compared to ATP is higher in cardiac muscle, and 2) the Ca-SPOC region clearly exists on the x-axis.

The molecular mechanism of SPOC has been primarily studied under the ADP-SPOC conditions using either a single skeletal myofibril or their small bundle. Under a phase-contrast microscope, two ends of the myofibril are twined to a pair of glass micro-needles, one of which is flexible and the other is rigid (Anazawa et al., 1992; Yasuda et al., 1996; see Figure 29.4b). The tension developed by the myofibril is determined from the deflection of the flexible needle (needle 1 in Figure 29.4b) and the mechanical impulse is applied by manipulating the rigid needle (needle 2 in Figure 29.4b). The interesting finding is that the ADP-bound cross-bridges function as an activator in the absence of Ca^{2+} (see the state change on the z-axis in the 3D state diagram shown in Figure 29.4a), which seems to be analogous to the rigor activation (Shimizu et al., 1992); in other words, the role of the ADP-bound cross-bridges is similar to that of rigor cross-bridges (Bremel and Weber, 1972).

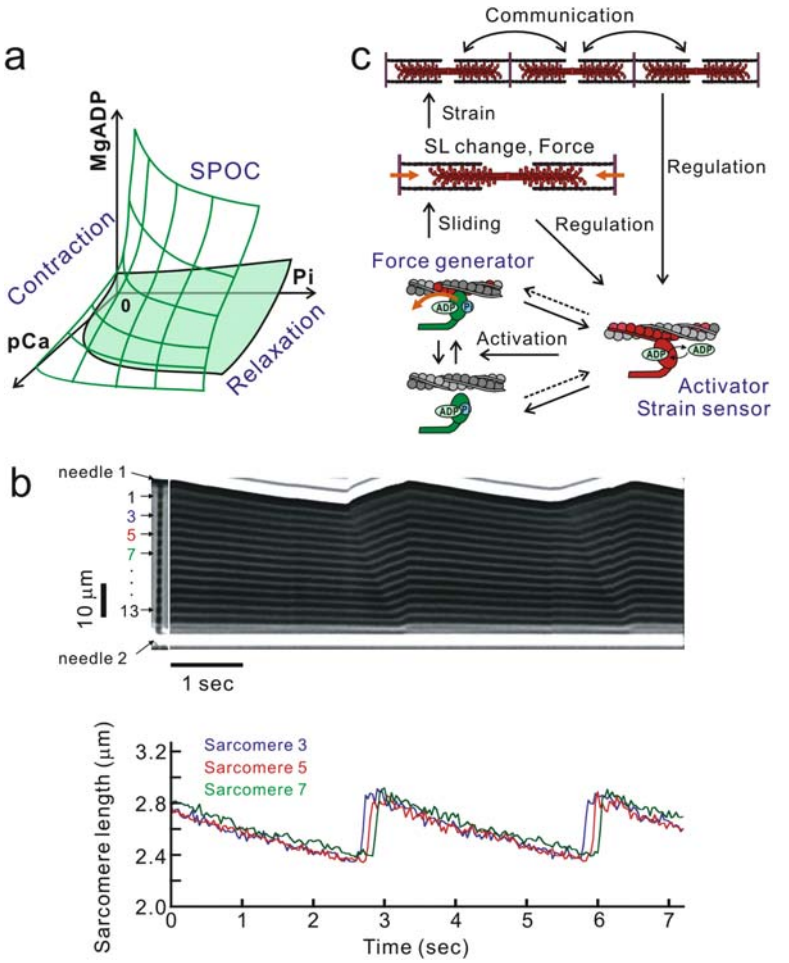

Figure 29.4. Schematic diagram showing the state of the contractile system of muscle. (a) 3D-state diagram showing the state of the contractile system of cardiac muscle against pCa (x-axis), the concentrations of Pi (y-axis) and MgADP (z-axis). The states are classified into three, i.e., contraction, relaxation and SPOC; in particular, we call the SPOC state on the y-z plane "ADP-SPOC" and the SPOC state along the x-axis "Ca-SPOC." (b) A typical pattern of ADP-SPOC as revealed by the auto-oscillation of sarcomere lengths in rabbit psoas myofibril. The kymograph was obtained by phase-contrast microscopy. Both ends of the myofibril were fixed to a pair of glass micro-needles; one is flexible (needle 1) and the other is stiff (needle 2). A propagation of the yielding phase of the sarcomere oscillation (SPOC wave) from the sarcomere #1 to #13 can be observed. (c) Schematic diagram showing the molecular aspects of feedback regulation in ADP-SPOC.

We have not fully clarified the molecular mechanism of SPOC yet, but, concerning the mechanism of length-dependent activation, we are now able to put forward the following hypothesis. 1) First, the activation at longer sarcomere lengths (in other words, inactivation at shorter sarcomere lengths) is expected to occur under the SPOC conditions. In fact, Endo (1972a,b) found that in skinned skeletal muscle fibers at the intermediate level of activation (pCa around 6) the higher tension is developed at longer sarcomere lengths. 2) Second, considering our model that can explain the essential

properties of the non-linear tension-length relationship at the intermediate level of activation (Ishiwata and Oosawa, 1974), we expect that the flexibility of the thin filaments, which depends on the binding of cross-bridges, may be important for the SPOC mechanism. In ADP-SPOC, the intermediate activation is realized due to the ADP-bound cross-bridges instead of binding of Ca^{2+} to Tn. If the flexibility of the thin filaments is increased by the ADP-bound cross-bridges, the positive feedback loop may occur as follows: as the sarcomere length changes, the occurrence probability of cross-bridge formation may change non-linearly due to the change in the distance between the thick and the thin filaments (cf. Figure 29.2a). Therefore, the cooperative activation (or deactivation) is expected to occur with an increase (or decrease) in the sarcomere length.

One apparent contradiction with the above considerations is that the flexibility of the reconstituted thin filaments does not increase upon the formation of rigor cross-bridges (the binding of HMM) in the absence of Ca^{2+} (see Figure 29.1). A possible explanation is that the flexibility of the thin filaments does increase at very low concentrations of ATP, where the so-called rigor activation occurs in the absence of Ca^{2+}, due to the coexistence of rigor and ATP-bound cross-bridges (practically, the ADP-Pi state of cross-bridges). Another possible reason is that, unlike the rigor cross-bridges, the ADP-bound cross-bridges do increase the flexibility of the filaments. Whether such inference is correct, must be examined in future.

Finally, it is to be noted that the activation state induced by the ADP-bound cross-bridges is very sensitive to the external mechanical impulse. Namely, the ADP-bound cross-bridges detach upon quick stretch of myofibril, so that the sarcomere is immediately relaxed. It results in the quick release of sarcomeres, which produces the saw-tooth waveform (Shimamoto et al., unpublished). It means that SPOC resonates with the external mechanical repetitive impulse; in other words, the SPOC period can be externally controlled within a certain region of frequencies. In addition, the state of each sarcomere under the SPOC conditions is influenced by the state of the contractile system surrounding the sarcomere. Such a situation is schematically summarized in Figure 29.4c. The ADP-bound cross-bridges are assumed to function as an activator that can activate the thin filaments even in the absence of Ca^{2+} and also function as a tension-sensitive regulator (Shimamoto et al., manuscript in preparation).

29.4.4. Physiological Significance of SPOC

It is interesting to examine whether SPOC has a physiological role in muscle function. To this end, we examined the properties of SPOC, namely, the SPOC period and the velocity of SPOC wave, in the demembranated cardiomyocytes prepared from several animals, i.e., rat, rabbit, dog, pig, and cow. As shown in Figure 29.5a, the sarcomere length oscillates with a saw-tooth waveform, which is common to all the species of muscles. To our surprise, we found that the period of SPOC has an excellent correlation (a linear relationship) with the period of resting heartbeat in each animal (Figure 29.5b–1), although the amplitude of sarcomere length oscillation varied only slightly between the species, implying that the higher the heartbeat is, the faster is the shortening velocity. On the other hand, the SPOC period exhibited nearly an inverse relation to the velocity of SPOC wave, implying that the latter has a linear relation to the heartbeat (Figure 29.5c). When the period of SPOC was measured at room temperature, e.g., 25°C, the period of ADP-SPOC was about 20 times slower than that of the heartbeat (Sasaki et al., 2005), but the period of Ca-SPOC was only

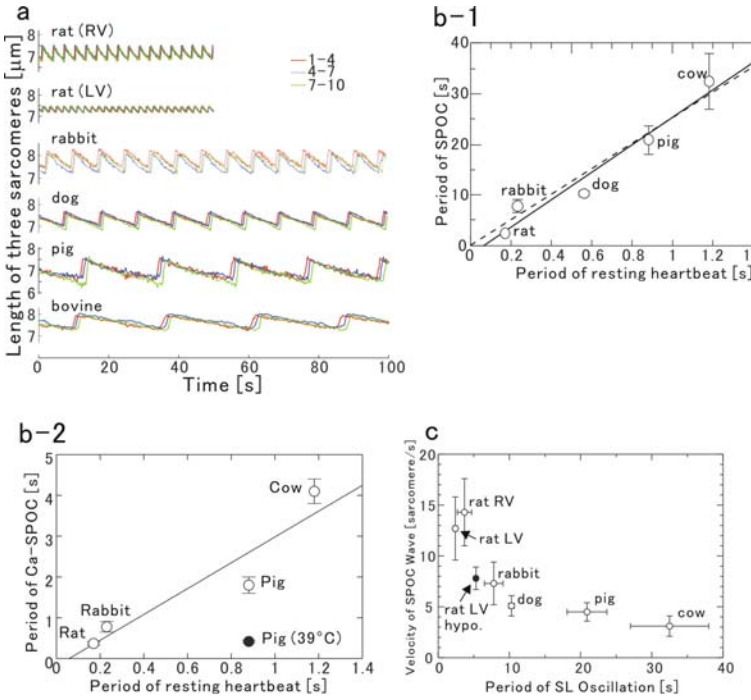

Figure 29.5. Characteristics of SPOC observed in the demembranated cardiomyocites. (a) A typical pattern of sarcomere length oscillation in ADP-SPOC observed in cardiac muscle fibers prepared from several animal species. (b) Relation between the period of SPOC (b-1, ADP-SPOC; b-2, Ca-SPOC) and the resting heartbeat of each animal. Modified from Sasaki et al. (2005) (b-1) and Sasaki et al. (2006) (b-2). (c) Relation between the period of SPOC and the velocity of SPOC wave under ADP-SPOC condition. The hypothyroid of rat (older than 10 weeks) were induced by drinking water containing 0.8 mg/ml propylthiouracil for more than 5 weeks.

three-fold slower than that of the heartbeat (Sasaki et al., 2006). Moreover, we found that the period of Ca-SPOC largely shortened with increasing temperature, and at the body temperature it fell exactly into the range of heartbeat (Figure 29.5b–2).

Though Ca-SPOC may play no significant role in skeletal muscle, there are good reasons to believe that Ca-SPOC may be an important factor for the mechanism of heartbeat: 1) Ca-SPOC occurs just within the physiological conditions of heartbeat. In particular, the level of Ca^{2+} concentration during heartbeat goes up and down in the region of the pCa values between <6 and >7, which exactly overlaps with the pCa region where Ca-SPOC occurs. 2) As described above, the period of SPOC (both ADP-SPOC and Ca-SPOC) has a linear relationship with the resting heartbeat of each animal. It means that the contractile machinery has been adapted to the physiological function of heartbeat in each animal. 3) The pattern of SPOC looks similar to that observed in the oscillation of sarcomeres during the heartbeat. 4) SPOC is synchronized with the external mechanical impulse, such as rapid stretch (Shimamoto et al., manuscript in preparation), and the mechanical boundary conditions, such as isotonic conditions (cf. Yasuda et al., 1996a); it is therefore plausible that these characteristics enable a long-range spatio-temporal

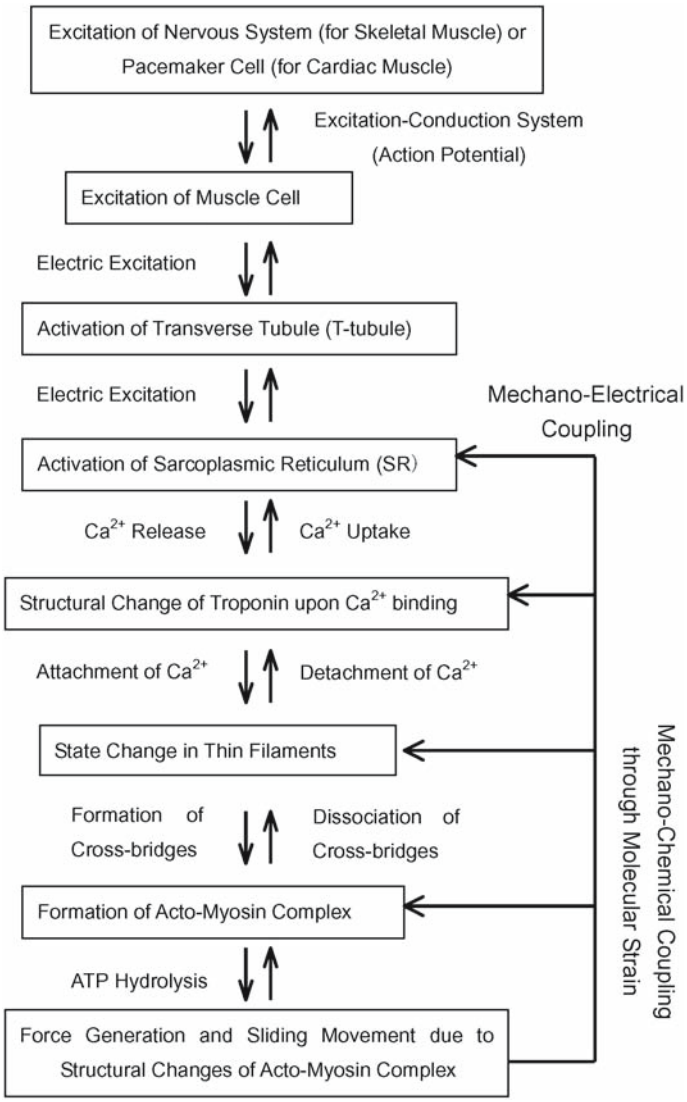

Figure 29.6. Hypothetical hierarchy in the regulation pathway in cardiac muscle. The rhythm of heartbeat is determined by the electrical impulse produced by pacemaker cells. In muscle cells, release and uptake of Ca^{2+} in SR are regulated by this electrical impulse. Ca^{2+} released in the cytoplasm binds to troponin, which turns the state of the thin filaments ON. In this sequential control mechanism, the contractile system is considered to be a force-producing machine that is regulated passively through the level of Ca^{2+}, i.e., pCa. The present study proposes that the contractile apparatus itself is an auto-oscillator that has an intrinsic oscillatory property with the period of oscillation characteristic of the heartbeat of each animal. This fact strongly suggests that in addition to the mechano-electrical feedback loops that may be relevant to the Ca^{2+} oscillation, there also exists a mechano-chemical feedback loop within the contractile apparatus. We hypothesize here that the ATPase enzymatic activities are modulated through the molecular strain that is induced by the force generation, which has already been hypothesized in the sliding theory of A. F. Huxley (1957); the direct experimental evidence has been obtained by studying the kinesin-microtubule interaction, where the ADP binding affinity of kinesin depended on the direction of the applied external force (Uemura and Ishiwata, 2003).

order of oscillation including the SPOC wave, so that it is expected that they are important for the macroscopic organization of the pumping function of the heart.

Next, a question arises: what is then the role of Ca^{2+} in the heartbeat, if the contractile apparatus is able to spontaneously oscillate without oscillation of Ca^{2+} concentration. It should be noted here that under steady SPOC conditions the metachronal oscillation wave in sarcomeres travels over several tens of sarcomeres in the fiber (SPOC wave). Therefore, various SPOC domains within the same fiber start to oscillate out of phase. An attractive idea that comes to mind here is that Ca^{2+} is necessary to ensure that the sarcomere oscillation occurs *in phase* over a large region of cardiac cell. In this sense, the real role of Ca^{2+} is to *synchronize* the oscillation of sarcomeres. This is an absolutely new concept on the mechanism of heartbeat: the contractile apparatus composed of actin, myosin, regulatory proteins and so on, is not a mere force generator that passively responds to Ca^{2+} as usually considered, but is actually a major player in the heartbeat. As summarized in Figure 29.6, there must exist several feedback loops in the mechanism of heartbeat; that is, the existence of feedback loops from the force generation to the SR function is now established. Additionally, the existence of Ca-SPOC strongly suggests that there must be a feedback loop within the force generation mechanism of the contractile apparatus. We thus propose that this oscillatory property, which is inherent to the contractile apparatus of the myocardium, is essential for the efficient functioning of the heart (Ishiwata et al., 2005; Sasaki et al., 2005, 2006).

29.5. CONCLUSION

In summary, we propose that the contractile apparatus is not a simple protein assembly, in which molecular motors independently generate tension; in fact, cooperativity exists not only between myosin motors, but within the thin filament as well. As a typical example supporting this idea, we focus on the auto-oscillation phenomena, especially on Ca-SPOC, which occurs within an intermediate range of Ca^{2+} concentrations under physiological conditions. The thin filament is usually considered to be a mere side player, or a mere track, on which the molecular motors produce tension. We are confident that SPOC is a key phenomenon for elucidating the mechanism of cooperativity operating in the assemblage composed of the cross-bridges and the thin filaments. Besides, we have proposed that the SPOC properties play an important role in the spatio-temporal organization of the heartbeat. It may be not easy to immediately accept this idea, however, we believe it is worth studying as a new concept that may open a new research field in muscle physiology.

29.6. ACKNOWLEDGMENT

We thank Dr. S. V. Mikhailenko for his critical reading of the manuscript. We also thank Ms. E. Wakabayashi for her excellent technical assistance on the SPOC experiments using diseased rats. This work was supported partly by Grants-in-Aid for Specially Promoted Research, the 21st Century COE Program and "Establishment of Consolidated Research Institute for Advanced Science and Medical Care" from the Ministry of Education, Sports, Culture, Science and Technology (MEXT) of Japan to S. I. and by

Grants-in-Aids for Young Investigator Research and Scientific Research in Priority Areas from the MEXT, Japan to M. S.

29.7. REFERENCES

Anazawa, T., Yasuda, K., and Ishiwata, S., 1992, Spontaneous oscillation of tension and sarcomere length in skeletal myofibrils. Microscopic measurement and analysis, *Biophys. J.* **61**:1099–1108.

Bremel, R. D., and Weber, A., 1972, Cooperative behavior within the functional unit of the actin filament in vertebrate skeletal muscle, *Nat. New Biol.* **238**:97–101.

Ebashi, S., 1972, Calcium ions and muscle contraction, *Nature* **240**:217–218.

Ebashi, S., and Endo, M., 1968, Calcium ions and muscle contraction, *Prog. Biophys. Mol. Biol.* **18**:123–183.

Ebashi, S., Endo, M., and Ohtsuki, I., 1969, Control of muscle contraction, *Quart. Rev. Biophys.* **2**:351–384.

Ebashi, S., and Kodama, A., 1965, A new protein factor promoting aggregation of tropomyosin, *J. Biochem.* **58**:107–108.

Ebashi, S., and Kodama, A., 1966, Interaction of troponin with F-actin in the presence of tropomyosin, *J. Biochem.* **59**:425–426.

Ebashi, S., Kodama, A., and Ebashi, F., 1968, Troponin. I. Preparation and physiological function, *J. Biochem.* **64**:465–477.

Egelman, E. H., Francis, N., and DeRosier, D. J., 1982, F-actin is a helix with a random variable twist, *Nature* **298**:131–135.

Endo, M., 1972a, Stretch-induced increase in activation of skinned muscle fibres by calcium, *Nat. New Biol.* **14**:211–213.

Endo, M., 1972b, Length dependence of activation of skinned muscle fibers by calcium, *Cold Spring Harb. Symp. Quant. Biol.* **37**:505–510.

Fabiato, A., and Fabiato, F., 1978, Myofilament-generated tension oscillations during partial calcium activation and activation dependence of the sarcomere length-tension relation of skinned cardiac cells, *J. Gen. Physiol.* **72**:667–699.

Fuchs, F., and Martyn, D. A. 2005. Length-dependent Ca^{2+} activation in cardiac muscle: some remaining questions, *J. Muscle Res. Cell Motil.* **26**:199–212.

Fujime, S., 1970, Quasi-elastic light scattering from solutions of macromolecules. II. Doppler broadening of light scattered from solutions of semi-flexible polymers, F-actin, *J. Phys. Soc. Jpn* **29**:751–759.

Fujime, S., 1972, Quasi-elastic scattering of laser light. A new tool for the dynamic study of biological macromolecules, *Adv. Biophys.* **3**:1–43.

Fujime, S., and Ishiwata, S., 1971, Dynamic study of F-actin by quasielastic scattering of laser light, *J. Mol. Biol.* **62**:251–265.

Fujita, H., and Ishiwata, S., 1998, Spontaneous oscillatory contraction without regulatory proteins in actin filament-reconstituted fibers, *Biophys. J.* **75**:1439–1445.

Fujita, H., Sasaki, D., Ishiwata, S., and Kawai, M., 2002, Elementary steps of the cross-bridge cycle in bovine myocardium with and without regulatory proteins, *Biophys. J.* **82**:915–928.

Fujita, H., Yasuda, K., Niitsu, S., Funatsu, T., and Ishiwata, S., 1996, Structural and functional reconstitution of thin filaments in the contractile apparatus of cardiac muscle, *Biophys. J.* **71**:2307–2318.

Fukuda, N., Fujita, H., Fujita, T., and Ishiwata, S., 1996, Spontaneous tension oscillation in skinned bovine cardiac muscle, *Pflügers Arch.* **433**:1–8.

Fukuda, N., Fujita, H., Fujita, T., and Ishiwata, S., 1998, Regulatory roles of MgADP and calcium in tension development of skinned cardiac muscle, *J. Muscle Res. Cell Motil.* **19**:909–921.

Fukuda, N., and Ishiwata, S., 1999, Effects of pH on spontaneous tension oscillation in skinned bovine cardiac muscle, *Pflugers Arch.* **438**:125–132.

Fukuda, N., Sasaki, D., Ishiwata, S., and Kurihara, S., 2001, Length dependence of tension generation in rat skinned cardiac muscle. Role of titin in the Frank-Starling mechanism of the heart, *Circulation* **104**:1639–1645.

Funatsu, T., Anazawa, T., and Ishiwata, S., 1994, Structural and functional reconstitution of thin filaments in skeletal muscle, *J. Muscle Res. Cell Motil.* **15**:158–171.

Funatsu, T., Higuchi, H., and Ishiwata, S., 1990, Elastic filaments in skeletal muscle revealed by selective removal of thin filaments with plasma gelsolin, *J. Cell Biol.* **110**:53–62.

Funatsu, T., Kono, E., Higuchi, H., Kimura, S., Ishiwata, S., Yoshioka, T., Maruyama, K., and Tsukita, S., 1993, Elastic filaments in situ in cardiac muscle: Deep-etch replica analysis in combination with selective removal of actin and myosin filaments, *J. Cell Biol.* **120**:711–724.

Gordon, A. M., Huxley, A. F., and Julian, F. J., 1966, The variation in isometric tension with sarcomere length in vertebrate muscle fibers, *J. Physiol.* **184**:170–192.

Higuchi, H., Yanagida, T., and Goldman, Y. E., 1995, Compliance of thin filaments in skinned fibers of rabbit skeletal muscle, *Biophys. J.* **69**:1000–1010.

Huxley, A. F., 1957, Muscle structure and theories of contraction, *Prog. Biophys. Biophys. Chem.* **7**:255–318.

Huxley, H. E., Stewart, A., Sosa, H., and Irving, T., 1994, X-ray diffraction measurements of the extensibility of actin and myosin filaments in contracting muscle, *Biophys. J.* **67**:2411–2421.

Isambert, H., Venier, P., Maggs, A. C., Fattoum, A., Kassab, R., Pantaloni, D., and Carlier, M. F., 1995, Flexibility of actin filaments derived from thermal fluctuations. Effect of bound nucleotide, phalloidin, and muscle regulatory proteins, *J. Biol. Chem.* **270**:11437–11444.

Ishiwata, S., 1973, A study on the F-actin, tropomyosin and troponin complex. I. Gel-filament transformation, *Biochim. Biophys. Acta* **303**:77–89.

Ishiwata, S., 1975, Doctoral Thesis, Nagoya University. "Study on muscle proteins – Principally, dynamic properties of actin filament studied by quasielastic scattering of laser light." pp. 229.

Ishiwata, S., 1978, Studies on the F-actin-tropomyosin-troponin complex. III. Effects of troponin components and calcium ion on the binding affinity between tropomyosin and F-actin, *Biochim. Biophys. Acta* **534**:350–357.

Ishiwata, S., 1998, Use of fluorescent probes, in: *Current Methods in Muscle Physiology-Advantages, Problems and Limitations-*, H. Sugi, ed., Oxford Univ. Press, Oxford, pp. 199–222.

Ishiwata, S., Anazawa, T., Fujita, T., Fukuda, N., Shimizu, H., and Yasuda, K., 1993, Spontaneous tension oscillation (SPOC) of muscle fibers and myofibrils. Minimum requirements for SPOC, *Adv. Exp. Med. Biol.* **332**:545–556.

Ishiwata, S., and Fujime, S., 1971, Effect of Ca^{2+} on dynamic properties of muscle proteins studied by quasi-elastic light scattering, *J. Phys. Soc. Jpn* **31**:1601.

Ishiwata, S., and Fujime, S., 1972, Effect of calcium ions on the flexibility of reconstituted thin filaments of muscle studied by quasielastic scattering of laser light, *J. Mol. Biol.* **68**:511–522.

Ishiwata, S., and Funatsu, T., 1985, Does actin bind to the ends of thin filaments in skeletal muscle? *J. Cell Biol.* **100**:282–291.

Ishiwata, S., Kinosita, Jr., K., Yoshimura, H., and Ikegami, A., 1987, Rotational motions of myosin heads in myofibril studied by phosphorescence anisotropy decay measurements, *J. Biol. Chem.* **262**: 8314–8317.

Ishiwata, S., and Kondo, H., 1978, Studies on the F-actin-tropomyosin-troponin complex. II. Partial reconstitution of thin filament by F-actin, tropomyosin and tropomyosin binding component of troponin (TNT), *Biochim. Biophys. Acta* **534**:341–349.

Ishiwata, S., Muramatsu, K., and Higuchi, H., 1985, Disassembly from both ends of thick filaments in rabbit skeletal muscle fibers. An optical diffraction study, *Biophys. J.* **47**:257–266.

Ishiwata, S., Okamura, N., Shimizu, H., Anazawa, T., and Yasuda, K., 1991, Spontaneous oscillatory contraction (SPOC) of sarcomeres in skeletal muscle, *Adv. Biophys.* **27**:227–235.

Ishiwata, S., and Oosawa, F., 1974, A regulatory mechanism of muscle contraction based on the flexibility change of the thin filament, *J. Mechanochem. Cell Motil.* **3**:9–17.

Ishiwata, S., Shimamoto, Y., Sasaki, D., and Suzuki, M., 2005, Molecular synchronization in actomyosin motors – From single molecules to muscle fibers via nanomuscle-, *Adv. Exp. Med. Biol.* **565**:25–36.

Ishiwata, S., and Yasuda, K., 1993, Mechano-chemical coupling in spontaneous oscillatory contraction of muscle, *Phase Transit.* **45**:105–136.

Kawai, M., and Ishiwata, S., 2006, Use of thin-filament reconstituted muscle fibres to probe the mechanism of force generation, *J. Muscle Res. Cell Motil.* 27:455–468.

Kinosita, K., Jr., Ishiwata, S., Yoshimura, H., Asai, H., and Ikegami, A., 1984, Submicrosecond and microsecond rotational motions of myosin head in solution and in myosin synthetic filaments as revealed by time-resolved optical anisotropy decay measurements, *Biochemistry* **23**:5963–5975.

Kojima, H., Ishijima, A., and Yanagida, T., 1994, Direct measurement of stiffness of single actin filaments with and without tropomyosin by in vitro nanomanipulation, *Proc. Natl. Acad. Sci. USA* **91**: 12962–12966.

Linke, W. A., Bartoo, M. L., and Pollack, G. H., 1993, Spontaneous sarcomeric oscillations at intermediate activation levels in single isolated cardiac myofibrils, *Circ. Res.* **73**:724–734.

McGough, A., Pope, B., Chiu, W., and Weeds, A., 1997, Cofilin changes the twist of F-actin: Implications for actin filament dynamics and cellular function, *J. Cell Biol*. **138**:771–781.

Molloy, J. E., 2005, Muscle contraction: actin filaments enter the fray, *Biophys. J.* **89**:1–2.

Nishizaka, T., Miyata, H., Yoshikawa, H., Ishiwata, S., and Kinosita, K., Jr., 1995, Unbinding force of a single motor molecule of muscle measured using optical tweezers, *Nature* **377**:251–254.

Nishizaka, T., Seo, R., Tadakuma, H., Kinosita, K., Jr., and Ishiwata, S., 2000, Characterization of single actomyosin rigor bonds – Load-dependence of lifetime and mechanical properties, *Biophys. J.* **79**: 962–974.

Ohtsuki, I., Maruyama, K., and Ebashi, S., 1986, Regulatory and cytoskeletal proteins of vertebrate skeletal muscle, *Adv. Protein Chem.* **38**:1–67.

Ohtsuki, I., Masaki, T., Nonomura, Y., and Ebashi, S., 1968, Periodic distribution of troponin along the thin filament, *J. Biochem.* **61**:817–819.

Okamura, N., and Ishiwata, S., 1988, Spontaneous oscillatory contraction of sarcomeres in skeletal myofibrils, *J. Muscle Res. Cell Motil*. **9**:111–119.

Oosawa, F., Fujime, S., Ishiwata, S., and Mihashi, K., 1972, Dynamic property of F-actin and thin filament, *Cold Spr. Harb. Symp. Quant. Biol.* **37**:277–285.

Prochniewicz, E., Janson, N., Thomas, D. D., and De La Cruz, E. M., 2005, Cofilin increases the torsional flexibility and dynamics of actin filaments, *J. Mol. Biol*. **353**:990–1000.

Prochniewicz-Nakayama, E., Yanagida, T., and Oosawa, F., 1983, Studies on conformation of F-actin in muscle fibers in the relaxed state, rigor, and during contraction using fluorescent phalloidin, *J. Cell Biol*. **97**: 1663–1667.

Sasaki, D., Fujita, H., Fukuda, N., Kurihara, S., and Ishiwata, S., 2005, Auto-oscillations of skinned myocardium correlating with heartbeat, *J. Muscle Res. Cell Motil.* **26**:93–101.

Sasaki, D., Fukuda, N., and Ishiwata, S., 2006, Myocardial sarcomeres spontaneously oscillate with the period of heartbeat under physiological conditions, *Biochem. Biophys. Res. Comm.* **343**:1146–1152.

Shimizu, H., Fujita, T., and Ishiwata, S., 1992, Regulation of tension development by MgADP and Pi without Ca^{2+}. Role in spontaneous tension oscillation of skeletal muscle, *Biophys. J.* **61**:1087–1096.

Stephenson, D. G., and Wendt, I. R., 1984, Length dependence of changes in sarcoplasmic calcium concentration and myofibrillar calcium sensitivity in striated muscle fibers, *J. Muscle Res. Cell Motil.* **5**: 243–272.

Suzuki, M., Fujita, H., and Ishiwata, S., 2005, A new muscle contractile system composed of a thick filament lattice and a single actin filament, *Biophys. J.* **89**:321–328.

Suzuki, N., Miyata, H., Ishiwata, S., and Kinosita, K., Jr., 1996, Preparation of bead-tailed actin filaments: Estimation of the torque produced by the sliding force in an in vitro motility assay, *Biophys. J.* **70**: 401–408.

Sweitzer, N. K., and Moss, R. L., 1990, The effect of altered temperature on Ca^{2+}-sensitive force in permeabilized myocardium and skeletal muscle. Evidence for force dependence of thin filament activation, *J. Gen. Physiol.* **96**:1221–1245.

Thomas, D. D., Seidel, J. C., and Gergely, J., 1979, Rotational dynamics of F-actin in submillisecond time range, *J. Mol. Biol*. **132**:257–273.

Thomas, D. D., Seidel, J. C., Hyde, J. S., and Gergely, J., 1975, Motion of subfragment-1 in myosin and its supramolecular complexes: saturation transfer electron paramagnetic resonance, *Proc. Natl. Acad. Sci. USA* **72**:1729–1733.

Tonomura, Y., Watanabe, S., and Morales, M. F., 1969, Conformational changes in the molecular control of muscle contraction, *Biochemistry* **8**:2171–2176.

Tsuda, Y., Yasutake, H., Ishijima, A., and Yanagida, T., 1996, Torsional rigidity of single actin filaments and actin-actin bond breaking force under torsion measured directly by in vitro micromanipulation**,** *Proc. Natl. Acad. Sci. USA* **93**:12937–12942.

Uemura, S., and Ishiwata, S., 2003, Loading direction regulates the affinity of ADP for kinesin, *Nat. Struct. Biol*. **10**:308–311.

Wakabayashi, K., Sugimoto, Y., Tanaka, H., Ueno, Y., Takezawa, Y., and Amemiya, Y., 1994, X-ray diffraction evidence for the extensibility of actin and myosin filaments during muscle contraction, *Biophys. J.* **67**: 2422–2435.

Yanagida, T., Nakase, M., Nishiyama, K., and Oosawa, F., 1985, Direct observation of motion of single F-actin filaments in the presence of myosin, *Nature* **307**:58–60.

Yasuda, K., Fujita, H., Fujiki, Y., and Ishiwata, S., 1994, Length regulation of thin filaments without nebulin, *Proc. Jap. Acad.* **70**, Ser. B.:151–156.

Yasuda, K., Shindo, Y., and Ishiwata, S., 1996a, Synchronous behavior of spontaneous oscillations of sarcomeres in skeletal myofibrils under isotonic conditions, *Biophys. J.* **70**:1823–1829.

Yasuda, R., Miyata, H., and Kinosita, K., Jr., 1996b, Direct measurement of the torsional rigidity of single actin filaments, *J. Mol. Biol*. **263**:227–236.

30

MUSCLE CONTRACTION MECHANISM BASED ON ACTIN FILAMENT ROTATION

Toshio Yanagida

Muscle contraction is caused by relative sliding movement between interdigitating actin and myosin filaments. It has been thought that myosin heads protruding from the myosin filament rotate between two orientations, while they repeat detachment from and attachment to actin filament coupled to the ATP hydrolysis cycle and the rotation of the head may cause the sliding. Recently atomic structure obtained from X-ray crystallography supports the rotation of the myosin head relative to the actin filament. A small conformational change in the ATP binding domain is transmitted to a neck domain that connects a motor domain (head) and tail domain, depending on the chemical state of nucleotide bound. Thus the neck domain acts as a lever-arm that can cause a displacement of 5–10 nm for the muscle myosin. This lever-arm swinging model has been a paradigm not only for the muscle myosin but also for unconventional myosins. Large stepsize of unconventional processive myosin V motor can be explained by its large lever arm within the frame of the lever-arm swinging model.

Since actin filaments was visualized using fluorescently labeled actin filaments, their smooth sliding movement along myosin molecules adsorbed on a slide glass can be visualized under fluorescence microscopy. Further development of this technique with a technique manipulating single actin filaments allowed elementary steps during single ATP molecules are hydrolyzed to be detected at single molecule level. The stepsize of muscle myosin for the elementary steps is 4–25 nm (Yanagida et al., 2000). Manipulation of single myosin heads instead of single actin filaments could reduce fluctuation of the probes, allowing the elementary steps to be scrutinized (Kitamura et al., 1999). The fluctuation of the probes is caused mainly due to compliant linkages existed in the experimental systems, expecially linkage between actin and the probes. by avoiding the compliant linkage between actin and probes. When single myosin molecules were manipulated using a scanning probe, the detailed processes of the rising phase of each displacement was resolved. In the rising phase, myosin heads do not move in a single step but make several steps of regular 5.5 nm step. on the binding site on actin monomer on the filament.

Formation of Soft Nanomachines, Core Research for Evolution Science and Technology, Japan Science and Technology Agency, Department of Biophysical Engineering, Osaka University, Soft Biosystem Group, Laboratories for Nanobiology, Graduate School of Frontier Biosciences, Osaka University, 1-3, Yamadaoka, Suita, Osaka 565-0871, Japan

Regulatory Mechanisms of Striated Muscle Contraction
Edited by Ebashi and Ohtsuki, Springer, 2007

The step occurs stochastically, mainly in one direction but occasionally inn opposite direction. Thus the movement of myosin heads is interpreted as a biased Brownian movement along the actin monomer on the filament. The total number of steps during the hydrolysis of single ATP molecules distributes within 5 steps and average value was 2.5 steps or 13 nm.

In muscle individual muscle myosin molecules which dissociate after each step movement, collaborate with many other myosin molecules in the filament. In the system containing numbers of myosin molecules in the filaments, the sliding distance between actin and myosin filaments during one ATP hydrolysis cycle was greater than 60 nm (Yanagida et al., 1985; Harada et al., 1990; Higuchi and Goldman 1991). The result has suggested cooperative action between myosin heads on the filament. In this report, the rotation of actin filaments is focused and its relation to the enhanced displacement per single ATP molecules is discussed.

30.1. CONFORMATIONAL CHANGES OF ACTIN REVEALED BY SINGLE MOLECULE FRET

Dynamically changing conformation of actin was measured using single molecule fluorescence resonance energy transfer (FRET) (Ishii et al., 1999). Actin was specifically labeled with tetramethylrhodamine (TMR) attached as a donor at Gln-41 in the DNase-I binding loop and IC5 attached as an acceptor at Cys-374 near the C terminus (Figure 30.1A) (Kozuka et al., 2006). In the time trajectory of the FRET signals from actin molecules in the filaments, the donor and acceptor fluorescence changed basically in opposite direction in accordance with the FRET mechanism; when the donor increases, the acceptor fluorescence decreases and vice versa (Figure 30.1B). The FRET efficiencies calculated from the donor and accepter fluorescence at every data point changed over a wide range from 0.2 to 0.7. The time course of the FRET efficiency suggested that actin molecules take several conformational states and the transition occurs in a time scale of seconds. In the time course, the FRET efficiency remained relatively constant for several seconds and then would change to a new FRET efficiency level for several seconds. The histograms of the FRET efficiencies of individual molecules show two or more peaks corresponding to different conformational states that illustrate this pattern in the time courses. All the data from numbers of molecules are summarized in a histogram (Figure 30.1C). There were two or more peaks in the histogram confirming that actin has multiple conformations. The histogram was fitted to a sum of two Gaussian distributions better than single Gaussian distribution. The fitting to two Gaussian distributions gave mean values of 0.27 (SD = 0.12) and 0.54 (SD = 0.12). Using the distribution of low and high FRET states, the time course data can be interpreted as fluctuation between the two states. The transition points are defined as the time when the FRET efficiency changes through a threshold determined by the mean value and the standard deviation. The duration time was fitted by a single exponential with rate constants of $0.24 \pm 0.04\,\mathrm{sec}^{-1}$ for the low FRET state and $0.34 \pm 0.05\,\mathrm{s}^{-1}$ for the high FRET state. Thus the time range for the transition between low and high FRET states were the order of seconds.

The existence of the two states is consistent with the conformational changes of actin associated with the myosin motility. The two states between which actin fluctuates are most likely the state that activates and inhibits myosin motility. As a state in which actin

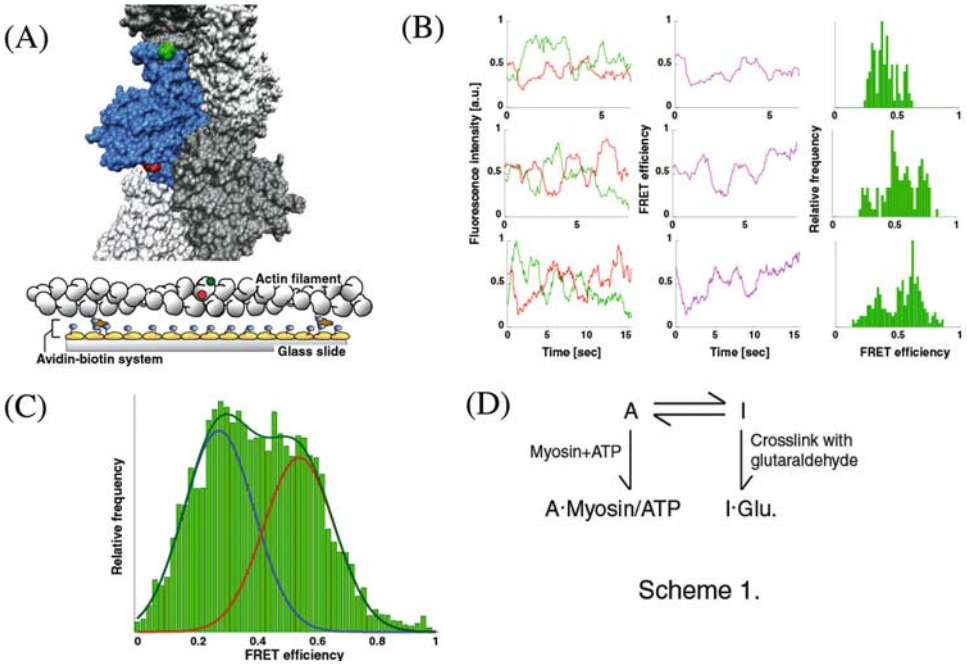

Figure 30.1. Dynamic conformation of actin. (A) The dynamic conformation of actin was measured using single molecule FRET with a donor at Gln 41 and an acceptor at Cys 374. The doubly labeled actin was polymerized with large excess of unlabeled actin (1:2000). F-actin was attached through an avdin-biotin system to a glass surface. (B) Time dependence of FRET from actin. (left) time dependence of donor (green) and acceptor (red) fluorescence. (middle) time dependence of FRET efficiency. (right) histogram of the FRET efficiency. Each row represents different molecule. (C) Histogram of the FRET efficiency summed over numbers of actin molecules. The histogram was best fit to two Gaussian distributions (blue and red) (D) Actin conformation varied between two conformational states A and I. When myosin is bount to actin in the presence of ATP, the population of the conformational state is shifted to active state for myosin motility and when actin is glutaraldehyde crosslinked, it is shifted to inactive state.

activates the myosin motility large amount of myosin V was added to actin filament in the presence of ATP. Under this condition the FRET efficiency varied to smaller extent as compared with the data in the absence of myosin. The FRET efficiency range (0.4–0.7) and mean value (~0.55) correspond to the high FRET efficiency state of actin filament alone. Low FRET efficiency value was hardly observed in the time trajectory. The actin filament chemically modified with glutaraldehyde was used for the state in which the motility of myosin is inhibited. Glutaraldehyde makes intramolecular and intermolecular cross-links through the amino groups that inhibited the motility of myosin without interfering with the actomyosin binding or with the actomyosin ATPase activity (Prochniewicz and Yanagida, 1990). The variation of the FRET efficiency with time was smaller than that of intact actin. The range of the FRET efficiency was mainly between 0.1 and 0.5, similar to the range of the low FRET efficiency state of non-cross-linked actin filaments. The population at the high FRET efficiency values was largely reduced. Thus the binding of myosin shifts the population to the high FRET state or the state that activates the myosin motility. The chemical crosslinking shifted the actin population to the low

FRET state or the state that inhibits the myosin motility. Considering these results together, it is concluded that actin fluctuates conformations between states that activate and inhibit the myosin motility (Figure 30.1D).

The change in the FRET efficiency due to the binding of myosin was mainly due to the distance change between the donor and acceptor probes. The distance between the donor and acceptor was calculated to be 6.2 nm from the mean FRET efficiency of 0.39 with assumption that the orientation of the fluorescence probes were randomized during measurement time (60 ms). This value agrees with the distance of 5.1 nm between the Gln-41 and Cys-374 sites estimated from a model for filamentous actin which is derived from X-ray fiber diffraction studies in association with the crystal structure of monomeric actin (Holmes et al., 2003) when one considers the additional distance between the amino acid positions and the dipoles of TMR and IC5 (~0.7 nm for TMR and ~1.2 nm for IC5). The contribution of the orientation changes to the FRET efficiency change seemed small, because single molecule polarization measurements showed that the change of the orientation of the probes with time was small and the contribution of changes in probe orientation to change in the FRET efficiency seemed small.

The conformational changes may involve the rotation of actin filament. DNase-I binding loop and the C-terminus where the fluorescent probes are attached are the locations where the conformational changes are most likely to occur according to structural studies. The atomic structure of the actin molecule shows that the structure of the DNase-I binding loop can change between a loop and a helix (Otterbein et al., 2001). Electron microscopy studies show a tilting of actin subunits (Galkin et al., 2002) and that the C-terminus can move between the inside and outside edge of the filament, which is consistent with their change in the layer line of diffraction originated from actin filaments in muscle. This change in the structure most likely leads to the rotation observed in actin filaments. Such changes may lead to a large variability in the repeat of the long pitch two-stranded actin helices. Many investigations have suggested that this variability in rotation is important for force generation with and without myosin.

30.2. BIASED BROWNIAN MOVEMENT OF MYOSIN

Using a scanning probe microscopy, we have shown that muscle myosin heads step stochastically along actin filaments with actin monomer repeats of 5.5 nm (Figure 30.2) (Kitamura et al., 1999). The direction of the steps is mainly in one direction but occasionally in opposite direction. The results were interpreted that the step movement along the actin monomer is thermally driven and the direction is biased to one direction. The number of steps in one displacement distributed 1–5 or 5–30 nm. In the presence of high load up to 4 pN, which was attained by using stiff needle, the number of the steps in a displacement decreased and the interval time increased, while the stepsize was constant, 5.5 nm (Kitamura et al., 2005). From the interval time between 5.5 nm steps at various force levels, the force-velocity curve of individual myosin heads was obtained. The force-velocity curve for individual myosin molecules is basically same as that of muscle. Thus the fundamental mechanical properties of muscle is originated from the stochastic nature of individual myosin molecules.

The 5.5 nm steps occurring stochastically in forward and backward directions are described using free energy landscape. Brownian particles are supposed to move in an

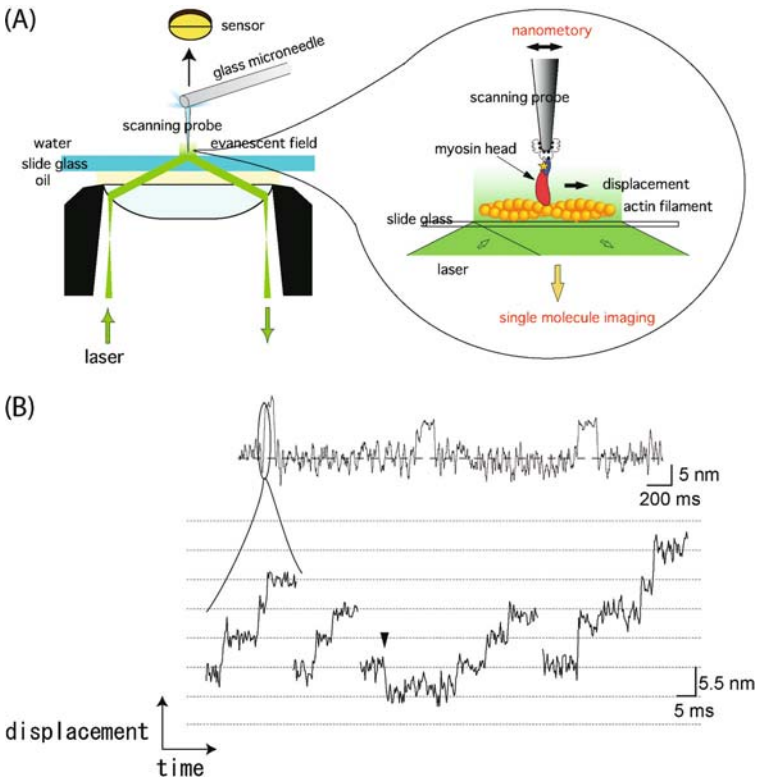

Figure 30.2. Substeps of muscle myosin within a displacement during the hydrolysis of single ATP molecules. (A) Single molecule of a myosin head was attached to a tip of a scanning probe. It was confirmed by single molecule imaging that attached molecules was single. The myosin head attached to the scanning probe was let interact with actin filaments immobilized on the slide glass. In the presence of ATP the single myosin head moved along an actin filament and its displacement was measured by monitoring the displacement of the tip of the scanning probe. (B) Typical trace of the displacement of the single myosin head. (top) stepwise displacement was coupled to the hydrolysis of single ATP molecules. (bottom) the trace in the rising phase was plotted in an expanded scale. Substeps were observed with the size of 5.5 nm.

asymmetric potential. When the particle has thermal energy greater than the activation barrier energy $u_+ + Fd_+$ for the forward step, and $u_- - Fd_-$ for the backward step, where u_+ and u_- an activation free energy barrier, F external force, and d_+ and d_- a characteristic distance for the forward and backward steps, respectively. The ratio of the numbers of the forward and backward steps N_f/N_b are related to the potential difference as $\Delta u - Fd = \ln(N_f/N_b)$, where $\Delta u = u_+ - u_-$, $d = d_+ + d_-$. As load increased, the ratio of the number of the forward step to the backward step decreased. The difference in the activation free energy between the forward to backward step was 2–3 k_BT. Several models have been proposed to explain the asymmetric potential. The conformational change in actin filament is one possibility. The other possibility is steric compatibility of the interaction between myosin and actinn filament. The myosin heads attached to the scanning probe bend and rotate around the axis of the actin filament when they move along a protofila-

ment of actin. Thus the binding to the binding site in the forward direction is favourable because myosin and actin are sterically compatible.

Similar 5.5 nm steps within single rising displacement were also observed for unconventional myosin V and VI using the same technique. Unlike muscle myosin, these two-headed myosins move successively with large stepsize of 36 nm in a hand-over-hand manner. A long neck region of myosin V is thought to be responsible for long stepsize but for myosin VI the neck region is too short to explain large stepsize. When single molecules of one-headed myosin V was attached to a scanning probe, stepwise movement was observed in the single rising displacement coupled to the hydrolysis of ATP. The stepsize of the substep was constant 5.5 nm regardless of experimental conditions. The 5.5 nm steps occurred in a stochastic manner and the interval time increased when the temperature decreased. The direction of the steps was mainly in one direction but occasionally in opposite direction. The difference between activation barrier energy between the forward and backward directions was 2–3 k_BT. Thus, the 5.5 nm steps are not only characteristic for muscle myosin but basic nature of the movement of myosin. The substep of myosin has been observed only with manipulation of single myosin molecules by a scanning microscope. The manipulation of actin filaments with a laser trap method, the substeps cannot be identified because of compliant linkage between protein molecules and beads which result in low signal to nosie ratio.

The total number of the 5.5 nm steps within an single ATPase-coupled displacement was limited less than 7 steps. There are several possible factors to stop the movement including a strain sensor, conformational changes and chemical reactions of nucleotide. Among them is geometrical restriction due to the protein arrangement in the measurements. The maximum number of the total steps, 7, is the number of the actin monomer contained in an half pitch of the filament. The myosin heads attached to a scanning probe binds to any of actin monomers in the filament configuration and moves along one of the actin protofilaments downwards the potential. Changing tracks to the other actin strand is unfavorable, since myosin head is required to bend and rotate. Finally the step movement of myosin head is blocked by the glass surface. Thus movement of myosin heads is restricted within a half pitch of the filament.

30.3. MYOSIN MOVEMENT IN MUSCLE ARRANGEMENT

In muscle, myosin molecules and actin filaments are arranged in organized manner. Myosin molecules assemble into the myosin filaments through their tail domain (Figure 30.3). The myosin heads protrude from the bundles of the tail domain every 14.3 nm in a helical arrangement with a pitch of 42.9 nm. The myosin and actn filaments are interdigitated and anchored at their ends to M- and Z-lines, respectively. An actin filament interacts with three surrounded myosin filaments. It has been reported that when the myosin and actin filaments are organized in this arrangement, the sliding distance per an ATP molecule is greater than 60 nm much longer than myosin heads isolated. The enhanced distance of myosin movement should be ascribed to the cooperative action between myosin molecules in this arrangement.

In the filament myosin heads are not allowed to move freely so the myosin heads behave rather like heads on the tip of a scanning probe. The rotation of actin filaments

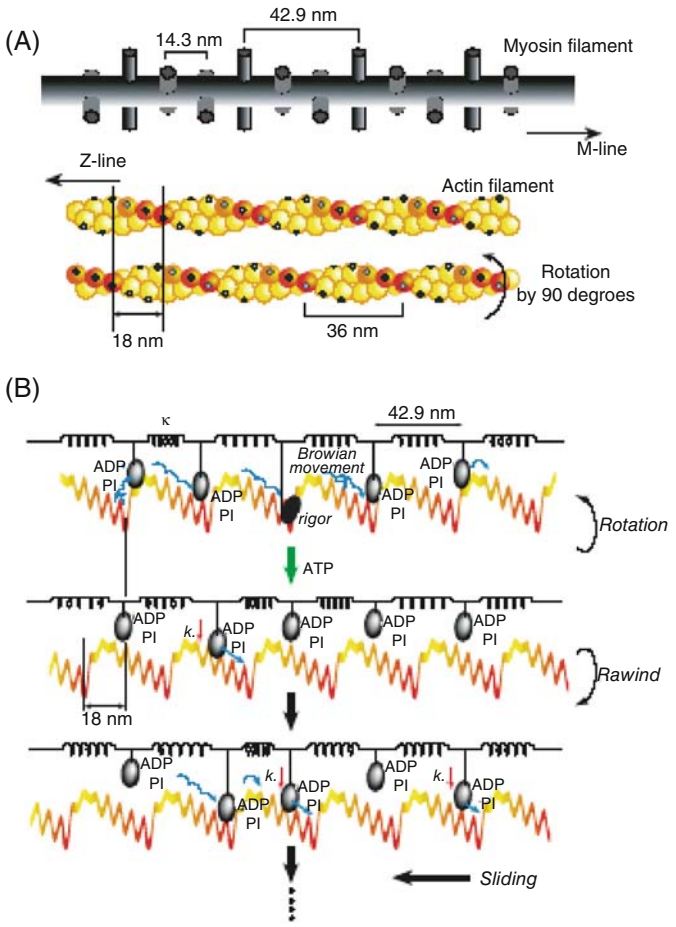

Figure 30.3. Enhanced displacement distance due to cooperative action between multiple myosin heads on the filament in muscle arrangement. (A) Arrangement of myosin filament. Myosin heads are protruded form the bundle of myosin tails. (B) Two-stranded actin filament rotates during force generation by myosin. (C) Qualitative explanation of cooperative action of myosin heads on the myosin filament. A myosin filament is represented by a row of myosin heads connected with springs. An actin filament is represented by a straight, periodic saw-tooth shape potentials along the half helical pitch. Cooperative action of myosin heads causes a long sliding distance per single ATP hydrolysis.

is also suppressed in muscle arrangement. In muscle, myosin heads move most likely in the same potential as described for the scanning probe measurements. In a half helical pitch, periodic potential is tilted along one strand of actin filament as in the scanning probe measurements and at the position where the strand reaches the opposite side of the myosin filament on the surface of actin filament, the potential jumps up to the original level. Thus the potential repeats with periodicity of a half pitch of the actin filament. In muscle most of myosin heads are in the weak binding state with Pi and ADP and stays near the bottom of the tilted potential. When the Pi and ADP from one of the heads is

released, actin filament rotates 90° as reported in muscle (Wakabayashi et al., 2001). The possibility of the rotation of actin filament was also suggested from the dynamic conformation of actin as mentioned above. The rotation of actin filaments changes the relative position of the myosin heads and actin filament and is equivalent with the shift of the potential by 3 actin monomers. Then myosin heads move again following the shifted potential slope. Then the binding of ATP molecule to myosin is followed, resulting in the dissociation of myosin from the actin filament and rewinding of the actin filament. After the rotation of the actin filament, one head moves towards the bottom of the potential. Then, two or three heads, dissociated from actin by the rotation, interact with the actin filament and exert force on the actin filament in the forward direction. The force is sufficient enough for other head to move to the next helical pitch. Thus myosin heads move for long distance.

The possibility was tested by simulating the movement of myosin in muscle arrangement. The simulation was performed by numerically solving the Langevin equation. The large displacement was demonstrated (Kitamura et al., 2005). In this case, the displacement is not coupled to the ATP hydrolysis.

30.4. CONCLUSIONS

This report showed that the movement of single muscle myosin head attached to a scanning probe occurs stochastically with actin monomer repeats of 5.5 nm. Recently similar substeps were observed for single headed myosin V and VI, suggesting that this mechanism is common for many types of myosins. The stepsize is limited within a half pitch of a half helical pitch of the actin filament for the myosin head attached to the scanning probe, whereas the stepsize is largely enhanced in muscle arrangement. The enhancement can be explained by cooperative action between the myosin head on the myosin filament. Also the rotation of actin filament is shown to play an important role. The rotation of the actin filament is suggested by observation of the dynamic structure of single actin molecules in the filament. Structural studies using EM suggested that the direction of the swinging of the lever arm is perpendicular to the longitudinal axis of the actin filament. In the actomyyosin motors, the rotational motion is converted to linear momtion. Evolutionary, the origin of the molecular motors may be a rotary motor and actomyosin motors are linear motors evolved from rotary motors.

30.5. REFERENCES

Galkin, V. E., VanLoock, M. S., Orlova, A., and Egelman, E. H., 2002. A new internal mode in F-actin helps explain the remarkable evolutionary conservation of actin's sequence and structure. *Curr. Biol.* **12**(7):570–575.

Harada, Y., Sakurada, Y., Aoki, T., Thomas, D. D., and Yanagida, T., 1990. Mechanochemmical coupling in actomyosin energy transduction studied by *in vitro* movement assay. *J. Mol. Biol.* **216**:49–68.

Higuchi, H., and Goldman, Y. E., 1991, Sliding distance between actin and myosin filaments per ATP hydrolyzed in skinned muscle fibers. *Nature* **35**:352–354.

Holmes, K. C., Angert, I., Kull, F. J., Jahn, W., and Schroder, R. R., 2003. Electron cryo-microscopy shoes how strong binding of myosin to actin releases nucleotide. *Nature* **425**(6956):423–427.

Ishii, Y., Yoshida, T., Funatsu, T., Wazawa, T., and Yanagida, T., 1999. Fluorescence resonance energy transfer between single fluorophores attached to a coiled-coil protein in aqueous solution. *Chem. Phys.* **247**:163–173.

Kitamura, K., Tokunaga, M., Esaki, S., Iwane, A. H., and Yanagida, T., 2005. Mechanism of mucle contraction based on stochastic properties of single actomyosin motors observed *in vitro*. *Biophysics* **1**:1–19.

Kitamura, K., Tokunaga, M., Iwane, A. H., and Yanagida, T., 1999. Single myosin head moves alon an actin filament with regular steps of 5.3 nanometers. *Nature* **397**:129.

Kozuka, J., Yokota, H., Arai, Y., Ishii, Y., and Yanagida, T., 2006. Dynamic polymorphism of single actin molecules in the actin filament. *Nat. Chem. Biol.* **2**(2):83–86.

Otterbein, L. R., Graceffa, P., and Dominguez, R., 2001. The crystal structure of uncomplexed actin in the ADP state. *Science* **293**(5530):708–711.

Prochniewicz, E., and Yanagida, T., 1990. Inhibition of sliding movement of F-actin by crosslinking emphasizes the role of actin structure in the mechanism of motility. *J. Mol. Biol.* **216**(3):761–772.

Wakabayashi, K., Ueno, Y., Takezawa, Y., and Sugimoto, Y., 2001. Muscle contraction mechanism: Use of X-ray synchrotron radiation. Nature Encyclopedia of life science pp. 1–11.

Yanagida, T., Arata, T., and Oosawa, F., 1985. Sliding distance induced by a myosin crossbridge during one ATP hydrolysis cycle. *Nature* **316**:366–369.

Yanagida, T., Esaki, S., Iwane, A. H., Inoue, Y., Ishijima, A., Kitamura, K., Tanaka, H., and Tokunaga, M., 2000. Single-motor mechanics and models of myosin motor. *Phil. Trans. R. Soc. Lond. B* **255**:441–447.

31

ON THE WALKING MECHANISM OF LINEAR MOLECULAR MOTORS

Kazuhiko Kinosita, Jr.[1], Katsuyuki Shiroguchi[1], M. Yusuf Ali[2], Kengo Adachi[1] and Hiroyasu Itoh[3,4]

31.1. WALKING LIKE A HUMAN?

Many of linear molecular motors, such as myosins and kinesins, have two "feet" (traditionally called "heads" or "motor domains") that bind to a motor-specific track and that each host a catalytic site for hydrolyzing ATP to power unidirectional movement along the track (Kinosita et al., 1998, 2005; Vale and Milligan, 2000; Mehta, 2001; Endow and Barker, 2003; Schliwa and Woehlke, 2003; Vale, 2003; Sablin and Fletterick, 2004). Some of the linear motors, such as conventional kinesin (Brady, 1985; Vale et al., 1985; Howard et al., 1989; Block et al., 1990; Svoboda et al., 1993), myosin V (Cheney et al., 1993; Mehta et al., 1999; Sakamoto et al., 2000), myosin VI (Kellerman and Miller, 1992; Wells et al., 1999; Rock et al., 2001; Nishikawa et al., 2002), and plant myosin XI (Tominaga et al., 2003), are processive, in that a single motor molecule proceeds along a filamentous track for many ATPase cycles without detaching from the track. That the two feet never detach simultaneously from the track (or the ground in case of a human) is an important feature of "walking," as opposed to "running" (Kinosita et al., 1998). In addition, at least for myosin V and conventional kinesin which are known to be processive, convincing evidence exists that these motors throw their two feet forward alternately in a hand-over-hand fashion (Yildiz et al., 2003, 2004; Asbury et al., 2003; Kaseda et al., 2003; Warshaw et al., 2005), just as a human does. In myosin V which has two long and stiff legs (we refer to as a "leg" the light-chain binding domain and associated light chains of myosin V; see Figure 31.1; in the literature this part is often referred to as a "lever arm"), fluorescence polarization measurements have indicated that each leg changes its orientation every time the myosin steps (Forkey et al., 2003), consistent with man-like walking. Recently we have succeeded in attaching a microtubule, as a micron-sized marker, to a leg of myosin V; we observed the microtubule to lean forward and backward

[1] Department of Physics, Faculty of Science and Technology, Waseda University, Okubo 3-4-1, Shinjuku-ku, Tokyo 169-8555, Japan, [2]Department of Physics, Faculty of Physical Sciences, Shahjalal University of Science and Technology, Sylhet-3114, Bangladesh, [3]Tsukuba Research Laboratory, Hamamatsu Photonics KK, and [4]CREST "Creation and Application of Soft Nano-Machine, the Hyperfunctional Molecular Machine" Team 13*, Tokodai, Tsukuba 300-2635, Japan

Regulatory Mechanisms of Striated Muscle Contraction
Edited by Ebashi and Ohtsuki, Springer, 2007

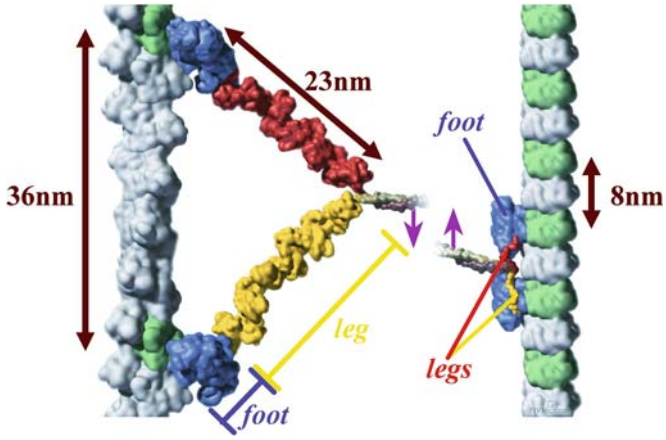

Figure 31.1. Structural models of myosin V (left) and conventional kinesin (right), adapted from Vale and Milligan (2000). Purple arrows show the direction of motor movement. Left, two feet (heads) of myosin V are shown in blue, the lead leg (light chain binding domain to which six calmodulin light chains are bound) in yellow, and the trail leg in red. The two legs merge with each other to form a coiled coil of α helices (colored gray). Each foot is bound primarily to an actin monomer in green, the front one being the thirteenth monomer from the rear one on the right-handed double helix of filamentous actin (gray). Right, two feet of conventional kinesin are shown in blue, the lead leg and trail leg in red and yellow, respectively. Kinesin's two legs also merge into a coiled coil (colored gray). Each foot is bound primarily to a β tubulin (light green; α tubulin in gray) in a protofilament of a microtubule.

on an actin filament as the motor stepped along the filament with an average step size of ~36 nm (Shiroguchi and Kinosita, 2005). All these observations indicate that two-foot processive motors do "walk," in that there are moments when both feet are landed on the track, one in front of the other, and that subsequent movements are lifting of the rear foot followed by landing on a position ahead of the pivoting foot. To what extent, then, does the walking mechanism of molecular motors resemble that of a human?

When a man walks, he relies heavily on the mass. Thus, he will allow gravity to pull his lifted foot down, instead of pushing it with his muscles. The foot that has come down will be carried forward by inertia, without requesting much help from muscles. If you attach a big balloon at his head to watch, from far above, how he moves forward, as done in a single-molecule assay, the balloon would move steadily forward with little sign of discrete stepping, because a human being normally exploits the inertia of the body to make movement as smooth as possible. Last but not least, a man does not have to cling to the ground to stay on, except possibly in a typhoon.

For biological molecules in an aqueous environment, mass is virtually absent, whether gravitational or inertial. A protein molecule never sinks toward the bottom of a tube, unless spun in an ultracentrifuge for long hours. This is because the mass is so small and the Brownian motion, or bombardment by surrounding water molecules, is so vigorous. A processive molecular motor must cling tenaciously to its track; otherwise the motor is immediately blown away by Brownian motion. Inertia is also negligible. In the absence of an external force, a protein molecule stops moving in a unique direction in a matter of 10^{-12} seconds, or within 0.1 nm, and begins to undergo a completely random Brownian fluctuations. This is due to the enormous viscous friction exerted by the aqueous

environment, compared to the inertia (Purcell, 1976). If you observe a molecule moving steadily in one direction, it must be pushed (or pulled) all the way by a force.

Another critical difference between a two-foot molecular motor and human being is that a molecular motor does not have a right and a left foot. The two feet, and the two legs, are completely identical. An expected consequence is that the motor would adopt precisely the same posture every time it steps, not every two steps as in human walking. A prediction that follows is that the motor body would rotate by 180° every time the motor steps (Howard, 1996), but this has not been observed so far (Hua et al., 2002; Ali et al., 2002, 2004).

The two identical legs of a molecular motor are joined at their base in twofold symmetry to form a coiled coil of α helices (Kozielski et al., 1997; Li et al., 2003; see Figure 31.1). If one foot points to the west, the other foot would point to the east. When the two feet bind to the track simultaneously, though, the two must be oriented in the same direction dictated by the structure of the binding sites on the track. Pointing both toes to a same direction is a natural posture for a human, but, for a molecular motor, doing so would require awkward bending and/or twisting of its legs (Kinosita et al., 2005). The legs thus must be flexible, yet they have to produce forward movement against a backward load.

31.2. HOW MOLECULAR MOTORS MAY WALK

31.2.1. Free Joints in the Legs

Orienting both toes forward is easy if there is a free joint(s) in the legs. For muscle myosin (myosin II), optical anisotropy decay measurements have revealed the existence of a free joint at the leg-hip junction, as shown in Figure 31.2 (Kinosita et al., 1984; Ishiwata et al., 1987). Electron micrographs of myosin V have indicated that this myosin also has a free joint at the leg-hip junction (Walker et al., 2000). The junction is the point at which the coiled coil of α helices branches into two individual helices (Figure 31.1), and thus melting of just one turn of the helix suffices to form a free joint, even though the rest of the helix is reinforced by light chains. In myosin VI, an upper part of the leg, unprotected by light chains, is flexible over ~80 amino-acid residues (Rock et al., 2005). In kinesin which lacks light chains that cover the legs, the entire portion of the legs (called "neck linkers" in the literature; see Figure 31.1) is likely flexible. In the original crystal structure (Kull et al., 1996), the leg portion of kinesin was disordered.

With the free joints, taking a standing posture with both feet on the track and both pointing forward will not result in an energy-consuming strain. Also, a free joint(s) in each leg implies that the body (the coiled coil portion) has a considerable freedom of rotation in the standing posture, around the axis of the body. A 180° rotation of the body in either direction can be achieved simply by crossing the two legs below the free joints. This would explain the above-mentioned failure in observing 180° rotations in processive motors: a slight hindrance against the rotation, likely introduced by the attachment of a probe for the observation, would suffice to induce leg crossing to counter the rotation (Kinosita et al., 2005).

With the free joints, then, does the motor gait appear similar to a human's except for the possible leg crossing? A free joint, made of single bonds between amino-acid residues, will allow rotation virtually in all directions unless hindered by steric constraints. Thus, a leg, once lifted, may go forward through many routes, passing the other leg on the left

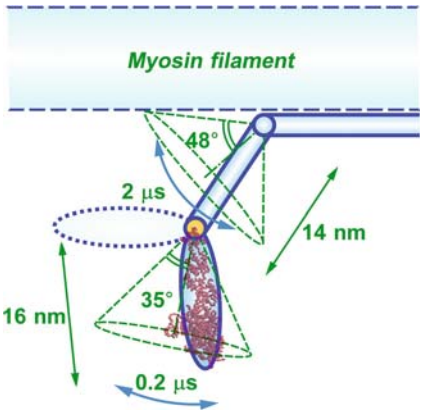

Figure 31.2. Rotational Brownian motion of muscle myosin (myosin II) on a myosin filament. In a muscle, many myosin molecules are bundled parallel to each other to form myosin filaments, from which myosin feet (and legs) protrude into surrounding medium. Rotational Brownian motion of the feet was assessed by attaching a dye molecule to the foot and measuring the absorption or phosphorescence anisotropy decay after pulsed and polarized excitation of the dye (Kinosita et al., 1984; Ishiwata et al., 1987). The motion could be modeled as wobbling of a prolate ellipsoid of size 16 nm in a cone of semiangle 35°, which in turn wobbles in another cone of semiangle 48°. The size of the prolate matches that of a foot-leg portion of myosin II, as shown in pink in the figure (the structure shown is that of scallop myosin binding MgADP·VO_4, from Houdusse et al., 2000). The result suggests that the two legs of myosin II are connected to the coiled coil (rods shown in blue solid lines in the figure) through a free joint (yellow).

or right side, or even from above as has been suggested in the electron micrographs of myosin V (Walker et al., 2000). The motion of the lifted leg must be a Brownian one, seeking all possible routes randomly and changing the direction continually. The lifted leg will move forward and backward basically with equal probabilities.

31.2.2. How to Move Forward

The hand-over-hand mechanism implies that a processive motor alternates between two-foot and one-foot bindings to the track, as has been demonstrated, for example, for kinesin (Kawaguchi and Ishiwata, 2001). To move forward and not backward, a molecular motor, without a brain, must make a correct choice mechanically at least twice in a cycle. Thus, when both feet are on the track, the motor must choose the correct foot (trail foot) to bring up. Then, the lifted foot must land on a forward, not backward, binding site. The prevailing theory for the choices is that a strain-dependent mechanism warrants the lifting of the trail foot and a lever action in the landed foot biases the motion of the lifted foot forward to assure forward landing.

31.2.3. Which Foot to Bring Up

When both feet of a processive molecular motor are landed on the track during normal walking, the chemical states of the two feet, whether they bind ATP, ADP plus phosphate, ADP, phosphate, or none, may well be different. Feet in different chemical states are expected to show different affinities for a landing site on the track. Thus, a

motor could in principle rely on the sequence of hydrolysis reaction to choose the correct foot to lift, the foot with a weak affinity, because the reaction phase on the trail foot is expected to be ahead of the phase on the lead foot. However, chemical reactions are stochastic and basically reversible. A choice relying solely on the simple phase difference cannot be robust: occasionally the two feet may fall into a same chemical state.

To warrant correct choice, or to insure a proper phase difference between the chemical reactions in the two feet, a motor probably exploits the difference in strain in the two feet (Hancock and Howard, 1999; Mehta, 2001). Because the two feet are connected to each other through the legs, the trail foot is pulled forward while the lead foot is pulled backward in the two-foot landing posture. The difference in the strain could modulate the affinity of the foot for the track, or the preference of the foot for a particular chemical state.

The expected strain dependence has recently been demonstrated in a persuasive experiment by Uemura and Ishiwata (2003). They pulled kinesin along a microtubule either forward or backward, and examined whether detachment of a bound foot required a weak or a strong force (Figure 31.3). Kinesin's affinity for a microtubule is known to be weak when it binds ADP (Hackney, 1994; Uemura et al., 2002). Under the physiological MgADP concentration of ~10^{-4} M, Uemura and Ishiwata found that a weak forward pull was sufficient to detach a bound foot from a microtubule, whereas a backward pull often had to be strong to induce detachment (Figure 31.3). Thus, from a two-foot landing state, a trail foot under a forward strain will be readily detached while a lead foot remains bound.

The ADP dependence of the strain effect (Figure 31.3, right) is revealing: a forward pull increases the affinity of a kinesin foot for ADP (dissociation constant 13 μM), whereas a backward pull decreases the affinity (dissociation constant 86 μM). The interpretation is

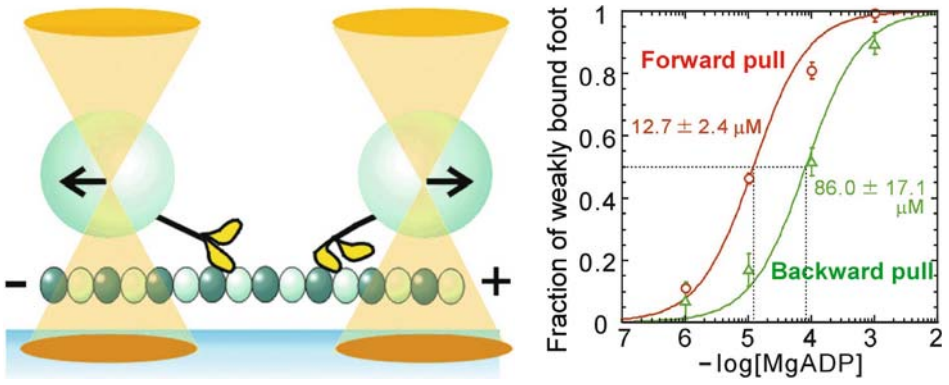

Figure 31.3. Strain-dependent detachment of kinesin from a microtubule, adapted from Uemura and Ishiwata (2003). A single kinesin molecule was attached to a plastic bead and the bead was pulled along a microtubule with optical tweezers at a constant speed. The kinesin repeatedly attached to and detached from the microtubule, and the force required for each unbinding event, presumably involving only one of the two feet under the experimental conditions employed, was estimated from displacement of the bead from the trap center. The unbinding force could be classified into a weak and a strong class, and the fraction of weakly bound events is plotted in the graph on the right, as a function of the MgADP concentration in the medium. When a foot binds MgADP, its affinity for a microtubule is expected to be low, compared to a foot without a nucleotide (or a foot binding ATP which was absent in this experiment).

as follows. Binding of ADP to a kinesin foot induces a conformational change of the foot such that its affinity for a microtubule decreases. By the law of action and reaction, then, inducing that conformational change by an external (or internal) agent should increase the affinity of the foot for ADP. A forward pull is just such an agent. A forward pull tends to change the conformation of the foot into the one that shows a low affinity for a microtubule and that also shows a high affinity for ADP (let us call this a lifting conformation). A backward pull, on the other hand, tends to stabilize the conformation with a high affinity for a microtubule and low affinity for ADP. A similar argument applies to F_1-ATPase, where ATP binding induces counterclockwise rotation and counterclockwise rotation increases the affinity for ATP (Yasuda et al., 2001; Kinosita et al., 2004).

Kinetically, two scenarios are possible: pulling a kinesin foot forward induces ADP binding, halfway toward the lifting conformation, and the ADP binding accelerates the conformational change to final foot lifting; or, a forward pull may lift a foot before it binds ADP and then the lifted foot binds ADP, which will prevent re-landing. Either way, the end result is a foot that binds ADP and that is dissociated from the microtubule. The choice between the two scenarios must be a stochastic one. Either may predominate over the other, but both must take place in the long run. In the world of molecules working with energies of the order of thermal energy, k_BT, where k_B is the Boltzmann constant and T the absolute temperature (e.g., a tenfold difference in affinity corresponds to a free-energy difference of $2.3\,k_BT$), anything can happen, albeit rarely (a process requiring $10\,k_BT$ would take place, in the absence of an external energy supply, once in exp(10) ~ 20000 trials, on the average).

Note that the argument above also applies to normal walking where the ADP state is reached by phosphate release from the ADP+phosphate state. Release of phosphate tends to induce the lifting conformation, and a forward pull promotes the phosphate release. By the law of action and reaction, a backward pull prevents the release of phosphate, keeping the foot landed.

Recently, strain-dependent detachment of a single foot of mouse myosin V from actin has directly been observed in a construct composed of a single foot connected to a single leg carrying six light-chain binding motifs (Veigel et al., 2005). A forward pull at 1.4 pN at 3 μM ATP reduced the lifetime of attachment from 390 ms to 170 ms, whereas a backward pull at 2.4 pN increased the lifetime to 733 ms. Similar, but somewhat different, results have been reported for single leg-foot constructs of chicken myosin V (Purcell et al., 2005). For the construct carrying six light-chain binding motifs, a forward pull at ~2 pN at 1000 μM ATP resulted in dissociation from actin at the rate of $15\,s^{-1}$, which was close to the rate at no load. A backward pull at ~2 pN, on the other hand, significantly reduced the dissociation rate to $1.5\,s^{-1}$. Results at 10 μM ATP were not grossly different. In the case of myosin (V), detachment of a foot is considered to result from the release of ADP followed by ATP binding (De la Cruz et al., 1999; Rief et al., 2000). Thus, a forward pull presumably changes the conformation of a landed foot to one having a low affinity for ADP, and a backward pull stabilizes the conformation having a high affinity for ADP.

31.2.4. Which Way to Land: Lever Action and Biased Diffusion

After the proper, trail foot is lifted, the next problem is to let the lifted foot choose a correct site for landing. With a free joint(s) in the legs, no force can operate on the

lifted foot to move it forward. The foot can move only by Brownian motion, which carries the foot in either direction, with an equal probability unless biased. Yet the foot must land on a forward, not backward, site.

A mechanism that is widely accepted, at least for myosin (V), is the lever action, or an ankle action in the landed foot. A chemical reaction in the landed foot of myosin, presumably phosphate release, induces forward bending of the ankle, resulting in leaning of the stiff leg forward (Figure 31.4). This lever action, originally proposed for myosin II (Huxley, 1969; Huxley and Simmons, 1971), moves the hip portion forward. The Brownian motion of the lifted leg is thus biased forward, because the pivot(s) for the random rotational Brownian motion (yellow ball in Figure 31.4) has now been displaced forward by the active (= energy consuming) ankle action in the landed foot.

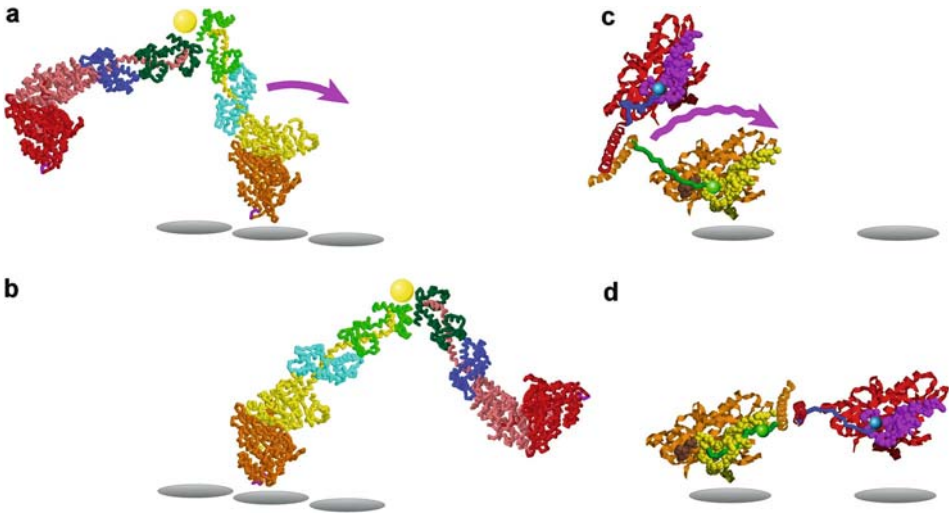

Figure 31.4. Lever action in two-foot motors which, in this figure, move toward right. (**a**, **b**) Scallop myosin. This myosin is non-processive, but its structure has been solved up to the leg portion. Postulated lever action is shown by an arrow: the dark-yellow leg (the long α-helix) rotates between *a* and *b*. Flexible joints likely exist around the location indicated by the yellow ball, beyond which the two α-helices form a coiled coil (not shown in the figure). Thus, the pink leg presumably undergoes rotational diffusion around the yellow ball. The lever action of the dark-yellow leg biases the Brownian motion of the red foot forward. Each figure is composed of two structures of scallop myosin subfragment 1 (S1), arranged arbitrarily. The orange foot/dark-yellow leg in *a* represents the structure of S1 binding MgADP·VO_4, and that in *b* is S1 without a nucleotide (Houdusse et al., 2000). The red foot/pink leg is S1 binding MgADP, which is supposed to mimic a structure immediately after detachment from actin (Houdusse et al., 1999). Cyan/blue, essential light chains; green/dark-green, regulatory light chains. The gray disks with a diameter of 5.5 nm represent myosin-binding sites on an actin filament. (**c**, **d**) Conventional kinesin. The blue and green legs ("neck linkers") between the balls are presumably flexible, and thus the red foot undergoes Brownian motion. The flexible green leg in *c* "docks" onto the dark-yellow portion of the orange foot, in an ATP-dependent process, through Brownian motion (wavy arrow). After docking (*d*), the Brownian motion of the red foot occurs around the green ball, and thus is biased toward the forward binding site. The docking is equivalent with the lever action in myosin. The docking site (magenta) in the red foot is yet to bind the blue leg (after landing). The gray disks with a diameter of 4 nm represent kinesin-binding sites on a microtubule. The figures are constructed from a structure of a dimeric kinesin (Kozielski et al., 1997) by assigning arbitrary structures to the neck linkers (except the green one in *d*) and orienting the central coiled coil (stalk) arbitrarily.

Structural evidence for the lever action includes, among others, early electron micrographs of myosin II which is not processive (Reedy et al., 1965), crystal structures of myosin II (Rayment et al., 1993; Houdusse et al., 1999, 2000), of myosin V (Coureux et al., 2003, 2004; Holmes et al., 2003) and of myosin VI (Ménétrey et al., 2005), and electron micrographs of myosin V (Walker et al., 2000; Burgess et al., 2002). Reversal of the motor direction by an artificial design of the ankle structure (Tsiavaliaris et al., 2004) strongly supports this biasing mechanism. Tilting of a (presumably landed) leg during walking has been demonstrated for myosin V (Forkey et al., 2003; Shiroguchi and Kinosita, 2005), although these observations do not necessarily show that tilting is the cause and not a result of forward motion. That tilting is an active, force producing event is best shown in single-molecule assays with a single-foot construct. For the processive motor myosin V, tilting results in a displacement (presumably of, or close to, the hip portion) of 20–25 nm (Moore et al., 2001; Veigel et al., 2002) that can take place against a backward load of more than 2 pN (Veigel et al., 2005). Another processive myosin, myosin VI that moves in the direction opposite to most other myosins (Wells et al., 1999), shows a single-leg displacement of 12 nm (Rock et al., 2005).

For kinesin without stiff legs, lever action in its genuine sense is not possible. Rice et al. (1999), however, have shown that the flexible leg of kinesin docks onto a landed foot upon binding of ATP. This will move forward the pivot for the Brownian motion of the lifted foot, biasing its diffusion forward (Figure 31.4). In effect, docking is equivalent to lever action.

31.2.5. Is the Lever Action Sufficient for Biasing?

It thus seems that the walking mechanism of molecular motors has basically been worked out. Strain-dependent lifting of the trail foot and a lever action in the landed foot/leg seem to warrant forward movement. Do we not miss something? The problem is this: biasing of diffusion by a lever action is unlikely to work under a high backward load.

Apparently the most serious example is myosin VI, which is processive and walks with long strides (Rock et al., 2001; Nishikawa et al., 2002), possibly the longest known of about 37 nm (Ali et al., 2004). The upper part of the legs of myosin VI is flexible over ~80 amino-acid residues with a contour length of 29 nm, and thus this portion cannot serve as a lever (Rock et al., 2005). The lower, presumably stiff light-chain binding part of the leg could form a lever, but its length (Ménétrey et al., 2005) seems to be at most ~10 nm. Yet myosin VI moves forward with step sizes of 30 ± 12 nm against a backward load of 1.7 pN (Rock et al., 2001). The backward load, presumably applied to the hip portion, would easily pull the hip backward, without suffering resistance from the flexible leg (Figure 31.5*a*). The pivot for the diffusion of the lifted leg would thus be on the rear side of the landed leg. The diffusion would be biased backward.

Kinesin with completely flexible legs faces a similar problem. The free-energy gain for docking is only a few k_BT (Rice et al., 2003). Thus, under a backward load, the landed leg would not be able to dock to bias the diffusion forward (Figure 31.5*b*).

The legs of myosin V are stiff, but not perfectly so. Its effective stiffness is 0.2 pN/nm (Veigel et al., 2002, 2005), implying that a backward pull at 2 pN will bring back the hip by 10 nm, almost canceling the forward bias (Figure 31.5*c*). Myosin V still moves forward under this load (Mehta et al., 1999; Rief et al., 2000).

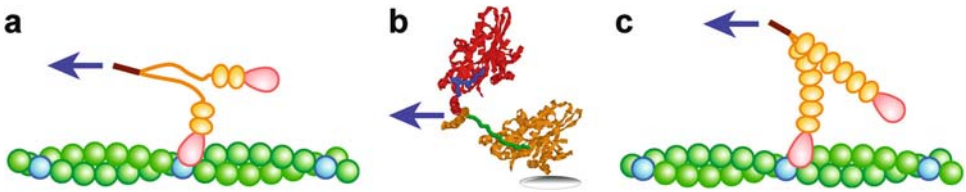

Figure 31.5. Moving against a backward force (arrows). (**a**) The upper part of the legs of myosin VI is flexible. Thus, a backward pull would bias the diffusion of the lifted foot toward a backward site. (**b**) The free-energy gain for docking in kinesin is only a few times k_BT. Thus, docking would readily be prohibited when the coiled-coil portion is pulled backward. (**c**) Under a backward force of 2 pN, the semi-rigid leg of myosin V is bent backward and the hip portion is pulled back by ~10 nm (Veigel et al., 2002). Forward bias for the diffusion of the lifted foot would thus be canceled.

There must be a mechanism, other than the lever action that moves the pivot forward, that warrants landing of the lifted foot on a forward site.

31.3. TOE UP-DOWN MECHANISM

31.3.1. Orienting the Lifted Sole Correctly

When a man lifts a foot while he walks, he immediately brings the toe down by unbending the ankle. When that foot is thrown forward, the sole will be correctly oriented for landing. Molecular motors may well adopt the same ankle action (Ali et al., 2004; Kinosita et al., 2005), because their sole must also be oriented correctly against a landing site on the track to allow stereospecific interactions between the two.

The lever action discussed above is forward bending of the ankle in a landed foot. The ankle, once bent, must be unbent in a walking cycle, in preparation for the next lever action. The unbending in this sense, for myosin, is often called "cocking" or "priming." Here we propose that unbending, or bringing the toe down, plays a more positive role of warranting landing on a correct, i.e. forward, site. The ankle action in a lifted foot (Figure 31.6*a*) may be equally, or possibly more, important than the ankle action in a landed foot.

Once the lifted toe is brought down, forward landing is natural because the sole is parallel to the track surface (Figure 31.6*b*), whereas backward landing would introduce a considerable strain in the leg (Figure 31.6*c*) and/or in the ankle. This is so even in the presence of a backward load. The load may pull back the hip portion to the rear side of the landed foot, but backward landing still results in a similar amount of strain (Figure 31.6*c*), whereas smooth forward landing ensues when the hip happens to move forward by Brownian motion. Of course forward motion of the hip should be infrequent under a high backward load, but this is consistent with the known load-dependent decrease in the stepping rate of molecular motors (Mehta et al., 1999; Visscher et al., 1999; Altman et al., 2004). In the case of myosin where landing sites are available close to a landed foot, the nearest being on the neighboring actin monomers at ±5.5 nm (see footmarks in Figure 31.6*b* and *c*; landing on a neighboring monomer, though, is not completely free of steric hindrance), landing under a high backward load might be on a nearby site. The motor then effectively stalls, as observed experimentally under a high load.

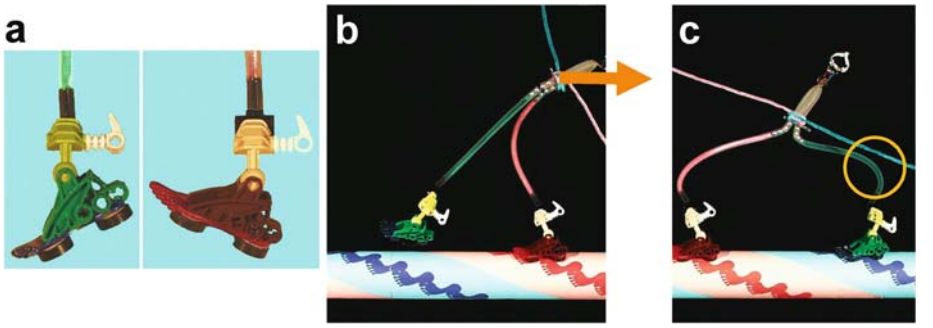

Figure 31.6. Ankle action in a walking molecular motor. (**a**) Ankle action, or toe up-down, changes the orientation of the sole relative to the leg. (**b**) With the lifted toe down, the sole becomes parallel to the track surface when the foot is thrown forward. Even when the hip is pulled backward (arrow), forward landing is assured, with a little bit of help by Brownian motion. (**c**) If the foot with its toe down is forced to land on a backward site, considerable strain, in the form of leg bending in the figure (orange circle), is introduced. Note that bending of the pink leg in *b* and *c* is due to the backward load (orange arrow) and does not contribute to biasing.

A nice feature of the toe up-down mechanism is that it will operate with flexible legs, as long as landing sites are far apart compared to the leg size (Ali et al., 2004; Kinosita et al., 2005). This seems to be the case for kinesin, for which the two flexible legs need to be fully extended to straddle two landing sites that are 8 nm apart (Figure 31.4*d*). As illustrated in Figure 31.7, a lifted foot with its toe down can land only on the forward site, because the orientation of the sole is restricted at the end of a fully extended leg. Here again, a backward load will pull back the pivot for the Brownian motion of the lifted foot, making forward landing infrequent. Backward landing would still be difficult, as shown in the second row in Figure 31.7. Note that, under a very high backward force, the toe up-down mechanism cannot warrant forward landing, but biased diffusion based on the lever action alone not only fails in warranting forward landing but would promote backward landing.

For myosin VI with two long legs that are stiff at the lower end but flexible in the upper portion, many landing sites are available on the actin track. This results in a broad distribution of step sizes (Rock et al., 2001; Nishikawa et al., 2002). With the toe down, backward landing should still be difficult, because a 36-nm back step would require an almost full extension of the legs and a shorter back step would require a bowlegged posture (Ali et al., 2004; Kinosita et al., 2005). Short steps, a few actin monomers backward or forward, may be allowed for myosin VI, but experimental detection of such short steps will be difficult.

When pulled back with a superstall force, a motor may walk backward as shown in Figure 31.7, bottom. The lead ankle would unbend (undock in the case of kinesin) and/or the lead leg would somehow be stretched to allow backward landing. Backward walking has indeed been observed for kinesin (Carter and Cross, 2005), although the high backward force often ripped the kinesin off the microtubule instead of allowing continuous backward steps. A similar observation has also been made on myosin V (Clemen et al., 2005), of which the legs are semi-rigid.

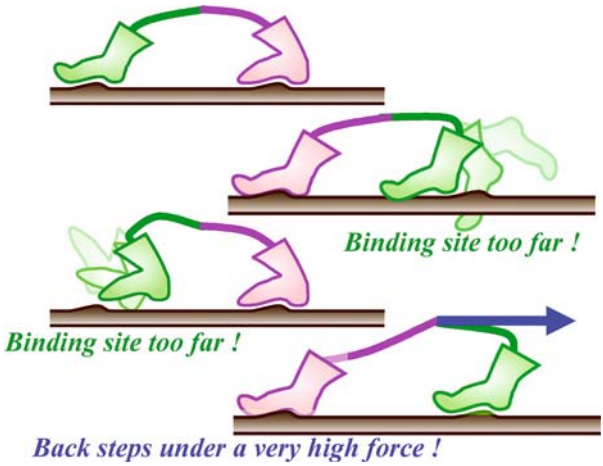

Figure 31.7. Toe up-down with flexible legs. If landing sites are far apart such that two-foot landing requires (almost) full extension of the two legs, with the lead toe down and trail toe up (top row), then a lifted foot (green in the second row) with its toe down cannot land on a backward site even if the other toe (pink) is also down. If, on the other hand, the toe remains up after lifting (green foot in the third row), forward landing would be prohibited. Under a very high backward load (fourth row), backward walking may take place if the lead ankle yields and/or the lead leg is somehow stretched. The backward walking will not be stable, because the lead foot tends to be detached. Recently, backward walking has indeed been observed for kinesin (Carter and Cross, 2005) and myosin V (Clemen et al., 2005).

31.3.2. Structural Evidence for Toe Up-Down

Is the toe up-down mechanism a mere conjecture? We note that crystal structures of linear motor proteins obtained so far are all without an associated track, and thus represent a structure of a lifted, not landed, foot. These structures do support the toe up-down mechanism (Figure 31.8), although they are often cited as a support for a lever action in a landed foot.

In Figure 31.8*a* and *b*, two crystal structures of scallop myosin (Houdusse et al., 2000) are compared. Although this myosin is not processive, structures of the processive myosin V are essentially similar to those of scallop myosin (Coureux et al., 2004). The foot in Figure 31.8*a* binds ADP and vanadate which is an analog of phosphate. Myosin is supposed to bind to actin when bound ATP is split into ADP and phosphate. Thus, the structure in Figure 31.8*a* represents the one prior to (and immediately after) binding to actin. As seen, the actin-binding site, or the sole, indicated by a purple bar is oriented in such a way that it faces the actin track when the leg leans backward or when the foot is thrown forward. This is a toe-down posture that warrants landing on a forward site. Figure 31.8*b*, on the other hand, shows a foot without a bound nucleotide. The lever action in a landed foot in myosin is considered to be driven by phosphate (and ADP) release, and thus the structure in Figure 31.8*b* presumably mimics the structure of a landed foot/leg prior to ATP-induced unbinding from actin. This structure, as seen, is a toe-up posture, which is to serve as a trail foot/leg in a two-foot landing phase.

In conventional kinesin, the docked structure (Figure 31.8*d*) presumably mimics a toe-up posture of a landed foot, because the docked leg (green) is extended in the

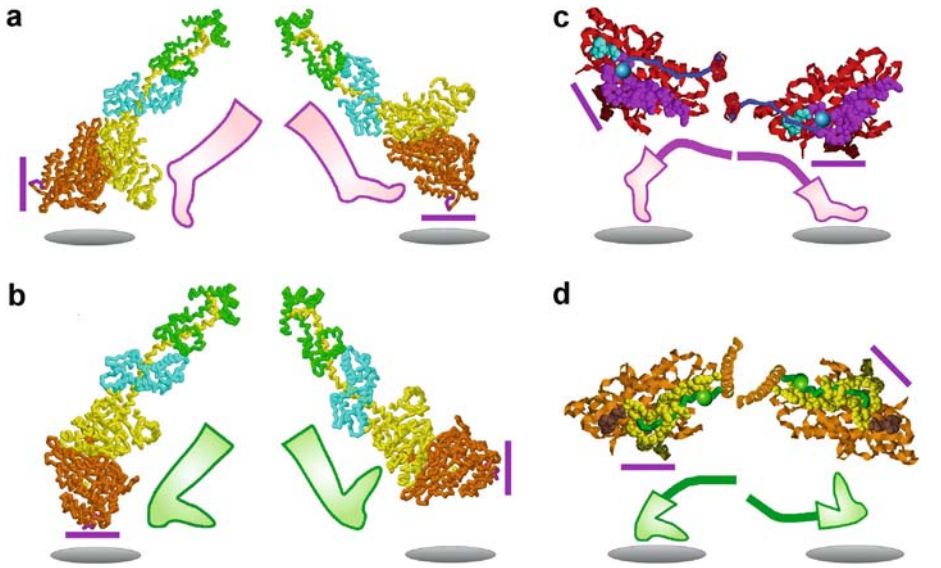

Figure 31.8. Structural evidence for toe up-down. **(a, b)** Myosin in a toe down **(a)** and toe up **(b)** conformation. Each panel shows two orientations of the same molecule. The leg/foot in *a* are the subfragment 1 (S1) of scallop myosin binding MgADP·VO_4, presumably representing a structure before and/or immediately after landing, and those in *b* are S1 without a nucleotide, probably mimicking a structure at the end of the lever action (Houdusse et al., 2000). Purple bars indicate the actin binding site, and gray disks represent myosin-binding sites on an actin filament. **(c, d)** Conventional kinesin with both feet in a toe down **(c)** and a toe up **(d)** conformation. The leg (neck linker) is shown in a backbone representation, and is undocked in *c* (blue) and docked in *d* (green). Atoms forming the docking site are shown in spheres (magenta in *c* and dark yellow in *d*). Cyan atoms in *c* show the position of an alternative docking site found in a related motor Eg5 (Turner et al., 2001). Large balls (blue in *c* and green in *d*) show the pivot for Brownian motion of the foot. Purple bars indicate the microtubule binding site, and gray disks represent kinesin-binding sites on a microtubule. The structures shown are one monomer in the dimeric kinesin structure (Kozielski et al., 1997), arranged in two arbitrary orientations in each panel; the α-helix in the coiled coil portion and the neck linker in *c* have been modified.

direction of motor movement to position the pivot (green sphere) on the forward side of the foot. This docked, toe-up posture is so designed as to serve as a trail foot/leg, as indicated by the green cartoon in Figure 31.8*d*. Upon lifting of the foot, the leg must undock to allow the lifted foot to reach the forward landing site. When undocked, the flexible leg will likely adopt all possible conformations excluding the docked conformation. Leg conformations close to the docked one will not be allowed, because of the interference with the residues forming the docking site. We consider the allowed, undocked conformations as toe-down postures (two examples shown in Figure 31.8*c*): these conformations, due to the steric interference, cannot serve as a trail foot/leg in two-foot landing, and these should include at least one conformation that serves as a lead foot/leg in two-foot landing (Figure 31.8*c*, right).

In an ADP-bound, and thus presumably lifted, foot of Eg5, a member of kinesin superfamily, the neck linker (leg) has been found to be docked onto a different site (cyan in Figure 31.8*c*) and assume an ordered structure (Turner et al., 2001; Sablin and Fletterick, 2004). For Eg5, this conformation likely dominates the toe-down postures. A

predominant conformation(s) may also exists in the toe-down postures of other two-foot kinesins including conventional kinesin, although the residues forming the alternative docking site appear to be unique to the Eg5 subfamily (Turner et al., 2001).

31.4. MECHANISMS THAT WARRANT FORWARD WALKING

We have discussed four mechanisms that together propel a two-foot, processive molecular motor forward: (1) a lever action that moves forward the pivot for diffusion of a lifted foot, (2) diffusion of the lifted foot, which is biased forward by the lever action unless a high backward load is applied, (3) toe up-down that biases landing toward a forward site, and (4) strain-dependent, preferential lifting of the trail foot. Of these, 1, 2, and 4 have been widely and extensively discussed in the literature.

Here we claim that 3 is equally important, particularly in the presence of a backward load. Under a high backward load, in particular, the role of lever action may well be auxiliary: preventing the pivot from moving too far back. With motors with flexible legs, even a small backward load should be sufficient to pull the hip portion to the rear side of the landed foot, neutralizing and even reversing the bias introduced by the lever action. Correct sole orientation dictated by toe up-down, evidenced by crystal structures, seems to be of vital importance in warranting forward walking. Quantitative appraisal of the toe up-down mechanism, such as the energy difference between the up and down postures or the dependence of diffusion and landing kinetics on the up/down states, awaits further studies.

In this article, we have focused on processive motors that have two identical feet. There are also one-foot motors, such as an unconventional kinesin KIF1A that moves processively along a microtubule, though not steadily in one direction (Okada et al., 2003), or myosin IXb (Inoue et al., 2002). The motion is essentially a one-dimensional biased diffusion on a filamentous track. Biasing in one direction requires force, as stated at the beginning. Production, within a motor, of a force that moves the motor forward, as opposed to a force that simply drives an internal conformational change, requires that part of a motor is firmly attached to the track against which the force operates. Thus, when a one-foot motor is in a biasing phase where the motor moves unidirectionally forward, the motor likely undergoes the following sequence: (i) one part of the motor is bound to the track, (ii) another part binds, resulting in two-spot binding, and (iii) the first part detaches, resulting in a net movement forward. This sequence is essentially the same as that in two-foot motors, except that the two binding events are not equivalent and that the motor may proceed to a diffusing phase after iii. Indeed, KIF1A has been shown to use two microtubule-binding loops alternately to bias its diffusion forward (Nitta et al., 2004). Conventional two-foot kinesin may also use the same tactics in a landed foot to move itself forward. That would be a lever action in the sense used in this article, in that it will move the pivot forward. Docking may not be the only way of moving kinesin' pivot forward.

31.5. ACKNOWLEDGMENTS

We thank M. Fukatsu for the toy model in Figure 31.6, and S. Ishiwata and the members of Kinosita lab for discussion. This work was supported in part by Grants-in-Aid from the Ministry of Education, Culture, Sports, Science and Technology of Japan.

M. Y. Ali was, and K. Shiroguchi is, a Research Fellow of the Japan Society for the Promotion of Science.

31.6. REFERENCES

Ali, M. Y., Uemura, S., Adachi, K., Itoh, H., Kinosita, K. Jr., and Ishiwata, S., 2002, Myosin V is a left-handed spiral motor on the right-handed actin helix, *Nat. Struct. Biol.* **9**:464–467.

Ali, M. Y., Homma, K., Iwane, A. H., Adachi, K., Itoh, H., Kinosita, K. Jr., Yanagida, T., and Ikebe, M., 2004, Unconstrained steps of myosin VI appear longest among known molecular motors, *Biophys. J.* **86**: 3804–3810.

Altman, D., Sweeney, H. L., and Spudich, J. A., 2004, The mechanism of myosin VI translocation and its load-induced anchoring, *Cell* **116**:737–749.

Asbury, C. L., Fehr, A. N., and Block, S. M., 2003, Kinesin moves by an asymmetric hand-over-hand mechanism, *Science* **302**:2130–2134.

Block, S. M., Goldstein, L. S. B., and Schnapp, B. J., 1990, Bead movement by single kinesin molecules studied with optical tweezers, *Nature* **348**:348–352.

Brady, S. T., 1985, A novel brain ATPase with properties expected for the fast axonal transport motor, *Nature* **317**:73–75.

Burgess, S., Walker, M., Wang, F., Sellers, J. R., White, H. D., Knight, P. J., and Trinick, J., 2002, The prepower stroke conformation of myosin V, *J. Cell Biol.* **159**:983–991.

Carter, N. J., and Cross, R. A., 2005, Mechanics of the kinesin step, *Nature* **435**:308–312.

Cheney, R. E., O'Shea, M. K., Heuser, J. E., Coelho, M. V., Wolenski, J. S., Espreafico, E. M., Forscher, P., Larson, R. E., and Mooseker, M. S., 1993, Brain myosin-V is a two-headed unconventional myosin with motor activity, *Cell* **75**:13–23.

Clemen, A. E.-M., Vilfan, M., Jaud, J., Zhang, J., Bärmann, M., and Rief, M., 2005, Force-dependent stepping kinetics of myosin-V, *Biophys. J.*, **88**:4402–4410.

Coureux, P.-D., Sweeney, H. L., and Houdusse, A., 2004, Three myosin V structures delineate essential features of chemo-mechanical transduction, *EMBO J.* **23**:4527–4537.

Coureux, P.-D., Wells, A. L., Ménétrey, J., Yengo, C. M., Morris, C. A., Sweeney, H. L., and Houdusse, A., 2003, A structural state of the myosin V motor without bound nucleotide, *Nature* **425**:419–423.

De La Cruz, E. M., Wells, A. L., Rosenfeld, S. S., Ostap, E. M., and Sweeney, H. L., 1999, The kinetic mechanism of myosin V, *Proc. Natl. Acad. Sci. USA* **96**:13726–13731.

Endow, S. A., and Barker, D. S., 2003, Processive and nonprocessive models of kinesin movement, *Annu. Rev. Physiol.* **65**:161–175.

Forkey, J. N., Quinlan, M. E., Shaw, M. A., Corrie, J. E. T., and Goldman, Y. E., 2003, Three-dimensional structural dynamics of myosin V by single-molecule fluorescence polarization, *Nature* **422**:399–404.

Hackney, D. D., 1994, Evidence for alternating head catalysis by kinesin during microtubule-stimulated ATP hydrolysis, *Proc. Natl. Acad. Sci. USA* **91**:6865–6869.

Hancock, W. O., and Howard, J., 1999, Kinesin's processivity results from mechanical and chemical coordination between the ATP hydrolysis cycles of the two motor domains, *Proc. Natl. Acad. Sci. USA* **96**: 13147–13152.

Holmes, K. C., Angert, I., Kull, F. J., Jahn, W., and Schröder, R. R., 2003, Electron cryo-microscopy shows how strong binding of myosin to actin releases nucleotide, *Nature* **425**:423–427.

Houdusse, A., Kalabokis, V. N., Himmel, D., Szent-Györgyi, A. G., and Cohen, C., 1999, Atomic structure of scallop myosin subfragment S1 complexed with MgADP: a novel conformation of the myosin head, *Cell* **97**, 459–470.

Houdusse, A., Szent-Györgyi, A. G., and Cohen, C., 2000, Three conformational states of scallop myosin S1, 2000, *Proc. Natl. Acad. Sci. USA* **97**, 11238–11243.

Howard, J., Hudspeth, A. J., Vale, R. D., 1989, Movement of microtubules by single kinesin molecules, *Nature* **342**:154–158.

Howard, J., 1996, The movement of kinesin along microtubules, *Annu. Rev. Physiol.* **58**:703–729.

Hua, W., Chung, J., and Gelles, J., 2002, Distinguishing inchworm and hand-over-hand processive kinesin movement by neck rotation measurements, *Science* **295**:844–848.

Huxley, A. F., and Simmons, R. M., 1971, Proposed mechanism of force generation in striated muscle, *Nature* **233**:533–538.

Huxley, H. E., 1969, The mechanism of muscular contraction, *Science* **164**:1356–1366.

Inoue, A., Saito, J., Ikebe, R., and Ikebe, M., 2002, Myosin IXb is a single-headed minus-end-directed processive motor, *Nat. Cell Biol.* **4**:302–306.

Ishiwata, S., Kinosita, K. Jr., Yoshimura, H., and Ikegami, A., 1987, Rotational motions of myosin heads in myofibril studied by phosphorescence anisotropy decay measurements, *J. Biol. Chem.* **262**: 8314–8317.

Kaseda, K., Higuchi, H., and Hirose, K., 2003, Alternate fast and slow stepping of a heterodimeric kinesin molecule, *Nat. Cell Biol.* **5**:1079–1082.

Kawaguchi, K., and Ishiwata, S., 2001, Nucleotide-dependent single- to double-headed binding of kinesin, *Science* **291**:667–669.

Kellerman, K. A., and Miller, K. G., 1992, An unconventional myosin heavy chain gene from *Drosophila melanogaster*, *J. Cell Biol.* **119**:823–834.

Kinosita, K. Jr., Ishiwata, S., Yoshimura, H., Asai, H., and Ikegami, A., 1984, Submicrosecond and microsecond rotational motions of myosin head in solution and in myosin synthetic filaments as revealed by time-resolved optical anisotropy decay measurements, *Biochemistry* **23**:5963–5975.

Kinosita, K. Jr., Yasuda, R., Noji, H., Ishiwata, S., and Yoshida, M., 1998, F_1-ATPase: a rotary motor made of a single molecule, *Cell* **93**:21–24.

Kinosita, K. Jr., Adachi, K., and Itoh, H., 2004, Rotation of F_1-ATPase: how an ATP-driven molecular machine may work, *Annu. Rev. Biophys. Biomol. Struct.* **33**:245–268.

Kinosita, K. Jr., Ali, M. Y., Adachi, K., Shiroguchi, K., and Itoh, H., 2005, How two-foot molecular motors may walk, *Adv. Exp. Med. Biol.* **565**:205–219.

Kozielski, F., Sack, S., Marx, A., Thormählen, M., Schönbrunn, E., Biou, V., Thompson, A., Mandelkow, E.-M., and Mandelkow, E., 1997, The crystal structure of dimeric kinesin and implications for microtubule-dependent motility, *Cell* **91**:985–994.

Kull, F. J., Sablin, E. P., Lau, R., Fletterick, R. J., and Vale, R. D., 1996, Crystal structure of the kinesin motor domain reveals a structural similarity to myosin, *Nature* **380**:550–555.

Li, Y., Brown, J. H., Reshetnikova, L., Blazsek, A., Farkas, L., Nyitray, L., and Cohen, C., 2003, Visualization of an unstable coiled coil from the scallop myosin rod, *Nature* **424**:341–345.

Mehta, A. D., Rock, R. S., Rief, M., Spudich, J. A., Mooseker, M. S., and Cheney, R. E., 1999, Myosin-V is a processive actin-based motor, *Nature* **400**:590–593.

Mehta, A., 2001, Myosin learns to walk, *J. Cell Sci.* **114**:1981–1998.

Ménétrey, J., Bahloul, A., Wells, A. L., Yengo, C. M., Morris, C. A., Sweeney, H. L., and Houdusse, A., 2005, The structure of the myosin VI motor reveals the mechanism of directionality reversal, *Nature* **435**: 779–785.

Moore, J. R., Krementsova, E. B., Trybus, K. M., and Warshaw, D. M., 2001, Myosin V exhibits a high duty cycle and large unitary displacement, *J. Cell Biol.* **155**:625–635.

Nishikawa, S., Homma, K., Komori, Y., Iwaki, M., Wazawa, T., Iwane, A. H., Saito, J., Ikebe, R., Katayama, E., Yanagida, T., and Ikebe, M., 2002, Class VI myosin moves processively along actin filaments backward with large steps, *Biochem. Biophys. Res. Commun.* **290**:311–317.

Nitta, R., Kikkawa, M., Okada, Y., and Hirokawa, N., 2004, KIF1A alternately uses two loops to bind microtubules, *Science* **305**:678–683.

Okada, Y., Higuchi, H., and Hirokawa, N., 2003, Processivity of the single-headed kinesin KIF1A through biased binding to tubulin, *Nature* **424**:574–577.

Purcell, E. M., 1976, Life at low Reynolds number, http://brodylab.eng.uci.edu/~jpbrody/reynolds/lowpurcell.html.

Purcell, T. J., Sweeney, H. L., and Spudich, J. A., 2005, A force-dependent state controls the coordination of processive myosin V, *Proc. Natl. Acad. Sci. USA* **102**:13873–13878.

Rayment, I., Rypniewski, W. R., Schmidt-Bäse, K., Smith, R., Tomchick, D. R., Benning, M. M., Winkelmann, D. A., Wesenberg, G., and Holden, H. M., 1993, Three-dimensional structure of myosin subfragment-1: a molecular motor, *Science* **261**:50–58.

Reedy, M. K., Holmes, K. C., and Tregear, R. T., 1965, Induced changes in orientation of the cross-bridges of glycerinated insect flight muscle, *Nature* **207**:1276–1280.

Rice, S., Cui, Y., Sindelar, C., Naber, N., Matuska, M., Vale, R., and Cooke, R., 2003, Thermodynamic properties of the kinesin neck-region docking to the catalytic core, *Biophys. J.* **84**:1844–1854.

Rice, S., Lin, A. W., Safer, D., Hart, C. L., Naber, N., Carragher, B. O., Cain, S. M., Pechatnikova, E., Wilson-Kubalek, E. M., Whittaker, M., Pate, E., Cooke, R., Taylor, E. W., Milligan, R. A., and Vale, R. D., 1999, A structural change in the kinesin motor protein that drives motility, *Nature* **402**:778–784.

Rief, M., Rock, R. S., Mehta, A. D., Mooseker, M. S., Cheney, R. E., and Spudich, J. A., 2000, Myosin-V stepping kinetics: A molecular model for processivity, *Proc. Natl. Acad. Sci. USA* **97**:9482–9486.

Rock, R. S., Ramamurthy, B., Dunn, A. R., Beccafico, S., Rami, B. R., Morris, C., Spink, B. J., Franzini-Armstrong, C., Spudich, J. A., and Sweeney, H. L., 2005, A flexible domain is essential for the large step size and processivity of myosin VI, *Mol. Cell* **17**:603–609.

Rock, R. S., Rice, S. E., Wells, A. L., Purcell, T. J., Spudich, J. A., and Sweeney, H. L., 2001, Myosin VI is a processive motor with a large step size, *Proc. Natl. Acad. Sci. USA* **98**:13655–13659.

Sablin, E. P., and Fletterick, R. J., 2004, Coordination between motor domains in processive kinesins, *J. Biol. Chem.* **279**:15707–15710.

Sakamoto, T., Amitani, I., Yokota, E., and Ando, T., 2000, Direct observation of processive movement by individual myosin V molecules, *Biochem. Biophys. Res. Commun.* **272**:586–590.

Schliwa, M., and Woehlke, G., 2003, Molecular motors, *Nature* **422**:759–765.

Shiroguchi, K., and Kinosita, K. Jr., 2005, Watching leg motion in walking myosin V, *Biophys. J.* **88**: 205A-205A.

Svoboda, K., Schmidt, C. F., Schnapp, B. J., and Block, S. M., 1993, Direct observation of kinesin stepping by optical trapping interferometry, *Nature* **365**:721–727.

Tominaga, M., Kojima, H., Yokota, E., Orii, H., Nakamori, R., Katayama, E., Anson, M., Shimmen, T., and Oiwa, K., 2003, Higher plant myosin XI moves processively on actin with 35 nm steps at high velocity, *EMBO J.* **22**:1263–1272.

Tsiavaliaris, G., Fujita-Becker, S., and Manstein, D. J., 2004, Molecular engineering of a backwards-moving myosin motor, *Nature* **427**:558–561.

Turner, J., Anderson, R., Guo, J., Beraud, C., Fletterick, R., and Sakowicz, R., 2001, Crystal structure of the mitotic spindle kinesin Eg5 reveals a novel conformation of the neck-linker, *J. Biol. Chem.* **276**: 25496–25502.

Uemura, S., and Ishiwata, S., 2003, Loading direction regulates the affinity of ADP for kinesin, *Nat. Struct. Biol.* **10**:308–311.

Uemura, S., Kawaguchi, K., Yajima, J., Edamatsu, M., Toyoshima, Y. Y., and Ishiwata, S., 2002, Kinesin–microtubule binding depends on both nucleotide state and loading direction, *Proc. Natl. Acad. Sci. USA* **99**:5977–5981.

Vale, R. D., 2003, Myosin V motor proteins: marching stepwise towards a mechanism, *J. Cell Biol.*, **163**: 445–450.

Vale, R. D., Reese, T. S., and Sheetz, M. P., 1985, Identification of a novel force-generating protein, kinesin, involved in microtubule-based motility, *Cell* **42**:39–50.

Vale, R. D., and Milligan, R. A., 2000, The way things move: looking under the hood of molecular motor proteins, *Science* **288**:88–95.

Veigel, C., Schmitz, S., Wang, F., and Sellers, J. R., 2005, Load-dependent kinetics of myosin-V can explain its high processivity, *Nat. Cell Biol.* **7**:861–869.

Veigel, C., Wang, F., Bartoo, M. L., Sellers, J. R., and Molloy, J. E., 2002, The gated gait of the processive molecular motor, myosin V, *Nat. Cell Biol.* **4**:59–65.

Visscher, K., Schnitzer, M. J., and Block, S. M., 1999, Single kinesin molecules studied with a molecular force clamp, *Nature* **400**:184–189.

Walker, M. L., Burgess, S. A., Sellers, J. R., Wang, F., Hammer, J. A., Trinick, J., and Knight, P. J., 2000, Two-headed binding of a processive myosin to F-actin, *Nature* **405**:804–807.

Warshaw, D. M., Kennedy, G. G., Work, S. S., Krementsova, E. B., Beck, S., and Trybus, K. M., 2005, Differential labeling of myosin V heads with quantum dots allows direct visualization of hand-over-hand processivity, *Biophys. J.* **88**:L30–L32.

Wells, A. L., Lin, A. W., Chen, L.-Q., Safer, D., Cain, S. M., Hasson, T., Carragher, B. O., Milligan, R. A., and Sweeney, H. L., 1999, Myosin VI is an actin-based motor that moves backwards, *Nature* **401**:505–508.

Yasuda, R., Noji, H., Yoshida, M., Kinosita, K. Jr., and Itoh, H., 2001, Resolution of distinct rotational substeps by submillisecond kinetic analysis of F_1-ATPase, *Nature* **410**:898–904.

Yildiz, A., Forkey, J. N., McKinney, S. A., Ha, T., Goldman, Y. E., and Selvin, P. R., 2003, Myosin V walks hand-over-hand: Single fluorophore imaging with 1.5-nm localization, *Science* **300**:2061–2065.

Yildiz, A., Tomishige, M., Vale, R. D., and Selvin, P. R., 2004, Kinesin walks hand-over-hand, *Science* **303**: 676–678.

32

MODELING OF THE F-ACTIN STRUCTURE

Toshiro Oda[1,2]*, Heiko Stegmann[3], Rasmus R. Schröder[4],
Keiichi Namba[5,6] and Yuichiro Maéda[1,2,7]

32.1. INTRODUCTION

Actin has been a major target for structural studies in biology since F. B. Straub discovered it in 1942.[1] This is probably because actin is one of the most abundant proteins in the eukaryotic cell as well as a key player in many physiological events, ranging from genetics to motility.

The scope of actin studies has gradually changed. Actin was initially characterized as a polymerizable muscle protein, because it was prepared by a cycle of polymerization and depolymerization from dry muscle powder. During this early period, it was found that monomeric actin (G-actin) would be transformed into filamentous actin (F-actin) by adding a neutral salt, a process that induces ATP hydrolysis.[2] The transformation was attributed to a type of condensation (fibrous condensation) between the monomeric state and polymerized state.[3] This idea was confirmed by the finding that a constant amount of actin monomer coexisted in an F-actin solution, thus indicating the existence of a critical concentration of actin for polymerization.[3,4] In the 1970s the dynamic properties of the individual ends of the filament were discovered together with their uni-directional elongation at the barbed-end (the fast growing end).[5,6] It was followed by the discovery of the treadmilling of subunits, which "flow" from the barbed-end to the pointed-end (slow growing end),[7,8] and of the ATP-capping at the barbed-end in the 1980s.[9,10]

Another line of studies involved the discovery and purification of cytoplasmic actin[11,12] in the 1960s. This discovery was the basis of cell biologist's interest in the aspects of actin in non-muscle cells. Advances in light microscopy and molecular biology permitted *in vivo* observations of actin motility under physiological conditions – such as Listeria motility or the movement of filopodia and lamellipodia. These observations revealed that the observed phenomena are linked to actin-based motility, which is controlled by

* Contact: Dr. Toshiro. E-mail: toda@spring8.or.jp; Voice: +81-791-58-1825; Fax : +81-791-58-1826.
[1] RIKEN Harima Institute, RIKEN SPring-8 center, 1-1-1 Kouto, Sayo, Hyogo 679-5148, Japan, [2]Actin-filament dynamics project, ERATO, JST, 1-1-1 Kouto, Sayo, Hyogo, Japan, [3]Carl Zeiss NTS GmbH, Carl-Zeiss-Str. 56, 73447 Oberkochen, [4]Max-Planck Institute of Biophysics, Max-von-Laue Str. 3, 60438 Frankfurt am Main, Germany, [5]Graduate School of Frontier Biosciences, Osaka University, 1-3 Yamadaoka, Suita, Osaka 565-0871, Japan, [6]Dynamic NanoMachine project, ICORP, JST, 1-3 Yamadaoka, Suita, Osaka 565-0871, Japan, and [7]Graduate School of Science, Nagoya University, Furo-cho, Chikusa, 464-8602 Nagoya, Japan

Regulatory Mechanisms of Striated Muscle Contraction
Edited by Ebashi and Ohtsuki, Springer, 2007

different kinds of actin-binding proteins.[13] Actin-binding proteins are key players for individual events. For example, formin connects the signal transferred by a G-protein to actin, which is the final target in this particular signal transduction pathway.[14] In the meantime other actin binding proteins, which control individual physiological events, have been found.

At present, actin research is pursued via a variety of biophysical and physiological approaches. To understand the details of the molecular mechanism of actin based motility or other physiological events, it is essential to obtain detailed structural information about F-actin. In the work presented here we determined the molecular structure of F-actin and derive an intrinsic regulatory mechanism of filament stability, which is incorporated in the structure of the filament. In the future it will be necessary to clarified also the relationship between the mechanisms intrinsic to F-actin and those derived from the various actin-binding proteins.

32.2. HISTRICAL ASPECTS OF STUDIES OF THE F-ACTIN STRUCURE

The analysis of the F-actin structure started immediately after actin was discovered. W. T. Astbury and colleagues recorded X-ray diffraction patterns from dry F-actin films in 1947.[15] Meridional arcs in the diffraction pattern were observed at a resolution range between 1/27 and 1/3.6 $Å^{-1}$. This suggested that the corpuscular units were not strung together in an arbitrary fashion, but always in the same way and with atomic precision.

To determine the arrangement of the constituents, C. C. Selby & R. S. Bear recorded X-ray diffraction patterns from dry clam adductor muscle in 1956.[16] The moderate-angle diffractions yielded by the whole muscle could be associated with the actin component, as confirmed by the patterns from a dried F-actin gel by C. Cohen and J. Hanson.[17] They searched for a selection rule that could account for the diffraction intensities in the pattern. They chose the selection rules of 15 nodes along 7 turns, or 13 nodes along 6 turns of the basic helix, although they could not decide whether it was a helical-net cell or a planar-net cell.

F. Oosawa and colleagues independently deduced that F-actin was a helical polymer by their biophysical studies in 1961.[18,19] They pointed out that at least two kinds of bonds between subunits in F-actin were required to explain the critical concentration because condensation does not occur in a 1-D system. The most probable arrangement would be a helical one, in which all subunits have the same environment.

Finally, J. Hanson & S. Lowy confirmed the helical structure of F-actin in 1963 by using electron microscopy:[20] Facts about the structure of F-actin they concluded are (a) F-actin consists of two helically-wound strands. (b) Each strand is composed of subunits that appear to be similar and approximately spherical. (c) The number of globular subunits per turn of the helical strand is 13 (i.e. the helical symmetry is 13 subunits / 6 turns of the left-handed basic helix), and the subunit arrangement corresponds to a model proposed earlier by C. C. Selby & R. S. Bear in 1956.[16]

To obtain a more refined structure, in 1970, P. B. Moore and colleagues calculated a three-dimensional (3D) map of negatively stained F-actin with the 3D image reconstruction technique of D. J. DeRosier and A. Klug[21] derived especially for electron microscopic (EM) images.[22] The reconstruction showed that the longitudinal contact is more pronounced than the interstrand contact. Considering the relative strength of the two

contacts, the issue of the relationship between the structure and the flexibility of F-actin was debated on basis of the available F-actin reconstruction in the 1980s, which generated the "lateral slipping" model[23] and the "random disorder" model.[24]

On the other hand, non-stained F-actin filaments in a frozen-hydrated state have been examined by electron cryo-microscopy (cryo-EM)[25,26] since the mid 1980s, but the resolution achieved for the 3D reconstructions was still only 20–30 Å. Recently, however, the methods in electron microscopy and image analysis have been developing at a remarkably high speed. Improvements in electron optics (such as field emission electron sources or imaging energy filters), image processing (e.g. novel back projection algorithms for filamentous structures[27–29]), and computing power may further improve obtainable resolution. As a consequence of these advances it was possible to detect several conformational changes of the actin subunit in F-actin induced by actin-binding proteins.[30] However, a high resolution structure of pure F-actin has not been reported yet.

32.3. THE CRYSTAL STRUCTURE OF THE ACTIN-DNase I COMPLEX AND THE FIRST ATOMIC MODEL FOR F-ACTIN

The turning point in structural biological research of the actin structure occurred in 1990. K. C. Holmes and colleagues solved the crystal structure of a DNase I – actin complex[31] and built an atomic model for the F-actin structure based on X-ray fiber diffraction data.[32] The importance of this work is not only marked by the first time determination of an actin crystal structure but also by the proposal of a model of the F-actin structure. This model has served as a working hypothesis, on which further studies on the F-actin structure were based.

K. C. Holmes and colleagues searched for such an orientation and position of the actin monomers in the filament that would account for the X-ray fiber diffraction patterns up to 8 Å resolution, obtained from well-oriented F-actin sols and the experimentally obtatined radius of gyration of F-actin.[32] They found only one unique orientation and position with a sufficiently small residual error between the model and the experimental pattern. They suggested also that the difference between the two actin structures, the one derived from the actin-DNase I complex and the other found in F-actin would be small. This conclusion formed the basis for following studies to refine the atomic model of F-actin and the actin-myosin complex.[33–35]

K. C. Holmes and colleagues also proposed the importance of the so-called hydrophobic plug, composed of actin residues 267–272, for the structural stability of F-actin.[32] In their model this hydrophobic plug protrudes from the actin surface and extends to a hydrophobic patch on the surface of opposite stand. The hypothesis is consistent with the results of biochemical experiments using yeast mutant actin by P. A. Rubenstein[36,37] and E. Reisler.[38]

To understand actin-involving physiological events precisely, one must know the detailed interactions between F-actin and actin-binding proteins. However, obtaining a detailed description of the structures involved has been difficult despite that many crystal structures of actin binding proteins which have been solved. The reason is the lack of accuracy of the available F-actin structures. Because the structures have been modelled at relatively low resolution, the details of the atomic interaction in the current F-actin models are

beyond the accuracy of the models. To understand the mechanisms of many cellular events in which the F-actin functions are involved, such as the interactions between F-actin and myosin,[35] an atomic model of the F-actin structure with highest accuracy is essential.

32.4. CURRENT APPROACHES TO THE STRUCTRAL ANALYSIS OF F-ACTIN[39]

How can one obtain an atomic model of F-actin structure with high accuracy?

Generally speaking, the most useful method to determine the atomic structure of protein complexes is protein crystallography. To use this excellent method, a crystal of F-actin is needed, but the crystallization is difficult because of many different reasons, one of them being the heterogeneous length of individual F-actin filaments. Several groups have tried to grow crystals of F-actin and derivatives. E. Reisler and colleagues solved the crystal structure of actin dimers that were cross-linked in F-actin, but the two actin molecules were not arranged in a helical manner.[40] Preparation of a mini-thin filament with a well-defined length has been reported but their crystallization has not yet been possible.[41]

Another approach is X-ray fiber diffraction from well-oriented sols, which can be used for the structural analysis of macromolecular complexes with helical symmetry.[42] Oriented sols are formed because densely packed filaments in soles are spontaneously aligned in parallel by an excluded volume effect. In the X-ray fiber diffraction field, the structural analysis of the cylindrical structure of tobacco mosaic virus (TMV), a rod-shaped virus made of a helical assembly of coat proteins and an RNA, is one of the most successful stories.[43–47] The analysis took more than 40 years, and finally the atomic structure was solved at 2.9 Å resolution in 1989.[48] At the same time, this success generated an extended methodology for fiber diffraction pattern analysis, such as the omit map method[49] and the solvent flattening method.[50] To fully utilize these methods, we need the intensity data along layer-lines, which can be extracted from the diffraction pattern. For the precise extraction of the layer-line intensities, diffraction patterns with sharp reflections are necessary. The quality of the patterns depends strongly on the orientation of the filament in the specimen sols. Therefore, we needed first to improve the orientation of F-actin in the sols (see below).

K. C. Holmes and colleagues used the same X-ray fiber diffraction approach for their structural analysis of F-actin. However, they treated the diffraction pattern as a whole, not the extracted layer-line intensities, to avoid possible errors connected with the extraction process. However, as a result, they could not use the available methodology to check the accuracy of the derived F-actin model.

32.4.1. Sample Preparation and Recording of X-ray Fiber Diffraction Patterns

In early structural studies the specimens of oriented filaments were prepared simply by controlling humidity,[17,51] because dehydration of specimens induces filament orientation. In the 1980s, D. Popp in Holmes' group improved the orientation combining protein concentration with laminar flow,[52] which also induces filament orientation at a low shear rate. From specimens prepared using this flow orientation method, they recorded X-ray

diffraction patterns and deduced a model of the F-actin structure.[32–35] However, the diffraction patterns available at that time were not sufficient for structural analysis at high resolution.

More recently we developed another procedure to obtain a better orientation of filament sols on the basis of some chemical and physical effects.[53] The strategy to produce a well-oriented filament sol is (a) to increase the filament concentration while maintaining the fluidity of the sols and (b) to make use of a strong external magnetic field. The average length of the filaments was controlled to be at around 0.6 μm by adding gelsolin during filament polymerization. The ionic strength should be as low as possible, typically 30 mM KCl, the filaments should be concentrated by very slow and long centrifugation, and the sols should be exposed to a strong magnetic field for further improvement in the orientation. The detailed procedure was described elsewhere.[53] The typical buffer conditions are 30 mM KCl, 1 mM $CaCl_2$, 0.5 mM ATP, 1 mM NaN_3 1 mM 2-mercaptoethanol and 10 mM Tris-acetate (pH 8.0).

X-ray diffraction patterns from well-oriented F-actin sols were recorded on Imaging Plate using synchrotron radiation at a wavelength of 1.0 Å at the beam-lines BL40B2 and BL41XU at SPring-8. The use of the extremely brilliant and parallel X-ray beams at SPring-8, resulting from the low emittance and low divergence of the photon sources, also helped to improve the quality of the diffraction patterns. We designed a special camera with a helium chamber, a small beam stop and a four-quadrant slit system to record diffraction patterns on Image Plates over a wide range of the diffraction space from low (400 Å) to high (2.5 Å) resolution with low background.

Figure 32.1 shows a typical X-ray diffraction pattern extending to 5.5 Å in resolution. The quality of the X-ray diffraction patterns, as compared with those of the previous studies, was improved with respect to the separation of the layer-lines. The average angle of the filament disorientation was about 1.7° in the present sols, as compared to 2.8° in those used in the previous studies.

The intensity peaks in the processed diffraction patterns were indexed by a pair of indices, *(n,l)*, where *n* is the Bessel order and *l* is the layer-line order. The helical symmetry of F-actin is slightly off the 13/-6, but we could not observe the separation of layer-lines induced by the difference. Layer-line intensity profiles were then extracted as

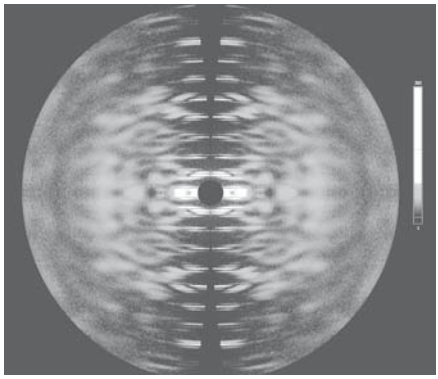

Figure 32.1. X-ray fiber diffraction pattern from a well-oriented F-actin sol.

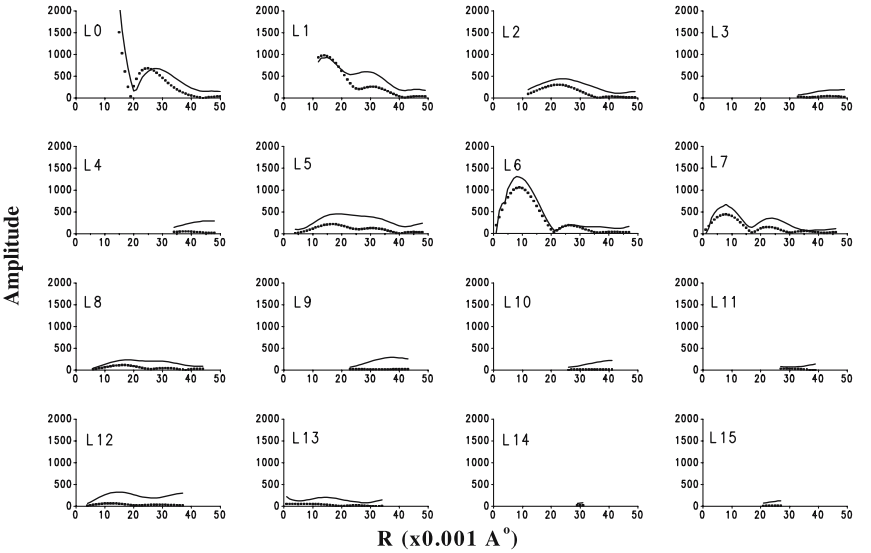

Figure 32.2. Amplitudes extracted from the X-ray fiber diffraction patterns of F-actin (continuous curve) and those (dotted curve) calculated from the reconstruction by electron cryo-microscopy using the single particle image analysis.

grouped layer-line intensities by deconvolution of the processed patterns,[54] which were indexed by 13/-6. The amplitude data within the area of 0.014 $Å^{-1}$, which is behind the beam stop, were replaced with scaled amplitudes calculated from the Lorenz model.[33] From X-ray diffraction patterns, layer-line amplitudes, i.e., the square-roots of layer-line intensities were extracted (Figure 32.2).

32.5. THE PHASE PROBLEM IN FIBER DIFFRACTION ANALYSIS

When modeling the F-actin structure we first have to determine the orientation of the actin subunit in the filament model. For this purpose, a 3D density map of the filament in real space is useful, and this reconstruction needs phase information in the same way as crystallography. In the fiber diffraction analysis, one uses the isomorphous replacement method[55] to deduce the phase information. However, in the case of F-actin, the application of isomorphous replacement is difficult, because the Bessel terms are extensively overlapping and their separation could only be achieved by using a large number of heavy atom derivatives. At least 16 heavy atom derivatives are needed for phasing up to 8 Å in resolution.

Another approach, electron microscopy and image analysis, would also be useful. X-ray fiber diffraction and electron cryo-microscopy are both independent and powerful tools for solving the structure of helical complexes of macromolecules, and each has unique advantages over the other. X-ray diffraction gives reliable amplitude data and electron cryomicroscopy gives reliable phases. The amplitude profiles obtained from

X-ray diffraction and electron microscopy are similar to each other, at least in the region up to 20 Å resolution, although the physics behind the scattering of X-ray photons and electrons is different.[56,57] Combination of X-ray amplitudes and EM phases is a reasonable strategy and has been applied to the structural analyses of TMV[58] and the flagellar filament,[59] demonstrating that the method can be used to obtain good quality 3D densities of high quality.

32.5.1. 3D Reconstruction by Electron Cryo-microscopy and Extraction of Phase Information

To obtain the phase information for F-actin, we used electron cryo-microscopy. Electron micrographs of individual F-actin filaments were selected and averaged applying conventional single particle algorithms and processed to produce a 3D reconstruction of F-actin as densities at each 3D-voxel in orthogonal coordinates. F-actin preparation, sample and microscopy conditions, image processing and the final 3D reconstruction are essentially identical to the work described for the case of decorated actin in Holmes *et al.*[35] The much lower resolution in the case of the F-actin reconstruction used here results from the smaller number of particles accepted in the final reconstruction (only 800 helical F-actin repeats). This reduction of data in the final set is mainly caused by the inferior quality of data, which was collection on a slow scan CCD camera, as compared to the collection on Image Plates used in the work on decorated actin. However, one should also keep in mind the relative mass of one actin helical unit cell (about 520 kDa) compared to that of one unit cell of decorated actin (about 1.56 MDa). The better alignment and obtainable resolution of decorated actin reflects therefore simply the higher mass (better SNR in the images).

The real space 3D reconstruction was converted into a density distribution in a helical lattice (Figure 32.3), in order to calculate structure factors (consisting of amplitudes and phases)[60] by a Fourier-Bessel transformation. The size of the corresponding helical lattice unit cell used here is 27.6 Å (in the direction of the filament axis), and 193.4 degrees (in azimuth, i.e. $(67–31) \times 360/67$). The radial size was arbitrarily set to 62 Å, since the radius of F-actin is only about 50 Å. This constraint implies that the electron densities beyond the radius of 62 Å are zero in the Fourier-Bessel transform. Therefore, the background level of the 3D reconstruction (ice density) was corrected accordingly, using the radial mass distribution of the F-actin (see the following paragraphs). The helical cell volume is expressed by the following inequality in cylindrical coordinates:

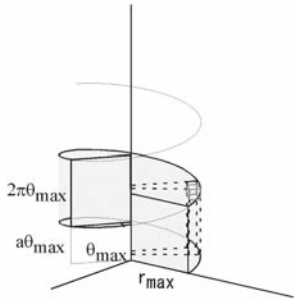

Figure 32.3. Helical lattice unit cell.

In the case that the thus resulting number of grid spacings on the radial helical axis would be less than 10, then this number was set to 10.

$$0 < r < r_{max},\ 0 < \theta < \theta_{max},$$
$$a \times \theta < z < a \times \theta + a \times 2\pi$$
$$\text{where } \theta_{max} = 2\pi \times \text{turn/subunit},$$
$$a = \text{repeat-distance}/(2\pi \times \text{turn})$$

In a next stepothogonal voxels are also defined in the helical cell. The radial helical axis was divided into the exact grid spacings of 2 Å size. The azimuth, $r\theta_{max}$ at the radius of r, was evenly divided into the nearest number of grid spacings (= $r\theta_{max}$/(quotient of $r\theta_{max}$/ 2 Å)). In the axial direction, the cell was as well evenly divided into the nearest number of grid spacings (= $a \times 2\pi$ / (quotient of $a \times 2\pi$/2 Å)). The area thus enclosed by the grid spacings in 3D was then defined as a voxel, which position was expressed by its center. For conversion of the orthogonal cell of the EM map into the helical cell, we choose lattice of $7 \times 7 \times 7$ orthogonal voxel and density of the helical voxel by the averaged density of the enclosed lattice points. A similar type of helical cell has been used in densities modification, such as solvent flattening.[59]

To calculate the Fourier-Bessel transform in cylindrical coordinates at an interval of 0.001 $Å^{-1}$, which corresponds to the sampling interval of the extracted X-ray amplitudes, all integrations have to be terminated at a radius of 62 Å. This can be facilitated simply by setting the electron density to zero at a radius larger than 62 Å. After background correction of the 3D reconstruction (ice density set to zero) the density of the reconstruction can then be corrected in the following way:

$$\rho_{corr} = \rho\ (\rho > 0),\ \rho_{corr} = 0\ (\rho \leq 0)$$

which also eliminates residual effects of the image formation (negative densities around protein as an effect of non-perfect matching of the image aberration corrections).The density correction was justified, as the corrected radial mass distribution of the EM-map was consistent with the radial distribution of the electron density deduced from the X-ray data (Figure 32.4). The density from the X-ray data was calculated by the Fourier-Bessel transform of the equatorial intensities that were phased by the use of phalloidin.[61–63] The correction did not affect either the volume or the overall shape of F-actin, but slightly affected the local shape.

32.5.2. Reconstruction of the Three-Dimensional Density Map of F-actin

A 3D density map of F-actin was reconstructed at 20 Å resolution by merging the X-ray amplitudes with the EM phases. The resulting map shows four clearly distinguished

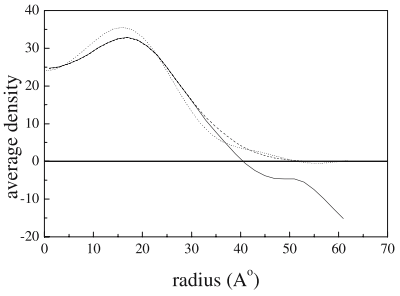

Figure 32.4. The averaged radial density distribution of F-actin deduced from the 3D reconstituted image of F-actin using cryo-EM without density correction (continuous curve), after background correction and density cut-off (dashed curve), and from the X-ray diffraction (dotted curve). The distribution from the X-ray diffraction was calculated by the Fourier-Bessel transform of the equatorial intensities.

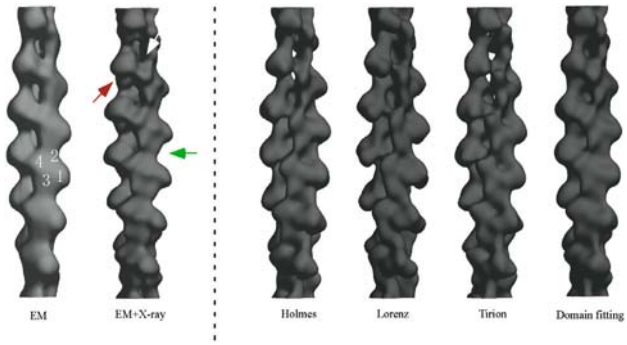

Figure 32.5. F-actin map at 20 Å in resolution. EM alone, X-ray amplitudes plus EM phase, Holmes model,[32] Lorenz model,[33] Tirion model,[34] and our new domain fitting model (for details see text). The red and green arrows point to local density differences between our new data and the previous F-actin models. The F-actin model maps were made via, calculation of structural factors from the atomic coordinates and map calculation from the structural factors up to 20 Å. (helical symmetry: 67/-31).

subdomains of actin, which is in contrast to either the less-featured density map obtained only from the EM data (Figure 32.5) or the previously published EM reconstruction.[26] This density map directly confirms the subunit orientation within F-actin proposed in the original Holmes model.[32] For reconstitution of the F-actin density map, the grouped amplitudes of the layer-lines were assigned to the lowest Bessel order in the group.

32.5.3. Comparison of the Density Map with Previous F-actin Models

The new density map obtained from combining X-ray and EM data was then compared by density cross-correlation to the three previous F-actin models – Holmes model,[32] Lorenz model[33] and Tirion model[34] (see Figure 32.5). The density cross-correlation in the helical cell is defined as follows.

$$Corr = \frac{\left(\rho_{obs} - \overline{\rho_{obs}}\right) \times \left(\rho_{calc} - \overline{\rho_{calc}}\right) \times V}{\left(\left(\rho_{obs} - \overline{\rho_{obs}}\right)^2 \times V \left(\rho_{calc} - \overline{\rho_{calc}}\right)^2 \times V\right)^{1/2}}$$

ρ_{obs} and ρ_{calc} represent the electron density of the reconstructed F-actin map and the calculated model map, respectively. V is the volume element of each voxel. The correlation coefficient depends strongly on the resolution of the 3D reconstruction. To match the resolution of the EM reconstruction all electron densities of the models were calculated at the resolution of 2 nm (0.05 $Å^{-1}$).

The correlation coefficients were approximately 0.9 for the three previous F-actin models, indicating that these F-actin models have an overall subunit orientation that agrees well with that of the new experimental map.

These three models are, however, significantly different from the new experimental map with respect to the following points. Firstly, the mass distribution at the interface between subdomain 2 and subdomain 1 of the upper subunit is different. While a substantial mass exists there in the experimental map (the green arrow in Figure 32.5), this region is empty in the Lorenz model with an occluded DNase-I loop. The Tirion model,

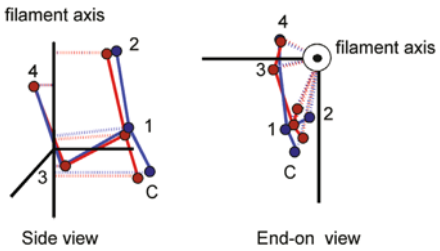

Figure 32.6. Shifts of the four domains and C-terminal region after the domain-fitting. The left panel is a side view, while the right panel is an end-on view. The blue circles indicate mass-centers of the domains in the original Holmes-model that was used as the initial model for the domain-fitting. The red circles are mass-centers in the domain fitting-model. Subdomain 1: 1–32, 70–144, 338–350, ADP and the divalent metal ion (Ca^{2+}). Subdomain 2: 33–69. Subdomain 3: 145–180. 270–337. Subdomain 4: 181–269. C-terminal region: 351–375.

which has a rotated and elongated DNase-I binding loop, has mass in this region (the green arrow in Figure 32.5), although the mass distribution is different from that of the new experimental density map. Our present map suggests that the DNase-I binding loop should not be compact but extended. Secondly, in each of these three models, the density is substantially lower than that in the new experimental map in the region between subdomain 4 and subdomain 1 of the diagonally-related subunit, *i.e.*, the contact region between the two long-pitch strands (the red arrow in Figure 32.5).

To improve the fitting of the crystallographic actin monomer model to our new experimental density, a domain fitting was performed by breaking the atomic model of Kabsch et al.[31] into five domains: the C-terminal part of subdomain 1; the rest of subdomain 1; and three other subdomains, 2, 3, and 4, followed by fitting each domain to our experimental map independently.

This domain fitting moved subdomain 2 by as much as 5 Å, making the overall shape of the actin subunit flatter, as pointed out previously.[33,64] The C-terminal region moved toward the filament axis by approximately 5 Å, narrowing the gap between the two strands. The rest of subdomain 1 also moved toward the filament axis by 3 Å (Figure 32.6). These modifications improved the matching, and the correlation coefficient with the density map increased from 0.91 to 0.94, at the expense of breaking the polypeptide chain. It should be noted here that the space between the two long-pitch strands in this model is significantly narrower than that in the previous models.

32.6. STRATEGY FOR THE REFINEMENT OF THE ATOMIC MODEL FOR F-ACTIN STRUCTURE

As described in the previous section a simple domain fitting model (rigid body fitting) improves fitting to the new experimental data, but does not produce a biochemically valid actin molecule (broken polypeptide chain). To overcome this problem we refined the actin crystal structure against our X-ray diffraction data up to 8 Å resolution using a combination of normal mode and molecular dynamics approaches. As a starting point for our refinement we used the orientation and position of the actin subunit in F-actin as determined in the domain fitting model (see last section). Model refinement then started with

the actin crystal structure against the X-ray diffraction data up to 8 Å resolution. In general, model refinement against low resolution data has the problem that the number of independent measurements is much smaller than the number of structural parameters of the atomic model to be refined, and thus this method has the potential danger of over-determination against the experimental data. To avoid this problem, one uses rigid body refinement or normal-mode based refinement.

In the rigid body refinement, one divides the atomic structure of protein into several domains with the help of biochemical information, after their positions and orientations are refined. The advantage of the method is the perfect stereochemistry within each domain, and structural errors are concentrated only in the connecting regions and extra constraints are necessary to avoid the possible breaking of the polypeptide chain. The method is useful when binding sites are expected to be present in the domain; for example, the modeling of F-actin to search for myosin binding sites. The F-actin refinements by Holmes[35] and by Lorenz[33] are basically along this line.

On the other hand, the normal mode-based refinement uses conformational changes along the vibrational directions of low-order modes that are found in a normal mode analysis of the protein. The normal mode analysis has been developed by Go and co-workers[65] and also by Brooks and Karplus[66] to study the motions of atoms within the structure of protein molecules. Recently, the elastic normal mode analysis of protein molecules has been developed,[67–69] in which a protein molecule is replaced by an α-carbon (Cα network. In the network, Cα atoms within a given distance are connected by springs with a common strength. This approximation results in a potential surface, which is much smoother than the exact potential surface, so that relatively large collective vibrations are expected. It has been pointed out that the large collective motions at slow frequencies most probably correlate with realistic, i.e. physiological conformational changes of proteins.[69,70]

Tirion *et al.*[34] started the structural modeling of macromolecular assemblies by utilizing the slow normal modes, as an approach different from the normal mode refinement in crystallography.[71,72] Recently, a similar refinement strategy was applied to the F-actin structure, in which the normal modes of F-actin, instead of G-actin, were used.[73] This method requires only a small number of structural parameters, and therefore it can be applied to low-resolution diffraction data with only a limited amount of information. Recently, the normal-mode based refinement has been combined with the elastic normal mode analysis, and this method has been frequently used especially in the real space image analysis, such as single particle EM image analysis.[74] It is expected that this method would allow a wider conformational space to be searched as compared to the use of the conventional normal modes. Our search procedure described here is along the same line. However, model building and refinement of the local conformation is beyond the capability of this analysis.

The molecular dynamics simulation was employed for optimizing the structure at the subunit-subunit contact regions against the X-ray diffraction data. Among the multiple models obtained by this fitting procedure, some common structural features were extracted, which may have significance.

32.6.1. Search for the Global Conformation of the Actin Subunit in F-actin

We searched for the most plausible global conformation of the actin subunit using 17 elastic normal modes of actin. This search was performed interactively in 2 steps:

(1) calculation of the normal modes based on the C_α network of the actin subunit within a C_α-C_α distance of 8 Å, followed by (2) minimization of the R-factor by altering the structure along the directions of vibrations of the normal modes. The R-factor was defined as the residual between the experimental diffraction pattern and those calculated from the model. This method permits conformational transitions beyond local minima of the R-factor, because the C_α network is updated after each cycle. The search was carried out against the diffraction intensities in a resolution range of 0.02–0.14 $Å^{-1}$. The model contained violations in the polypeptide stereochemistry. The violations were removed by minimizing the conformational energy within the harmonic C_α-atom position (10 kcal/mol) and the helical symmetry by using FX-PLOR.[75]

The resulting conformations of the models originating from TMR-ADP-actin,[76] open state actin[77] and tight state actin[78] were all alike, although the detailed conformations in the subunit-subunit contact regions showed significant variations. A common property of the resulting structure was the closure of the nucleotide-binding cleft. In order to identify other conformational alterations, the resulting model originating from TMR-ADP-actin was aligned to the large domain core (subdomains 3 & 4) of the original TMR-ADP-actin structure. The small and large domain cores are those defined by Page *et al.*[79] Four major structural changes were observed: (1) A "scissors-like motion" shifts the nucleotide-binding cleft and brings the small domain and large domains closer together (Figure 32.7A). (2) A "propeller-like motion" skews the small domain relative to the large domain (Figure 32.7B). The two prominent modes of motions described here as "scissors-like motion" and "propeller-like motion" occur around the residue Gln 137 and the α-helix formed by residues 331–337. (3) Subdomain 4 is rearranged relative to the rest of the large domain. The α-helices consisting residues 180–194 and 203–216 are tilted and skewed around Ala 181 and Ile 212, respectively (Figures 32.7A & 7C). (4) The α-helical DNase-I binding loop of residues 38–52 rotates relative to the rest of the small domain core about the hinge residues Val 35 and Ala 68.

32.6.2. Search for the Local Conformations of the Actin-Actin Contact Regions in F-actin

To obtain more detailed information about possible local conformations that fit to the X-ray diffraction data, we further performed simulated annealing of molecular

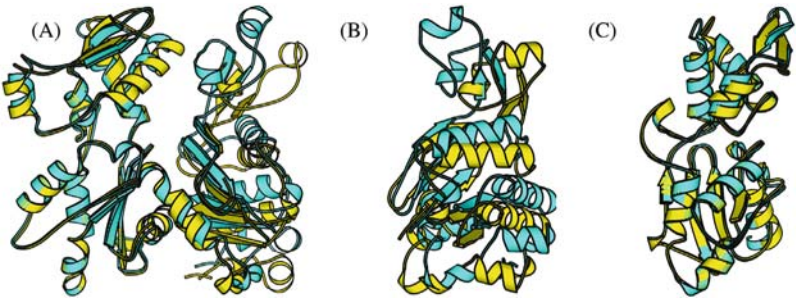

Figure 32.7. Comparison of the conformational change between the resulting model originated from TMR-ADP-actin (cyan) and crystal structure of TMR-ADP-actin (yellow). (A) front view (B) side view from the small domain (C) side view from the large domain. This figure was made using MOLSCRIPT.[82]

dynamics (MD) simulation by FX-PLOR. The annealing was carried out from 2000 K. To avoid destroying the core structure of the actin molecule, we allowed movement of only such regions, where the RMSDs of the C_α-atoms from the average of the three refined models were over 1 Å (110–114, 166–170, 192–208, 223–251, 318–325), as well as movement of the hydrophobic plug (263–273), the projection (283–292) and the C-terminal region (350–375). The other C_α atom positions were fixed during these MD trials. This procedure assumed two components of the energy term. One was the conformational energy including the subunit-subunit contacts, which is restricted by the helical symmetry. The other was the residual of diffraction amplitudes between the observed experimental data and those calculated from the models. The weight of the diffraction term gradient was set to one half of the conformational energy one. Twenty-five individual MD trials did not converge in a single model. These multiple conformations are probably resulting from the complexity of the energy surface. The structural information about F-actin obtainable from those trials is therefore not given by the details of each model but rather their common features, i.e., features shared by those model conformations. Some details of the subunit-subunit contacts are also shared by the majority of the final F-actin models. The subunit-subunit contact regions are defined by a separation between any two chains (in terms of the Cα–Cα distance) of 8 Å or less, as frequently used as the criterion in the Cα network.[68] The residues that met this criterion in more than 50% of the MD trials were classified as the member of the contact regions in Figure 32.8.[39]

The main "axial" contact between the two subunits along the long-pitch strand is made between a large depression formed by residues 60–63, 202–205, and 243–246 of the lower subunit, and the projection formed by residues 322–325 of the upper subunit (here the slow-growing end of F-actin is on the upper side). The other contacts, consisting of 41–48, 148–149, 166–169 and 322–325, support the main contact. The "diagonal" contacts across two long-pitch strands are formed between three pairs of regions. One is between the loop of residues 194–197 and the α-helix of residues 110–115 of the upper-diagonal subunit. The second is between the hydrophobic plug of residues 266–267 and residues 172–173. The third is between residues 269–271 of the hydrophobic plug of the upper subunit, and residues 202–205 of the lower-diagonal subunit. The most important point revealed from our new F-actin model is the crucial role played by subdomain 4. The filament formation is likely to induce the rearrangement of the two α-helices composed of residues 181–194 and 203–216 within subdomain 4, which substantially

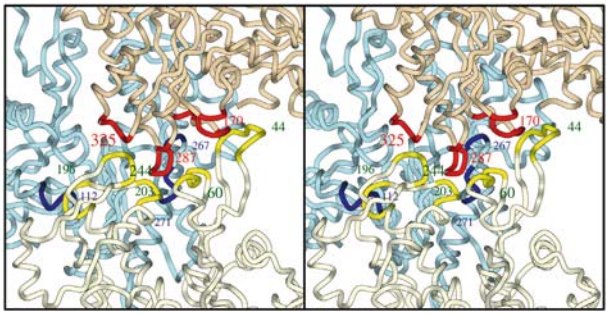

Figure 32.8. Subunit-subunit contact in F-actin. Pink, white and sky-blue express 3 different subunits. Red, yellow and blue express the contact chains.

influences the subunit-subunit contacts both along the long-pitch strand and across the two strands, as well as the conformation of the nucleotide binding cleft. Consistent with this, the folding topology of subdomain 4 is shared with a bacterial actin-like protein, ParM,[80] which forms a helical filament, and also with MreB,[81] which forms a straight filament.

32.7. REFERNCE

1. F. B. Straub. Actin, *Studies Int. Med. Chem. Univ. Szeged*. **2**, 3–15 (1942).
2. F. Straub, and G. Feuer. Adenosinetriphosphate the functional group of actin, *Biochim. Biophys. Acta* **4**, 455–470 (1950).
3. F. Oosawa, S. Asakura, K. Hotta, N. Imai, and T. Ooi. G-F transformation of actin as a fibrous condensation, *J. Polymer Sci*. **37**(3), 323–336 (1959).
4. F. Oosawa. Size distribution of protein polymers, *J. Theor. Biol*. **27**(1), 69–86 (1970).
5. D. T. Woodrum, S. A. Rich, and T. D. Pollard. Evidence for biased bidirectional polymerization of actin filaments using heavy meromyosin prepared by an improved method, *J. Cell Biol*. **67**(1), 231–237 (1975).
6. H. Kondo, and S. Ishiwata. Uni-directional growth of F-actin, *J. Biochem. (Tokyo)*. **79**(1), 159–171 (1976).
7. A. Wegner. Head to tail polymerization of actin, *J. Mol. Biol*. **108**(1), 139–150 (1976).
8. N. Selve, and A. Wegner. Rate of treadmilling of actin filaments in vitro, *J. Mol. Biol*. **187**(4), 627–631 (1986).
9. M. F. Carlier, D. Pantaloni, and E. D. Korn. Evidence for an ATP cap at the ends of actin filaments and its regulation of the F-actin steady state, *J. Biol. Chem*. **259**(16), 9983–9986 (1984).
10. M. F. Carlier, D. Pantaloni, and E. D. Korn. The mechanisms of ATP hydrolysis accompanying the polymerization of Mg-actin and Ca-actin, *J. Biol. Chem*. **262**(7), 3052–3059 (1987).
11. S. Hatano, and F. Oosawa. Extraction of an actin-like protein from the plasmodium of a myxomycete and its interaction with myosin A from rabbit striated muscle, *J. Cell. Physiol*. **68**(2), 197–202 (1966).
12. S. Hatano, and F. Oosawa. Isolation and characterization of plasmodium actin, *Biochim. Biophys. Acta* **127**(2), 488–498 (1966).
13. T. D. Pollard, and G. G. Borisy. Cellular motility driven by assembly and disassembly of actin filaments, *Cell*. **112**(4), 453–465 (2003).
14. S. H. Zigmond. Formin-induced nucleation of actin filaments, *Curr. Opin. Cell Biol*. **16**(1), 99–105 (2004).
15. W. T. Astbury, S. V. Perry, R. Reed, and L. C. Spark. An electron microscopy and X-ray study of actin., *Biochim. Biophys. Acta* **1**, 379–392 (1947).
16. C. C. Selby, and R. S. Bear. The structure of actin-rich filaments of muscles according to X-ray diffraction, *J. Biophys. Biochem. Cytol*. **2**(1), 71–85 (1956).
17. C. Cohen, and J. Hanson. An X-ray diffraction study of F-actin, *Biochim. Biophys. Acta* **21**(1), 177–178 (1956).
18. F. Oosawa, S. Asakura, and T. Ooi. Physical Chemistry of muscle protein "actin," *Prog. Theor. Phys. Suppl*. **17**, 14–34 (1961).
19. F. Oosawa, and M. Kasai. A theory of linear and helical aggregations of macromolecules, *J. Mol. Biol*. **4**, 10–21 (1962).
20. J. Hanson, and J. Lowy. The structure of F-actin of actin filaments isolated from muscle, *J. Mol. Biol*. **6**, 46–60 (1963).
21. D. J. DeRosier, and A. Klug. Reconstruction of three dimensional structure from electron micrographs, *Nature* **217**(5124), 130–134 (1968).
22. P. B. Moore, H. E. Huxley, and D. J. DeRosier. Three-dimensional reconstruction of F-actin, thin filaments and decorated thin filaments, *J. Mol. Biol*. **50**(2), 279–295 (1970).
23. A. Bremer, R. C. Millonig, R. Sutterlin, A. Engel, T. D. Pollard, and U. Aebi. The structural basis for the intrinsic disorder of the actin filament: the "lateral slipping" model, *J. Cell Biol*. **115**(3), 689–703 (1991).

24. E. H. Egelman, N. Francis, and D. J. DeRosier. F-actin is a helix with a random variable twist, *Nature* **298**(5870), 131–135 (1982).
25. J. Trinick, J. Cooper, J. Seymour, and E. H. Egelman. cryo-electron microscopy and three-dimensional reconstruction of actin filament, *J. Microsc.* **141**(Pt 3), 349–360 (1986).
26. R. A. Milligan, M. Whittaker, and D. Safer. Molecular structure of F-actin and location of surface binding sites, *Nature* **348**(6298), 217–221 (1990).
27. E. H. Egelman. A robust algorithm for the reconstruction of helical filaments using single-particle methods, *Ultramicroscopy* **85**(4), 225–234 (2000).
28. A. Narita, T. Yasunaga, T. Ishikawa, K. Mayanagi, and T. Wakabayashi. Ca(2+)-induced switching of troponin and tropomyosin on actin filaments as revealed by electron cryo-microscopy, *J. Mol. Biol.* **308**(2), 241–261 (2001).
29. D. Paul, A. Patwardhan, J. M. Squire, and E. P. Morris. Single particle analysis of filamentous and highly elongated macromolecular assemblies, *J. Struct. Biol.* **148**(2), 236–250 (2004).
30. E. H. Egelman. Molecular evolution: actin's long lost relative found, *Curr. Biol.* **11**(24), R1022–R1024 (2001).
31. W. Kabsch, H. G. Mannherz, D. Suck, E. F. Pai, and K. C. Holmes. Atomic structure of the actin:DNase I complex, *Nature* **347**(6288), 37–44 (1990).
32. K. C. Holmes, D. Popp, W. Gebhard, and W. Kabsch. Atomic model of the actin filament, *Nature* **347**(6288), 44–49 (1990).
33. M. Lorenz, D. Popp, and K. C. Holmes. Refinement of the F-actin model against X-ray fiber diffraction data by the use of a directed mutation algorithm, *J. Mol. Biol.* **234**(3), 826–836 (1993).
34. M. M. Tirion, D. ben-Avraham, M. Lorenz, and K. C. Holmes. Normal modes as refinement parameters for the F-actin model, *Biophys. J.* **68**(1), 5–12 (1995).
35. K. C. Holmes, I. Angert, F. J. Kull, W. Jahn, and R. R. Schroder. Electron cryo-microscopy shows how strong binding of myosin to actin releases nucleotide, *Nature* **425**(6956), 423–427 (2003).
36. X. Chen, R. K. Cook, and P. A. Rubenstein. Yeast actin with a mutation in the "hydrophobic plug" between subdomains 3 and 4 (L266D) displays a cold-sensitive polymerization defect, *J. Cell Biol.* **123**(5), 1185–1195 (1993).
37. R. Musib, G. Wang, L. Geng, and P. A. Rubenstein. Effect of polymerization on the subdomain 3/4 loop of yeast actin, *J. Biol. Chem.* **277**(25), 22699–22709 (2002).
38. A. Shvetsov, R. Musib, M. Phillips, P. A. Rubenstein, and E. Reisler. Locking the hydrophobic loop 262–274 to G-actin surface by a disulfide bridge prevents filament formation, *Biochemistry* **41**(35), 10787–10793 (2002).
39. T. Oda. Structural analysis of filamentous macromolecular complexes: in the case of actin filament, *Seitai no kagaku* **56**(6), 581–587 (2005).
40. D. S. Kudryashov, M. R. Sawaya, H. Adisetiyo, T. Norcross, G. Hegyi, E. Reisler, and T. O. Yeates. The crystal structure of a cross-linked actin dimer suggests a detailed molecular interface in F-actin, *Proc. Natl. Acad. Sci. USA* **102**(37), 13105–13110 (2005).
41. H. Gong, V. Hatch, L. Ali, W. Lehman, R. Craig, and L. S. Tobacman. Mini-thin filaments regulated by troponin-tropomyosin, *Proc. Natl. Acad. Sci. USA* **102**(3), 656–661 (2005).
42. K. C. Holmes. Solving the structure of macromolecular complexes with the help of X-ray fiber diffraction diagrams, *J. Struct. Biol.* **115**(2), 151–158 (1995).
43. D. L. D. Casper. The radial density distribution in the tobacco mosaic virus particle, *Nature* **177**(4516), 928 (1956).
44. R. E. Franklin. Location of the ribonucleic acid in the tabacco mosaic virus particles, *Nature* **177**(4516), 928–930 (1956).
45. K. C. Holmes, G. J. Stubbs, E. Mandelkow, and U. Gallwitz. structure of tobacco mosaic virus at 6.7 A resolution, *Nature* **254**(5497), 192–196 (1975).
46. G. Stubbs, S. Warren, and K. Holmes. Structure of RNA and RNA binding site in tobacco mosaic virus from 4-A map calculated from X-ray fibre diagrams, *Nature* **267**(5608), 216–221 (1977).
47. K. Namba, and G. Stubbs. Structure of tobacco mosaic virus at 3.6 A resolution: implications for assembly, *Science* **231**(4744), 1401–1406 (1986).
48. K. Namba, R. Pattanayek, and G. Stubbs. Visualization of protein-nucleic acid interactions in a virus. Refined structure of intact tobacco mosaic virus at 2.9 A resolution by X-ray fiber diffraction, *J. Mol. Biol.* **208**(2), 307–325 (1989).

49. K. Namba, and G. Stubbs. Difference Fourier syntheses in fiber diffraction, *Acta Cryst.* **A43**(Pt 4), 533–539 (1987).
50. K. Namba, and G. Stubbs. Solving the phase problem in fiber diffraction. Application to tobacco mosaic virus at 3.6 A resolution, *Acta Cryst.* **A41**(Pt 3), 252–262 (1985).
51. V. V. Lednev. Structure and function of the thin filaments of the cross-striated muscle of vertebrates. structural parameters of F-actin, *Biofizika* **19**(1), 116–121 (1974).
52. D. Popp, V. V. Lednev, and W. Jahn. Methods of preparing well-orientated sols of f-actin containing filaments suitable for X-ray diffraction, *J. Mol. Biol.* **197**(4), 679–684 (1987).
53. T. Oda, K. Makino, I. Yamashita, K. Namba, and Y. Maeda. Effect of the length and effective diameter of F-actin on the filament orientation in liquid crystalline sols measured by X-ray fiber diffraction, *Biophys J.* **75**(6), 2672–2681 (1998).
54. I. Yamashita, F. Vonderviszt, Y. Mimori, H. Suzuki, K. Oosawa, and K. Namba. Radial mass analysis of the flagellar filament of Salmonella: implications for the subunit folding, *J. Mol. Biol.* **253**(4), 547–558 (1995).
55. G. J. Stubbs, and R. Diamond. The phase problem for cylindrically averaged diffraction patterns. Solution by isomorphous replacement and application to tobacco mosaic virus, *Acta Cryst.* **A31**(Pt 6), 709–718 (1975).
56. M. F. Smith, and J. P. Langmore. Quantitation of molecular densities by cryo-electron microscopy. Determination of the radial density distribution of tobacco mosaic virus, *J. Mol. Biol.* **226**(3), 763–774 (1992).
57. Y. Mimori, I. Yamashita, K. Murata, Y. Fujiyoshi, K. Yonekura, C. Toyoshima, and K. Namba. The structure of the R-type straight flagellar filament of Salmonella at 9 A resolution by electron cryomicroscopy, *J. Mol. Biol.* **249**(1), 69–87 (1995).
58. T. W. Jeng, R. A. Crowther, G. Stubbs, and W. Chiu. Visualization of alpha-helices in tobacco mosaic virus by cryo-electron microscopy, *J. Mol. Biol.* **205**(1), 251–257 (1989).
59. K. Namba, I. Yamashita, and F. Vonderviszt. Structure of the core and central channel of bacterial flagella, *Nature* **342**(6250), 648–654 (1989).
60. A. Klug, F. H. Crick, and H. W. Wyckoff. Diffraction by helical structure, *Acta Cryst.* **11**(Pt 3), 199–213 (1958).
61. T. Oda, Z. D. Crane, C. W. Dicus, B. A. Sufi, and R. B. Bates. Dolastatin 11 connects two long-pitch strands in F-actin to stabilize microfilaments, *J. Mol. Biol.* **328**(2), 319–324 (2003).
62. D. L. D. Casper. The radial density distribution in the tobacco mosaic virus particle, *Nature* **177**(4516), 928 (1956).
63. R. E. Franklin. Location of the ribonucleic acid in the tabacco mosaic virus particles, *Nature* **177**, 928–930 (1956).
64. A. Orlova, and E. H. Egelman. A conformational change in the actin subunit can change the flexibility of the actin filament, *J. Mol. Biol.* **232**(2), 334–341 (1993).
65. N. Go, T. Noguti, and T. Nishikawa. Dynamics of a small globular protein in terms of low-frequency vibrational modes, *Proc. Natl. Acad. Sci. USA* **80**(12), 3696–3700 (1983).
66. B. Brooks, and M. Karplus. Harmonic dynamics of proteins: normal modes and fluctuations in bovine pancreatic trypsin inhibitor, *Proc. Natl. Acad. Sci. USA* **80**(21), 6571–6575 (1983).
67. M. M. Tirion. Large amplitude elastic motions in proteins from a single-parameter, atomic analysis, *Phys. Rev. Lett.* **77**(9), 1905–1908 (1996).
68. I. Bahar, A. R. Atilgan, and B. Erman. Direct evaluation of thermal fluctuations in proteins using a single-parameter harmonic potential, *Fold Des.* **2**(3), 173–181 (1997).
69. F. Tama, and Y. H. Sanejouand. Conformational change of proteins arising from normal mode calculations, *Protein Eng.* **14**(1), 1–6 (2001).
70. C. Xu, D. Tobi, and I. Bahar. Allosteric changes in protein structure computed by a simple mechanical model: hemoglobin T⟨–⟩R2 transition, *J. Mol. Biol.* **333**(1), 153–168 (2003).
71. R. Diamond. On the use of normal modes in thermal parameter refinement: theory and application to the bovine pancreatic trypsin inhibitor, *Acta Crystallogr. A* **46**(Pt 6), 425–435 (1990).
72. A. Kidera, and N. Go. Normal mode refinement: crystallographic refinement of protein dynamic structure. I. Theory and test by simulated diffraction data, *J. Mol. Biol.* **225**(2), 457–475 (1992).
73. Y. Wu, and J. Ma. Refinement of F-actin model against fiber diffraction data by long-range normal modes, *Biophys J.* **86**(1 Pt 1), 116–124 (2004).

74. F. Tama, M. Valle, J. Frank, and C. L. Brooks, 3rd. Dynamic reorganization of the functionally active ribosome explored by normal mode analysis and cryo-electron microscopy, *Proc. Natl. Acad. Sci. USA* **100**(16), 9319–9323 (2003).
75. H. Wang, and G. Stubbs. Molecular dynamics in refinement against fiber diffraction data, *Acta Crystallogr A* **49**(3), 504–513 (1993).
76. L. R. Otterbein, P. Graceffa, and R. Dominguez. The crystal structure of uncomplexed actin in the ADP state, *Science* **293**(5530), 708–711 (2001).
77. J. K. Chik, U. Lindberg, and C. E. Schutt. The structure of an open state of beta-actin at 2.65 A resolution, *J. Mol. Biol.* **263**(4), 607–623 (1996).
78. C. E. Schutt, J. C. Myslik, M. D. Rozycki, N. C. Goonesekere, and U. Lindberg. The structure of crystalline profilin-beta-actin, *Nature* **365**(6449), 810–816 (1993).
79. R. Page, U. Lindberg, and C. E. Schutt. Domain motions in actin, *J. Mol. Biol.* **280**(3), 463–474 (1998).
80. F. van den Ent, J. Moller-Jensen, L. A. Amos, K. Gerdes, and J. Lowe. F-actin-like filaments formed by plasmid segregation protein ParM, *EMBO J.* **21**(24), 6935–6943 (2002).
81. F. van den Ent, L. A. Amos, and J. Lowe. Prokaryotic origin of the actin cytoskeleton, *Nature* **413**(6851), 39–44 (2001).
82. P. J. Kraulis. MOLSCRIPT: a program to produce both detailed and schematic plots of protein structures, *J. Appl. Cryst* **24**(5), 946–950 (1991).

Participants in the international symposium “Regulatory Proteins of Striated Muscle – Structure, Function and Disorder (33rd NIPS Conference),” held at the Okazaki Conference Center, Okazaki, Japan, October 25–28, 2005, to celebrate the 40th anniversary of Professor Ebashi’s discovery of troponin.

SUBJECT INDEX

W

X